

N73- 27899
NASA CR-114607
DOUGLAS MDC-J4371

STUDY OF QUIET TURBOFAN STOL AIRCRAFT
FOR
SHORT-HAUL TRANSPORTATION

FINAL REPORT
VOLUME II
AIRCRAFT

JUNE 1973

Prepared Under Contract No. NAS2-6994

for

ADVANCED CONCEPTS AND MISSIONS DIVISION
NATIONAL AERONAUTICS AND SPACE ADMINISTRATION
MOFFETT FIELD, CALIFORNIA 94035

Douglas Aircraft Company - Long Beach

FOREWORD

This document is one of six volumes which comprises the final report of a contract study performed for NASA, "Study of Quiet Turbofan STOL Aircraft for Short-Haul Transportation," by the Douglas Aircraft Company, McDonnell Douglas Corporation.

The NASA technical monitor for the study was R. C. Savin, Advanced Concepts and Missions Division, Ames Research Center, California.

The Douglas program manager for the study was L. S. Rochte. He was assisted by study managers who prepared the analyses contained in the technical volumes shown below.

Volume I	Summary	
Volume II	Aircraft	L. V. Malthan
Volume III	Airports	J. K. Moore
Volume IV	Markets	G. R. Morrissey
Volume V	Economics	M. M. Platte
Volume VI	Systems Analysis	J. Seif

The participation of the airline subcontractors, (Air California, Allegheny, American and United), throughout the study was coordinated by J. A. Stern.

The one year study, initiated in May 1972, was divided into two phases. The final report covers both phases.

TABLE OF CONTENTS

	Page
TABLE OF CONTENTS	iii
LIST OF FIGURES	ix
LIST OF TABLES	xviii
SUMMARY	1
INTRODUCTION	3
SYMBOLS AND ABBREVIATIONS	5
1.0 AIRCRAFT ANALYSIS STUDY PLAN	11
2.0 AIRCRAFT DESIGNS	15
2.1 Parametric Aircraft	15
2.1.1 Performance Ground Rules	16
2.1.2 Direct Operating Cost Ground Rules	19
2.1.3 Sizing Results	19
2.1.4 Parametric Results	26
2.2 Final Design Aircraft	41
2.2.1 Final Design Aircraft Performance Ground Rules	43
2.2.2 Aircraft Sizing	45
2.2.3 Configuration Descriptions	57
2.2.4 Final Design Aircraft Weight and Performance	75
2.3 System Analysis Aircraft	86
2.3.1 Aircraft Configurations	86
2.3.2 Noise Contours	88
3.0 AIRCRAFT TRADE STUDIES	103
3.1 Aircraft Noise Study	104
3.1.1 Aircraft Analysis	104

TABLE OF CONTENTS (Cont'd)

	Page
3.1.2 Results	112
3.1.3 Conclusions	115
3.2 Configuration Studies	115
3.2.1 Aspect Ratio Study - EBF	115
3.2.2 Boundary Layer Control for USB STOL Leading Edge Protection	120
3.3 Performance Trade Offs	125
3.3.1 Cruise Performance Optimization	125
3.3.2 Trade Factors	125
3.4 Landing Ground Rules Study	130
3.5 Avionics Studies	145
3.5.1 Avionics Baseline	145
3.5.2 Avionics Tradeoffs	145
3.5.3 STOL A.T.C. Environment	156
3.6 Ride Qualities Study	161
3.7 Alternate Missions	163
3.8 Advanced Composite Materials Study	168
3.8.1 Aircraft Resizing	168
3.8.2 Structural Description	169
3.8.3 Conclusions	175
3.9 Military/Commercial Commonality	176
4.0 QCSEE COORDINATION AND ENGINE SELECTION	185
4.1 Engine/Airframe Coordination	185
4.2 Engine Selection	185

TABLE OF CONTENTS (cont'd)

	Page
4.2.1 Engine Selection Criteria	185
4.2.2 Selection Approach	187
4.2.3 Engines for Final Design Aircraft	188
4.2.4 Engines for EBF Aircraft	188
4.2.5 Engine for Upper Surface Blown Flap	194
4.2.6 Engine for Mechanical Flap	194
4.2.7 Engines for Augmentor Wing	195
5.0 AIRLINE COORDINATION	199
6.0 STOL TECHNOLOGY ASSESSMENT	203
6.1 Critical Technology	203
6.1.1 Critical Acoustic Technology	203
6.1.2 Critical Propulsion System Technology	204
6.2 High Payoff Technology	207
6.2.1 High Payoff Propulsion System Technology	207
6.2.2 High Payoff Aerodynamic Technology	208
6.2.3 High Payoff Structure and Materials Technology	209
6.2.4 Ice Protection	210
7.0 CONCLUSIONS	211
REFERENCES	215
 APPENDIX	
A PRELIMINARY BASEPOINT AIRCRAFT	219
B AERODYNAMIC SUBSTANTIATION - FINAL DESIGN AIRCRAFT	225
B.1 Performance Analysis Methods	225
B.1.1 Takeoff	225
B.1.2 Landing	227

TABLE OF CONTENTS (Cont'd)

	Page
B.1.3 Aircraft Sizing	230
B.2 High Lift Configuration Aerodynamic Characteristics.	238
B.2.1 Externally Blown Flap	239
B.2.2 Upper Surface Blowing	249
B.2.3 Conventional Mechanical Flap Systems	254
B.2.3.1 3000 Foot (914 m) Field Length	254
B.2.3.2 4000 Foot (1219 m) Field Length	256
B.2.3.3 CTOL Field Length	256
B.2.4 Augmentor Wing	260
B.2.5 Ground Effects	263
B.3 High Speed Aerodynamic Characteristics	268
C ACOUSTIC ANALYSIS - FINAL DESIGN AIRCRAFT	275
C.1 Introduction	275
C.2 Acoustic Technology	275
C.2.1 Noise Sources	275
C.2.2 Duct Linings	276
C.2.3 1980 Technology Factors	280
C.3 Aircraft Noise Levels	282
C.3.1 EBF Concept	282
C.3.2 Upper Surface Blowing Concept	287
C.3.3 Mechanical Flap Concept	288
C.3.4 Augmentor Wing Concept	291
C.3.5 Internally Blown Jet Flap Concept	293
C.3.6 Conventional Takeoff and Landing Aircraft (CTOL)	296

TABLE OF CONTENTS (Cont'd)

	Page
D	
PROPULSION INSTALLATION SUBSTANTIATION - FINAL DESIGN AIRCRAFT	299
D.1 Propulsion Installation	299
D.1.1 Externally Blown Flap	299
D.1.2 Upper Surface Blowing	303
D.1.3 Augmentor Wing	311
D.1.4 Mechanical Flap	317
D.2 Installed Engine Performance (General)	320
D.2.1 Inlet Pressure Loss	321
D.2.2 Fan Duct and Nozzle Losses	321
D.2.3 External Aerodynamic Losses	321
D.2.4 Airbleed and Mechanical Power Extraction	323
D.3 Installed Engine Performance Particular to the Augmentor Wing	323
D.3.1 High Lift Configuration	323
D.3.2 Cruise Configuration	325
D.3.3 Fan Exhaust Losses	325
D.3.4 Primary Exhaust System Losses	325
D.4 Installation Loss Analyses	326
D.5 Installed Propulsion System Performance Data	326
E	
MASS PROPERTIES DATA	337
E.1 Weights, Dimensional and Structural Data	338
E.2 Weight Substantiation	338
E.2.1 Wing Structure	344
E.2.2 Tail Structure	344
E.2.3 Fuselage Structure	348

TABLE OF CONTENTS (Cont'd)

	Page
E.2.4 Landing Gear	348
E.2.5 Flight Control and Hydraulics	348
E.2.6 Nacelle, Pylon, and Propulsion	353
E.2.7 Instruments	355
E.2.8 APU, Pneumatics, and Air Conditioning	357
E.2.9 Electrical System	357
E.2.10 Avionics	357
E.2.11 Furnishings	357
E.2.12 Ice Protection	366
E.2.13 Operational Items	366
E.3 Balance and Moments of Inertia	369
F FINAL DESIGN AIRCRAFT CONTROL SYSTEM, HANDLING QUALITIES, AND FLIGHT ENVELOPE	389
F.1 Control System	389
F.2 Flying Qualities	391
F.2.1 Longitudinal	391
F.2.2 Lateral-Directional	395
F.3 STOL Flight Envelope	403
F.4 Conclusions	405
G RIDE QUALITIES	407
G.1 Introduction Ride Qualities	407
G.2 Longitudinal Axis	408
G.3 Lateral/Directional Axes	414
G.4 Conclusions - Ride Qualities	424

LIST OF FIGURES

		Page
1-1	Aircraft Analysis Study Plan	12
2-1	Parametric Aircraft Sizing Mission Profile	18
2-2	Externally Blown Flap Parametric Aircraft Sizing	20
2-3	Externally Blown Flap Parametric Aircraft Sizing	21
2-4	Augmentor Wing Parametric Aircraft Sizing	23
2-5	Upper Surface Blown Flap Parametric Aircraft Sizing	24
2-6	Mechanical Flap Parametric Aircraft Sizing	25
2-7	Internally Blown Flap Parametric Aircraft Sizing	27
2-8	Parametric Wing Loading and Thrust-to-Weight Variations . . .	37
2-9	Parametric Direct Operating Cost Variation with Field Length	39
2-10	Parametric Takeoff Gross Weight Variation with Field Length	40
2-11	Sizing Mission Profile	44
2-12	Externally Blown Flap STOL Aircraft Sizing - 150 Psgr, 3000 ft Runway	46
2-13	Externally Blown Flap STOL Aircraft Sizing - 200 Psgr, 3000 ft Runway	48
2-14	Externally Blown Flap STOL Aircraft Sizing - 100 Psgr, 3000 ft Runway	49
2-15	Externally Blown Flap STOL Aircraft Sizing - 150 Psgr, 2000 ft Runway	50
2-16	Mechanical Flap STOL Aircraft Sizing - 150 Psgr, 3000 ft Runway	52
2-17	Mechanical Flap STOL Aircraft Sizing - 150 Psgr, 4000 ft Runway	53
2-18	Augmentor Wing STOL Aircraft Sizing - 150 Psgr, 2000 ft Runway	55
2-19	Upper Surface Blown Flap STOL Aircraft Sizing - 150 Psgr, 2000 ft Runway	56

LIST OF FIGURES (Cont'd)

	Page
2-20 Externally Blown Flap Aircraft - Final Design - 100 Passengers - 3000 Ft. (915 m) Field Length	58
2-21 Externally Blown Flap Aircraft - Final Design - 150 Passengers - 3000 ft (915 m) Field Length	59
2-22 Externally Blown Flap Aircraft - Final Design 200 Passengers - 3000 ft (915 m) Field Length	60
2-23 Externally Blown Flap Aircraft - Final Design 150 Passengers - 2000 ft (610 m) Field Length	61
2-24 Upper Surface Blown Aircraft - Final Design 150 Passengers - 2000 ft (610 m) Field Length	62
2-25 Augmentor Wing Aircraft - Final Design 150 Passengers - 2000 ft (610 m) Field Length	63
2-26 Mechanical Flap Aircraft - Final Design 150 Passengers - 3000 ft (914 m) Field Length	64
2-27 Mechanical Flap Aircraft - Final Design 150 Passengers, 4000 ft (1219 m) Field Length	65
2-28 CTOL Aircraft - Final Design - 150 Passengers, 7500 ft (2286 m) Field Length	66
2-29 100 Passenger Interior - Final Design Aircraft	71
2-30 150 Passenger Interior - Final Design Aircraft	72
2-31 200 Passenger Interior - Final Design Aircraft	73
2-32 Externally Blown Flap STOL Aircraft Cruise Performance . . .	78
2-33 Time, Distance, and Fuel to Climb from Sea Level	79
2-34 Time, Distance, and Fuel to Descend to Sea Level	80
2-35 Reserve Fuel vs Distance to Alternate	81
2-36 Design Takeoff Gross Weight - Field Length Comparison - Final Design Aircraft	82
2-37 Direct Operating Cost - Field Length Comparison - Final Design Aircraft	83
2-38 Wing Loading: Thrust-to-Weight Relationship - Final Design Aircraft	85

LIST OF FIGURES (Cont'd)

		Page
2-39	Typical EPNL-Distance Curves	89
2-40	Single Event EPNL Contours	91
2-41	Effect of Field Length on 90 EPNdB Noise Contour	92
2-42	Comparison of Externally Blown Flap and Mechanical Flap STOL	93
2-43	Comparison of Externally Blown Flap Systems Analysis - Aircraft and Final Design Aircraft - 90 EPNdB Noise Contour .	94
2-44	Effect of Sideline Noise Level on 90 EPNdB Noise Contour	95
2-45	Single Event EPNL Contours - E.150.2000 - 4 Allison PD287-3 Engines	97
2-46	Single Event EPNL Contours - U.150.2000 - 4 Allison PD287-22 Engines	98
2-47	Single Event EPNL Contours - M.150.3000 - 2 Allison PD287-23 Engines	99
2-48	Single Event EPNL Contours - A.150.4000 - 4 Allison PD287-23 Engines	100
2-49	Single Event EPNL Contours - A.150.2000 - 4 Allison PD287-43 Engines	101
2-50	Single Event EPNL Contours - 1980 Advanced Technology CTOL	102
3-1	Noise Study Engine Cutaway Drawings	106
3-2	Noise Trade Off Results - EBF Configuration	114
3-3	Effect of Aspect Ratio on Aircraft Sizing	119
3-4	Effect of Leading Edge Boundary Layer Control on $\Delta C_{L_{max}}$	122
3-5	Effect of Leading Edge Boundary Layer Control on T/W Required	122
3-6	Direct Operating Cost Variation with Cruise Mach Number . . .	126
3-7	Cruise Altitude Optimization	127

LIST OF FIGURES (Cont'd)

	Page
3-8 Landing Field Length Versus Wing Loading	131
3-9 Effect of Landing Ground Rules on Aircraft Sizing	132
3-10 Effect of Approach Sink Rate on Landing Field Length	134
3-11 Effect of Touchdown Sink Rate on Landing Field Length.	137
3-12 Effect of Deceleration Rate on Landing Field Length.	138
3-13 Effect of Field Length Factor on Landing Field Length.	141
3-14 Effect of Ground Effect on Landing Field Length.	142
3-15 Parametric - Final Landing Ground Rules Comparison	144
3-16 Upgraded Third Generation Conus ATC System	158
3-17 Direct Operating Cost Penalty for Extended Range Capability - Externally Blown Flap Aircraft.	167
3-18 Composite Structure Aircraft	172
3-19 Composite Application to STOL Baseline	173
3-20 Military STOL Transport.	177
3-21 Commercial Derivative of Military Transport	178
3-22 Fuselage Cross Section	180
4-1 Fan Exhaust Velocity	190
4-2 Effect of Fan Pressure Ratio on Direct Operating Cost.	192
4-3 Effect of Engine Cycle Parameters on Direct Operating Cost - 1.2 Fan Pressure Ratio Engines.	193
4-4 Effect of Engine Cycle Parameters on Direct Operating Cost - 2.5 Fan Pressure Ratio Engines.	196
A-1 Basepoint Parametric Aircraft - Externally Blown Flap - Externally Blown Flap - Passengers: 100, Field Length (ft): 2000	220
A-2 Basepoint Parametric Aircraft - Upper Surface Blown Jet Flap - Passengers: 100, Field Length (ft): 2000.	221

LIST OF FIGURES (Cont'd)

	Page
A-3 Basepoint Parametric Aircraft - Augmentor Wing - Passengers: 100, Field Length 2000 ft (610 m)	222
B-1 Sample Takeoff Time History	226
B-2 Takeoff Field Length Definition	228
B-3 Landing Field Length Definition	229
B-4 Sample Flare Time History	232
B-5 Aircraft Sizing Process	233
B-6 Sizing Mission Profile	235
B-7 Sample Sizing Mission Summary Printout	236
B-8 Sample Direct Operating Cost Breakdown Printout	237
B-9 Externally Blown Flap Trimmed Lift and Drag Characteristics - Takeoff Configuration	240
B-10 Externally Blown Flap Trimmed Lift and Drag Characteristics - Landing Configurations	241
B-11 Externally Blown Flap Trimmed Lift and Drag Characteristics - Landing Configuration	242
B-12 Externally Blown Flap Trimmed Lift and Drag Characteristics - Takeoff Configuration	243
B-13 Externally Blown Flap Trimmed Lift and Drag Characteristics - Landing Configuration	244
B-14 Externally Blown Flap Trimmed Lift and Drag Characteristics - Landing Configuration	245
B-15 Externally Blown Flap Longitudinally, Laterally and Directionally Trimmed Lift and Drag Characteristics - Takeoff Configuration	246
B-16 Externally Blown Flap Longitudinally, Laterally and Directionally Trimmed Lift and Drag Characteristics - Landing Configuration	247
B-17 Externally Blown Flap Longitudinally, Laterally and Directionally Trimmed Lift and Drag Characteristics - Landing Configuration	248

LIST OF FIGURES (Cont'd)

	Page
B-18 Comparison of Pitching Moments - EBF and Upper Surface Blowing Configurations	250
B-19 Comparison of EBF and Upper Surface Blowing Configuration Lift Curves.	252
B-20 Comparison of EBF and Upper Surface Blowing Configuration Drag Polars	253
B-21 Mechanical Flap Trimmed Lift and Drag Characteristics - 3000 ft Field Length Configuration	257
B-22 Mechanical Flap Trimmed Lift and Drag Characteristics - 4000 ft Field Length Configuration	258
B-23 Mechanical Flap Trimmed Lift and Drag Characteristics - CTOL Configuration	259
B-24 Augmentor Wing Trimmed Lift and Drag Characteristics - Takeoff Configuration	264
B-25 Augmentor Wing Trimmed Lift and Drag Characteristics - Landing Configuration	265
B-26 Estimated Cruise-Configuration Drag Characteristics.	271
B-27 Estimated Cruise-Configuration Drag Characteristics.	272
B-28 Estimated Cruise-Configuration Drag Characteristics.	273
B-29 Estimated Cruise-Configuration Drag Characteristics.	274
C-1 Preliminary Design Chart for Acoustically Treated Inlet and Discharge Ducts.	278
D-1 Externally Blown Flap Engine Installation.	300
D-2 Upper Surface Blowing Engine Installation.	304
D-3 Augmentor Wing Engine Installation	312
D-4 Augmentor Wing Ducting Installation.	315
D-5 Mechanical Flap Engine Installation.	318
D-6 Fan Bleed-Heat Exchanger Effectivity	324
D-7 Gross Thrust and Ram Drag at Takeoff Power - Externally Blown Flap.	329

LIST OF FIGURES (Cont'd)

	Page
D-8 Gross Thrust and Ram Drag at Takeoff Power - Upper Surface Blowing	330
D-9 Gross Thrust and Ram Drag at Takeoff Power - Augmentor Wing	331
D-10 Gross Thrust and Ram Drag at Takeoff Power - Mechanical Flap	332
D-11 Generalized Net Thrust and Fuel Flow - Externally Blown Flap	333
D-12 Generalized Net Thrust and Fuel Flow - Upper Surface Blowing	334
D-13 Generalized Net Thrust and Fuel Flow - Augmentor Wing	335
D-14 Generalized Net Thrust and Fuel Flow - Mechanical Flap	336
E-1 Weight Trend - Wing Box	345
E-2 Weight Trend - Wing Group	346
E-3 Weight Trend - Tail Group	347
E-4 Weight Trend - Fuselage Structure	349
E-5 Weight Trend - Landing Gear	351
E-6 Weight Trend - Flight Controls and Hydraulic System	352
E-7 Pylon Unit Weight Comparison	354
E-8 Weight Trend - Instruments	356
E-9 Weight Trend - APU, Air Conditioning, Pneumatics	358
E-10 Weight Trend - Electrical Group	359
E-11 Weight Trend - Furnishings	365
E-12(a) Balance Diagram - 100 Pax EBF 3000 ft (914 m) Field Length	373
E-12(b) Balance Diagram - 150 Pax EBF 2000 ft (610 m) Field Length	374

LIST OF FIGURES (Cont'd)

	Page
E-12(c) Balance Diagram - 150 Pax EBF 3000 ft (914 m) Field Length	375
E-12(d) Balance Diagram - 200 Pax EBF 3000 ft (914 m) Field Length	376
E-12(e) Balance Diagram - 150 Pax AW 2000 ft (610 m) Field Length	377
E-12(f) Balance Diagram - 150 Pax USB 2000 ft (610 m) Field Length	378
E-12(g) Balance Diagram - 150 Pax MF 3000 ft (914 m) Field Length	379
E-12(h) Balance Diagram - 150 Pax MF 4000 ft (1220 m) Field Length	380
E-13 Vertical Center of Gravity	381
E-14 Airplane Pitching Moment of Inertia	382
E-15 Airplane Roll Moment of Inertia	383
E-16 Sample Problem Charts and Nomographs	386
F-1 Landing Flare Time History	393
F-2 RH Outboard Engine Cut Time History During Takeoff	397
F-3 RH Outboard Engine Cut Time History During Takeoff	398
F-4 RH Outboard Engine Cut Time History During Waveoff	399
F-5 RH Outboard Engine Cut Time History During Waveoff	400
F-6 Typical STOL Mode Operating Conditions	404
G-1 Longitudinal Ride Control System (Approach).	410
G-2 Basic Aircraft Normal Acceleration/Vertical Gust	411
G-3 Power Spectrum of Normal Acceleration.	412
G-4 Normal Acceleration/Vertical Gust.	413
G-5 Power Spectrum of Normal Acceleration.	415
G-6 Aircraft Normal Acceleration Activity in Turbulence.	416

LIST OF FIGURES (Cont'd)

	Page
G-7 Lateral Control System	419
G-8 Basic Aircraft Lateral Acceleration Activity - Lateral Acceleration/Beta Gust	420
G-9 Basic Aircraft Lateral Acceleration Activity - Power Spectrum of Lateral Acceleration	421
G-10 Effect of Yaw Rate + Lateral Acceleration Feedback to Rudder - Lateral Acceleration/Beta Gust	422
G-11 Basic Aircraft Lateral Acceleration Activity - Lateral Acceleration/Beta Gust	423
G-12 Basic Aircraft Lateral Acceleration Activity - Power Spectrum of Lateral Acceleration	425
G-13 Aircraft Lateral Acceleration - Activity in Turbulence	426

LIST OF TABLES

		Page
2-1	Aircraft Parametric Analysis - Externally Blown Flap - Allison PD287-3 Engines	28
2-2	Aircraft Parametric Analysis - Externally Blown Flap - GE-19/F6A Engines	29
2-3	Aircraft Parametric Analysis - Upper Surface Blown Flap - Allison PD287-22 Engines	30
2-4	Aircraft Parametric Analysis - Augmentor Wing - Allison PD287-43 Engines	31
2-5	Aircraft Parametric Analysis - Augmentor Wing - GE-19/F9A Engines	32
2-6	Aircraft Parametric Analysis - Internally Blown Jet Flap - Allison PD287-43 Engines	33
2-7	Aircraft Parametric Analysis - Mechanical Flap - Allison PD287-23 Engines.	34
2-8	Aircraft Parametric Analysis - CTOL - Twin Engine - 1380 Statute Mile Range	35
2-9	Final Design Aircraft Matrix	42
2-10	Final Design Aircraft Performance Summary	76
2-11	Final Design Aircraft Weight Summary	77
2-12	Characteristics Summary of Aircraft Families.	87
2-13	Noise Footprint Area Comparison	96
3-1	Engine Characteristics for Acoustics Study	105
3-2	Installation Losses for Aircraft Noise Level Trade Study (EBF Only).	109
3-3	Weight Breakdown - Aircraft Noise Study	110
3-4	Acoustic Trade Study Aircraft Summary	111
3-5	EBF STOL Noise Trade Study - EPNL @ 500 ft (152 m) Sideline - 4 Engines @ 20,000 lb (44,200 N)/Engine.	113
3-6	Treatment Definition - L/H	113

LIST OF TABLES (Cont'd)

	Page
3-7 EBF STOL Noise Trade Study - Engine Hardwall Noise Levels, 500 ft (152 m) Sideline - 4 Engines at 20,000 lb (44,200 N)/Engine	113
3-8 Aspect Ratio Study Aircraft	117
3-9 Wing Aspect Ratio Study Weight Summary	118
3-10 Leading Edge Slat vs Blown Leading Edge Flap Summary . . .	123
3-11 Sizing Trade Factors	128
3-12 Growth Factors	128
3-13 Comparison of Various Landing Ground Rules	133
3-14 Breguet 941 Sink Rate Comparisons	136
3-15 DC - Series Aircraft Deceleration Capability	136
3-16 Comparison of Operational and Maximum Performance Landing Distance on Breguet 941	140
3-17 Avionics Equipment List	146
3-18 Summary of Cost & Weight Savings for STOL Avionics	157
3-19 Externally Blown Flap STOL Aircraft - Extended Range Capability Performance Summary	164
3-20 Extended Range Capability Weight Summary	165
3-21 Advanced Materials Aircraft Weight Comparison	170
3-22 Advanced Materials Aircraft Summary	171
3-23 Cost Weight Commonality Comparison - Military STOL vs Model 24C	181
3-24 Aircraft Characteristics - Military STOL vs Model 24C . .	182
4-1 Final Design Aircraft Engine Characteristics	189
A-1 Preliminary Basepoint Aircraft Performance Summary	223
B-1 Final Aircraft Approach Margins	231
B-2 Mechanical Flap Engine-Out Lateral-Directional Trim Increments in Drag Coefficient	260

LIST OF TABLES (Cont'd)

	Page
B-3	Estimated Ejector Parameters 263
B-4	Low Speed Drag Breakdown - Final Design Aircraft 270
C-1	Noise Reduction Improvements from Technological Advancements 281
C-2	Noise Levels of Externally Blown Flap Airplane 286
C-3	Noise Level of Upper Surface Blowing Concept 289
C-4	Noise Level of Mechanical Flap Airplane. 290
C-5	Noise Level of Augmentor Wing Airplane 294
C-6	Noise Levels of Internally Blown Jet Flap. 295
C-7	Noise Level of Conventional Takeoff and Landing Airplane . . 297
D-1	Engine Support Structure Schemes for USB Lift Concept. . . . 307
D-2	Installation Losses 322
D-3	Installation Losses 327
D-4	Summary of Engine Losses for Propulsive Lift Configurations 328
E-1	Group Weight Summary 339
E-2	Dimensional and Structural Data 342
E-3	STOL Fuselage Weight Penalties and Unit Ratios 350
E-4	STOL Nacelle Weight Correlation 355
E-5	Avionics Weight Summary. 360
E-6	STOL Furnishings Weight. 364
E-7	Weight Summary - Ice Protection System 367
E-8	Operational Items Weight Summary 368
E-9	Weight, Balance and Principal Axis Summary 370
G-1	Longitudinal Transfer Functions 409
G-2	Lateral Transfer Functions 417

SUMMARY

Aircraft parametric analyses were completed on five different lift concepts for a short haul transportation system. Design parameters included: three field lengths, three passenger capacities, various cruise speeds, a range of 575 statute miles (926 km), and a noise goal of 95 PNdB at 500 feet (152 m) sideline. More than 200 parametric aircraft were generated which were then screened for their applicability to the short haul system. Most of the aircraft were eliminated due to very low wing loadings, very high thrust-to-weight ratios, or high operating costs. The remainder were subjected to a systems analysis evaluation from which eight candidate STOL aircraft were selected for more detailed analysis.

These eight candidate aircraft were resized based on improved weight and drag information and revised performance groundrules, and then subjected to detailed economic, market, systems analyses, and airport compatibility studies. The results of these studies are reported in the various other volumes comprising the NASA Systems Study final report. These aircraft are termed "system analysis aircraft".

Aircraft trade studies were performed on noise level, cruise performance, landing ground rules, avionics, ride quality, alternate missions, effects of composite materials and feasibility of military/commercial commonality. After several iterations to refine performance and weights, a number of final design aircraft emerged that had sideline noise levels ranging from 95 to 98 EPNdB compared to the 95 EPNdB of the systems analysis aircraft. Relaxing the design sideline noise goal significantly reduced aircraft direct operating costs, particularly when engine treatment level

was reduced. Other trade studies showed:

- o The landing ground rules and ground effects have a marked impact on aircraft sizing especially for the shorter design field lengths.
- o A STOL short haul aircraft could be designed to fly extended ranges with no significant penalty to its basic short range economics.
- o The use of composite materials can significantly reduce aircraft size and weight but further cost studies are required to determine economic viability.
- o A commercial STOL aircraft based upon a high degree of commonality with a military STOL transport appears to be economically feasible and could produce a viable short-haul aircraft.

The engine data used in the study were furnished by General Electric and Detroit Diesel Allison who are the two engine contractors in the NASA QCSEE study program. Four airlines - Air California, Allegheny, American and United - cooperated in the study and provided valuable assistance in assuring airline realism.

The critical technology areas where research and development should be emphasized include propulsive lift related acoustics, variable pitch fan engine technology and the aerodynamics of the upper surface blowing concept.

INTRODUCTION

This report summarizes in part the work accomplished under NASA Contract NAS 2-6994, "Study of Quiet Turbofan STOL Aircraft for Short Haul Transportation", which began May 8, 1972 and is culminated by this report. The objectives of the study were:

- o Determine relationships between STOL characteristics and economic and social viability of short-haul air transportation.
- o Identify critical technology problems to introduce STOL short-haul systems.
- o Define representative aircraft configurations, characteristics and costs.
- o Identify high payoff technology areas to improve STOL systems.

This volume summarizes the analyses of the aircraft designs which were generated to fulfill these objectives. The baseline aircraft characteristics are documented and significant trade studies presented.

The STOL lift concepts studied are analyzed in the context of a complete STOL transportation system. This system analysis work is presented in four companion volumes and a summary volume;

Volume I	Summary
Volume III	Airport Analysis
Volume IV	Market Analysis
Volume V	Economics Analysis
Volume VI	Systems Analysis

The contracted effort was conducted in coordination with the Quiet Clean STOL Experimental Engine (QCSEE) study program (Contract NAS 3-16726 and NAS 3-16727) managed by the NASA-Lewis Research Center. Douglas evaluated the candidate engines studied by both QCSEE contractors (General Electric and Detroit Diesel Allison) in the framework of the subject system study. Technical liaison with the QCSEE contractors was maintained throughout the study.

The contracted effort was equally divided between the aircraft analyses and the systems analyses efforts. The study consisted of the derivation of a large number of parametric aircraft representing several candidate propulsive and conventional lift systems and a wide matrix of design requirements. These aircraft were evaluated by the systems evaluation and aircraft design processes and narrowed to eight selected STOL aircraft. These eight aircraft and an additional advanced CTOL aircraft used for comparative purposes were then submitted to detailed short haul systems evaluation. Many aircraft trade studies were also conducted to refine these baseline designs.

SYMBOLS & ABBREVIATIONS

A_y	Lateral acceleration
A_z	Normal acceleration
APU	Auxiliary power unit
AR	Aspect ratio
ASKM	Available seat kilometer
ASSM	Available seat statute mile
ATC	Air Traffic Control
AW	Augmentor wing
BPR	Bypass ratio
BLC	Boundary layer control
C_D	Drag coefficient
C_{D_0}	Zero lift parasitic drag coefficient - zero lift parasitic drag/ $q S_w$
CG	Center of gravity
C_j	Jet momentum coefficient - mv/qS_w
C_L	Lift coefficient - lift/ qS_w
CTOL	Conventional takeoff and landing
C_μ	Gross thrust coefficient = gross thrust/ qS_w
C_{μ_0}	Ram drag coefficient = ram drag/ qS_w
C_v	Nozzle velocity coefficient
dB	decibel
D	Drag
DOC	Direct operating cost
EBF	Externally blown flap
EPNL	Effective perceived noise level
EPNdB	Effective perceived noise level in decibels
F	Thrust force
FAR	Federal Air Regulations

SYMBOLS & ABBREVIATIONS (Cont'd)

FL	Field length
FPR	Fan pressure ratio
fps	Feet per second
H	Height of duct flow channel
h_{CRUISE}	Cruise altitude
HP	Horsepower
$H_w(s)$	Turbulence model along W axis
$H_\beta(s)$	Turbulence model along Y axis
IAS	Indicated air speed
in	Inch
IBF	Internally blown flap
L	Length of duct flow channel
lb	Pound
K_{AZ}	Normal acceleration gain
K_θ	Pitch rate gain
KIAS	Indicated airspeed in knots
kg	Kilogram
LFL	Landing field length
m	Meter
\dot{m}	Mass flow measured
M	Mach number
MAC	Mean aerodynamic chord
MDOF	Multiple degree of freedom
MF	Mechanical flap
mps	Meters per second
n	Load factor
N	Newton

SYMBOLS & ABBREVIATIONS (Cont'd)

OEW	Operators empty weight
P	Pressure
PL	Payload, pounds
PNdB	Perceived noise level in decibels
PNL	Perceived noise level
Psgr	Passengers
q	Free stream dynamic pressure
S	Area; La Place operator
S_w	Wing area
SDOF	Single degree of freedom
st mi	Statute miles
STOL	Short takeoff and landing
t	Time
T	Temperature
t/c	Thickness ratio
$T_{1/10}$	Time to damp to one-tenth amplitude
$T_{1/2}$	Time to damp to one-half amplitude
TEU	Trailing edge up
TOFL	Takeoff field length
TOGW	Takeoff gross weight
T/W	Thrust-to-weight ratio
USB	Upper surface blown flap
v	Velocity
V	Velocity
V_1	Decision speed
V_{MIN}	Minimum operating speed
V_{MC}	Minimum control speed

SYMBOLS & ABBREVIATIONS (Cont'd)

W	Weight
W_G	Gust velocity along W axis
w	Mass flow
W/S	Wing loading
$Z.F.W.$	Zero fuel weight
Δn	Incremental load factor
α	Angle of attack
β	Side slip angle
β_G	Gust velocity along Y axis
γ	Flight path angle; static thrust turning efficiency
δ	Pressure relative to sea level standard
δ_A	Aileron displacement
δ_e	Elevator displacement
δ_F	Flap angle
δ_R	Rudder displacement
δ_{SP}	Spoiler deflection
δ_w	Control wheel deflection
ζ	Dampening ratio
θ	Aircraft pitch attitude; total flap deflection, relative absolute temperature
$\dot{\theta}$	Aircraft pitch rate
Λ	Sweep angle
λ	Taper ratio
μ	Coefficient of friction
ν	Static thrust turning angle
τ	Ratio of gross thrust to takeoff gross thrust, static turning efficiency

SYMBOLS & ABBREVIATIONS (Cont'd)

ϕ	Aircraft roll attitude
$\ddot{\phi}$	Roll acceleration
Φ_G	Gross thrust augmentation ratio
Φ_{G_i}	Ideal gross thrust augmentation ratio = $\Phi_G \times C_v$
Φ_w	Augmentor entrainment ratio
$\dot{\psi}$	Aircraft yaw rate
$\ddot{\psi}$	Yawing acceleration
ω_n	Undamped natural frequency

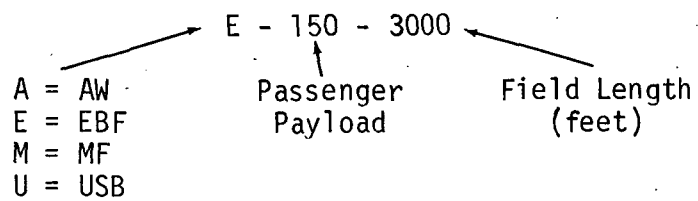
Subscripts

A	Air, airplane trimmed
CR	Cruise
T.E.	Trailing edge
T.O.	Takeoff
a	Air
am	Ambient
avg	Average
ea	Elastic axis
f	Fuel
g	Gross
i	Isentropically expanded
max	Maximum
n	Net
o	Free stream, standard sea level
r	Ram

SYMBOLS & ABBREVIATIONS (concluded)

t Total
ult Ultimate
w Wing
0,2,3,8,28 Engine station position

STOL Aircraft Model Designation



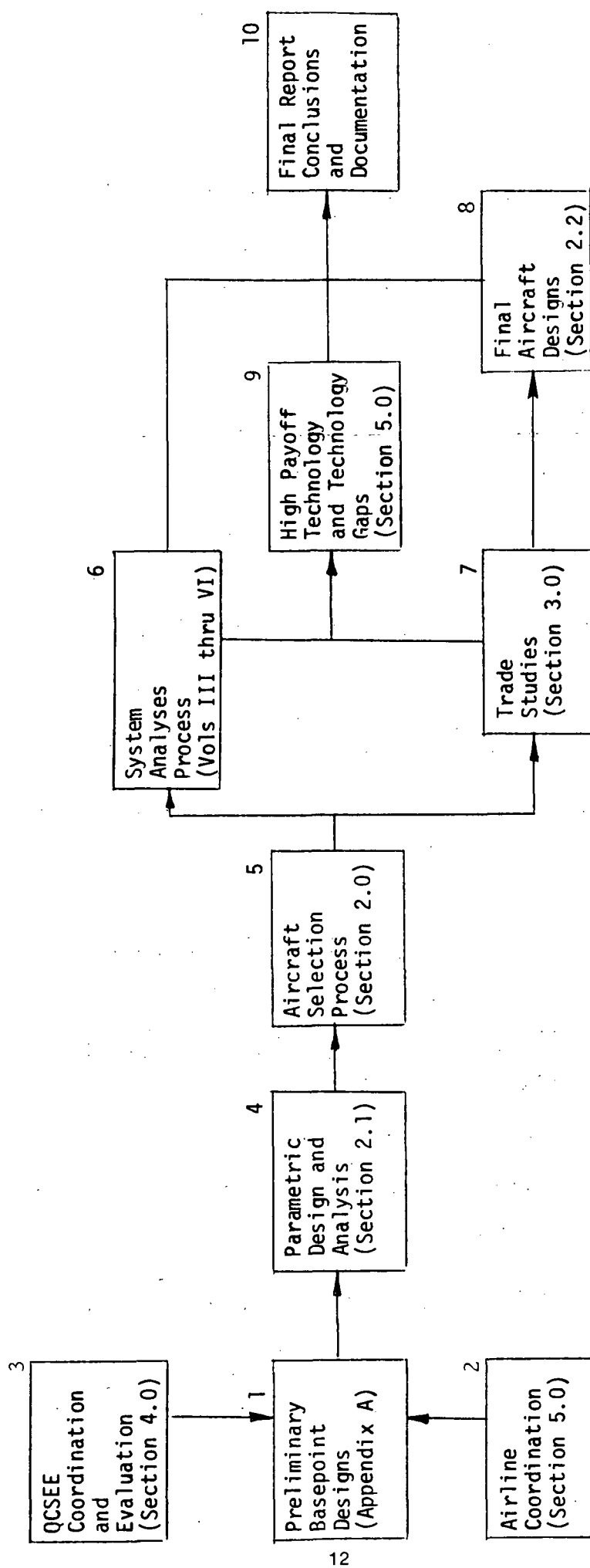
1.0 AIRCRAFT ANALYSIS STUDY PLAN

The aircraft analysis consisted of the generation and analysis of a broad spectrum of aircraft based on a number of high lift systems and a broad range of design requirements. This analysis began with the generation of a large number of parametric aircraft and progressed with the narrowing down of these aircraft to a limited set of designs which were subjected to detailed trade studies and analyses. The selection process was conducted with the aid of the systems analyses evaluations described in the companion volumes. At each step in the study, great care was taken to assure that realism in the designs was reflected.

This process is shown in Figure 1-1 and is described by the following steps:

- o A number of basepoint aircraft were developed and analyzed at the beginning of the study to assure an in-depth understanding of the aircraft characteristics such as weight, drag, high lift, propulsion, and acoustics (Block 1). These aircraft were designed for 100 passengers and a 2000 foot (610 m) field length and represented one aircraft each for the EBF, USB, AW and CTOL aircraft. To insure the use of realistic designs in the study extensive coordination with the airline subcontractors (United, American, Allegheny and Air California) was maintained and the results reflected in the baseline designs (Block 2). Also the QCSEE parametric study engines resulting from the General Electric and Allison contracts with NASA-Lewis were evaluated and the best engines used for the study aircraft (Block 3).

FIGURE 1-1 AIRCRAFT ANALYSIS STUDY PLAN



- o Based on the above basepoint analyses over 200 parametric aircraft designs were generated encompassing the various lift systems and the specified range of design requirements with the use of special STOL oriented computer programs (Block 4).
- o With the use of screening criteria such as operating costs, gross weight, wing loading, thrust loading and system analysis criteria, the parametric aircraft were successively narrowed to 8 specific STOL aircraft designs (Block 5).
- o These selected aircraft were then refined and subjected to detailed systems analyses (Block 6 as reported in the companion volumes).
- o A number of significant trade studies were conducted using one or more of the 8 selected detailed study aircraft (Block 7).
- o The results of these trade studies were then incorporated into a refined set of 8 final design aircraft for which detailed substantiation data is presented in the appendices of this report (Block 8). An additional advanced CTOL aircraft was synthesized for comparison purposes and use in the system analysis process.
- o Based on the results of the study work, an assessment of the technological gaps which must be filled before a STOL short-haul system can be implemented was determined (Block 9).

2.0 AIRCRAFT DESIGNS

2.1 Parametric Aircraft

In accordance with the study plan discussed in Section 1.0, preliminary basepoint aircraft were sized to assure a realistic basis for the aerodynamic, propulsion, acoustic and weight data used in the parametric study. The major characteristics of these aircraft are summarized in Appendix A. These aircraft used QCSEE study engines as supplied by General Electric and Detroit Diesel Allison. The best engine was selected for each lift concept by the evaluation process discussed in Section 4.0. These preliminary designs were reviewed with the airline participants and appropriate changes incorporated.

Parametric aircraft were then generated for the STOL high lift candidates, and included:

Externally Blown Flap (EBF)

Upper Surface Blowing (USB)

Augmentor Wing (AW)

Internally Blown Flap (IBF)

Mechanical Flap (MF)

The design requirements to which these aircraft systems were designed were:

Payload - 50, 100 and 200 passengers

Field Length - 1500 (457), 2000 (610) and 3000 feet (915 meters)

Noise Criteria - 95 PNdB at 500 feet (152 m) sideline distance

Design Range - 575 statute miles (926 km)

The aerodynamic, acoustic, propulsion and weight methodology is consistent with that used for the final design aircraft (Appendices B, C,

D and E respectively).

The parametric aircraft sizing process involves calculating takeoff and landing performance to determine combinations of T/W and W/S that meet the design requirements. A minimum direct operating cost criteria was used to select the optimum W/S - T/W combination for each set of requirements and lift system. Over 200 parametric aircraft were evaluated. Some of the more pertinent ground rules used to size these aircraft are described below.

2.1.1 Performance Ground Rules. - Takeoff field length is defined as the greater of:

- (1) $1.15 \times$ all engine takeoff distance to 35 foot (10.7 m) height.
- (2) Distance to 35 foot (10.7 m) height with critical engine failure at V_1 .
- (3) Distance to accelerate to V_1 and then decelerate to a stop.

The following constraints were used in calculating takeoff field length:

- (1) Rolling friction, $\mu = 0.025$
- (2) Fuselage angle of attack \leq ground limit = 15°
- (3) Rotation rate, $\dot{\theta} \leq 5^\circ/\text{sec}$
- (4) $C_L \leq 0.9 C_{L_{\max}}$
- (5) No deceleration during air run to 35 feet (10.7 m)
- (6) Five knot (2.75 m/sec) early rotation may not give greater takeoff field length
- (7) Accelerate - Stop distance based on three second delay after reaching V_1 followed by a deceleration of $0.4g$ to a stop.

Takeoff flap angle settings were optimized in determining the T/W required for each configuration. Takeoff performance was calculated at sea level on a 95°F (35°C) day.

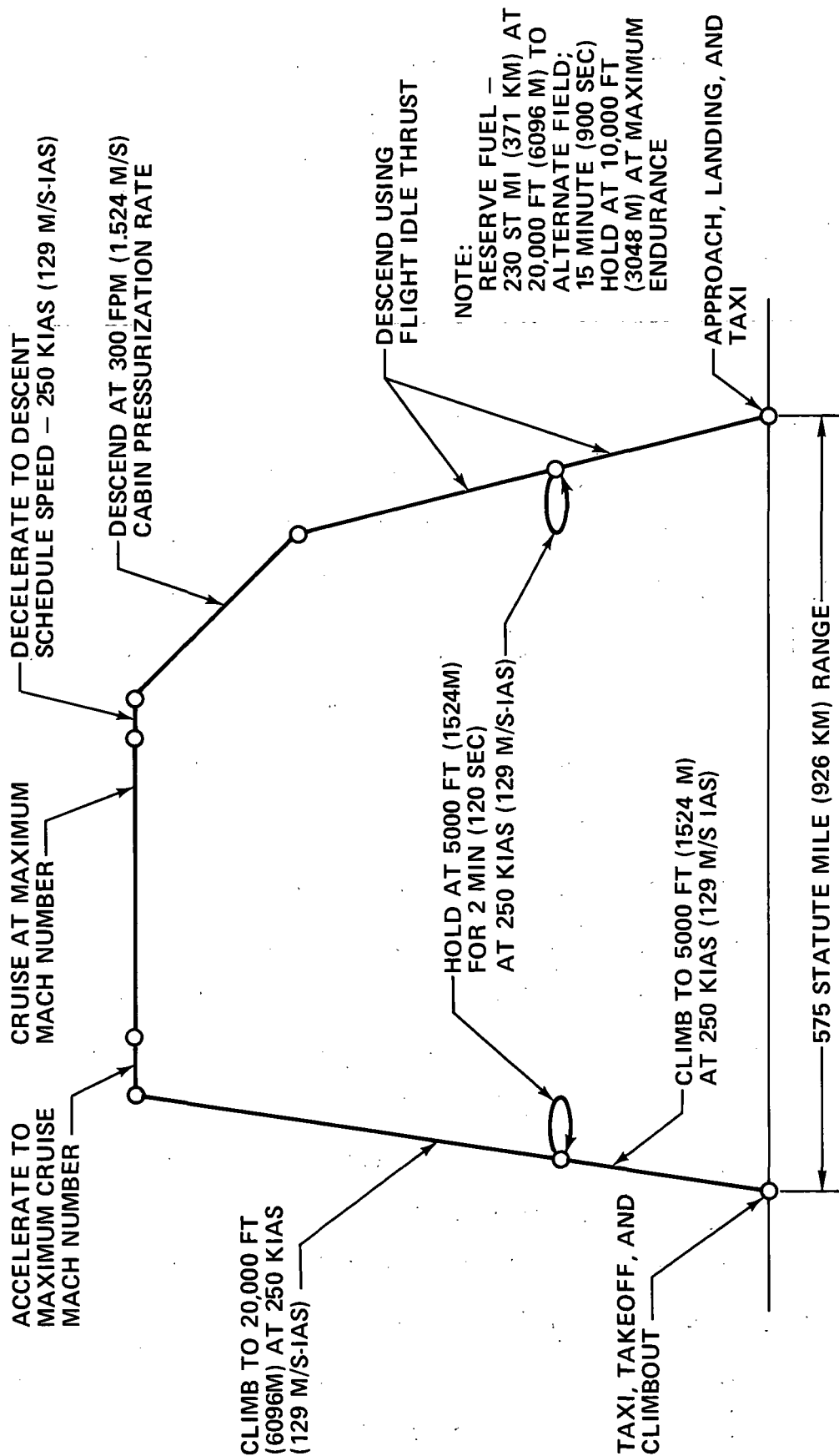
Landing field length is defined as landing distance over a 35 foot (10.7 m) obstacle divided by a 0.6 factor. The landing calculations were governed by the following constraints:

- (1) Approach sink speed = 800 fpm (4.06 m/sec)
- (2) Touchdown sink speed = 3 fps (.915 m/sec)
- (3) Rotation rate during flare, $\dot{\theta} \leq 5^\circ/\text{sec}$
- (4) Fuselage angle of attack \leq ground limit = 15°
- (5) Deceleration device effectiveness delay = 1 second
- (6) Deceleration rate = 0.35g

The load factor required to perform the flare maneuver was obtained from the use of direct lift control and rotation of the aircraft. Approach margins were selected to provide adequate maneuver capabilities in the event of an engine failure. Landing performance, like takeoff performance, was calculated for sea level, 95°F (35°C) conditions.

The mission profile used in sizing the parametric aircraft is shown in Figure 2-1. A computer program was used to iterate the weight, thrust and drag data to determine the characteristics, such as TOGW, OEW, wing area, engine size and fuel burned for an aircraft that satisfies the requirements of the mission profile. Mission performance was calculated for standard day conditions. Parametric tail sizing, based on previous STOL aircraft analyses at Douglas, is handled internally in the mission program. When a solution has been found, the program also calculates a direct operating cost breakdown.

PARAMETRIC AIRCRAFT SIZING MISSION PROFILE



PR3-STOL-1647

FIGURE 2-1.

2.1.2 Direct Operating Cost Ground Rules. - Direct operating costs (DOC) were used throughout the aircraft analysis as one of the prime criteria for aircraft optimization and selection. Two sets of DOC ground rules are used in these volumes; those for the aircraft analyses and those for the system analyses. The aircraft analyses ground rules were used throughout the aircraft studies reported in this volume. The aircraft analyses ground rules assume a production run of 300 aircraft and a 20 percent profit margin compared to 400 aircraft and a 10 percent margin used for the systems analysis work. The DOCs quoted in the companion volumes will therefore be somewhat lower than those quoted in this volume. Valid aircraft comparisons, however, are rendered by the use of the DOC criteria in this volume. Absolute values of DOC should be obtained from Volume V - Economic Analysis where a complete dissertation on the ingredients of the DOC equations will be found.

2.1.3 Sizing Results. -

EXTERNALLY BLOWN FLAP

Two typical aircraft sizing plots for the externally blown flap configuration using Allison and General Electric engines are shown in Figures 2-2 and 2-3, respectively. In order to keep STOL aircraft competitive in terms of speed with conventional turbine powered transport aircraft, a minimum acceptable cruise Mach number of 0.70 at 20,000 feet (6096 meters) was arbitrarily chosen as a design requirement for the parametric aircraft. This speed requirement was the critical sizing constraint primarily for the parametric externally blown flap aircraft with Allison engines. Wing loading and thrust-to-weight ratio were increased beyond those required for a balanced takeoff-landing condition in order to provide for sufficient cruise thrust. Cruise Mach number is low due to the very high thrust lapse rate of the high

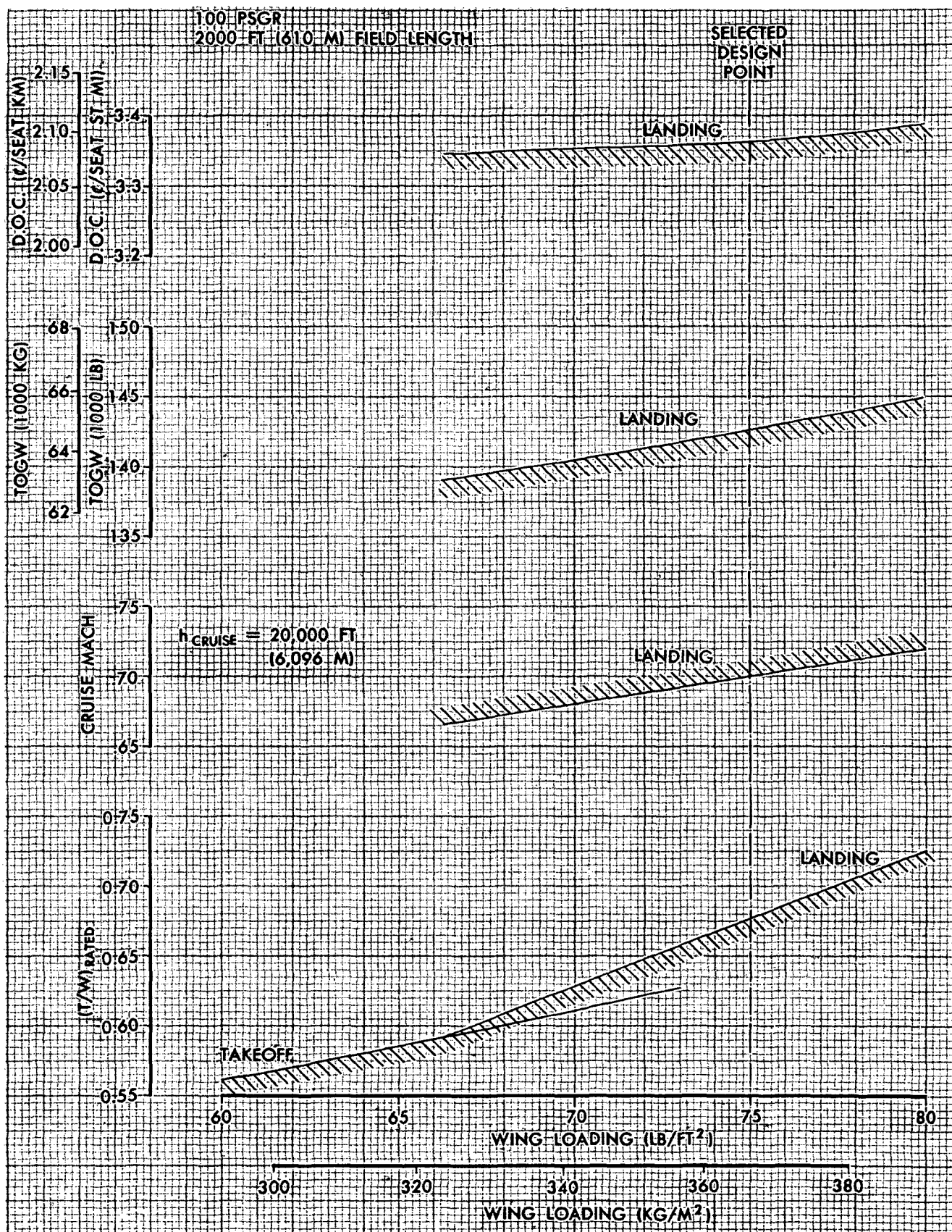


FIGURE 2-2: EXTERNALLY BLOWN FLAP PARAMETRIC AIRCRAFT SIZING—ALLISON ENGINES

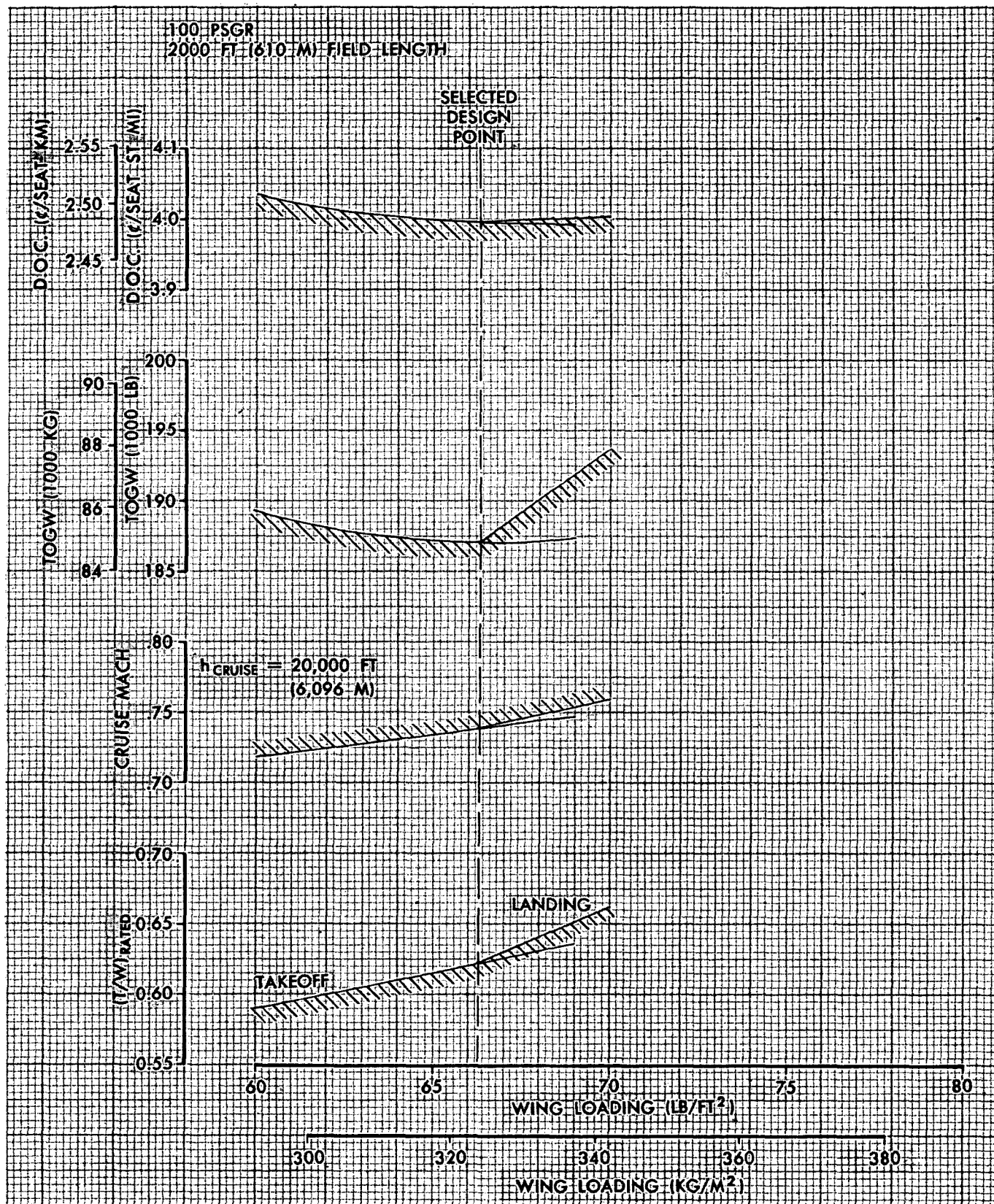


FIGURE 2-3. EXTERNALLY BLOWN FLAP PARAMETRIC AIRCRAFT
SIZING—GENERAL ELECTRIC ENGINES

bypass, low pressure ratio variable pitch fan engine and the acoustic treatment required to achieve the 95 PNdB 500 foot (152 m) sideline noise level. The General Electric variable pitch fan engines with the same pressure ratio have a lower bypass ratio (11.5 vs 17.4) and a lower lapse rate. The General Electric engined aircraft are therefore sized for a balanced takeoff-landing, minimum direct operating cost condition, and have Mach numbers greater than 0.70. The higher gross weights of the aircraft with General Electric engines compared to those with Allison engines is due to considerably higher installed engine weight and SFC.

AUGMENTOR WING

The higher pressure ratio augmentor wing engines give this configuration much greater cruise speed capability than the externally blown flap. The aircraft were sized for minimum DOC which in these cases occurs at a balanced takeoff and landing condition as shown in the sample sizing plot (Figure 2-4).

UPPER SURFACE BLOWN FLAP

This configuration behaves much like the externally blown flap in that the aircraft were sized by the 0.70 Mach number limit and are landing critical. A typical sizing plot is shown in Figure 2-5.

MECHANICAL FLAP

A 1500 foot (457 meter) field length appears impractical for this type of configuration due to the very low wing loadings required. Aircraft were therefore sized at 2000 (610, 3000 (914) and 4000 feet (1219 meters). Aircraft were sized by minimum DOC which occurs at the balanced landing-takeoff condition as shown in Figure 2-4. The 2000 foot (610 meter) field

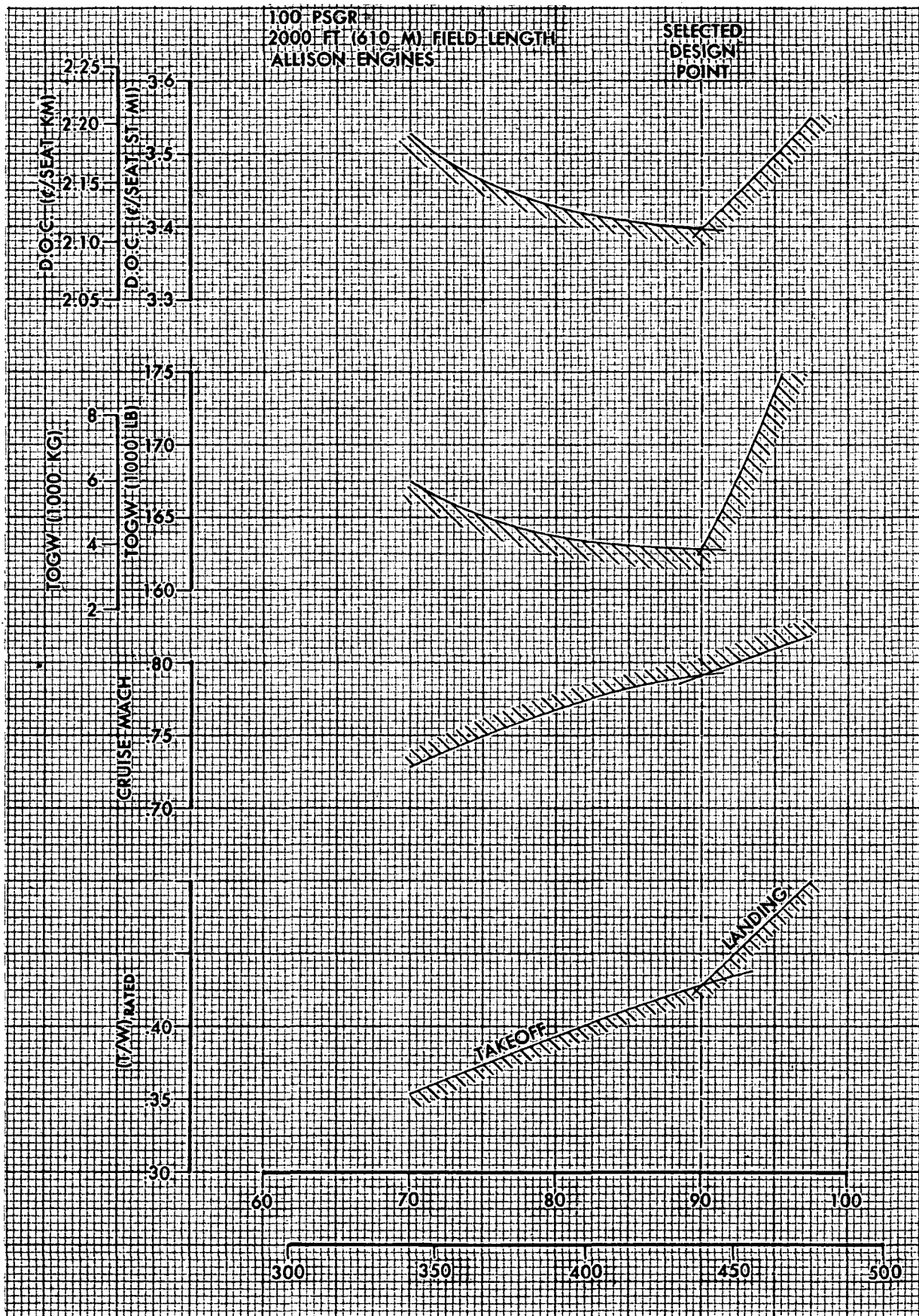


FIGURE 2-4. AUGMENTOR WING PARAMETRIC AIRCRAFT SIZING

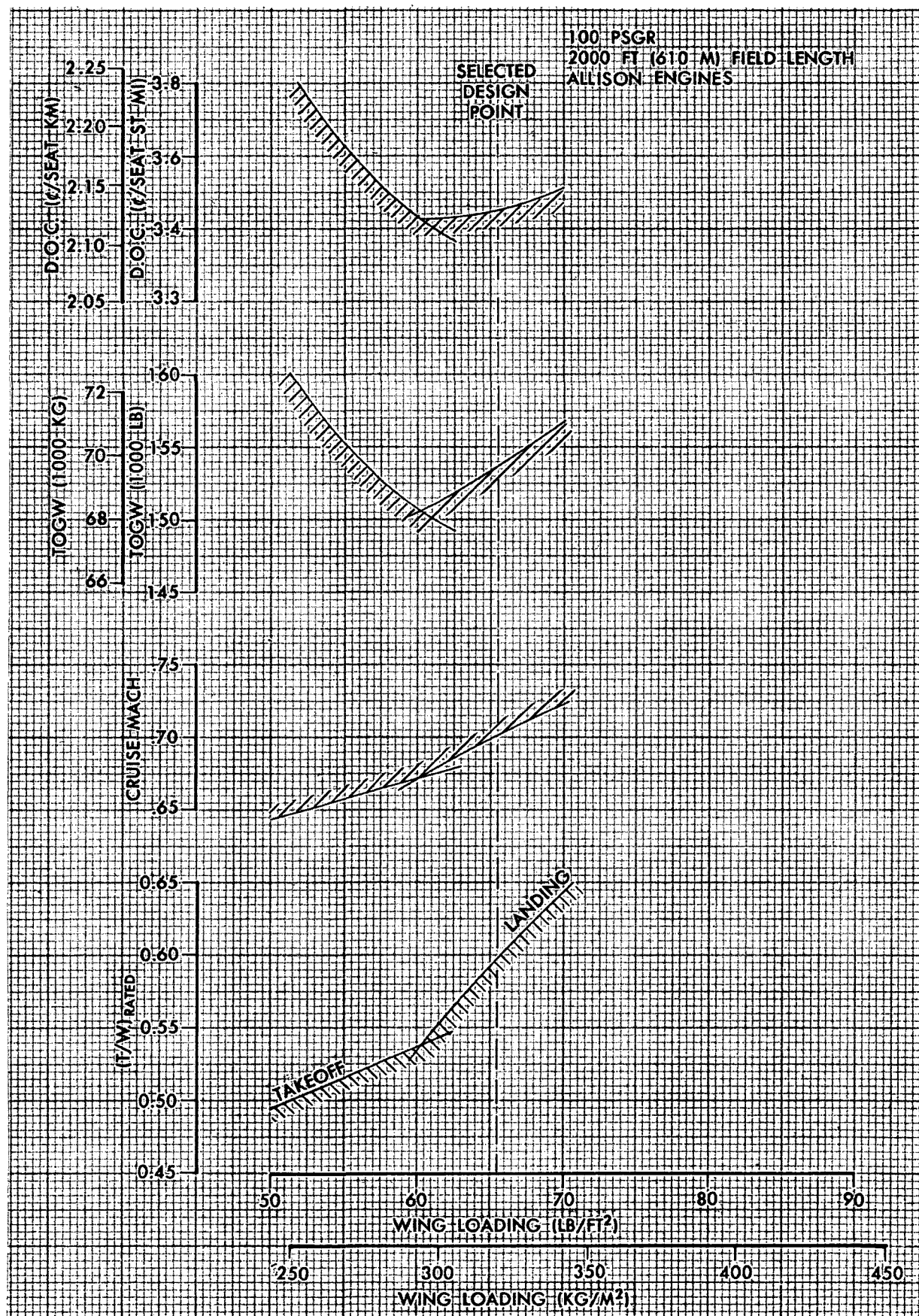


FIGURE 2-5. UPPER SURFACE BLOWN FLAP PARAMETRIC AIRCRAFT SIZING

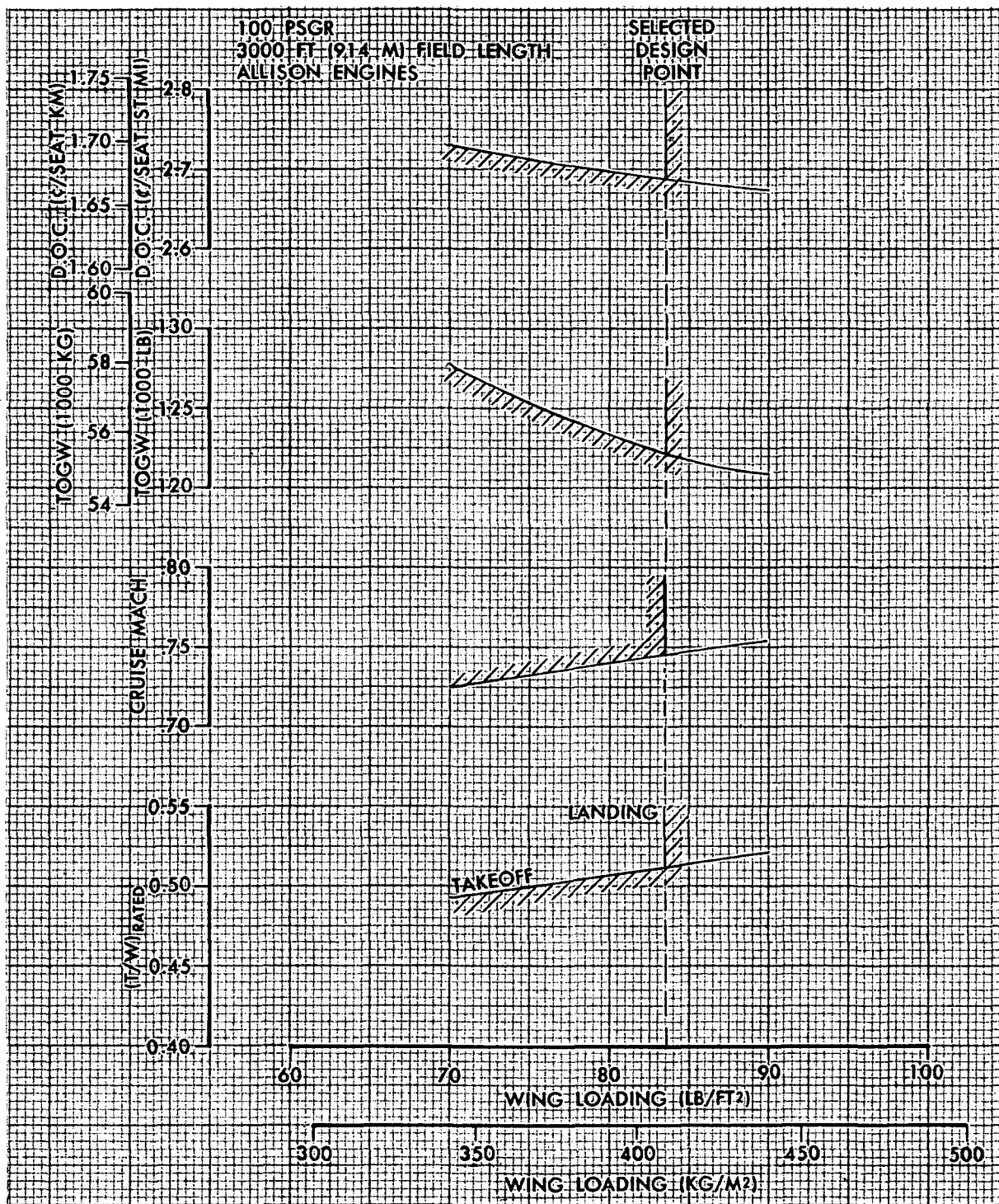


FIGURE 2-6. MECHANICAL FLAP PARAMETRIC AIRCRAFT SIZING

length aircraft are also limited by Mach number and the 200 passenger, 2000 foot (610 meter) field length aircraft required an increase in T/W to achieve $M = 0.70$ in cruise.

INTERNALLY BLOWN FLAP

This configuration is very similar to the augmentor wing and only one aircraft was sized. The minimum DOC occurs for a takeoff critical condition as shown in Figure 2-7.

CTOL

Two CTOL aircraft were sized for comparison purposes. These aircraft, of 100 and 200 passenger capacity, are twin engine configurations designed to meet the FAR Part 36 minus 14 EPNdB sideline noise levels. This approximately corresponds to a 500 foot sideline noise level of 98 EPNdB. They are both sized at a wing loading of 120 psf (580 kg/m^2) for a 1380 statute mile (1932 km) mission with a cruise speed of $M = 0.78$ at 30,000 feet (9150 m).

2.1.4 Parametric Results. - A summary of the basic characteristics of 53 selected parametric aircraft having minimum DOCs while meeting specified design constraints by the proper choice of W/S and T/W is shown in Tables 2-1 through 2-8. In general, Allison engines were used because more complete parametric engine data was available from Allison than General Electric. Both Allison and General Electric based aircraft were generated for the externally blown flap and augmentor wing concepts.

In some cases resulting aircraft configurations were not considered practical and were not retained. For instance, the General Electric EBF

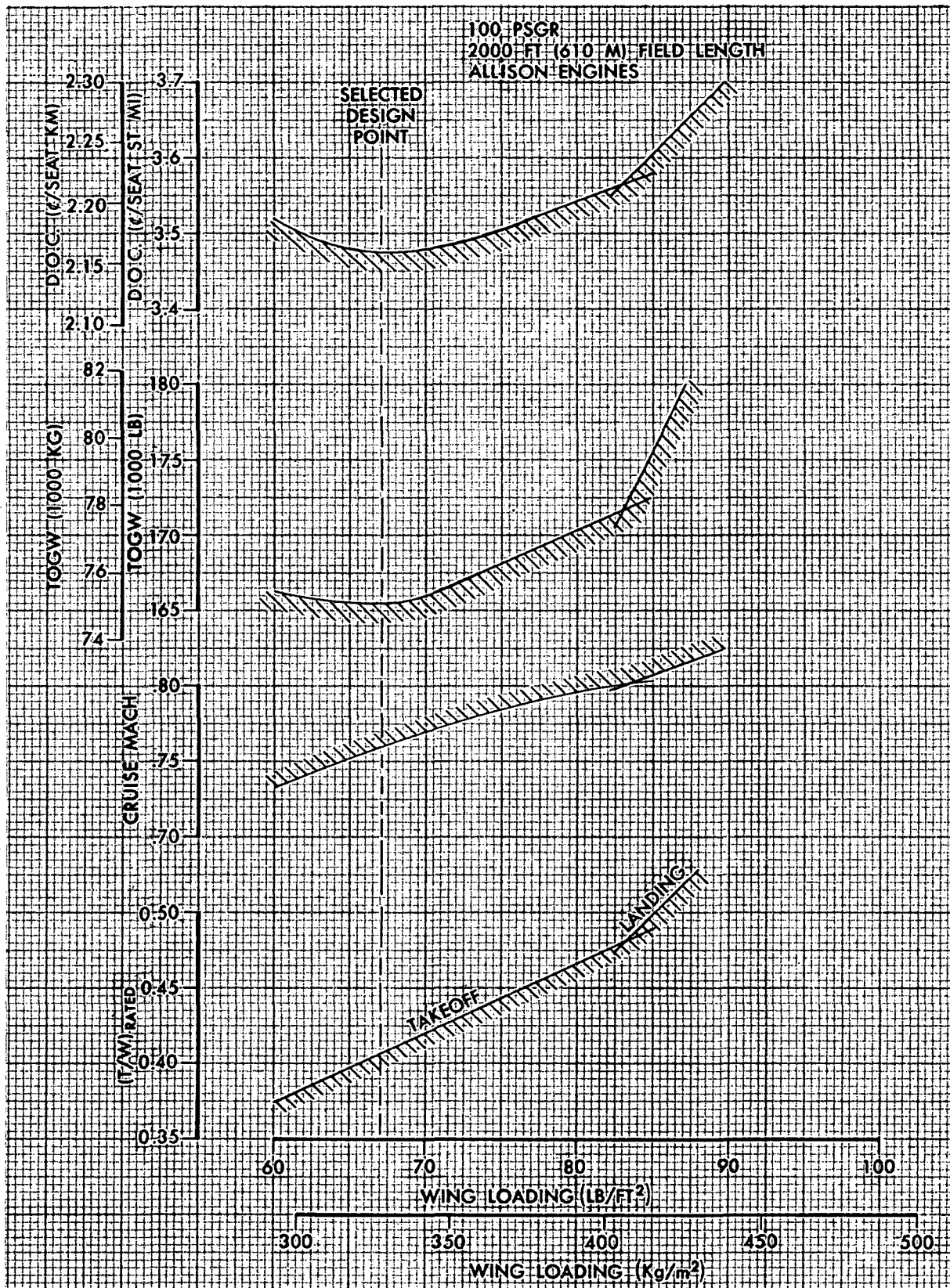


FIGURE 2-7. INTERNALLY BLOWN FLAP PARAMETRIC AIRCRAFT SIZING

Table 2-1
AIRCRAFT PARAMETRIC ANALYSIS
EXTERNALLY BLOWN FLAP
Allison PD287-3 Engines

		Field Length - Ft (M)			
		1,500	(457)	2,000	(610)
50 Passengers	TOGW	108,300	(49,100)	82,800	(37,550)
	SW	1,850	(171.9)	1,060	(98.5)
	FN	20,400	(90,750)	14,590	(64,900)
	W/S	58.5	(285.5)	78.0	(381.0)
	T/W	.740		.705	
	MCR DOC	5.93	(3.69)	5.03	(3.13)
100	TOGW	190,600	(86,450)	142,600	(64,700)
	SW	3,285	(305.2)	1,900	(176.5)
	FN	35,210	(156,600)	24,170	(107,500)
	W/S	58.0	(283.0)	75.0	(366.0)
	T/W	.739		.678	
	MCR DOC	4.19	(2.60)	3.36	(2.09)
200	TOGW	345,400	(156,650)	266,500	(120,900)
	SW	5,755	(534.6)	3,460	(321.4)
	FN	65,750	(292,450)	46,000	(204,600)
	W/S	60.0	(293.0)	77.0	(376.0)
	T/W	.762		.692	
	MCR DOC	3.20	(1.99)	2.55	(1.58)
		1,500	(457)	2,000	(610)
50 Passengers	TOGW	108,300	(49,100)	82,800	(37,550)
	SW	1,850	(171.9)	1,060	(98.5)
	FN	20,400	(90,750)	14,590	(64,900)
	W/S	58.5	(285.5)	78.0	(381.0)
	T/W	.740		.705	
	MCR DOC	5.93	(3.69)	5.03	(3.13)
100	TOGW	190,600	(86,450)	142,600	(64,700)
	SW	3,285	(305.2)	1,900	(176.5)
	FN	35,210	(156,600)	24,170	(107,500)
	W/S	58.0	(283.0)	75.0	(366.0)
	T/W	.739		.678	
	MCR DOC	4.19	(2.60)	3.36	(2.09)
200	TOGW	345,400	(156,650)	266,500	(120,900)
	SW	5,755	(534.6)	3,460	(321.4)
	FN	65,750	(292,450)	46,000	(204,600)
	W/S	60.0	(293.0)	77.0	(376.0)
	T/W	.762		.692	
	MCR DOC	3.20	(1.99)	2.55	(1.58)

DOC calculations are for 575 st mi (926 km) stage length

Table 2-2
AIRCRAFT PARAMETRIC ANALYSIS
EXTERNALLY BLOWN FLAP
GE-19/F6A Engines

		Field Length - Ft (M)			
		1,500 (457)	2,000 (610)	3,000 (914)	
50 Passengers	TOGW				
	Lb (Kg)				
	Ft ² (M ²)				
	FN (Newtons)	166,600 (75,550)	108,200 (49,100)	84,400 (38,300)	
	Lb (Kg)	3,450 (320.5)	1,630 (151.4)	800 (74.3)	
	Lb/Ft ² (Kg/M ²)	26,300 (117,000)	16,900 (75,150)	12,600 (56,050)	
100	W/S	48.3 (236.0)	66.3 (323.5)	95.8 (467.5)	
	T/W	.631	.623	.599	
	MCR	.71	.73	.73	
	DOC	7.75 (4.82)	5.67 (3.52)	4.80 (2.99)	
	TOGW				
	Lb (Kg)				
200	Ft ² (M ²)				
	FN (Newtons)	275,700 (125,050)	187,100 (84,850)	145,100 (65,800)	
	Lb (Kg)	5,710 (530.5)	2,820 (262.0)	1,510 (14.0)	
	Lb/Ft ² (Kg/M ²)	43,500 (193,500)	29,100 (129,450)	21,700 (96,550)	
	W/S	48.3 (236.0)	66.3 (323.5)	95.8 (467.5)	
	T/W	.631	.623	.599	
	MCR	.71	.74	.76	
	DOC	5.46 (3.39)	3.99 (2.48)	3.26 (2.02)	
	TOGW				
	Lb (Kg)				
	Ft ² (M ²)				
	FN (Newtons)				
	Lb (Kg)				
	Lb/Ft ² (Kg/M ²)				
	W/S				
	T/W				
	MCR				
	DOC				
	TOGW				
	Lb (Kg)				
	Ft ² (M ²)				
	FN (Newtons)				
	Lb (Kg)				
	Lb/Ft ² (Kg/M ²)				
	W/S				
	T/W				
	MCR				
	DOC				
	TOGW				
	Lb (Kg)				
	Ft ² (M ²)				
	FN (Newtons)				
	Lb (Kg)				
	Lb/Ft ² (Kg/M ²)				
	W/S				
	T/W				
	MCR				
	DOC				
	TOGW				
	Lb (Kg)				
	Ft ² (M ²)				
	FN (Newtons)				
	Lb (Kg)				
	Lb/Ft ² (Kg/M ²)				
	W/S				
	T/W				
	MCR				
	DOC				
	TOGW				
	Lb (Kg)				
	Ft ² (M ²)				
	FN (Newtons)				
	Lb (Kg)				
	Lb/Ft ² (Kg/M ²)				
	W/S				
	T/W				
	MCR				
	DOC				
	TOGW				
	Lb (Kg)				
	Ft ² (M ²)				
	FN (Newtons)				
	Lb (Kg)				
	Lb/Ft ² (Kg/M ²)				
	W/S				
	T/W				
	MCR				
	DOC				
	TOGW				
	Lb (Kg)				
	Ft ² (M ²)				
	FN (Newtons)				
	Lb (Kg)				
	Lb/Ft ² (Kg/M ²)				
	W/S				
	T/W				
	MCR				
	DOC				
	TOGW				
	Lb (Kg)				
	Ft ² (M ²)				
	FN (Newtons)				
	Lb (Kg)				
	Lb/Ft ² (Kg/M ²)				
	W/S				
	T/W				
	MCR				
	DOC				
	TOGW				
	Lb (Kg)				
	Ft ² (M ²)				
	FN (Newtons)				
	Lb (Kg)				
	Lb/Ft ² (Kg/M ²)				
	W/S				
	T/W				
	MCR				
	DOC				
	TOGW				
	Lb (Kg)				
	Ft ² (M ²)				
	FN (Newtons)				
	Lb (Kg)				
	Lb/Ft ² (Kg/M ²)				
	W/S				
	T/W				
	MCR				
	DOC				
	TOGW				
	Lb (Kg)				
	Ft ² (M ²)				
	FN (Newtons)				
	Lb (Kg)				
	Lb/Ft ² (Kg/M ²)				
	W/S				
	T/W				
	MCR				
	DOC				
	TOGW				
	Lb (Kg)				
	Ft ² (M ²)				
	FN (Newtons)				
	Lb (Kg)				
	Lb/Ft ² (Kg/M ²)				
	W/S				
	T/W				
	MCR				
	DOC				
	TOGW				
	Lb (Kg)				
	Ft ² (M ²)				
	FN (Newtons)				
	Lb (Kg)				
	Lb/Ft ² (Kg/M ²)				
	W/S				
	T/W				
	MCR				
	DOC				
	TOGW				
	Lb (Kg)				
	Ft ² (M ²)				
	FN (Newtons)				
	Lb (Kg)				
	Lb/Ft ² (Kg/M ²)				
	W/S				
	T/W				
	MCR				
	DOC				
	TOGW				
	Lb (Kg)				
	Ft ² (M ²)				
	FN (Newtons)				
	Lb (Kg)				
	Lb/Ft ² (Kg/M ²)				
	W/S				
	T/W				
	MCR				
	DOC				
	TOGW				
	Lb (Kg)				
	Ft ² (M ²)				
	FN (Newtons)				
	Lb (Kg)				
	Lb/Ft ² (Kg/M ²)				
	W/S				
	T/W				
	MCR				
	DOC				
	TOGW				
	Lb (Kg)				
	Ft ² (M ²)				
	FN (Newtons)				
	Lb (Kg)				
	Lb/Ft ² (Kg/M ²)				
	W/S				
	T/W				
	MCR				
	DOC				
	TOGW				
	Lb (Kg)				
	Ft ² (M ²)				
	FN (Newtons)				
	Lb (Kg)				
	Lb/Ft ² (Kg/M ²)				
	W/S				
	T/W				
	MCR				
	DOC				
	TOGW				
	Lb (Kg)				
	Ft ² (M ²)				
	FN (Newtons)				
	Lb (Kg)				
	Lb/Ft ² (Kg/M ²)				
	W/S				
	T/W				
	MCR				
	DOC				
	TOGW				
	Lb (Kg)				
	Ft ² (M ²)				
	FN (Newtons)				
	Lb (Kg)				
	Lb/Ft ² (Kg/M ²)				
	W/S				
	T/W				
	MCR				
	DOC				
	TOGW				
	Lb (Kg)				
	Ft ² (M ²)				
	FN (Newtons)				
	Lb (Kg)				
	Lb/Ft ² (Kg/M ²)				
	W/S				
	T/W				
	MCR				
	DOC				
	TOGW				
	Lb (Kg)				
	Ft ² (M ²)				
	FN (Newtons)				
	Lb (Kg)				
	Lb/Ft ² (Kg/M ²)				
	W/S				
	T/W				
	MCR				
	DOC				
	TOGW				
	Lb (Kg)				
	Ft ² (M ²)				
	FN (Newtons)				
	Lb (Kg)				
	Lb/Ft ² (Kg/M ²)				
	W/S				
	T/W				
	MCR				
	DOC				
	TOGW				
	Lb (Kg)				
	Ft ² (M ²)				
	FN (Newtons)				
	Lb (Kg)				
	Lb/Ft ² (Kg/M ²)				
	W/S				
	T/W				
	MCR				
	DOC				
	TOGW				
	Lb (Kg)				
	Ft ² (M ²)				
	FN (Newtons)				
	Lb (Kg)				
	Lb/Ft ² (Kg/M ²)				
	W/S				
	T/W				
	MCR				
	DOC				
	TOGW				
	Lb (Kg)				
	Ft ² (M ²)				
	FN (Newtons)				
	Lb (Kg)				
	Lb/Ft ² (Kg/M ²)				

Table 2-3
AIRCRAFT PARAMETRIC ANALYSIS
UPPER SURFACE BLOWN FLAP
Allison PD287-22 Engines

		Field Length - Ft (M)				
		1,500	(457)	2,000	(610)	3,000 (914)
50 Passengers	TOGW	124,500	(56,450)	89,300	(40,500)	73,100 (33,150)
	SW	2,430	(225.7)	1,290	(119.8)	700 (65.0)
	FN	20,590	(91,600)	14,140	(62,900)	11,400 (50,700)
	W/S	51.2	(250.0)	69.0	(337.0)	104.3 (509.0)
	T/W	.662		.633		.623
	MCR	.70		.70		.70
100	DOC	6.27	(3.90)	5.06	(3.14)	4.50 (2.80)
	TOGW	236,400	(107,250)	153,500	(69,650)	120,900 (54,850)
	SW	4,580	(425.5)	2,340	(217.4)	1,290 (119.8)
	FN	39,430	(175,400)	22,950	(102,100)	16,740 (74,450)
	W/S	51.6	(252.0)	65.5	(320.0)	93.7 (457.5)
	T/W	.667		.598		.554
200	MCR	.70		.70		.70
	DOC	4.77	(2.96)	3.43	(2.13)	2.88 (1.79)
	TOGW			314,000	(142,450)	229,200 (103,950)
	SW			4,510	(419.0)	2,420 (224.8)
	FN			50,240	(223,500)	32,190 (143,200)
	W/S			69.7	(340.5)	94.8 (463.0)
	T/W			.640		.562
	MCR			.70		.60
	DOC			2.82	(1.75)	2.15 (1.34)

DOC calculations are for 575 st mi (926 km) stage length

Table 2-4
AIRCRAFT PARAMETRIC ANALYSIS
AUGMENTOR WING
Allison PD287-43 Engines

		Field Length - Ft (M)				
		1,500	(457)	2,000	(610)	3,000 (914)
50 Passengers	TOGW					
	SW	125,000	(56,700)	96,000	(43,550)	78,000 (35,400)
	FN	1,950	(181.1)	1,070	(99.4)	710 (66.0)
	W/S	13,300	(59,150)	10,300	(45,800)	7,000 (31,150)
	T/W	64.4	(314.5)	90.0	(439.5)	110.0 (537.0)
	MCR	.425		.427		.357
	DOC	.77	(3.72)	.78	(3.10)	.73 (2.81)
100	TOGW					
	SW	204,000	(92,550)	163,000	(73,950)	131,000 (59,400)
	FN	3,170	(294.5)	1,810	(168.1)	1,190 (110.6)
	W/S	21,700	(96,550)	17,400	(77,400)	11,700 (52,050)
	T/W	64.4	(314.5)	90.0	(439.5)	110.0 (537.0)
	MCR	.425		.427		.357
	DOC	.77	(2.53)	.79	(2.11)	.76 (1.81)
200	TOGW					
	SW	372,000	(168,750)	295,000	(133,800)	239,000 (108,400)
	FN	5,750	(534.2)	3,280	(304.7)	2,170 (201.6)
	W/S	39,500	(175,700)	31,500	(140,100)	21,300 (94,750)
	T/W	64.4	(314.5)	90.0	(439.5)	110.0 (537.0)
	MCR	.425		.427		.357
	DOC	.76	(1.96)	.79	(1.59)	.76 (1.33)

DOC calculations are for 575 st mi (926 km) stage lengths

Table 2-5
AIRCRAFT PARAMETRIC ANALYSIS
AUGMENTOR WING
GE-19/F9A Engines

		Field Length - Ft (M)					
		1,500	(457)	2,000	(610)	3,000	(914)
50 Passengers	TOGW	Lb	(Kg)				
	SW	Ft ²	(M ²)				
	FN	Lb	(Newtons)				
	W/S	Lb/Ft ²	(Kg/M ²)				
	T/W						
	MCR DOC	¢/ASSM	(¢/ASKM)				
100	TOGW	Lb	(Kg)				
	SW	Ft ²	(M ²)				
	FN	Lb	(Newtons)				
	W/S	Lb/Ft ²	(Kg/M ²)				
	T/W						
	MCR DOC	¢/ASSM	(¢/ASKM)				
200	TOGW	Lb	(Kg)				
	SW	Ft ²	(M ²)				
	FN	Lb	(Newtons)				
	W/S	Lb/Ft ²	(Kg/M ²)				
	T/W						
	MCR DOC	¢/ASSM	(¢/ASKM)				

DOC calculations are for 575 st mi (926 km) stage lengths

Table 2-6
 AIRCRAFT PARAMETRIC ANALYSIS
 INTERNALLY BLOWN JET FLAP
 Allison PD287-43 Engines

Field Length Payload	Ft (M) Passengers	2,000 100	(610)
TOGW	Lb (Kg)	165,500	(75,050)
Sw	Ft ² (M ²)	2,470	(229.5)
Fn	Lb/Eng (Newtons/Eng)	16,760	(74,550)
W/S	PSF (Kg/M ²)	67	(327.0)
T/W		.405	
Mcr		.76	
DOC @ 575 st mi (926 km)	¢/ASSM (¢/ASKM)	3.48	(2.16)

Table 2-7
AIRCRAFT PARAMETRIC ANALYSIS
MECHANICAL FLAP
Allison PD287-23 Engines

		Field Length - Ft (M)				
		2,000	(610)	3,000	(914)	4,000 (1,219)
50 Passengers	TOGW					
	SW	110,100	(49,950)	73,200	(33,200)	
	FN	2,229	(207.1)	876	(81.4)	
	W/S	13,930	(61,950)	9,340	(41,550)	
	T/W	49.4	(241.0)	83.5	(407.5)	
	MCR	.506		.511		
100	DOC	.70	(3.52)	4.40	(2.73)	
	TOGW	168,500	(76,450)	122,400	(55,500)	110,400 (50,100)
	SW	3,410	(316.8)	1,466	(136.2)	920 (85.5)
	FN	21,310	(94,800)	15,630	(69,550)	14,090 (62,750)
	W/S	49.4	(241.0)	83.5	(407.5)	120.0 (586.0)
	T/W	.506		.511		.510
200	MCR	.70	(2.25)	.74	(1.74)	.76
	DOC	3.62		2.81		2.60 (1.61)
	TOGW	286,300	(129,850)	222,000	(100,700)	205,100 (93,050)
	SW	5,796	(538.4)	2,658	(246.9)	1,710 (158.9)
	FN	37,940	(168,750)	28,360	(126,150)	26,180 (116,450)
	W/S	49.4	(241.0)	83.5	(407.5)	120.0 (586.0)
	T/W	.530		.511		.510
	MCR	.70	(1.61)	.75	(1.26)	.77
	DOC	2.59		2.02		1.89 (1.17)

DOC calculations are for 575 st mi (926 km) stage lengths

Table 2-8
AIRCRAFT PARAMETRIC ANALYSIS

CTOL
TWIN ENGINE
1380 STATUTE MILE RANGE

Field Length	ft (m)	7,500 (2,286)	8,500 (2,591)
Payload	passengers	100	200
TOGW	lb (kg)	129,500 (58,740)	220,800 (100,150)
SW	ft ² (m ²)	1,080 (100)	1,840 (171)
FN	lb/eng (kg/eng)	26,500 (12,020)	40,400 (18,330)
W/S	lb/ft ² (kg/m ²)	120 (586)	120 (586)
T/W		0.409	0.366
M _{CR}		0.78	0.78
DOC @ 1380 S MI (1932 km)	¢/ASSM (¢/ASKM)	2.08 (1.29)	1.43 (0.89)

aircraft for the 1500 foot (457 m) field length - 200 passenger case (Table 2-2) was over 400,000 pounds (181,440 kg) takeoff gross weight and is therefore not shown. The mechanical flap aircraft for the 1500 foot (457 m) field length cases required thrust-to-weight ratios in the neighborhood of unity and are therefore not shown (Table 2-7). Only a single internally blown flap aircraft is shown (Table 2-6) because the IBF system is so similar to that of the augmentor wing.

Variations in thrust-to-weight ratio (T/W) and wing loading (W/S) data from the previous tables for the 100 passenger aircraft are shown in Figure 2-8. The externally blown flap and upper surface blown flap configurations show the expected trend, i.e., as field length increases, W/S tends to increase and T/W to decrease. The externally blown flap aircraft have greater T/W ratios than those of the upper surface blown flap aircraft. Since these aircraft, with similar high lift characteristics, were sized in the parametric studies by a cruise requirement of 0.70 Mach number at 20,000 feet (6096 meters), the higher lapse rate of the EBF engines results in a higher required W/S and T/W .

There was almost no variation in T/W with field length for the mechanical flap and shorter field length augmentor wing aircraft, the performance being attained by W/S changes alone. These parametric aircraft were sized at the intersection of the takeoff and landing critical lines, as illustrated in Figures 2-4 and 2-6, and the constant T/W is due to the low landing restricted wing loadings and the relatively low engine thrust lapse rate. The wing loadings of the mechanical flap aircraft are lower than those of the powered lift systems of the same field length due to the

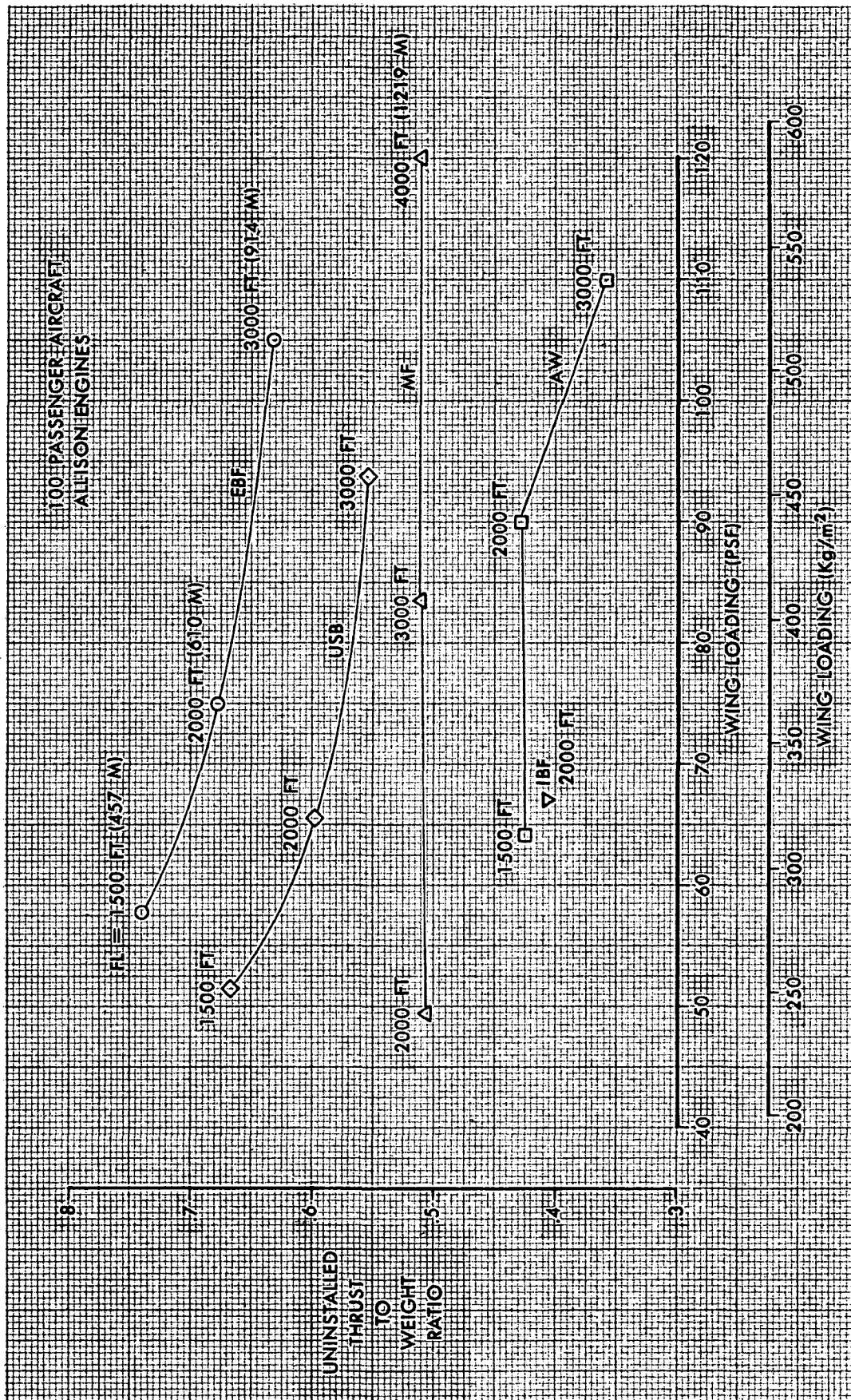


FIGURE 2-8. PARAMETRIC WING LOADING AND THRUST-TO-WEIGHT VARIATIONS

relatively poorer high lift performance in landing associated with the mechanical flap.

The 3000 foot (914 m) field length augmentor wing is not shown on the same level as the 1500 (457) and 2000 (610 m) aircraft because the minimum DOC occurred at a W/S lower than that of the takeoff-landing line intersection. The augmentor wing aircraft have relatively low T/W and high W/S because of the very low lapse rate of the high pressure ratio engines and the thrust augmentation obtained from the augmentor.

These W/S - T/W relationships do not change significantly for other passenger capacities. The only variations are due to small changes in the drag levels for different sizes of aircraft.

Direct operating cost and takeoff gross weight as a function of field length and passenger payload are shown in Figures 2-9 and 2-10, respectively. Each of the powered high lift systems exhibit similar characteristics with respect to DOC. The cost values are sufficiently close that the best configuration for a given field length and payload is not evident. The slope of the DOC - field length curves for the mechanical flap are steeper than those for the powered lift systems. Based on the parametric ground rules, the mechanical flap has higher DOC for field lengths below 2500 feet (821 m), but a lower DOC for field lengths above 3000 feet (610 m) compared to the powered systems. This conclusion was modified somewhat by more detailed analysis of the final design aircraft.

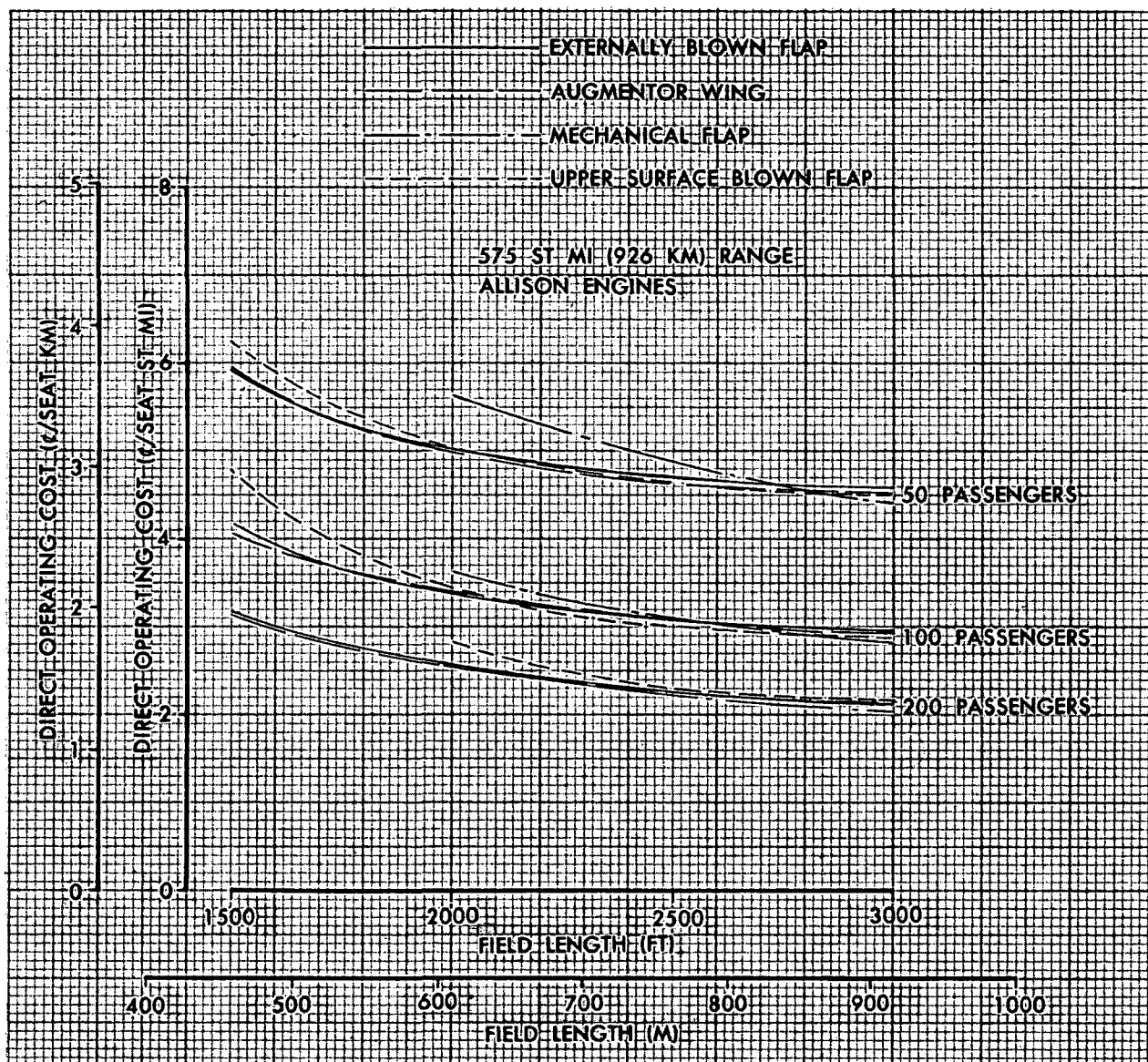


FIGURE 2-9. PARAMETRIC DIRECT OPERATING COST VARIATION WITH FIELD LENGTH

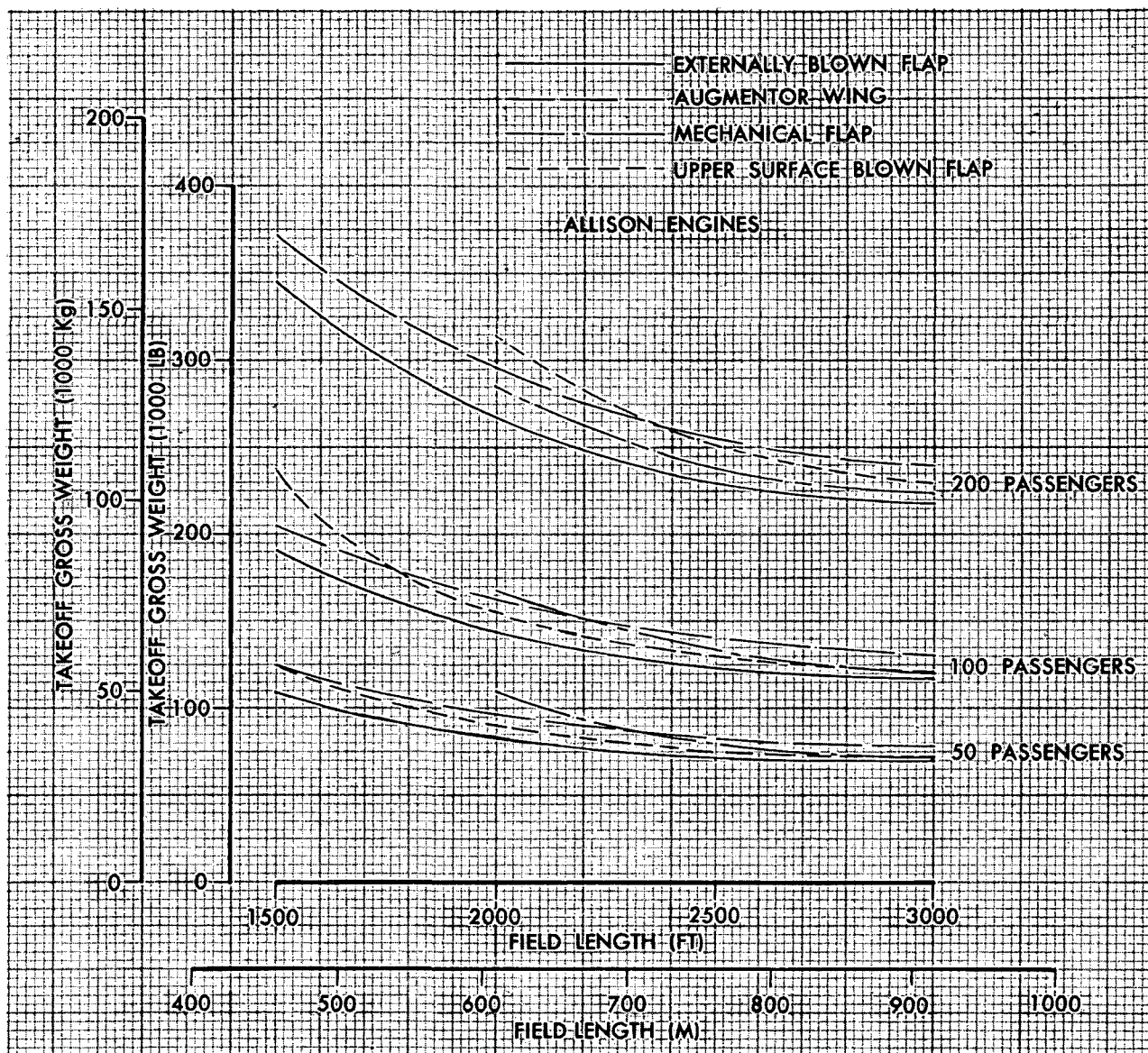


FIGURE 2-10. PARAMETRIC TAKEOFF GROSS WEIGHT VARIATION WITH FIELD LENGTH

2.2 Final Design Aircraft

As a result of aircraft and system analysis work accomplished for the parametric study, Douglas and NASA jointly eliminated from consideration aircraft candidates based on criteria of DOC, gross weight, wing loading, thrust loading and configuration considerations. Table 2-9 shows the results of this selection process with a total of eight short haul aircraft resulted from this selection process for detailed analysis.

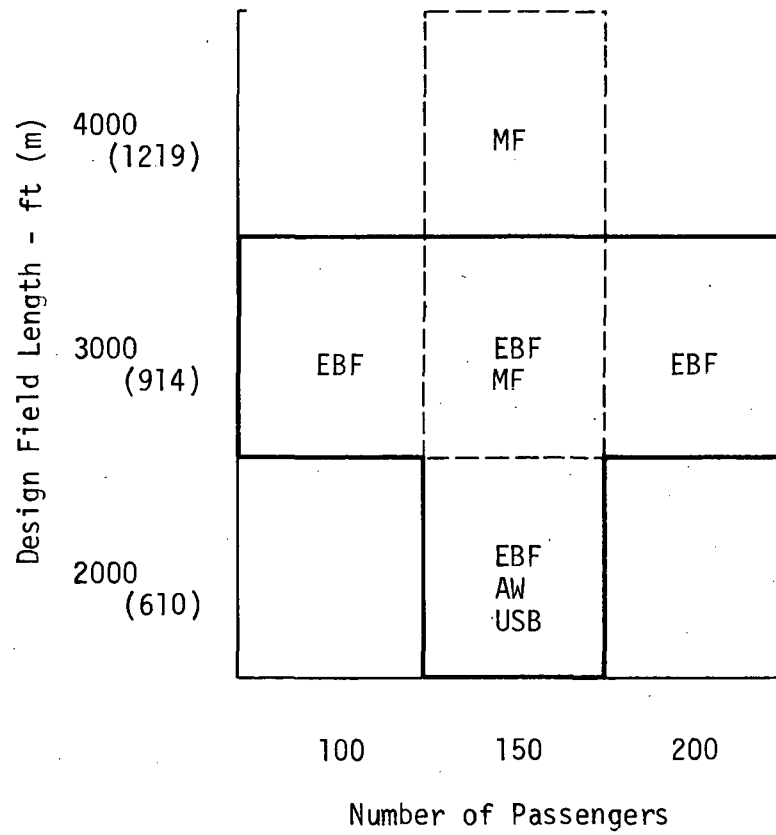
The EBF system was used to provide a comparison between the design requirements of field length and of passenger payload because of the extensive data base existing for this system. The 150 passenger 3000 foot (914 m) field length EBF aircraft was used as a basis for the trade studies presented in Section 3.0. A comparison of propulsive lift systems is made at the 150 passenger, 2000 foot (610 m) field length as shown in Table 2-9. In addition a CTOL aircraft was synthesized for comparison purposes. This aircraft was designed for a 150 passenger payload, a range of 1380 statute miles (2220 km) and a field length of 7500 feet (2260 m).

As a result of the acoustic trade study discussed in Section 3.1, the 95 PNdB 500 foot (152 m) sideline noise requirement used for the parametric aircraft was relaxed somewhat so that the final design aircraft have 500 foot (152 m) sideline EPNdB values ranging between 95 and 98.

The engine selection rationale and a description of the selected engine characteristics are presented in Chapter 4. Engineering data and methods substantiation for these final design aircraft are contained in the appendix material.

Table 2-9

FINAL DESIGN AIRCRAFT MATRIX



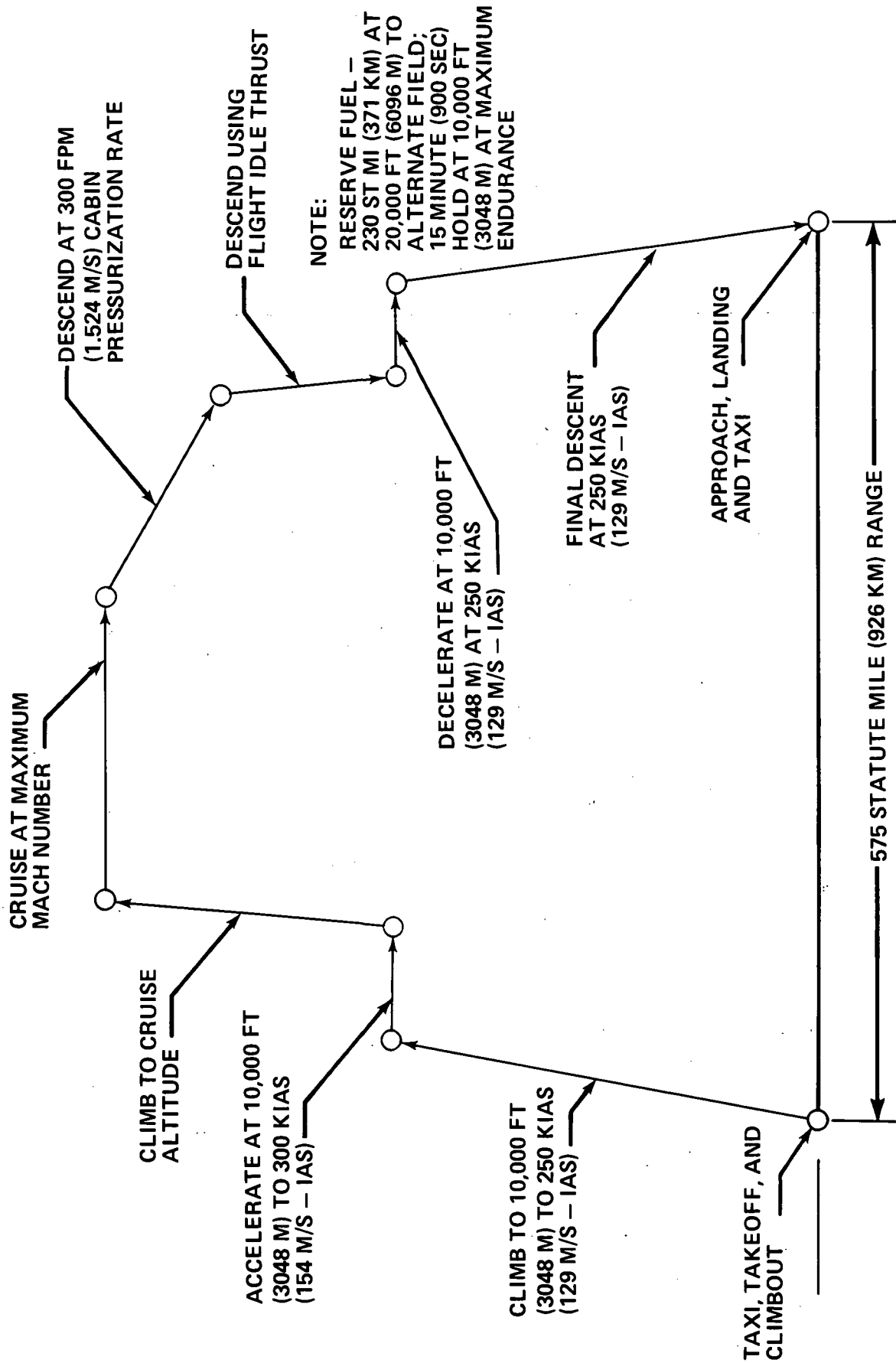
2.2.1 Final Design Aircraft Performance Ground Rules. - The performance ground rules used for the final design aircraft are the same as those discussed in paragraph 2.1.1 except for the following:

- o Ground effects were included in the takeoff and landing calculations in accordance with the following restrictions:
 - $C_L \leq 100\%$ of $C_{L_{max}}$ in ground effect
 - $C_L \leq 90\%$ of $C_{L_{max}}$ out of ground effect
- o The sink speed in approach was increased from 800 to 900 fpm (4.06 to 4.57 m/sec). Justification for this change is given later in Section 3.4.
- o The sink speed at touchdown was increased from 3 to 10 fps (0.91 to 3.05 m/sec) to represent landing field length certification conditions. Justification for this change is also given in Section 3.4.

The mission profile used to size the final design aircraft is shown in Figure 2-11. This profile differs from that used for the parametric aircraft (Figure 2-1) as follows:

- o Hold segments at 5000 feet (1524 m) were eliminated. Takeoff and landing allowances were correspondingly increased.
- o Climb and descent speed above 10,000 feet (3048 m) was increased from 250 to 300 KIAS (129 to 154 m/sec). Climb Mach number

SIZING MISSION PROFILE



PR3-STOL-1591

FIGURE 2-11

was restricted to less than or equal to initial maximum cruise Mach.

- o Cruise altitude was optimized for minimum DOC at design range instead of being fixed at 20,000 feet (6096 m).

A more detailed discussion of the performance methods and ground rules used in sizing the final design aircraft is presented in Appendix B.

2.2.2 Aircraft Sizing. - The principle criterion used in aircraft sizing was direct operating cost at the design range. Design wing loading, climb speed and cruise altitude were selected on this basis. The cruise segment of the mission was flown at maximum cruise Mach numbers with Mach number increasing slightly as fuel is burned off. The quoted values for cruise Mach number are those at the initial cruise weight.

Externally Blown Flap

The four final design externally blown flap (EBF) aircraft are all four engine, high wing configurations with a 25 degree swept wing. An aspect ratio of 8 was chosen based on the results of an aspect ratio trade study discussed in Section 3.2.

Minimum direct operating cost (DOC) for the 150 passenger 3000 foot (914 m) field length aircraft occurs at the intersection of the takeoff and landing critical lines at a wing loading of 102 lb/ft² (498 kg/m²) as shown in Figure 2-12. At this wing loading, selected as the design point, takeoff and landing field length are both 3000 feet (914 m). The DOC vs wing loading curve is very flat, an increase of 5 percent in design wing loading increasing the direct operating cost by less than 1/3 of one percent. The low cruise

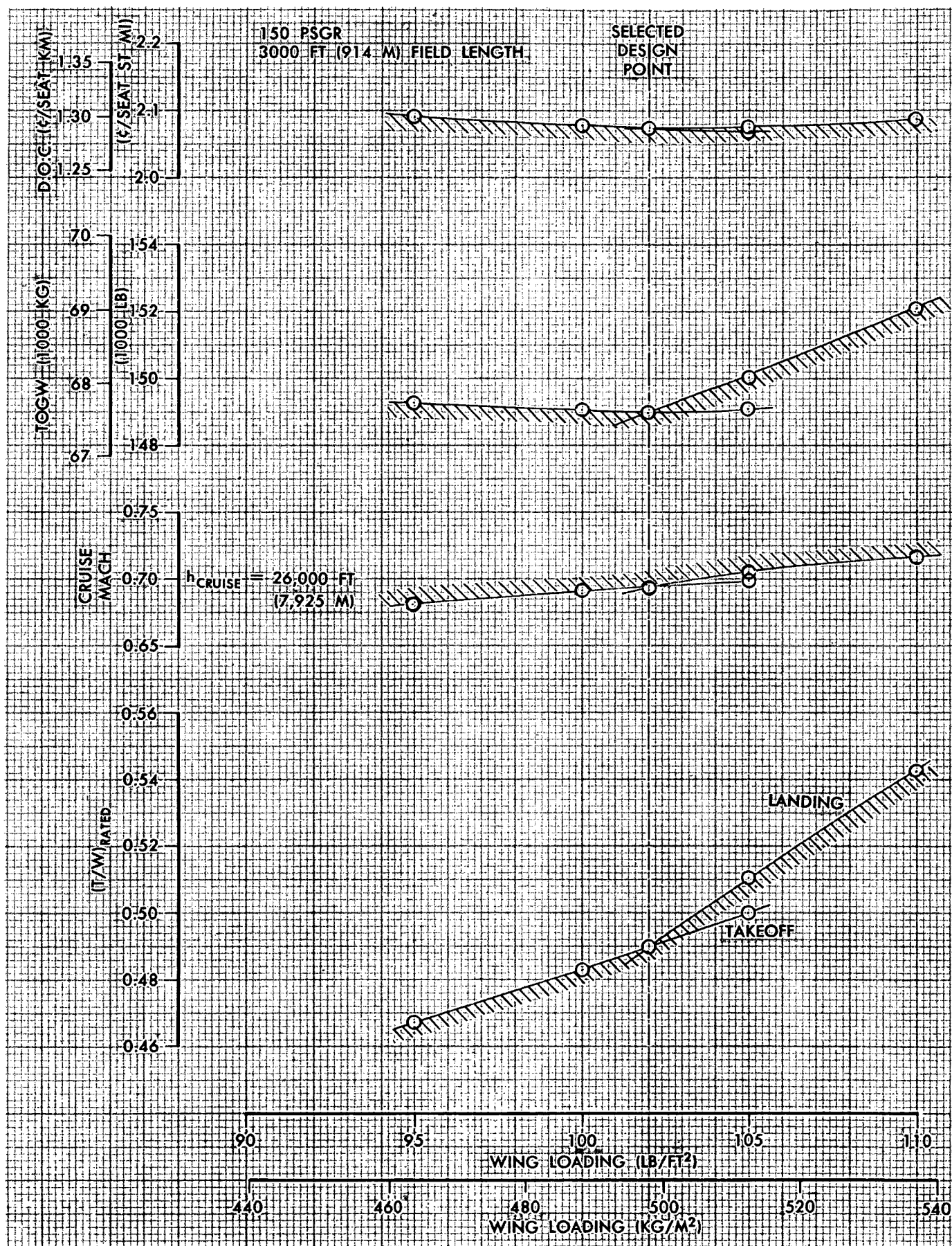


FIGURE 2-12. EXTERNALLY BLOWN FLAP STOL AIRCRAFT SIZING.

Mach number of 0.69 at 25,000 feet (7925 m) at the selected design point, is due to the severe thrust lapse of the high bypass ratio prop-fan engine.

The sizing chart for the EBF 200 passenger, 3000 foot (915 meter) field length airplane (Figure 2-13), is very similar to that for the 150 passenger aircraft. The relative displacements of the thrust-to-weight ratio vs wing loading curves for the two aircraft are due to the influence of ground effects on aircraft size. Ground effects are more severe for the larger aircraft causing the thrust-to-weight line for takeoff to move downward due to the reduction in drag during the ground roll and the landing line to move upward due to the decrease in lift during the flare maneuver. Minimum direct operating cost again occurs at the takeoff-landing intersection, at a wing loading of 100 lb/ft^2 (488 kg/m^2).

Minimum direct operating cost for the EBF 100 passenger 3000 foot (914 m) field length aircraft does not occur at the takeoff-landing line intersection but at a higher wing loading on the landing critical line as shown in Figure 2-14. This is because the increase in cruise Mach number more than offsets the increase in takeoff gross weight in determining direct operating cost. The intersection, at a wing loading of 105 lb/ft^2 (513 kg/m^2) was chosen as the design point, however, on the basis of aircraft geometry considerations. At wing loadings higher than 105 lb/ft^2 (513 kg/m^2) the engine-to-engine and engine-fuselage spacing becomes sufficiently small to cause large increases in interference drag.

The sizing chart for the EBF 150 passenger 2000 foot (610 m) field length aircraft is shown in Figure 2-15. The selected design point, chosen for minimum direct operating cost, occurs on the landing line at a wing

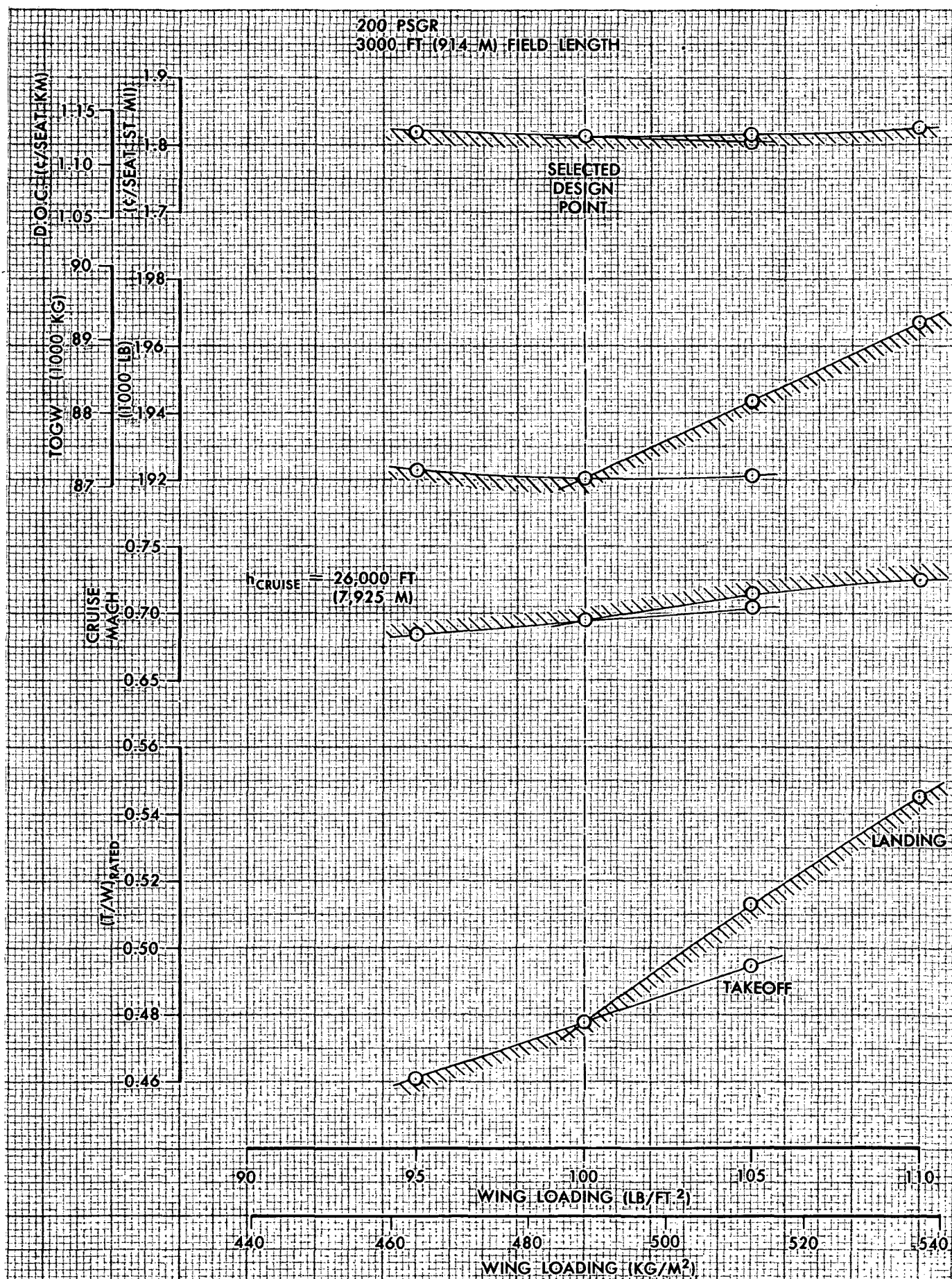


FIGURE 2-13. EXTERNALLY BLOWN FLAP STOL AIRCRAFT SIZING

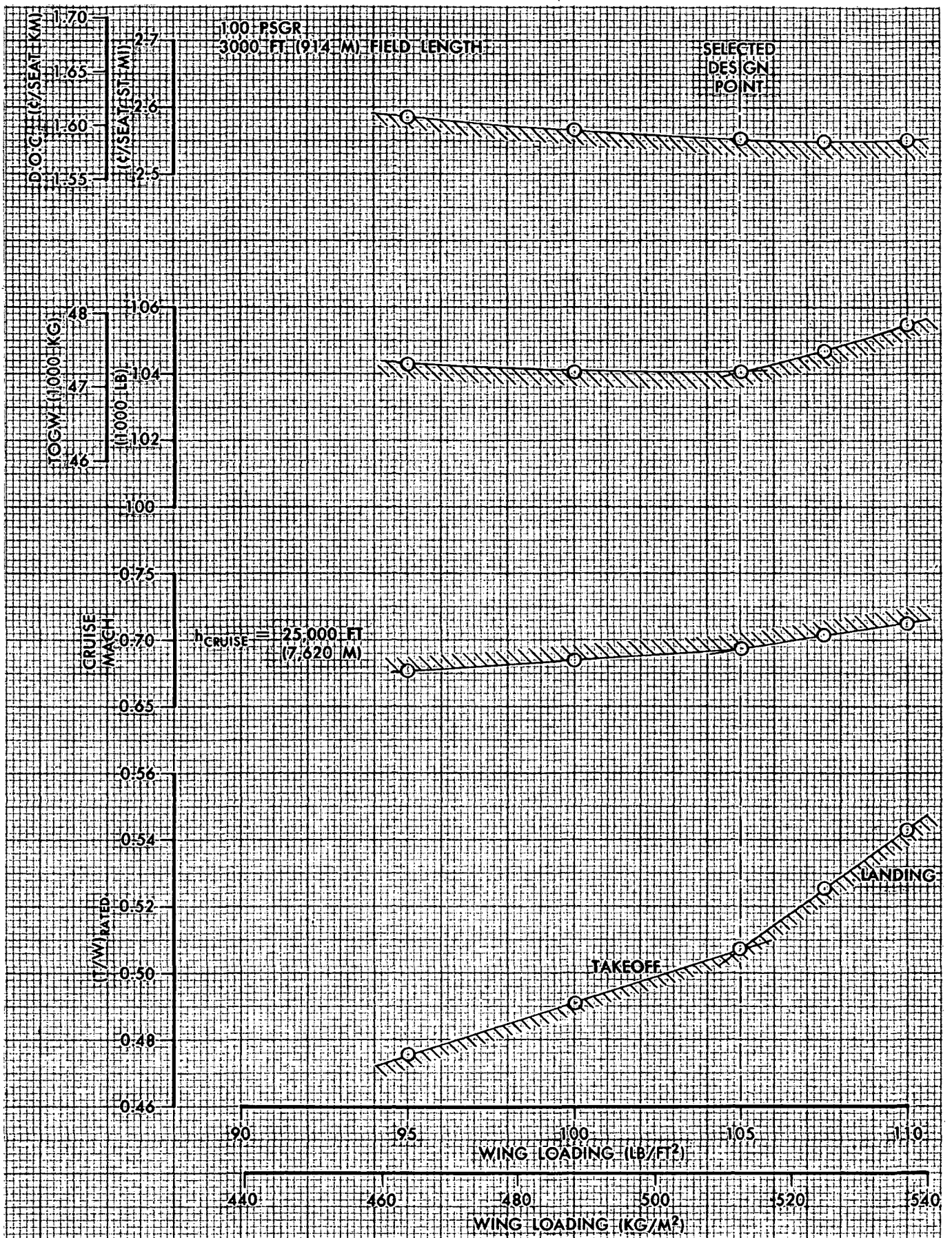


FIGURE 2-14. EXTERNALLY BLOWN FLAP STOL AIRCRAFT SIZING

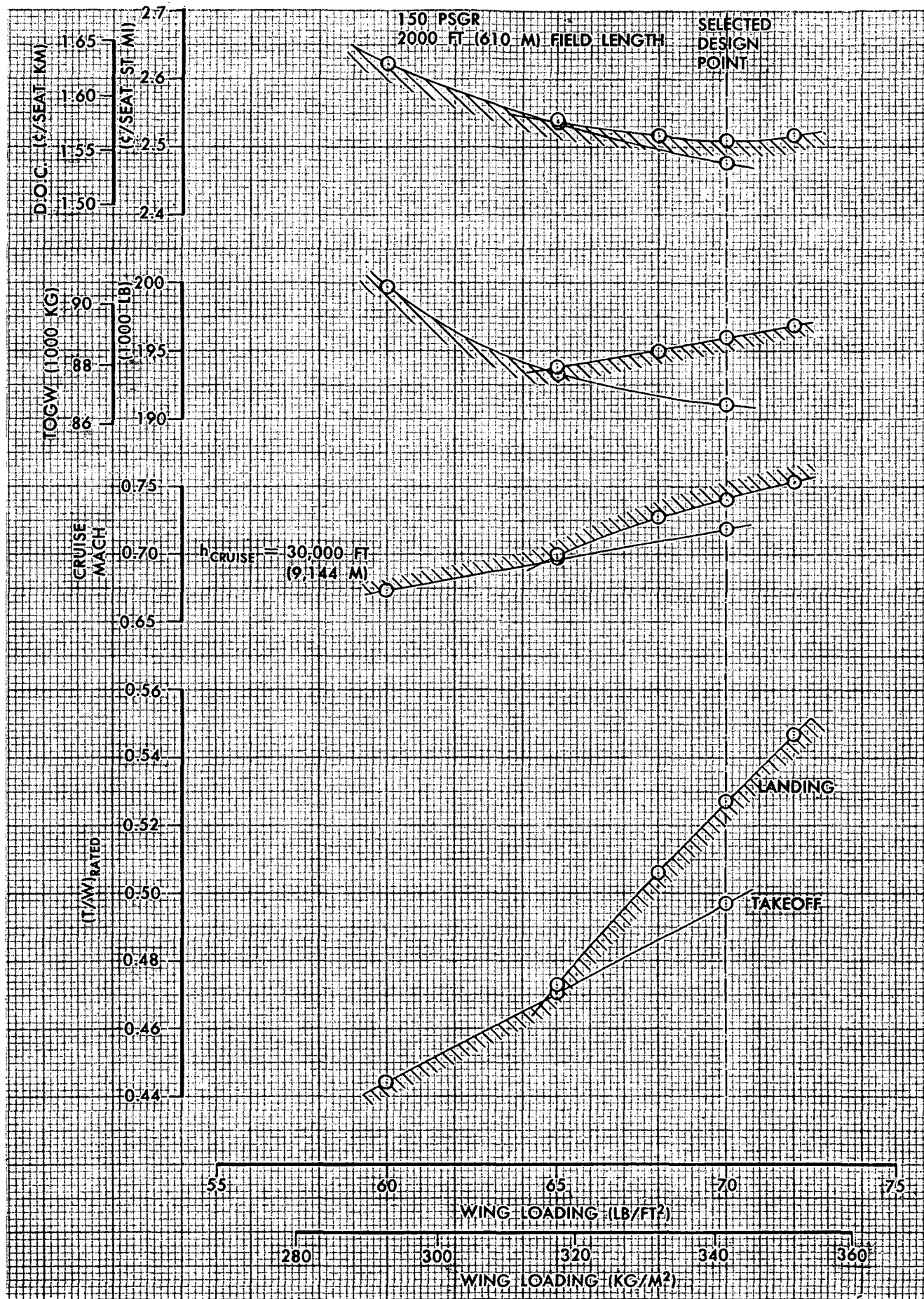


FIGURE 2-15. EXTERNALLY BLOWN FLAP STOL AIRCRAFT SIZING

loading of 70 lb/ft^2 (342 kg/m^2). The DOC tradeoff between increased weight and thrust on one hand and cruise speed on the other at these low wing loadings favors an increase in wing loading above the takeoff-landing intersection. Direct operating cost is much more sensitive to wing loading for the 2000 foot (610 m) field length aircraft than it was for the 3000 foot (915 m) cases. The steep slope of the DOC vs wing loading for the takeoff line indicates that a change in landing ground rules could significantly alter the aircraft direct operating costs. Even though wing loadings are low compared to the 3000 foot (914 m) field length aircraft, cruise Mach number for the 2000 foot (610 m) design point is noticeably higher due to the rapid increase in thrust-to-weight required by selection of the sizing point on the landing critical line.

Mechanical Flap

The final design mechanical flap STOL aircraft are high wing, twin-engine configurations with no flap cutouts. An aspect ratio of 9 was selected to meet the one engine failed second segment climb gradient requirement.

Both aircraft were designed to carry 150 passengers, one from a 3000 foot (915 m) field length and one from a 4000 foot (1220 m) field length. The sizing plots are shown in Figures 2-16 and 2-17. Since these aircraft have essentially no powered lift, the landing lines are almost vertical, i.e., an increase in thrust-to-weight ratio will not noticeably improve landing performance. The takeoff-landing line intersections were chosen as the selected design points for minimum direct operating cost. Cruise Mach numbers are similar to those for the externally blown flap STOL

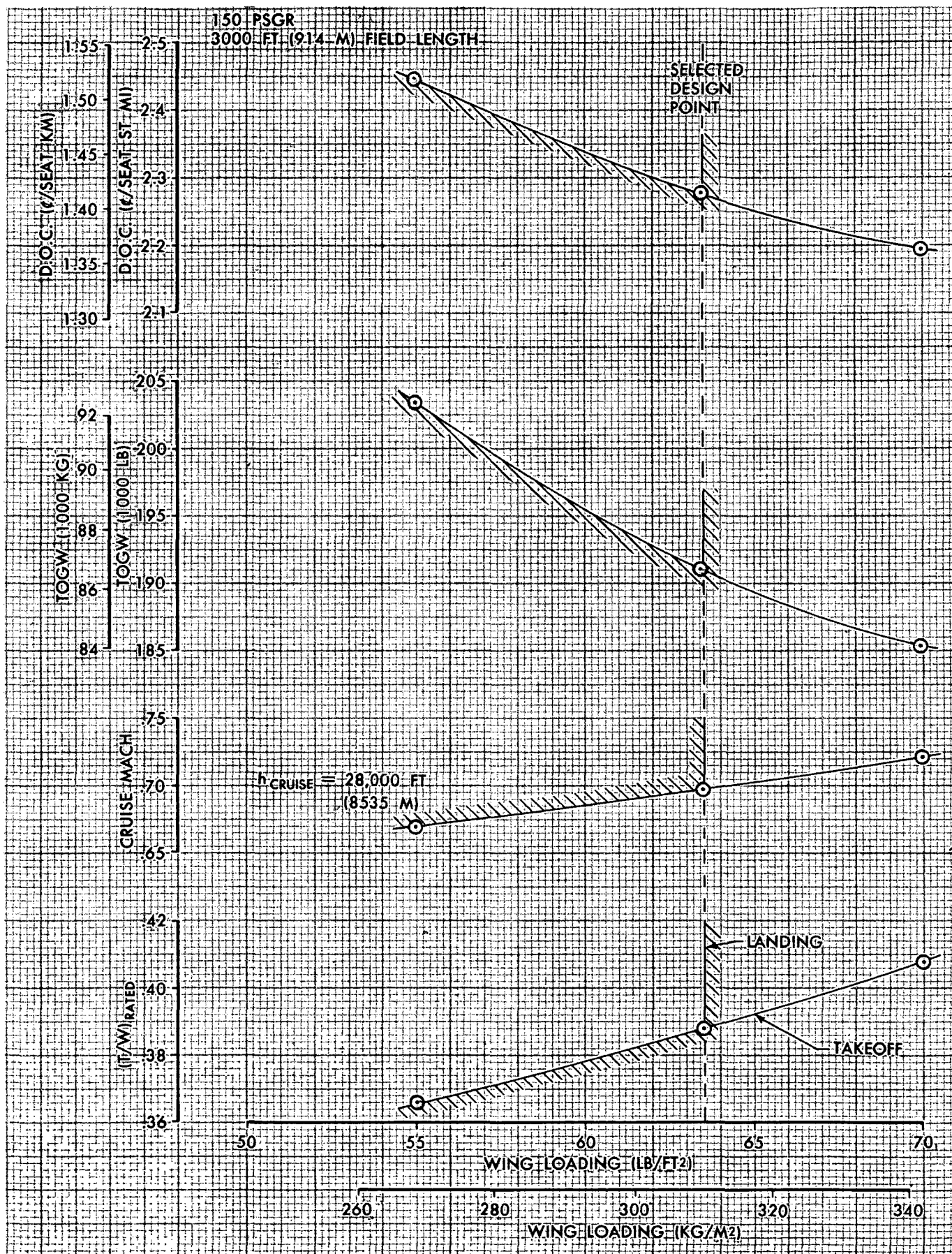


FIGURE 2-16. MECHANICAL FLAP AIRCRAFT SIZING

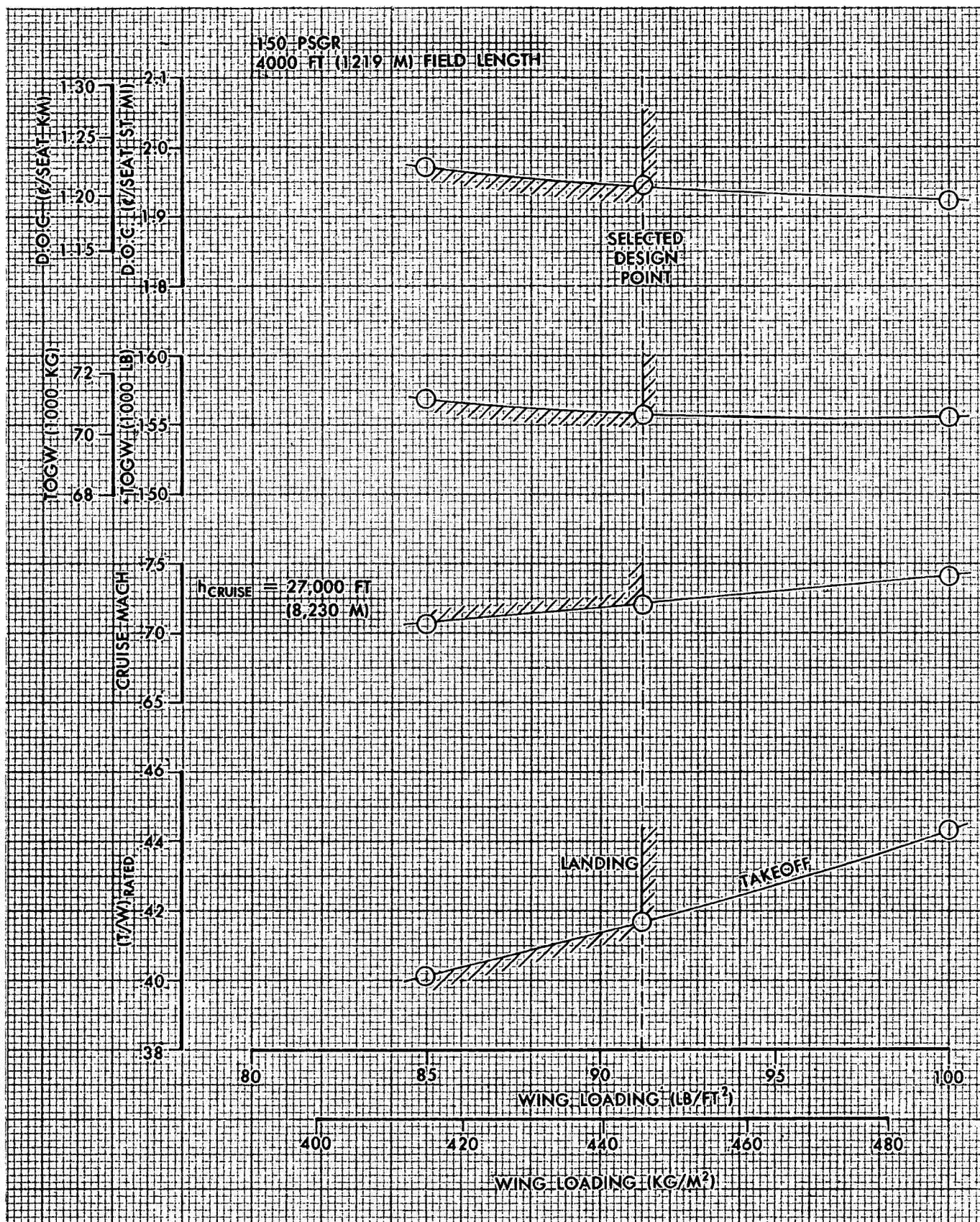


FIGURE 2-17. MECHANICAL FLAP STOL AIRCRAFT SIZING

aircraft due to the low thrust-to-weight ratios which in turn are due to the low wing loadings.

Any improvement in maximum lift capability or a relaxation of the landing ground rules would increase the design wing loading and reduce weight and direct operating costs, particularly for the 3000 foot (914 m) field length aircraft. Further work on this configuration should be channeled in the direction of improving high lift performance.

Augmentor Wing

An aspect ratio of 6.5 was selected for the AW 150 passenger 2000 foot (610 m) field length aircraft on the basis of high lift data availability (Ref. 1). The selected design point, chosen to minimize DOC, occurs at the intersection of the takeoff and landing critical lines at a wing loading of 77.5 lb/ft^2 (378 kg/m^2). The landing line is quite steep, imposing fairly severe economic penalties if a higher wing loading were selected. The very low lapse rate of the Allison PD287-43 engine provides a maximum cruise Mach number of 0.78, about 12 percent higher than that of the externally blown flap or mechanical flap STOL aircraft. On the other hand, the takeoff gross weight for the augmentor wing is high due to the poor engine SFC and high propulsion system weight.

Upper Surface Blown Flap

The USB, 150 passenger, 2000 foot (610 m) field length aircraft sizing chart, Figure 2-19, looks very similar to that for the corresponding EBF aircraft. The design point, selected for minimum DOC at a wing loading of 67 psf (327 kg/m^2), occurs on the landing critical line as it did for the externally blown flap aircraft. Also like the EBF, this aircraft would show

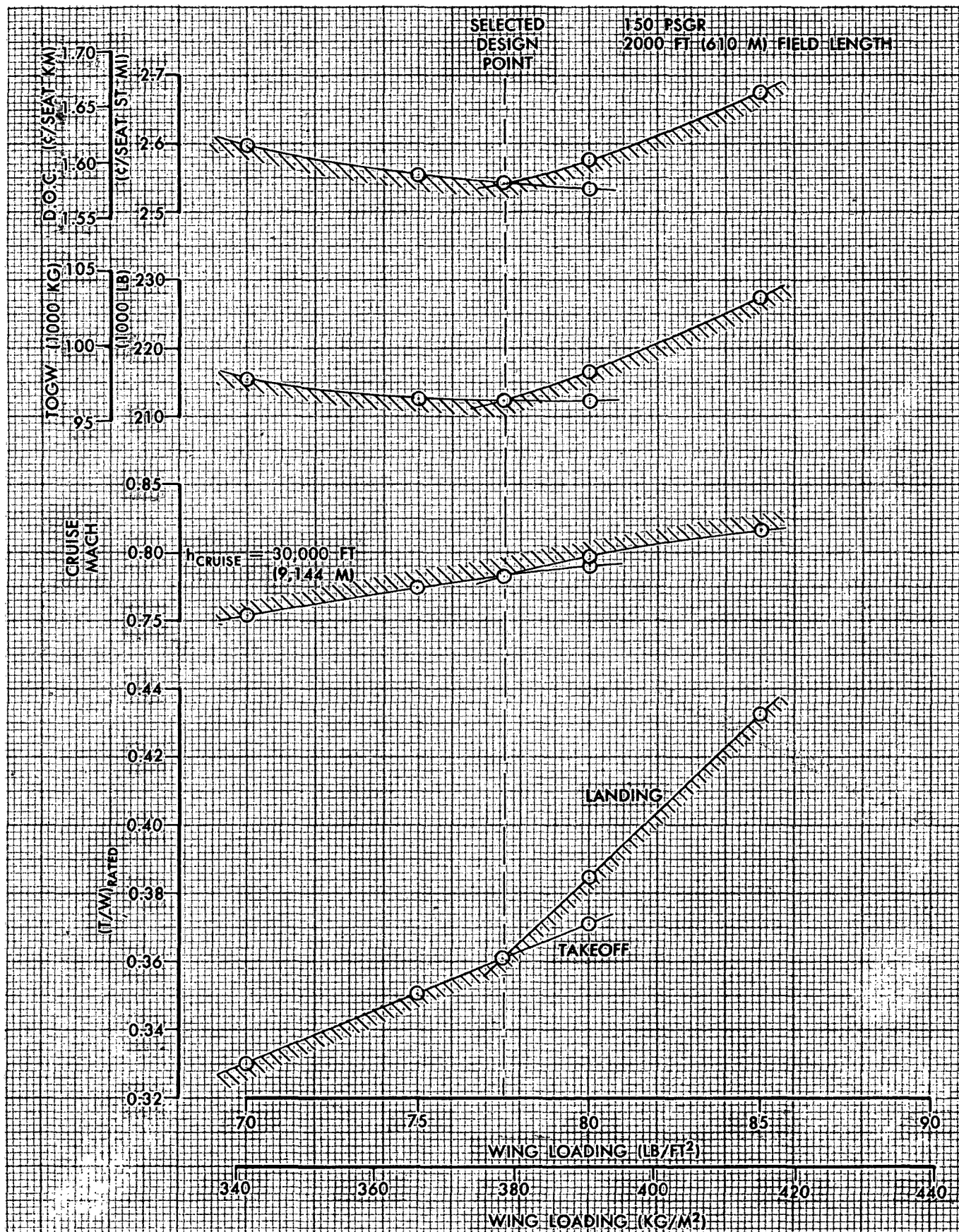


FIGURE 2-18. AUGMENTOR WING STOL AIRCRAFT SIZING

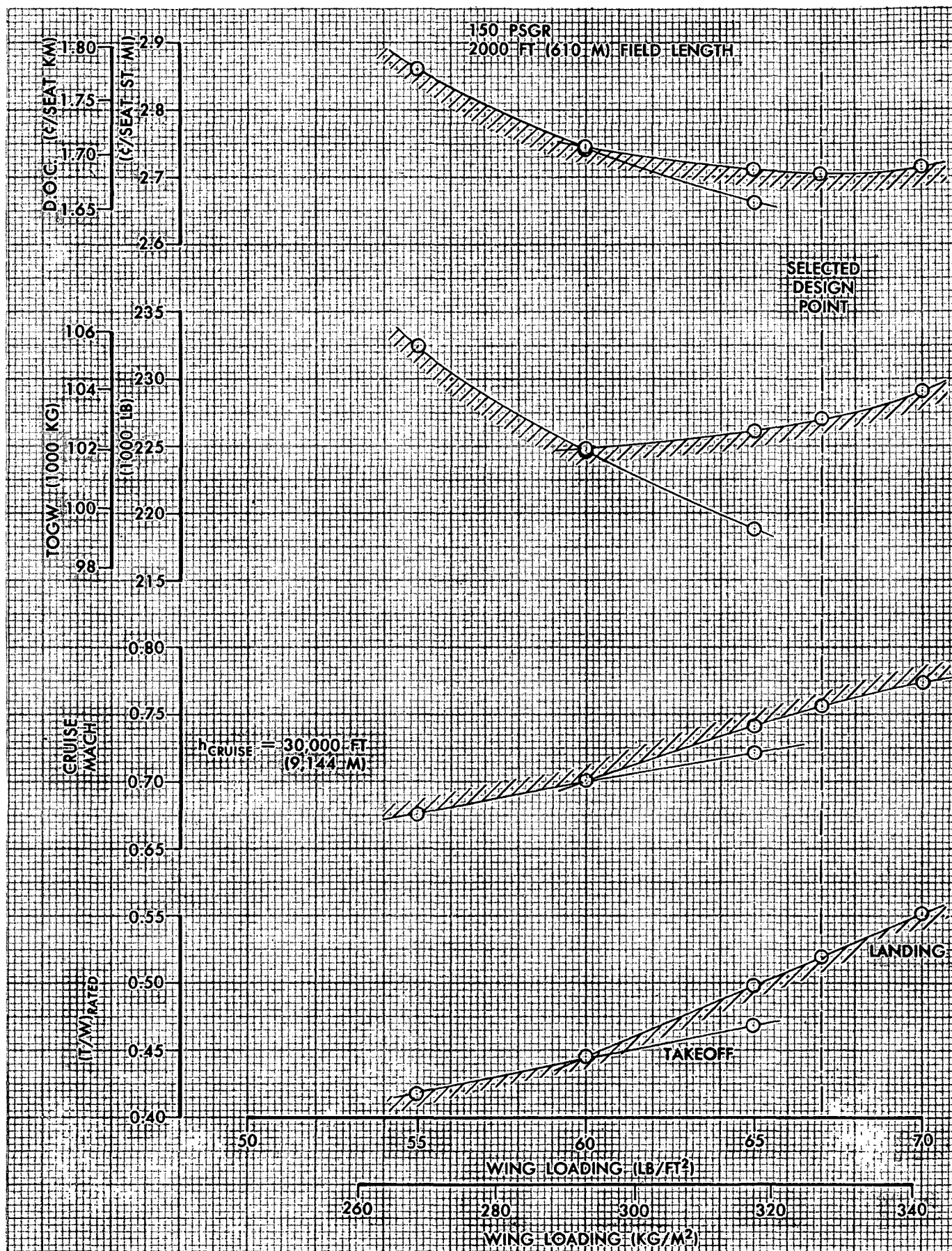


FIGURE 2-19. UPPER SURFACE BLOWN FLAP STOL AIRCRAFT SIZING

a noticeable improvement in DOC if the landing high lift performance could be improved or the landing ground rules relaxed.

Cruise Mach number is slightly higher than that for the EBF aircraft, 0.76 vs 0.74. The weight of the USB aircraft, however, is considerably more than that of the EBF aircraft and consequently direct operating costs are noticeably higher.

CTOL Aircraft

An advanced CTOL aircraft was sized for comparison purposes only and for this reason detailed sizing optimization studies were not performed. The aircraft was sized to carry 150 passengers for ranges up to 1380 statute miles (2224 km) and meet FAR Part 36 minus 14 PNdB sideline noise levels. A wing loading of 110 psf (537 kg/m^2) and an aspect ratio of 9 were chosen to provide a 7500 foot (2286 m) field length capability and a cruise Mach number of 0.80 at 30,000 feet (9144 m).

2.2.3 Configuration Descriptions. - The brief configuration descriptions given in this section are based upon extensive configuration studies conducted during the contract. Engineering three-view drawings of each of the eight STOL final design aircraft and the advanced CTOL aircraft are shown in Figures 2-20 through 2-28.

High Lift Systems

Externally Blown Flap - The EBF airplane has flaps extending from the fuselage side to 75 percent of the wing semi-span and occupy 35 percent of the wing chord when retracted. Each flap has two segments hinged independently to give a large chord-wise expansion and 3 percent chord gaps

FINAL DESIGN AIRCRAFT

EXTERNALLY BLOWN FLAP AIRCRAFT

100 PASSENGERS-3000 FT. (914 M.) FIELD LENGTH

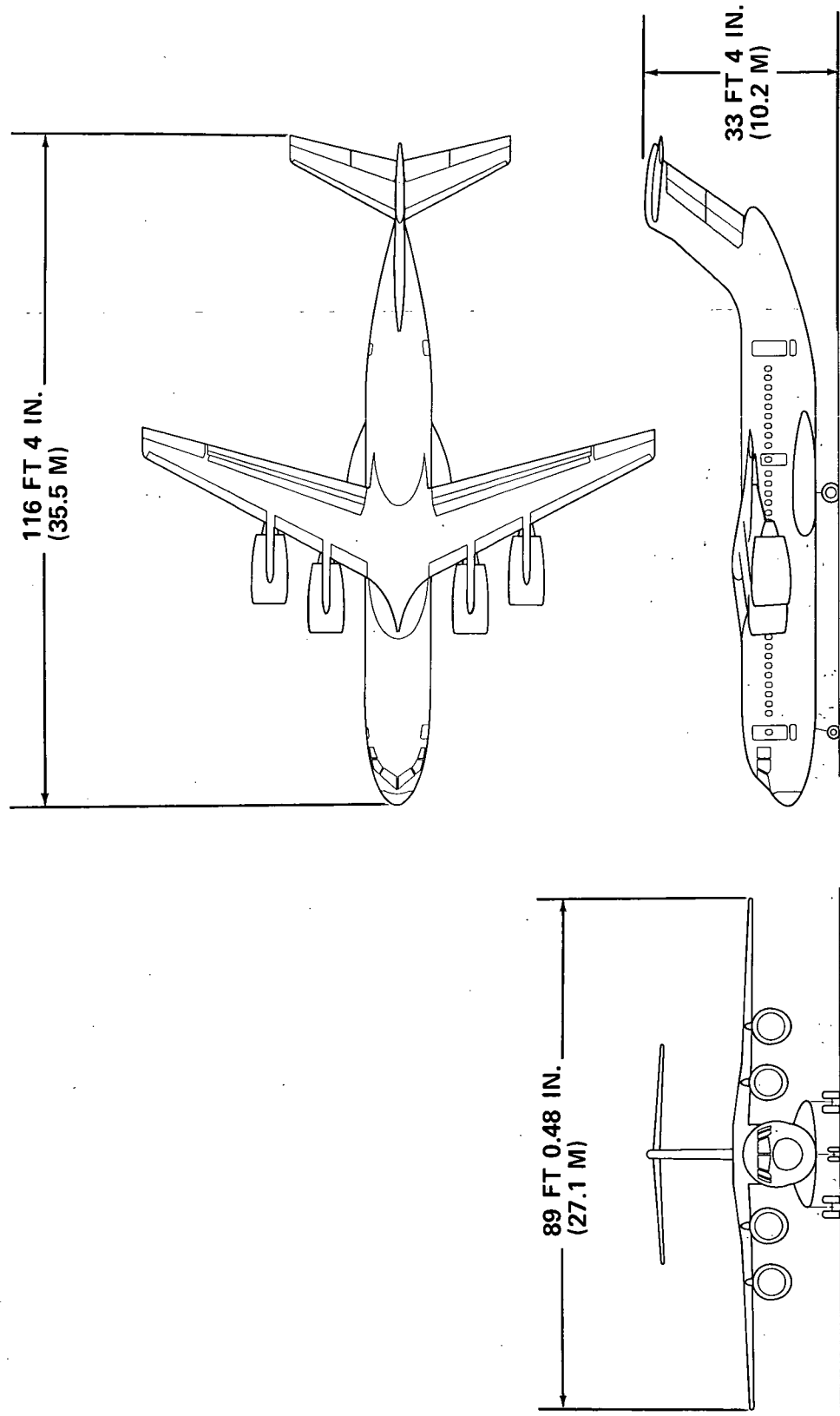


FIGURE 2-20

FINAL DESIGN AIRCRAFT
EXTERNALLY BLOWN FLAP AIRCRAFT
 150 PASSENGERS - 3000 FT (914 M) FIELD LENGTH

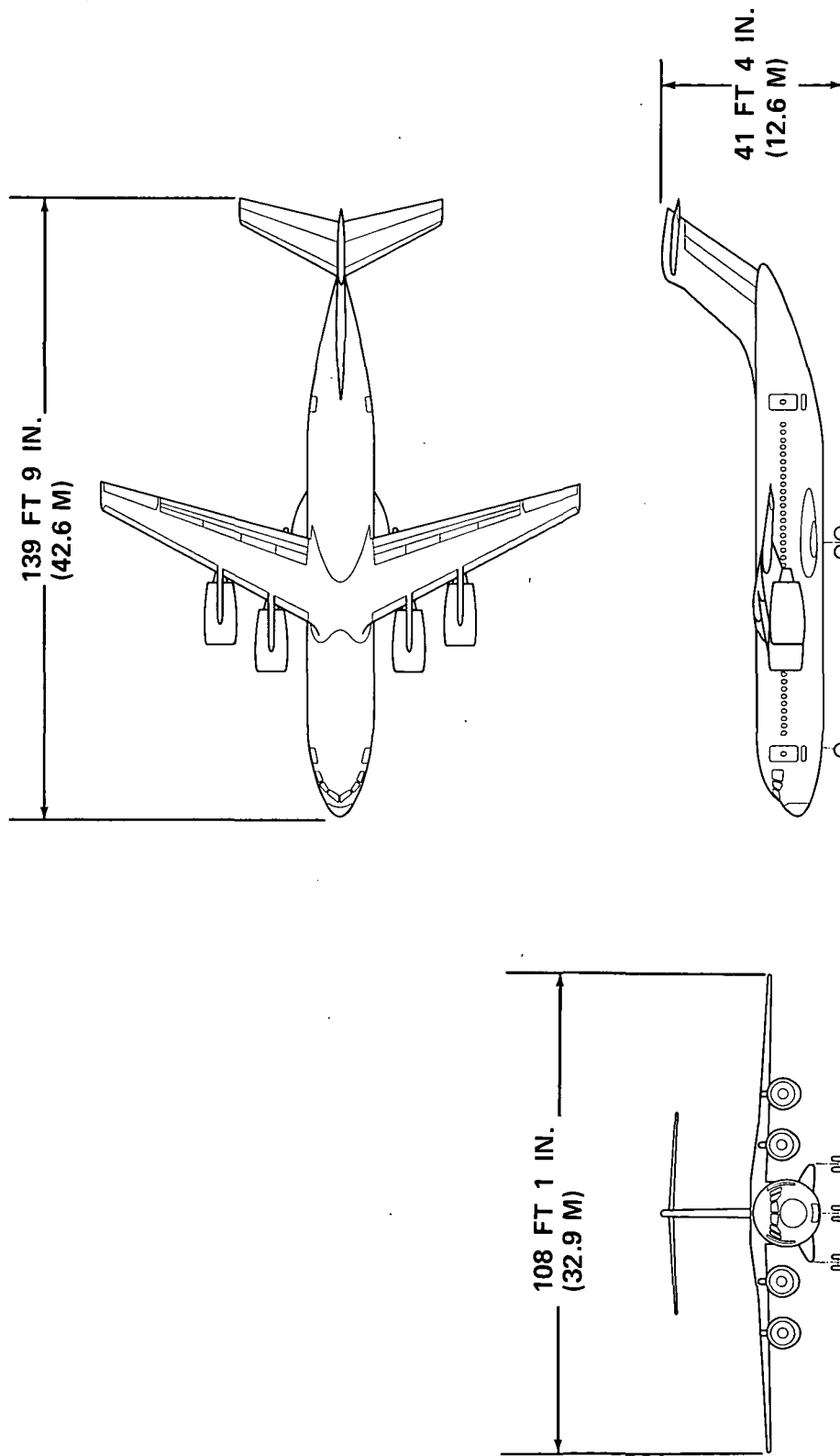


FIGURE 2-21

PR3-STOL-15128

FINAL DESIGN AIRCRAFT

EXTERNALLY BLOWN FLAP AIRCRAFT

200 PASSENGERS - 3000FT. (914 M.) FIELD LENGTH

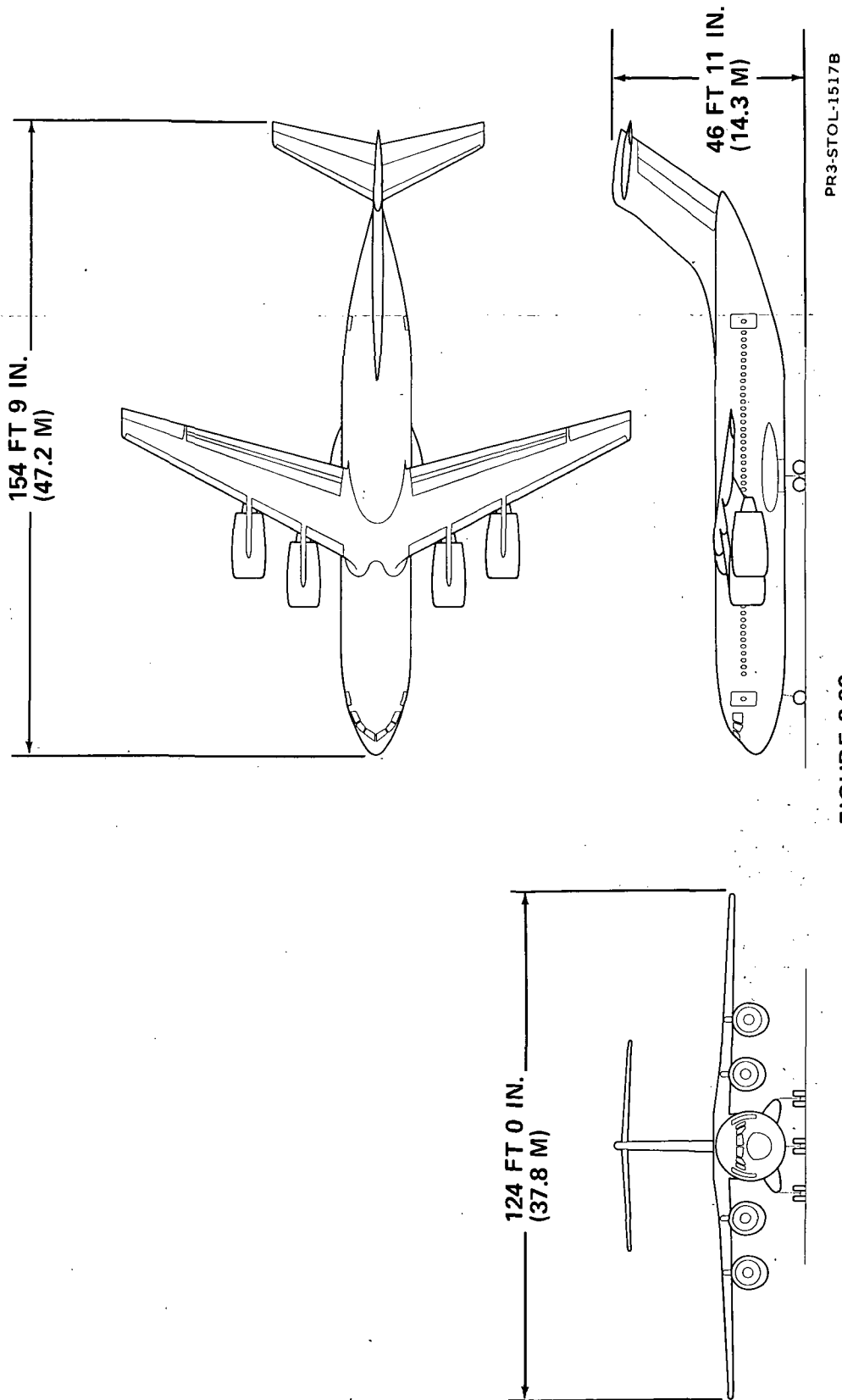


FIGURE 2-22

FINAL DESIGN AIRCRAFT

EXTERNALLY BLOWN FLAP AIRCRAFT

150 PASSENGERS - 2000 FT. (610M.) FIELD LENGTH

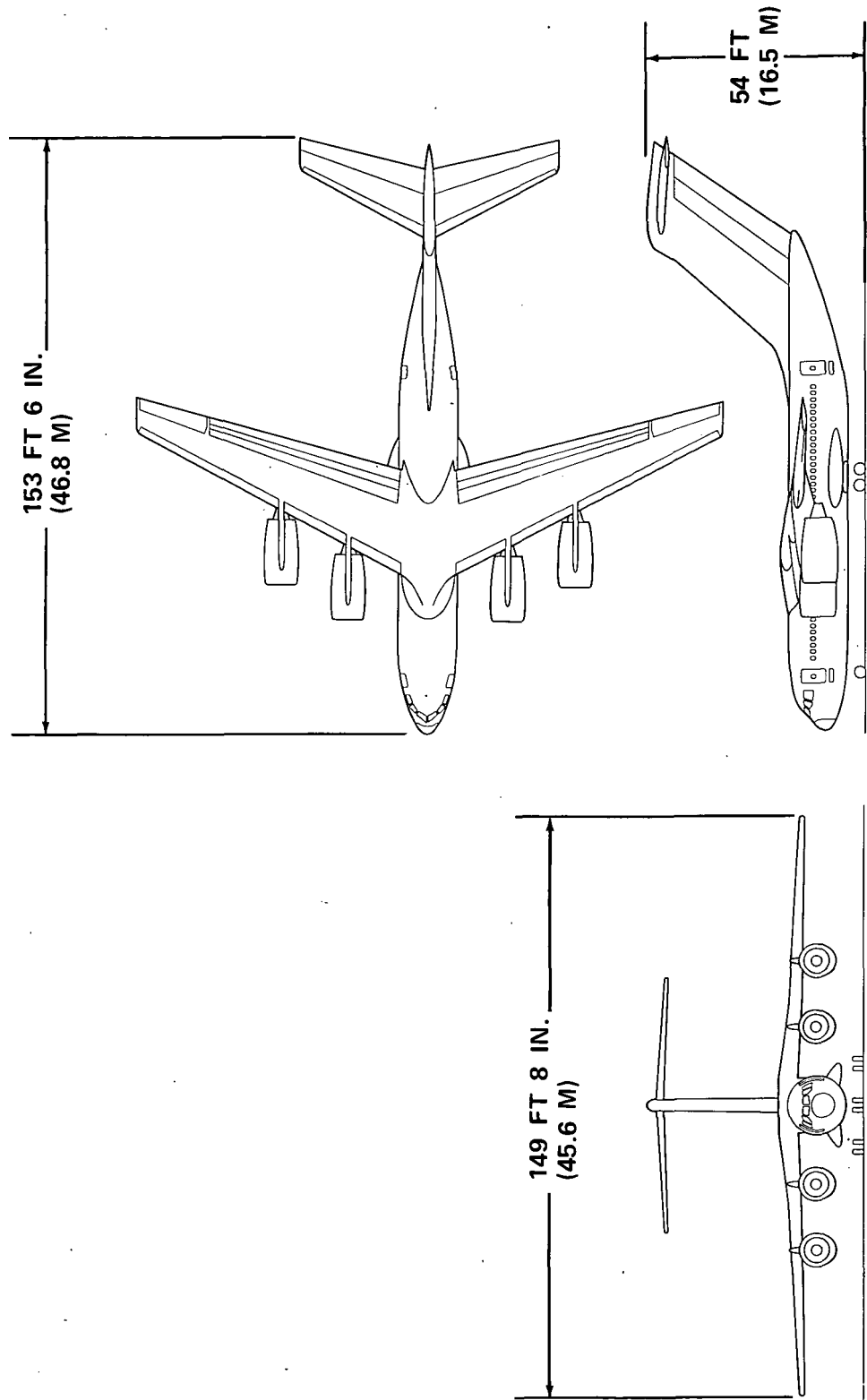


FIGURE 2-23

FINAL DESIGN AIRCRAFT

UPPER SURFACE BLOWN AIRCRAFT

150 PASSENGERS - 2000 FT (610 M) FIELD LENGTH

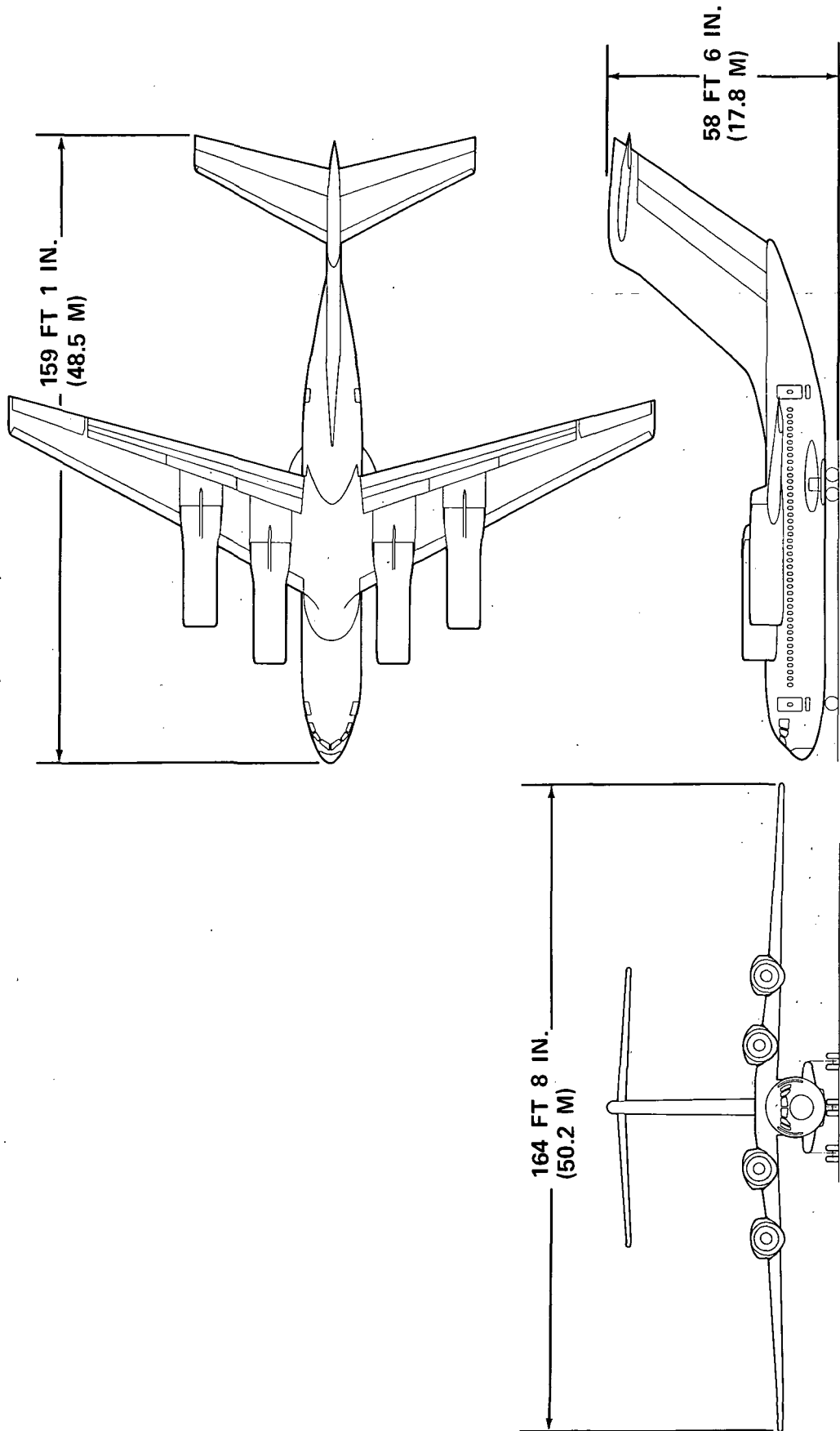


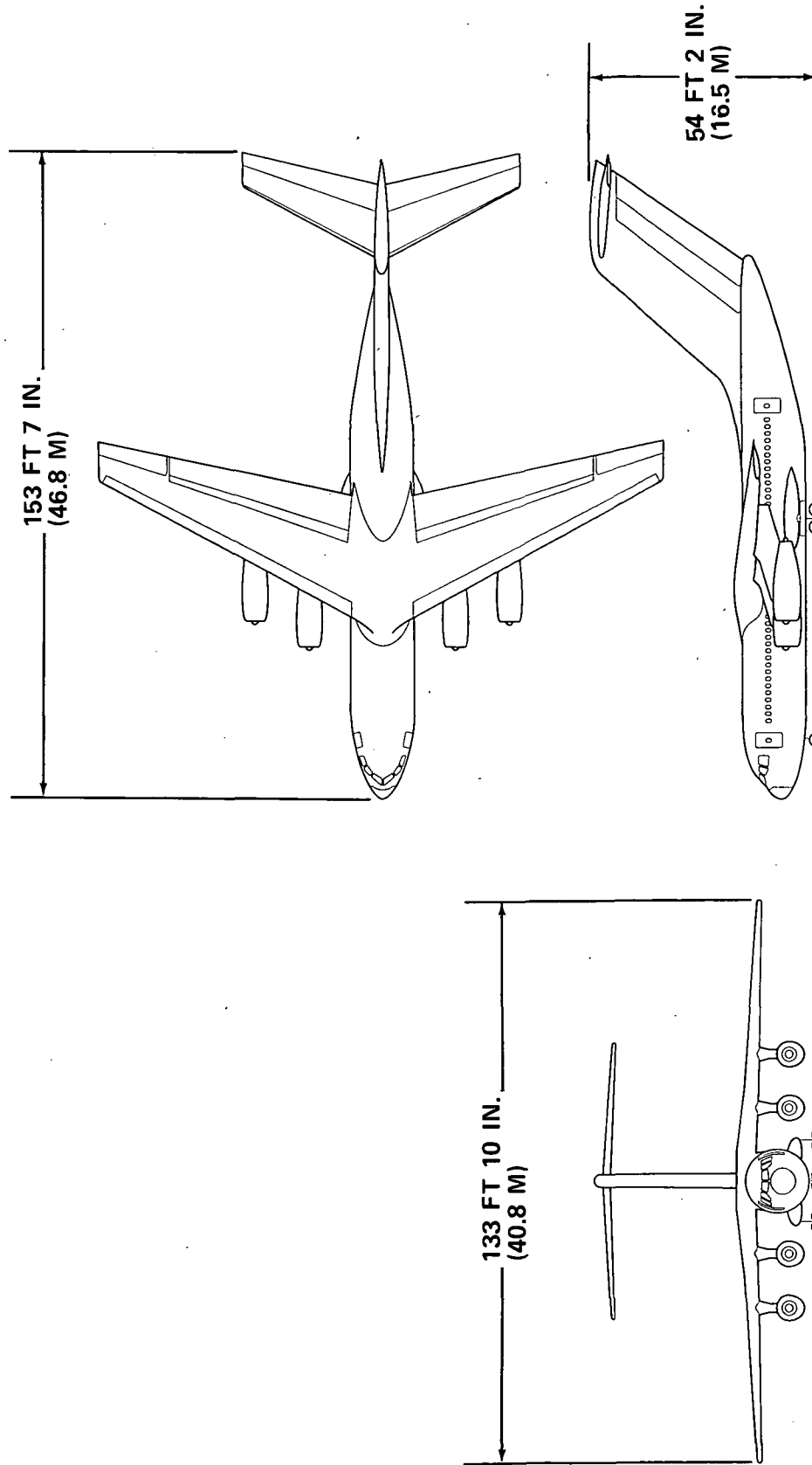
FIGURE 2-24

PR3-STOL-1646B

FINAL DESIGN AIRCRAFT

AUGMENTOR WING AIRCRAFT

150 PASSENGERS - 2000 FT (610 M) FIELD LENGTH



PR3-STOL-1458 B

FIGURE 2-25

FINAL DESIGN AIRCRAFT

MECHANICAL FLAP AIRCRAFT

150 PASSENGERS • 3000 FT (914 M) FIELD LENGTH

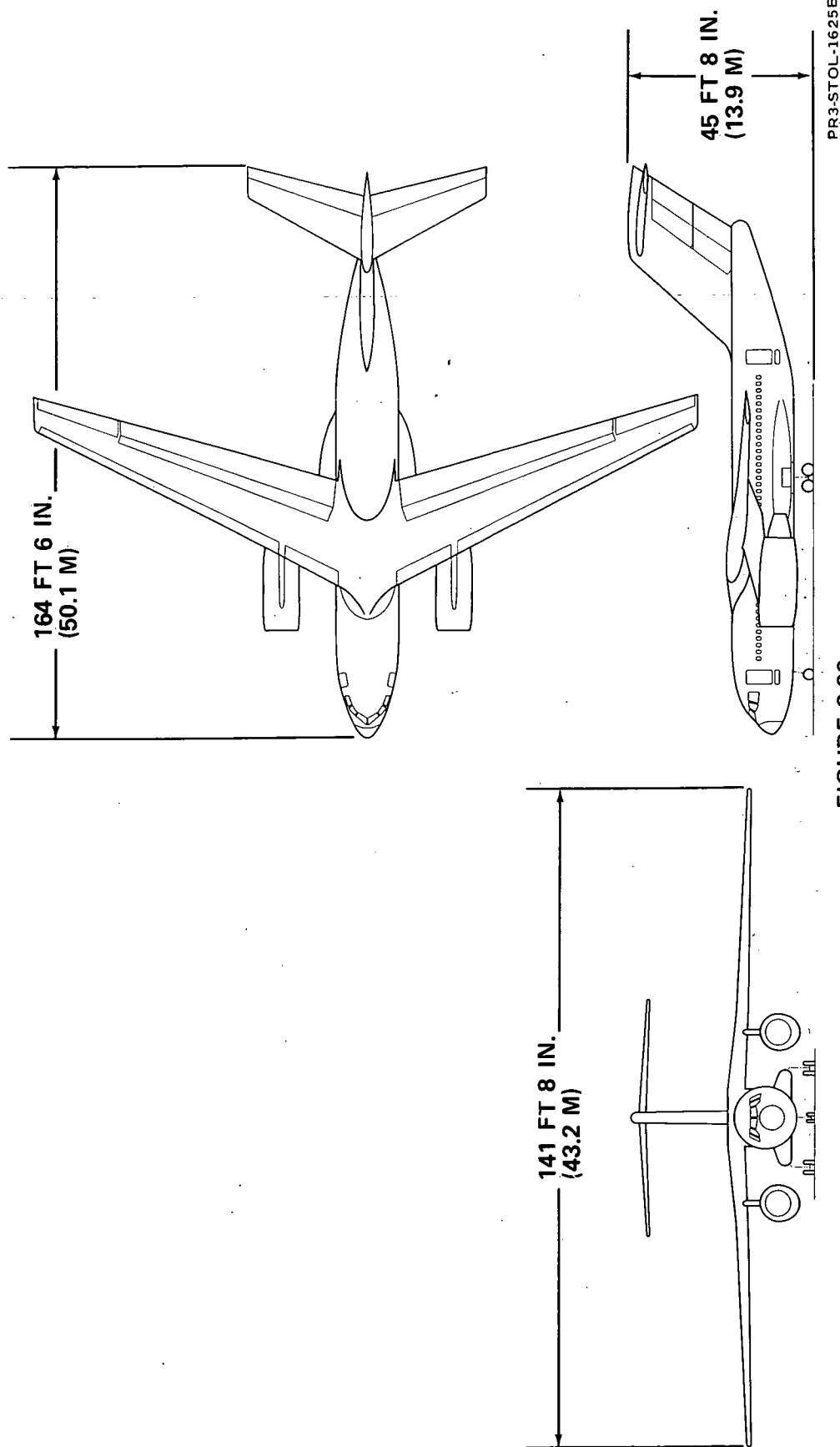
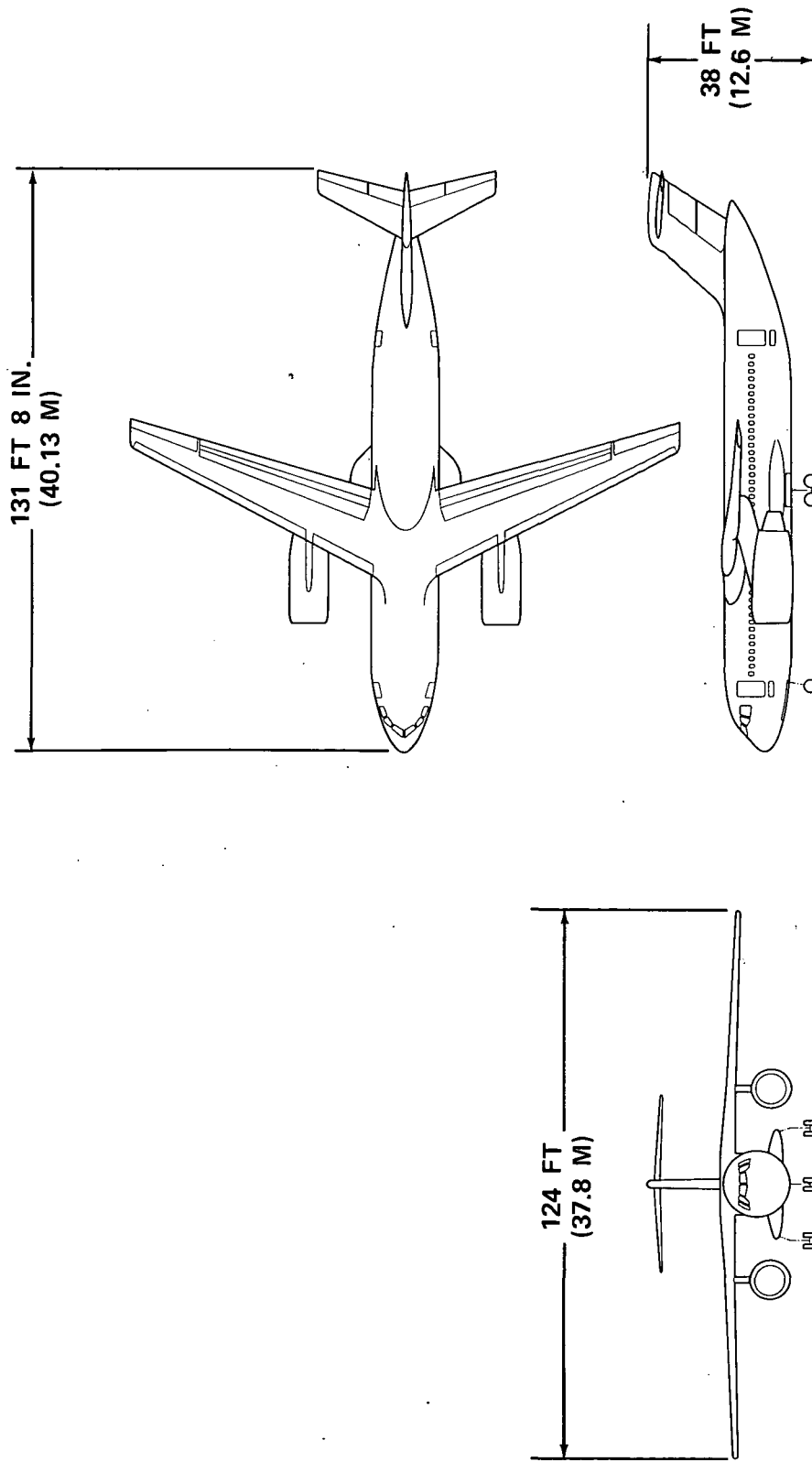


FIGURE 2-26

FINAL DESIGN AIRCRAFT

MECHANICAL FLAP AIRCRAFT

150 PASSENGERS 4000 FT (1220 M) FIELD LENGTH



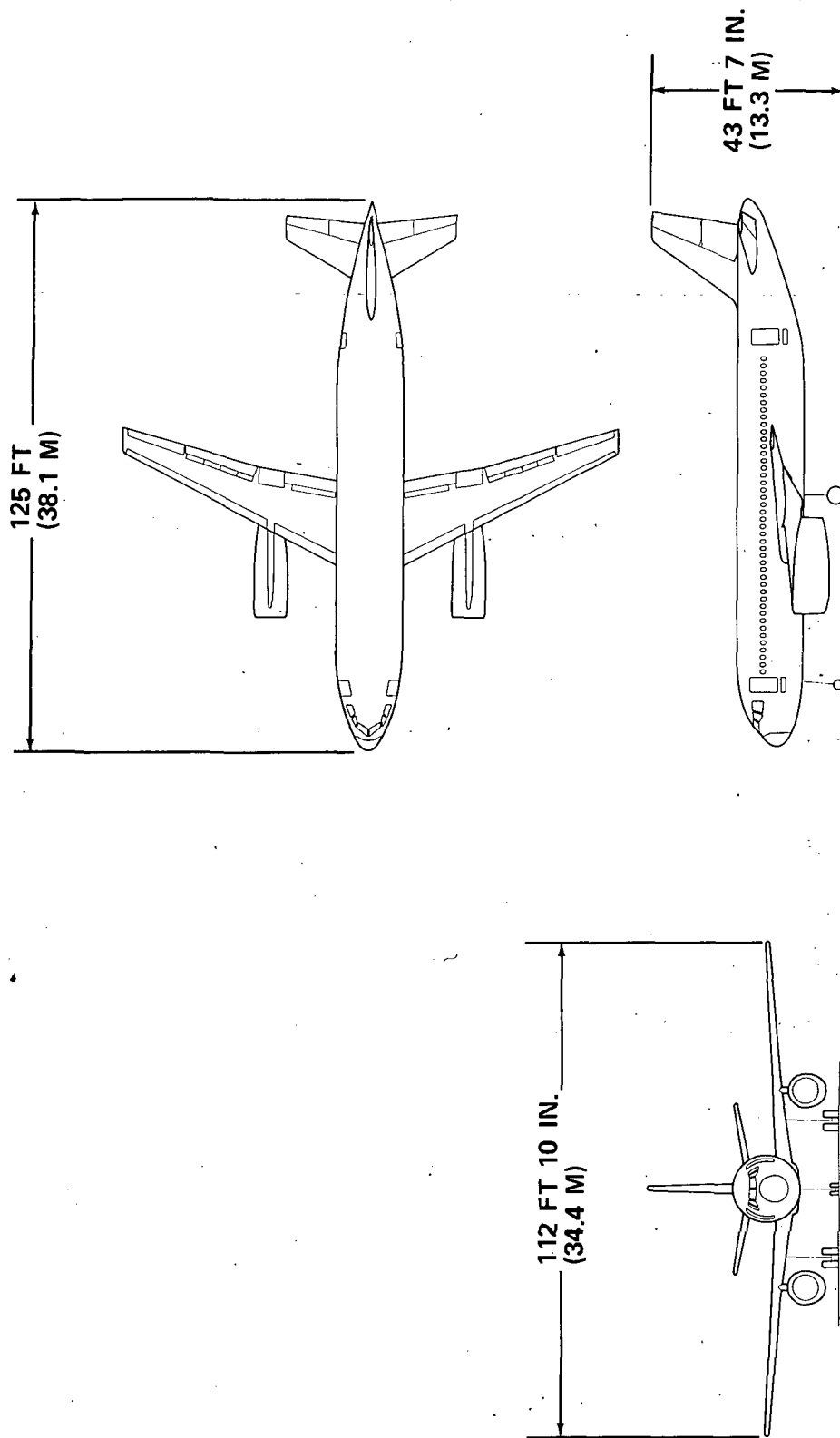
PR3-STOL-1676 B

FIGURE 2-27

FINAL DESIGN AIRCRAFT

CTOL AIRCRAFT

150 PASSENGERS - 7500 FT. (2286 M.) FIELD LENGTH



PR3-STOL-1455 B

FIGURE 2-28

between segments. Spoilers are used for direct lift control in the approach mode and are normally drooped for takeoff. Leading edge flaps are used behind the engines and leading edge slats outboard. The engines are located well inboard to reduce engine-out asymmetric effects. The location of the outboard engine at 50 percent of the wing semi-span allows sufficient spacing to avoid significant interference drag penalties. The engine fan exits are located at approximately 10 percent of the wing chord forward of the wing leading edge and are positioned as high as possible for high turning efficiency without the fan exhaust impinging on the deflected leading edge flaps or introducing significant scrubbing losses in cruise flight.

Upper Surface Blowing - The flaps located behind the engines are similar to the EBF flaps except that the components are arranged to provide a continuous, smooth, relatively large radius coanda surface without slots. Outboard of the engines, the flap is similar to the EBF flap except that the flap gaps are only 2 percent of the wing chord because this part of the wing is unblown. The engine exhaust is ejected parallel to and close to the wing upper surface, separated from it by a vented insulating layer which tapers to zero thickness at the spoiler hinge line.

Augmentor Wing - For the augmentor wing configuration, all of the fan airflow is diverted to independent plenums in the wing which feed discreet high aspect ratio flap nozzles and secondary aileron BLC plenums. The augmentor flap technology presented in Reference 1 was used in selecting the ejector and nozzle geometries. The engines are mounted on pylons to permit the use of an uninterrupted leading edge slat and to minimize cruise interference drag.

Mechanical Flap - The mechanical flap high lift system uses a large chord ratio two segment flap similar to that of the EBF except that the gaps are smaller. The engines are mounted low enough to avoid exhaust impingement on the flaps at takeoff setting. The leading edge has full span slats similar to those used on the DC-10 airplane.

CTOL - Hinged expanding double slotted flaps, similar to DC-10 flaps, are used and occupy 28 percent of the wing chord when retracted. An inboard aileron behind the engine serves as a gate to avoid exhaust impingement on the flap. Leading edge slats are interrupted only by the engine pylon and are otherwise continuous. A reduction in $C_{L_{max}}$ requirements with the longer field length results in less adverse ground effects and permits the use of a conventional low wing configuration.

Engine Arrangements

Four engines are used with all propulsive lift systems and are positioned to avoid significant interference drag. On the EBF airplane, the outboard engine is limited to 50 percent of the semi span for safe control with one engine out and on the augmentor wing is limited to 45 percent of the semi span due to duct size limitations.

Only two engines are required for the mechanical flap and CTOL configurations. The use of two engines in lieu of three or four has significant economic and operational advantages including lower maintenance costs and higher aircraft dispatch reliability.

Wing Configurations

Advanced technology supercritical wing sections having an average thickness of 13.9 percent are used on all configurations. All front spars

are located at 13 percent of the theoretical root chord increasing linearly to 28 percent at the tip to allow the use of a 25 percent tip chord leading edge slat.

The rear spar location is influenced by the flap system used. It is at 57 percent chord on the EBF, USB, and 4000 foot (1219 m) field length MF airplanes. The rear spar is at 52 percent chord on the 3000 foot (914 m) field length MF airplanes to allow use of an unextended flap chord of 42 percent. The rear spar is located further forward on the augmentor wing airplane to provide sufficient space for housing the ducting between the wing structural box and the augmentor flap. It is located at 50 percent chord at the wing root decreasing linearly to 45 percent at the outboard engine location then increasing linearly to 60 percent chord at the tip. The CTOL airplane uses a rear spar location of 65 percent chord.

An aspect ratio of 8.0 was chosen for all four-engined configurations except the augmentor wing. The augmentor wing aircraft was limited to an aspect ratio of 6.5 so that the wing cross section would be of sufficient size to accommodate ducting large enough to avoid excessive ducting losses. An aspect ratio of 9.0 was chosen for the two-engined airplanes to reduce the influence of induced drag on second segment climb performance.

Tail Arrangement and Sizing

Because of the severe downwash conditions associated with propulsive lift systems, a "T" tail is necessary to achieve satisfactory longitudinal stability. Empennage surfaces were primarily sized by control requirements for pitch and yaw acceleration. A double hinged rudder and a leading edge flap on the horizontal stabilizer are used to help reduce tail areas. A

fuselage mounted horizontal tail, similar to that on the DC-10 is used on the CTOL airplane.

Fuselage Arrangement

The fuselage arrangements described below are the result of extensive review and coordination between Douglas Aircraft and its airline subcontractors, American Airlines, United Air Lines, Allegheny Airlines and Air California. These interior designs meet the projected requirements for commercial STOL transport aircraft by their expected users as summarized in Section 5.

Interior arrangements are shown for the 100, 150 and 200 passenger fuselages in Figures 2-25, 2-26 and 2-27, respectively. Fuselage dimensions were selected by the need for sufficient fuselage length for passenger and crew access and baggage loading relative to the proximity of the large engines. Longer fuselages also help to reduce the size of the very large tail surfaces needed for the shorter field lengths.

For passenger comfort, DC-9 seats are used at 34 inch pitch. These seats are one inch wider per passenger than DC-8 or B707/727/737 seats. An aisle width of 20 inches was chosen, consistent with current wide body airplanes. Buffet, lavatory, coat space, entry doors and attendants seats are located at both ends of the airplane in accordance with airline suggestions. Large windows are used in every bay as on the DC-10.

The under floor compartments are sized to accommodate standard belly containers where practical. Bulk cargo only is assumed for the basic airplane weight empty calculations.

[illegible]

PR3-STOL-1516 A

150 PASSENGER INTERIOR

FINAL DESIGN AIRCRAFT

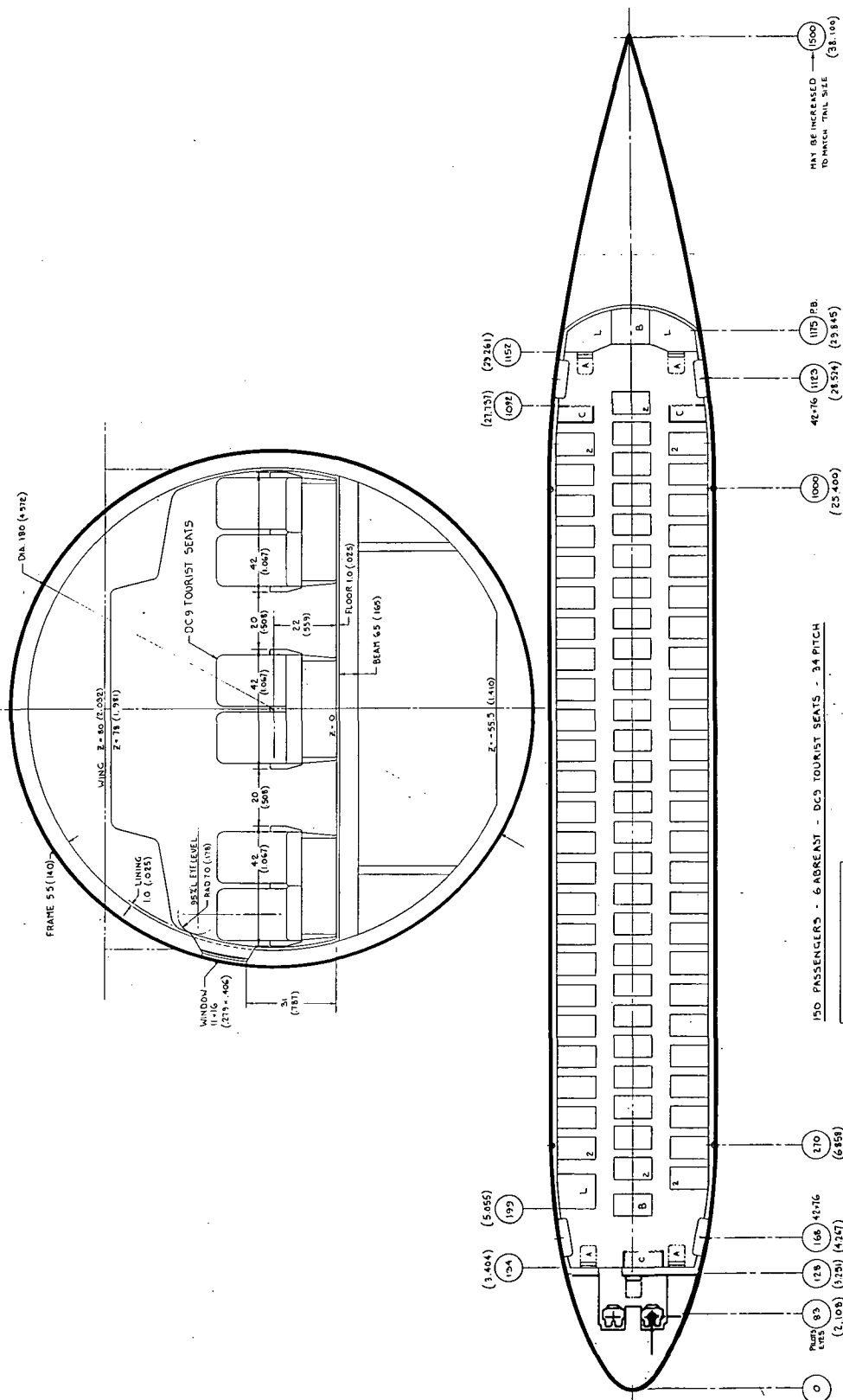


FIGURE 2-30

PR3-STOL-1515 B

200 PASSENGER INTERIOR

FINAL DESIGN AIRCRAFT

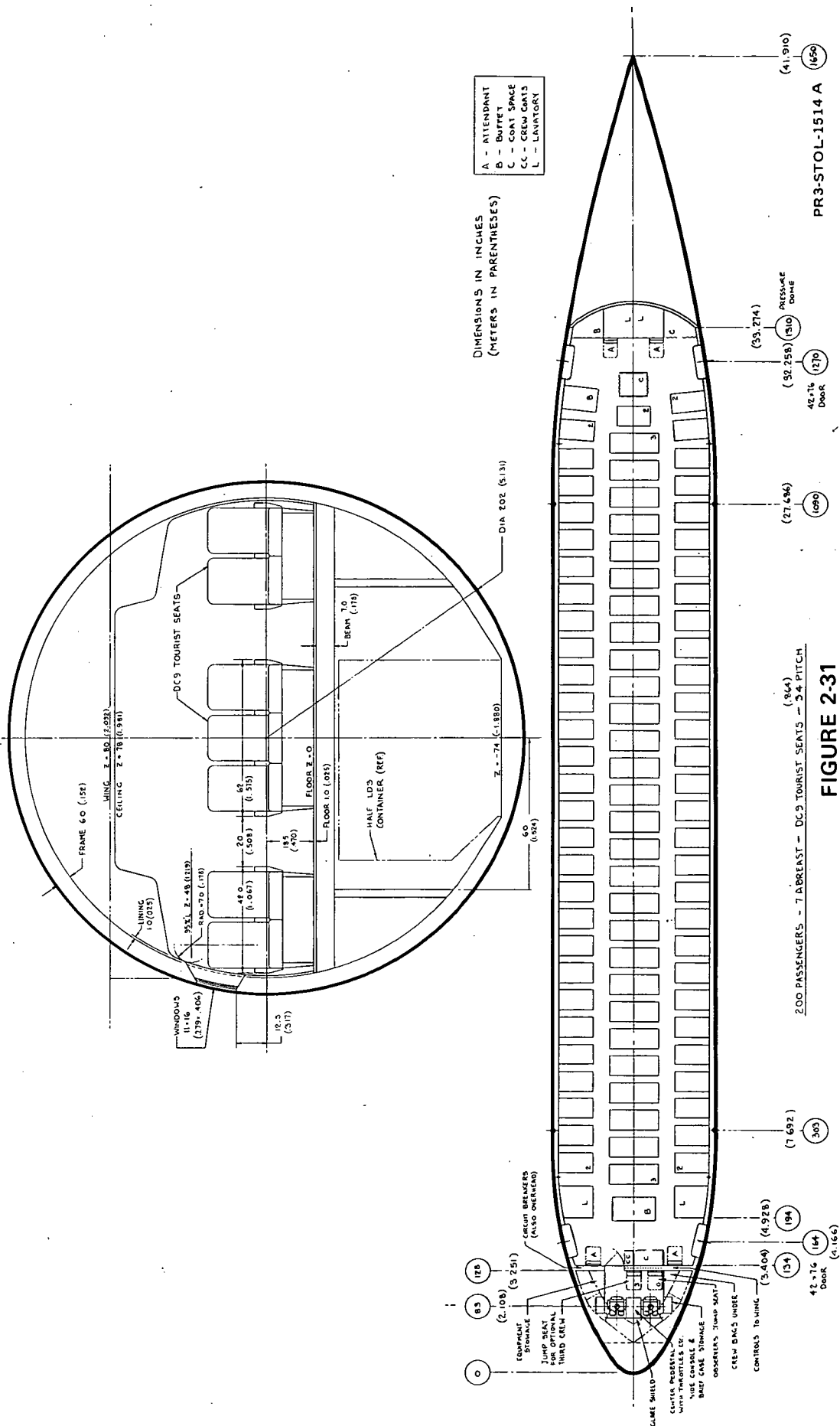


FIGURE 2-31

The cockpits are arranged for operation with two crew members. Jump seats are provided for an optional third crewman and for an observer. The third crewman's seat is positioned midway between the pilots seats behind the center pedestal so that he can reach all center pedestal controls including throttles and could monitor systems on the overhead panel. In addition, he could assist in check list procedures and provide a third pair of eyes for avoidance of mid-air collisions. The observer's seat position is suitable for observing all crew procedures as would be required by a check pilot.

Gear Arrangement

The nose and main gear tires are sized for the use of pressures low enough to achieve acceptable tire wear. Wheel spacing should permit landing on any airfield usable by a DC-9, such as one having runways with ten inches (.254 m) of concrete or 25 inches (.635 m) of flexible paving with a C.B.R. rating of 9.0.

Gear stroke is larger than normal to absorb frequent high energy STOL landings, to extend aircraft life and to minimize passenger discomfort.

2.2.4 Final Design Aircraft Weight and Performance. -

Performance summaries for the eight final design aircraft and the CTOL are presented in Table 2-10. Table 2-11 is a summary of the major weight items which make up these STOL aircraft. More detailed information on the weight breakdown is available in Appendix E.

An example of off design performance is shown in Figures 2-32 through 2-35. This particular set of data is for the 150 passenger, 3000 foot (914 m) field length externally blown flap final design aircraft. This type of information was calculated for all of the systems analysis aircraft discussed in the next chapter and used extensively in the airline planning, scheduling, economic and operations analysis work described in the companion volumes of this report.

Figures 2-36 and 2-37 compare the final aircraft in terms of takeoff gross weight and operating cost. At a field length of 2000 feet (610 m), the EBF configuration is lighter than either the USB or AW. The higher TOGW for the AW aircraft is due to the weight of the complicated propulsion-lift system and high fuel fraction. The high USB weight results from the heavy propulsion system installation. The DOC trends for these aircraft follow the same pattern as the TOGW, but the variation in operating cost between the different configurations is less due to the high cruise speeds of the heavier aircraft.

The EBF is lighter than the MF aircraft at a field length of 3000 feet (914 m), but the reduced initial and maintenance costs associated with the twin engine MF configuration cause the DOC spread between them to narrow. The MF is competitive with the propulsive lift systems for field lengths greater than 3000 feet (914 m).

TABLE 2-10. FINAL DESIGN AIRCRAFT PERFORMANCE SUMMARY

Configuration	EBF				MF		AW	USB	CTOL
	100	150	200	150	150	150			
Passengers	3000 (914)	3000 (914)	3000 (914)	2000 (610)	3000 (914)	4000 (1220)	150 2000 (610)	150 2000 (610)	150 - -
Design Field Length Ft (M)	PD287-3 (47,200)	PD287-3 (67,600)	PD287-3 (87,100)	PD287-3 (88,900)	PD287-23 (86,600)	PD287-23 (70,700)	PD287-43 (96,400)	PD287-22 (103,000)	BPR 6 155,800 (70,600)
Engine	991 (92.1)	1461 (135.7)	1920 (178.4)	2800 (260.1)	3007 (279.4)	1708 (158.7)	2743 (254.8)	3390 (314.9)	1414 (131.4)
Design TOGW Lb (Kg)	104,100 (47,200)	149,000 (67,600)	192,000 (87,100)	196,000 (88,900)	191,000 (86,600)	155,800 (70,700)	212,600 (96,400)	227,100 (103,000)	155,800 (70,600)
Wing Area Ft ² (M ²)	13,200 (58,720)	18,260 (81,220)	22,920 (101,950)	25,830 (114,900)	36,990 (164,540)	32,450 (144,340)	19,200 (85,410)	29,490 (131,180)	26,770 (119,080)
Thrust/Engine Lb (N)	105.0 (512.7)	102.0 (498.0)	100.0 (488.2)	70.0 (341.8)	63.5 (310.0)	91.2 (445.3)	77.5 (378.4)	67.0 (327.1)	110.0 (537.1)
Wing Loading Lb/Ft ² (Kg/M ²)	0.508	0.490	0.478	0.527	0.387	0.417	0.361	0.519	0.344
Thrust to Weight Ratio	4	4	4	4	2	2	4	4	2
Number of Engines	8.0	8.0	8.0	8.0	9.0	9.0	6.5	8.0	9.0
Aspect Ratio	0.69	0.69	0.69	0.74	0.70	0.72	0.78	0.76	0.80
Cruise Mach Number	25,000 (7620)	26,000 (7925)	26,000 (7925)	30,000 (9144)	28,000 (8534)	27,000 (8230)	30,000 (9144)	30,000 (9144)	30,000 (9144)
Cruise Altitude Ft (M)	3000 (914)	3000 (914)	3000 (914)	1865 (568)	3000 (914)	4000 (1220)	2000 (610)	1820 (555)	7500 (229)
TOFL Ft (M)	3000 (914)	3000 (914)	3000 (914)	2000 (610)	3000 (914)	4000 (1220)	2000 (610)	2000 (610)	5750 (175)
LFL Ft (M)	5.5	5.5	5.5	7.1	5.4	4.5	7.3	7.1	3.0
Approach Path Angle Deg	9.0	8.8	8.5	11.2	8.8	9.5	11.2	11.6	7.9
Takeoff Climbout Angle Deg	96	96	96	96	97	97	95	98	90**
Noise*	2.55 (1.59)	2.08 (1.29)	1.81 (1.13)	2.51 (1.56)	2.28 (1.41)	1.95 (1.21)	2.55 (1.58)	2.71 (1.68)	1.79 (1.11)
D.O.C. @ 575 st mi (926 km)									

*500 Ft (152 m) sideline

**FAR-36 Noise measuring locations, no cutback

TABLE 2-11

[illegible]

* PAYLOAD @ 200 LBS/PAX (90.7 kg/PAX)
** JP-4 @ 6.7 LBS/GAL (802.9 kg/m³)

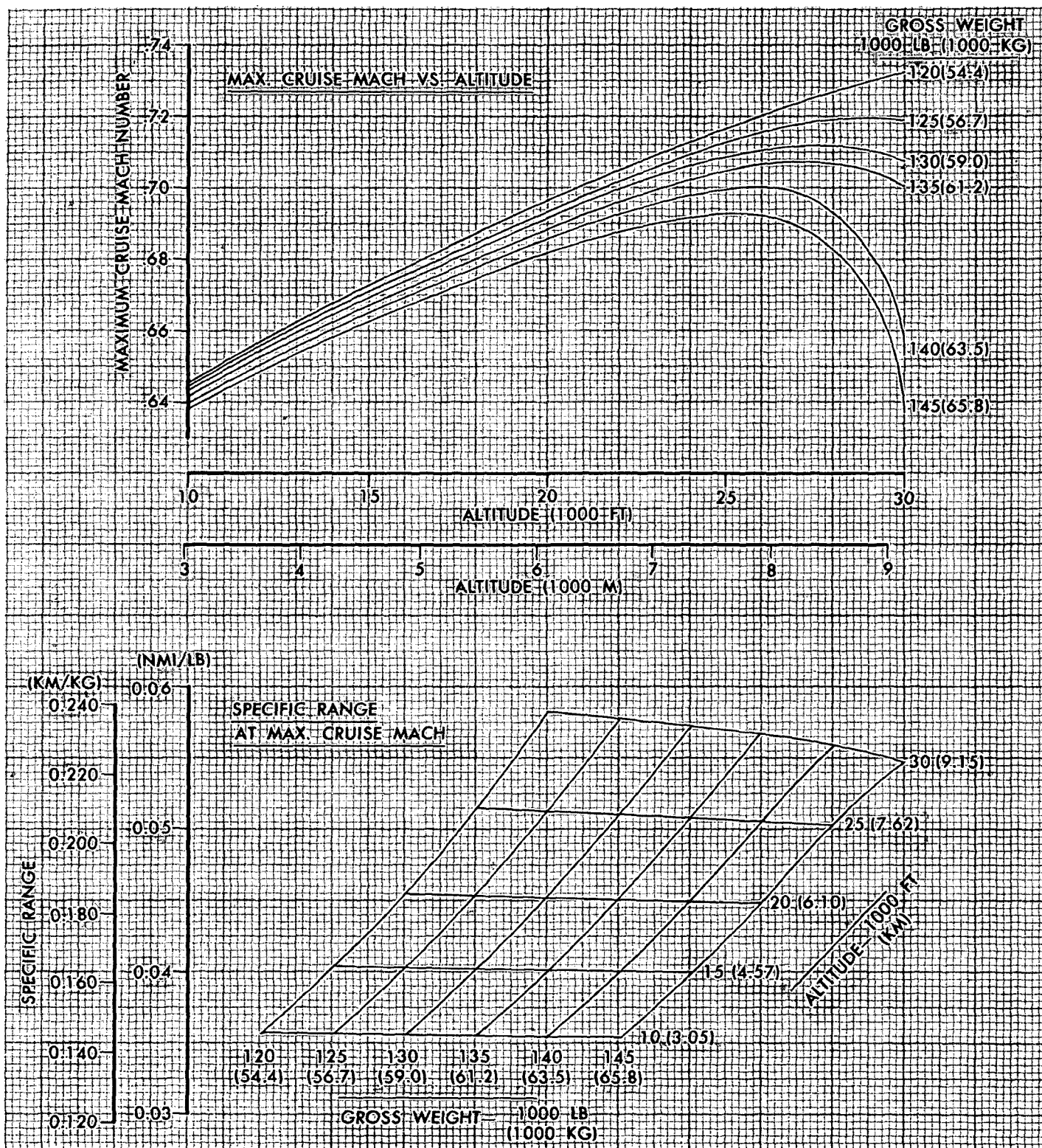


FIGURE 2-32. EXTERNALLY BLOWN FLAP STOL AIRCRAFT CRUISE PERFORMANCE
 150 PASSENGERS, 3000 FT (914 M) FIELD LENGTH
 FINAL DESIGN AIRCRAFT

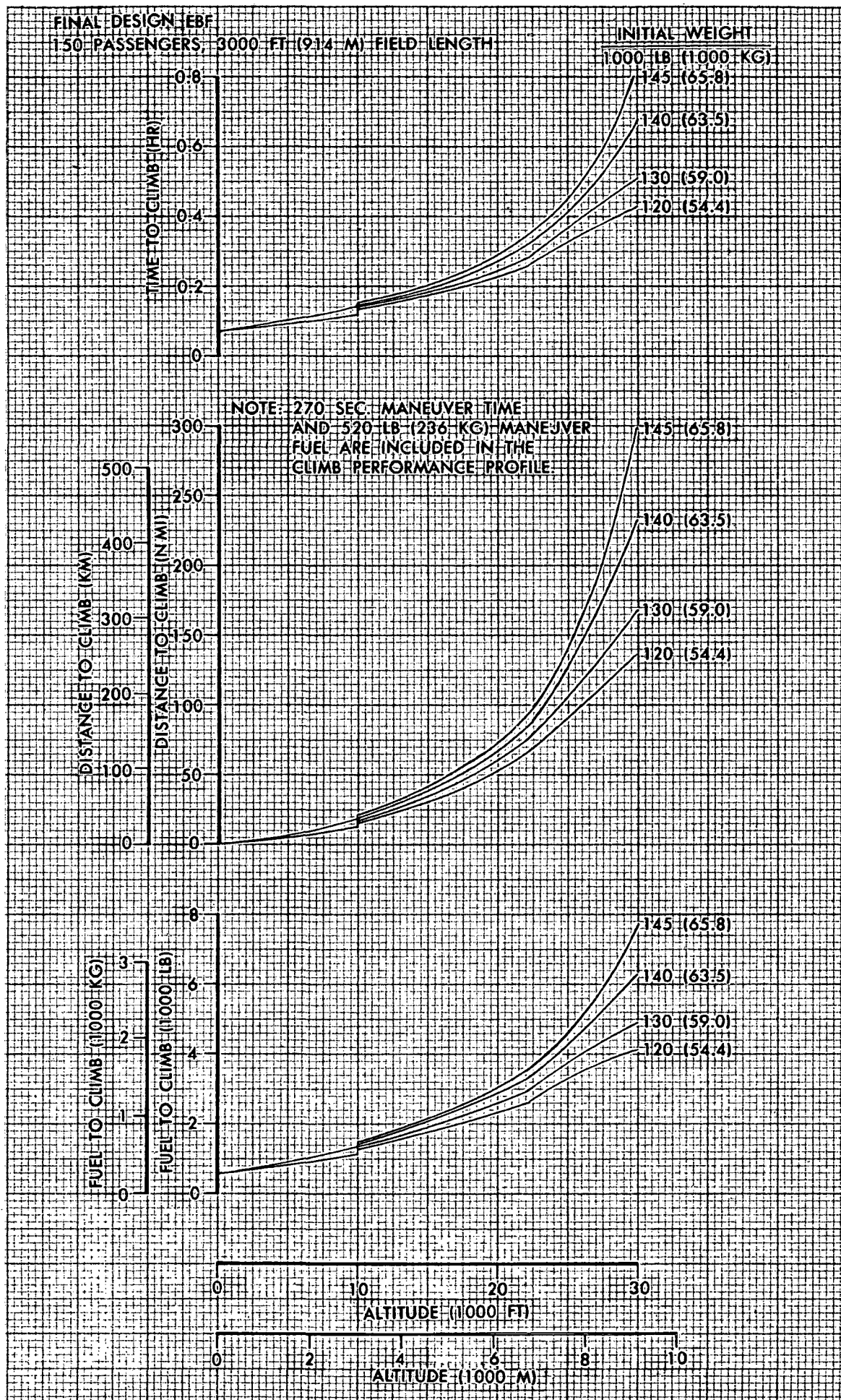


FIGURE 2-33. TIME, DISTANCE, AND FUEL TO CLIMB FROM SEA LEVEL

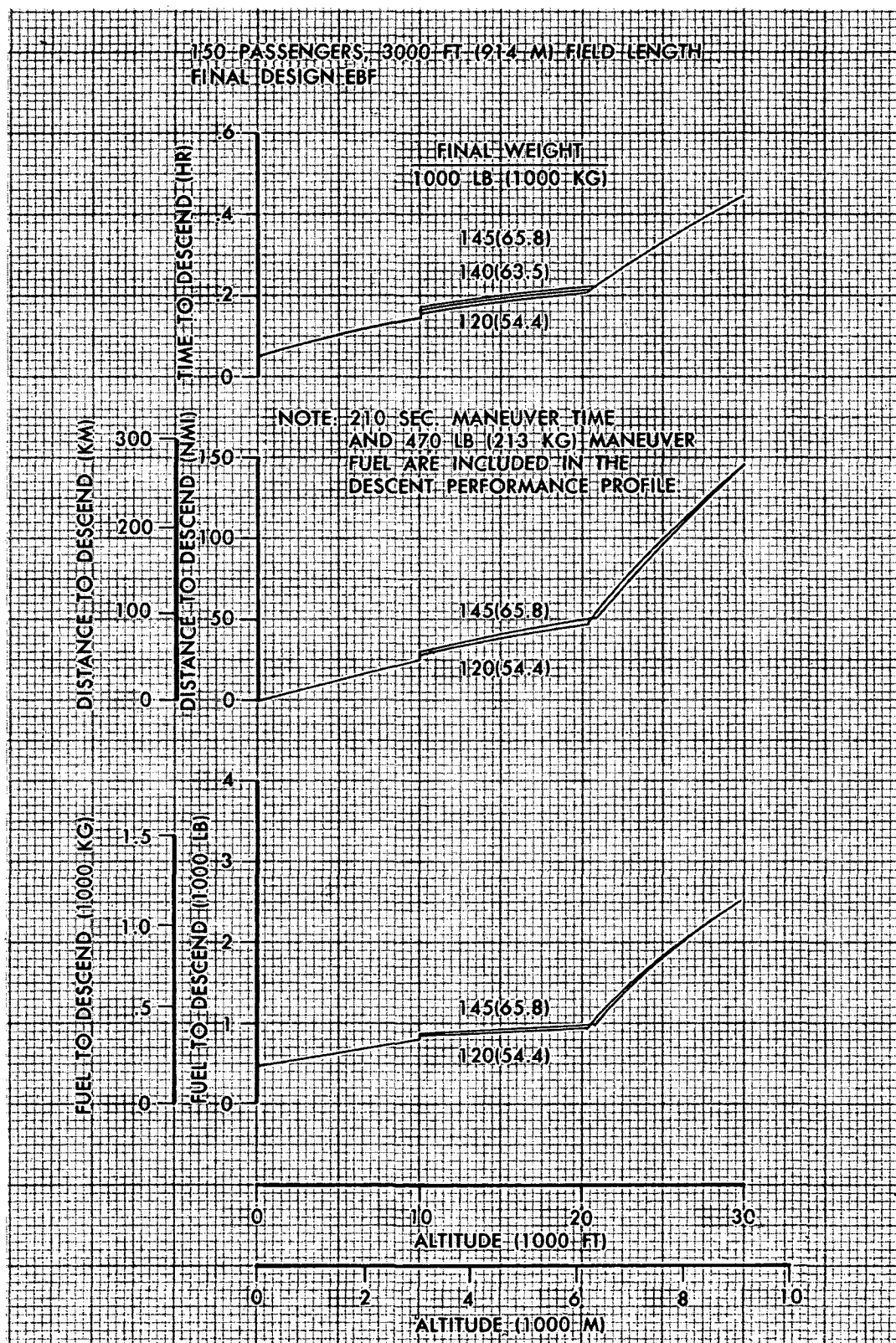


FIGURE 2-34. TIME, DISTANCE, AND FUEL TO DESCEND TO SEA LEVEL

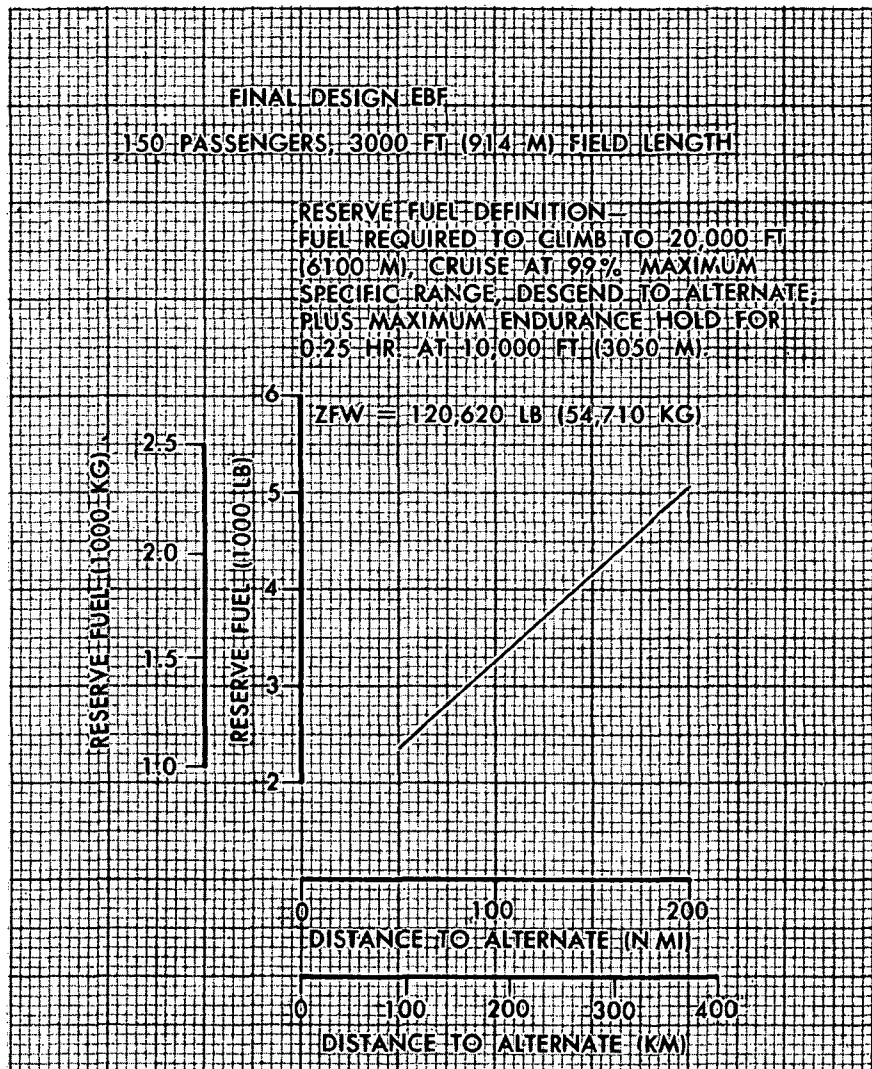
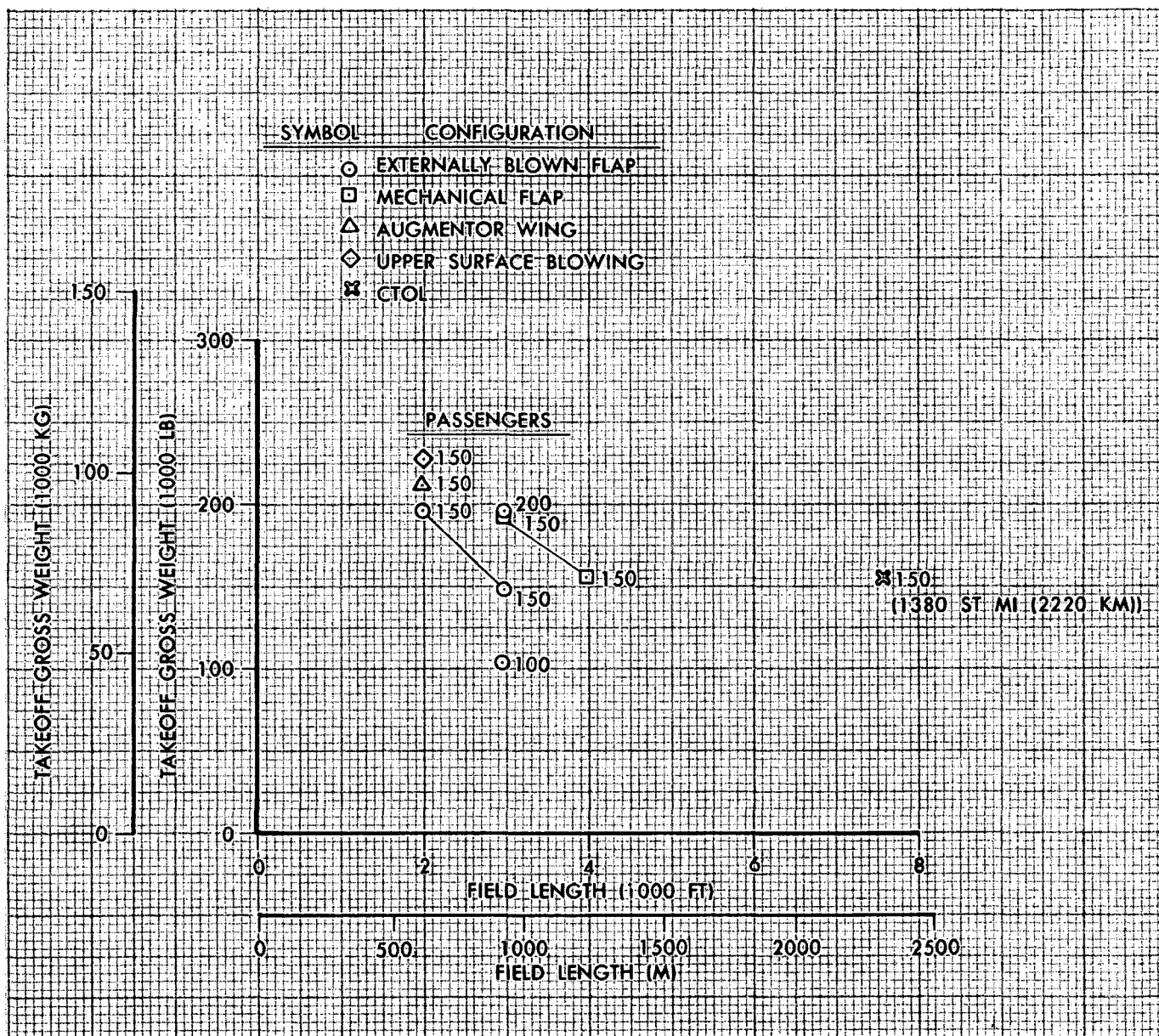


FIGURE 2-35. RESERVE FUEL VS. DISTANCE TO ALTERNATE



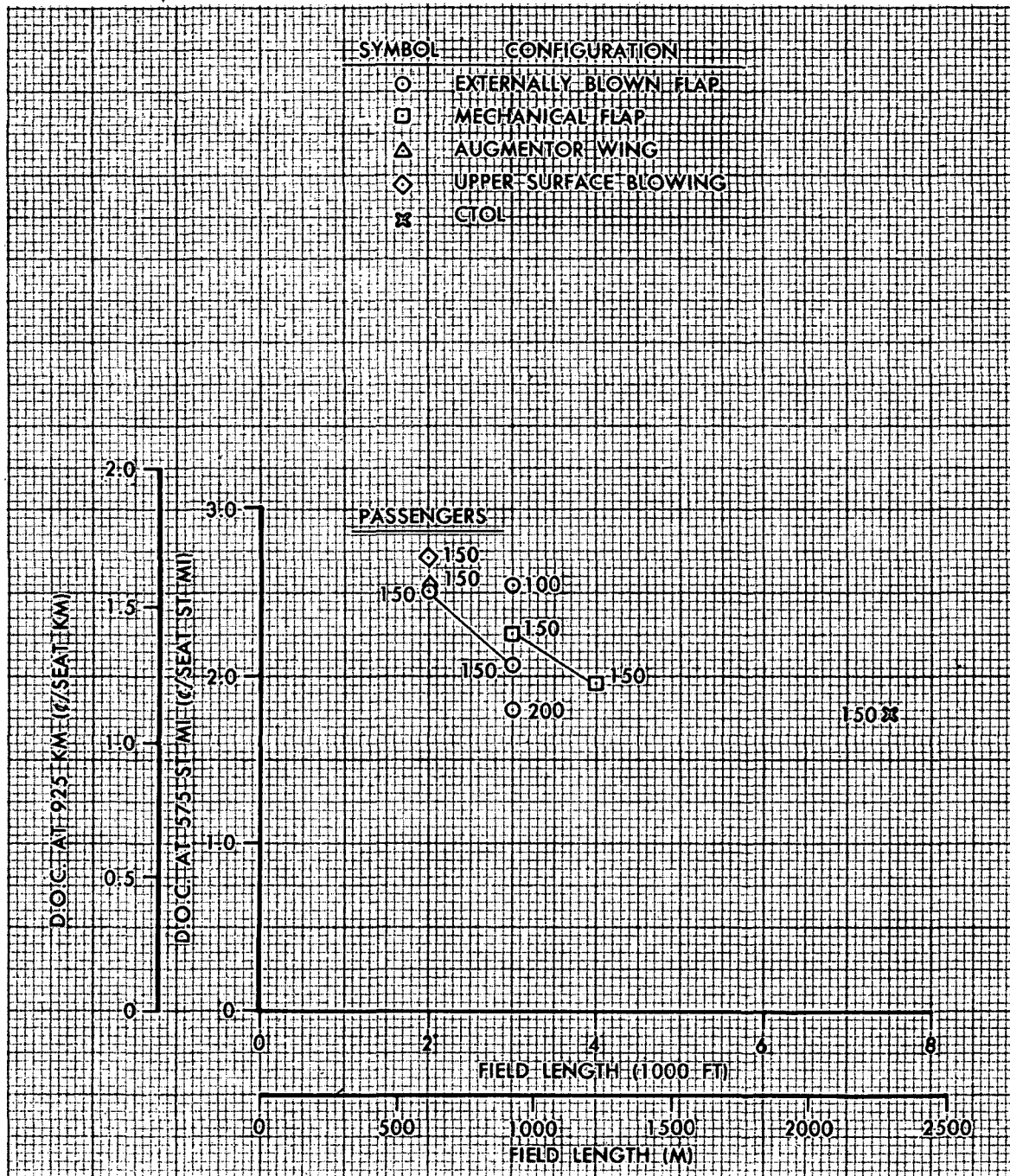
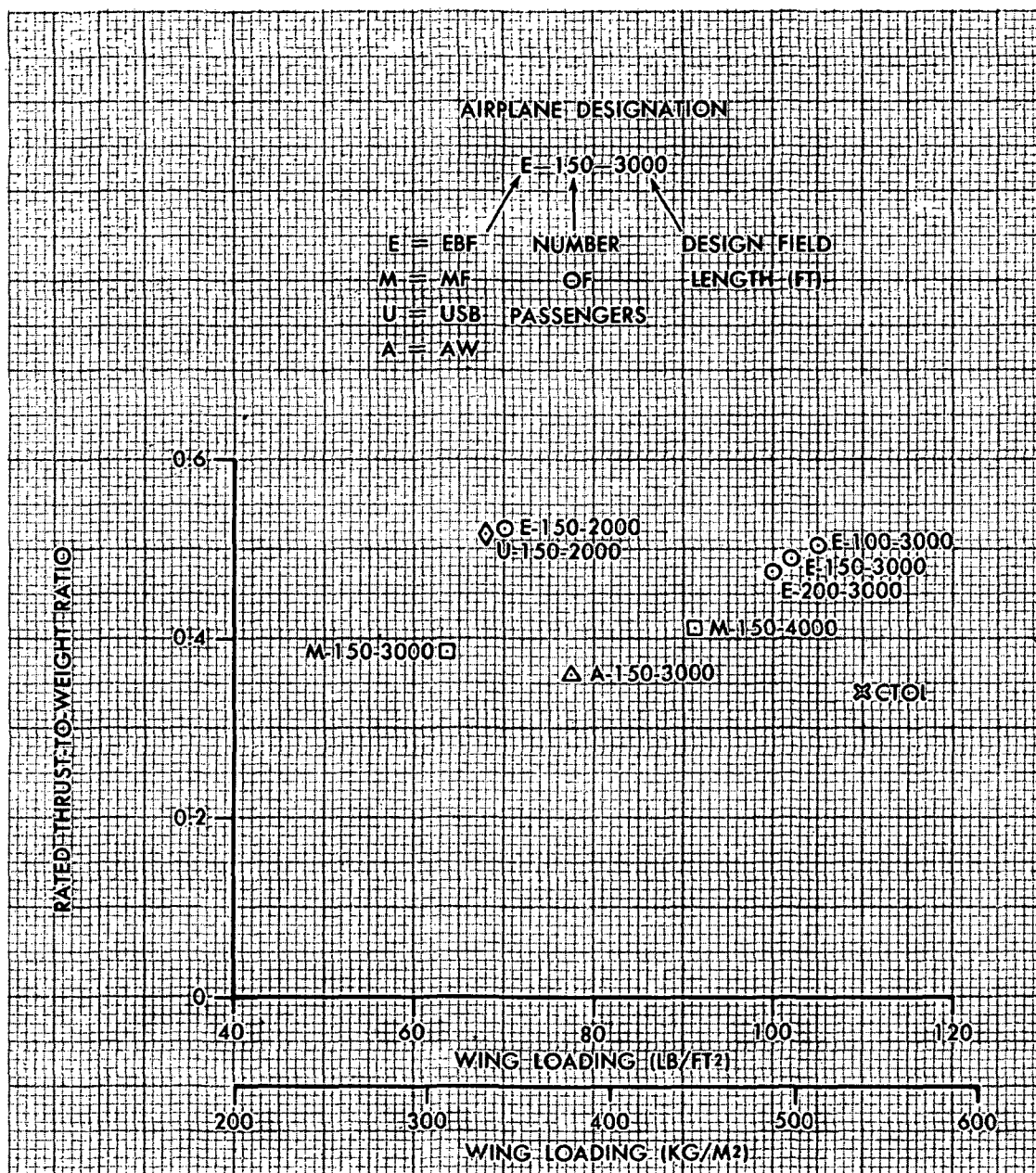


FIGURE 2-37 DIRECT OPERATING COST—FIELD LENGTH COMPARISON
FINAL DESIGN AIRCRAFT

The W/S - T/W relationship is presented in Figure 2-38. The T/W ratios do not vary greatly for a given high lift configuration. Variations in field length are primarily due only to changes in wing loading. The three 3000 foot (914 m) field length EBF aircraft illustrate the effect of passenger capacity on W/S and T/W. W/S and T/W decrease as aircraft size is increased due to the influence of aircraft size on ground effects. Ground effects are more severe for the larger aircraft, because of the lower wing height to span ratios.



**FIGURE 2-38. WING LOADING: THRUST-TO-WEIGHT RELATIONSHIP
FINAL DESIGN AIRCRAFT**

2.3 System Analysis Aircraft

2.3.1 Aircraft Configurations. - In accordance with the study plan discussed in Section 1.0, a family of aircraft were derived (after the completion of the parametric aircraft) to be used in the derivation and evaluation of the complete STOL short haul transportation system summarized in the companion volumes. These aircraft are called the System Analysis Aircraft and differ in detail from their counterpart Parametric Aircraft (Section 2.1) and Final Design Aircraft (Section 2.2). They are based on detailed updated weight, drag, and acoustic analyses conducted during the parametric study time period, and are designed to meet 95 EPNdB on the 500 foot (152 m) sideline. The drag, acoustic, propulsion and weight methods used to define these system analysis aircraft are compatible in every respect with the Appendices material which are intended to substantiate the final design aircraft.

A comparison between these system analysis aircraft, which are used throughout the companion volumes, and the parametric and final design aircraft is shown in Table 2-12. Only two parametric aircraft, however, have a direct correspondence in terms of payload and field length as shown in the table.

Off design performance was calculated to support the system analysis of the total short haul transportation system summarized in the companion volumes of this report. An example of these performance calculations is contained in Section 2.4.

TABLE 2-12
CHARACTERISTICS SUMMARY OF AIRCRAFT FAMILIES

	E 100.3000			E 200.3000			E 150.3000			E 150.2000		
	Parametric	System Analysis	Final Design	Parametric	System Analysis	Final Design	System Analysis	Final Design	System Analysis	Final Design	System Analysis	Final Design
TOGW	Lb (Kg)	117,900 (53,500)	104,100 (47,300)	216,600 (98,000)	221,400 (104,000)	192,000 (87,100)	163,300 (74,100)	149,000 (67,600)	206,200 (93,400)	196,000 (87,900)	206,200 (93,400)	196,000 (87,900)
Wing Area	Ft ² (M ²)	1,122 (104.3)	991 (92)	2,060 (192)	2,214 (206)	1,920 (179)	1,633 (152)	1,461 (136)	3,100 (288)	2,800 (260)	3,100 (288)	2,800 (260)
Wing Loading	Lb/Ft ² (Kg/M ²)	105 (513)	105 (513)	105 (513)	100 (488)	100 (488)	100 (488)	102 (498)	66.5 (324)	70.0 (342)	66.5 (324)	70.0 (342)
Rated Thrust/Engine	Lb (Newtons)	18,570 (82,500)	14,520 (64,600)	34,130 (152,000)	28,780 (128,000)	22,925 (102,000)	21,270 (94,500)	18,260 (81,100)	26,830 (119,000)	25,830 (115,000)	26,830 (119,000)	25,830 (115,000)
Thrust Loading		0.63	0.501	0.63	0.520	0.478	0.521	0.490	0.521	0.527	0.521	0.527
500 Foot (152 M) Sideline Noise		95 PNdB	95 EPNdB	95 PNdB	95 EPNdB	96 EPNdB	95 EPNdB	96 EPNdB	95 EPNdB	97 EPNdB	95 EPNdB	97 EPNdB
Wing Aspect Ratio		7.0	8.0	7.0	8.0	8.0	8.0	8.0	8.0	8.0	8.0	8.0
Cruise Altitude	Ft (M)	20,000 (6,100)	25,000 (7,620)	20,000 (6,100)	25,000 (7,620)	26,000 (7,930)	25,000 (7,620)	26,000 (7,930)	25,000 (7,620)	30,000 (9,150)	25,000 (7,620)	30,000 (9,150)
Max. Cruise Speed	MN	0.70	0.67	0.70	0.70	0.69	0.70	0.69	0.68	0.68	0.68	0.74

	U 150.2000		A 150.2000		M 150.3000		M 150.4000		C 150.7500	
	System Analysis	Final Design	System Analysis	Final Design	System Analysis	Final Design	System Analysis	Final Design	System Analysis	Final Design
TOGW	Lb (Kg)	232,800 (105,600)	227,100 (102,000)	211,300 (95,900)	212,600 (96,400)	191,000 (86,600)	154,100 (69,800)	155,800 (70,700)	159,600 (72,400)	155,600 (70,600)
Wing Area	Ft ² (M ²)	3,881 (361)	3,390 (315)	2,471 (230)	2,743 (255)	3,007 (279)	1,525 (142)	1,708 (159)	1,450 (135)	1,414 (132)
Wing Loading	Lb/Ft ² (Kg/M ²)	60 (293)	67 (327)	85.5 (417)	77.5 (378)	63.5 (310)	101 (493)	91.2 (445)	110 (537)	110 (537)
Rated Thrust/Engine	Lb (Newtons)	27,480 (122,000)	29,490 (131,000)	22,200 (98,700)	19,200 (85,300)	36,990 (164,500)	34,390 (153,000)	32,450 (144,300)	29,350 (130,500)	26,770 (119,000)
Thrust Loading		0.472	0.519	0.420	0.361	0.387	0.447	0.417	0.368	0.344
500 Foot (152 M) Sideline Noise		95 EPNdB	98 EPNdB	95 EPNdB	95 EPNdB	97 EPNdB	95 EPNdB	97 EPNdB	95 EPNdB	98 EPNdB
Wing Aspect Ratio		8.0	8.0	6.5	6.5	9.0	9.0	9.0	8.0	9.0
Cruise Altitude	Ft (M)	30,000 (9,150)	30,000 (9,150)	29,000 (8,750)	30,000 (9,150)	28,000 (8,540)	26,000 (7,930)	27,000 (8,230)	32,000 (9,770)	30,000 (9,150)
Max. Cruise Speed	MN	0.70	0.76	0.79	0.78	0.72	0.76	0.72	0.80	0.80

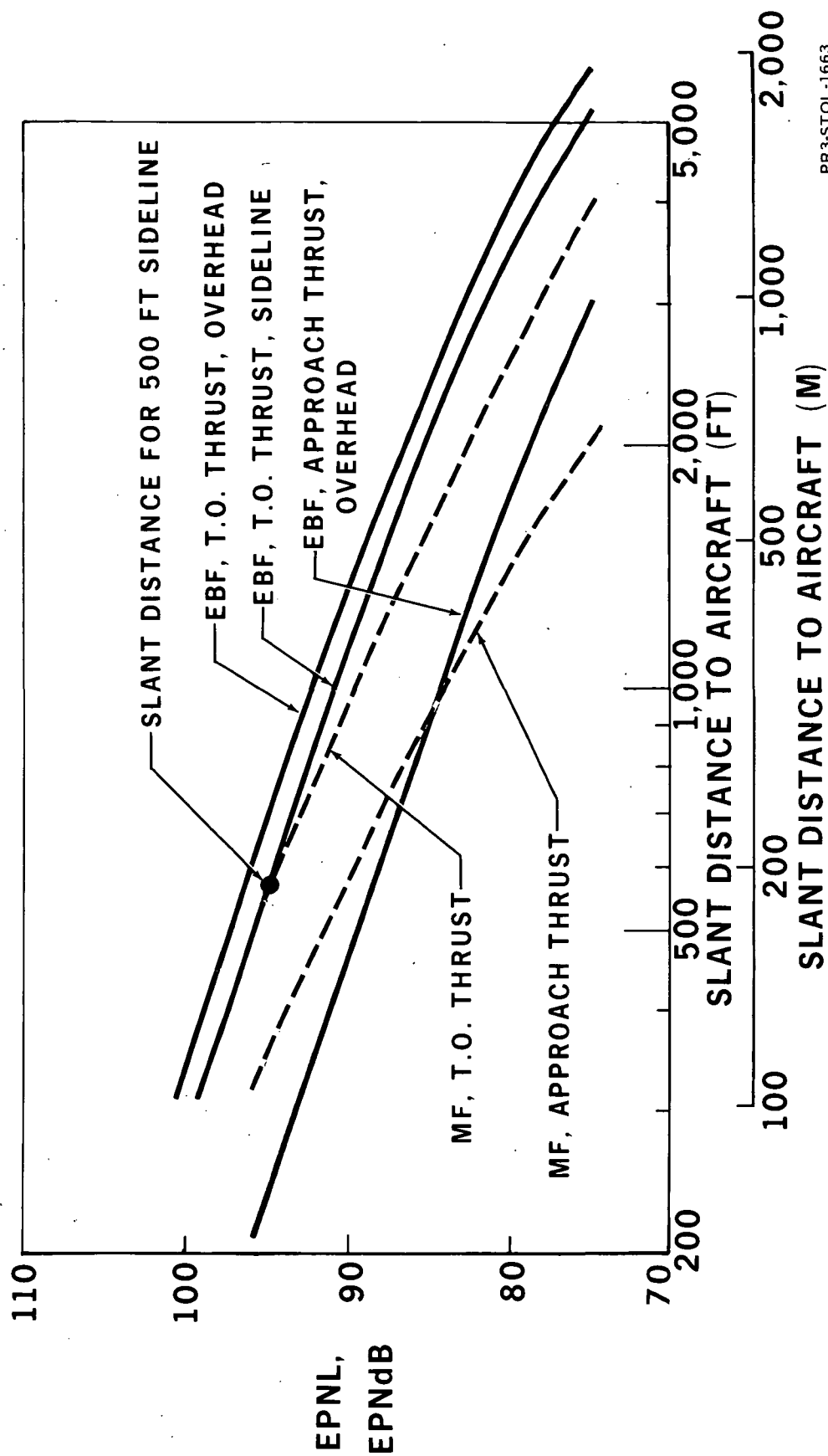
2.3.2 Noise Contours. - Noise contours ranging from 75 to 95 EPNdB were developed for the system analysis airplanes and are used extensively in Volume III. However, very little flight test noise data exists at the 75 EPNdB levels because of the less objectionable nature of these low noise levels. Therefore little empirical data exists with which to verify the EPNL-Distance curves at these long distances from the noise source. This problem does not affect the validity of the 90 to 95 EPNdB contours.

Spherical directivity was used for all of the short haul concepts except the EBF systems. For these aircraft the "viewfactor" or non-spherical directivity between sideline and directly below the aircraft lengthens the noise contour (see Appendix C for a discussion of the viewfactor for the EBF concept). The higher noise level below the aircraft compared to the sideline requires that the aircraft climb to a higher altitude to close the noise contour then would be predicted based on the sideline noise level.

All of the short haul system analysis aircraft were designed to a 95 EPNdB 500 foot (152 m) sideline noise level. This means that the only variables which affect the area of the contour are the takeoff and approach climb angles and the slope of the EPNL-Distance curve. A typical EPNL distance curve is shown on Figure 2-39 for the EBF and mechanical flap concepts. The difference in slope between the concepts is caused by different engine cycles and by the low frequency flap interaction noise generated by powered lift. This shallower slope is generally applicable to all of the powered lift aircraft.

Noise contours were developed by combining a fixed distance to the selected contour with the airplane flight path data. For a straight line

TYPICAL EPNL - DISTANCE CURVES



PR3-STOL-1663

FIGURE 2-39

flight path the resultant shape of the contour is semi-elliptical for either takeoff or landing. Allowances have been made for ground attenuation and the time duration correction along the runway during ground roll. Figure 2-40 shows the 75 through 95 EPNdB contours for the EBF airplane. The "coke bottle" effect along the runway is caused by the ground attenuation and time duration during ground roll. The minimum width contour occurs near the end of the runway because the airplane is still on the ground with ground attenuation of the noise but has a high velocity to shorten the time duration.

The takeoff field length has a major impact on the area of the noise contour. Figure 2-41 shows the difference for the 3000 foot (914 m) and 4000 foot (1219 m) mechanical flap airplanes. The 3000 foot (914 m) contour is shortened both because of the shorter ground distance and the higher thrust-to-weight ratio resulting from the shorter field length. The effect of the EBF viewfactor discussed above is shown on Figure 2-42 where the mechanical flap and EBF airplanes are compared. Some of the difference in contour length is caused by the steeper climb angle of the mechanical flap.

The effect of reducing the level of treatment is shown in Figure 2-43 for the EBF 3000 foot (914 m) field length system analysis and final design airplanes. The final design airplane is one EPNdB noisier on a 500 foot (152 m) sideline. Figure 2-44 shows the 90 EPNdB contour for the EBF airplane designed for a sideline noise level of 95, 100 and 105 EPNdB. Table 2-13 gives the areas and climb gradients for the system analysis aircraft and for the final design EBF 150 passenger, 3000 foot (914 m) field length aircraft and an advanced CTOL aircraft. The 75, 80, 85, 90 and 95 EPNdB contours for all the systems analysis airplanes are shown in Figures 2-36 and 2-45 through 2-50. The 100 and 200 passenger 3000 foot field length (914 m) EBF airplane would have the same contour as the E,150,3000 airplane.

SINGLE EVENT EPNL CONTOURS

E : 150 : 3000 4 ALLISON PD 287-3 ENGINES

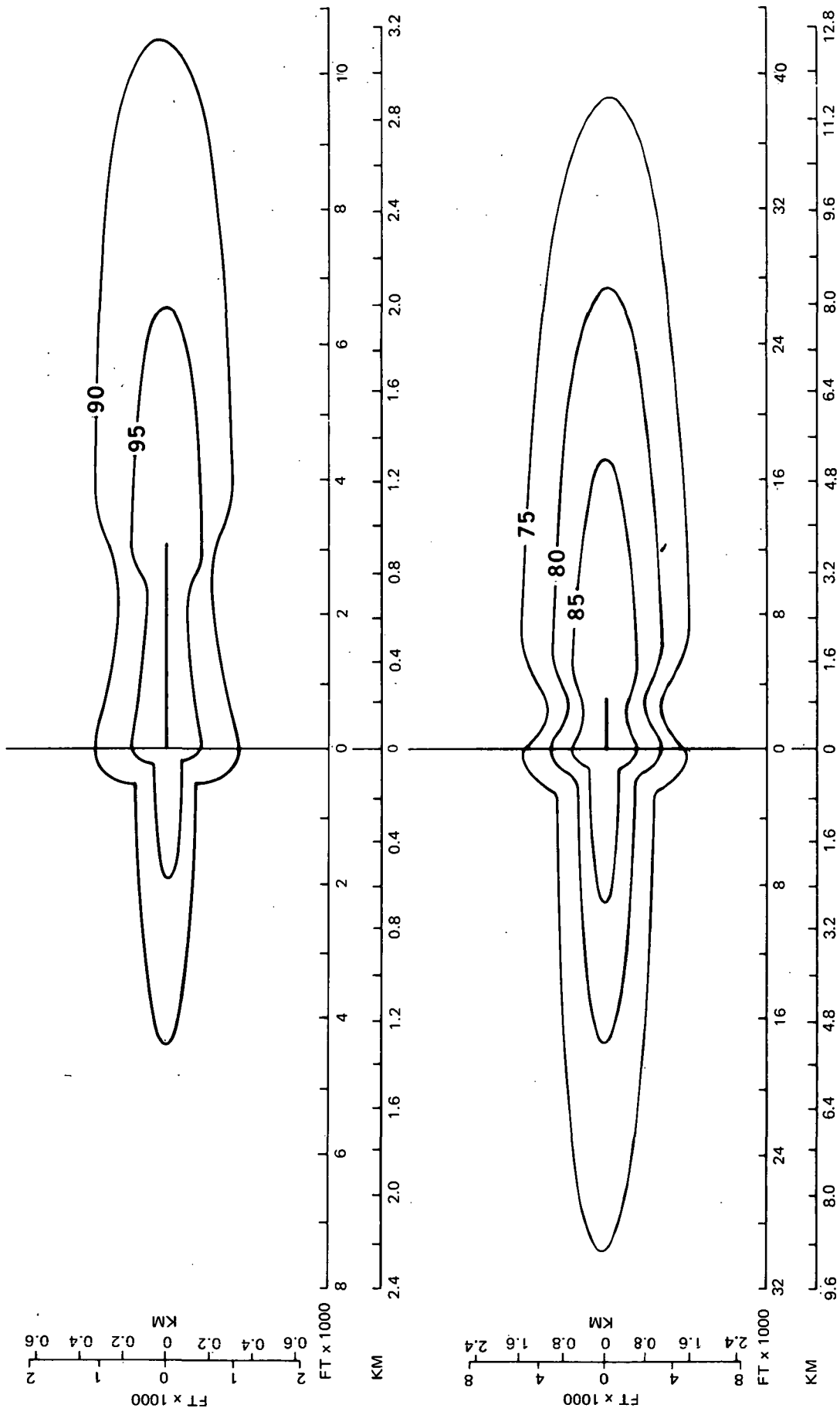


FIGURE 2-40

EFFECT OF FIELD LENGTH ON 90 EPNdB NOISE CONTOUR

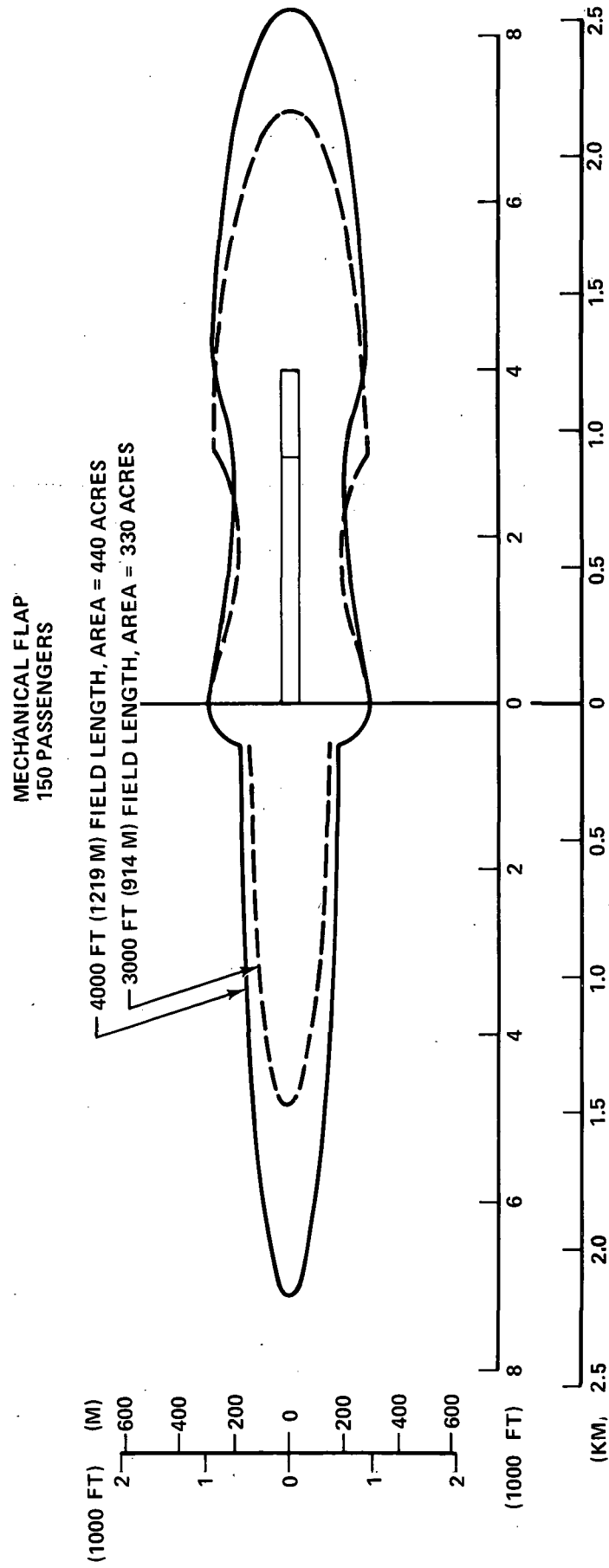


FIGURE 2-41

PR3-STOL-1665 B

COMPARISON OF EXTERNALLY BLOWN FLAP AND MECHANICAL FLAP STOL

90 EPNdB NOISE CONTOURS

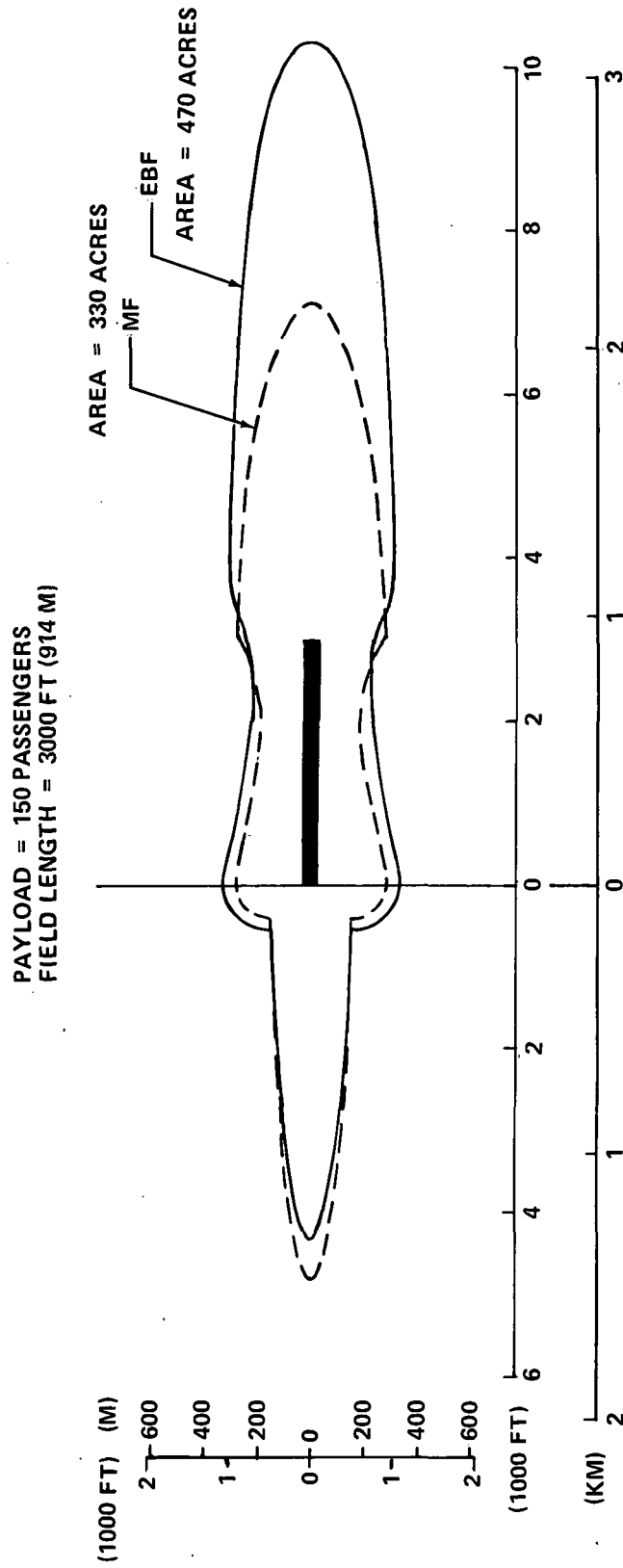


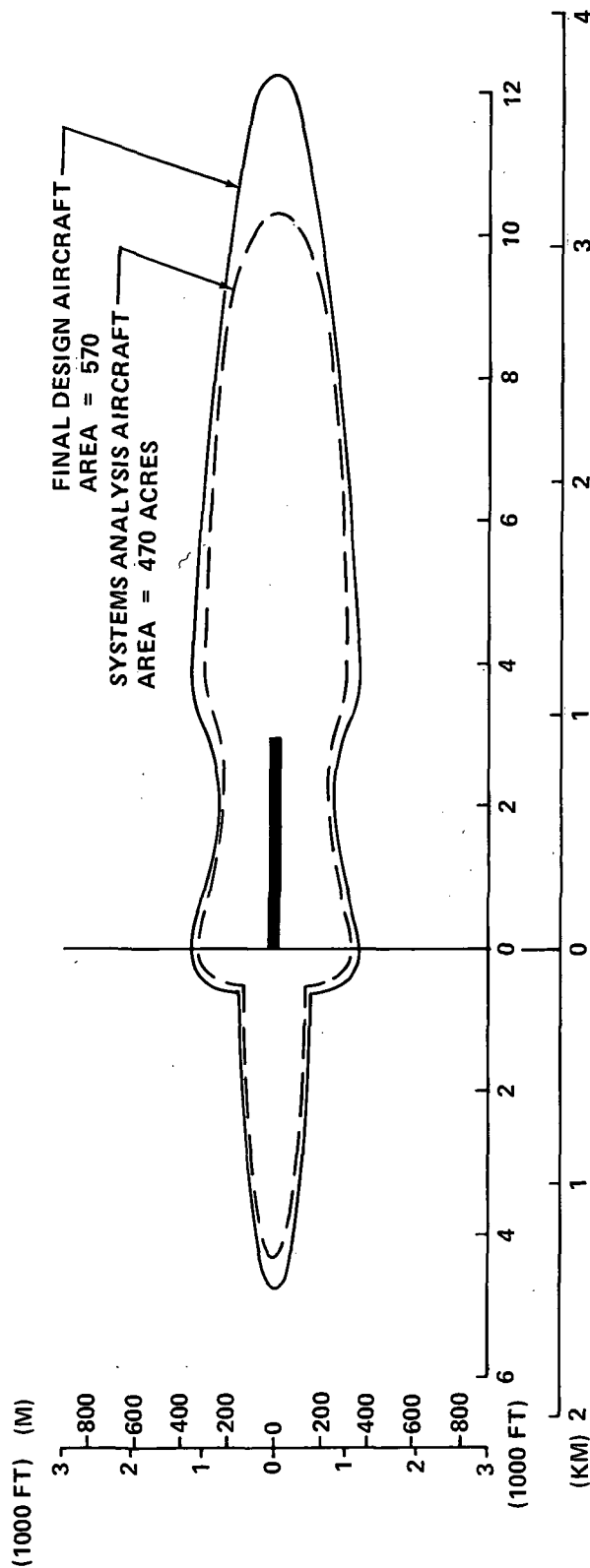
FIGURE 2-42

PR3-STOL-1662 A

COMPARISON OF EXTERNALLY BLOWN FLAP SYSTEMS ANALYSIS AIRCRAFT AND FINAL DESIGN AIRCRAFT

90 EPNdB NOISE CONTOUR

EXTERNALLY BLOWN FLAP
PAYLOAD = 150 PASSENGERS
FIELD LENGTH = 3000 FT (914 M)



PR3-STOL-1667B

FIGURE 2-43

EFFECT OF DESIGN SIDELINE NOISE LEVEL ON 90 EPNdB NOISE CONTOUR

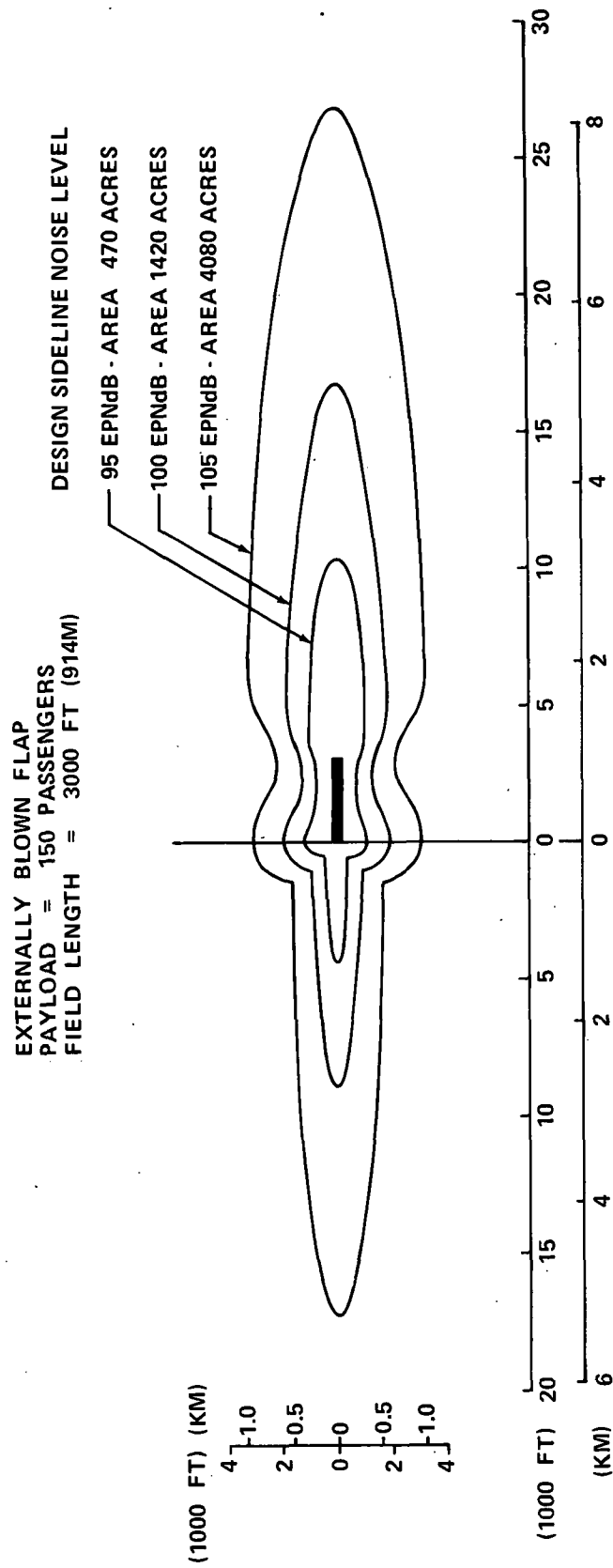


FIGURE 2-44

PR3-STOL-1666A

Table 2-13

NOISE FOOTPRINT AREA COMPARISON
Systems Analysis Aircraft

Configuration	Payload Passengers	Field Length ft (m)	Noise Footprint Area in Acres (Hectares)				
			95 EPNdB	90 EPNdB	85 EPNdB	80 EPNdB	75 EPNdB
EBF	100	3000 (914)	134 (54)	474 (192)	1421 (575)	4083 (1652)	9920 (4015)
EBF	150	3000 (914)	134 (54)	474 (192)	1421 (575)	4083 (1652)	9920 (4015)
EBF	200	3000 (914)	134 (54)	474 (192)	1421 (575)	4083 (1652)	9920 (4015)
EBF	150	2000 (610)	102 (41)	358 (144)	1184 (479)	3456 (1399)	8333 (3372)
MF	150	3000 (914)	128 (52)	326 (132)	813 (329)	1939 (785)	4454 (1803)
MF	150	4000 (1219)	166 (67)	435 (176)	1037 (420)	2726 (1103)	5370 (2173)
USB	150	2000 (610)	109 (44)	371 (150)	1229 (497)	3584 (1450)	8627 (2491)
AW	150	2000 (610)	102 (41)	288 (117)	838 (339)	2426 (982)	6893 (2790)
CTOL	150	7000 (2134)	390 (158)	928 (376)	2144 (868)	4794 (1940)	10573 (4279)

SINGLE EVENT EPNL CONTOURS

E : 150 : 2000 4 ALLISON PD 287-3 ENGINES

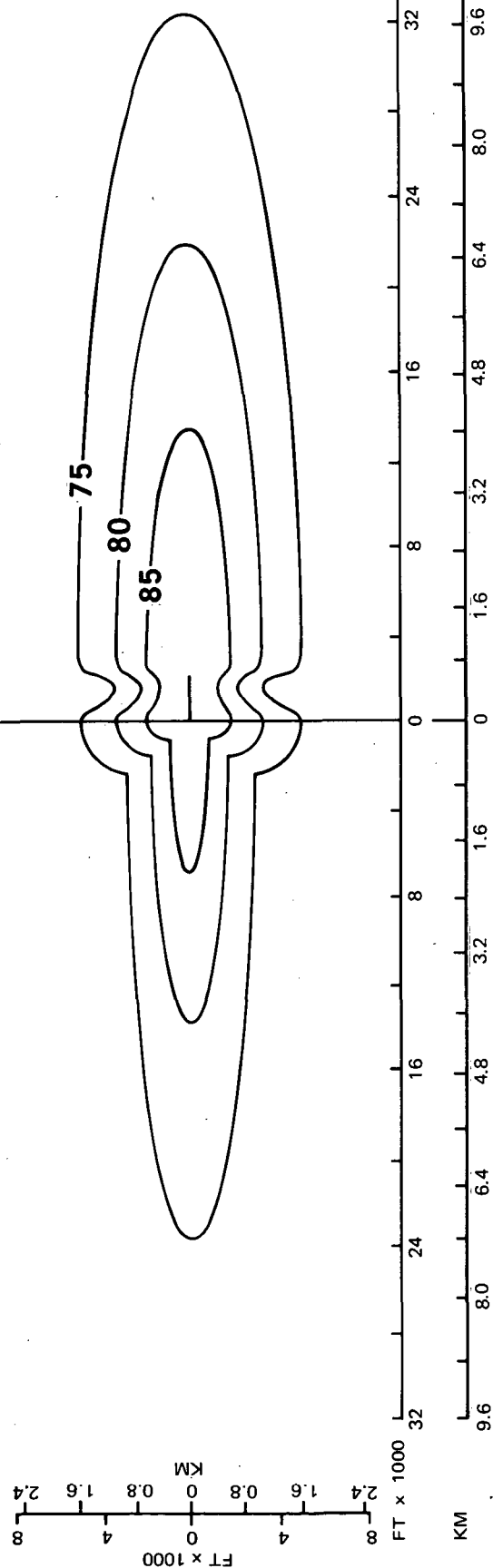
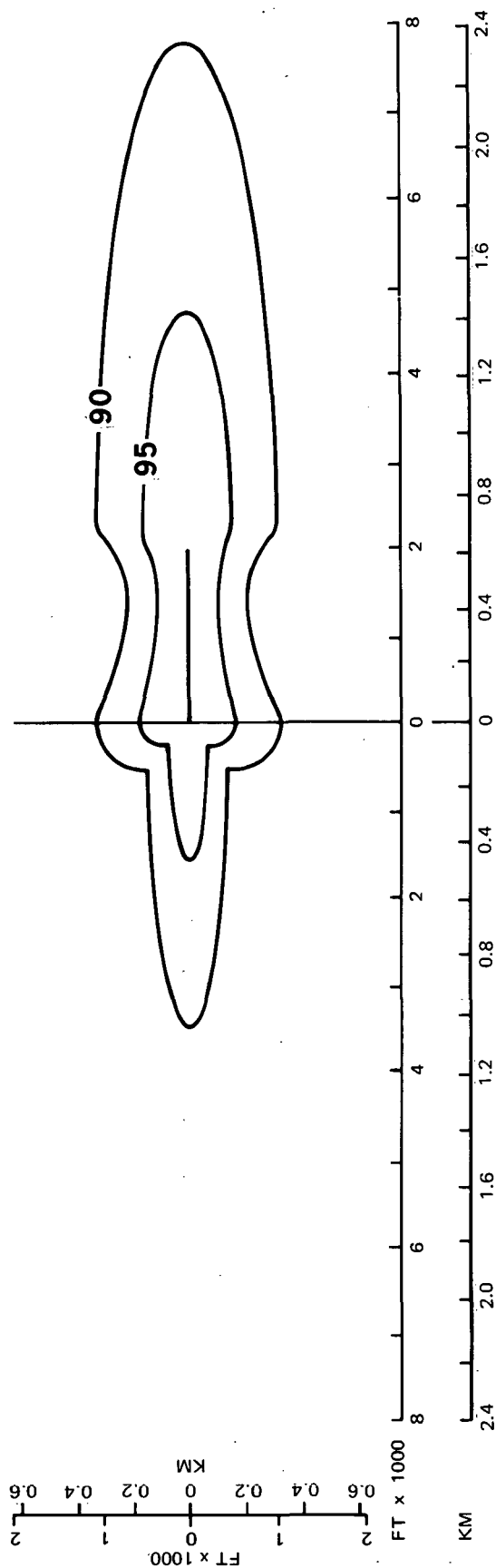
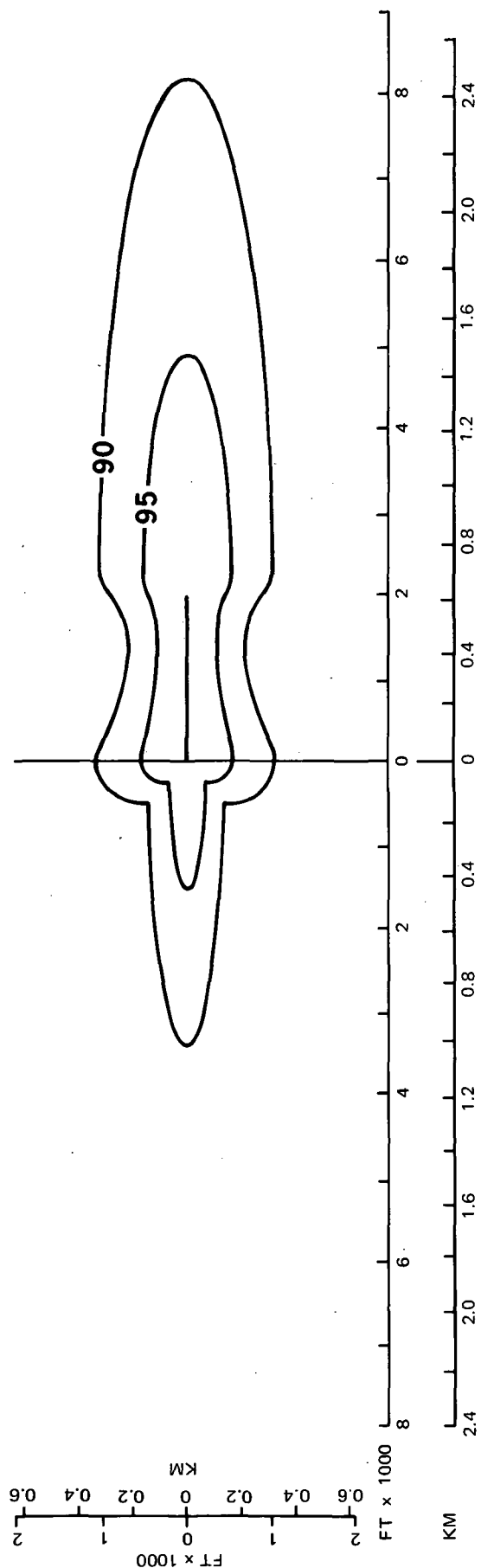


FIGURE 2-45

SINGLE EVENT EPNL CONTOURS

U : 150 : 2000 4 ALLISON PD 287-22 ENGINES



SINGLE EVENT EPNL CONTOURS

M : 150 : 3000 2 ALLISON PD 287-23 ENGINES

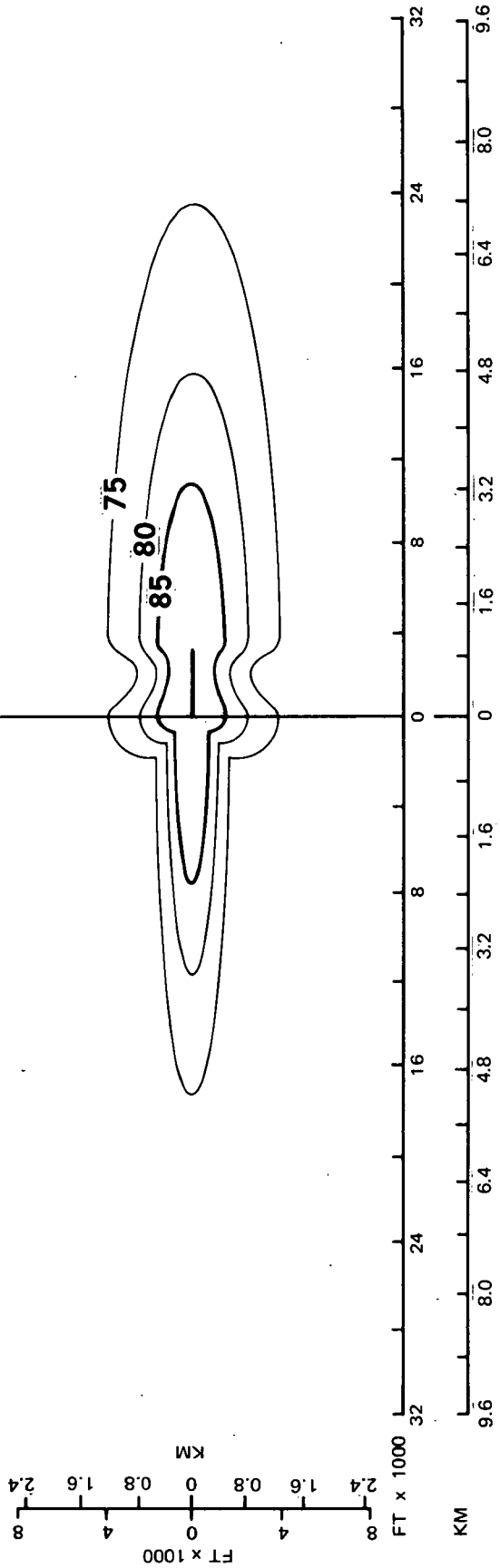
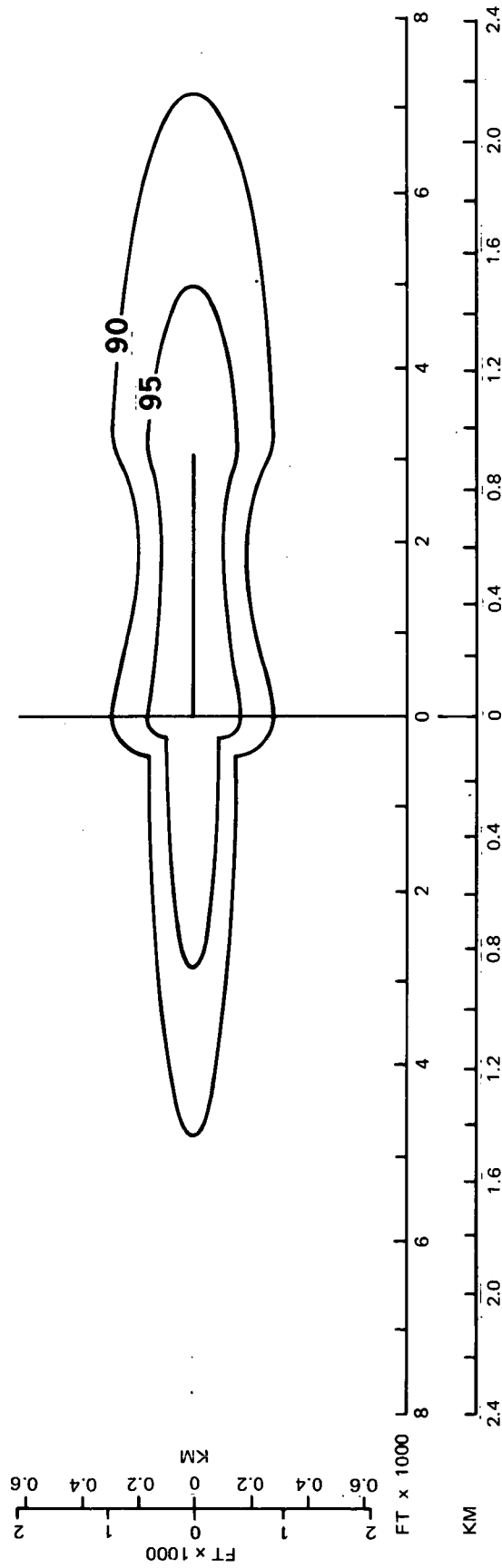


FIGURE 2-47

SINGLE EVENT EPNL CONTOURS

M : 150 : 4000 2 ALLISON PD 287-23 ENGINES

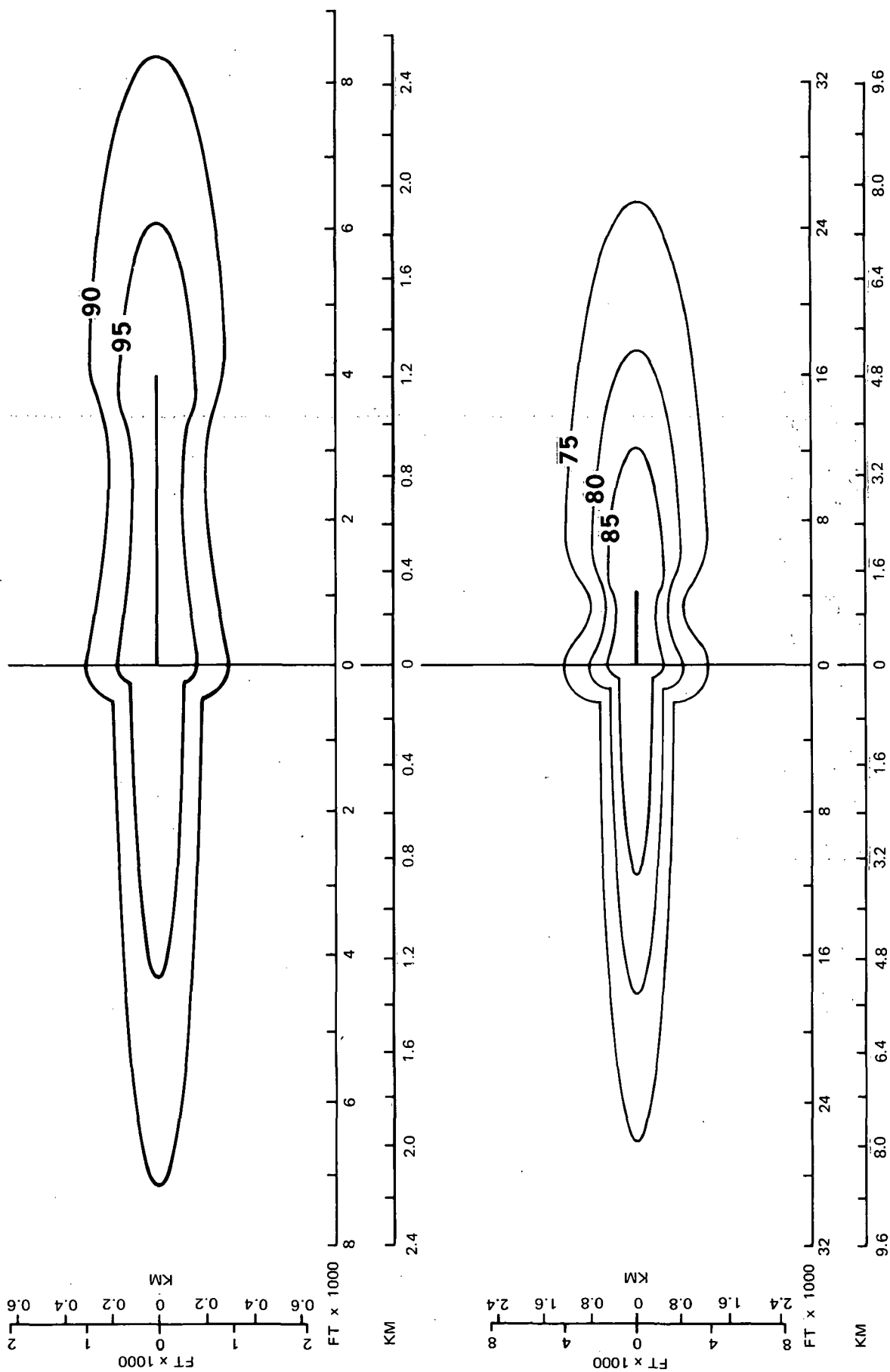


FIGURE 2-48

SINGLE EVENT EPNL CONTOURS

A : 150 : 2000 4 ALLISON PD 287-43 ENGINES

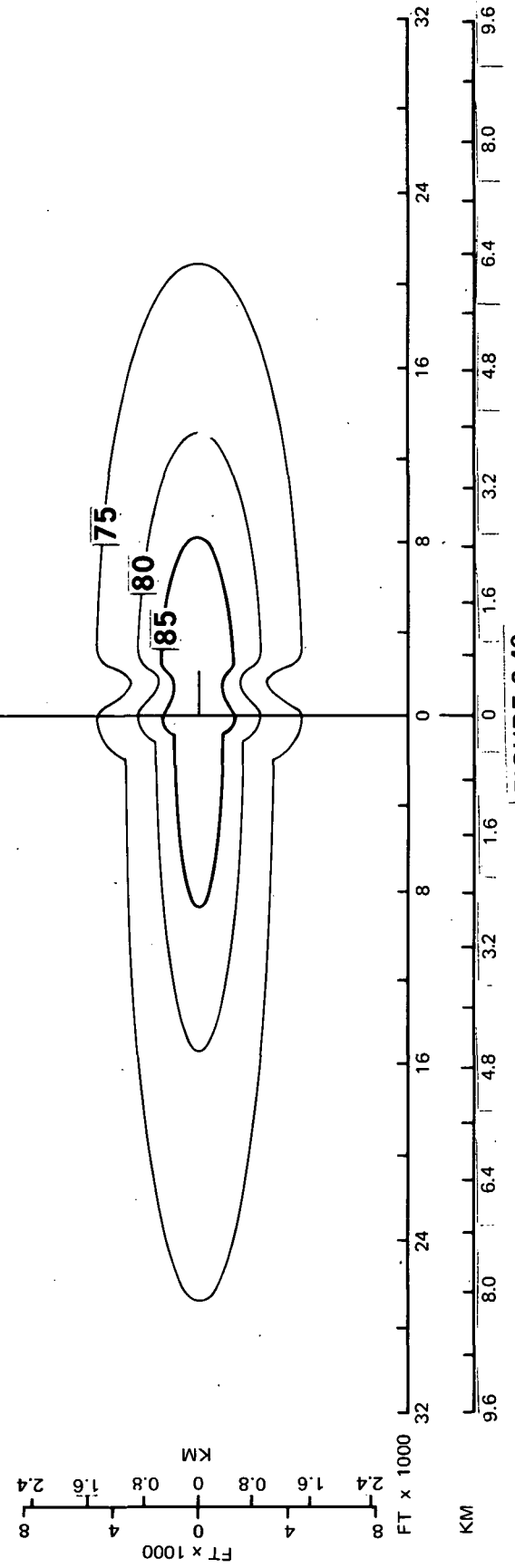
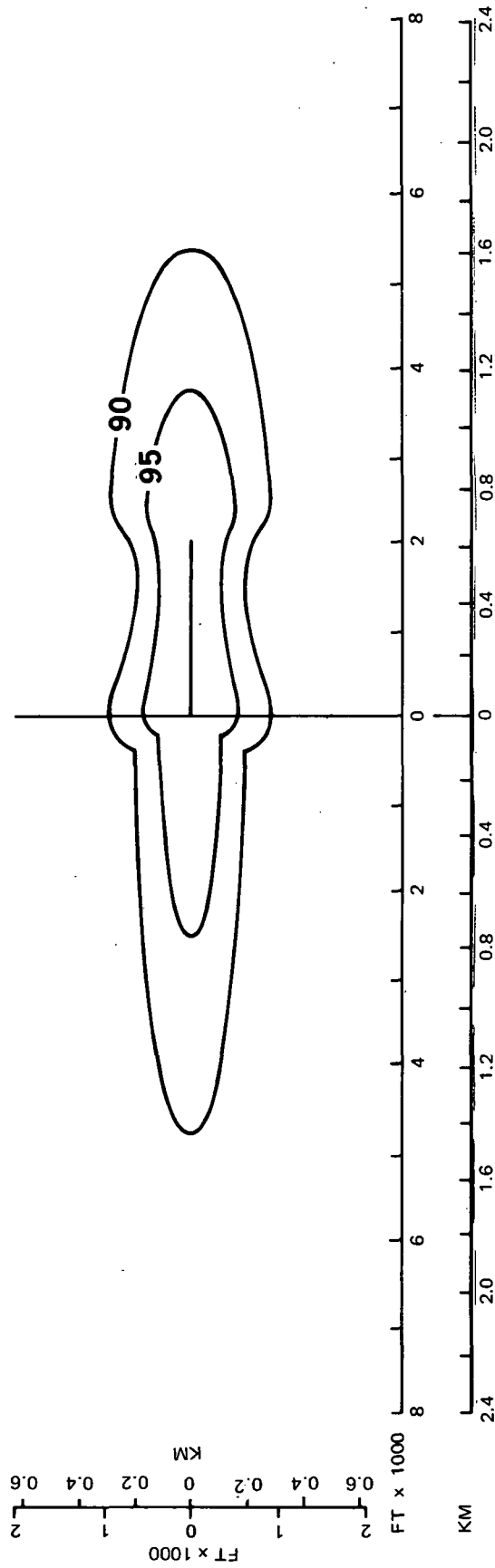


FIGURE 2-49

SINGLE EVENT EPNL CONTOURS

1980 ADVANCED TECHNOLOGY CTOL

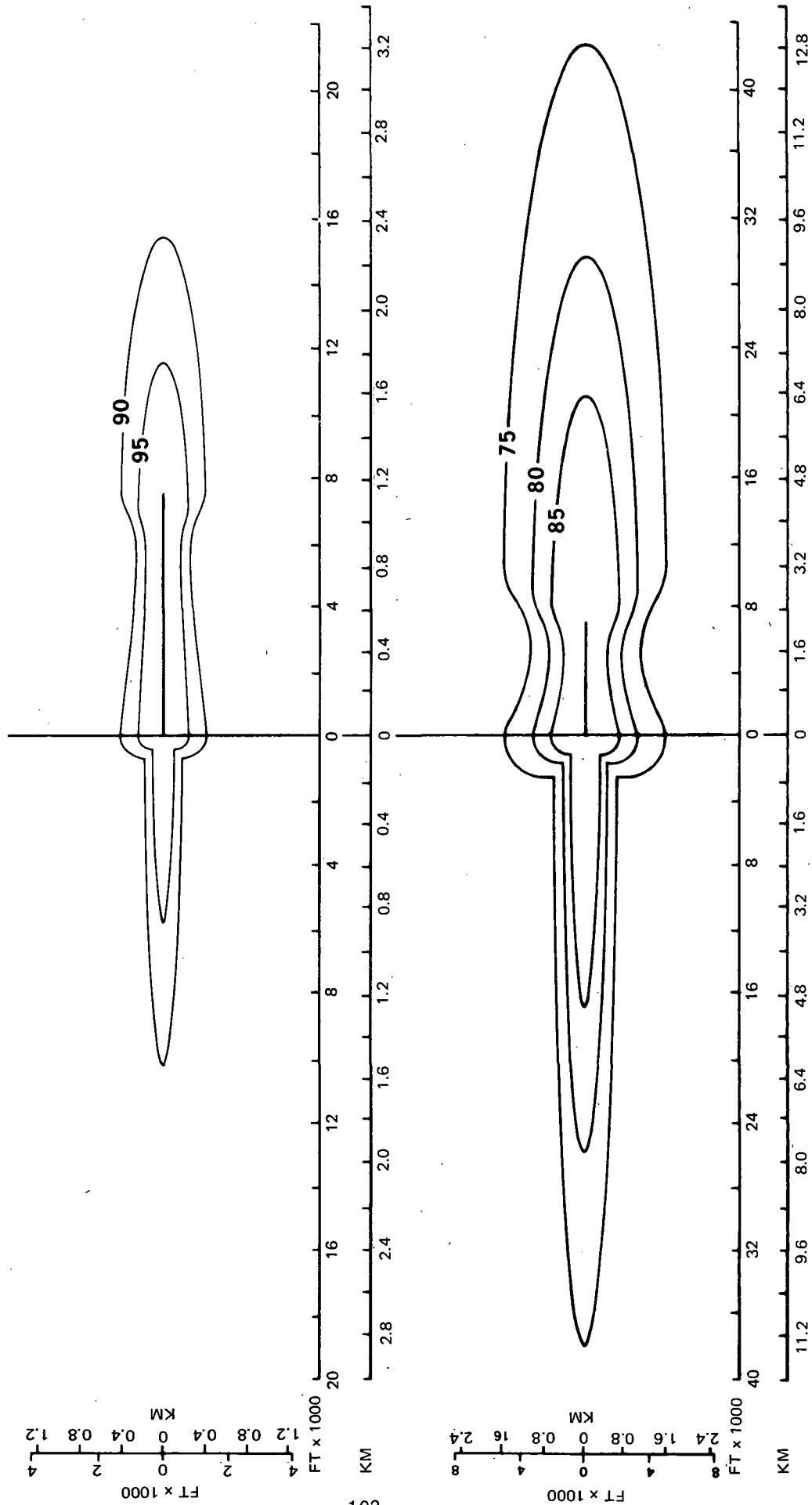


FIGURE 2-50

3.0 AIRCRAFT TRADE STUDIES

Significant design and trade studies conducted prior to the establishment of the final design aircraft are summarized in this section. Some of the results are incorporated in the final baseline aircraft and some are left as design options requiring further in-depth investigations before inclusion in the basic designs. Included in this section are the following studies:

- o Aircraft noise level
- o Configuration trade offs
- o Performance trade offs such as cruise altitude and speed
- o Landing ground rules and their impact upon aircraft sizing
- o Avionics trades such as CAT I, II vs. III
- o Ride quality studies to determine pertinent technology needs
- o Extended range aircraft
- o Use of composite materials
- o Commonality of a military STOL transport with its commercial STOL derivative

3.1 Aircraft Noise Study

3.1.1 Aircraft Analysis. - Because of the critical impact of the design noise level on aircraft sizing and economics, an acoustic trade off study was conducted. The study determines this impact relative to engine treatment level and engine cycle characteristics for a baseline EBF aircraft. Three engine cycles were selected for study; a variable-pitch fan engine with a fan pressure ratio of 1.25, a variable-pitch fan engine with a fan pressure ratio of 1.32, and a fixed pitch engine with a fan pressure ratio of 1.57. The engine cycle characteristics of these engines are summarized in Table 3-1. For each engine, three levels of acoustic treatment were used; none (hardwall), wall treatment only, and treatment which reduced the rotating machinery noise to the level of the jet and flap interaction noise.

Nacelle designs were generated for each of the nine above cases and were developed with the same core as those discussed for the design aircraft (Appendix D). Cutaway drawings of these designs is shown in Figure 3-1. A summary of the engine losses is given in Table 3-2. The methods used to determine these losses are discussed in Appendix D. Engine pod weight estimates developed for these designs are shown in Table 3-3 for a constant engine size. These estimates were scaled when used to size aircraft designs.

Aircraft were sized by the methods presented in Section 2.0 and Appendix B. The characteristics of the resized aircraft are shown in Table 3-4. One notable effect of the different engine cycles is the significantly higher Mach number achieved with the high fan pressure ratio engine.

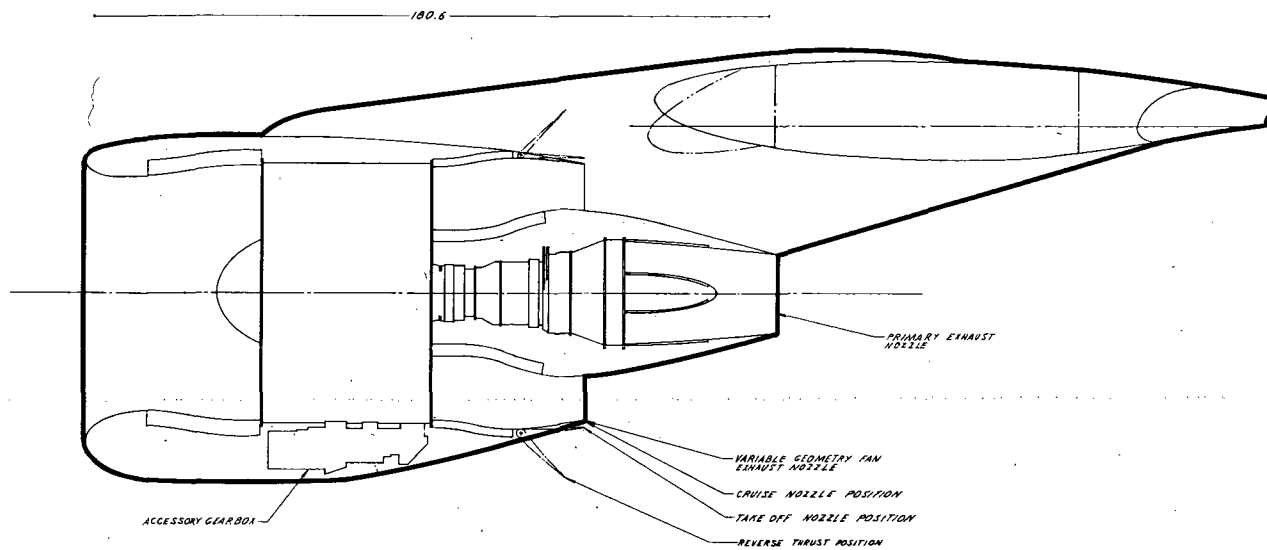
Table 3-1
ENGINE CHARACTERISTICS FOR ACOUSTICS STUDY

Engine Type	Variable-Pitch	Variable-Pitch	Fixed-Pitch
Fan Pressure Ratio	1.25	1.32	1.57
Bypass Ratio	17	13	6
W_{fan} , lbs/sec (kg/sec) ⁽¹⁾⁽²⁾	969 (440)	863 (391)	570 (259)
V_{fan} , ft/sec (m/sec) ⁽²⁾	655 (200)	732 (223)	939 (286)
W_{pri} , lbs/sec (kg/sec) ⁽¹⁾⁽²⁾	57 (26)	63 (28.5)	98 (44.5)
V_{pri} , ft/sec (m/sec) ⁽²⁾	690 (210)	700 (213)	1324 (404)
Tip Speed, ft/sec (m/sec)	750 (229)	900 (274)	1550 (472)
No. of fan blades	17	23	44

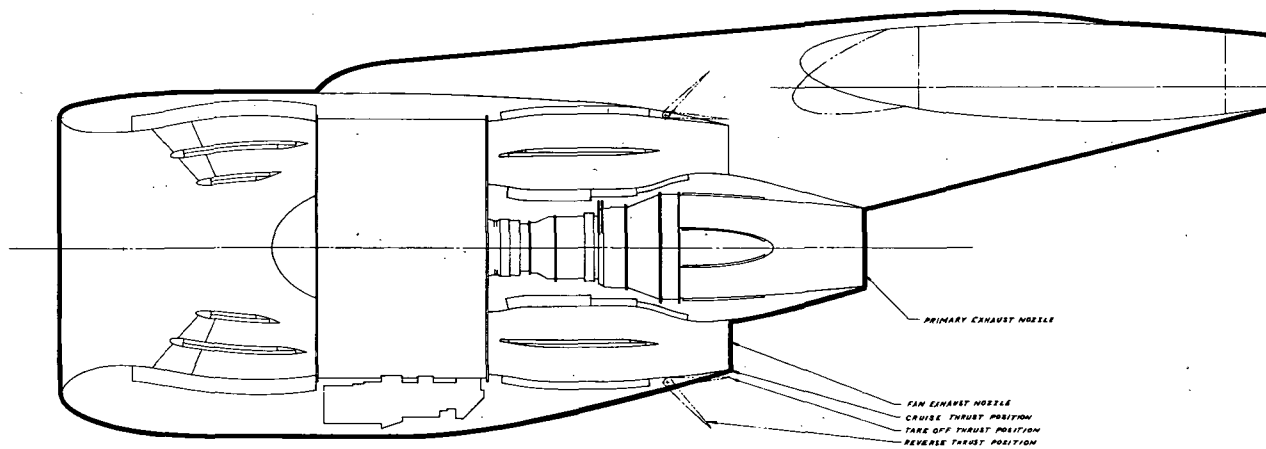
1. For 20,000 lbs (89,000 N) SLS takeoff thrust
2. SL, Std. day, $M_0 = 0.15$

Figure 3-1 NOISE STUDY ENGINE CUTAWAY DRAWINGS

Fan Pressure Ratio 1.25

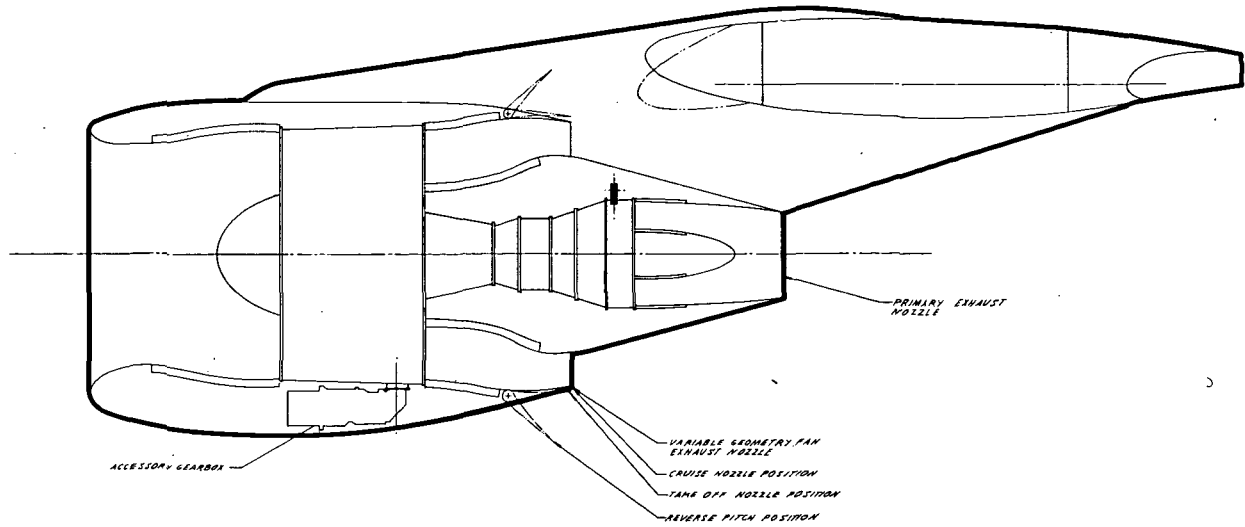


Wall Treatment Only

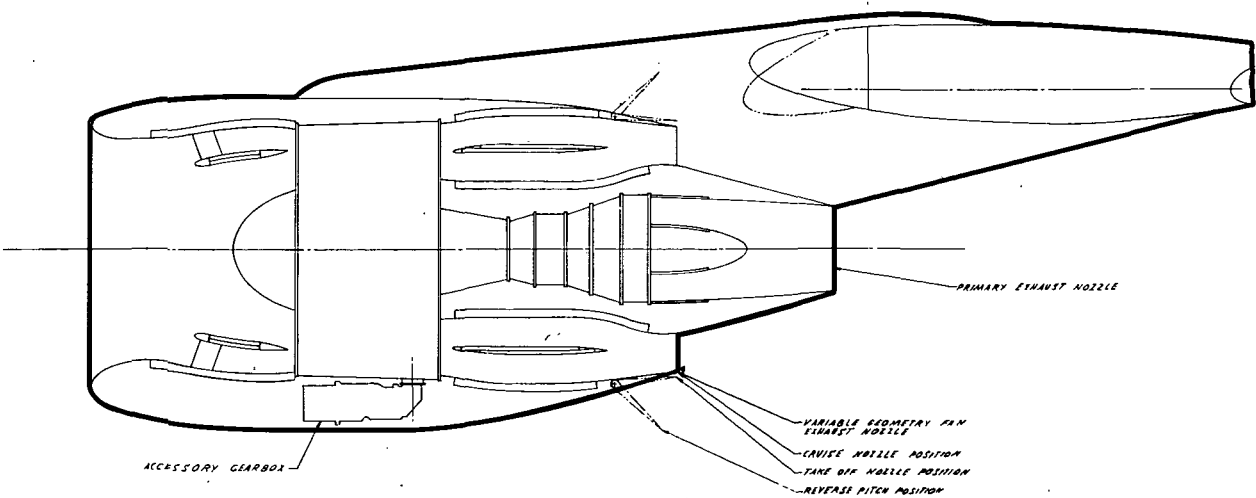


Extensive Treatment

Figure 3-1 NOISE STUDY ENGINE CUTAWAY DRAWINGS (Continued)
Fan Pressure Ratio 1.32

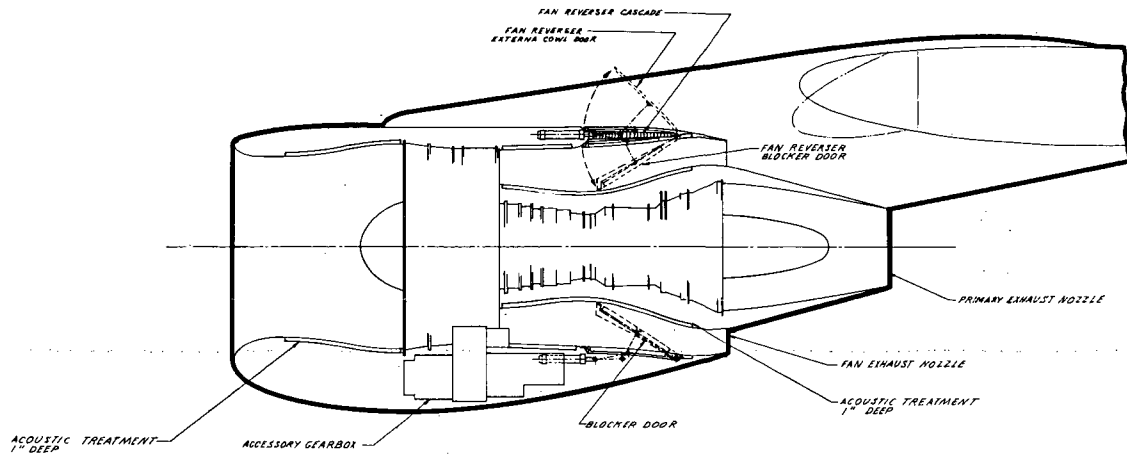


Wall Treatment Only

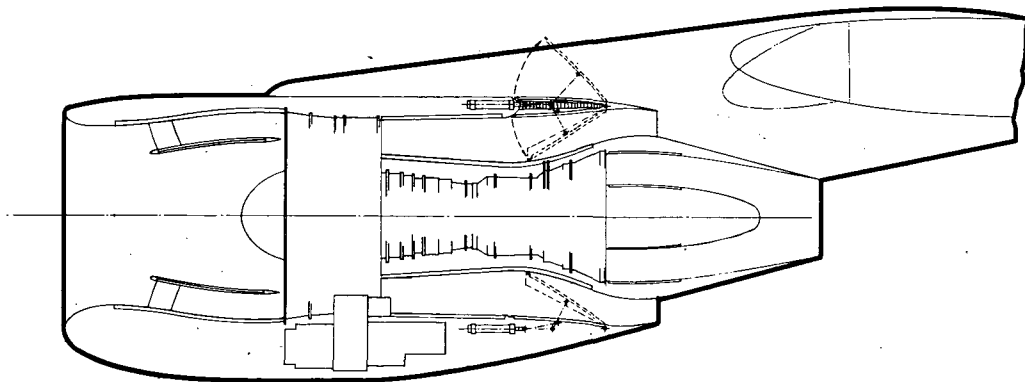


Extensive Treatment

Figure 3-1 NOISE STUDY ENGINE CUTAWAY DRAWINGS (Continued)
Fan Pressure Ratio 1.57



Wall Treatment Only



Extensive Treatment

TABLE 3-2 - INSTALLATION LOSSES FOR AIRCRAFT NOISE LEVEL TRADE STUDY (EBF ONLY)

ENGINE	TREATMENT	INLET LOSS		FAN DUCT	PRIMARY DUCT	NOZZLE VELOCITY COEFF.		DRAGS		
		Takeoff $\frac{\Delta P_T}{q_i}$	Cruise $\frac{\Delta P_T}{q_j}$			$C_{V \text{ DUCT}}$	$C_{V \text{ PRI}}$	$\frac{D}{q_o}$	$\frac{D}{q_{\text{FAN}}}$	$\frac{D}{q_{\text{PRI}}}$
Variable-Pitch FPR = 1.25	N.T.	.024	.0122	.026	.0262	.978	.977	1.061	.272	.042
	W.T.	.025	.0132	.0324	.0454	.978	.977	1.061	.272	.042
	E.T.	.052	.043	.0852	.0507	.978	.977	1.243	.2065	.042
Variable-Pitch FPR = 1.32	N.T.	.028	.017	.0276	.0315	.978	.977	1.019	.304	.044
	W.T.	.03	.019	.0349	.0385	.978	.977	1.019	.304	.044
	E.T.	.042	.0325	.1000	.042	.978	.977	1.114	.2368	.044
Fixed-Pitch FPR = 1.57	N.T.	.029	.017	.0454	.0437	.978	.985	.851	.213	.040
	W.T.	.031	.019	.0576	.0437	.978	.985	.851	.213	.040
	E.T.	.0555	.046	.0697	.0682	.978	.985	.951	.206	.040

NOTE: (1) * Denotes dynamic pressure at duct inlet.

(2) N.T. - No Treatment

W.T. - Wall Treatment

E.T. - Rotating machinery noise treatment to approximate level of jet and flap interaction noise.

CONFIGURATION

[illegible]

Table 3-3
AIRCRAFT WEIGHT SUMMARY
Resized Aircraft

[illegible]

Table 3-4 ACOUSTIC TRADE STUDY AIRCRAFT SUMMARY
Externally Blown Flap, 150 Passengers
3000 Ft (914M) Field Length, 575 St.Mi. (926 Km) Range

	FPR = 1.25				FPR = 1.32				FPR = 1.57			
	None	Wall	Max		None	Wall	Max		None	Wall	Max	
W/S Lb/Ft ² (Kg/M ²)	102 (498)	102 (498)	102 (498)		102 (498)	102 (498)	102 (498)		102 (498)	102 (498)	102 (498)	
T/W	0.481	0.483	0.500		0.469	0.470	0.480		0.442	0.443	0.449	
TOGW Lb (kg)	148,330 (67,280)	149,660 (67,880)	159,210 (72,220)		147,940 (67,100)	148,750 (67,470)	154,090 (69,890)		149,000 (67,580)	149,430 (67,780)	152,780 (69,300)	
S _w Ft ² (M ²)	1454 (135.1)	1467 (136.3)	1561 (145.0)		1450 (134.7)	1458 (135.4)	1511 (140.4)		1461 (135.7)	1465 (136.1)	1498 (139.2)	
Fn Lb/Engine (N/Engine)	17,840 (79,360)	18,060 (80,330)	19,910 (88,560)		17,340 (77,130)	17,490 (77,800)	18,490 (82,250)		16,460 (73,220)	16,550 (73,620)	17,150 (76,290)	
OEW Lb (kg)	101,420 (46,000)	102,550 (46,520)	110,280 (50,020)		100,710 (45,680)	101,390 (45,990)	105,760 (47,970)		99,790 (45,260)	100,130 (45,420)	102,820 (46,640)	
MEW Lb (kg)	98,580 (44,710)	99,710 (45,230)	107,430 (48,730)		97,870 (44,390)	98,550 (44,700)	102,910 (46,680)		96,950 (43,980)	97,290 (44,130)	99,980 (45,350)	
M _{cr}	0.70	0.70	0.70		0.73	0.73	0.73		0.79	0.79	0.79	
h _{cr} Ft (M)	25,000 (7620)	25,000 (7620)	25,000 (7620)		25,000 (7620)	25,000 (7620)	25,000 (7620)		27,000 (8230)	27,000 (8230)	27,000 (8230)	
D.O.C. ϕ /ASSM (ϕ /ASKM)	2.06 (1.28)	2.08 (1.29)	2.19 (1.36)		2.03 (1.26)	2.04 (1.27)	2.09 (1.30)		1.92 (1.20)	1.93 (1.20)	1.97 (1.22)	

DOC calculations are for 575 st mi (926 km) stage length

The acoustic results for the nine aircraft are shown in Table 3-5, based on the acoustic channel definitions tabulated in Table 3-6 and the noise component breakdown shown in Table 3-7. As with the final design aircraft, 1980 acoustic technology is assumed.

3.1.2 Results. - The results of this trade study are summarized in Figure 3-2, showing the 500 foot (152 m) sideline EPNdB values resulting from the acoustic treatment used plotted as a function of takeoff gross weight and direct operating cost. It is evident that the addition of wall treatment to a nacelle significantly reduces the noise emitted by the engines at a very small penalty whereas the inclusion of additional ring treatment yields only nominal acoustic payoffs at a substantial penalty to the aircraft. This effect causes a sharp knee in the curve to exist at the wall-treatment-only point. This characteristic is true for the complete range of engine cycles studied. This knee in the curve is caused by the engine turbomachinery noise being suppressed below the level of the flap interaction noise. This flap interaction noise becomes dominant when extensive nacelle acoustical treatment is used, so the key to obtaining further noise reduction is to develop a means of suppressing the noise generated by the flap.

From a TOGW standpoint it is seen that an engine cycle with a fan pressure ratio of 1.32 is slightly better than the other cycles studied (wall treatment only case). From the economics standpoint the DOC penalty increases essentially linearly as the sideline noise is decreased. The lower DOC for the FPR = 1.57 engine relative to the other study engines results from the significantly higher Mach number associated with the low thrust lapse of that engine and the lower engine cost associated with a fixed pitch engine.

Table 3-5

EBF STOL NOISE TRADE STUDY
 EPNdB @ 500 ft (152 m) Sideline
 4 Engines @ 20,000 lb (44,200N)/Engine

Engine	Acoustic Treatment		
	Hardwall	Wall Treatment*	Extensive Treatment*
FPR = 1.25	104	98	95
FPR = 1.32	108	102	100
FPR = 1.57	117	111	110
*Includes 1980 Technology			

Table 3-6

TREATMENT DEFINITION - L/h

Engine	Inlet		Fan Discharge		Turbine	
	Wall	Extensive	Wall	Extensive	Wall	Extensive
FPR = 1.25	.44	1.5	1.3	3.5	2.6	3.0
FPR = 1.32	.5	1.0	1.4	4.0	1.7	2.0
FPR = 1.57	.6	2.5	4.6	5.2	-	2.0

Table 3-7

EBF STOL NOISE TRADE STUDY
 Engine Hardwall Noise Levels, 500 ft (152 m) Sideline
 4 Engines at 20,000 lb (44,200 N)/Engine

Source	Maximum Perceived Noise Level, PNdB		
	FPR = 1.25	FPR = 1.32	FPR = 1.57
Inlet	100	104	117
Fan Discharge	103	107	116
Turbine Discharge	98	99	99
Jet	89	94	108
Flap Interaction	<u>100</u>	<u>105</u>	<u>113</u>
Total	106	110	119

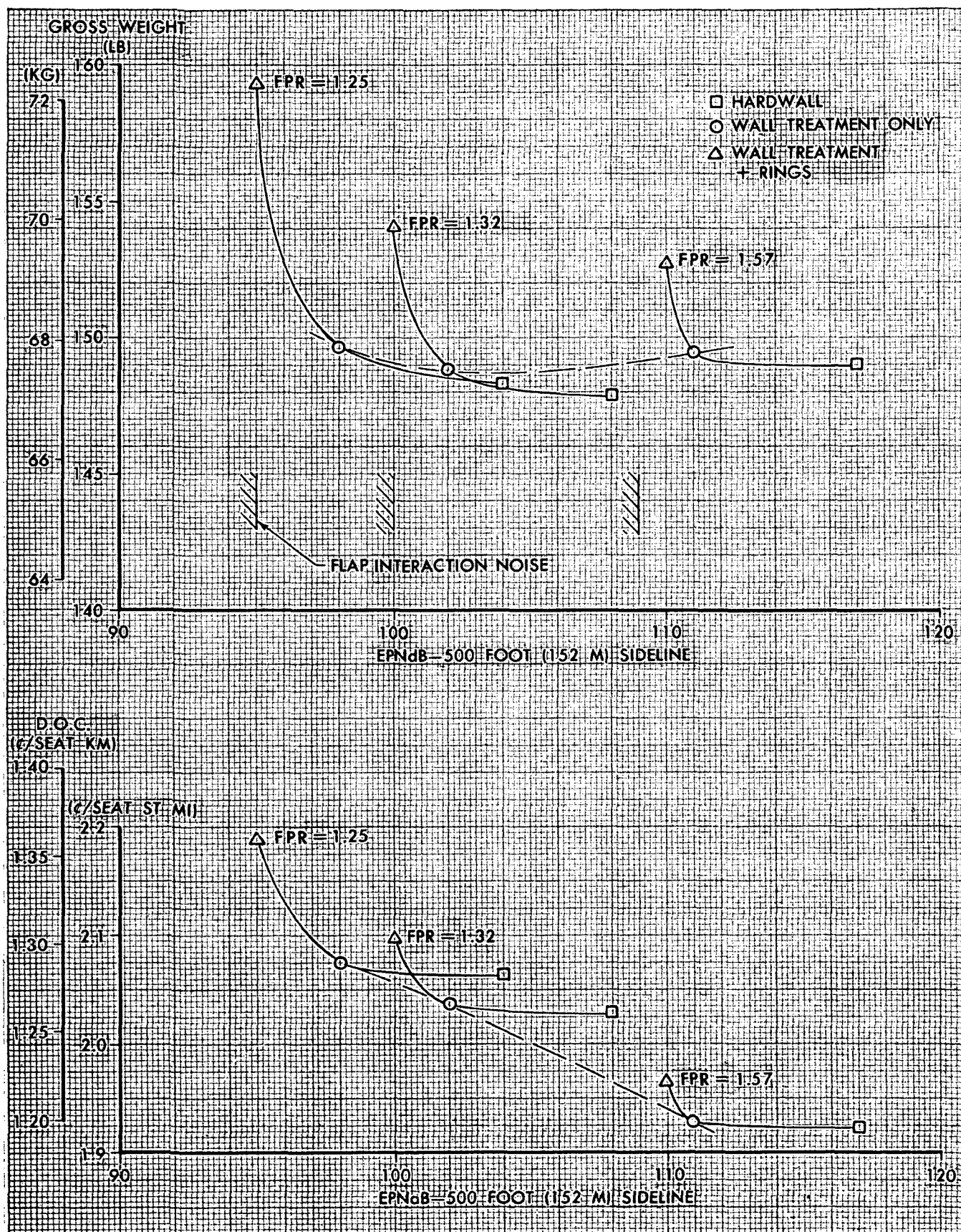


FIGURE 3-2. NOISE TRADE OFF RESULTS—EBF CONFIGURATION

3.1.3 Conclusions. - Unless effective and practical methods to suppress jet exhaust noise and flap interaction noise can be developed, the noise from externally blown (EBF and USB) type of powered lift systems exhibit a flap interaction "noise floor". Efforts to achieve aircraft noise levels near or below this floor by applying extensive acoustic treatment to the engine nacelle result in larger performance and economic penalties for a rather small decrease in total airplane noise level. The extensive nacelle treatment does give substantial suppression of turbomachinery noise but the flap interaction noise dominates the total noise level. The flap interaction noise level was calculated from extrapolations of small scale static test data. Large scale flyover and static flap noise testing is required to determine flight effects and correlate between static and flyover data. The economics of quiet powered lift STOL aircraft is dependent upon an accurate assessment of flap interaction noise.

The results of this trade study, using the flap noise estimating procedures discussed in Appendix C, have been incorporated into the final design aircraft (Section 2.2). Acoustic rings are therefore not included in the engine pod designs for the final design EBF and USB aircraft and these configurations tend to have 500 foot (152 m) sideline noise levels somewhat higher than 95 EPNdB. However, the final design EBF and USB aircraft have a lower gross weight and better economics than the parametric or system analysis aircraft which were designed for 95 PNdB or EPNdB, respectively.

3.2 Configuration Studies

3.2.1 Aspect Ratio Study - EBF. - The choice of wing aspect ratio is based on the tradeoff between increased aerodynamic efficiency and structural

weight as aspect ratio is increased. The influence of aspect ratio on the sizing of a 150 passenger, 3000 foot (914 m) field length externally blown flap STOL aircraft was examined.

High lift aerodynamic data for aspect ratios of 7, 8 and 9 was used in calculating takeoff and landing performance to determine thrust-to-weight ratio as a function of wing loading for a 3000 foot (914 m) field length. Parametric weight data were prepared for the three aspect ratios. Wing flutter weight penalties, which were a function of aspect ratio, wing loading, and wing area, were included in the parametric weights data to reflect any increases in wing box weight needed to satisfy stiffness requirements. The primary effect of aspect ratio on high speed drag is a change in induced drag. Other drag changes are of secondary importance and were not included. The performance calculations were performed in the same manner as described for the final design aircraft in Appendix B.

Minimum direct operating cost for the three aircraft occurred at the intersection of the takeoff and landing critical lines. These aircraft for the three aspect ratios are summarized in Table 3-8 with a weight breakdown in Table 3-9. Direct operating cost is not very sensitive to aspect ratio as shown in Figure 3-3. Based on this curve, an aspect ratio of 8.0 was chosen for sizing the final design externally blown flap STOL aircraft. It should be noted that the earlier parametric aircraft were based on an aspect ratio of 7.0.

Since the aerodynamic characteristics of the upper surface blowing aircraft are similar to those of the EBF aircraft, a similar aspect ratio trend for the USB configuration may be expected.

Table 3-8

ASPECT RATIO STUDY AIRCRAFT

Externally Blown Flap Configuration

$$\lambda = .3, t/c_{avg} = .139, \Lambda = 25^\circ$$

Aspect Ratio	7	8	9
Passengers	150	150	150
Design Field Length ft (m)	3,000 (914)	3,000 (914)	3,000 (914)
Engine	PD287-3	PD287-3	PD287-3
TOGW	149,860 (67,970)	149,030 (67,600)	149,440 (67,780)
Wing Area ft ² (m ²)	1,521 (141.3)	1,461 (135.7)	1,448 (134.5)
Thrust/Engine lb (N)	18,860 (83,890)	18,260 (81,220)	17,820 (79,270)
W/S lb/ft ² (kg/m ²)	98.5 (481)	102.0 (498)	103.2 (504)
T/W	0.504	0.490	0.477
Cruise Mach Number	0.70	0.69	0.69
Cruise Altitude ft (m)	26,000 (7,925)	26,000 (7,925)	26,000 (7,925)
D.O.C. @ 575 st mi (926 km)	2.085 (1.295)	2.076 (1,290)	2.081 (1.293)

Table 3-9

WING ASPECT RATIO STUDY WEIGHT SUMMARY

	Aspect Ratio					
	7.0		8.0		9.0	
	English	Metric	English	Metric	English	Metric
GEOMETRY DATA						
Wing Area	1,521	141.3	1,461	135.7	1,448	134.5
Wing Loading	98.5	481	102	498	103	504
Horiz/Vert Tail Area	419/312	38.9/29.0	419/319	38.9/29.6	421/332	39.1/30.8
Horiz/Vert Tail Volume	1.257/.1218	1.257/.1218	1.426/.1238	1.426/.1238	1.540/.1229	1.540/.1229
SLS Thrust (uninst)/TOGW	.50	.50	.49	.49	.48	.48
SLS Thrust (uninst)/Eng	18,865	83,911	18,260	81,176	17,820	79,263
Mission Fuel Weight/TOGW	.113	.113	.110	.110	.107	.107
	1b	kg	1b	kg	1b	kg
WEIGHT DATA						
Wing	17,710	8,033	18,070	8,196	19,175	8,698
Tail	4,580	2,078	4,625	2,098	4,715	2,139
Fuselage	23,430	10,628	23,405	10,616	23,445	10,634
Landing Gear	6,295	2,855	6,260	2,840	6,275	2,846
Propulsion System	19,305	8,756	18,690	8,478	18,240	8,274
Remaining Weight	28,750	13,040	28,720	13,027	28,700	13,018
Manufacture Empty Weight	100,070	45,390	99,770	45,255	100,550	45,609
Operational Items	2,850	1,293	2,840	1,288	2,840	1,288
Operational Empty Weight	102,920	46,683	102,610	46,543	103,390	46,897
Mission Payload	30,000	13,608	30,000	13,608	30,000	13,608
Mission Zero Fuel Weight	132,920	60,291	132,610	60,151	133,390	60,505
Mission Fuel Weight	17,070	7,702	16,390	7,434	16,010	7,262
STOL Takeoff Gross Weight	149,990	67,993	149,000	67,585	149,400	67,767

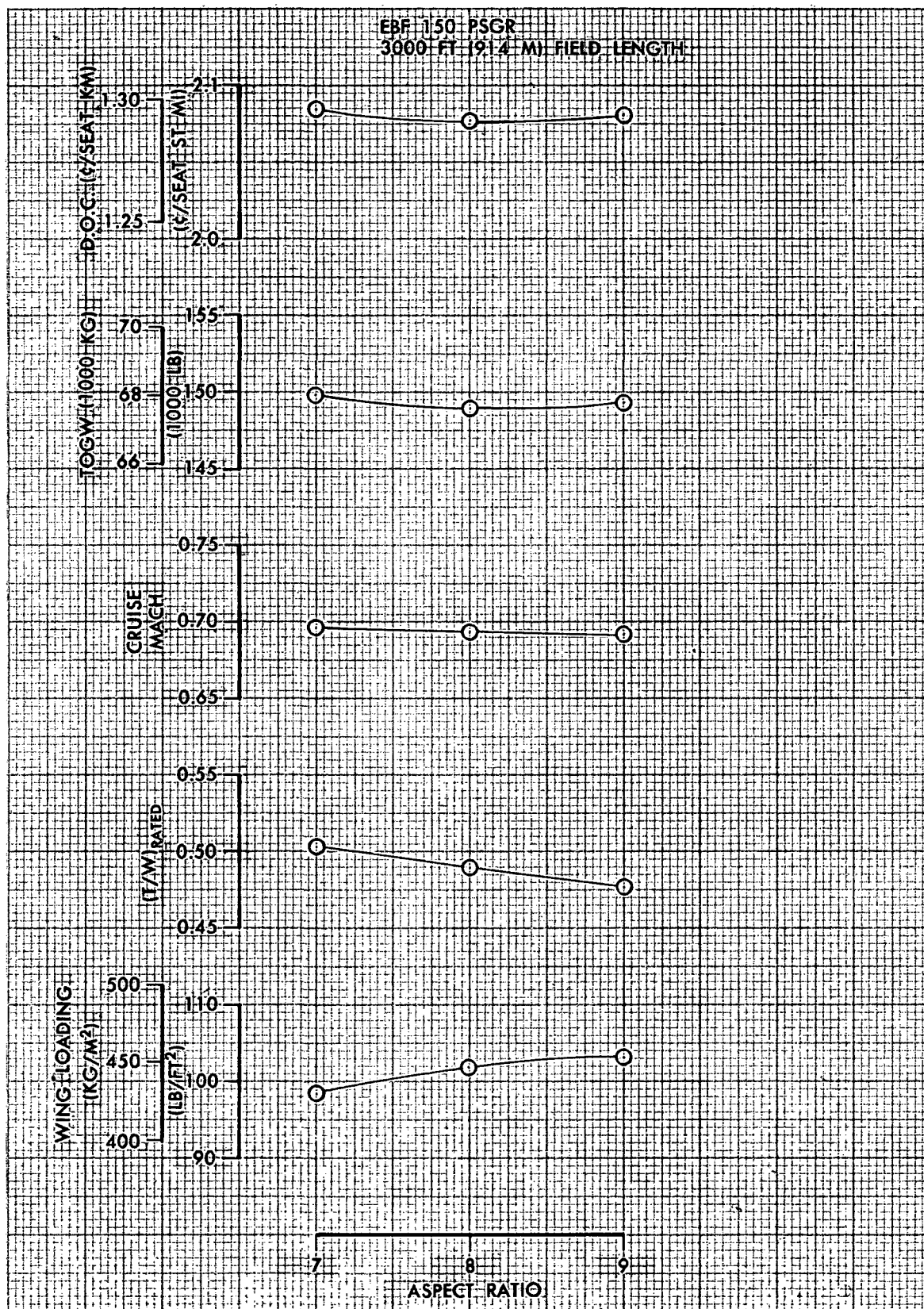


FIGURE 3-3. EFFECT OF ASPECT RATIO ON AIRCRAFT SIZING

3.2.2 Boundary Layer Control for USB STOL Leading Edge Protection. - STOL aircraft landing performance is dependent on the ability to achieve high $C_{L_{max}}$ values. The upper surface blown flap configuration requires some type of wing leading edge protection, either mechanical slats or leading edge boundary layer control (BLC), to prevent flow separation at high angles of attack.

Two different leading edge USB configurations were considered in this study. The first configuration incorporates a full span leading edge slat. The second utilizes a 15 percent chord drooped leading edge with boundary layer control blowing at the knee.

For the full span leading edge slat configuration, it was assumed that the losses in maximum lift due to nacelle interference can be reduced with further development work but, based on Douglas experience, not entirely eliminated. For this case the upper surface blowing high lift aerodynamic characteristics are estimated to be identical to the externally blown flap characteristics except that a penalty of $\Delta C_{L_{max}} = -.20$ is assumed for all flap deflections.

Figure 3-4 shows the incremental improvement in maximum lift coefficient that can be achieved with leading edge BLC. These values are relative to the EBF $C_{L_{max}}$ levels where the initial value of $\Delta C_{L_{max}}$ at zero leading edge blowing is the sum of the estimated nacelle interference effects and the result of replacing the outboard slat with a drooped leading edge. For this case the upper surface blowing high lift aerodynamic characteristics were estimated as follows:

- 1) The EBF aerodynamic characteristics were used where C_μ is based on the installed engine thrust plus a 50 percent recovery of the leading edge blowing.
- 2) Maximum lift coefficients are the sum of the EBF levels plus the incremental values from Figure 3-4.

In addition to the improvement in $C_{L_{max}}$ that can be achieved with a BLC system, there is a possible weight advantage since the BLC nozzles and associated ducting may weigh less than a full span slat.

High pressure air is required to choke the flow at the nozzle. This air must be bled from the engine core rather than from the fan ducts due to the low fan pressure ratio of the PD287-22 engine. This will result in a loss in engine thrust which will tend to offset the gain in $C_{L_{max}}$.

Figure 3-5 shows the thrust-to-weight ratio required to attain 2000 foot (610 m) field length performance at a W/S of 65 lb/ft^2 (317 kg/m^2) as a function of C_μ at the slot. The calculations for the blown leading edge system are based on the following assumptions:

1. 15 percent pressure drop in duct
2. 90 percent nozzle coefficient
3. 50 percent thrust recovery.

The minimum required T/W with leading edge blowing occurs at a $C_{\mu_{SLOT}}$ of 0.010. This T/W is still higher than that required for the leading edge slat configuration. Table 3-10 shows that the weight advantage of the BLC system just about offsets the T/W penalty.

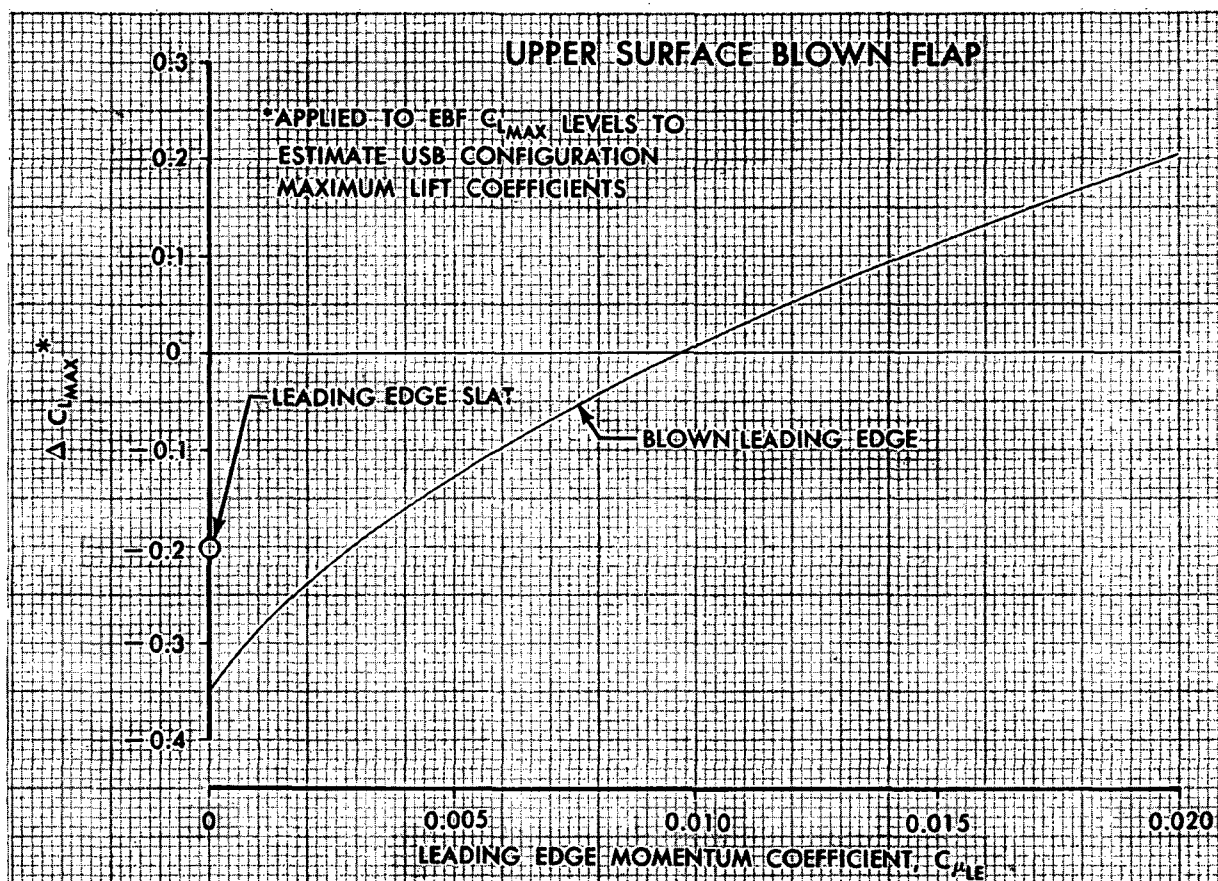


FIGURE 3-4. EFFECT OF LEADING EDGE BOUNDARY LAYER CONTROL ON ΔC_{LMAX}

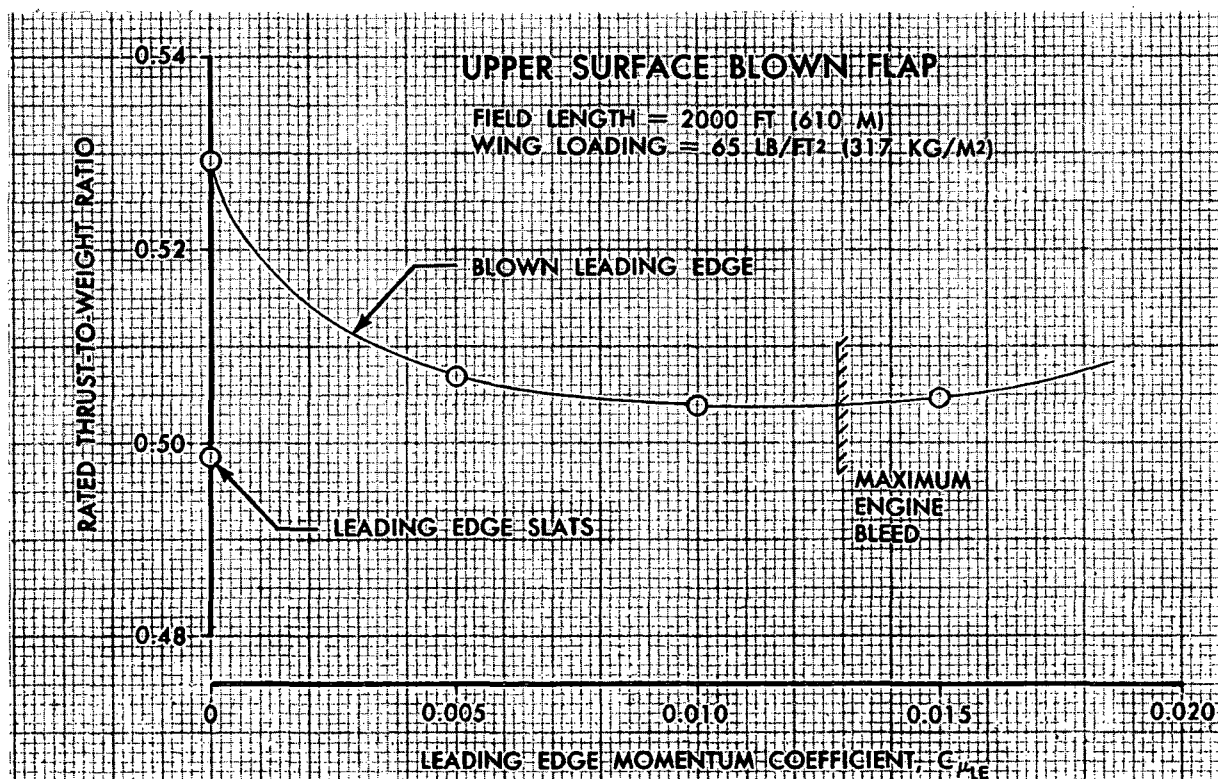


FIGURE 3-5. EFFECT OF LEADING EDGE BOUNDARY LAYER CONTROL ON T/W REQUIRED

Table 3-10

LEADING EDGE SLAT VS BLOWN LEADING EDGE FLAP SUMMARY

	Leading Edge Slat		Blown Leading Edge Flap	
	English	Metric	English	Metric
GEOMETRY DATA: Wing Area - ft ² (m ²) Wing Loading - lb/ft ² (kg/m ²) Horiz/Vert Tail Area - ft ² (m ²) Horiz/Vert Tail Volume SLS Thrust (uninst)/TOGW - lb/lb (N/kg) SLS Thrust (uninst)/Eng - lb (N) Mission Fuel Weight/TOGW	3,480 65 1048/1247 1.0250/.1170 .498 28,160 .1071	323.8 317 97.36/115.9 1.0250/.1107 4.88 125,262 .1071	3,489 65 1055/1250 1.0278/.1169 .504 28,570 .1075	324.1 317 98.01/116.1 1.0278/.1169 4.94 127,086 .1075
	1b (42,350) 1,614 1,777 1,035 -- 37,924 (14,490) (31,870) (9,500) (35,280) (1,155) (34,305)	kg (19,210) 732 806 470 -- 17,202 (6,572) (14,456) (4,309) (16,003) (524) (15,560)	1b (41,885) 1,014 -- 2,325 511 38,035 (14,560) (31,870) (9,525) (35,795) (1,460) (34,305)	kg (18,999) 460 -- 1,055 232 17,252 (6,604) (14,456) (4,321) (16,236) (662) (15,560)
	168,950 3,030	76,634 1,375	169,400 3,030	76,838 1,375
	171,980 30,000	78,009 13,608	172,430 30,000	78,213 13,608
	201,980 24,220	91,617 10,986	202,430 24,370	91,821 11,054
	226,200	102,603	226,800	102,875
WEIGHT DATA: Leading Edge Str Slat Droop L.E. Flap Plenum and Nozzles Remaining Wing Structure Tail Fuselage Landing Gear Propulsion System Pneumatic System Remaining Weight Manufacturer Empty Weight Operational Items Operational Empty Weight Mission Payload Mission Zero Fuel Weight Mission Fuel Weight STOL Takeoff Gross Weight				

The differences between these two aircraft are sufficiently small that the best solution is not apparent considering the accuracy of the analysis. Other considerations such as anti-icing, noise, maintenance, etc. would probably be deciding factors. If lower bypass ratio, higher pressure ratio engines were used, the blown leading edge system would appear more favorable than it does with the PD287-22 engine because the thrust loss due to bleed would not be as severe.

3.3 Performance Trade Offs

Trade studies including the optimization of cruise altitude and Mach number and aircraft sizing sensitivities are discussed in the following paragraphs.

3.3.1 Cruise Performance Optimization. - The selection of cruise Mach number and altitude for the sizing mission was based on the minimization of direct operating cost (DOC). Figure 3-6 shows the variation in direct operating cost with cruise Mach number for a 150 passenger, 3000 foot (914 m) field length, externally blown flap STOL aircraft. Minimum DOC occurs when the aircraft is sized to fly at maximum cruise Mach number.

The variation in direct operating cost with cruise altitude for this same aircraft is shown in Figure 3-7. There is an optimum cruise altitude, in this case 26,000 feet (7,925 m), for minimum DOC. This altitude corresponds to that for maximum Mach number.

Optimization studies of this type were performed during the sizing of all the final design aircraft.

3.3.2 Trade Factors. - Table 3-11 shows the sensitivity of takeoff gross weight and direct operating cost to five percent incremental changes in the significant parameters affecting aircraft sizing. These factors were calculated for the final baseline 150 passenger, 3000 foot (914 m) field length EBF aircraft but similar trends would be shown for the other configurations.

Growth factors, defined as $\Delta\text{TOGW}/\Delta\text{Empty Weight}$, are presented in Table 3-12 for several of the final baseline aircraft. The higher growth

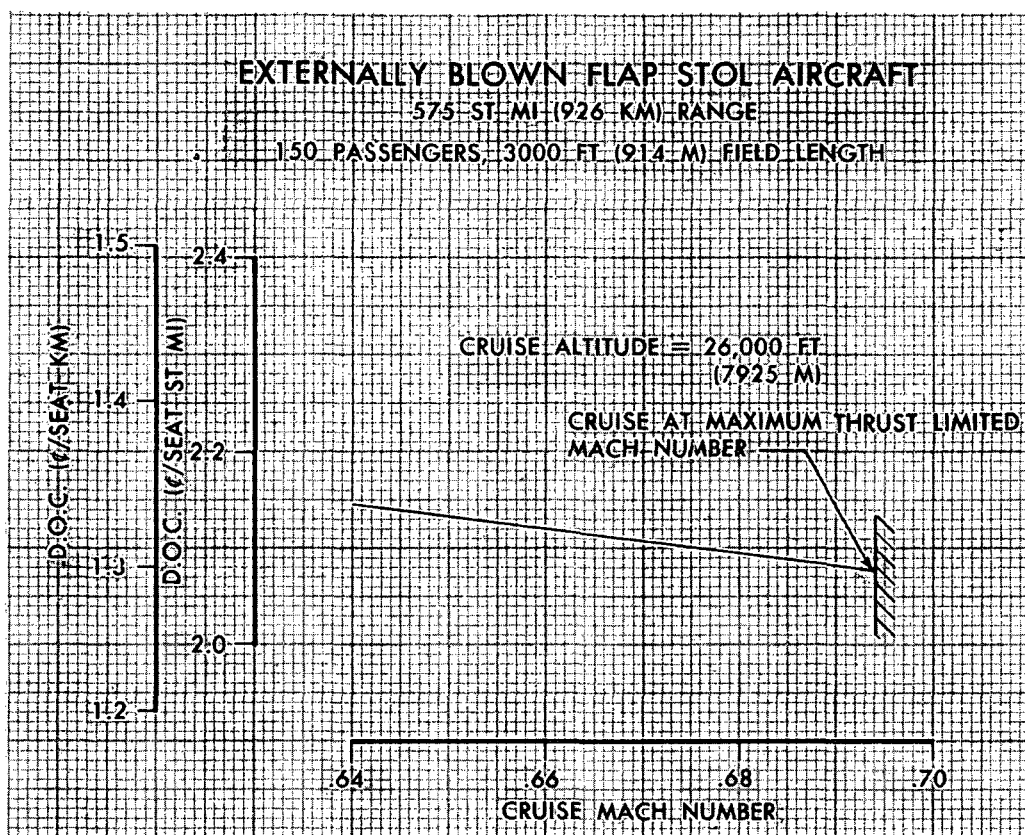


FIGURE 3-6. DIRECT OPERATING COST VARIATION WITH CRUISE MACH NUMBER

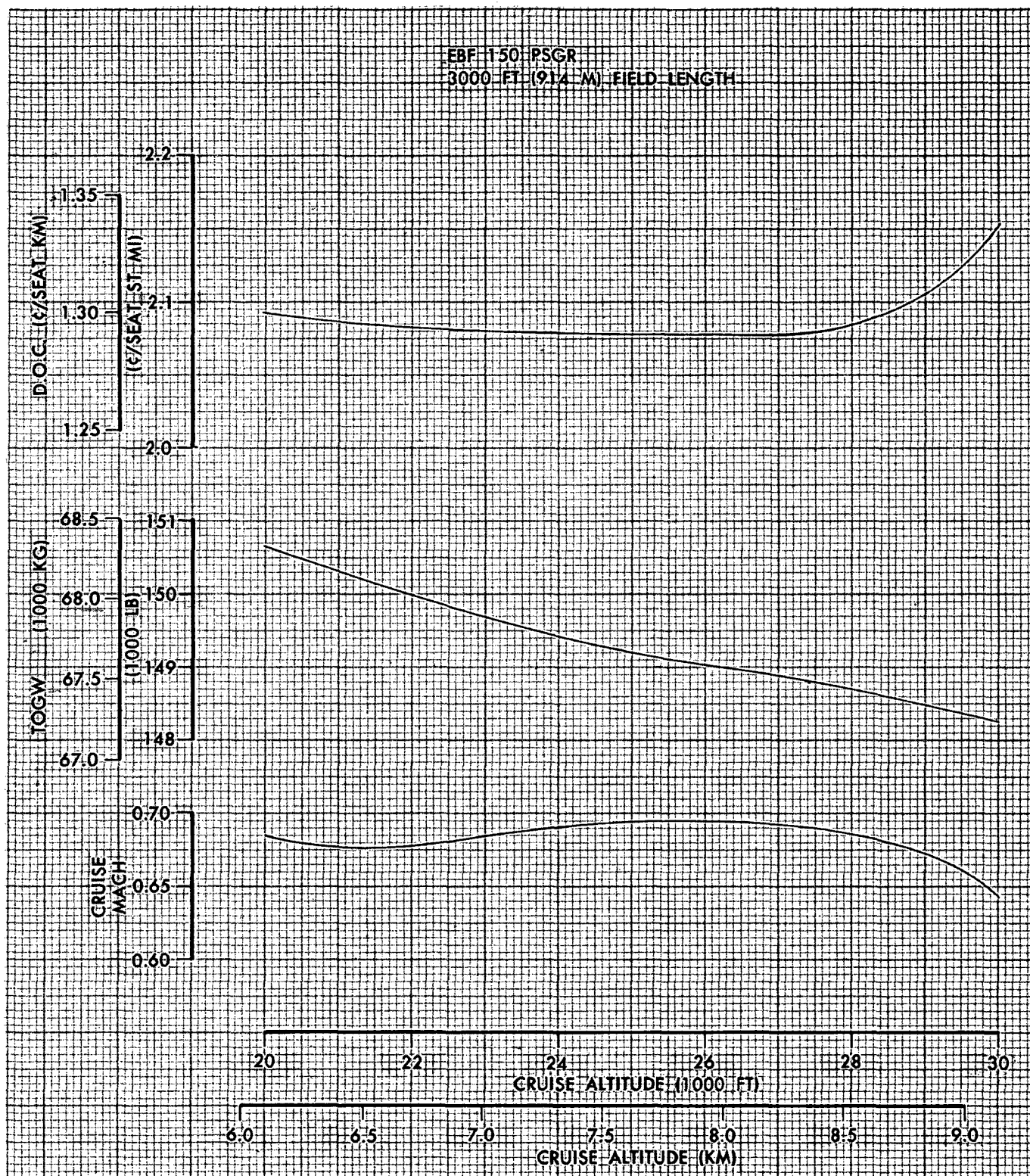


FIGURE 3-7. CRUISE ALTITUDE OPTIMIZATION

Table 3-11

SIZING TRADE FACTORS

Externally Blown Flap STOL
150 passengers, 3000 foot (914 m) field length

A 5 percent increase in	will produce changes in		
	<u>TOGW</u>	and	<u>DOC</u> of
Airframe Weight	+ 5.1 %		+ 3.2 %
Propulsion System Weight	+ 1.2 %		+ 0.6 %
Parasite and Compressibility Drag	+ 0.4 %		+ 1.5 %
T/W	+ 1.6 %		+ 0.4 %
Maximum Continuous Thrust	+ 0.4 %		- 0.7 %
SFC	+ 0.9 %		+ 0.8 %
Tail Volumes	+ 0.2 %		+ 0.2 %

Table 3-12

GROWTH FACTORS

<u>Configuration</u>	<u>Payload pax</u>	<u>Field Length ft (m)</u>	<u>Growth Factor</u>
EBF	150	2000 (609)	2.40
EBF	150	3000 (914)	1.85
MF	150	4000 (1219)	1.90
CTOL	150	7500 (2286)	1.75

factors associated with the shorter field lengths indicate that the change in aircraft weight due to the use of composite materials, for example, will be more dramatic for shorter design field lengths.

3.4 Landing Ground Rules Study. - The landing ground rules, as originally specified for the study were found to have an adverse effect on aircraft sizing and are evaluated in this section. The ground rules as specified were:

- 800 fpm (4.06 m/s) approach sink rate
- flare to 3 fps (.915 m/s) at touchdown
- one second delay before deceleration device effectiveness
- decelerate at 0.35g to a stop.

Landing distance calculated using the above rules is divided by the conventional 0.6 factor to determine field length. This approach represents a major departure in certification philosophy. To date, certified landing field length has been based on a maximum performance landing divided by the 0.6 factor. The above ground rules represent a normal operational landing which is then divided by 0.6. The results of this procedure are to cause STOL aircraft to be landing critical by substantial margins. Figure 3-8 shows landing field lengths as a function of wing loading for these ground rules for 1500 (457), 2000 (610) and 3000 foot (914 meter) takeoff field lengths. The resulting wing loading for balanced field lengths produce large weight and cost penalties, particularly for the shorter field lengths. This penalty is shown in Figure 3-9 for the 2000 foot (610 meter) case. These weight and cost penalties, 10 to 15 percent in this case, will unduly bias the study results in favor of longer field lengths.

These ground rules are compared to previous requirements in Table 3-13. The parametric study requirements are usually more restrictive than any of the others. Figure 3-10 shows the effect of approach sink rate on landing field length. Increasing the approach sink rate above 800 fpm (4.06 m/s) increases the design wing loading only slightly.

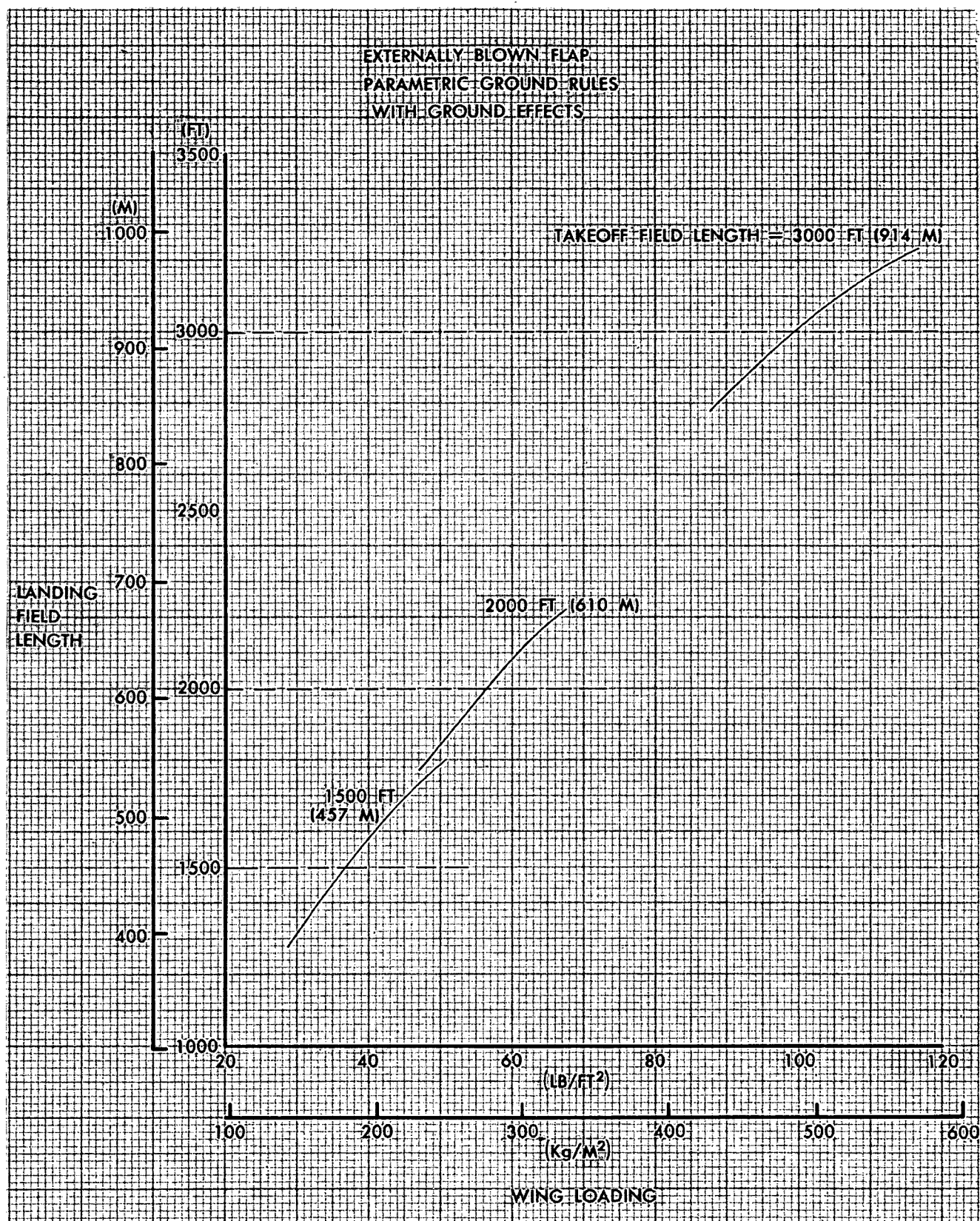


FIGURE 3-8. LANDING FIELD LENGTH VERSUS WING LOADING

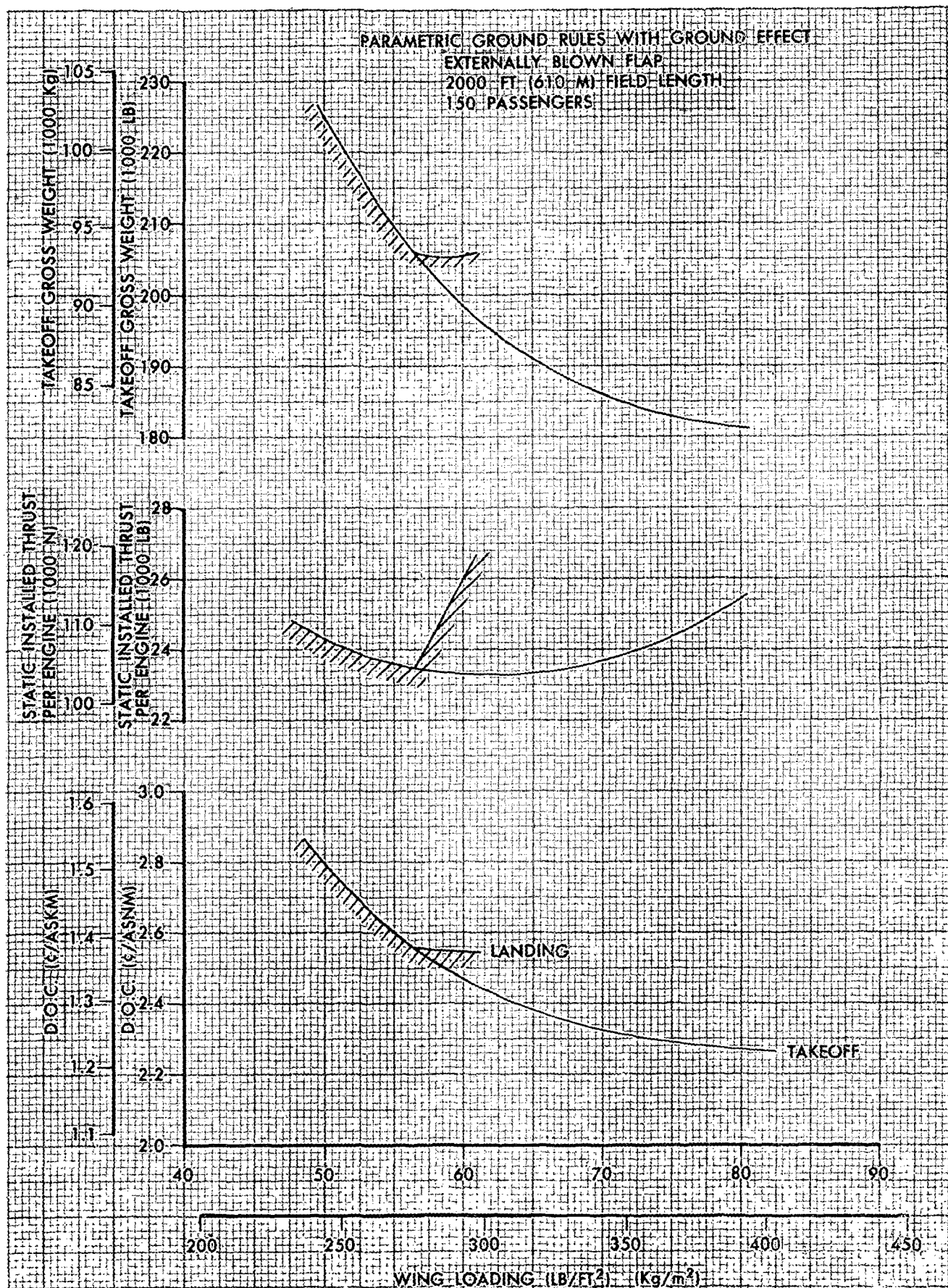


FIGURE 3-9. EFFECT OF LANDING GROUND RULES ON AIRCRAFT SIZING
 (TYPICAL)

Table 3- 13
COMPARISON OF VARIOUS LANDING GROUND RULES

	STOL Study	FAR Part 25 & Part 121	Part XX	Breguet 941
Approach Sink Rate	800 fpm (4.06 mps)	None	None	None
Touch Down Sink	3 fps (.915 mps)	None	3 fps (.915 mps)	Deleted
Braking Devices Delay	1 sec	Those "that may reasonably be expected in service"	Same as Part 25	Same as Part 25
Deceleration	0.35 g	None	None	None
Factor	1/0.6	1/0.6	--	1/0.6

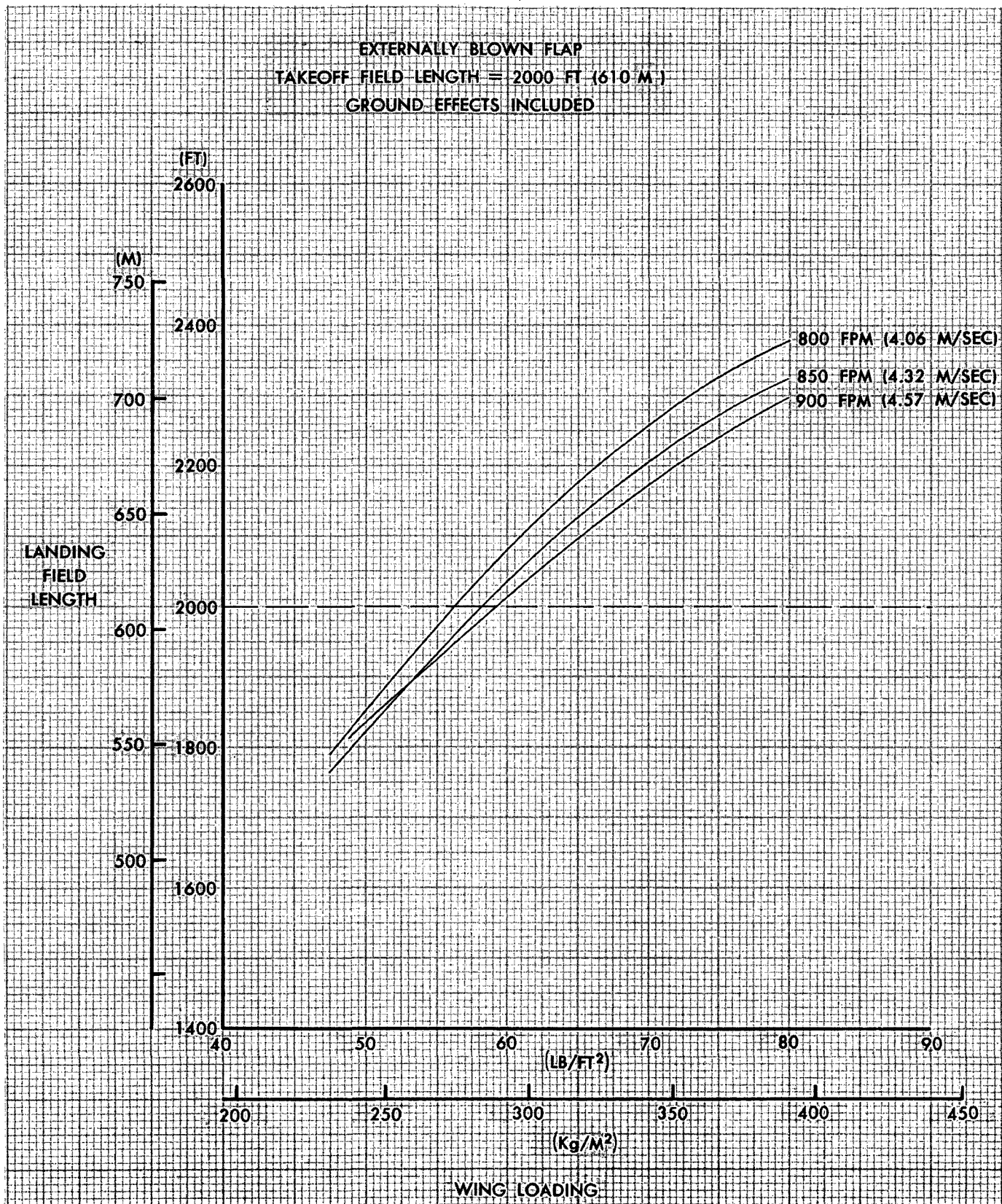


FIGURE 3-10. EFFECT OF APPROACH SINK RATE ON LANDING FIELD LENGTH

An increase in approach angle is offset by a longer flare distance. An approach sink rate of 900 fpm (4.57 m/s), as selected for final design work, provides a small but useful benefit in aircraft sizing and is below the accepted operational limit of 1000 fpm (5.08 m/s).

The touchdown vertical sink speed of 3 fps (.915 m/s) is restrictive even for normal STOL operations. Average normal operation sink speeds for the Breguet 941 are 4 (1.22) to 5.5 fps (1.28 m/s) as shown in Table 3-14. Figure 3-11 shows the impact of touchdown sink speed on the design wing loading for a 2000 foot (610 m) field length externally blown flap aircraft. Increasing touchdown sink rate from 3 fps (.915 m/s) to 10 fps (3.05 m/s) allows a 10 lb/ft^2 (48.7 kg/m^2) increase in W/S and is more in line with conventional practice. The DC-8, DC-9 and DC-10 series aircraft have a structural design sink speed of 10 fps (3.05 m/s) and landing field length performance was certified using the design limit. The STOL aircraft have a gear design limit of 15 fps (4.57 m/s) so that use of 10 fps (3.05 m/s) is quite conservative.

Deceleration time delay and average deceleration rate achieved during certification tests of recent Douglas commercial transports is shown in Table 3-15. Figure 3-12 shows the effect of deceleration rate on design wing loading. Large benefits are available if the deceleration rate can be increased. The specified one second delay and 0.35g deceleration represent reasonable, if somewhat conservative, values based on recent experience, but efforts to increase deceleration capability and/or reduce the actuation delay have potentially large rewards.

Table 3- 14

BREGUET 941 SINK RATE COMPARISONS

FAA NAFEC Flight Program Average (74 Landings)	-	4.1 FPS	(1.25 MPS)
$\bar{x} + 3\sigma$	-	10.2 FPS	(3.11 MPS)
Breguet Operational Data Average (32 Landings)	-	5.5 FPS	(1.68 MPS)

Table 3- 15

DC - SERIES AIRCRAFT DECELERATION CAPABILITY

Aircraft	Equivalent Time Delay (Sec.)	Average Decel Rate (g)
DC-9-30	0.6	.39g
DC-9-30 (improved anti-skid system)	-	.47g
DC-10-10	1.6	.39g

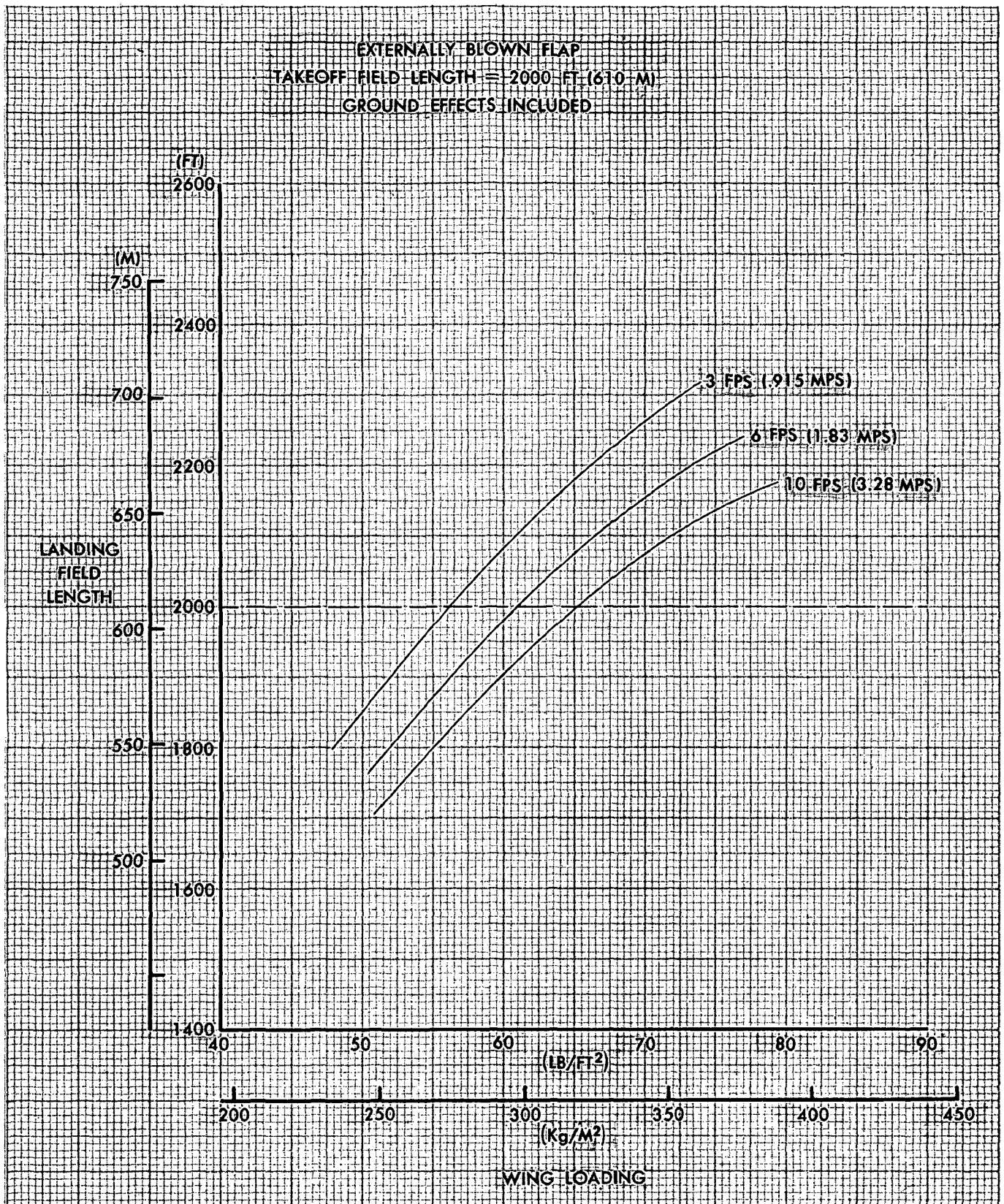


FIGURE 3-11. EFFECT OF TOUCHDOWN SINK RATE ON LANDING FIELD LENGTH

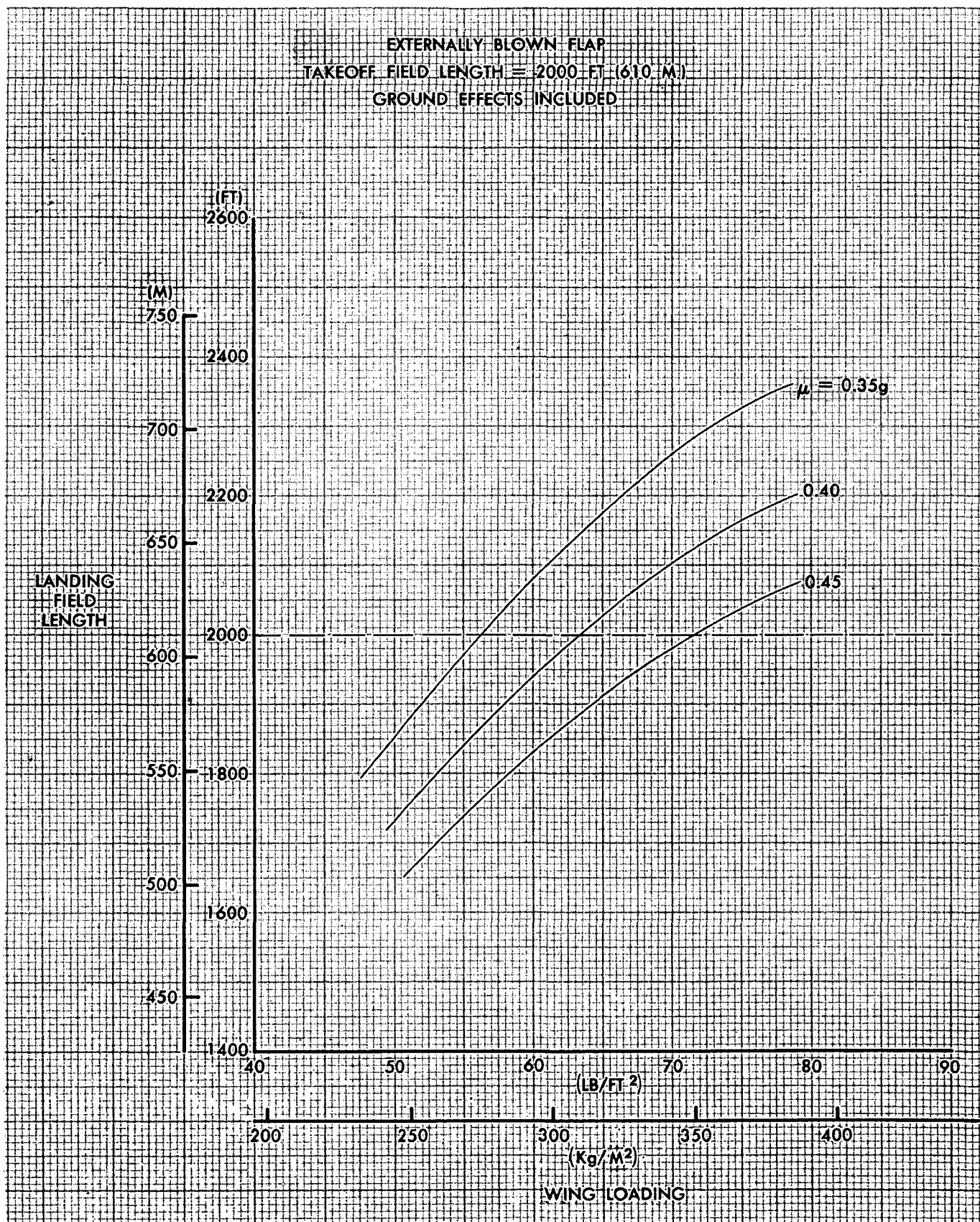


FIGURE 3-12. EFFECT OF DECELERATION RATE ON LANDING FIELD LENGTH

The 0.6 time-honored field length factor has been substantiated by studies using the Breguet 941 as shown in Table 3-16. This aircraft demonstrated a factor of 0.64 between operational and maximum effort landings. Figure 3-13 shows the direct relationship between this factor and design wing loading. Much additional actual flight experience with STOL aircraft is necessary to justify any change from the 0.6 factor.

On powered lift STOL aircraft, the ground effect phenomenon has been shown to be adverse in landing. A loss in lift experienced during the flare maneuvers when approaching the ground necessitates high flare heights and consequently long air run distances to achieve low touchdown sink rates. The impact of ground effects on an externally blown flap STOL aircraft are shown in Figure 3-14 for a 3 fps (.915 mps) touchdown sink rate.

There has been some concern, however, about the use of wind tunnel ground effects data for the prediction of aircraft flare characteristics for the following reasons:

- (1) There is an aerodynamic time lag required for the wing lift distribution to readjust to a height change of the wing above the ground plane. This time lag will be manifested as an effective reduction in the ground effects as the aircraft enters the ground proximity during approach.
- (2) The attitude of a flight aircraft relative to the ground plane and flight path angle differs from that in a wind tunnel. This difference is also expected to reduce the effective ground effects of the flight aircraft.

Table 3- 16

COMPARISON OF OPERATIONAL AND MAXIMUM PERFORMANCE
LANDING DISTANCE ON BREGUET 941

(43,000 lbs (94,600 kg) Gross Weight, 35 ft (10.7 m) Obstacle)

Operational Landing Distance (Mean + 3 σ value from 154 landings)	1,450 ft. (442 m)
Maximum Performance (17 landings)	930 ft. (283 m)
$\frac{\text{Maximum Performance Distance}}{\text{Operational Distance}} =$.64

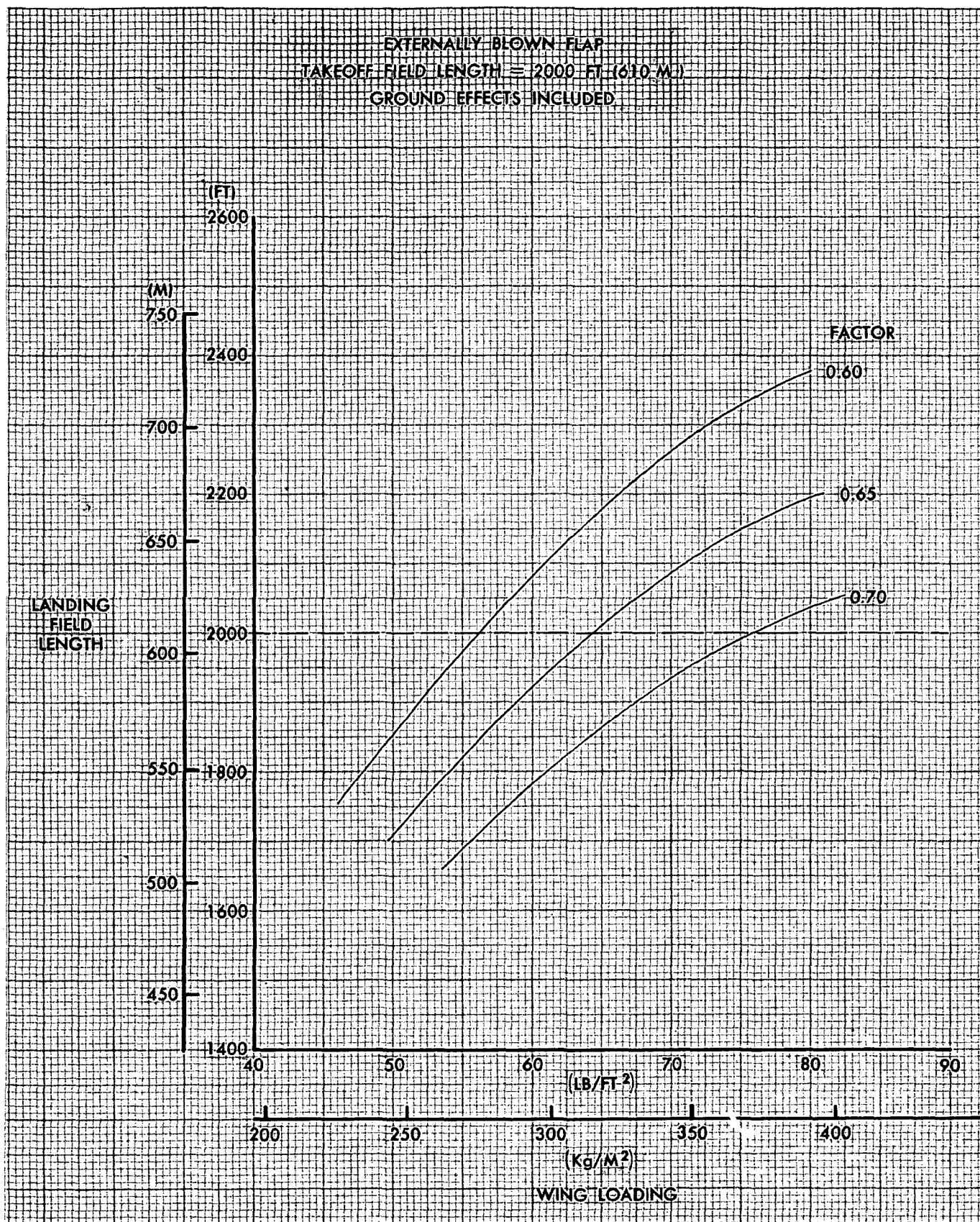


FIGURE 3-13. EFFECT OF FIELD LENGTH FACTOR ON LANDING FIELD LENGTH

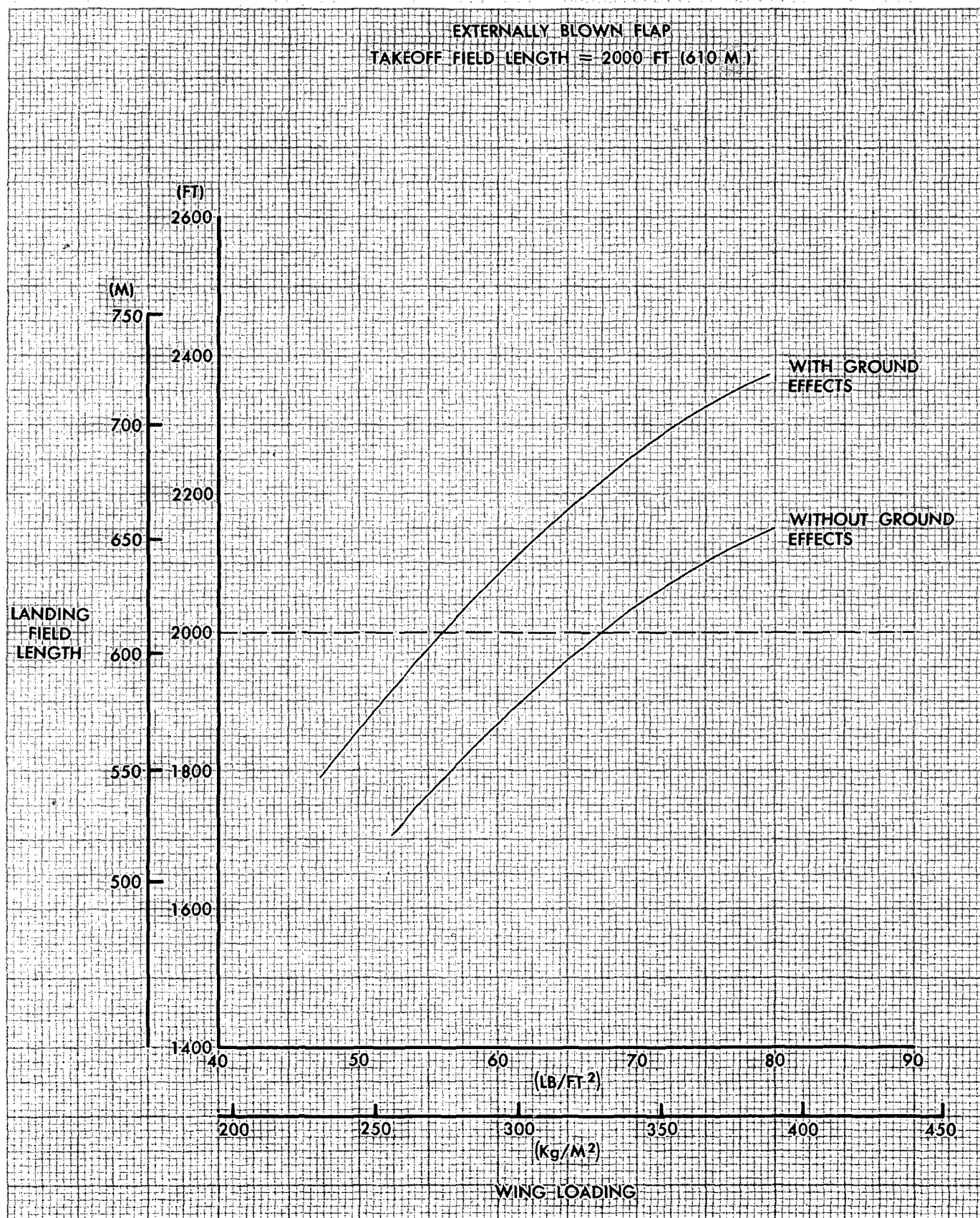


FIGURE 3-14. EFFECT OF GROUND EFFECT ON LANDING FIELD LENGTH

These effects are generally recognized by NASA and contractor personnel but are not fully understood nor quantitized at the present time.

The parametric sizing calculations do not include ground effects in order not to be unduly pessimistic. Ground effects are included in the final design work but are not as significant due to the compensating effects of the higher touchdown sink rate of 10 fps (3.05 m/s) in lieu of 3 fps (.915 m/s). A comparison of the parametric and final ground rules are shown in Figure 3-15. Elimination of ground effects from the parametric sizing calculations results in the parametric aircraft being similar to the final designs.

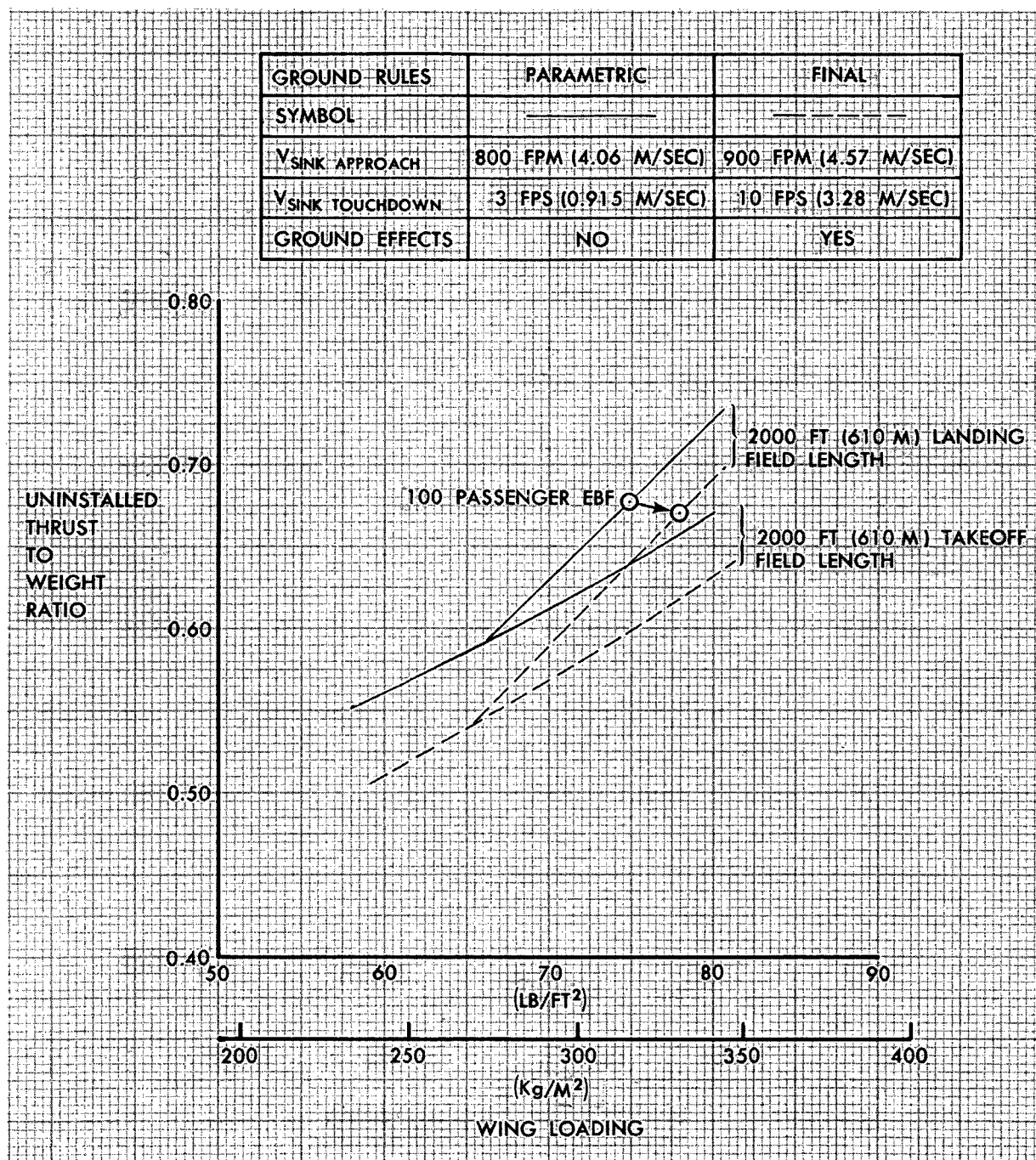


FIGURE 3-15. PARAMETRIC—FINAL LANDING GROUND RULES COMPARISON

3.5 Avionics Studies

3.5.1 Avionics Baseline. - A determination of the avionics requirements for STOL aircraft has been made from studies based on trends and forecasts in equipment characteristics, performance, reliability and costs. Included in the studies was an analysis of the navigation, guidance, control and flight management requirements for conformance with applicable ARINC specifications. Table 3-17 shows an equipment list for the STOL avionics referenced to present commercial and ARINC standards. This avionics system will provide category III A Fail Operational All Weather Operations (including Autoland).

3.5.2 Avionics Tradeoffs. - A trade-off study was made to reduce the avionics sophistication to meet the minimum requirements for Cat. II and IFR. The reduction was achieved as follows:

Cat. II (Fail Safe)

1. Third channel of the triplex Flight Guidance and Control system deleted.
2. Third vertical gyro deleted.
3. Third Air Data Computer deleted.
4. One Radio Altimeter system deleted.

I.F.R.

1. One Flight Guidance system deleted.
2. Simple Head-Up Display system only.
3. Delete remaining Radio Altimeter system.
4. One Microwave Landing System deleted.
5. One I.L.S. receiver deleted.

CODE: Source of Price

V - Vendor B - Buyer E - Estimate

K - Procurement Records

Table 3-17

AVIONICS EQUIPMENT LIST

SYSTEM: INTEGRATED FLIGHT GUIDANCE & CONTROL SYSTEM

ITEM NO.	WBS COST CODE	DESCRIPTION	PART NUMBER	VENDOR	NO. per A/C	RECURRING UNIT COST	SHIPSET COST	C O D E	REMARKS
1		IFGCS, INCLUDING:			1		386,707	V	
1a		FLT GUIDANCE & CONTROL SUBSYSTEM (SCAS, AP/FD, A/T, TMS, AREA NAV)		SPERRY			(168,207)		
1b		FLT INSTRUMENT SUBSYSTEM (EADI, EHSI, SYMBOL GENERATOR)		SPERRY			(52,100)		
1c		ELEVATOR LOAD FEEL SUBSYSTEM		SPERRY			(4,500)		
1d		ATTITUDE & HEADING REF. SUBSYSTEM		SPERRY			(29,850)		
1e		AIR DATA SUBSYSTEM (CRT DISPLAY, ADC)		SPERRY			(75,450)		
1f		SPOILER SUBSYSTEM ELECTRONICS		SPERRY			(8,600)		
1g		ACTUATORS		SPERRY	5		(16,000)		
2		HEAD-UP DISPLAY, INCLUDING					(32,000)	V	
2a		DEFLECTION AMPLIFIER	AO5A0149-1	CONDUCTRON					
2b		PROJECTION UNIT	AO5A0152-1	CONDUCTRON					
2c		CONTROL UNIT	AO5A0153-1	CONDUCTRON					

Table 3-17 (Cont'd)

AVIONICS EQUIPMENT LIST

SYSTEM: INTEGRATED FLIGHT GUIDANCE & CONTROL SYSTEM

[illegible]

CODE: Source of Price

V - Vendor B - Buyer E - Estimate

K - Procurement Records

Table 3-17 (Cont'd)
AVIONICS EQUIPMENT LIST

SYSTEM: AVIONICS

ITEM NO.	WBS COST CODE	DESCRIPTION	PART NUMBER	VENDOR	NO. per A/C	RECURRING UNIT COST	SHIPSET COST	C O D E	REMARKS
1a		VHF COMM TRANSCEIVER	522-4088-001 (618M-2B)	COLLINS	2	3925	7850	B	ARINC 546
1b		VHF COMM CONTROL PANEL	G3006	GABLES	2	615	1230	B	
1c		VHF ANTENNA	DMC50-3b	DORNE & MARGOLIN	2	200	400	B	
2a		SELCAL DECODER	NA-136	MOTOROLA	1	930	930	B	
2b		SELCAL CONTROL PANEL	G3009	GABLES	1	130	130	B	
2c		SELCAL CHIME	3001-1A	GARDIN ELECTRIC MFG CO.	1	15	15	B	
3a		MARKER BEACON RECEIVER	2087821-2802 (MKA-28C)	BENDIX	1	575	575	V	
3b		MARKER ANTENNA	522-0854-003 (37X-2)	COLLINS	1	72	72	B	
4a		PA AMPLIFIER	522-4538-002 (346D-1B)	COLLINS	2	1092	2184	B	ARINC 560
4b		ENTERTAINMENT TAPE REPRODUCER	108002-0008	SUNDSTRAND	1	4300	4300	B	ARINC 539A
5a		FLIGHT INTERPHONE AMPLIFIER	G3122(B)	GABLES	1	165	165	B	
5b		SERVICE INTERPHONE AMPLIFIER	G3122(B)	GABLES	1	165	165	B	

CODE: Source of Price

V - Vendor B - Buyer E - Estimate

K - Procurement Records

Table 3-17 (Cont'd)

AVIONICS EQUIPMENT LIST

SYSTEM: AVIONICS

ITEM NO.	WBS COST CODE	DESCRIPTION	PART NUMBER	VENDOR	NO. per A/C	RECURRING UNIT COST	SHIPSET COST	C O D E	REMARKS
5c		AUDIO CONTROL PANEL	G3004(A)	GABLES	4	543	2172	B	
6a		FLIGHT RECORDER	ED743830-1	HAMILTON STANDARD	1	3200	3200	B	ARINC 573-1
6b		ACCELEROMETER, TRIAXIAL	ED743831-1	HAMILTON STANDARD	1	800	800	B	
6c		FLIGHT DATA ENTRY PANEL	ED742986-1	HAMILTON STANDARD	1	900	900	B	
6d		FLIGHT DATA ACQUISITION UNIT (FDAU)	ED742951-1	HAMILTON STANDARD	1	4800	4800	B	
7a		VOICE RECORDER	103600	SUNDSTRAND	1	1500	1500	B	ARINC 557
7b		VOICE RECORDER CONTROL UNIT	103610-1	SUNDSTRAND	1	450	450	B	
8a		ILS RECEIVER	2070724-3203 (RIA-32)	BENDIX	2	3552	7104	V	ARINC 578
8b		GS ANTENNA	S41422-5	SENSOR SYSTEMS	2	100	200	B	
8c		ILS CONTROL PANEL	1990013-4	BENDIX	1	2000	2000	B	
9a		VOR RECEIVER	2070750-3301 (RVA-33A)	BENDIX	2	3500	7000	B	ARINC 579
9b		VOR/DME CONTROL PANEL	G3547(A)	GABLES	2	1000	2000	V	

CODE: Source of Price

V - Vendor B - Buyer E - Estimate

K - Procurement Records

Table 3-17 (Cont'd)
AVIONICS EQUIPMENT LIST

SYSTEM: AVIONICS

ITEM NO.	WBS COST CODE	DESCRIPTION	PART NUMBER	VENDOR	NO. per A/C	RECURRING UNIT COST	SHIPSET COST	CODE	REMARKS
9c		VOR/LOC ANTENNA COUPLER	100C0178	DAICO IND.	2	316	632	B	
9d		ANTENNA COUPLER	100C2035	DAICO IND.	2	104	208	B	
10a		ATC TRANSPONDER	787-6211-001 (621A-6)	COLLINS	2	3993	7986	B	ARINC 572
10b		ATC CONTROL PANEL	G3005	GABLES	1	315	315	B	
10c		ATC ANTENNA, BLADE	DMNI50-2	DORNE & MARGOLIN	2	26	52	B	
11a		RADIO ALTIMETER TRANSCEIVER	2067631-5151 (ALA-51A)	BENDIX	2	6240	12,480	V	ARINC 552A
11b		RADIO ALTIMETER INDICATOR	2067635-0703 (INA-51A)	BENDIX	2	1500	3000	V	
11c		ANTENNA, RADIO ALTIMETER	2070057-0701 (ANA-51D)	BENDIX	4	168	672	V	
12a		DME INTERROGATOR	522-4209-002 (860E-3)	COLLINS	2	8778	17,556	B	ARINC 568
12b		ANTENNA, DME	DMNI50-2	DORNE & MARGOLIN	2	26	52	B	
13a		ADF RECEIVER	777-1492-001 (51Y-7)	COLLINS	1	3267	3267	B	ARINC 570
13b		ADF CONTROL PANEL	787-6366-004 (614B-12)	COLLINS	1	756	756	B	

CODE: Source of Price

V - Vendor S - Buyer E - Estimate

K - Procurement Records

Table 3-17 (Cont'd)

AVIONICS EQUIPMENT LIST

SYSTEM: AVIONICS

ITEM NO.	WBS COST CODE	DESCRIPTION	PART NUMBER	VENDOR	NO. per A/C	RECURRING UNIT COST	SHIPSET COST	C O D E	REMARKS
13c		ANTENNA, LOOP	792-6010-001 (137A-6C)	COLLINS	1	342	342	B	
13d		ANTENNA COUPLER, SENSE	622-0346-001	COLLINS	1	141	141	B	
14a		WEATHER RADAR R/T UNIT	2070410-0106 (RDR-1F)	BENDIX	1	10,000	10,000	V	ARINC 564-1
14b		CONTROL PANEL, WEATHER RADAR	G2756	GABLES	1	472	472	B	
14c		INDICATOR, WEATHER RADAR	2070411-0105 (PPI-IL)	BENDIX	1	5000	5,000	V	
14d		ANTENNA, WEATHER RADAR	2070409-0101 (ANT-IT)	BENDIX	1	6510	6510	V	
15a		COLLISION AVOIDANCE SYSTEM	TBD	TBD	1	5000	5000	E	ARINC 590
16a		MICROWAVE LANDING GUIDANCE SYSTEM (SINGLE)	TBD	TBD	2	8000	16,000	E	COST BASED ON RTCA DO-148 MICROWAVE LANDING SYSTEM STUDY

CODE: Source of Price

V - Vendor B - Buyer E - Estimate

K - Procurement Records

SYSTEM: MISC. COCKPIT INSTRUMENTS

Table 3-17 (Cont'd)

AVIONICS EQUIPMENT LIST

ITEM NO.	WBS COST CODE	DESCRIPTION	PART NUMBER	VENDOR	NO. per A/C	RECURRING UNIT COST	SHIPSET COST	C O D E	REMARKS
1a		ATTITUDE INDICATOR, STANDBY	705-7-V9	SFENA	1	2000	2000	V	
1b		INVERTER, STATIC	TSG-420-101	SFENA	1	350	350	V	
2a		COMPASS, STANDBY	C4E	U.S. GAUGE	1	100	100	B	
3		FUEL FLOW INDICATOR	8DJ180LWC1	G.E.	1	1,756	1,756	K	
4		ENGINE N ₁ INDICATOR	8DJ202LW1	G.E.	1	2,917	2,917	K	
5		ENGINE N ₂ INDICATOR	8DJ186LWC1	G.E.	1	1,779	1,779	K	
6		ENGINE EGT INDICATOR	8DJ185LWB1	G.E.	1	1,784	1,784	K	
7		ENGINE EPR INDICATOR	8DJ184LWD1	G.E.	1	1,781	1,781	K	
8		ENGINE OIL PRESSURE INDICATOR	VIL-OC4A	U.S. GAUGE	4	163	652	K	
9		ENGINE OIL QUANTITY INDICATOR	8DJ172LWD1	G.E.	4	220	880	K	
10		FUEL FLOW TRANSMITTER	9-114-02	EDC	4	736	2,944	B	
11		ENGINE N ₁ TACH GENERATOR	9053M20P02	G.E.	4	798	3,192	E	

CODE: Source of Price

V - Vendor B - Buyer E - Estimate
K - Procurement Records

Table 3-17 (Cont'd)
AVIONICS EQUIPMENT LIST

SYSTEM: MISC. COCKPIT INSTRUMENTS

ITEM NO.	WBS COST CODE	DESCRIPTION	PART NUMBER	VENDOR	NO. per A/C	RECURRING UNIT COST	SHIPSET COST	C O D E	REMARKS
12		ENGINE N ₂ TACH GENERATOR	9015M78P02	G.E.	4	789	3,192	B	
13		ENGINE EPR TRANSMITTER	ED747599-1	HAM. STD.	1	1,175	1,175	K	
14		ENGINE EPR TRANSDUCER	ED747600-1	HAM. STD.	4	921	3,684	K	
15		BRAKE PRESSURE INDICATOR	AGK-10/A-27-51	BENDIX	2	250	500	V	
16		HYDRAULIC PRESSURE INDICATOR	AGK-10/A-27-51	BENDIX	3	250	750	V	
17		HYDRAULIC QTY. INDICATOR	9807-47	T.A. EDISON	3	105	315	K	
18		FLAP/SLAT POSITION INDICATOR	8DJ225WAA1	G.E.	1	1,700	1,700	K	
19		SURFACE POSITION INDICATOR	520642	WESTON	1	800	800	K	
20a		CLOCK, ELECTRONIC, DIGITAL	AL5580-P1	A.W. HAYDON	2	450	900	B	
20b		TIME BASE, ELECTRONIC	E31832-P1	A.W. HAYDON	1	1,320	1,320	B	
21a		MASTER WARN & CAUTION CONTROLLER	102300-1	ACTRON	1	3,716	3,716	V	
21b		MASTER WARN & CAUTION ANNUN.	102100-13	ACTRON	1	3,158	3,158	V	

Source of Price
V - Vendor B - Buyer E - Estimate
X - Procurement Records

SYSTEM: MISC. COCKPIT INSTRUMENTS

Table 3-17 (Cont'd)
AVIONICS EQUIPMENT LIST

[illegible]

CODE: Source of Price

V - Vendor B - Buyer E - Estimate

K - Procurement Records

SYSTEM: OPTIONAL AVIONICS

Table 3-17 (Cont'd)
AVIONICS EQUIPMENT LIST

ITEM NO.	WBS COST CODE	DESCRIPTION	PART NUMBER	VENDOR	NO. per A/C	RECURRING UNIT COST	SHIPSET COST	C O D E	REMARKS
1a		HF TRANSCEIVER	522-1501-041 (618T-2)	COLLINS	2	7551	15,102	B	ARINC 533
1b		CONTROL PNL, HF	522-2457-036 714E-3	COLLINS	2	312	624	B	
1c		COUPLER, ANTENNA, HF	(4905-1) 792-6140-001	COLLINS	2	7026	14,152	B	
1d		ANTENNA, ADAPTER, HF	(599H-5) 792-6464-001	COLLINS	1	312	312	B	
1e		MOUNT, COUPLER, ANTENNA, HF	(790S-4) 792-6461-001	COLLINS	1	375	375	B	
		DIGITAL DATA LINK INTERFACE			1		~15,000		

Table 3-18 provides a summary of the weight and cost savings per airplane by these reductions in avionics sophistication.

3.5.3 STOL ATC Environment. - Operating the STOL aircraft within the framework of the FAA's National Aviation System Plan will require it to function within the same air traffic control (ATC) environment that will exist for CTOL aircraft in the 1980/85 time period. Plans for the upgraded third generation ATC system scheduled for implementation during 1980/85 stress increased automation, two way data-link traffic flow control, computer aided rerouting, area navigation and microwave landing guidance systems. Reference to Figure 3-16 shows the third generation ATC system now being developed for the 1980's.

In the 1980/85 centrally managed ATC system, the responsibility for navigating STOL and CTOL aircraft will rest with the pilot and the responsibility for organizing a safe and expeditious flow of STOL and CTOL traffic into the terminal area will rest with the ATC controller. With the application of automatic controls, the controller on the ground and the STOL and CTOL pilots in the air will manage the air traffic navigation and control using automatic, semi-automatic or manual methods based upon computer derived planning information.

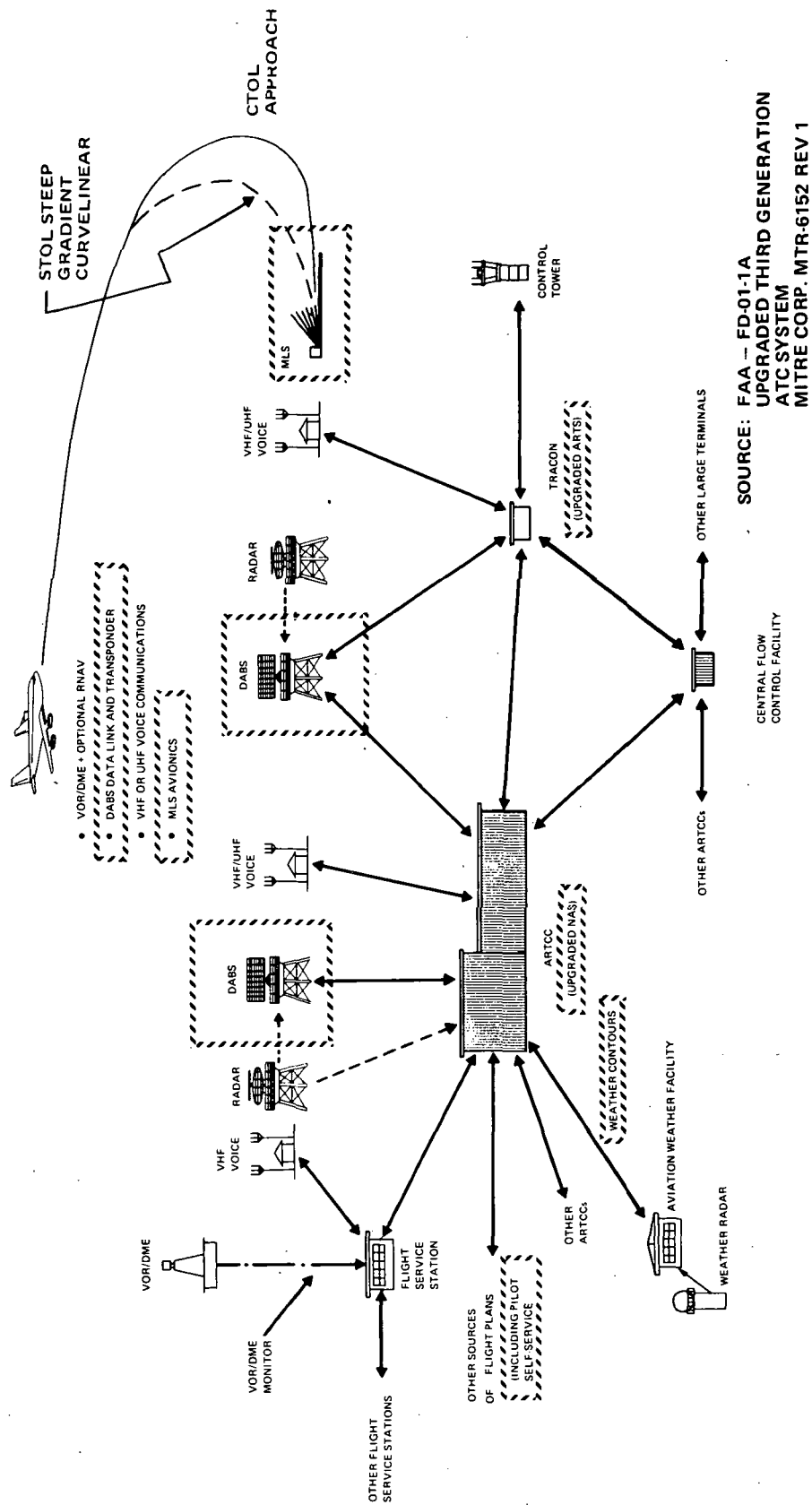
During automatic operation, the computer will determine and communicate ATC instructions to the STOL pilot. Semi-automatic operations will involve the automatic control of controller-delegated functions and/or require controller's approval of computer derived ATC instructions before they are transmitted to the aircraft.

TABLE 3-18

SUMMARY OF COST & WEIGHT SAVINGS FOR STOL AVIONICS

AVIONICS SUBSYSTEM	CAT III		CAT II		IFR		IFR (Less Weather Radar)	
	WEIGHT 1b (kg)	COST \$	WEIGHT 1b (kg)	COST \$	WEIGHT 1b (kg)	COST \$	WEIGHT 1b (kg)	COST \$
IFGCS	702 (318)	386,707	661 (300)	311,707	610 (277)	291,707	610 (277)	291,707
Comm & Nav	665 (302)	140,583	646 (293)	132,507	507 (230)	104,093	457 (207)	82,093
Engine Insts & Misc Cockpit Instst	159 (72)	43,945	159 (72)	43,945	159 (72)	43,945	159 (72)	43,945
TOTALS	1,526 (692)	571,235	1,466 (665)	488,159	1,276 (579)	439,745	1,226 (556)	417,745

UPGRADED THIRD GENERATION CONUS ATC SYSTEM



INDICATES A CHANGE FROM
PARAMETRIC TO FINAL
BASELINE SYSTEM

PR3-STOL-1586 A

FIGURE 3-16

The STOL pilot will have the option to direct his aircraft in response to ATC clearances by an automatic, semi-automatic or manual operation. An automatic operation will allow ATC instructions to be fed directly into the airborne computer and simultaneously display instructions to the pilot. The ATC instructions will not control the STOL craft until verified by the pilot. Semi-automatic operations will require pilot acceptance of the displayed ATC instructions before they are given to the airborne computer. Manual operation relates to the pilot receiving and complying with ATC instructions without the aid of an automatic airborne device. The 1980/85 ground systems will be capable of communicating simultaneously via a universal air-ground digital communications system and a Discrete Address Beacon System (DABS) to accommodate the different and varying needs of STOL and CTOL aircraft users.

In this time period, closely spaced non-conflicting flight paths will be established to maximize capacity in congested areas. STOL aircraft will need to be equipped with airborne guidance and control systems capable of accurately following such paths and each other. The number and use of closely spaced flight paths within any given area (arrival, departure, transition, enroute) will depend upon the associated ATC procedures and whether STOL aircraft diverge from or converge to a particular location and the amount of airspace that is available.

The ability of one STOL aircraft to follow another, referred to as "station keeping" will be utilized by ATC when in-trail operations are required.

Improved avionics air data systems will allow the use of one thousand feet vertical separation criteria in both low and high altitude corridors.

Airborne computers, area navigation and microwave landing systems will provide the STOL aircraft pilot with the ability to follow any ATC assigned four dimensional flight path including high angle curvilinear approaches to touchdown.

3.6 Ride Qualities Study

The major objective of this study was to investigate the ride qualities characteristics of a typical low wing loading EBF type aircraft and to explore the effects of various stability and control augmentation concepts on aircraft response in turbulence. The intention was to identify some of the potential problems which arise in attempting to provide satisfactory ride qualities for STOL aircraft with low values of wing loading.

This section is a summary of the conclusions of this study with the technical justification presented in Appendix G.

This initial study concentrated on aircraft dynamic behavior in the approach mode and used the Dryden turbulence model from the flying qualities specification MIL-F-8785B (Reference 2) to provide external disturbances. A basic RMS value of 10 ft/sec (3.05 m/s) was chosen for the turbulence model as representing a realistic level of gust activity for the approach mode.

Use of the elevator for gust suppression was investigated utilizing pitch rate and normal acceleration feedback. Normal acceleration feedback to elevator although providing reduced aircraft activity in turbulence created basic stability problems unless the gains were maintained at a relatively low value thus limiting system effectiveness.

A much more effective technique for reducing aircraft normal acceleration activity in turbulence was to use normal acceleration feedback to spoiler surfaces and to utilize pitch rate feedback to elevator as a means of providing the necessary damping signals. Since the use of spoiler surfaces for this function is feasible only for the approach mode it is

necessary to explore alternate solutions for cruise and transition flight regimes.

For the lateral/directional axes for the approach mode, several stability and control configurations were investigated. Lateral acceleration feedback to rudder was found to be undesirable for the approach mode due primarily to destabilizing effects on the basic airframe spiral and dutch roll mode.

The use of roll rate and roll attitude feedback to the ailerons in conjunction with a conventional yaw damper (yaw rate feedback to rudder) proved to be very effective for reducing aircraft lateral acceleration activity in turbulence. This type of system also provides adequate stability for basic airframe spiral and dutch roll modes in the approach configuration. Since the basic airframe spiral mode normally has adequate stability in the cruise flight regime, lateral acceleration feedback to the rudder may prove to be an effective technique for these flight conditions.

3.7 Alternate Missions

The capability of extending the range of a STOL aircraft by flying from longer runways with increased fuel load would provide an airline with increased marketability and scheduling flexibility. This capability is not free, however, since a penalty in structural weight must be paid to maintain aircraft design load factor at the higher gross weights.

Two 150 passenger externally blown flap aircraft were synthesized for comparison to the final design EBF 150 passenger, 3000 foot (914 m) field length aircraft. They were designed with 3000 foot (914 m) STOL capability for ranges up to 575 statute miles (926 km) and, by loading extra fuel, to fly from longer fields with maximum ranges of 1035 and 1380 statute miles (1668 and 2224 km) with maximum payload.

The fuel allowance for the reserve hold segment of the sizing mission was increased from 0.25 hours at 575 statute miles (926 km) to 0.50 hours at 1035 statute miles (1668 km) and 0.75 hours at 1380 statute miles (2224 km) to provide contingency fuel comparable to CTOL aircraft at the longer ranges. Operational items were increased at the two longer ranges by 480 and 960 pounds (218 and 435 kg), respectively, to provide additional passenger services normally associated with longer flights.

A performance summary comparing the three aircraft is shown in Table 3-19 and a weight summary in Table 3-20. Increases in manufacturers empty weight (MEW) of 820 and 1215 pounds (372 and 551 kg) respectively were necessary to provide the required structural beefup for the 1035 and 1380 statute mile (1668 and 2224 km) range capability. The associated cost penalties at 575 statute miles (926 km) for the two aircraft, 0.4 and 0.6 percent, are

Table 3-19

EXTERNALLY BLOWN FLAP STOL AIRCRAFT
EXTENDED RANGE CAPABILITY PERFORMANCE SUMMARY

	Base	1035 St.Mi. (1668 m)	Extended Range	1380 St.Mi. (2224 m)	Extended Range
Passengers	150	150	150	150	150
Field Length ft (m)	3,000 (914)	3,000 (914)	3,540 (9,079)	3,000 (914)	4,090 (1,247)
Range st mi (km)	575 (925)	575 (926)	1,035 (1,668)	575 (926)	1,380 (2,224)
TOGW lb (kg)	149,000 (67,600)	149,900 (68,000)	159,800 (72,500)	150,400 (68,200)	168,300 (76,300)
Wing Area ft ² (m ²)	1,461 (135.7)	1,470 (136.6)	1,470 (136.6)	1,474 (136.9)	1,474 (136.9)
Thrust/Engine lb (N)	18,260 (81,220)	18,370 (81,710)	18,370 (81,710)	18,420 (81,940)	18,420 (81,940)
W/S lb/ft ² (kg/m ²)	102.0 (498)	102.0 (498)	108.7 (531)	102.0 (498)	114.2 (558)
T/W	0.490	0.490	0.460	0.490	0.44
Aspect Ratio	8.0	8.0	8.0	8.0	8.0
Cruise Mach Number	0.69	0.69	0.67	0.69	0.65
Cruise Altitude ft (m)	26,000 (7,925)	26,000 (7,925)	26,000 (7,925)	26,000 (7,925)	26,000 (7,925)
D.O.C. @ 575 st mi (926 km) ϕ /ASSM (ϕ /ASKM)	2.08 (1.29)	2.09 (1.30)	1.88 (1.17)	2.09 (1.30)	1.84 (1.14)

TABLE 3-20

EXTENDED RANGE CAPABILITY WEIGHT SUMMARY

	Mission Range - statute miles (km)					
	Base Case Weight		Extended Range Weight			
	English 575	Metric 926	English 1035	Metric 1667	English 1380	Metric 2222
<u>GEOMETRY DATA</u> Wing Area Wing Loading (STOL/CTOL) Horiz/Vert Tail Area Horiz/Vert Tail Volume SLS Thrust (uninst)/TOGW (CTOL/STOL) SLS Thrust (uninst)/Eng Mission Fuel Weight/TOGW	1,461 102 419/319 1.426/.1238 .49 18,260 .110	135.7 498 38.9/29.6 1.426/.1238 .49 81,220 .110	1,470 102/109 421/322 1.419/.1237 .46/.49 18,370 .162	136.6 498/530.6 39.1/29.9 1.419/.1237 .46/.49 81,710 .162	1,474 102/114 421/323 1.416/.1237 .44/.49 18,420 .199	136.9 498/557.6 39.1/30.0 1.416/.1237 .44/.49 81,940 .199
	1b	kg	1b	kg	1b	kg
	18,070 4,625 23,405 6,260 18,690 28,720	8,196 2,098 10,616 2,840 8,478 13,027	18,465 4,655 23,605 6,300 18,795 28,770	8,376 2,111 10,707 2,858 8,525 13,050	18,585 4,665 23,765 6,330 18,850 28,790	8,430 2,116 10,780 2,871 8,550 13,059
	99,770 2,840 102,610 30,000 132,610 16,390 149,000	45,255 1,288 46,543 13,608 60,151 7,434 67,585	100,590 3,325 103,915 30,000 133,915 25,885 159,800	45,627 1,508 47,135 13,608 60,743 11,741 72,484	100,985 3,800 104,785 30,000 134,785 33,515 168,300	45,806 1,723 47,529 13,608 61,137 15,202 76,339
	149,000	67,585	149,900	67,993	150,400	68,220
	STOL Takeoff Gross Weight					
<u>WEIGHT DATA</u> Wing Tail Fuselage Landing Gear Propulsion System Remaining Weight						
Manufacture Empty Weight						
Operational Items						
Operational Empty Weight						
Mission Payload						
Mission Zero Fuel Weight						
Mission Fuel Weight						
Takeoff Gross Weight						

extremely small as illustrated by the DOC-Range curves of Figure 3-17. On the longer range routes, however, they are not very efficient when compared to an advanced CTOL aircraft. The 27 percent increase in direct operating cost (DOC) over the CTOL aircraft at 1380 statute miles (2224 km) is due to a number of factors including higher gross weight of the EBF aircraft, increased initial and maintenance cost of four engines vs two, different design noise criterion, and the large difference in cruise speed (primary effect). Initial cruise Mach number for the EBF STOL aircraft was 0.69 at the 575 statute mile (926 km) design range. This drops to 0.65 at 1380 statute miles (2224 km) due to the decrease in thrust-to-weight ratio at the higher gross weights compared to 0.80 for the CTOL. Direct operating cost becomes increasingly sensitive to cruise speed as range is increased.

The takeoff field lengths for the extended range aircraft, 4090 feet (1247 m) at the takeoff gross weight for a 1380 statute mile (2224 km) flight, are still shorter than most existing airport runways.

In summary, the cost penalties to a STOL aircraft for providing extended range capability are very small, but these aircraft will tend to be at an economic disadvantage on longer routes when compared to a CTOL aircraft. If an airline's route structure demands range flexibility it may be better from a total airline cost viewpoint to occasionally use a STOL aircraft with extended range capability on a few longer range routes rather than to buy two types of aircraft.

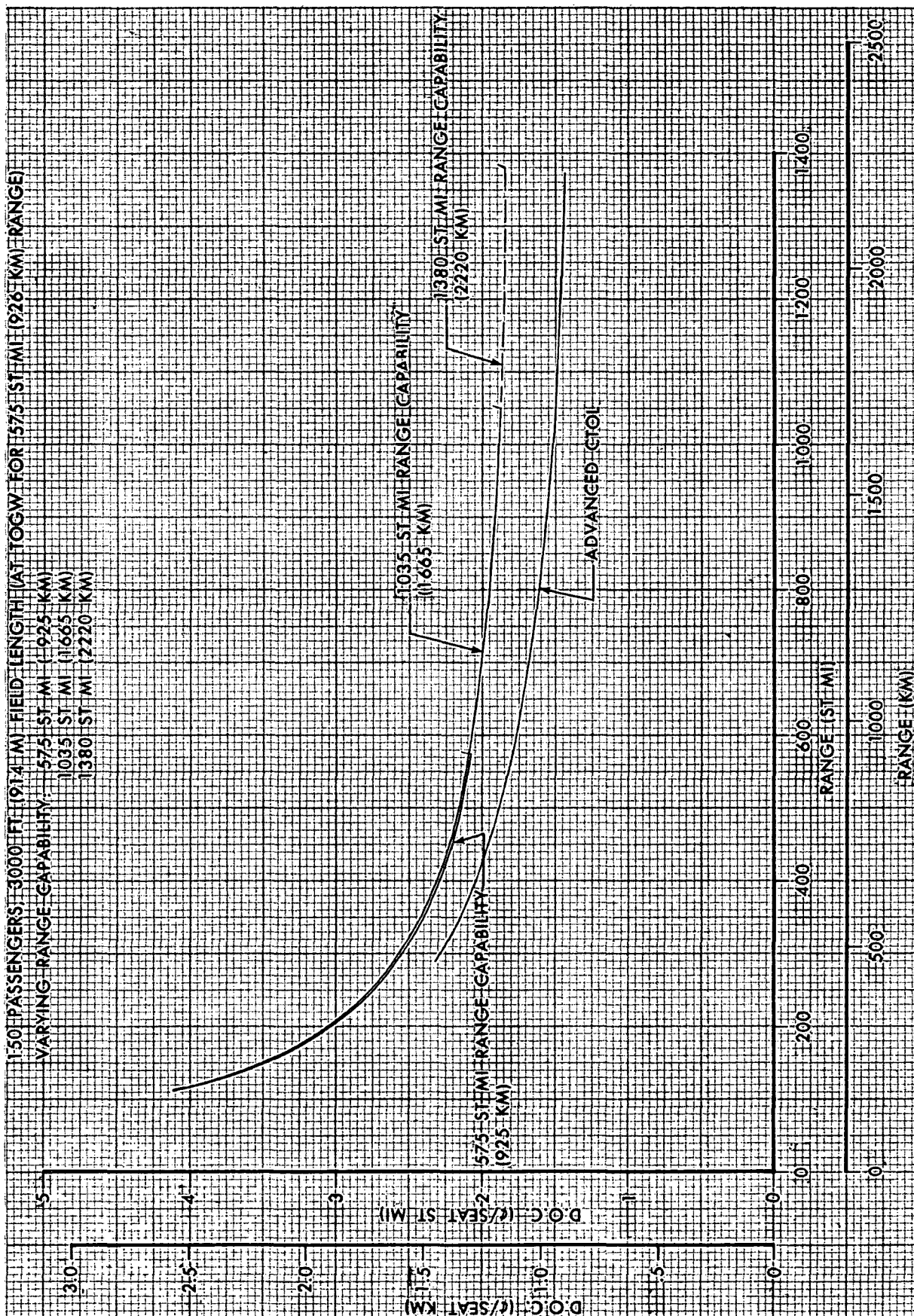


FIGURE 3-17. DIRECT OPERATING COST PENALTY FOR EXTENDED RANGE CAPABILITY
EXTERNALLY BLOWN FLAP AIRCRAFT

3.8 Advanced Composite Materials Study

This section presents results of a study to assess the impact of application of advanced composite materials to a typical STOL aircraft structure. The final design EBF 150 passenger, 3000 foot (915 m) field length aircraft was used as a base for the study. The information summarized in this section is based on an extension to the prime contract entitled "A Study of the Costs and Benefits of the Application of Composite Materials to Civil STOL Aircraft", Contract NAS2-6994-1. The details of the composite study may be found in its final report.

Materials considered in the study are limited to advanced composites, although other materials show advantageous application as demonstrated in References 3 and 4. Comparison of specific strengths and stiffnesses of metals and composites demonstrates a marked advantage for composite. While specific properties do not present a complete picture for assessment of material applications, when the leverage of resizing due to reduced structural weight is considered, composite materials have a greater potential than metals and justifies their detailed consideration.

3.8.1 Aircraft Resizing. - Using the detailed structural analyses performed for the above referenced composite study, the baseline 150 passenger, 3000 foot (914 m) field length EBF aircraft was redesigned using advanced composites. The composite aircraft was designed to meet the same performance requirements as that of the final design conventional metal structure airplane.

A summary size and weight breakdown for the composite airplane is given in Table 3-21, and is compared to the baseline metal airplane. A summary of performance characteristics for the two airplanes is given in Table 3-22. It is seen that the gross weight is reduced from 149,000 pounds (67,600 kg) to 132,300 pounds (60,000 kg), or approximately an 11 percent reduction. A planview comparison of the composite airplane compared to the baseline airplane is shown in Figure 3-18. It should be noted that the fuselage size is constrained by passenger requirements and cannot be physically reduced.

3.8.2 Structural Description. - The approach to structural design for the composite study considered a wide application of composite materials in the airframe primary structure. The applications developed are shown in Figure 3-19. Design concepts considered are keyed to manufacturing capabilities that are improvements of existing procedures, rather than development of new techniques. Despite the necessary remaining development required to realize the anticipated applications, the designs discussed are felt to be practicably obtained within the study time period.

The composite fuselage has honeycomb skin panels with an aluminum core and graphite/epoxy face sheets. No stringers are required and the honeycomb panels are supported on fiberglass zee-section frames. Frame caps are reinforced with unidirectional graphite.

Major frames for landing gear support and wing attachment utilize aluminum fittings and the adjacent portion of the frame is also fabricated of aluminum. This portion is in turn spliced to composite upper and lower frame segments.

Table 3-21

ADVANCED MATERIALS AIRCRAFT WEIGHT COMPARISON

VEHICLE DESCRIPTION	CONVENTIONAL	COMPOSITE	PERCENTAGE CHANGE
Wing Area ft ² (m ²)	1,461 (136)	1,285 (119)	- 12.0
Horizontal Tail Area ft ² (m ²)	419 (38.9)	385 (35.8)	- 8.1
Vertical Tail Area ft ² (m ²)	319 (29.6)	272 (25.3)	- 14.7
Rated Thrust per Engine lb (N)	18,250 (81,180)	16,410 (73,000)	- 10.1
Wing Loading lb/ft ² (kg/m ²)	102 (498)	103 (503)	+ 1.0
Rated Thrust Loading	0.490	0.496	+ 1.2
WEIGHTS			
Wing	18,070 (8,196)	12,798 (5,805)	- 29.2
Horizontal Tail	2,580 (1,170)	1,809 (820)	- 29.9
Vertical Tail	2,045 (928)	1,235 (560)	- 39.6
Fuselage	23,405 (10,616)	19,531 (8,859)	- 16.6
Landing Gear	6,260 (2,839)	5,559 (2,522)	- 11.2
Propulsion	18,691 (8,479)	15,086 (6,843)	- 19.3
Fuel System	779 (353)	731 (332)	- 6.2
Aux. Power Unit	950 (431)	950 (431)	0
Flight Controls	3,500 (1,588)	3,297 (1,495)	- 5.8
Instruments	1,175 (533)	1,175 (533)	0
Hydraulics	1,278 (580)	1,204 (546)	- 5.8
Pneumatics	1,007 (456)	949 (430)	- 5.8
Electrical	2,590 (1,175)	2,590 (1,175)	0
Avionics	1,760 (798)	1,760 (798)	0
Furnishings	13,690 (6,210)	13,690 (6,210)	0
Air Conditioning	1,430 (649)	1,430 (649)	0
Ice Protection	530 (240)	496 (225)	- 6.4
Handling Gear	30 (14)	30 (14)	0
MFG. EMPTY WEIGHT	99,770 (45,255)	84,320 (38,247)	- 15.5
Operator's Items	2,840 (1,288)	2,820 (1,279)	- 0.7
OPER. EMPTY WEIGHT	102,610 (46,543)	87,140 (39,526)	- 15.1
Payload	30,000 (13,608)	30,000 (13,608)	0
Fuel	16,390 (7,434)	15,160 (6,876)	- 7.5
TAKEOFF WEIGHT	149,000 (67,585)	132,300 (60,010)	- 11.2

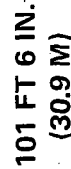
Table 3-22

ADVANCED MATERIALS AIRCRAFT SUMMARY
Externally Blown Flap Configuration

Structure		Conventional	Composite
Passengers		150	150
Design Field Length	ft (m)	3,000 (914)	3,000 (914)
Engine (4)		PD287-3	PD287-3
TOW	lb (kg)	149,000 (67,600)	132,300 (60,000)
Wing Area	ft ² (m ²)	1,461 (136)	1,285 (119)
Rated Thrust/Engine	lb (N)	18,260 (81,220)	16,410 (73,000)
W/S	lb/ft ² (kg/m ²)	102 (498)	103 (503)
T/W		0.490	0.496
Aspect Ratio		8	8
Cruise Mach Number		0.69	0.68
Cruise Altitude	ft (m)	26,000 (7,925)	25,000 (7,620)
D.O.C. @ 575 st mi (926 km)	φ/ASSM (φ/ASKM)	2.08 (1.29)	2.05 (1.19)

EXTERNALLY BLOWN FLAP

150 PASSENGERS



PR3-STOL-1674 A

COMPOSITE APPLICATION TO STOL FINAL DESIGN

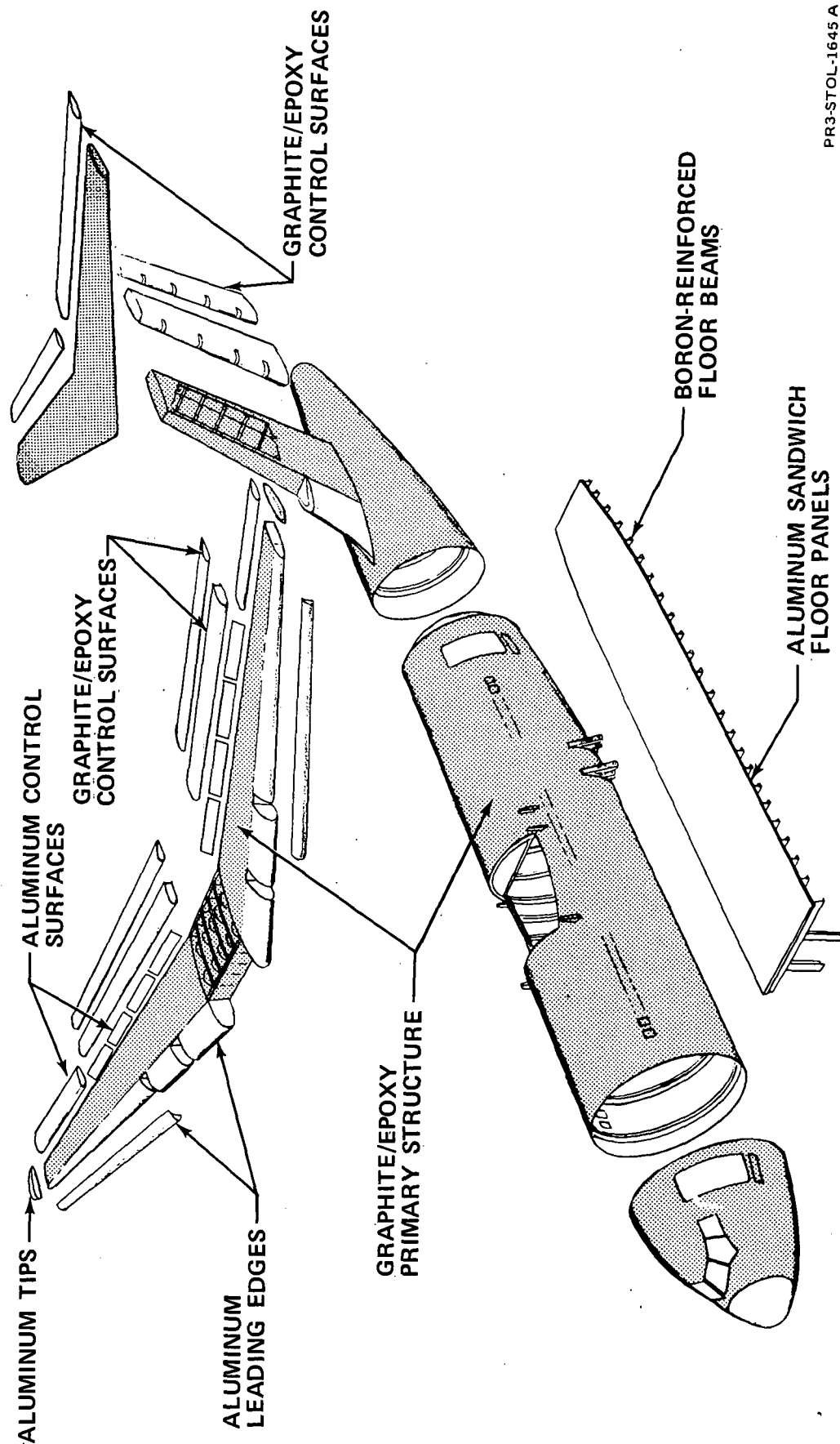


FIGURE 3-19

PR3-STOL-1645 A

The wing consists of a multi-rib structural box, two-segment flaps, ailerons, and leading edge structure with leading edge slats and an inboard drooped leading edge. The wing structural box is of composite construction with graphite/epoxy faced honeycomb sandwich skin, spars, and ribs. Bulkheads support flap and aileron loads. These control surfaces are supported by aluminum fittings which are attached by bolts to the composite structure.

The skin panels are made from an aluminum honeycomb core with graphite/epoxy face sheets. Inserts of unidirectional graphite in the spar cap areas assist in carrying bending loads. Spar caps are fabricated from a graphite/epoxy layup with a predominance of 0° fibers. Spars and ribs are also fabricated as honeycomb panels and bonded on assembly. The upper skin panel is bolted and bonded to the assembly of the ribs, spars, and lower panel. Engine pylons are attached to their support bulkheads through aluminum fittings bolted to the pylon and wing structure.

Control surfaces are primarily full-depth honeycomb construction with a thin composite skin for the smaller surfaces, such as rudders and elevators. Large control surfaces such as the flaps are built of honeycomb spars and skin panels. Metal components shown were selected primarily for lightning protection and environmental considerations with the spoiler and aileron designs chosen from cost considerations.

The empennage is also fabricated from graphite/epoxy composites. The horizontal stabilizer is a multi-rib, two spar design consisting of a multi-rib substructure, and upper and lower skins. The vertical stabilizer is a multi-rib design with front and rear spars to support the horizontal

surfaces at the upper end of the vertical stabilizer. This construction is similar to that of the wing with skins, spars and ribs fabricated as honeycomb panels.

3.8.3 Conclusions. - The use of composite materials for primary aircraft structure will produce a significant reduction in TOGW compared to an all metal airplane. It is expected that even greater weight savings would exist for those configurations with higher all metal weights or shorter field lengths due to their higher growth factors. Growth factors are discussed in Section 3.3.

Final data from the STOL Composites Study are not complete, but preliminary results indicate that the composite airplane will develop a slightly lower DOC than the baseline design. In general, manufacturing costs for the composite airplane are less than the baseline airplane, but are nearly offset by increased material costs. Maintenance costs for the composite airplane, which may be significantly higher than those for an all metal aircraft, are currently being evaluated.

While detailed conclusions must await completion of the economic analysis, it is tentatively concluded that under the ground rules of the STOL Composite Study, applications of advanced composites to primary airframe structure can be cost-effective.

3.9 Military/Commercial Commonality

An analysis was made to investigate the economic tradeoffs of military/commercial commonality. A typical aircraft designed to meet a military STOL transport mission is shown in Figure 3-20. This aircraft is designed to operate from 2000 foot (610 m) fields, based on military takeoff and landing requirements, with a payload of 28,000 pounds (12,700 kg) and fuel for 575 statute miles (926 km) plus normal military reserves. From this design, a commercial transport was derived having the same general dimensions as shown in Figure 3-21. The commercial transport would carry 151 passengers for a design range of 575 statute miles (926 km), and can operate from 2700 foot (823 m) length fields based on the takeoff and landing criteria used for the final design aircraft. The military STOL transport is an externally blown flap configuration powered by four advanced technology engines rated at 18,900 pounds (84,000 N) at sea level standard (SLS) day conditions. This engine has a bypass ratio of six, and the installation has no acoustical treatment.

The commercial derivative airplane (Model 24C) has an engine which uses the same engine core as the military transport. The military engine, which has a fan pressure ratio of about 1.6, is replaced for commercial use by a variable pitch fan with a 1.32 fan pressure ratio. The resulting engine has a bypass ratio of about 13.5 and is rated at 24,000 pounds (106,700 N) at sea level standard day conditions. The variable pitch fan is used for thrust reversing on this aircraft. With acoustical treatment lining the internal nacelle walls, but without treated rings, the aircraft has an estimated sideline noise level of 102 EPNdB at 500 feet (152 m) assuming 1980 technology.

MILITARY STOL TRANSPORT

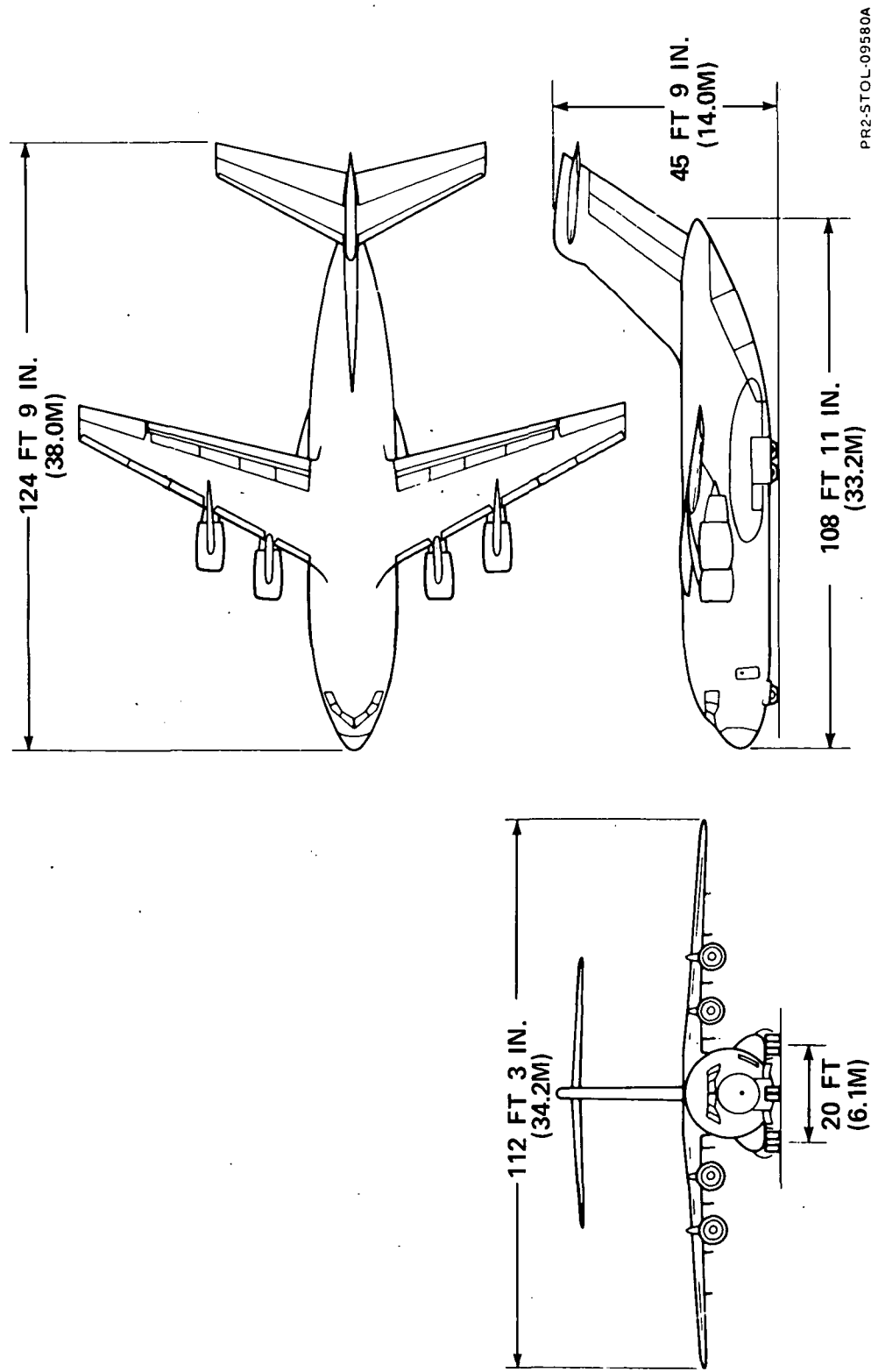


FIGURE 3-20

MODEL 24C

GENERAL ARRANGEMENT

COMMERCIAL DERIVATIVE OF MILITARY TRANSPORT

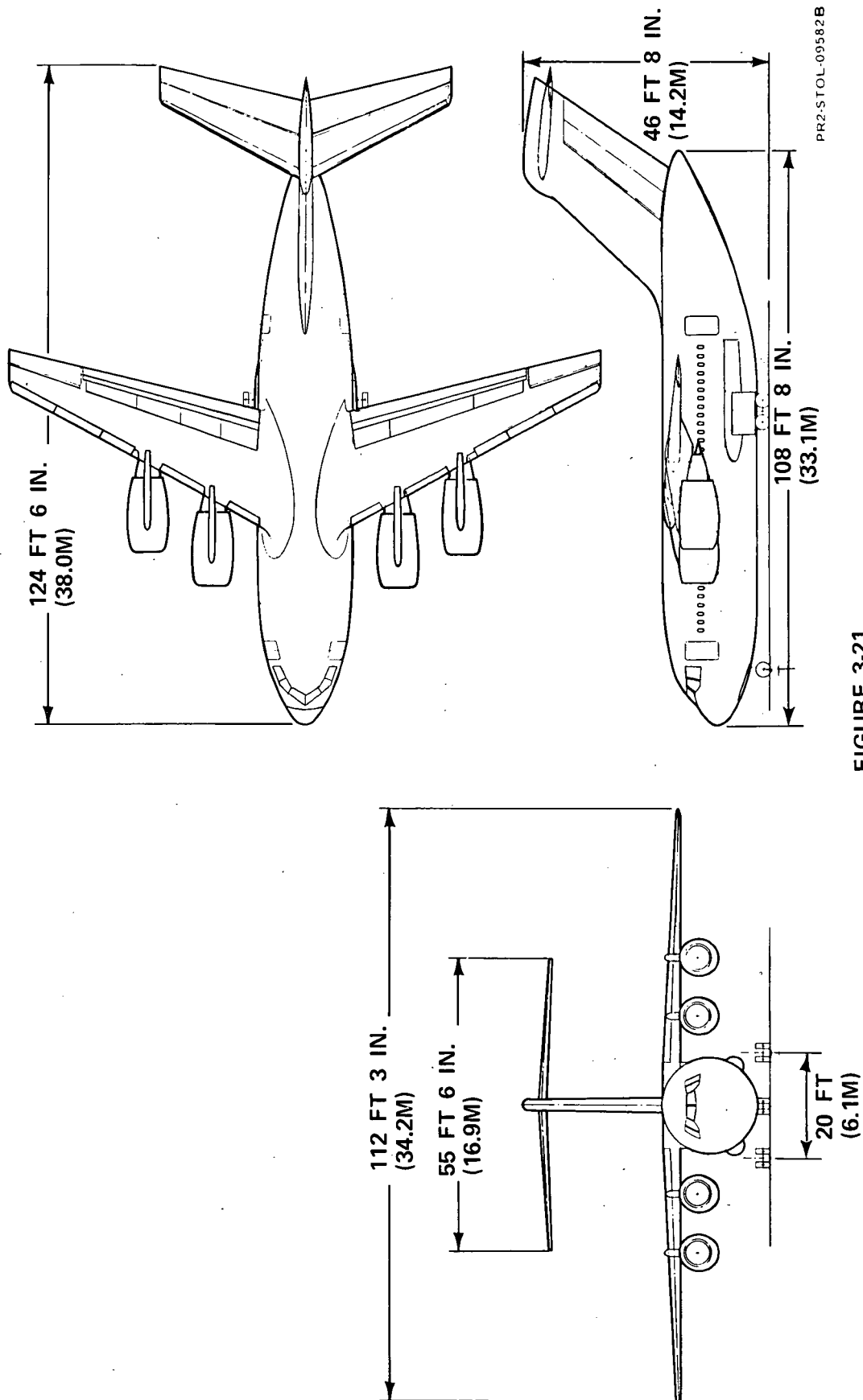


FIGURE 3-21

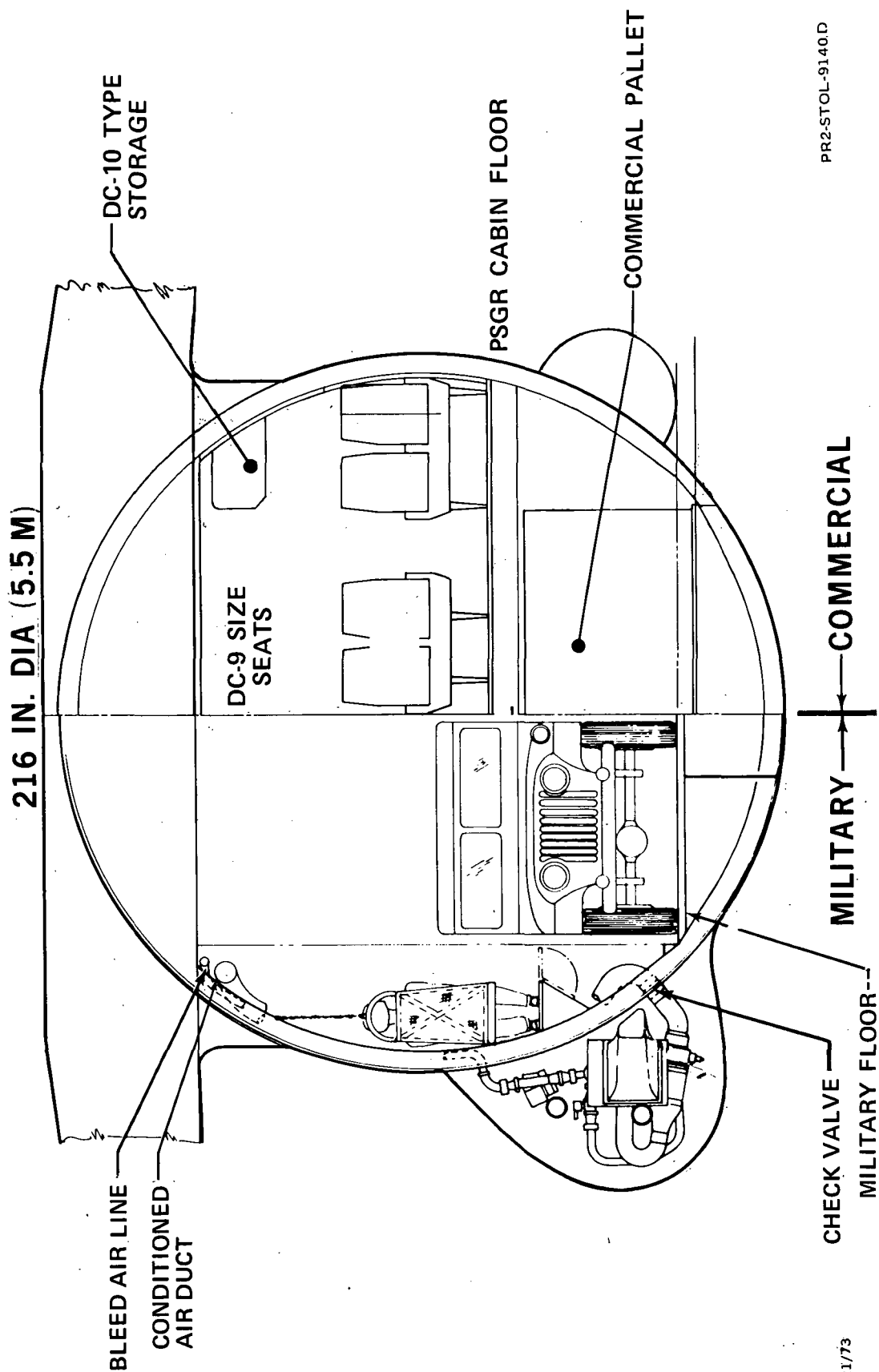
Adding acoustically absorptive rings in the inlet and fan discharge ducts would reduce the overall noise only slightly but DOC would be increased approximately ten percent.

The military STOL transport fuselage has a diameter of 216 inches (5.5 m) which allows a double aisle and 151 passenger 8-abreast seating in the commercial version. The military aircraft is typical of cargo configurations featuring low cargo floors to facilitate loading through a rear clam-shell door. A comparison of the military and commercial cross sections is shown in Figure 3-22. The military configuration does not permit landing gear retraction into the belly compartment and leads to a sponson type gear fairing. Although the same shell size is used in the commercial aircraft, the floor is located higher which permits space for baggage, cargo, and landing gear retraction into the belly compartment. The wing, vertical and horizontal tail are 100 percent common. Some of the other components, such as, wing and tail attach structure in the fuselage, the pilot's compartment, flight controls, and the various systems have commonality in varying degrees. The engine pylon stations in the military version were located slightly further outboard than normally would be required in order to provide proper spacing for the larger diameter engines of the commercial derivative.

Table 3-23 is a detailed weight breakdown of the two aircraft and shows that 44.5 percent of the commercial cost weight and 48.6 percent of the military cost weight are common parts of the two aircraft. Table 3-24 compares the characteristics of the military STOL transport and the commercial Model 24C. The T/W ratios are based on the uninstalled sea level standard engine thrust ratings. The high cruise Mach number of 0.78 compared to 0.69

FUSELAGE CROSS SECTION

151 PSGR DC-9 SEATS



PR2-STOL-9140 D

2/21/73

FIGURE 3-22

TABLE 3-23

COST WEIGHT COMMONALITY COMPARISON
MILITARY STOL VS MODEL 24C

DETAIL WEIGHTS: UNIT OF MASS	MILITARY STOL		COMMON		NEW		MODEL 24C	
	LBS	kg	LBS	kg	LBS	kg	LBS	kg
Wing	18,140	8,228	18,140	8,228	--	--	18,140	8,228
H-Tail	3,490	1,583	3,490	1,583	--	--	3,490	1,583
V-Tail	3,250	1,474	3,250	1,474	--	--	3,250	1,474
Fuselage	25,610	11,617	4,540	2,059	20,370	9,240	24,910	11,299
Landing Gear	8,130	3,688	--	--	6,880	3,121	6,880	3,121
Propulsion	18,780	8,518	--	--	24,345	11,043	24,345	11,043
Fuel System	1,260	572	795	361	--	--	795	361
Aux Power Unit	650	295	580	263	140	64	720	327
Flight Controls	4,230	1,919	3,830	1,737	200	91	4,030	1,828
Instruments	1,740	789	870	395	870	395	1,740	790
Hydraulic System	1,710	776	1,520	689	90	41	1,610	730
Pneumatic System	580	263	535	243	185	84	720	327
Electrical (incl. Lighting System)	2,230	1,011	2,120	962	865	392	2,985	1,354
Avionics	2,100	953	700	317	1,060	481	1,760	798
Furnishings	6,470	2,935	300	136	12,870	5,837	13,170	5,973
Air Conditioning	880	399	880	399	600	272	1,480	671
Ice Protection	590	267	580	263	10	5	590	268
Handling Fittings	150	68	15	7	20	9	35	16
Manufacture Empty Weight	99,990	45,355	42,145	19,116	68,505	31,075	110,650	50,191
Less: Rolling Assembly	3,040	1,379			1,820	825	1,820	825
Dry Engines	10,280	4,663			14,225	6,453	14,225	6,453
Cost Weight	86,670	39,313	42,145	19,116	52,460	23,797	94,605	42,913
Operator Items	1,540	698					2,910	1,320
Operational Empty Weight	101,530	46,053					113,560	51,511
Cost Weight Commonality (%)	48.6						44.5	

TABLE 3-24

AIRCRAFT CHARACTERISTICS
Military STOL vs Model 24C

	Military STOL	Model 24C
Takeoff Gross Weight	1b (kg)	164,350 (74,550)
Operational Empty Weight	1b (kg)	113,560 (51,510)
Payload	1b (kg) - psgr	151
Wing Area	ft ² (m ²)	1,800 (167)
Wing Loading	1b/ft ² (kg/m ²)	91.3 (446)
Aspect Ratio		7
Engine Thrust	1b (n)	24,000 (106,760)
T/W		0.584
Field Length	ft (m)	2,700 (823)
Cruise Mach No.		0.78
Cruise Altitude	ft (m)	28,000 (8,534)
DOC @ 575 st mi (926 km)	¢/ASSM (¢/ASKM)	2.15 (1.34)

for the final EBF design aircraft results from the large engine thrust available which results from the use of a core common with the military engine.

It should be noted that the Model 24C is quite different from the 150 passenger, 3000 foot (915 m) field length final design aircraft, (see Table 2-11). There are differences in fuselage cross section, wing area, aspect ratio, thrust to weight ratio, and wing loading to name a few. A comparison of the DOC show the final design aircraft value to be 2.08 ¢/ASSM (1.29 ¢/ASKM) and the Model 24C to be 2.15 ¢/ASSM (1.34 ¢/ASKM). The final design aircraft is closer to optimum for the short-haul mission, while the Model 24C with its extra thrust, larger wing, and wider fuselage has a far greater potential for stretching both range and passenger payload.

In a stretched version of Model 24C, the seating capacity could increase to 220 seats with a fuselage length increase of only 26 feet (7.9 m), while the range could be increased to 1500 statute miles (2420 km). Previous Douglas studies have shown that with such an increase in design range and passenger payload the direct operating costs could be reduced by 63 percent.

Economic studies (Volume V) showed that an aircraft such as the Model 24C would cost approximately 5 percent less in a combined military/commercial program and that airframe development costs could be reduced by approximately 50 percent. These costs are based on a 400 unit production for the commercial aircraft and assumed engine commonality only in the engine core. These costs do not include engine development. The commercial program, for

noise reasons, would have to bear the costs of development of a high bypass ratio variable pitch fan engine thus reducing somewhat the potential cost savings. The attractiveness of commonality could obviously be enhanced if the military and commercial aircraft could be so designed as to use the same power plant.

4.0 QCSEE COORDINATION AND ENGINE SELECTION

4.1 Engine/Airframe Coordination

Close coordination was maintained with the QCSEE study program engine contractors. A primary purpose was to mutually identify the most suitable engine for the various propulsive lift concepts studied. The engine companies provided parametric engine data. These data were evaluated and engine cycles selected for the study aircraft. Part of this coordination was providing the engine companies with information on engine/airframe interfaces. One of the items of concern was the engine thrust response required for powered lift aircraft. The NASA Ames S-16 three degree of freedom moving base simulator was used by NASA, McDonnell Douglas and Lockheed pilots to evaluate different engine response rates. The conclusion reached by McDonnell Douglas is that rapid engine response is beneficial. Some form of warning to the pilot showing that an engine failure had occurred is necessary since the engine instrumentation was outside of the pilot's normal field of view. It would be difficult for the pilot to initially differentiate between a gust and engine failure, and if stability augmentation was used there could be a time delay unless some warning occurred. It is possible the warning could be tied into existing engine instrumentation.

4.2 Engine Selection

4.2.1 Engine Selection Criteria. - Studies and analyses were conducted to select propulsion systems for two basic purposes. The first was to evaluate the parametric engines of the "Quiet Clean STOL Experimental Engine Study Program" (QCSEE) Task I. The second purpose was to define the propulsion systems for further study and use in the Douglas aircraft study.

The engine selection criteria used to fulfill the basic study objectives were:

- (1) A design noise level of 95 EPNdB on a 500 foot (152 m) sideline for the aircraft.
- (2) Minimum aircraft direct operating cost for a 575 statute mile (926 km) range mission.
- (3) Engine installations that are suitable for commercial airline operations and practices.

The first criterion is established in the RFP and represents a noise level that is significantly below present aircraft levels. It is a common belief that aircraft noise levels of this magnitude may be required in order to have community acceptance of aircraft at terminals close to populated areas.

The second criterion is used to identify the most economical engine cycle. Since the short haul aircraft will have to compete with other means of air and ground transportation, minimizing the operating costs is essential. Direct operating costs were used to identify the most suitable engine for a given powered-lift system.

The third criterion is used to ensure that the selected engines, if developed, could be used by commercial airlines. For this, judgment, based on past and present experience and knowledge of airline operations and practices, was applied. As part of this effort, study results were reviewed with airline personnel for their comments.

4.2.2 Selection Approach. - Engines were selected from quantitative and qualitative assessments for each lift concept. The engines defined by the two QCSEE engine contractors were evaluated, and typical engines were used to determine installation factors. Douglas conducted these engine installation studies to make realistic evaluations of the propulsion system on a commercial aircraft. Conceptual design drawings were made in sufficient detail to enable reliable performance and weight estimates to be made. Aerodynamic lines are based on the present design practices used on the DC-10, with modifications for differences associated with the short haul aircraft. Since there are no known means to significantly improve subsonic nacelle aerodynamics, existing technology was employed.

The installation configurations also provide required volume allocations for the power plant subsystems including ice protection, hydraulic pumps, generators, starters, actuators, and pneumatic ducting. Inherent in the configurations is the ability to meet present commercial aircraft requirements for maintenance and inspection while achieving maximum nacelle and pylon commonality to minimize production and spare parts costs. The weight estimates include allowances for all necessary components, accessories, and access panels, though these are not all indicated on the drawings.

The installed performance and weights based on these installation drawings were used in aircraft studies to determine relative direct operating cost. The direct operating cost calculations are with the modified ATA formula specified by NASA and used throughout this volume.

The cycle parameters which were varied were fan pressure ratio, turbine inlet temperature, overall pressure ratio, and primary exhaust velocity.

(With these values specified, the bypass ratio becomes a dependent variable.) Installed engine performance for each cycle combination considered was estimated from the uninstalled engine performance values supplied by the engine manufacturer and available at the time the study was conducted. Losses included were inlet and fan duct pressure drop, bleed, exhaust nozzle losses, and drag of the engine pod and pylon.

4.2.3 Engines for Final Design Aircraft. - The engines selected for the final design aircraft and their respective thrust levels are shown in Table 4-1. Thrust level determination is described in Section 2.2 and Appendix B. Engine cycle selection is discussed below.

4.2.4 Engines for EBF Aircraft. - The goal that the aircraft sideline noise not exceed 95 EPNdB at 500 foot (152 m) was the most influential factor in determining the engine cycle for aircraft using the EBF lifting system. By the method currently used to estimate flap interaction noise level (Appendix C), the magnitude of this source is 95 PNdB when the fan exhaust velocity is about 650 ft/sec (198 m/sec). At an aircraft speed of 0.15 Mach number, this velocity is reached with a 1.25 fan pressure ratio, as shown in Figure 4-1. For the engine selection study, all engine installations were designed to meet the 95 EPNdB limit. A velocity decayer nozzle was used when the fan pressure ratio was greater than 1.25 to reduce the exhaust impingement velocities on the flap.

For engines with variable pitch fans from 1.15 to 1.25 pressure ratio, and with fixed-pitch fans from 1.3 to 1.5, installed performance and weight were estimated, and direct operating costs calculated using the modified ATA equation. The variation of DOC with engine fan pressure ratio is shown

Table 4-1

FINAL DESIGN AIRCRAFT ENGINE CHARACTERISTICS

Lift System	Engine Type	Fan P.R.	Bypass Ratio	No. of Pass.	Field Length ft (m)	No. of Engines	Thrust lbs (Newtons)
EBF	PD287-3	1.25	17.5	100	3000 (914)	4	13,200 (58,700)
EBF	PD287-3	1.25	17.5	150	3000 (914)	4	18,260 (81,200)
EBF	PD287-3	1.25	17.5	200	3000 (914)	4	22,930 (102,000)
EBF	PD287-3	1.25	17.5	150	2000 (610)	4	25,830 (114,900)
USB	PD287-22	1.30	14.8	150	2000 (610)	4	29,490 (131,200)
AW	PD287-43	3.0	2.8	150	2000 (610)	4	19,200 (85,400)
MF	PD287-23	1.5	9.0	150	3000 (914)	2	36,710 (163,300)
MF	PD287-23	1.5	9.0	150	4000 (1219)	2	33,160 (147,500)

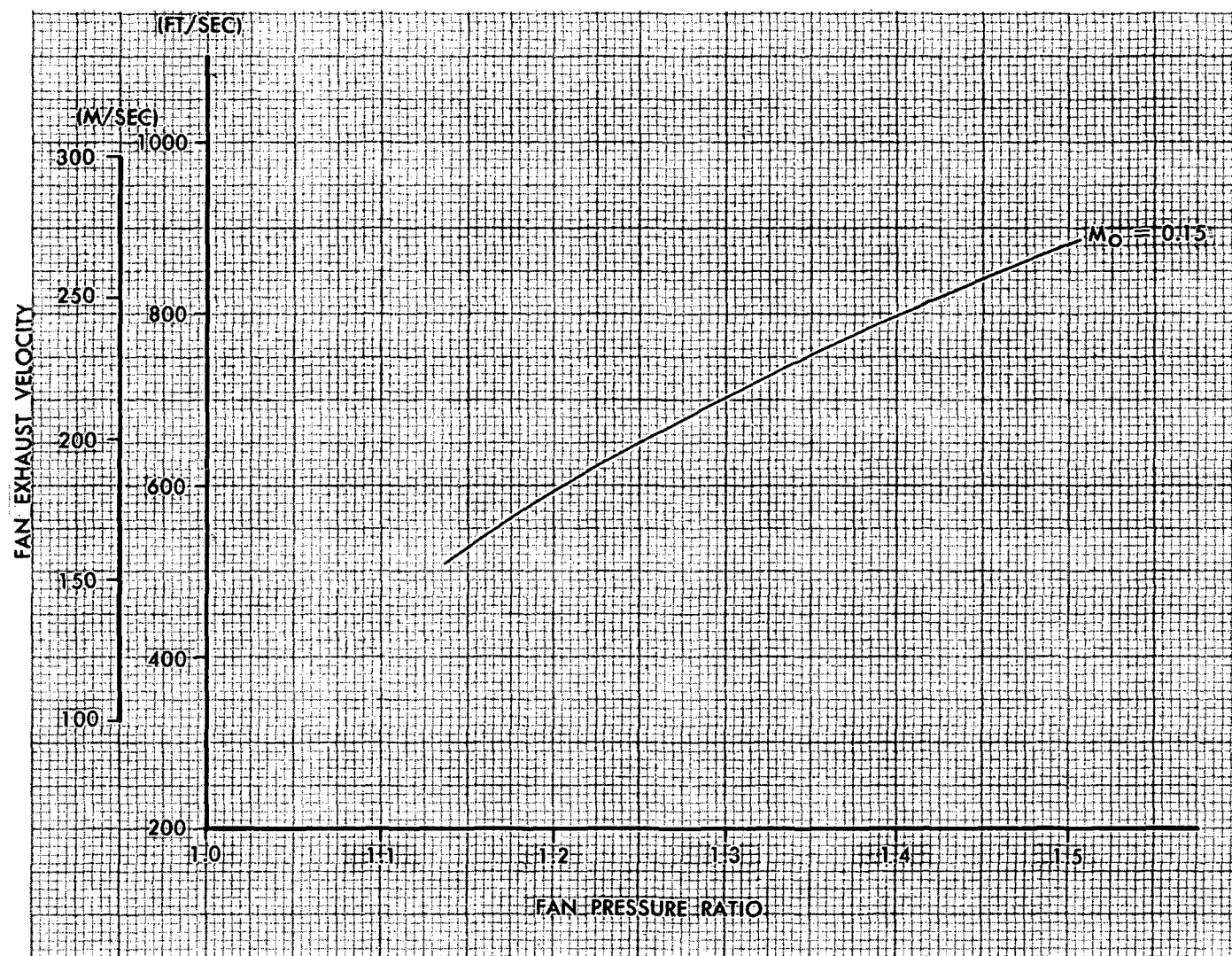


FIGURE 4-1. FAN EXHAUST VELOCITY

in Figure 4-2.

An engine with a variable-pitch fan with a fan pressure ratio of 1.25 resulted in the lowest DOC. The variable-pitch fan type engine has a lower installed weight because the variable-pitch feature permits the elimination of a thrust reverser.

Figure 4-3 shows the effect of varying turbine inlet temperature, overall pressure ratio, and primary velocity. The optimum turbine inlet temperature is in the 2200-2400°F (1200-1320°C) range. Increasing turbine inlet temperature above this range does not increase performance or thrust/weight significantly because of the necessity of compromising the engine cycle to keep the primary exhaust velocity low. Also, the higher turbine inlet temperatures result in greater maintenance costs.

DOC is relatively insensitive to overall pressure ratio as shown in Figure 4-3. A primary jet velocity of 900 ft/sec (274 m/sec) resulted in the lowest DOC. It is believed that this velocity can be compatible with a 95 EPNdB noise limit, if the primary jet is directed so as not to impinge on the flap at takeoff.

The study results show that the variable-pitch fan engine with a fan pressure ratio of 1.25 is the best engine of those considered for the externally blown flap aircraft. Increasing the fan pressure ratio above 1.25 will further reduce the direct operating cost by reducing the sensitivity of performance to inlet and nozzle losses and allowing increased cruise speeds. The limit of 1.25 was established due to the flap interaction noise. It is too early to state unequivocally that this is a true limit due to the numerous possibilities of modifying the flap to reduce the noise source strength.

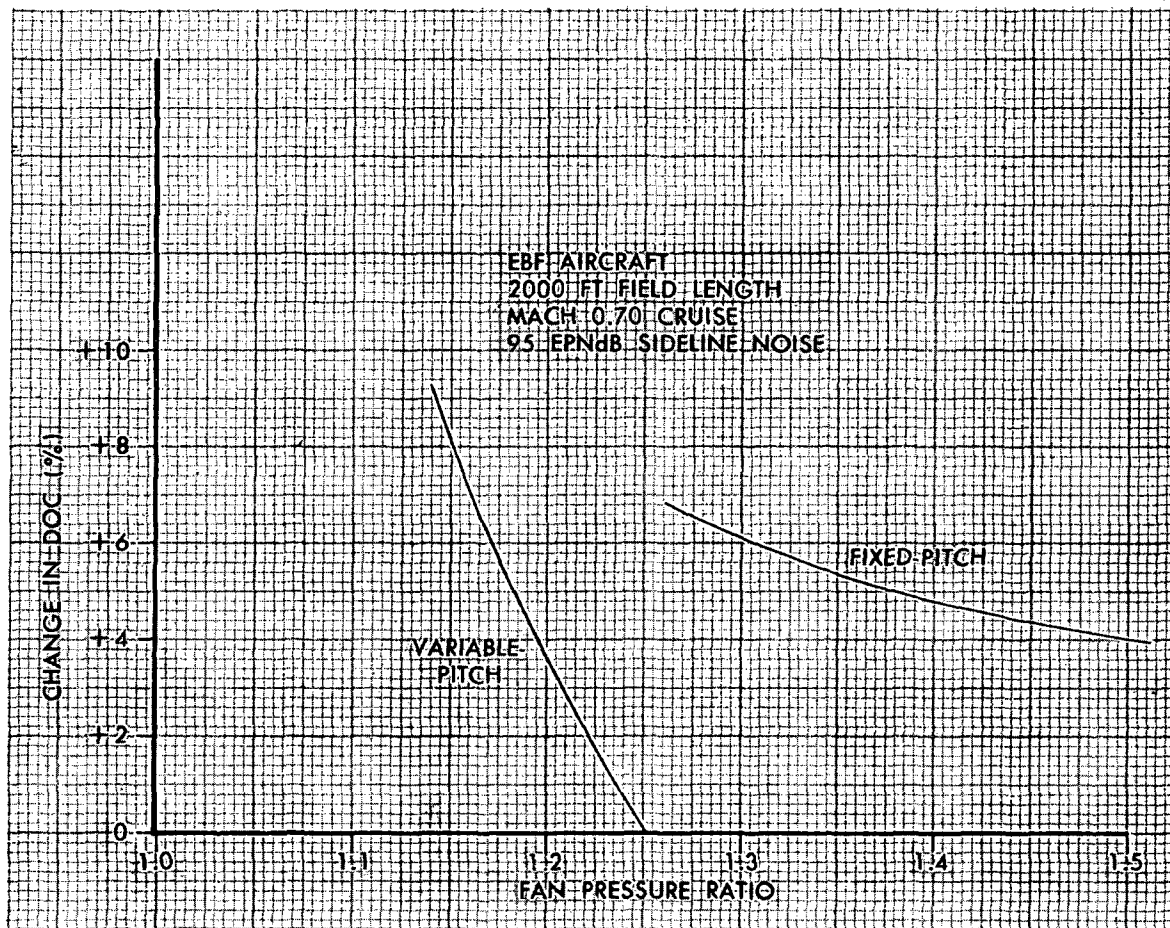


FIGURE 4-2. EFFECT OF FAN PRESSURE RATIO ON DIRECT OPERATING COST

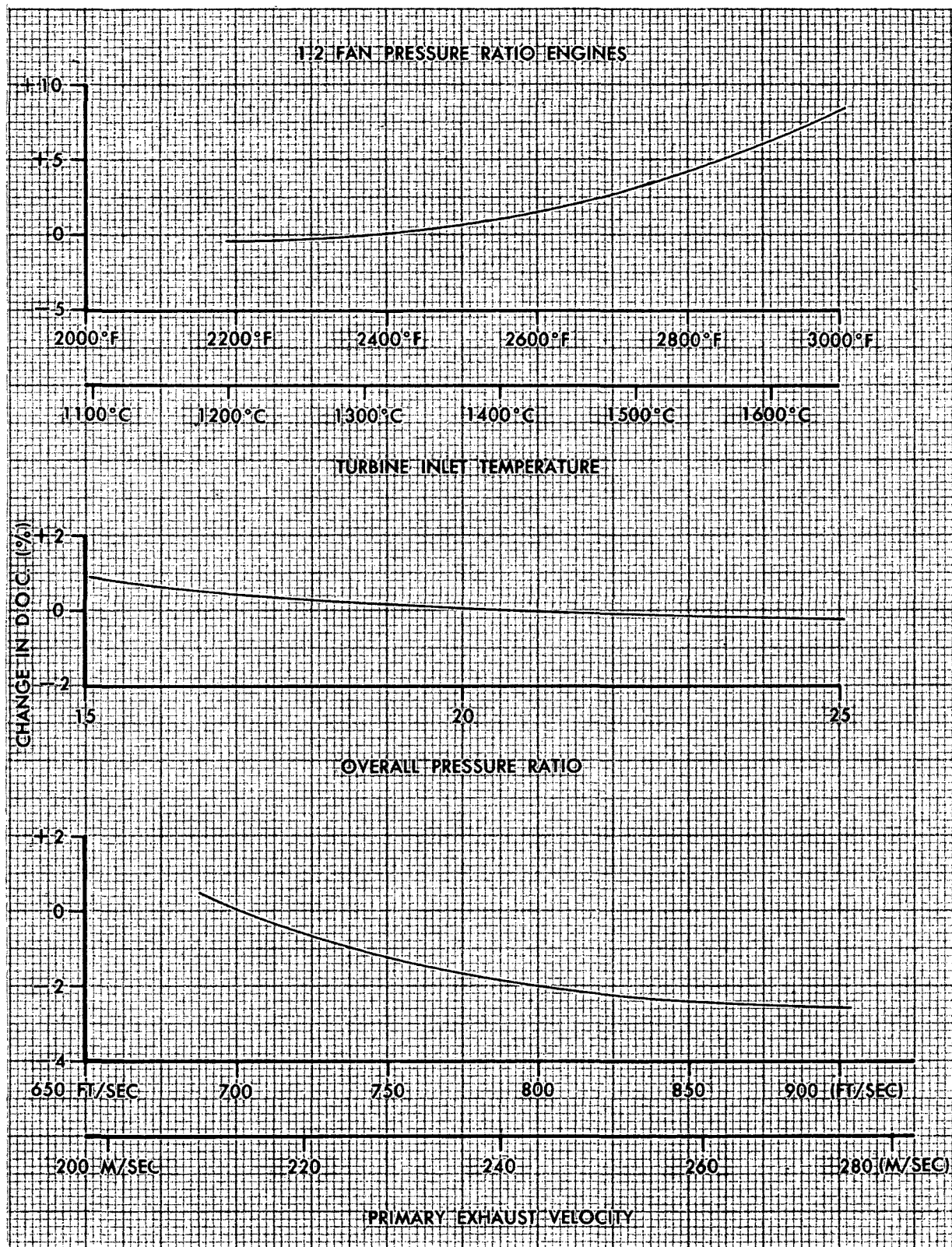


FIGURE 4-3. EFFECT OF ENGINE CYCLE PARAMETERS
ON DIRECT OPERATING COST OF
EBF AIRCRAFT

4.2.5 Engine for Upper Surface Blown Flap. - The highest fan pressure ratio consistent with the noise level requirement will result in the minimum DOC, over the range considered. Early model tests indicated some shielding effect from the wing for flyover noise. If subsequent studies show the wing also provides some shielding for sideline noise, the fan pressure ratio may go as high as 1.3 and still meet a 95 EPNdB requirement. It was assumed that this will be the case, and an engine with a fan pressure ratio of 1.3 was used for the upper surface blowing aircraft.

While a variable-pitch fan shows an advantage over a fixed-pitch fan for an EBF installation because of the reverser weight saving, the situation is different for the USB installation. In this case a mixed flow engine exhaust was found to provide the lightest weight approach since the complexity of separating the fan and the primary flow during reverse operation eliminates the weight savings of the variable pitch feature. A fixed-pitch engine was selected to minimize DOC for the USB.

4.2.6 Engine for Mechanical Flap. - The mechanical flap airplane was designed for a two-engine configuration, which put a constraint on the engine selection that was not a factor for the powered-lift systems. This was a limit on the maximum diameter, involving two factors: (1) the maximum diameter which can be shipped routinely and (2) engine ground clearance. The maximum diameter which can be shipped without special permits in many states is 96 inches (2.44 m). This proved to be a more difficult requirement than the ground clearance for which a certain amount of flexibility is possible. The maximum diameter limitation was imposed on the DC-10 and is expected to be mandatory with short haul aircraft with their more widely distributed airports with minimum maintenance facilities.

The engine which meets the diameter limitation in the 36,000 pound (160,000 N) thrust range is one with a fan pressure ratio of 1.5.

There may be payload/field length combinations where a four engine MF aircraft using lower fan pressure ratio engines and a corresponding lower acoustic treatment level would be competitive with a two engine aircraft with 1.5 FPR engines. This could be a subject for subsequent study.

4.2.7 Engines for Augmentor Wing. - The selection of the fan pressure ratio for the augmentor wing aircraft is constrained by the available duct volume in the wing and pylon. (The ducting installation is discussed in Appendix D.) Past studies and those conducted as a part of this contracted effort have shown that for a two-flow engine in which all the fan air is ducted to the wing (fan thrust is about 80 percent of the total thrust), a fan pressure ratio of 3.0 can barely be accommodated. Reducing the pressure increases the duct volume required. Boeing design studies under NASA Contract (Reference 1) show that augmentor nozzles with pressure ratios at or below 2.8 are acceptable for noise. Since the drop between the engine and augmentor nozzles is about 14 percent, the fan pressure ratio of 3.0 results in a pressure ratio of 2.6 at the augmentor nozzles. For the two-flow engines, it is concluded that a fan pressure ratio of 3.0 is acceptable whereas a value of 2.5 would result in significant wing penalties.

The effect of other augmentor wing engine cycles parameters on DOC is shown in Figure 4-4. The augmentor wing engine should have the highest primary jet velocity consistent with meeting the noise limit. The direct operating cost varies insignificantly between an overall pressure ratio of

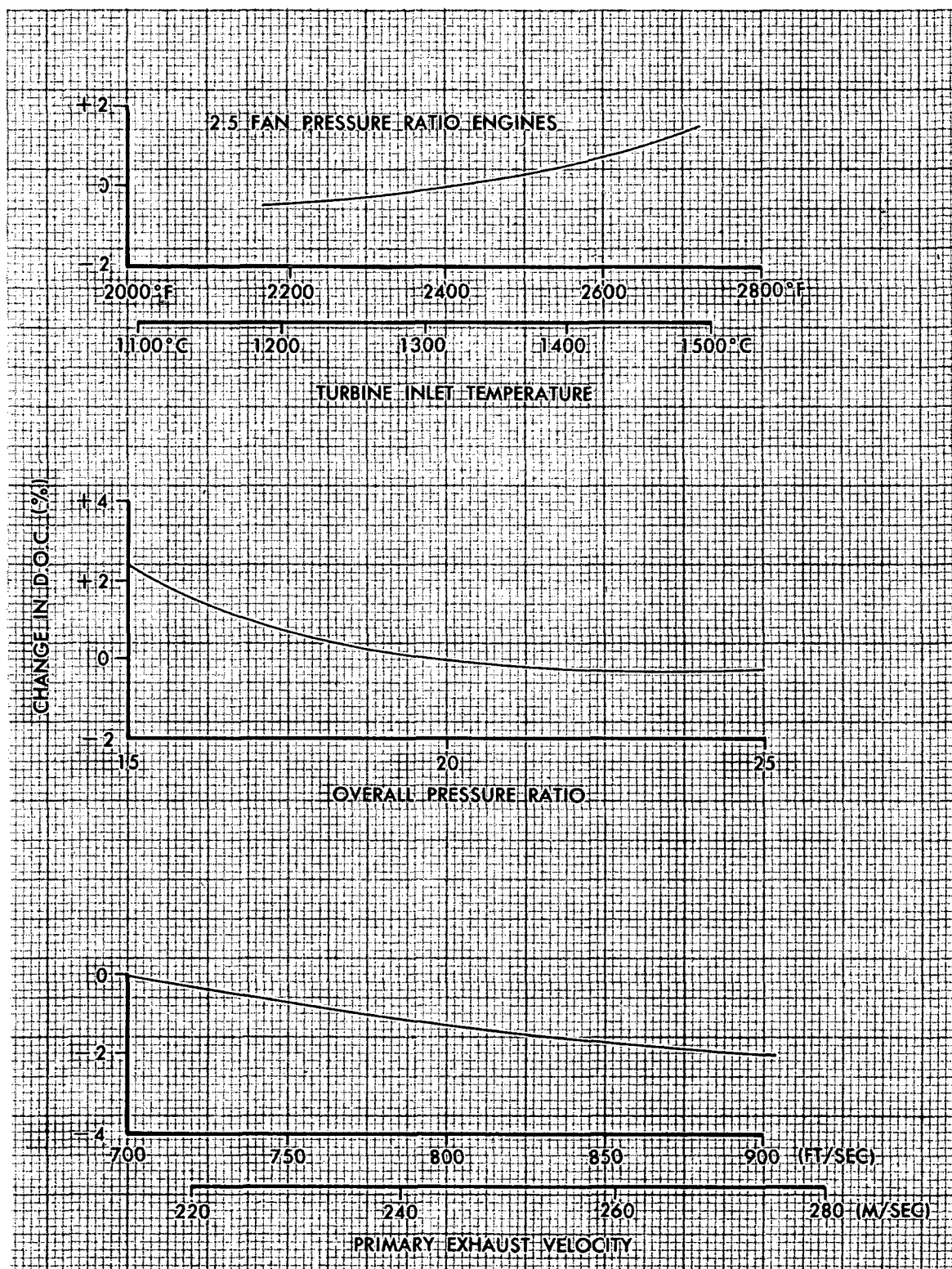


FIGURE 4-4. EFFECT OF ENGINE CYCLE PARAMETERS ON DIRECT OPERATING COST OF AUGMENTOR WING AIRCRAFT

20 to 25. The higher value of overall pressure ratio implies some benefit for use over longer ranges.

The complexity of the three-flow engine is greater than that of the two-flow engine. Although the duct volume limitation in the wing is relieved, the same components in the wing and pylon are required, with their size somewhat reduced. Within the engine pod, the complexity increases. Douglas studies show that a three-flow engine will require a thrust reverser for the wing flow (the forward thrust of this stream is 40 to 60 percent of the total), and for the low pressure fan flow (50 to 30 percent of the total), and possibly a spoiler on the primary flow as well. In a two-flow engine, the cascades for reversing the wing flow occupy the nacelle space ordinarily used for low pressure fan reverser cascades. A suitable means for reversing the fan flow in combination with the forward thrust wing flow has not been identified. Another area of increased installation complexity is the access to the gas generator. The means by which visual inspections can be readily accomplished are complicated on the three-flow engine because of the multiple ducting required.

The three-flow engine is different from any known turbofan engine in present use. This in itself presents the possibility of unforeseen difficulties which may result in significant performance or weight penalties. For example, a back pressure change on the wing flow will affect the forward thrust fan flow due to aerodynamic coupling. The proper exit area match can be accomplished at takeoff power setting by a trial and error process. The discharge coefficients of the augmentor flow and the fan flow, however, are likely to change at a different rate as power is reduced. This combined

with the increased inlet distortion characteristic of STOL aircraft due to the wing upwash may result in engine dynamic stability problems.

Since the two-flow engine can be integrated with the airframe in a reasonable manner, there was no reason to prefer the three flow engine with its increased complexity.

5.0 AIRLINE COORDINATION

In order to ensure airline realism in the study aircraft, four airlines evaluated the candidate designs and applied airline requirements to the aircraft designs and layouts. In order to obtain an airline cross section in the evaluation, two trunk lines (American and United Air Lines), a local carrier (Allegheny Airlines) and an intra-state airline (Air California) were contracted by Douglas.

Communication was maintained with all airline subcontractors throughout the study in order to ensure this realism in the aircraft designs. The airline comments have been most helpful and instructive in the study work. A primary impact has been in the structuring of the interior arrangements of the aircraft. Strong suggestions concerning the operational aspects of STOL aircraft were also received.

Some of the major operational suggestions resulting from this coordination are:

- o It is believed technically possible to certify the STOL aircraft with a flight crew of two.
- o STOL aircraft must have unusually high reliability because of their economic vulnerability to other modes of transportation in the event of excessive delay time.
- o A strong preference has been expressed for low wing aircraft. This comment is primarily motivated by customer appeal considerations and ditching requirements.

A summary of the more detailed airline comments which affect the vehicle configuration are summarized as follows:

WING LOCATION

- o A high wing configuration is undesirable from the ditching standpoint.
- o Overhead hatches are required for escape with a high wing. (not incorporated in study aircraft).
- o High wing disadvantages may be compensated to some extent by greater passenger appeal, due to the improved view.
- o Airframe maintenance is easier and more economical with low wings.

ENGINE/FUSELAGE CONFIGURATION

- o Additional cabin insulation may be needed because of the proximity of the engines to the passenger cabin.
- o Shielding may be needed to protect the passengers against failure of rotating engine components.
- o Engine foreign object damage is more likely with a low wing.
- o Engine intakes should be well clear of the passenger entry door for safety and rapid passenger loading.
- o Areas of specific consideration but no distinct airline requirements
 - Wing mounted engines are preferred
 - Fuselage mounted engines are better for boarding and evacuation
 - Engine access for maintenance should be at eye level
 - Engine removal - straight down

PASSENGER SEATING ARRANGEMENT

- o Flexibility in seat pitch between 34-38 inch (86-97 cm) is desirable. 34-inch (86 cm) pitch with 20 inch (51 cm) aisle is below current standard for short haul operations. Seat pitch requirements will vary with individual airline operations.
- o Provision for movable cabin divider is required
- o Single 20-inch (51 cm) aisle is satisfactory depending on capacity
- o All-coach 6-abreast single aisle seating is acceptable but dual aisle is preferred.

- o 5-abreast seating with doubles and triples similar to DC-9 is acceptable

PASSENGER AMENITIES

- o Lavatories required forward and aft;
 - Minimum 2 lavatories for 75 passengers
 - One lavatory/50 passengers for one hour flight, one lavatory/40 passengers for more than one hour
 - Two lavatories minimum required for 100 passengers, with one lavatory forward and two aft desired.
- o Buffets required forward and aft;
 - Two buffets required with space for supplies, meals and beverages for 100 passengers.
 - Two coffee/beverage units required per 100 passengers for up to one hour. For more than one hour add hot meal service.
- o Coat space required;
 - One required near each main entrance with one inch of coat rod per passenger.
- o Air stairs are necessary at main passenger entries.

DOORWAYS

- o FAR should permit 2 type "A" exits for each side with credit for a total of 4 type A exits. Present rules do not permit double width door fed from a single aisle.
- o Minimum door width is 34 inches (86 cm) for a passenger carrying a bag.

FLIGHT CREW

- o With adequate systems aids the airplane should be certified for operation with 2 crew members.
- o Design systems for two man crew, calculate DOC for both two and three man crew.

BAGGAGE AND FREIGHT

- o Rapid baggage loading and unloading capability with convenient passenger drop-off and pick-up is desired.

- o Carry-on garment and baggage provisions are desirable. These provisions may be limited to under seat and coat space provision only or combined with enclosed overhead stowage depending on individual airline requirements.
- o Cargo Provisions
 - Should not compromise passenger compartment.
 - Cargo containers are not required, but could be optional with consideration for interchangeability with other aircraft models.
 - Weight and balance characteristics should be compatible with varying passenger/cargo configurations.
 - Unlikely to be used with quick turn-around operation.
 - Provision for mail is required.

These requirements and suggestions have been incorporated where possible in the aircraft design arrangements as described in Section 2.2.3.

6.0 STOL TECHNOLOGY ASSESSMENT

The broad nature of this study coupled with the in-depth analysis of the aircraft systems, provides an excellent basis for an assessment of STOL technology. In the following paragraphs, the assessment is divided into "critical technology" requirements which must be satisfied before a STOL system can be implemented and "high payoff technology" which will yield significant benefits if developed. This division is in keeping with the basic study objectives presented in the introduction.

6.1 Critical Technology

6.1.1 Critical Acoustic Technology. -

Noise Design Criteria - The single most important technical problem facing the aircraft industry today is reducing aircraft noise. The most widely used aircraft community-noise design criterion available today is Part 36 of the FAR with the effective perceived noise level (EPNdB) as the noise-rating scale. While this criterion is clearly an improvement over the previous chaotic situation, it is inadequate for future airplanes, especially those intended to serve a new short-haul market. Although there are at present certification noise standards for transport aircraft, these standards do not take into account community acceptance factors such as the psychoacoustics - the characteristics and the duration and time frequency of the noise source. The present three-point measuring system may be acceptable, however, if appropriate adjustments of the distances to the measuring points reflects the community acceptance aspects of future short-haul STOL aircraft operating from airports near population centers. The 500 foot (152 m) sideline criteria used for this study is clearly inadequate from a community acceptance standpoint.

Research is required to establish proper noise-rating scales and noise-measurement locations to ensure minimum community reaction and to permit more accurate evaluation of alternative aircraft designs. The research should include laboratory and operational evaluation and social surveys with the goal of relating severity of annoyance and number of people annoyed to appropriate aircraft design parameters.

Noise of Powered-Lift Systems - For airplanes that generate propulsive lift by blowing on, over, or through the wing and flap surfaces, significant noise is generated by mechanisms that today are poorly understood. No effective, economically feasible method has been developed to achieve substantial reductions in any of these sources of noise. Preliminary indications are that large suppressions may well be needed to achieve acceptable community noise levels. Laboratory and large scale tests (static and flyover) are required to identify sources of noise and their directivity patterns under and to the side of the flight paths, and to develop practical noise-suppression systems.

6.1.2 Critical Propulsion System Technology. - The various propulsive lift concepts have different technology advancement requirements. General improvements such as lighter, quieter engines are beneficial to all transport aircraft and are not identified here.

Variable Pitch Fan Technology - All of the lift concepts except the externally blown flap use turbomachinery essentially similar to existing turbofan engines albeit with quieter fans. The externally blown flap, however, shows performance improvements by the use of a variable pitch fan. This type of fan has been developed for low thrust and low fan pressure ratio by the Europeans and model fan testing has been conducted in the U. S. Technology

advancement is required to establish the capability to produce variable pitch fan engines of the thrust level required for short haul transport aircraft. Concomitant with the need to advance the technology is the need to demonstrate that a variable pitch fan will perform as intended with flight-weight hardware. Such a demonstration would be required before such an engine could be committed to production.

The variable pitch fan requires a variable area nozzle to change the engine match between takeoff and cruise. In addition, this variable area nozzle should open and function as an inlet in the reverse thrust mode. The use of a variable area nozzle changes the design requirements. Current fixed-area nozzles are designed to maintain a fairly constant discharge coefficient to obtain good cruise performance. The variable area feature of the high bypass ratio engine eliminates this requirement, and permits a more flexible approach to nozzle design. The means of using this to advantage requires exploration.

Augmentor Wing Ducting and Nozzle System - The augmentor wing requires technology advancement in order to be able to design the wing flow ducting with its multiplicity of discharge slots to assure the necessary level of noise reduction. Since the wing nozzles have a large perimeter-to-flow-area ratio, the means for engine matching needs to be established. The effects of thermal expansion, duct pressure and wing deflections on the engine match should be determined. This system also requires a flow diverter valve for transition between the powered lift and cruise modes. The valve must maintain its functional position in the event of an actuation system failure. Pressure losses need to be minimized and inspection and maintenance provision included.

Thrust Reverser - All lift concepts require advancements in thrust reversing technology. To improve low speed reversing capabilities, directional flow control to minimize re-ingestion and ground impingement at very low forward speeds is needed. Each of the lift concepts requires a different type of reverser.

- a. The externally blown flap aircraft uses fan pitch change to obtain reverse thrust. The variable area fan nozzle associated with the variable pitch engine must be designed to act as an inlet in the reverse thrust mode.
- b. The augmentor wing uses a low bypass ratio engine and has a takeoff thrust-to-gross weight ratio of about 0.4. With only fan flow reversing and an effectiveness of 50 percent, the static reverse thrust-to-aircraft gross weight would be only 8 percent. This combination of a relatively low bypass ratio and aircraft thrust loading results in the need for both fan and primary flow reversers with a high degree of efflux directional control. The augmentor wing fan reverser also requires a forward thrust flow blocker which is remote from the reverser cascades. This flow blocker must be synchronized with the reverser cascade covers.
- c. The mechanical flap aircraft requires a fan thrust reverser similar to present CTOL concepts except for the need to have improved low speed capabilities of minimum re-ingestion and flow ground impingement.
- d. The upper surface blowing concept can use either a fan-only thrust reverser or a reverser in the common fan and primary duct section. A fan-only reverser could be similar to that required for the mechanical flap aircraft. A common-duct reverser was selected in this study since the required variable

area nozzle can also function as a reverser/flow diverter.

Although common-nozzle reversers are in existence, present designs are not suitable for operation below 60 knots (31 m/sec), and the possibility of combining the thrust reverser and variable area nozzle appears attractive for the USB installation.

Upper Surface Blowing - Further investigations are required to define nozzle shapes, chordwise nozzle positions and Coanda flow turning relationships which produce acceptably low cruise thrust scrubbing losses and good high-lift characteristics at low noise levels. Boundary layer control on the trailing edge flap may be useful in achieving the high turning angles necessary for landing. Chordwise fences used on the cambered upper surface of the wing/flap may help to achieve a more two-dimensional Coanda flow with resulting higher turning angles. USB wash effects on the empennage, with engines on and one engine out, should be evaluated. Both chordwise and spanwise BLC on the leading edge should be investigated for achieving high CL_{max} values.

6.2 High Payoff Technology

6.2.1 High Payoff Propulsion System Technology. -

Emissions - Although aircraft operations add only a minor amount of pollutants to the atmosphere, primarily during ground operations and while flying at low altitudes, the release of engine exhaust emissions has become a major environmental issue. The presence of irritating oxidants in the urban atmosphere has been ascribed to the interaction of hydrocarbons (HC) and nitrogen oxides (NOX) in the presence of sunlight. It may be easier to reduce emissions of hydrocarbons than NOX, and such action may be sufficient to reduce smog

irritants. Additional studies should be made to determine the impact of NOX on the environment, in the presence of varying amounts of reactive hydrocarbons. Engine combustor design, and research and development, should be continued on a high priority basis directed toward the reduction of all harmful jet engine emissions. Special emphasis should be placed on the reduction of nitrogen oxides. One possible way to control NOX emissions is to restrict the cycle pressure ratio of the engines. However, restricting the pressure ratio below that required by other considerations will have a serious impact on the performance of the airplane and, therefore, the direct operating costs to the airlines. A study should be made to assess direct operating cost as a function of NOX control by pressure ratio variations.

6.2.2 High Payoff Aerodynamic Technology. -

Ground Effect - Accurate knowledge of the ground effects during takeoff and landing has a major impact on the design of propulsive lift systems. Additional research is required to determine the influence of ground effect on the landing flare maneuver, the use of direct lift control systems, the margin of approach speed to stall speed, and available load factor required for commercial operations. The aircraft with shorter design field lengths tend to be more sensitive to ground effects since their design wing loadings are limited by landing performance. In addition to weight and cost penalties associated with these low wing loadings, ride quality is only marginal in turbulent air. At present, no upper surface blowing (USB) high lift aerodynamic wind tunnel data in-ground effect are available. Test information is needed pertaining to the stability of the USB Coanda turning process in ground effect and in the dynamic ground effect maneuver.

Hybrid Configurations - Hybrid configurations using a combination of high lift concepts should be investigated. For example, as stated in the previous section, the USB with blowing on the trailing edge flap is essentially a combination of USB with the jet flap principle. This hybrid could possibly produce high turning efficiencies.

Canard configurations could offer advantages in longitudinal trim and maneuvering capability. Control configured vehicles utilizing a combination of controls such as wing flaps and canards might prove very efficient. Studies should be made to determine whether canard and multiple control systems can be coupled mechanically or electronically to achieve longitudinal control throughout the aircraft lift range. Canard-wing position and various planform studies are necessary to determine configurations with acceptable canard - wing interference effects. Use of sensors and electronically-activated flaps, canard surfaces, elevators, and engine thrust may be a means to provide the highest possible climb rate to minimize climb-out noise footprints.

6.2.3 High Payoff Structure and Materials Technology. - Reduction of structural weight through the application of new emerging materials has a great potential for improvement of system economics, as demonstrated in Reference 5. The weight saving potential of advanced composites is significantly greater than that of other materials, as discussed in the Structures and Materials section of that report. As discussed in Reference 6, principal barriers to extensive application of advanced composites to aircraft structures are high costs and lack of experience for broad applications on primary structure.

An area that requires attention is the validation of advanced composites to promote acceptability, both to manufacturers and airlines. Generally, this validation will require implementation of a wide range of programs that develop production and operating experience. Expected payoffs for this technology application include reduced weight, improved manufacturability, and increased reliability through improved fatigue behavior. However, if an economically viable composite aircraft is to evolve, a breakthrough in composite economics is required.

6.2.4 Ice Protection. - All commercial aircraft for which all-weather certification is desired must comply with the ice protection provisions of Part 25 of the FAA regulations. STOL aircraft will normally fly shorter ranges than CTOL aircraft and thus spend a higher percent of their operating time at lower altitudes where severe icing is more frequently encountered. Thus, icing conditions which exceed the specified standards will be encountered more often. For example, freezing rain/drizzle, that is found more often at the lower altitudes, is not covered in the current regulations. There is concern, therefore, that STOL aircraft requirements for visibility, controllability, and performance may be more sensitive to ice accumulation than CTOL aircraft and that current regulations may not provide proper safety margins for STOL.

The meteorological standards and methods of showing compliance with safety regulations will require a thorough study as applied to the new STOL aircraft. Tests are also required to show the effects of icing on the various lift system components, such as: leading edge flaps and slats, high deflection trailing edge flaps, direct lift and direct drag controls, and the leading edge of the augmentor wing upper flap.

7.0 CONCLUSIONS

This study has provided a broad basis upon which each aircraft concept was evaluated in the environment of a complete short haul transportation system. In addition, an in-depth analysis in each engineering discipline provided a basis of validity in the aircraft designs. Airline subcontractors and engine company discourse also helped to provide design realism. It is felt therefore that the conclusions drawn from the study are valid and that they will serve as a guide to the development of the short haul market.

Major conclusions of the study are:

1. Work reported in this and the other companion volumes indicates that the first generation STOL/short haul aircraft should be designed to no less than a 3000 foot (914 m) field length and to a payload of 150 passengers or more. The economic penalties for designing to 1500 to 2000 foot (457 to 610 m) field lengths are large and the definitive requirement for this type of STOL performance is not well substantiated. The passenger size is primarily a tradeoff between frequency of service and operating economics.
2. The sensitivity of aircraft operating costs to design noise level places a high priority on continuing research directed toward the development of accurate methods of predicting the levels and spectral content of STOL aircraft noise sources and the development of efficient methods of reducing the noise from dominant sources. Noise radiated from the powered lift

system is currently the least understood of the major noise sources, and its study warrants the most emphasis. Large-scale static and flight testing of powered lift systems is recommended to improve the understanding of powered-lift noise.

3. The externally blown flap, upper surface blowing and mechanical flap systems are competitive at the 3000 foot (914 m) field lengths and require more detailed study in order to select the best high lift approach. Augmentor wing designs are the most complex systems evaluated in the study.
4. A new, quiet, clean, high bypass ratio, variable-pitch fan engine is required for the STOL system. This engine is most applicable to the EBF, upper surface blowing and mechanical flap systems.

Additional conclusions are:

- o For all STOL aircraft studied, significant reductions in community noise are possible by the selective use of operational techniques as discussed in Volume III of this report. These techniques can be highly variable depending upon specific airport environments. For the EBF and USB systems additional considerations should be given to the use of configuration changes during takeoff because of the prominence of propulsive lift noise.
- o Weight growth factors (e.g., change in gross weight per change in dead weight) are greater for STOL aircraft than for conventional CTOL aircraft. Thus larger weight reductions and

economic payoffs are possible from weight savings techniques (e.g., composite applications) for STOL aircraft than for CTOL designs.

- o Ground effects for propulsive lift systems based on wind tunnel data are large and adverse, particularly in the landing mode. Until these effects are better understood, high wing designs such as those proposed in this report are considered to be the more conservative approach.
- o STOL certification requirements need to be developed and must be firm before a STOL system can be implemented. The nature of many certification requirements is such that a flight demonstration program will be necessary.
- o The greatest STOL technology gaps are for the development of the aerodynamic and acoustic characteristics of the upper surface blowing concept and for the reduction of flap interaction noise for the externally blown flap concept.
- o The airlines believe that short haul aircraft can be certified for a flight crew of two with adequate systems aids. Emphasis should therefore be made to increase cockpit automation for checklist procedures and system control to reduce crew work load.
- o Short haul aircraft must have unusually high dispatch reliability because of their vulnerability to competitive modes of transportation in the event of excessive time delays. As a design goal,

more maintenance action should be deferrable for short haul aircraft than for long haul aircraft because of the short stage lengths of the short haul system.

- o The extensive use of advanced composite materials will result in significantly lower aircraft weight and a slight decrease in operating cost as compared to a conventional metal structure aircraft based on preliminary study results. Offsetting these advantages are the high risks involved in the development of new primary structure materials.

REFERENCES

1. Roepcke, F. A. and Kelley, G. S., Design Integration and Noise Studies for Jet STOL Aircraft, Volume II, NASA CR-114284, 1972.
2. Anon., Flying Qualities of Piloted Airplanes, MIL-F-8785B (ASG), August 7, 1969.
3. Lehman, G. M., et al., "Study to Assess the Utility of Advanced Materials in Aircraft Structures", (U), AFML-TR-67-383 (Secret), October 1967.
4. Matt, C. W., "Cost Considerations Regarding the Use of Advanced Materials in Aircraft Structures", ASME Paper 67-WA/AV-5, 1967.
5. Douglas Aircraft Co., "Advanced Transport Technology Economic Evaluation", NASA Contract NAS1-10705.
6. Anon., "Panel Reports of Composites Recast, An Air Force/NASA Long Range Planning Study", 22 Feb. 1972.
6. Phelps, A. E., Letko, W., and Henderson, R. L., Preliminary Low-Speed Wind-Tunnel Investigation of a Semispan STOL Jet Transport Wing with an Upper-Surface Blown Jet Flap, NASA Langley Working Paper 1022, January 1972.
8. Falarski, Michael, and Koenig, David G., Aerodynamic Characteristics of a Large Scale Model with a Swept Wing and Augmented Jet Flap, NASA TMX-62029, 1971.
9. Falarski, Michael D., and Koenig, David G., Longitudinal and Lateral Stability and Control Characteristics of a Large-Scale Model with a Swept Wing and Augmented Jet Flap, NASA TMX-62-145, 1972.
10. Campbell, J. M., Lawrence, R. L., and O'Keefe, J. V., Design Integration and Noise Studies for Jet STOL Aircraft - Volume III Static Test Program, NASA CR-114285 (Boeing Report D6-40552-3), May 1972.
11. Wang, T., Wright, F., and Mahal, A., Design Integration and Noise Studies for Jet STOL Aircraft, Volume IV, NASA CR-114286, 1972.
12. Volger, R. D., Wind-Tunnel Investigation of a Four-Engine Externally Blowing Jet-Flap STOL Airplane Model, NASA TN D-7034, December 1970.
13. Manhart, J. K., et al., Investigation of DC-8 Nacelle Modifications to Reduce Fan-Compressor Noise in Airport Communities, Part III, Static Tests of Noise Suppressor Configurations, NASA CR-1708, December 1970.
14. Zwieback, E. L., et al., Investigation of DC-8 Nacelle Modifications to Reduce Fan-Compressor Noise in Airport Communities, Part IV, Flight Acoustical and Performance Evaluations, NASA CR-1708, December 1970.

15. Anon., Study and Development of Turbofan Nacelle Modifications to Minimize Fan-Compressor Noise Radiation, Volume IV, Flightworthy Nacelle Development, NASA CR-1714, January 1971.
16. Marsh, A. H., et al., Investigation of DC-8 Nacelle Modifications to Reduce Fan-Compressor Noise in Airport Communities, Part II, Design Studies and Duct-Lining Investigations, NASA CR-1706, December 1970.
17. Rice, E. J., Attenuation of Sound in Soft-Walled Circular Ducts, pp. 229 to 249 in Aerodynamic Noise, University of Toronto Press, May 1968.
18. Rice, E. J., A Model for the Acoustic Impedance of a Perforated Plate Liner with Multiple Frequency Excitation, NASA TMX-67950, October 1971.
19. Anon., Aircraft Engine Noise Reduction Conference, NASA Lewis Research Center, 16-17 May 1972.
20. Rice, E. J., et al., Acoustic and Aerodynamic Performance of a 6-Foot Diameter Fan for Turbofan Engines, Volume II, Performance with Noise Suppressors, NASA TN D-6178, February 1971.
21. Dorsch, R. G., et al., Blown-Flap Noise Research, AIAA Paper No. 72-129, January 1972.
22. Putman, T. W., and Lasagna, P. L., Externally Blown Flap Impingement Noise, AIAA Paper No. 72-654, June 1972.
23. Maglieri, D. J., et al., Preliminary Measurements of the Noise Characteristics of Some Jet-Augmented-Flap Configurations, NASA Memo 12-4-58L, 1959.
24. Dorsch, R. G., et al., Blown-Flap Noise Research, AIAA Paper No. 71-745, June 1971.
25. Putnam, T. W., et al., A Full-Scale Investigation of Externally Blown-Flap Impingement Noise, NASA Flight Research Center Working Paper, FWP-25, August 1971.
26. Gibson, F. W., Noise Measurements of Model Jet-Augmented Lift Systems, NASA TN D-6710, April 1972 (Also NASA LWP-981, August 1971).
27. Chestnutt, D., et al., Noise Generation by Plates in the Presence of Jets, Part D of NASA LWP-989, September 1971.
28. Olsen, W. A., et al., Noise Produced by a Small-Scale Externally Blown Flap, NASA TN D-6636, March 1972.

29. Reshotko, M., Olsen, W. A., and Dorsch, R. G., Preliminary Noise Tests of the Engine-Over-The-Wing Concept, I 30° - 60° Flap Position, NASA TMX-68032, March 1972.
30. Reshotko, M., Olsen, W. A., and Dorsch, R. G., Preliminary Noise Tests of the Engine-Over-The-Wing Concept, II 10° - 20° Flap Position, NASA TMX-68104, June 1972.
31. Anon., Aircraft Engine Noise Reduction Conference - Figure Preprints, Lewis Research Center, Cleveland, Ohio, May 16-17, 1972.
32. Harkonen, D. L., Wintermeyer, C. F., and Wright, F. L., Static Tests of a 0.7 Scale Augmentor Wing Flap for the Modified C-8A Airplane - Test Results and Analysis, NASA CR 114315 (Boeing Report D6-24850), May 1971.
33. Dorsch, R. G., Krejsa, E. A., and Olsen, W. A., Blown Flap Noise Research, AIAA Paper No. 71-745, June 1971.
34. Kelley, G. S., and Gerend, R. P., Propulsion Systems for Commercial STOL Aircraft, AIAA Paper No. 71-746, June 1971.
35. Gibson, F. W., Noise Measurements of Model Jet-Augmented Lift Systems, NASA TN D-6710, April 1972. (Also NASA LWP-981, August 1971.).
36. O'Keefe, J. V., and Kelley, G. S., Design Integration and Noise Studies for Jet STOL Aircraft, Volume I, Program Summary, NASA CR-114283 (Boeing Report D6-40552-1), May 1972.
37. Anon., Aircraft Engine Noise Reduction Conference - Figure Preprints, NASA Lewis Research Center document, May 1972.
38. Anon., Design Integration and Noise Study for a Large STOL Augmentor Wing Transport, Boeing Report D6-60139, August 1971.
39. O'Keefe, J. V., Nickson, T., and True, H. C., A Comparative Study of Augmentor Wing, Ejector Nozzle, and Power Jet Flap Low Noise STOL Concepts, Presented American Acoustical Society, December 1972.
40. McKinney, John S., Simulation of Turbofan Engine, Technical Report AFAPL-TR-67-125, November 1967.
41. Douglas Aircraft Company, Commercial STOL Weight Comparison Study - Turbofan Vs Turboprop, Report DAC-67692, 31 January 1969.
42. Douglas Aircraft Company, Commercial STOL Mass Properties Study, Report MDC-J0273, 6 March 1970.

43. Douglas Aircraft Company, Mass Properties Report - Advanced Medium STOL Transport, Report MDC-J5466, 14 January 1972.
44. Douglas Aircraft Company, Mass Properties Report - NASA QUESTOL, Report MDC-J5577, 15 June 1972.
45. Douglas Aircraft Company, Mass Properties Report - Advanced STOL Transport (Medium), Report MDC-J5652, 14 August 1972.
46. Anon., Flying Qualities of Piloted V/STOL Aircraft, MIL-F-83300, December 31, 1970.
47. Anon., Recommendations for V/STOL Handling Qualities with an Addendum Containing Comments on the Recommendations, NATO AGARD Report 408A, October 1964.
48. Innis, R. C., Holzhauser, C. A., and Quigley, H. C., Airworthiness Considerations for STOL Aircraft, NASA TN D-5594, January 1970.
49. Holloway, R. B., Brumaghim, S. H., "Tests and Analysis Applicable to Passenger Ride Quality of Large Transport Aircraft". Symposium on Vehicle Ride Quality, NASA TMX-2620, page 91-113, October 1972.

APPENDIX A

PRELIMINARY BASEPOINT AIRCRAFT

To insure a high degree of realism in the parametric aircraft, preliminary basepoint aircraft designs were generated for the matrix mid-point design requirements of 100 passengers and 2000 foot (610 meters) field length for each of the lift systems:

Externally blown flap	(EBF)
Upper surface blowing	(USB)
Augmentor wing	(AW)
Internally blown flap	(IBF)
Mechanical flap	(MF)

For the EBF and AW aircraft both General Electric Company and Detroit Diesel Allison Task I QCSEE engines were used making a total of seven hard point design aircraft. An additional basepoint CTOL design was studied. The selection of the proper QCSEE Study engine for each case is discussed in Section 4.0 of the report.

These basepoint aircraft incorporate the results of coordination with the airline subcontractors as discussed in Section 5.0.

Three-view drawings of these designs are shown in Figures A-1 through A-3 for the externally blown flap, upper surface blowing and augmentor wing aircraft, respectively. A performance summary of these hard point aircraft including the CTOL design is shown in Table A-1.

The basepoint airplanes were designed for a cruise speed of not less than $M = 0.7$ and a range of 575 statute miles (926 km). Each airplane was designed to meet the noise target of 95 PNdB at a sideline distance of 500 feet (152 meters).

BASEPOINT PARAMETRIC AIRCRAFT

EXTERNALLY-BLOWN FLAP

PASSENGERS: 100

FIELD LENGTH 2000 FT (610M)

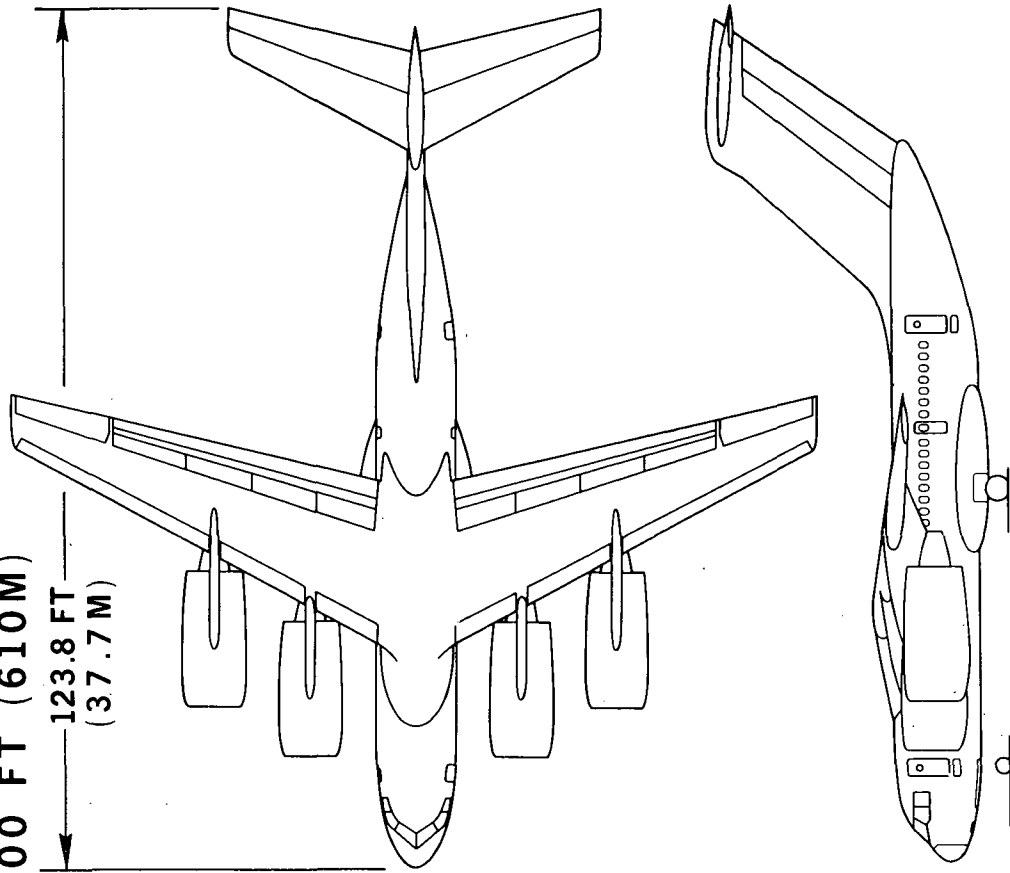
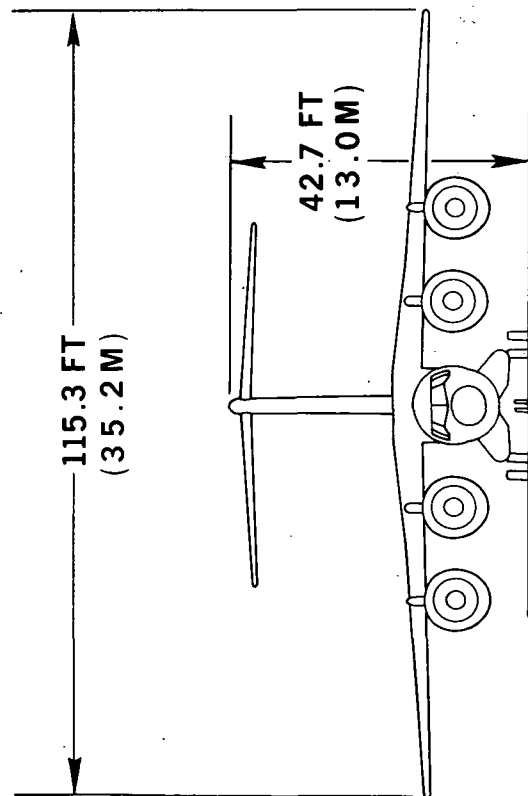
FOUR VP PROPFAN ENGINES

ALLISON PD287-3

BYPASS RATIO 17.4

PRESSURE RATIO 1.25

SLS THRUST (107,700N)



PR2-STOL-9918

FIGURE A-1

BASEPOINT PARAMETRIC AIRCRAFT

UPPER SURFACE BLOWN JET FLAP

PASSENGERS: 100 FIELD LENGTH 2000 FT (610M)

FOUR TURBOFAN ENGINES

ALLISON PD287-22

BYPASS RATIO 14.8

PRESSURE RATIO 1.3

SLS THRUST (102,000N)

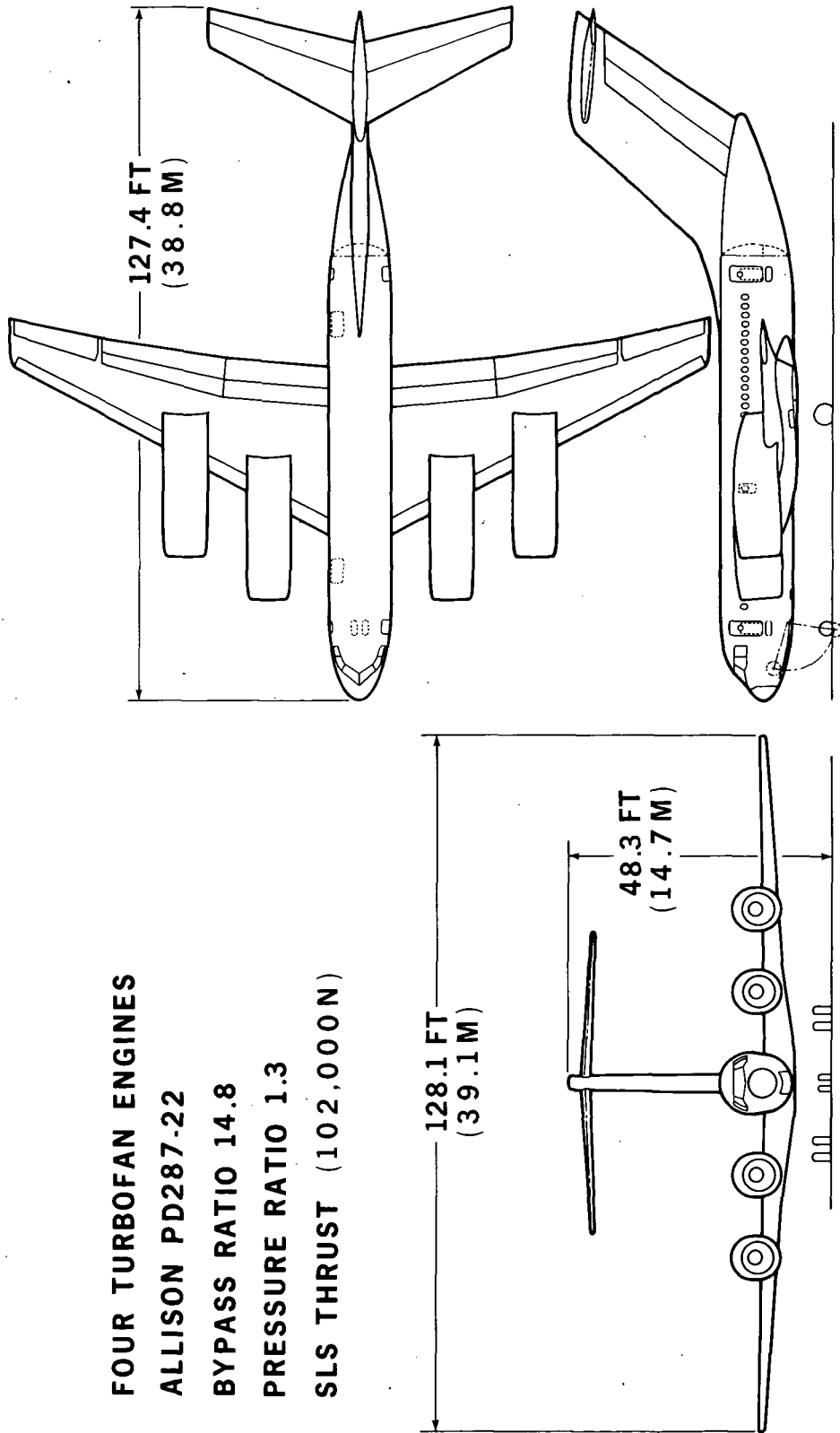


FIGURE A-2

PR2-STOL-9956

BASEPOINT PARAMETRIC AIRCRAFT

AUGMENTOR - WING

PASSENGERS: 100, FIELD LENGTH 2000 FT (610 M)

FOUR TURBOFAN ENGINES

ALLISON PD287.43

BYPASS RATIO 2.8

PRESSURE RATIO 3.0

SLS THRUST 22,200 LB (98,800 N)

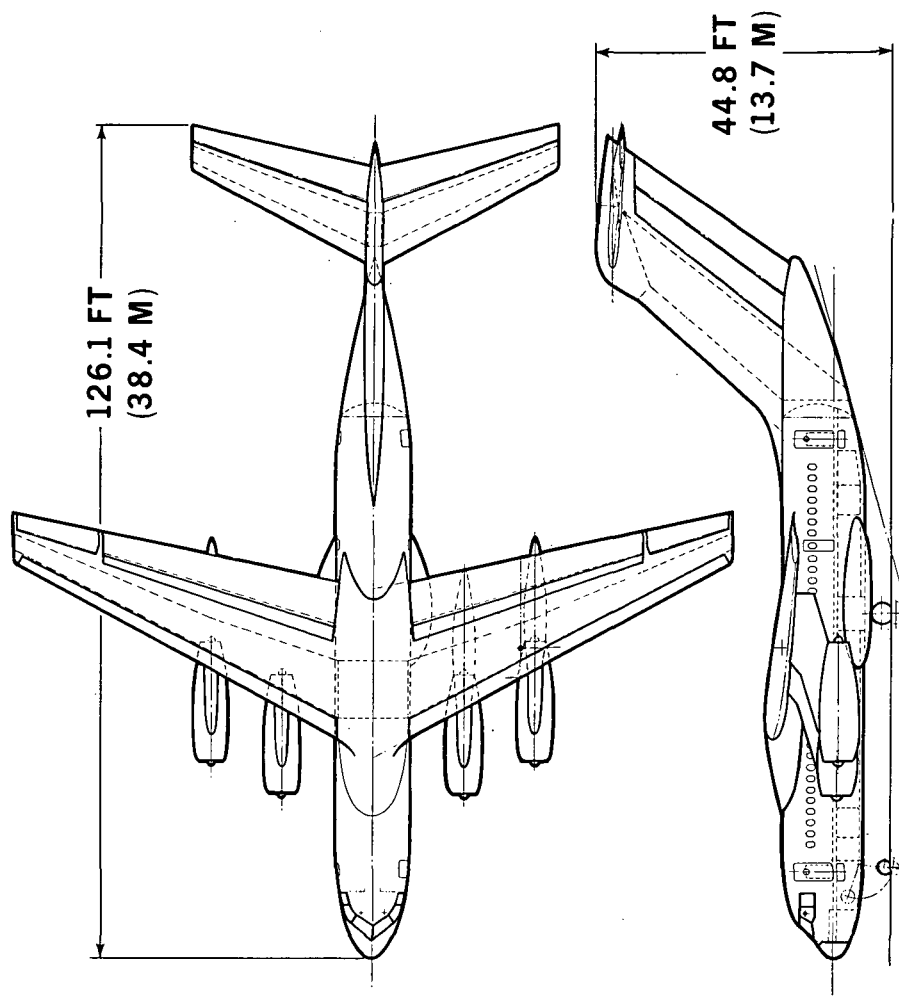
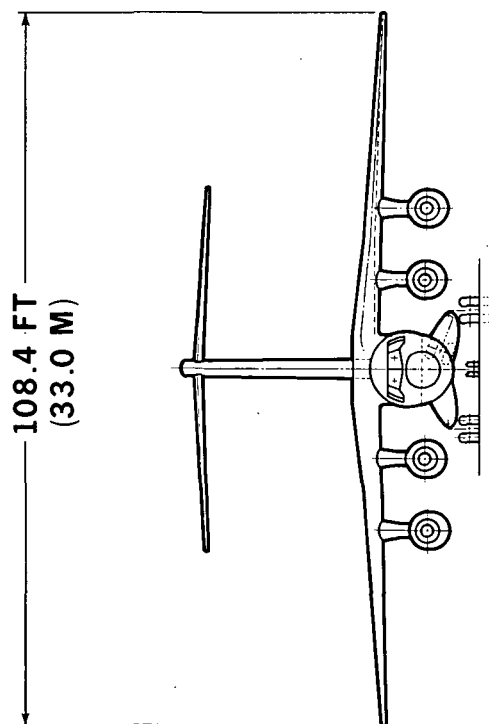


FIGURE A-3

PR2-STOL-9955A

Table A-1

PRELIMINARY BASEPOINT AIRCRAFT PERFORMANCE SUMMARY

	HARDPOINT DESIGNS					
	EBF	USB	AW	IBF	MF	CTOL
Range	St Mi (Km)		575 (927)			1380 (1932)
Field Length	Ft (M)		2,000 (610)			7500 (2285)
Passengers			100			100
TOGW	Lb (Kg)	142,600 (64,700)	162,800 (73,800)	189,200 (85,800)	165,500 (75,100)	129,500 (58,700)
OEW	Lb (Kg)	101,600 (46,100)	111,300 (50,500)	135,100 (61,300)	114,600 (52,000)	77,300 (35,100)
Fuel	Lb (Kg)	21,000 (9,500)	31,500 (14,300)	34,100 (15,500)	30,900 (14,000)	32,200 (14,600)
Wing Area	Ft ² (M ²)	1,900 (177)	1,810 (168)	2,366 (220)	2,470 (229)	1,080 (100)
Wing Loading	Lb/Ft ² (Kg/M ²)	75 (366)	90 (439)	80 (391)	67 (327)	120 (586)
Engine		(4)Allison PD287-3	(4)Allison PD287-43	(4)GE19/F9	(4)Allison PD287-43	(2)Hybrid Engine
Rated Thrust/Eng	Lb (Newtons)	24,200 (107,650)	17,400 (77,400)	20,700 (92,100)	16,760 (74,550)	26,500 (117,900)
Thrust Loading		0.678	0.427	0.438	0.405	0.409
Max Cruise Speed	MN	0.70	0.79	0.80	0.76	0.78
DOC	¢/ASSM (¢/ASKM)	3.36 (2.09)	3.40 (2.11)	3.85 (2.39)	3.48 (2.16)	2.08 (1.29)

APPENDIX B

AERODYNAMIC SUBSTANTIATION - FINAL DESIGN AIRCRAFT

B.1 PERFORMANCE ANALYSIS METHODS

B.1.1 Takeoff

STOL takeoff performance was estimated by calculating the time history of the takeoff flight path. This method allows for recognition of changes in aerodynamic characteristics and flight limitations which occur during the maneuver. The calculations are governed by the following assumptions:

1. The aircraft is assumed to be a point mass, i.e., second order rotational dynamics have been ignored and the analysis is essentially two dimensional.
2. The forces acting on the aircraft are summed in the longitudinal and normal directions and are a function of true airspeed, flight path angle, angle of attack and height above the ground.
3. Any restriction on speed, acceleration, attitude, etc. may be imposed as desired.
4. The path is generated by numerical integration of the forces acting on the aircraft over small increments in time using a digital computer.

The time history of a typical takeoff case is shown in Figure B-1. In this example, engine failure occurs prior to the start of rotation and limitations on angle of attack and longitudinal acceleration are recognized during the air run.

Takeoff field length is defined as the greater of:

1. $1.15 \times$ all engine takeoff distance to 35 foot (10.7 m) height.
2. Distance to 35 foot (10.7 m) height with critical engine failure at V_1 .
3. Distance to accelerate to V_1 and then decelerate to a stop.

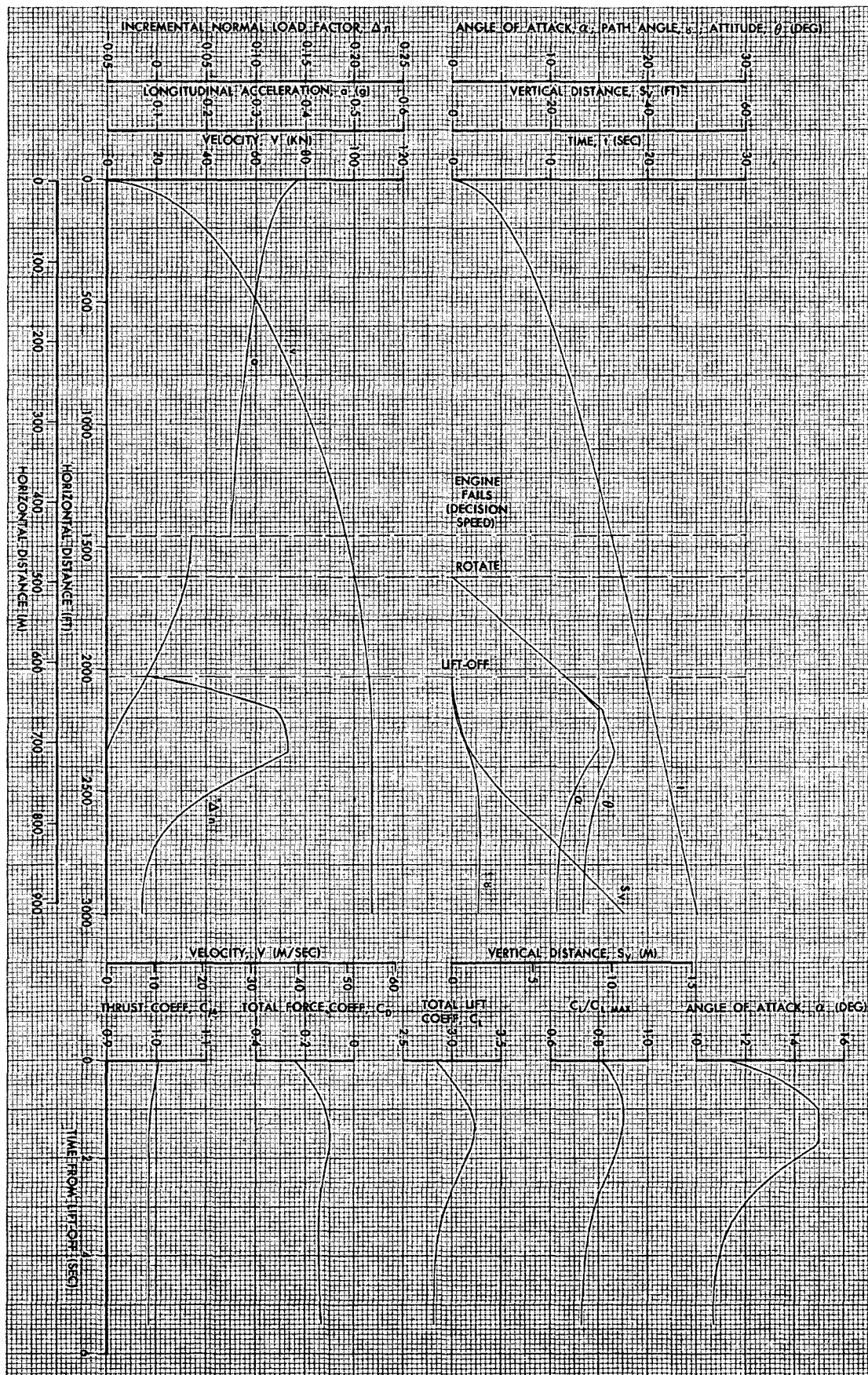


FIGURE B-1. SAMPLE TAKEOFF TIME HISTORY

The following constraints were used in calculating the takeoff field lengths for the final design aircraft.

1. Rolling friction, $\mu = 0.025$
2. Fuselage angle of attack \leq ground limit = 15°
3. Rotation rate, $\dot{\theta} \leq 5^\circ/\text{sec}$
4. $C_L \leq 90\%$ of $C_{L_{\max}}$ out of ground effect
5. $C_L \leq 100\%$ of $C_{L_{\max}}$ in ground effect
6. No deceleration during air run to 35 feet (10.7 m) height
7. Five knot (2.57 m/sec) early rotation may not give greater takeoff field length
8. Accelerate-stop distance based on three second delay after reaching V_1 followed by a deceleration of 0.4g to a stop.

The takeoff computer program, in addition to calculating takeoff time histories, will automatically vary rotation and decision speeds to determine takeoff field lengths as defined above and illustrated in Figure B-2. Additional capabilities exercised during the sizing of the final design aircraft include optimization of flap angle and the ability to select the thrust loading required for a given wing loading and field length. Takeoff performance was calculated for sea level, 95°F (35°C) conditions.

B.1.2 Landing

The methods and assumptions used in calculating landing field lengths are essentially the same as those used for takeoff performance. The landing maneuver consists of three segments; approach, flare and ground roll as shown in Figure B-3. Landing field length is defined as the landing distance over a 35-foot (10.7 m) obstacle divided by a 0.6 factor, i.e., a 3000 foot (914 m) field length requires a landing distance of 1800 feet (549 m).

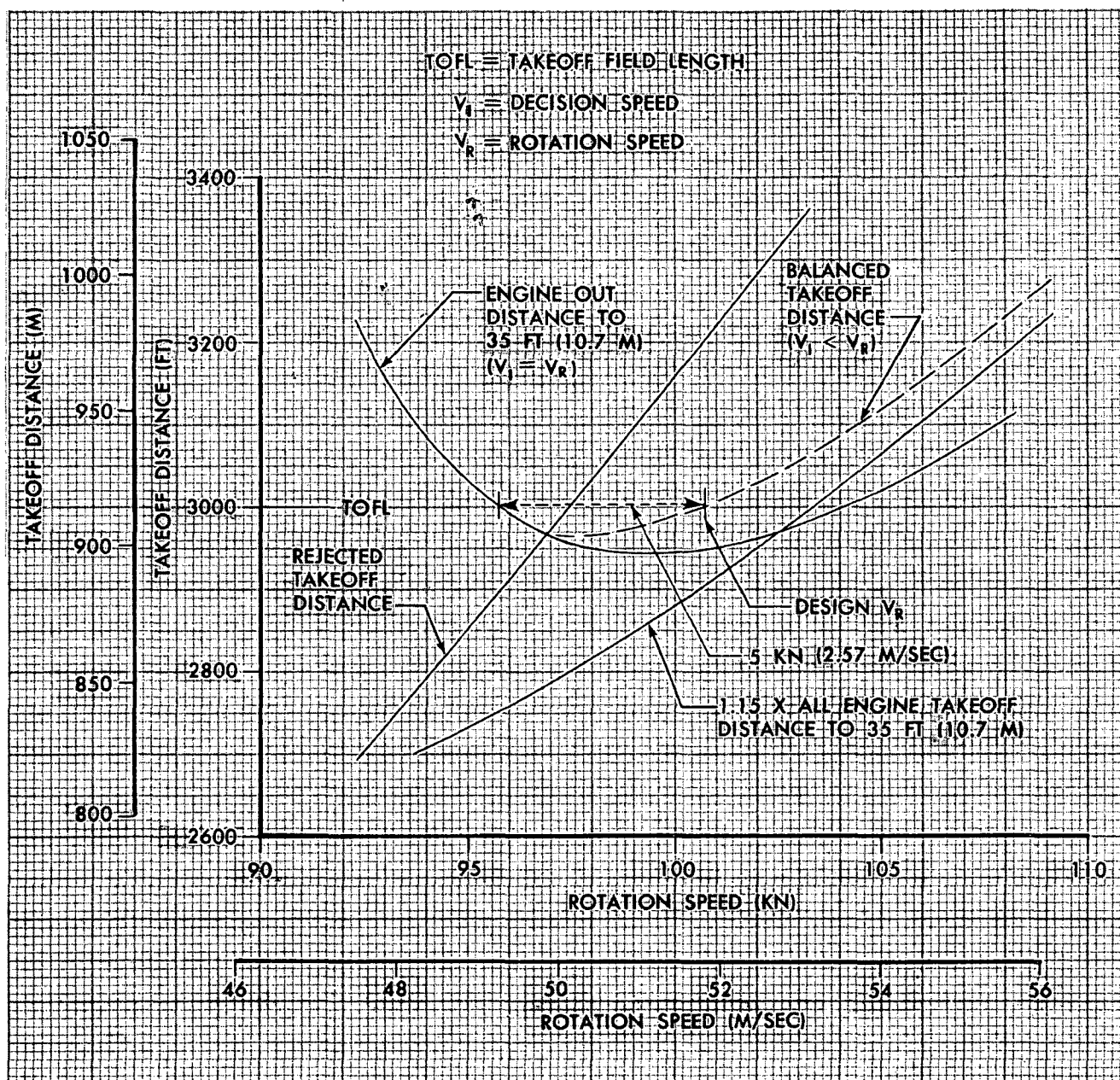


FIGURE B-2. TAKEOFF FIELD LENGTH DEFINITION

LANDING FIELD LENGTH DEFINITION

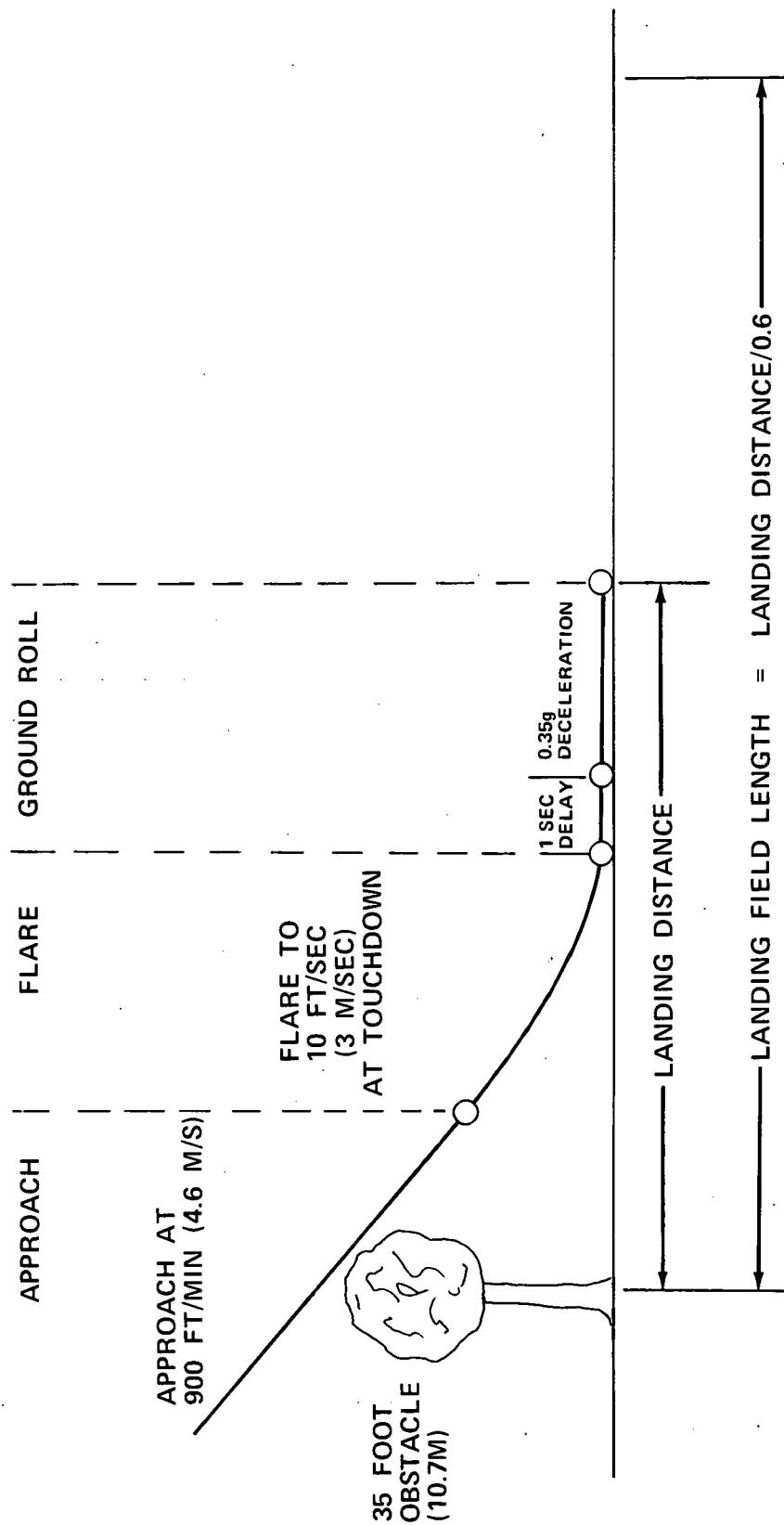


FIGURE B-3

PR3-STOL-1494

Approach margins, selected to provide adequate maneuver capabilities in the event of an engine failure are summarized in Table B-1 for the nine final design aircraft. These margins in addition to the 900 fpm (4.57 m/sec) approach sink rate define the approach conditions.

The flare maneuver is governed by the following constraints:

1. Fuselage angle of attack \leq ground limit = 15°
2. Rotation rate, $\leq 5^\circ/\text{sec}$
3. $C_L \leq 100\%$ of $C_{L_{\max}}$ in ground effect

A typical flare time history is shown in Figure B-4. The flare maneuver was accomplished by retracting the DLC spoilers at the flare height and rotating the aircraft at $5^\circ/\text{sec}$. As the aircraft approaches the ground, C_L and C_D tend to drop off due to ground effect.

The ground roll consists of one second at constant speed from touch-down to deceleration device effectiveness followed by a constant deceleration of $0.35g$ to a stop. Landing, like takeoff, was calculated for sea level, 95°F (35°C) conditions.

B.1.3 Aircraft Sizing

The sizing process is illustrated by Figure B-5. Thrust-to-weight and wing loading combinations which satisfy the takeoff and landing field length requirements together with parametric weight data ($\text{OEW} = f(\text{TOGW}, W/S, T/W)$), installed thrust and fuel flow maps, and drag and tail sizing information are used as inputs to a computer program which performs the aircraft sizing calculations. This program was specifically developed by Douglas Aircraft Company during the last five years for the sizing of STOL aircraft in the advanced design stage. The methods used are essentially those of classical airplane performance. The mission profile used for airplane sizing

Table B-1

FINAL AIRCRAFT APPROACH MARGINS

Configuration	Field Length ft (m)	Approach Speed kn (m/sec)	V_{APR}/V_{STALL}	Angle of Attack Margin (deg)	Available Load Factor g	Percent of Gross Takeoff Thrust Used in Approach
EBF	2000	76 (39)	1.33	11	1.33	65
EBF	3000	97 (50)	1.33	11	1.33	65
MF	3000	97 (50)	1.30	16	1.64	40
MF	4000	116 (60)	1.30	16	1.63	46
AW	2000	74 (38)	1.30	15	1.34	75
USB	2000	75 (39)	1.35	15	1.33	65
CTOL	7500	132 (68)	1.30	14	1.63	47

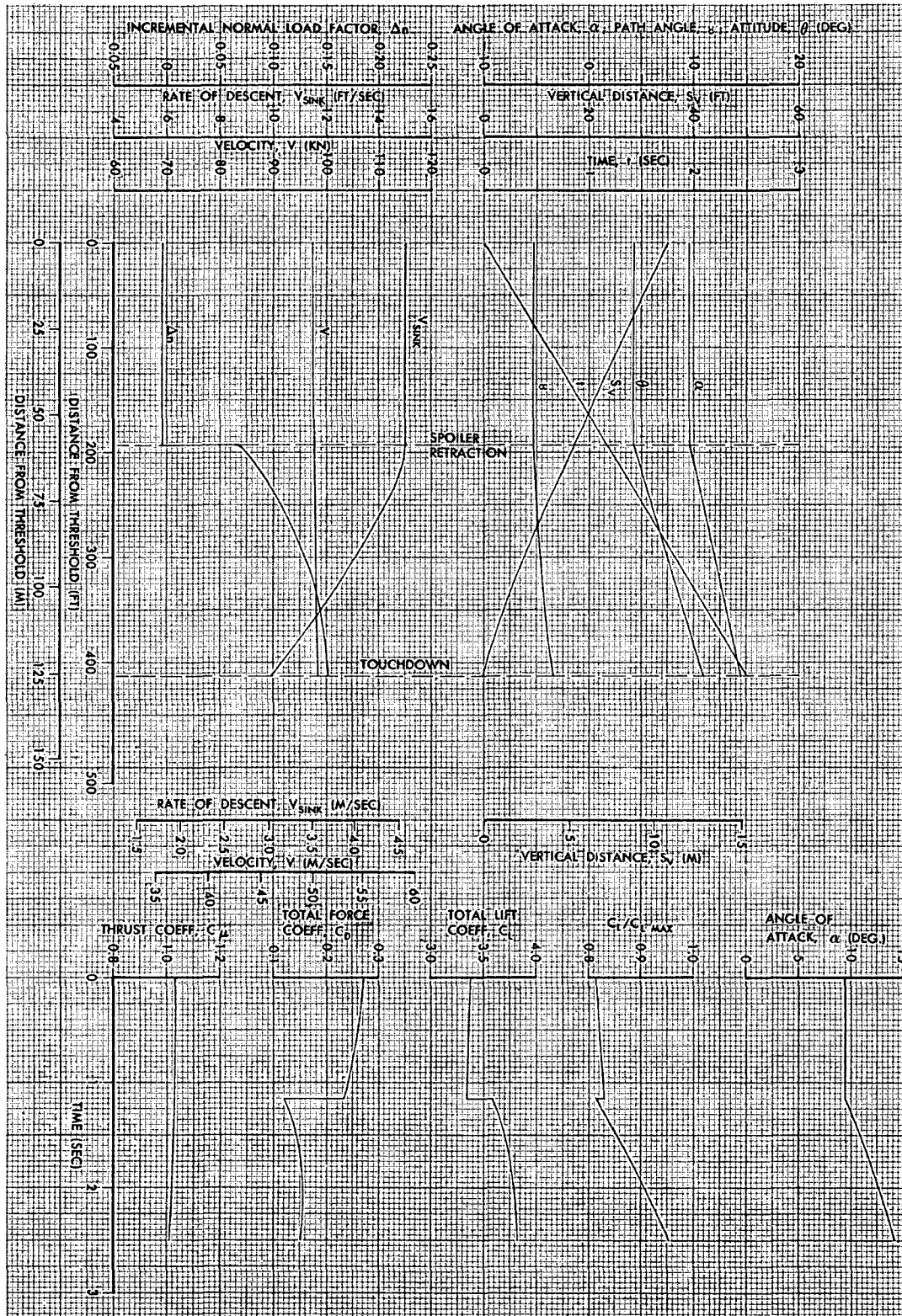


FIGURE B-4. SAMPLE FLARE TIME HISTORY

AIRCRAFT SIZING PROCESS

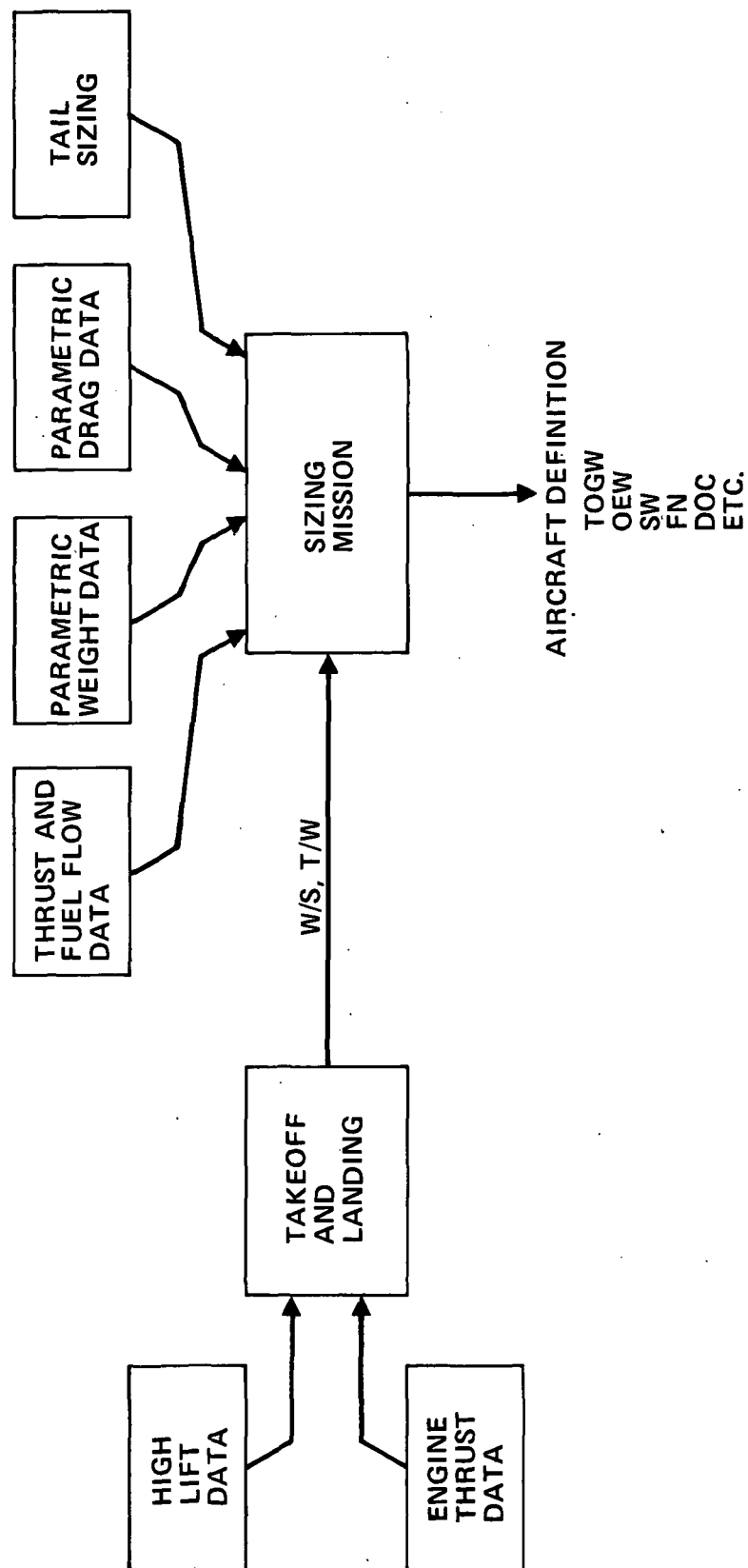
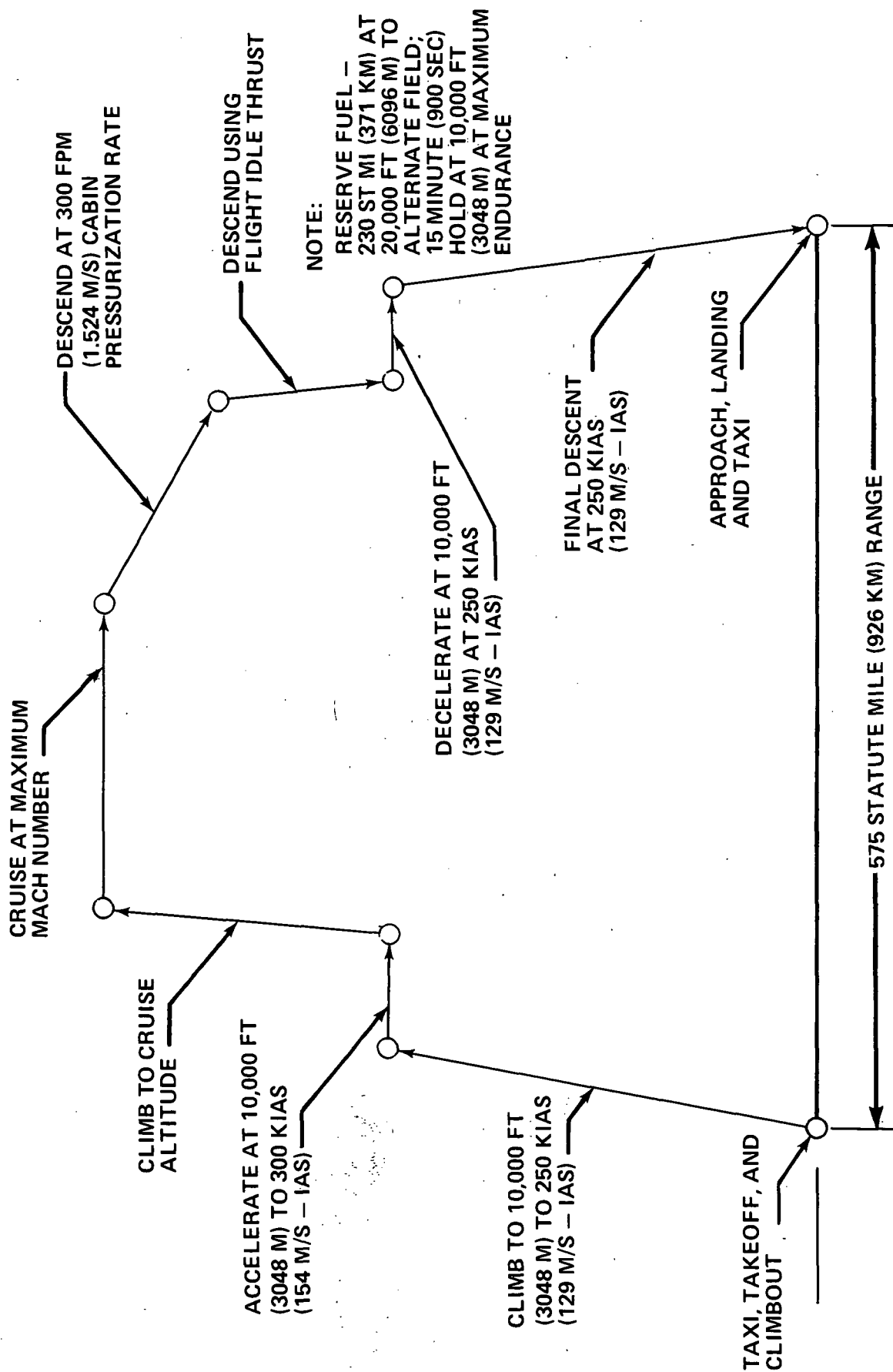


FIGURE B-5

is shown in Figure B-6. The computer program was used to calculate 2 degree of freedom mission time histories, iterating on the weight, thrust, drag and tail sizing data to determine the characteristics such as TOGW, wing area, engine size, OEW, fuel burned, etc. of an aircraft which satisfies the requirements of the mission profile with the desired payload. When a solution has been found, the program calculates a direct operating cost (DOC) breakdown. The computer printout of a mission segment summary and a DOC breakdown for a typical sizing mission are shown in Figures B-7 and B-8.

Cruise altitude and climb Mach number were optimized to minimize DOC for the final design aircraft. Mission performance was calculated for standard day conditions.

SIZING MISSION PROFILE



PR3-STOL-1591

FIGURE B-6

SAMPLE SIZING MISSION SUMMARY PRINTOUT

KSJA - MISSION ANALYSIS

M C D O N N E L L D O U G L A S C O R P O R A T I O N

MARCH 3, 1973

REFERENCE RUN 1 CASE 1
NASA SYSTEMS STUDY (ERE) DCCG=F(M,CL) 1C-26-72 LEVEL

TAKEOFF WT = 149032. THRUST/ENG = 18256. BLOCK TIME = 1.41915 (T-MP) TIME= 0.0
WING AREA = 1461.09 NO. OF ENG = 4.00000 BLOCK FUEL = 11526.2 (T-MP) FUEL= 0.0
PAYLOAD = 30000. ENGINE SIZE= 0.91290 BLOCK DIST = 500.00 (T-MP) DIST= 0.0
O.F.W. = 102613. WF MULT. = 1.00000 F (DRAG) = 32.3634 (T-B) TIME = 0.86810 MP W/S = 0.0
TOGW/SW = 102.001 FN MULT. = 1.00000 AR = 8.00000 (T-B) FUEL = 4892.9 MP T/W = 0.0
THRUST/TOGW= 0.48999 FUEL/TOGW = 0.11017 F = 0.76739 (T-B) DIST = 200.00 MP FUEL/WT = 0.0

MISSION SEGMENT	FINAL WEIGHT(LB)	SEGMENT TIME(HR)	SEGMENT FUEL(LB)	SEGMENT DIST(NM)	INITIAL HP(FT)	FINAL HP(FT)	INITIAL MACH	FINAL MACH	TEMPERATURE
TEMPERATURE ALLOWANCE	148511.	0.07500	520.29	0.0		10000.	0.37794	0.45227	0.0
CLIMB	147699.	0.06155	812.44	16.515	0.	10000.	0.45227	0.54105	0.0
ACCELERATION	147557.	0.01169	142.50	3.724	10000.	26000.	0.54105	0.69000	0.0
CLIMB	143587.	0.34660	3870.00	153.808	10000.	26000.	0.69000	0.69413	32.
SPEED POWER	143586.	0.01239	100.13	5.139	26000.	26000.	0.69413	0.69413	0.0
ACCELERATION	143586.	0.00572	4096.70	211.475	26000.	32574.	0.69413	0.70081	0.0
SPEED POWER	143586.	0.00102	1.75	0.425	26000.	26000.	0.70081	0.69000	0.0
OPT ALTITUDE	139488.								
CRUISE	138491.	0.13823	997.20	57.137	26000.	20758.	0.69000	0.66074	
DECELERATION	138344.	0.05890	146.14	21.923	20758.	10000.	0.66074	0.54105	
TIME START	139315.	0.01013	28.38	3.202	10000.	10000.	0.54105	0.45227	
DESCENT	137974.	0.09963	341.36	26.653	10000.	0.	0.45227	0.37794	
DESCENT	137505.	0.05830	468.30	0.0					T-TMIN=-0.00018
ALLOWANCE									
BLOCK POINT	133829.	0.61810	3675.94	200.001	20000.	20000.	0.52932	0.52424	0.0
TEMPERATURE	132612.	0.25000	1216.94	0.0	10000.	10000.	0.31754	0.31608	
CRUISE									
HOLD									

VH = 1.4262 VV = 0.1238

NUMBER OF ITERATIONS = 8
CALCULATION TIME = 0.3602 MINUTES
ACCUMULATED TIME = 0.4676 MINUTES

PR3-STOL-1639

FIGURE B-7

SAMPLE DIRECT OPERATING COST BREAKDOWN PRINTOUT

K5JA - MISSION ANALYSIS

W C D O N N E L L D O U G L A S C O R P O R A T I O N

MARCH 3, 1973

DIRECT OPERATING COST

OPERATIONAL ITEMS (LR)	=	2841.	ROLLING ASSEMBLY FACTOR	=	0.0	PASSENGER & BAGGAGE WT	=	200.00
CARGO WEIGHT (LB)	=	0.	OIL PRICE (\$/LB)	=	0.92600	FUEL PRICE (\$/LR)	=	0.01800
AIRFRAME COST (\$/LR)	=	105.052	MISCELLANEOUS COST (\$)	=	0.	LABOR RATE (\$/HR)	=	6.0000
INSURANCE RATE	=	0.02000	DEPRECIATION PERIOD (YR)	=	12.000	RESIDUAL VALUE FACTOR	=	0.0
UTILIZATION (HR/YR)	=	2500.	OPERATOR EMPY WT (LB)	=	102613.	PAYLOAD (LR)	=	30000.
BURDEN FACTOR	=	1.8000	CRUISE ENGINE S.O.F.	=	0.2500	LIFT ENGINE S.O.F.	=	0.2000
CRUISE THRUST / ENGINE	=	18256.	NUMBER OF ENGINES	=	4.0000			

NUMBER OF SEATS	=	150.000	DEPRECIATION, FLIGHT EQUIPMENT	=	(\$/BLK HR)
CENTS/SEAT MILE	=	2.38097	COMPLETE AIRCRAFT	=	421.719
CENTS/TON MILE	=	23.8097	AIRFRAME SPARES	=	31.419
DOLLARS/MILE	=	3.58406	CRUISE ENGINE SPARES	=	26.883
DOLLARS/BLK HOUR	=	1263.064	LIFT ENGINE SPARES	=	0.0
DOLLARS/FLIGHT CYCLE	=	1792.48	SURTOTAL.....	=	480.021
MAX TAKEOFF GROSS WEIGHT (LR)	=	149032.	HOURLY MAINTENANCE, FLIGHT EQUIPMENT (\$/FLT HR)		
CRUISE ENGINE WEIGHT (LR/ENG)	=	2723.63	AIRFRAME LABOR	=	19.721
LIFT ENGINE WEIGHT (LR/ENG)	=	0.0	CRUISE ENGINE LABOR	=	19.672
CROSS SHAFTING WEIGHT	=	0.0	LIFT ENGINE LABOR	=	0.0
CRUISE ENGINE COST (\$/ENG)	=	806491.	CROSS SHAFTING LABOR	=	0.0
LIFT ENGINE COST (\$/ENG)	=	0.	AIRFRAME MATERIAL	=	21.773
AIRFRAME COST (\$)	=	9425587.	CRUISE ENGINE MATERIAL	=	60.487
AIRCRAFT COST (\$)	=	12651550.	LIFT ENGINE MATERIAL	=	0.0
MANEUVER TIME (HR)	=	0.13330	BURDEN	=	70.907
BLACK TIME (HR)	=	1.41915	SURTOTAL.....	=	192.560
BLACK FUEL (LR)	=	11526.17	CYCLIC MAINTENANCE, FLIGHT EQUIPMENT (\$/FLT CYCLE)		
FLIGHT TIME (HR)	=	1.28585	AIRFRAME LABOR	=	33.425
RANGE (NAUTICAL MILES)	=	500.00	CRUISE ENGINE LABOR	=	15.259
BLACK SPEED (KNOTS)	=	352.323	LIFT ENGINE LABOR	=	0.0
FUEL COST (\$/FLT CYCLE).....	=	207.471	AIRFRAME MATERIAL	=	44.112
FLYING OPERATIONS (LESS FUEL)		(\$/BLK HR)	CRUISE ENGINE MATERIAL	=	48.389
PILOT & CREW COST	=	190.432	LIFT ENGINE MATERIAL	=	0.0
OIL COST	=	0.500	BURDEN	=	87.629
HULL INSURANCE	=	101.213	SURTOTAL.....	=	228.813
SURTOTAL.....	=	301.144			

FIGURE B-8

PR3-STOL-1640

B.2 High Lift Configuration Aerodynamic Characteristics

The high lift system concepts evaluated during Phase II of this study may be grouped into two broad categories:

I. Externally Blown Flap and Mechanical Flap Systems:

- a. Classical externally blown flap (EBF) systems with engines generally forward of and below the wing, with significant exhaust impingement on the flaps.
- b. Upper surface blowing systems (USB) involving exhaust flow over the wing and Coanda flow turning.
- c. Conventional mechanical flap systems with little or no exhaust impingement.

II. Internally Blown Flap Systems:

- a. Ejector-augmented flap systems currently being developed as the augmentor wing.

In the first category, the Douglas externally blown flap powered wind tunnel model data, with appropriate modifications, represents a suitable baseline for estimating the high lift aerodynamic characteristics of EBF, USB and the 3000 foot (914 m) field length mechanical flap configuration. The USB characteristics may be considered to be adequately represented by the externally blown flap powered data with small adjustments, based on comparisons between Douglas EBF data and the USB data presented in Reference 7. The mechanical flap system characteristics may be derived from unpowered (zero thrust) externally blown flap configuration data. DC-10 type flap high lift characteristics were used as the base for the longer field length mechanical flap configurations.

The second category contains a variation of the classical jet flap. The system involves ducting all of the fan airflow through the wing to nozzles near the flap knee. The ejector-augmented system exhaust is turned partially by Coanda effect, but primarily by the walls of the inclined ejector. This system delivers a relatively uniform jet sheet to the flap trailing edge. The ejector-augmented flap system characteristics have been derived from the ejector-augmented flap configuration data from Reference 8.

B.2.1 Externally Blown Flap. - The externally blown flap high lift longitudinal aerodynamic characteristics were estimated based on Douglas powered-model low speed wing tunnel data acquired in the Canadian National Research Council (NRC) 30 foot V/STOL wind tunnel.

These data were adjusted to reflect a reduction of flap chord/wing chord ratio from 0.42 on the model to 0.35 on the aircraft using the Elementary Vortex Distribution (EVD) powered lifting surface theory and related Douglas static test data. The EVD method was also used to adjust the aspect ratio from 7.0 to 8.0.

No corrections were applied for Reynold's number. The increase in Reynold's number to airplane flight values will probably improve the wing section maximum lift values, especially outboard of the flap and engine exhaust region, and possibly result in some improvement in aileron effectiveness at high angles of attack. Accurate evaluation of these effects is not possible and neglecting them is believed to be conservative.

The trimmed lift and drag characteristics for the aspect ratio 8 EBF configurations are presented in Figures B-9 through B-17. Figures B-9 through B-14 present the all engines operating case, with and without DLC spoilers. Figures B-15 through B-17 present an outboard engine out (three

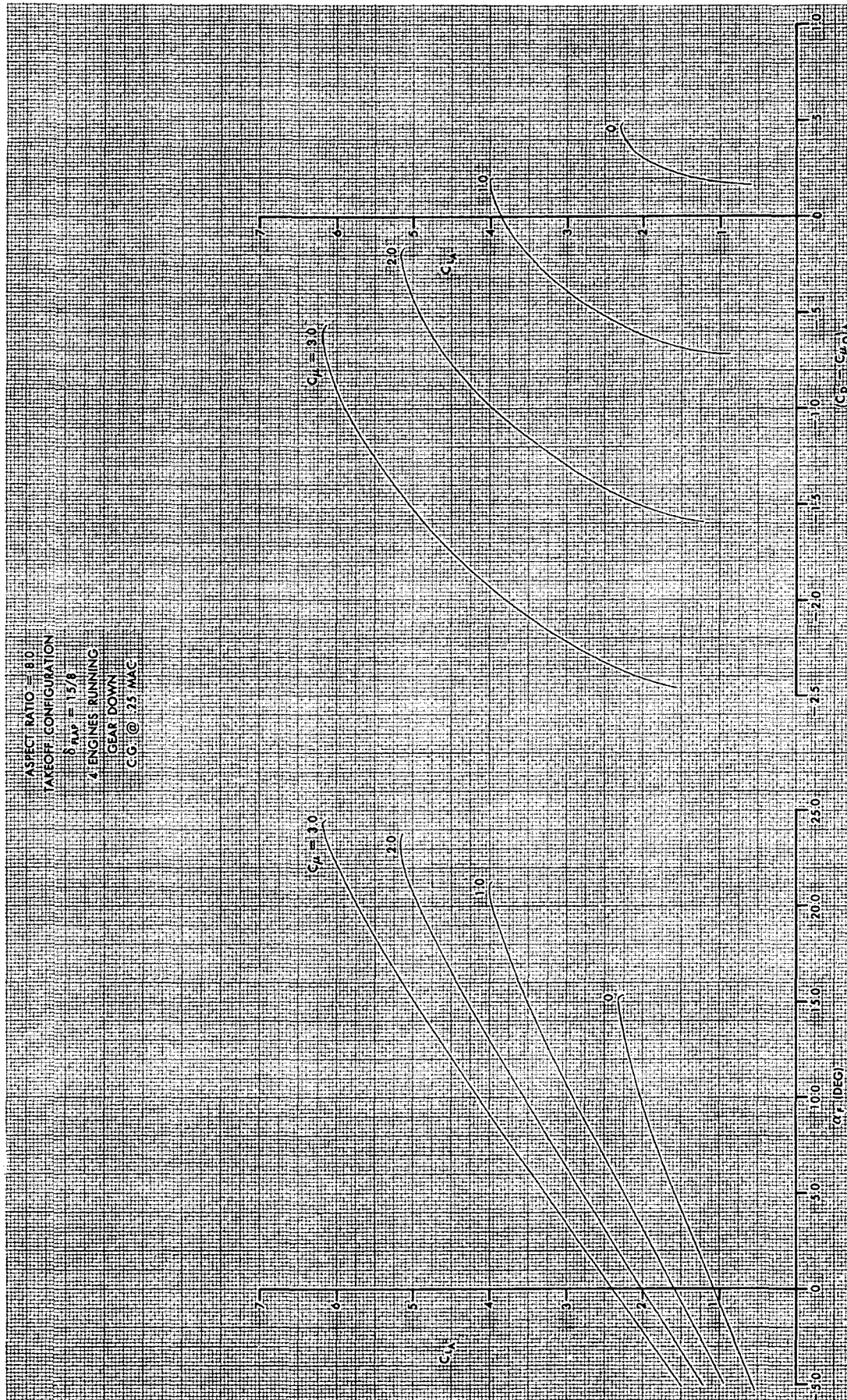


FIGURE B-9. EXTERNALLY BLOWN FLAP TRIMMED LIFT AND DRAG CHARACTERISTICS

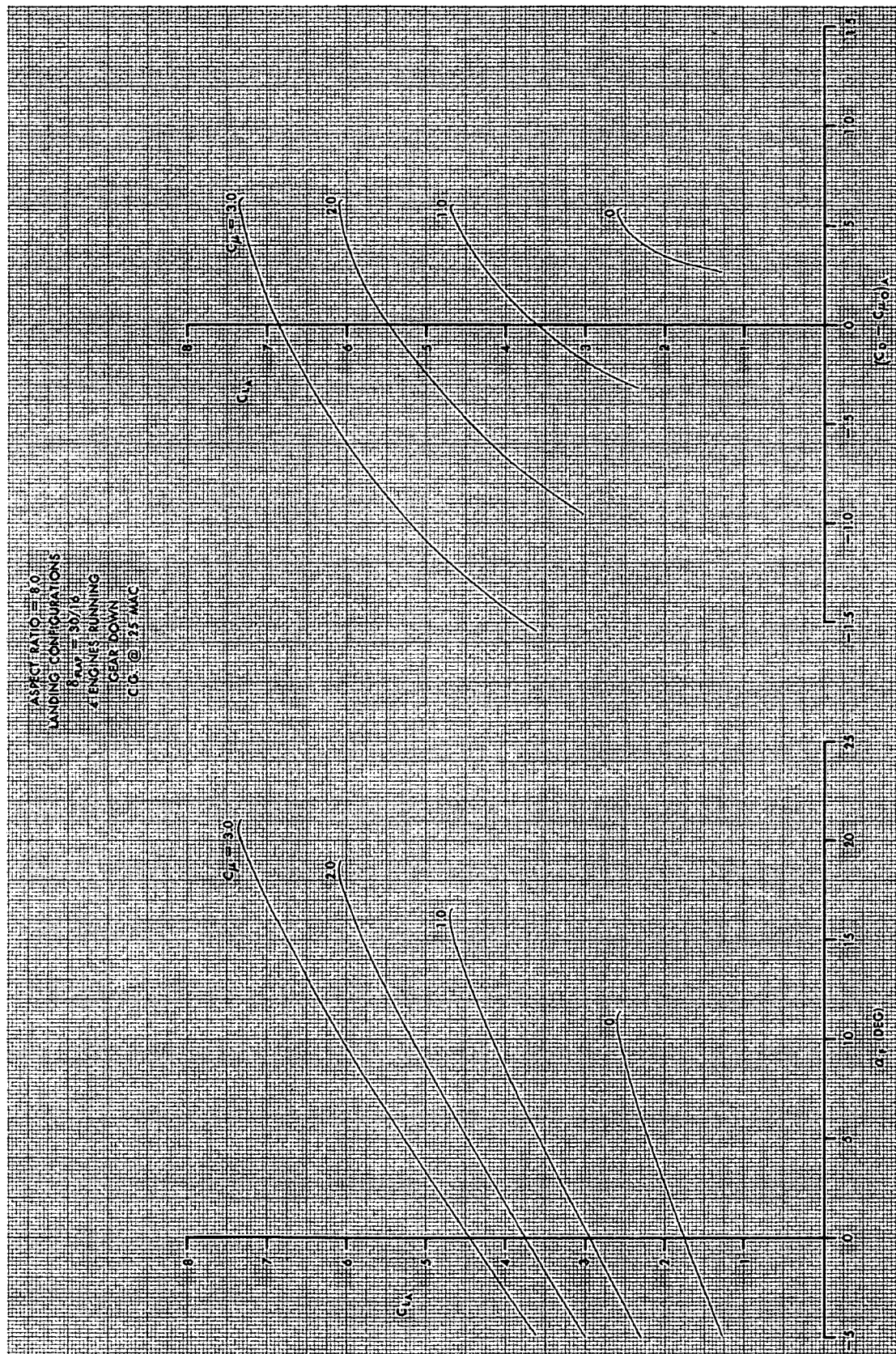


FIGURE B-10. EXTERNALLY BLOWN FLAP TRIMMED LIFT AND DRAG CHARACTERISTICS

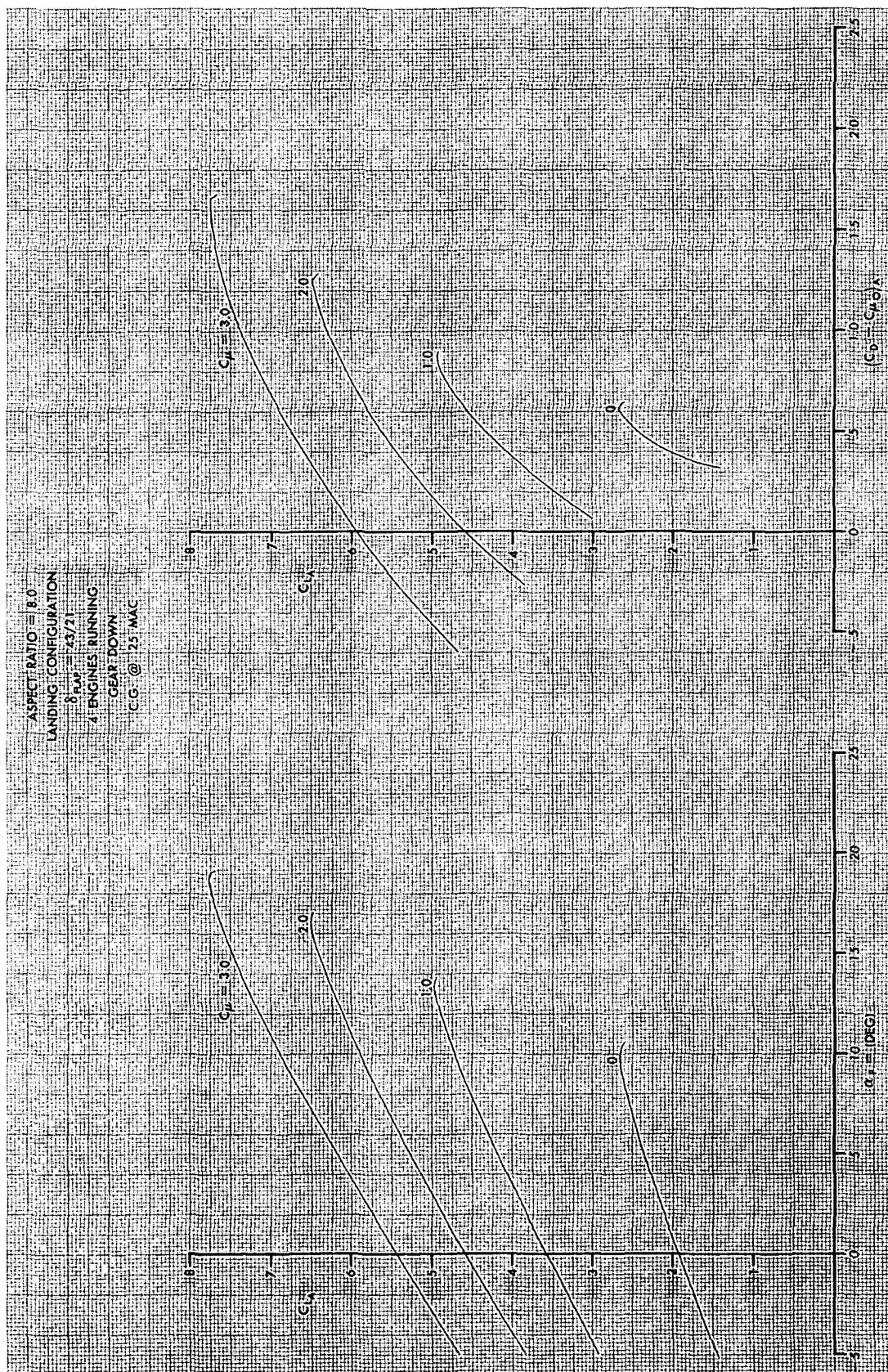


FIGURE B-11. EXTERNALLY BLOWN FLAP TRIMMED LIFT AND DRAG CHARACTERISTICS

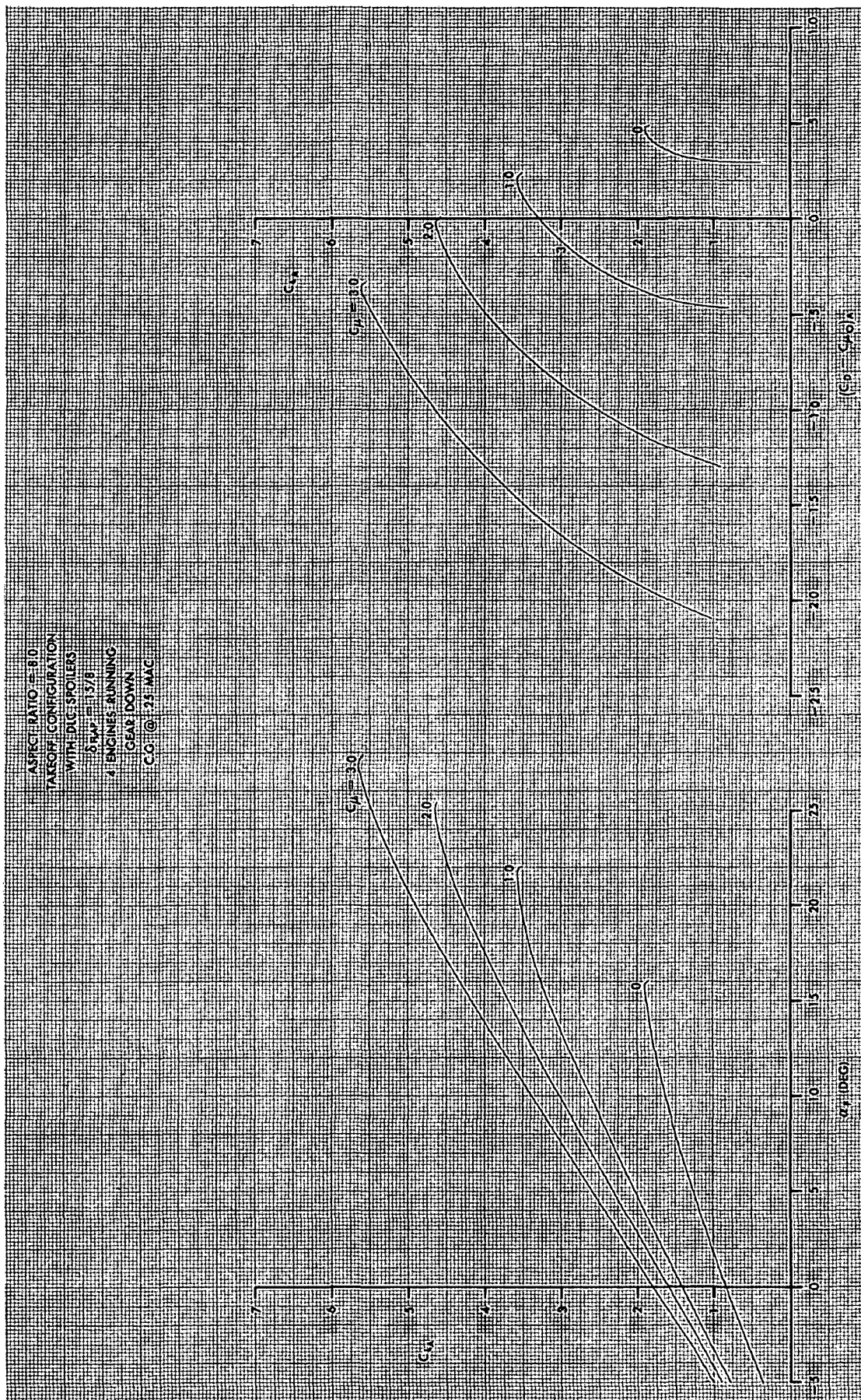


FIGURE B-12. EXTERNALLY BLOWN FLAP TRIMMED LIFT AND DRAG CHARACTERISTICS

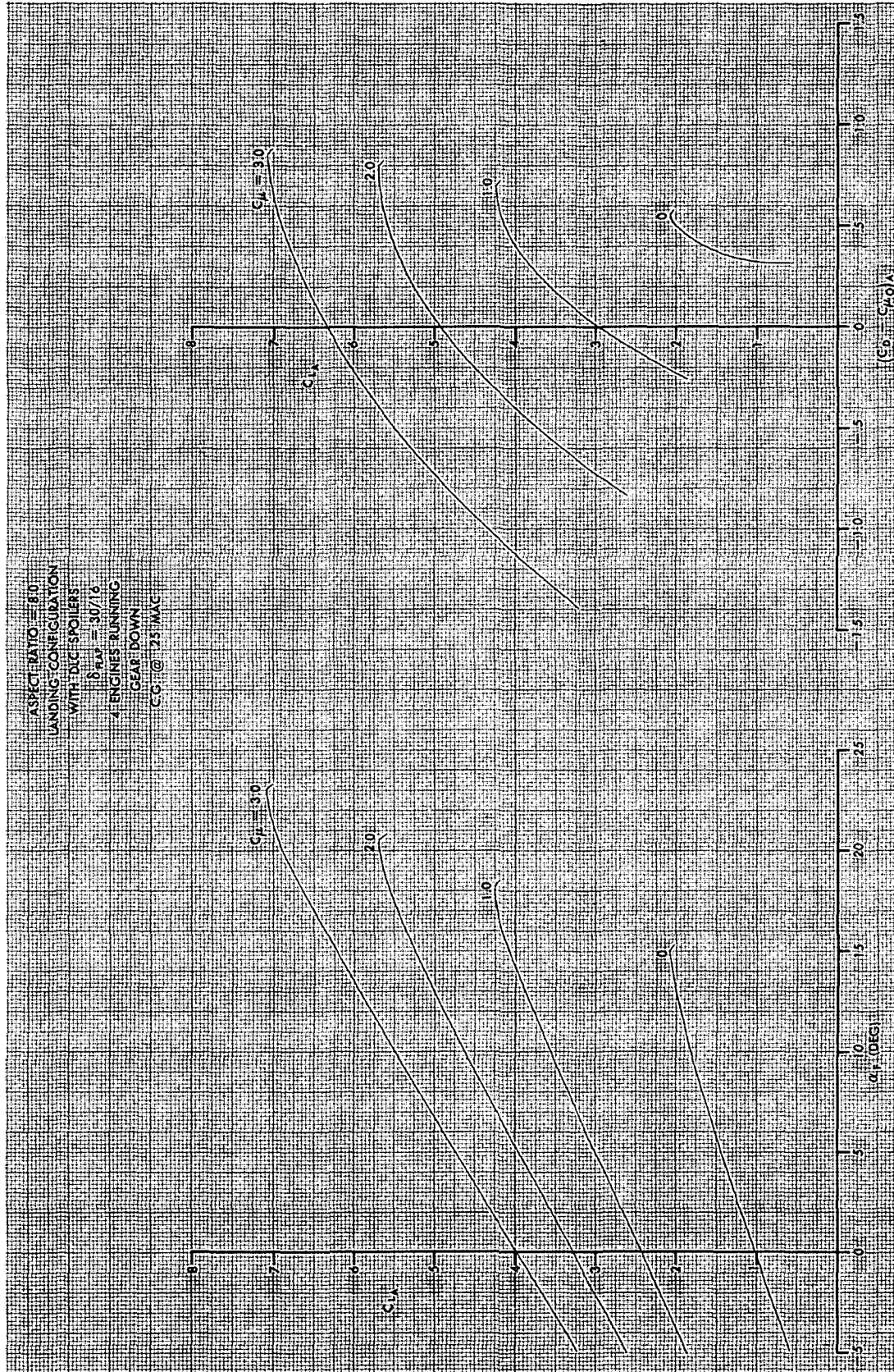


FIGURE B-13. EXTERNALLY BLOWN FLAP TRIMMED LIFT AND DRAG CHARACTERISTICS

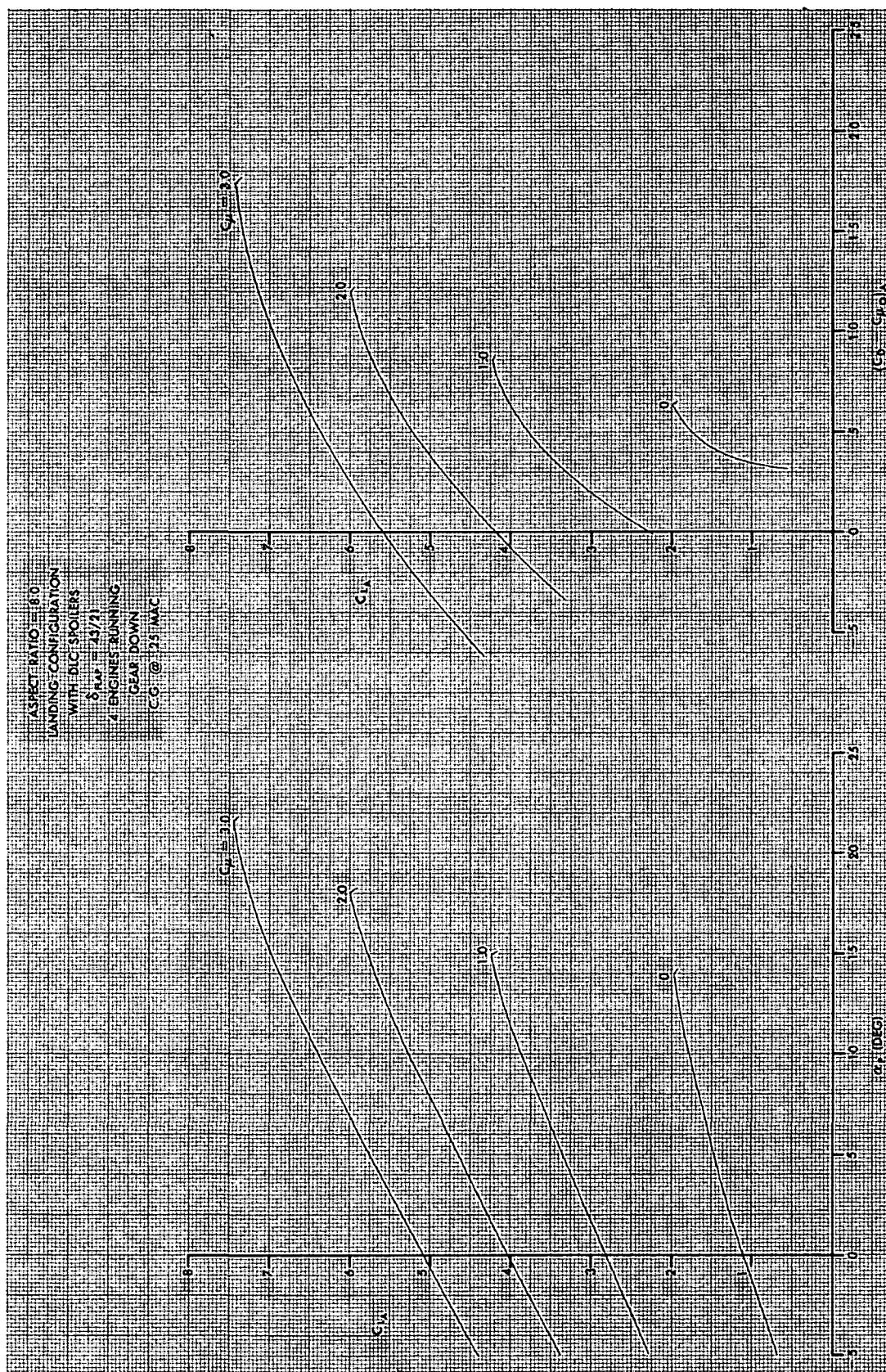


FIGURE B-14. EXTERNALLY BLOWN FLAP TRIMMED LIFT AND DRAG CHARACTERISTICS

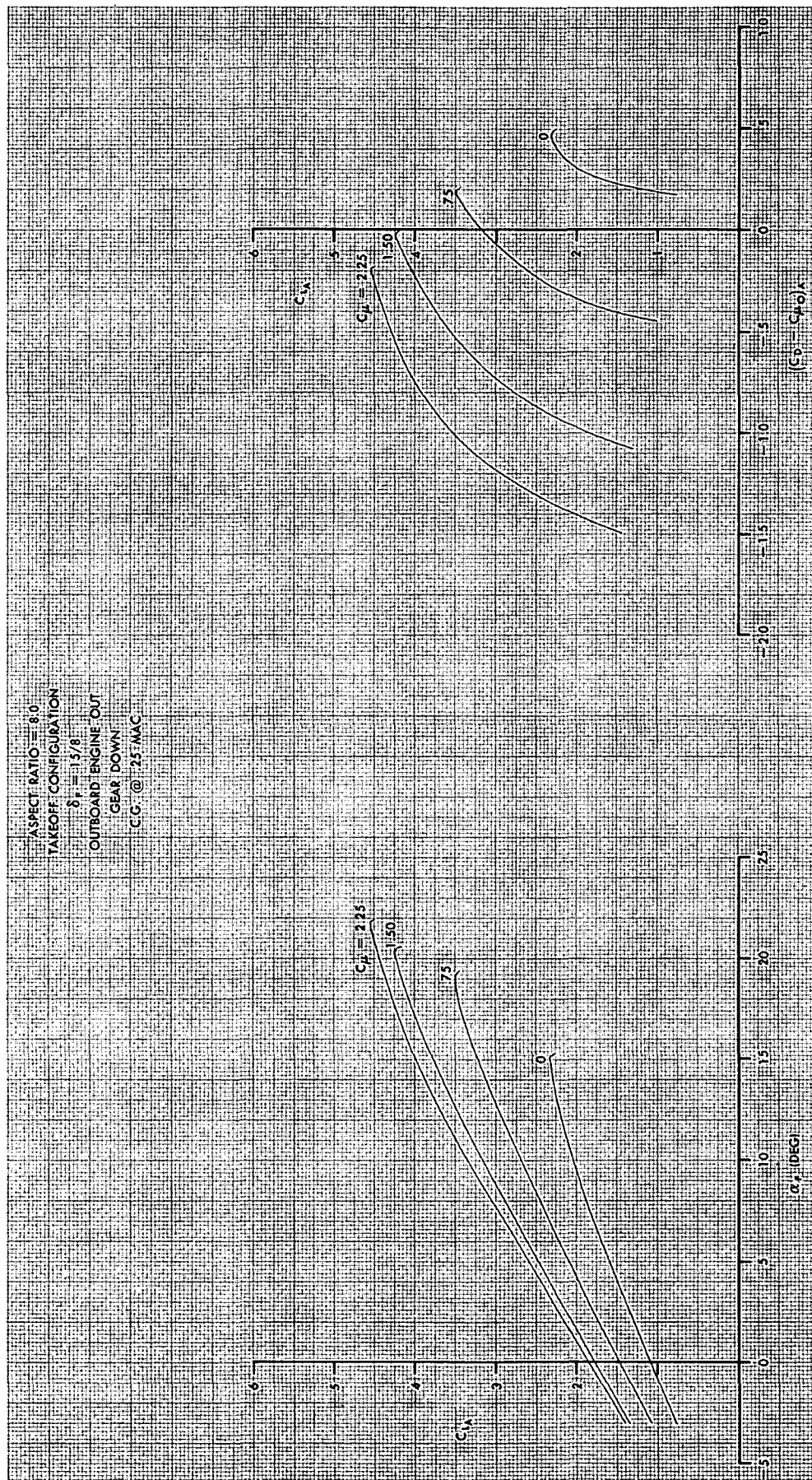


FIGURE B-15. EXTERNALLY BLOWN FLAP LONGITUDINALLY, Laterally AND DIRECTIONALLY TRIMMED LIFT AND DRAG CHARACTERISTICS

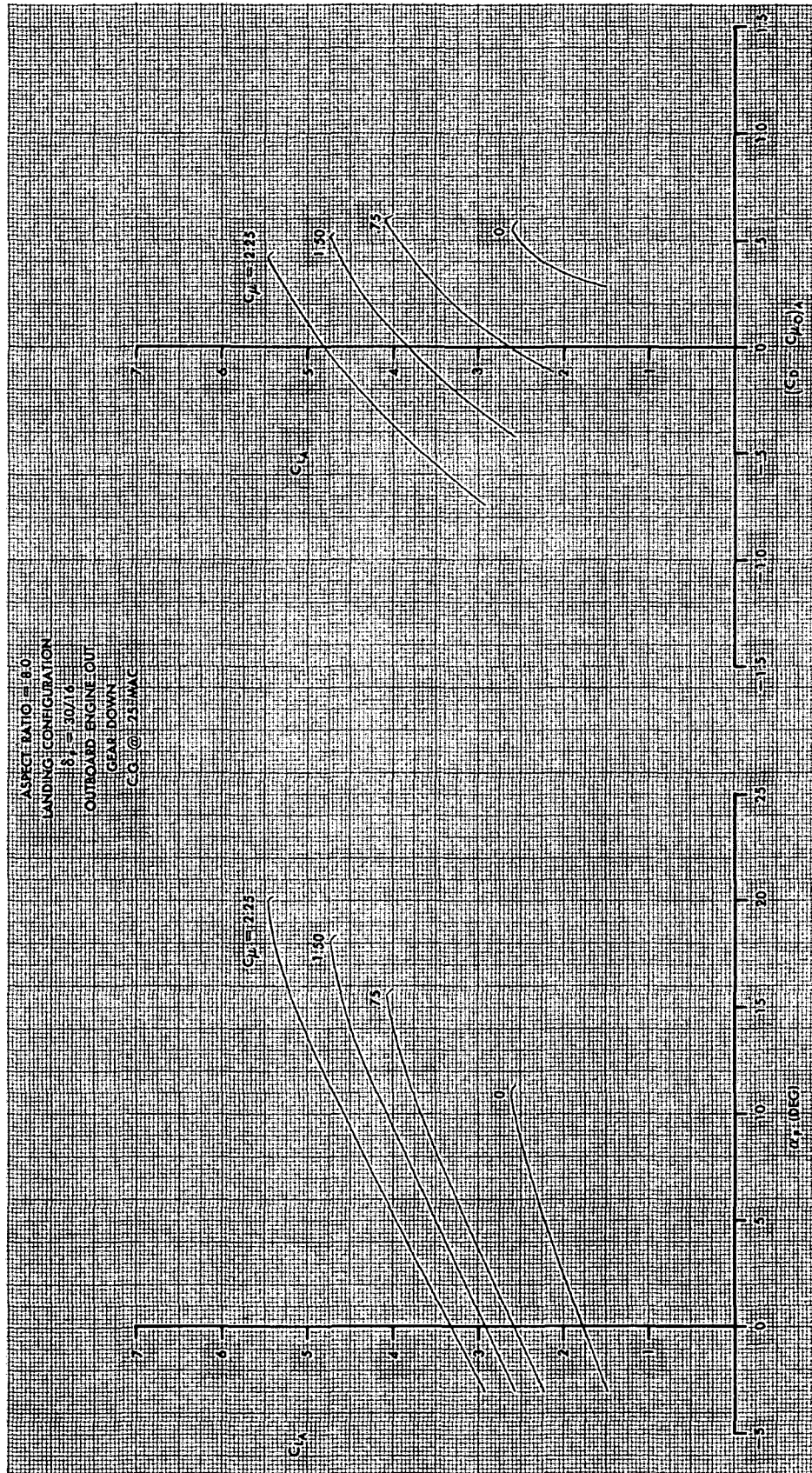


FIGURE B-16. EXTERNALLY BLOWN FLAP LONGITUDINALLY, Laterally AND
DIRECTIONALLY TRIMMED LIFT AND DRAG CHARACTERISTICS

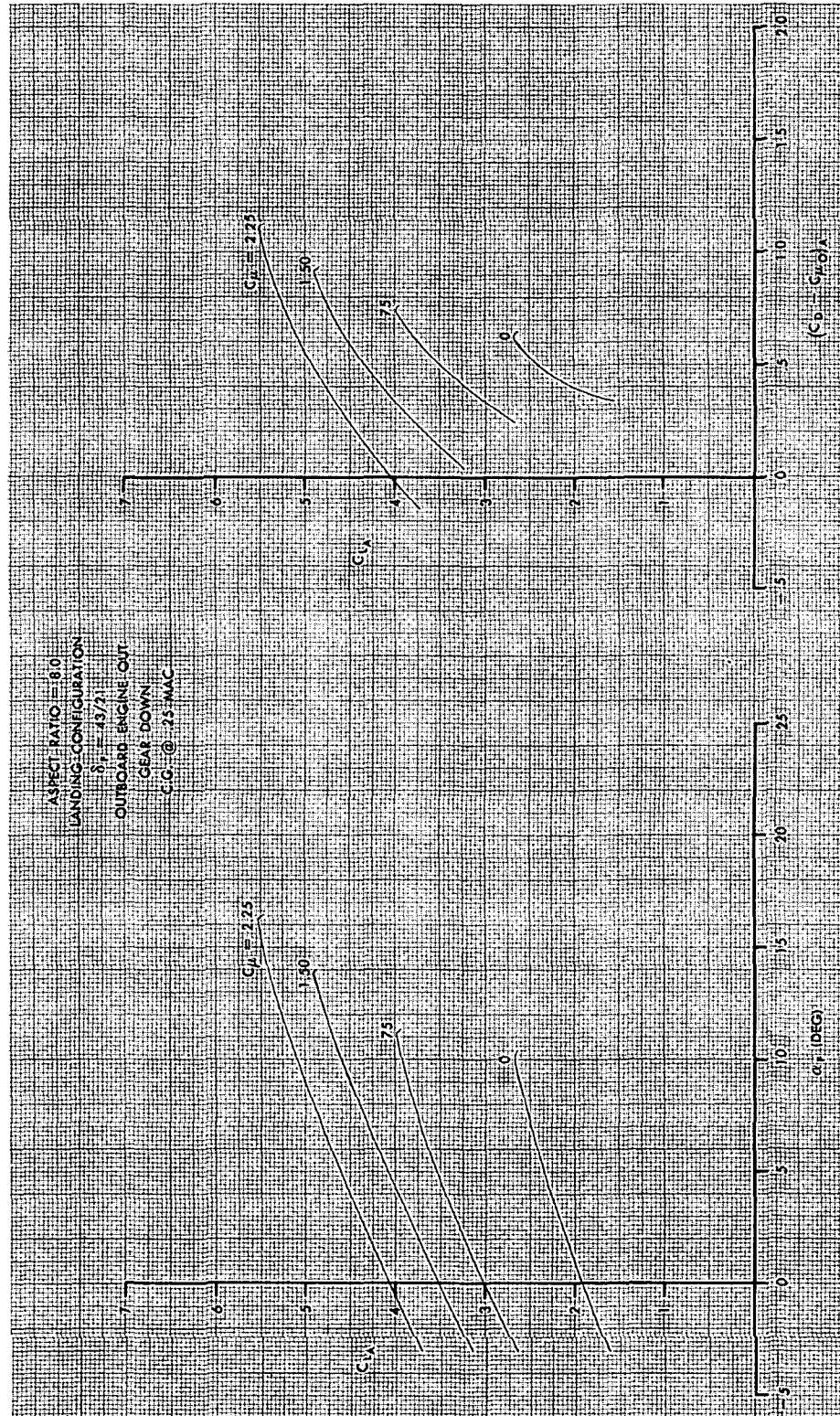


FIGURE B-17. EXTERNALLY BLOWN FLAP LONGITUDINALLY, Laterally AND DIRECTIONALLY TRIMMED LIFT AND DRAG CHARACTERISTICS

engines running) case, which are trimmed longitudinally, laterally and directionally.

B.2.2 Upper Surface Blowing. - A detailed comparison has been made between the aerodynamic characteristics of the USB configuration presented in Reference 7 and those of a Douglas EBF model. The results of this comparison indicate that the major differences are:

- (1) The power-on nose down pitching moments produced by the USB model are lower in magnitude than those of the Douglas EBF model.
- (2) The USB model data indicated a relatively severe loss in maximum lift capability, presumably due to the interference effects of the over-wing nacelle installation.
- (3) The effectiveness of the USB flap in turning the engine exhaust decreases sharply at high flap deflections.

The lower values of negative pitching moments (Figure B-18) due to the application of power for the NASA USB configuration appear to be primarily due to the shape of the Coanda surface, or flap. The flap is a simple-hinge plain flap with a trailing edge extension approximately as long as the flap chord. The extension is tangent to the relatively flat upper surface of the flap. The resulting surface consists of an abrupt bend (small radius) at the leading edge of the surface, followed by a long flat run. The loading due to exhaust turning on this type of shape is probably concentrated near the point of turning, or the leading edge of the flap. The blown portion of the USB flap does not extend as far outboard as that for the externally blown flap configuration, which would further decrease the severity of the nose down pitching moments due to power in this swept-wing comparison.

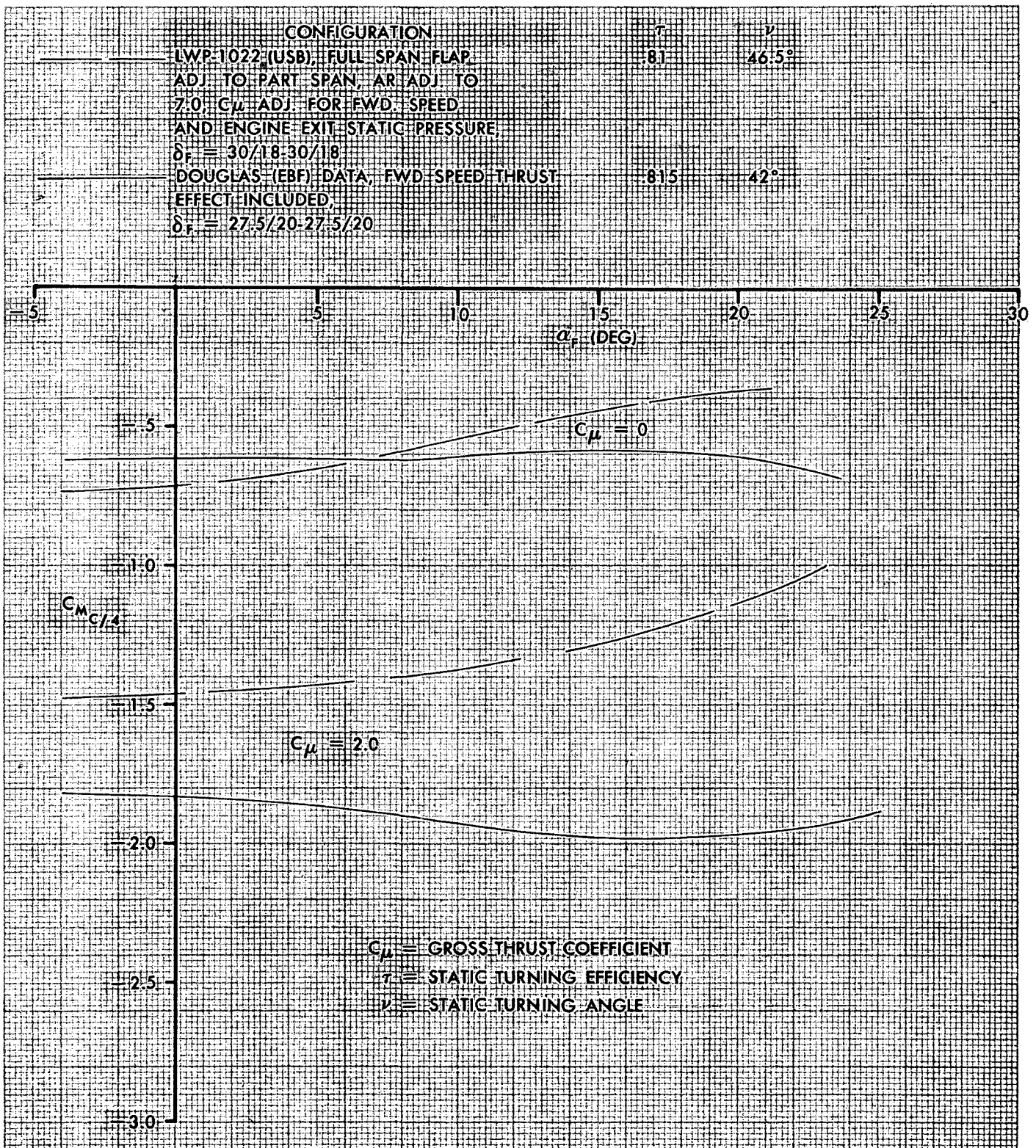


FIGURE B-18. COMPARISON OF PITCHING MOMENTS
EBF AND UPPER SURFACE BLOWING CONFIGURATIONS

The loss in maximum lift capability of the USB configuration indicated in the comparison shown in Figures B-19 and B-20 is probably due to the interruption of the leading edge device by the over-wing nacelle. It is anticipated that this loss could be reduced through further developmental wind tunnel testing.

The USB static turning characteristics presented in NASA LWP 1022 (Reference 7) indicate that a severe loss in turning effectiveness occurs between the takeoff and landing flap deflection levels. This loss in turning effectiveness of the NASA model is considered to be a direct result of using a very small Coanda turning radius on the flap upper surface.

The Douglas USB flap design concept involves flap components similar to the externally blown flap, but arranged behind the engines to form a smoothly cambered flap with a large Coanda radius value. The flap outboard of the engines is identical to that used on the mechanical flap configuration. It is anticipated that this flap will maintain a high degree of turning effectiveness over the required ranges of flap deflection and thrust with no requirement for supplemental slot blowing on the flap. The similarity between the Douglas upper surface blowing and externally blown flap contours, in conjunction with the similar planforms and engine spanwise locations, suggest that the pitching moment characteristics for the two concepts will be very similar.

A full span leading edge slat is provided to prevent flow separation at high angles of attack.

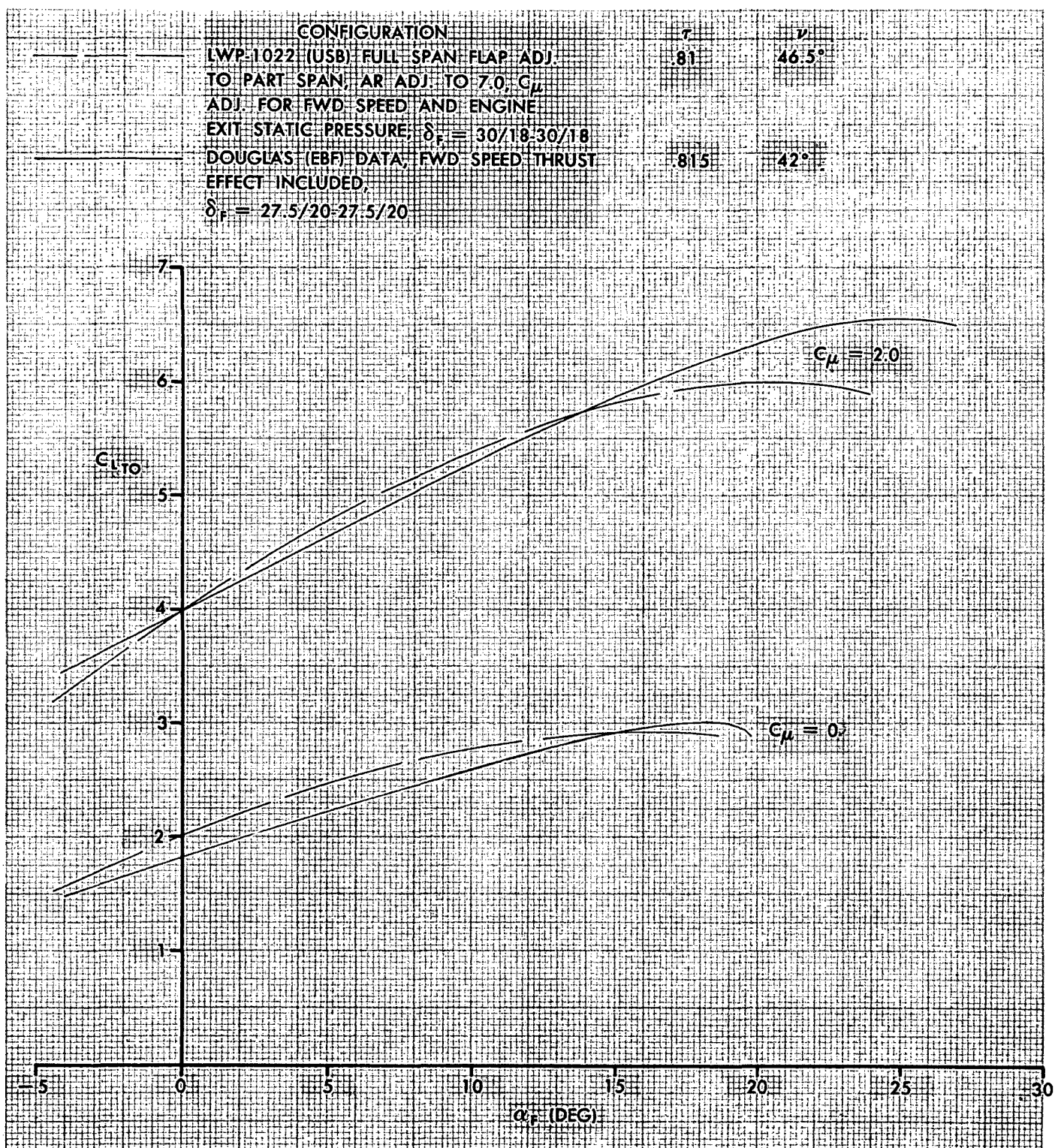


FIGURE B-19. COMPARISON OF EBF AND UPPER SURFACE BLOWING CONFIGURATION LIFT CURVES

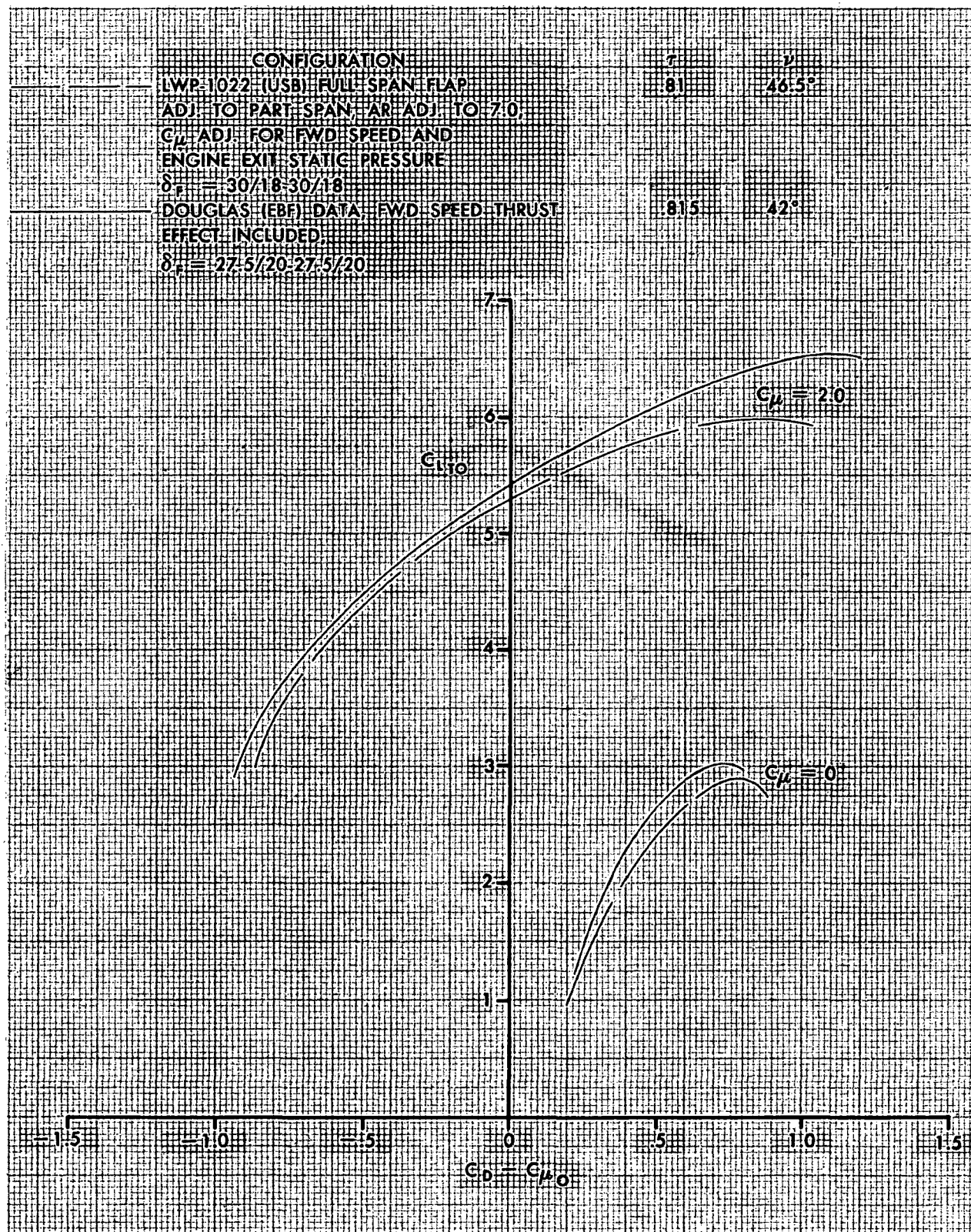


FIGURE B-20. COMPARISON OF EBF AND UPPER SURFACE BLOWING CONFIGURATION DRAG POLARS

It was assumed that the losses in maximum lift due to nacelle interference can be reduced with further development work but based on Douglas experience, not entirely eliminated. For this case the upper surface blowing high lift aerodynamic characteristics are estimated to be identical to the externally blown flap characteristics except that a penalty of $\Delta C_{L_{\max}} = -.20$ is assumed for all flap deflections.

B.2.3 Conventional Mechanical Flap Systems. - Aircraft sized to 3000 foot (914 m), 4000 foot (1219 m), and CTOL field lengths are included in this study. The following paragraphs describe the high lift aerodynamic characteristics used for these field lengths.

B.2.3.1 3000 Foot (914 m) Field Length - For this field length, it is appropriate to use high lift aerodynamic characteristics derived from a large flap chord (high flap power) configuration. Douglas externally blown flap ($C_{\mu} = 0$) model data with a nested flap chord/wing chord ratio of .42 were used as the data base. These data were adjusted to reflect the effect of Reynolds number on maximum lift coefficient, the effect of an increase in aspect ratio from 7.0 to 9.0 using the EVD method, and the following differences between the mechanical flap configuration and the externally blown flap model.

- (1) The mechanical flap aircraft has smaller flap gaps than those used on the EBF.
- (2) The mechanical flap engines are located further from the wing than the engines on the EBF configuration.
- (3) The mechanical flap uses a full span slat leading edge device, whereas the externally blown flap configuration uses a leading edge flap inboard and a slat outboard.

The effect of flap gap on the unpowered model lift, drag, and pitching moment were extracted from flap arrangement studies conducted on a Douglas EBF model and applied to the model data used to predict the aerodynamic characteristics. The typical effect of reducing the flap gaps to conventional values is a small increase in lift with no change in the lift-to-drag ratio.

The nacelle height for the mechanical flap configuration has been selected so that no exhaust impingement occurs at the highest nominal takeoff flap setting ($\delta_F = 25$ degrees). It is estimated that the interference effects resulting from minor exhaust impingement on the landing flaps can be neglected in this study.

The effect of replacing the inboard leading edge flap with a slat was estimated using relationships derived from wind tunnel tests of similar configurations utilizing full span slats.

The effects of Reynolds number on maximum lift coefficient are based on comparisons of low Reynolds number wind tunnel test data and flight test data for the DC-9 configurations. It is considered appropriate to apply this adjustment to the unpowered lifting system, whereas it was not applied for the externally blown flap system. The uncertainties related to nacelle interference and exhaust flow entrainment on the sensitivity of the externally blown flap system to scale effects led to the conservative assumption that the Douglas EBF model maximum lift capability is representative of that which will be demonstrated by the full scale externally blown flap configuration.

The estimated longitudinally trimmed lift and drag characteristics for the 3000 foot (914 m) field length mechanical flap high lift configurations are presented in Figure B-21. The lateral-directional aerodynamic engine out trim increments are not included in Figure B-21 since the thrust effects are handled separately in the performance analysis. The estimated engine out lateral-directional trim increments used in the performance analysis are tabulated in Table B-2.

B.2.3.2 4000 Foot (1219 m) Field Length - As field length increases, it is appropriate to use a more conventional mechanical flap configuration. Estimated aerodynamic characteristics for a DC-10 type flap system with a nested flap chord ratio of .35 and a wing aspect ratio of 9.0 were used as the data base.

The estimated longitudinally trimmed lift and drag characteristics for the 4000 foot (1219 m) field length mechanical flap high lift configurations are presented in Figure B-22. The lateral-directional trim increments presented in Table B-2 are applicable for these configurations.

B.2.3.3 CTOL Field Length - This field length is representative of existing mechanical flap configurations. Estimated aerodynamic characteristics for a DC-10 type flap system with a nested flap chord ratio of .28 and a wing aspect ratio of 9.0 were used as the data base.

The estimated longitudinally trimmed lift and drag characteristics for the CTOL field length mechanical flap high lift configurations are presented in Figure B-23. The lateral-directional trim increments presented in Table B-2 are also applicable for these configurations.

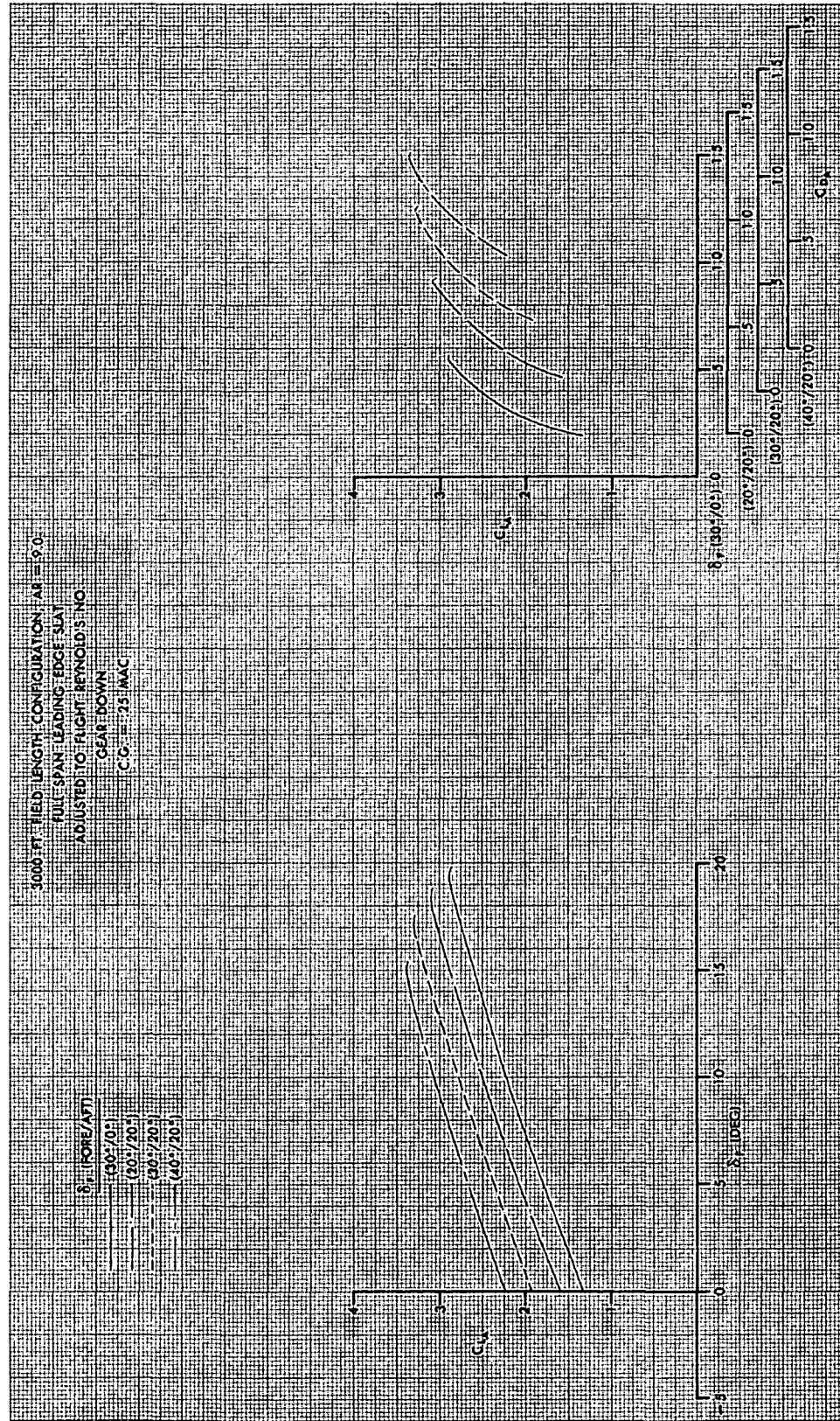


FIGURE B-21. MECHANICAL FLAP TRIMMED LIFT AND DRAG CHARACTERISTICS

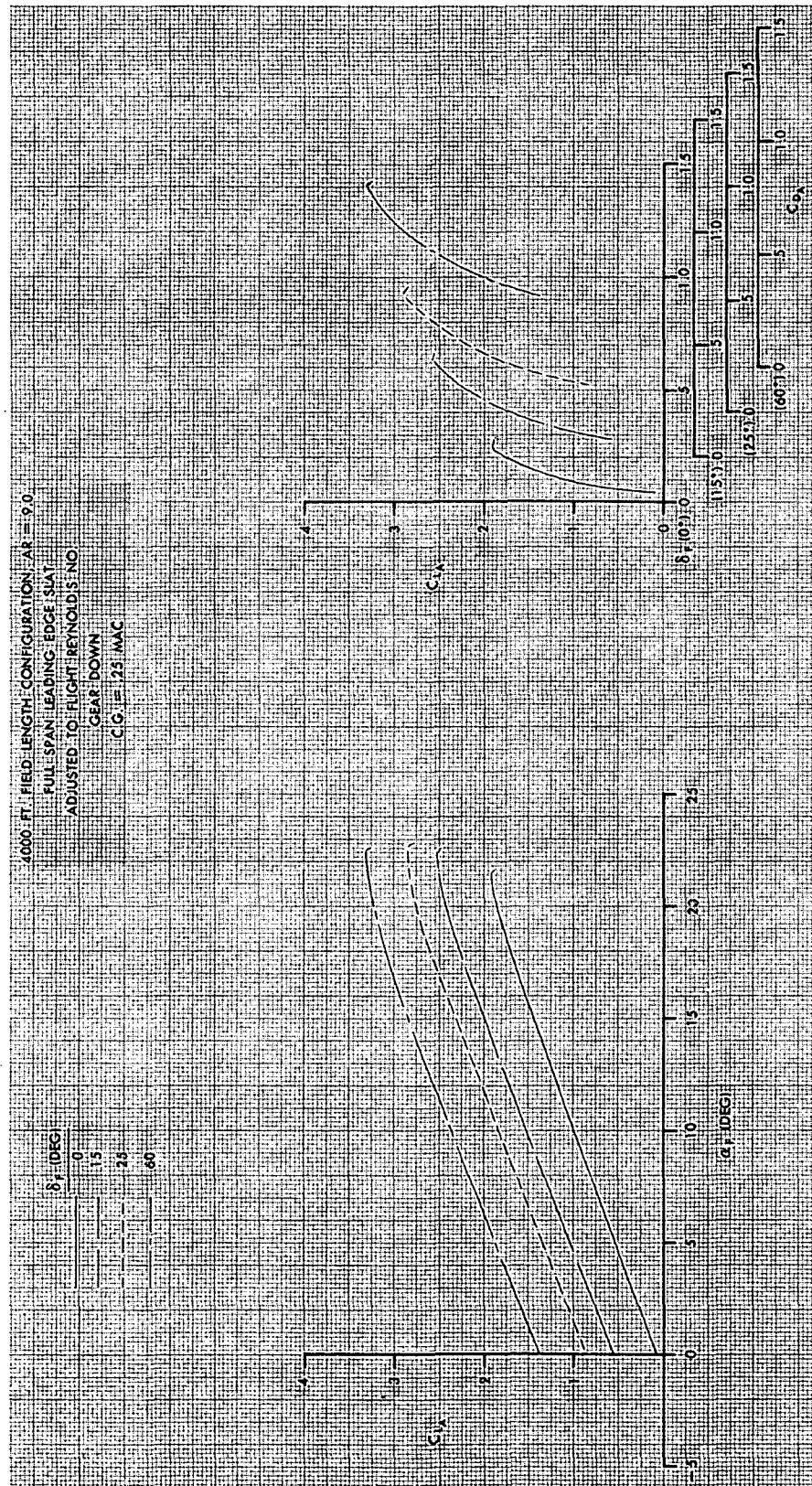


FIGURE B-22. MECHANICAL FLAP TRIMMED LIFT AND DRAG CHARACTERISTICS

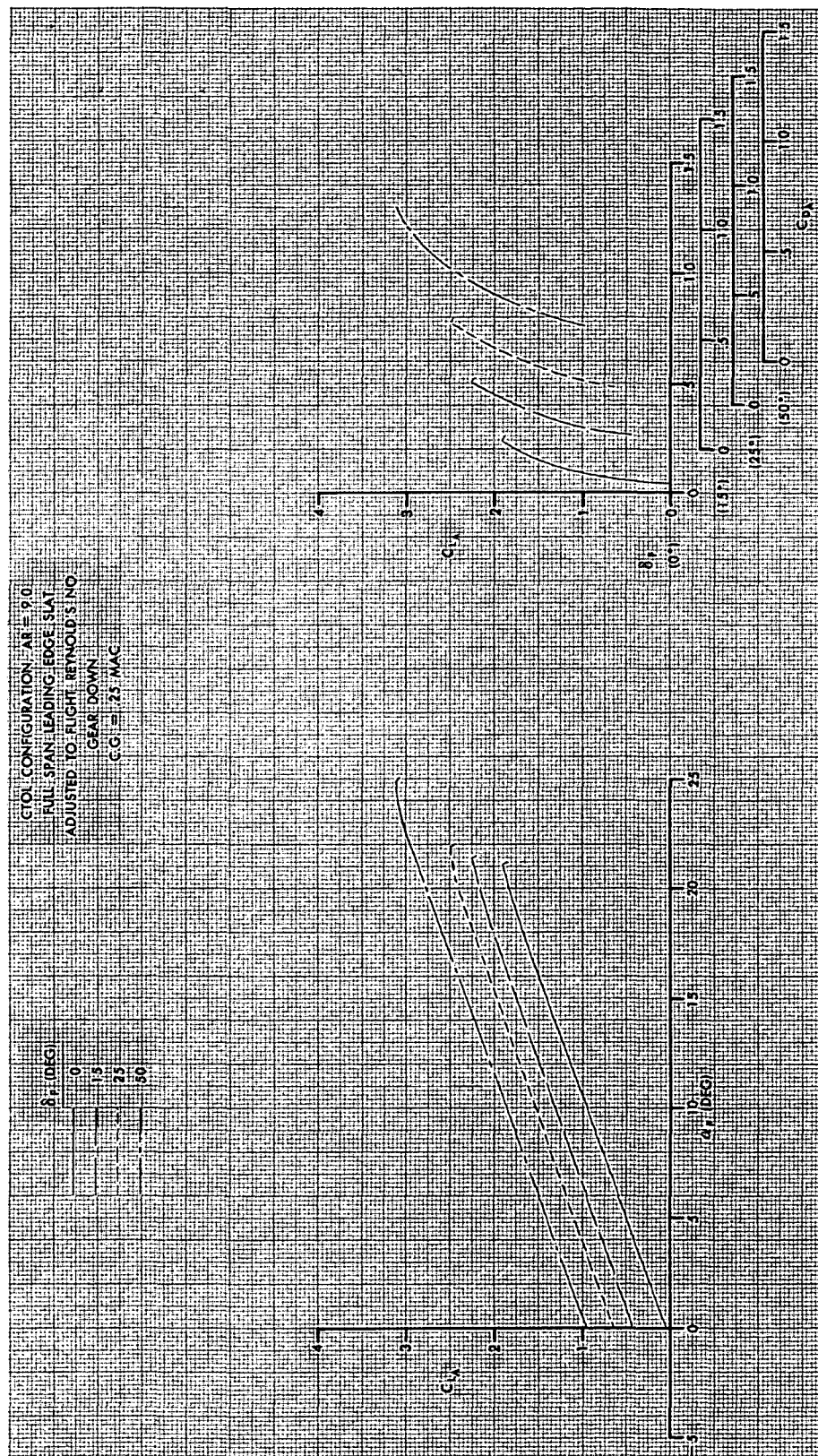


FIGURE B-23. MECHANICAL FLAP TRIMMED LIFT AND DRAG CHARACTERISTICS

TABLE B-2

MECHANICAL FLAP ENGINE-OUT LATERAL-DIRECTIONAL TRIM INCREMENTS
IN DRAG COEFFICIENT

α_F	$C_{\mu} = 0.25$	0.50	0.75
0°	$\Delta C_D = 0.006$	0.017	0.032
10°	0.006	0.017	0.033
20°	0.007	0.018	0.035

B.2.4 Augmentor Wing - The aerodynamic characteristics of the augmentor wing high lift configurations were estimated using the data from References 1, and 8 through 11. The model test data presented in Reference 8 were adjusted to reflect the differences between the model and the current study configurations, and interpreted as outlined in the following paragraphs.

The model test data presented in Figures 18 through 22 of Reference 8 were adjusted to reflect the aspect ratio and flap chord ratio changes, using the EVD method. These corrections were limited to lift, drag and pitching moment changes in the unseparated wing flow regime. The effects of body-to-span ratio, flap span ratio, and taper ratio are small and were estimated to be compensating in nature, and were therefore neglected.

In the non-linear portion of the lift curves, the wing planform effects on maximum lift were estimated to be negligible. The effect of reducing the flap chord ratio of 0.27 was evaluated by assuming the change in maximum lift was one-half the change in flap power at zero angle of attack.

The cruise configuration zero-lift angle of attack for the study vehicle was based on high speed wind tunnel test results for a similar configuration. The lift curves presented in Reference 8 were shifted 3.5 degrees to a lower angle of attack to account for the differences in zero-lift angle of attack in the cruise configuration.

The static calibration data presented in Reference 9 were used to calculate the trailing edge momentum coefficient, $C_{\mu_{TE}}$, as a function of the isentropic jet momentum coefficient, C_{J_i} . The sum of the losses in the aileron blowing system, due to nozzle C_V , scrubbing and turning, was estimated to be 19 percent, so the equation for $C_{\mu_{TE}}$ is:

$$C_{\mu_{TE}} = .95 C_{J_i} \phi_{G_i} + .05 C_{J_i} \quad (.81)$$

where ϕ_{G_i} = ideal gross thrust augmentation ratio.

The ejector entrainment ratio, ϕ_w , was calculated using one-dimensional full-mixing ejector theory. The estimated forward speed effects

on ϕ_{G_i} and ϕ_w for the model are small and were neglected.

The ram drag of the augmentor model was estimated and removed from the adjusted model data, and the results were compared to theoretical characteristics predicted by the EVD method. The model data, interpreted as described, did not correlate well with theory. Specifically, the ratio $\Delta(C_D - C_{\mu_0})/\Delta C_{\mu_{TE}}$ was not consistent with theory, which suggests that the forward speed values of ϕ_{G_i} obtained with the model were significantly larger than those calculated using simple ejector theory. Based on the higher static augmentation ratios reported in References 10 and 11 for this flap geometry, the estimated values of $C_{\mu_{TE}}$ for the adjusted model test data were increased by 10 percent and again compared to theory. The correlation was improved.

The values of ϕ_{G_i} and ϕ_w used to transform the model data from jet momentum coefficient and simple drag coefficient form into trailing edge momentum and $(C_D - C_{\mu_0})$ coefficient form were based on the static calibration data presented in References 10 and 11.

The full scale airplane values of ϕ_{G_i} and ϕ_w are based on the technology reported in Reference 1. The 1978 technology level values of ϕ_{G_i} presented in Reference 1 were adjusted for forward speed effects using ejector theory and the corresponding values of ϕ_w were estimated.

The values of ϕ_{G_i} and ϕ_w used in this study are presented in Table B-3.

TABLE B-3
ESTIMATED EJECTOR PARAMETERS

$V_0 = 80$ Knots

δ_F	Nozzle Pressure Ratio	ϕ_{G_1}	ϕ_w
32°	1.6	1.38	3.05
	2.1	1.33	2.94
	2.6	1.30	2.74
41°	1.6	1.34	2.96
	2.1	1.31	2.85
	2.6	1.28	2.70
51°	1.6	1.31	2.90
	2.1	1.27	2.80
	2.6	1.25	2.63
61°	1.6	1.28	2.80
	2.1	1.24	2.70
	2.6	1.23	2.55
71°	1.6	1.25	2.68
	2.1	1.22	2.58
	2.6	1.20	2.48

The estimated longitudinally trimmed lift and drag characteristics for the augmentor wing high lift configurations are presented in Figures B-24 and B-25. A small lateral-directional trim penalty of $\Delta C_D = 0.005$ due to a slight engine out asymmetry was included in the engine out performance calculations.

B.2.5 Ground Effects. - The free air aerodynamic characteristics previously presented were corrected for the influence of ground by two sets of empirical equations.

The first set of empirical equations were derived from power-on EBF model data obtained in the Langley Research Center Wind Tunnel with a moving ground plane, as reported in Reference 12. The effect of ground on the

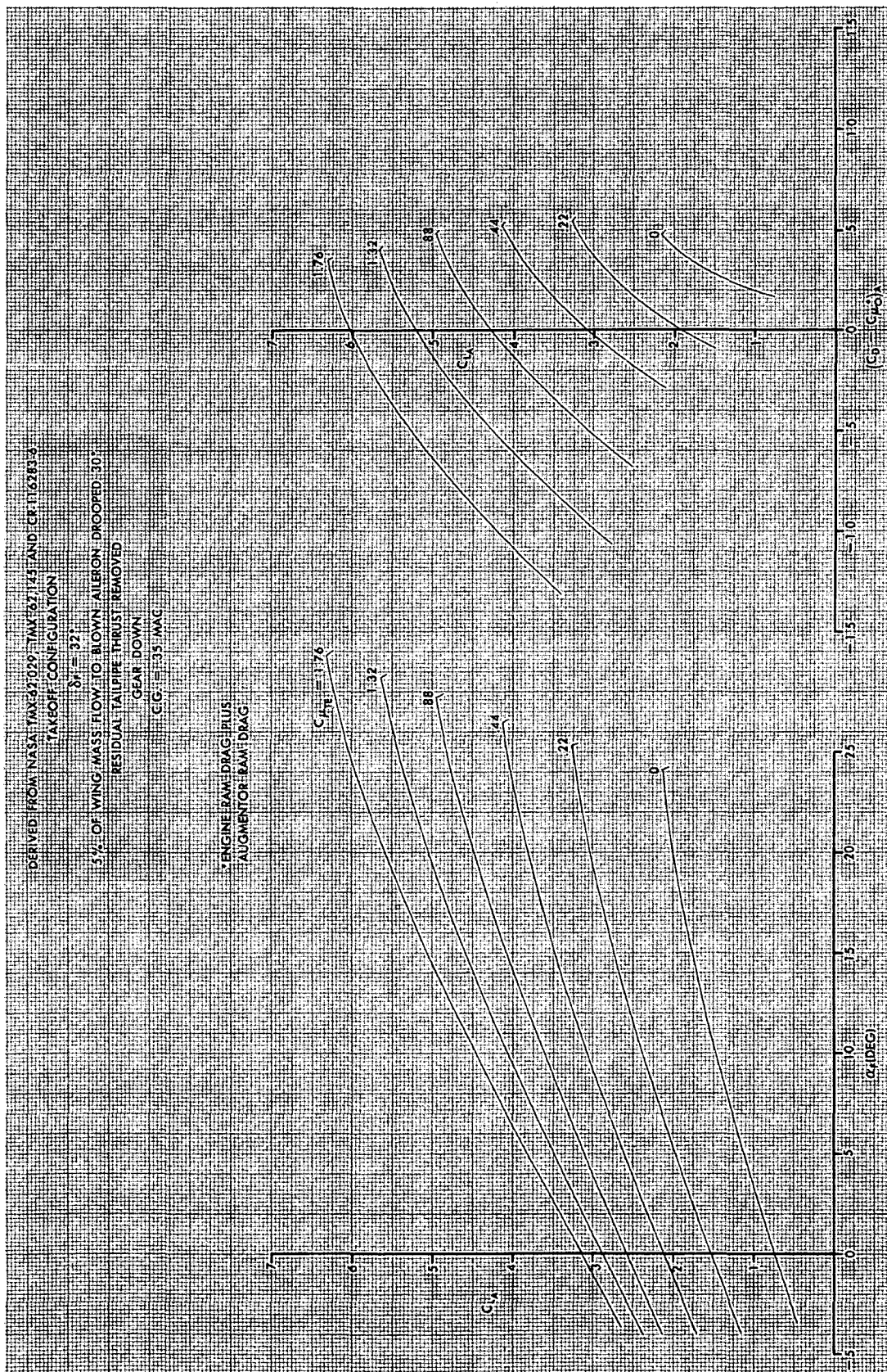


FIGURE B-24. AUGMENTOR WING TRIMMED LIFT AND DRAG CHARACTERISTICS

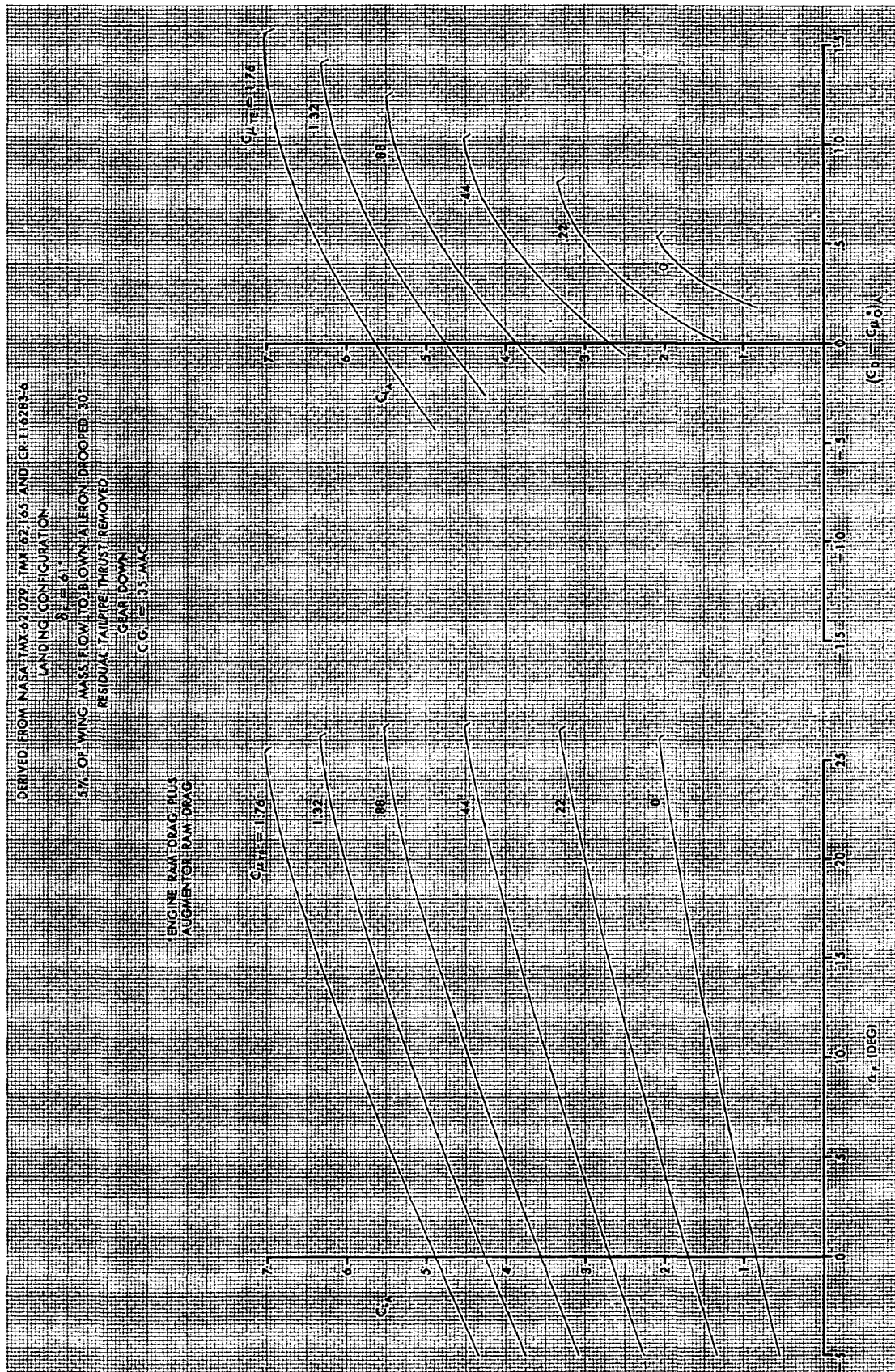


FIGURE B-25. AUGMENTOR WING TRIMMED LIFT AND DRAG CHARACTERISTICS

aerodynamic characteristics including the effect on longitudinal trim are summarized in the following equations which are applicable to all the powered high lift systems.

$$C_{L_T} \leq 1.59, \Delta C_L = K(0.072)$$

GROUND
EFFECT

$$C_{L_T} > 1.59, \Delta C_L = K[-0.1(C_{L_T} - 1.59)^2 + 0.072]$$

GROUND
EFFECT

where

$$K = e^{-5.728(h/b - 0.179)}$$

$$K = e$$

h = Height above ground

b = wing span

$$C_{L_T} = C_{L_{h/b=\infty}} - (\tau C_\mu) \sin(\alpha_F + \nu)$$

τC_μ = thrust at the trailing edge

ν = static thrust turning angle

$$\text{if } \Delta C_L > 0.096K^2, \Delta C_D = 0$$

GROUND
EFFECT

GROUND
EFFECT

$$\text{if } \Delta C_L < 0.096K^2, \Delta C_D = - \left[\frac{\Delta C_L - 0.096K^2}{-2.34 - 0.23(1-K)} \right]^{0.675}$$

GROUND
EFFECT

GROUND
EFFECT

$$\alpha_{\text{STALL IN GROUND}} = (1-K) \alpha_{\text{STALL } h/b=\infty} + \left[22.6 - 0.1 \times \delta_{F_{\text{TOT}}} \right] K$$

where

$$K' = 0.1372 \left[\frac{1}{h/b - 0.054} - 0.12 \right]$$

$$\text{if } \alpha_{\text{STALL IN GROUND}} > \alpha_{\text{STALL } h/b = \infty}, C_{L_{\text{max IN GROUND}}} = C_{L_{\text{max } h/b = \infty}} + \left(\frac{\Delta C_{L \text{ GROUND EFFECT}}}{\alpha_{\text{STALL } h/b = \infty}} \right) \alpha_{\text{STALL IN GROUND}}$$

$$\text{if } \alpha_{\text{STALL IN GROUND}} \leq \alpha_{\text{STALL } h/b = \infty}, C_{L_{\text{max IN GROUND}}} = 3/4 \times 1 + 1/4 \times 2$$

where

$$1 = \left[C_{L_{\infty}} + \frac{\Delta C_{L \text{ GROUND EFFECT}}}{\alpha_{\text{STALL IN GROUND}}} \right] \alpha_{\text{STALL IN GROUND}}$$

$$2 = \left[C_{L_{\infty}} + \frac{\Delta C_{L \text{ GROUND EFFECT}}}{\left(\alpha_{\text{STALL IN GROUND}} \right)^{-4^\circ}} \right] \left(\alpha_{\text{STALL IN GROUND}} \right)^{-4^\circ}$$

The second set of empirical equations were derived from power-off data of Reference 12. The effect of ground on the aerodynamic characteristics including the effect on longitudinal trim are summarized in the following equations which are applicable to mechanical flap systems.

$$\frac{\Delta C_{L \text{ GROUND EFFECT}}}{\alpha_{\text{STALL IN GROUND}}} = \frac{\Delta C_{L_{\text{TOG}}} + \left[\frac{0.104 K_L^{1.5} - 0.27 \Delta C_{L_{\text{TOG}}}}{3.5} \right]}{\alpha_{\text{STALL IN GROUND}}}$$

where $\Delta C_{L_{\text{TOG}}}$ = incremental tail off lift coefficient due to ground effects.

where

$$C_{L_{\infty}} \leq 1.0, \Delta C_{L_{TOG}} = K_L (0.045)$$

$$C_{L_{\infty}} > 1.0, \Delta C_{L_{TOG}} = K_L \left\{ -0.092 [C_{L_{\infty}} - 1.0]^2 + 0.045 \right\}$$

$$K_L = 1.53 e^{-h/b(3.5)}$$

$$\Delta C_D = - \left[\frac{\Delta C_{L_{TOG}} - 0.08 K_L^2}{2.1} \right]^{0.8}$$

GROUND EFFECT

The in-ground-effect stall angle of attack and $C_{L_{max}}$ equations of the previous section also apply to mechanical flap systems.

B.3 High Speed Aerodynamic Characteristics

The cruise drag characteristics for the final configurations have been estimated by the well-established Douglas drag prediction procedure for jet transport aircraft. The cruise drag consists of the zero-lift parasite drag and the drag due to lift at Mach numbers below those at which compressibility effects exist, plus the drag due to compressibility. The zero-lift parasite drag and the drag due to lift are evaluated at 0.5 Mach number, but at the Reynolds number corresponding to the design cruise points; in this way, the compressibility drag, which accounts for any drag increase at Mach numbers above 0.5, does not include a Reynolds number variation with Mach number.

A breakdown of the estimated zero-lift parasite drag and a tabulation of the induced drag efficiency factors for the final configurations are

shown in Table B-4. The total estimated trimmed cruise-configuration drag characteristics (zero-lift parasite, lift-dependent, and compressibility drag) for the final configurations are shown in Figures B-26 through B-29 for a wide range of lift coefficients and Mach numbers.

TABLE B-4
LOW SPEED DRAG BREAKDOWN – FINAL DESIGN AIRCRAFT

Configuration	EBF					AW	USB	CTOL	MF	
	100	150	200	3000	2000				150	150
Passengers										
Field Length										
Ft										
(M)										
Wing Area										
Ft ²										
(M ²)										
EQUIVALENT PARASITE DRAG AREA, D/q ₀ ~ Sq. Ft. (Sq. Meters)										
Fuselage										
Friction, Form, Roughness*	6.70	10.29	11.63	10.00	10.07	10.30	10.24	10.03	9.34	10.03
Canopy	(0.623)	(0.956)	(1.081)	(0.930)	(0.936)	(0.957)	(0.952)	(0.932)	(0.915)	(0.932)
Aft-Fuselage Upsweep	0.04	0.07	0.07	0.06	0.06	0.06	0.06	0.06	0.06	0.06
Gear Pods	(0.004)	(0.007)	(0.007)	(0.006)	(0.006)	(0.006)	(0.006)	(0.006)	(0.006)	(0.006)
Wing	0.72	1.50	1.72	0.64	0.85	1.44	0.31	1.79	1.30	1.79
Friction, Form, Roughness	(0.067)	(0.139)	(0.160)	(0.059)	(0.079)	(0.134)	(0.029)	(0.166)	(0.121)	(0.166)
Flap Hinge Fairings	2.11	1.71	1.69	2.13	1.60	2.76	-	1.68	1.35	1.68
Horizontal Tail	(0.196)	(0.159)	(0.157)	(0.198)	(0.149)	(0.256)	-	(0.156)	(0.172)	(0.156)
Friction, Form, Roughness	6.07	8.00	11.10	15.36	14.76	15.93	8.44	10.20	17.05	10.20
Elevator Hinge Fairings	(0.564)	(0.744)	(1.032)	(1.428)	(1.372)	(1.481)	(0.784)	(0.948)	(1.585)	(0.948)
Vertical Tail	0.30	0.40	0.56	0.77	0.74	0.80	0.42	0.51	0.35	0.51
Friction, Form, Roughness	(0.028)	(0.037)	(0.052)	(0.071)	(0.069)	(0.074)	(0.039)	(0.048)	(0.079)	(0.048)
Nacelles & Pylons (Unscrubbed)	2.01	2.60	3.18	5.28	5.55	5.60	1.95	2.09	3.95	2.09
Friction, Form, Roughness	(0.187)	(0.242)	(0.296)	(0.491)	(0.516)	(0.521)	(0.181)	(0.194)	(0.367)	(0.194)
Subtotal	0.10	0.13	0.16	0.26	0.28	0.28	0.10	0.10	0.20	0.10
Friction, Form, Roughness	(0.009)	(0.012)	(0.015)	(0.024)	(0.026)	(0.026)	(0.009)	(0.009)	(0.018)	(0.009)
Miscellaneous Items	1.25	1.98	2.77	4.93	5.05	5.59	1.30	2.01	3.37	2.01
Excrescences (7.1% of Subtotal)	(0.116)	(0.184)	(0.257)	(0.456)	(0.469)	(0.52)	(0.121)	(0.187)	(0.313)	(0.187)
Air Conditioning (0.7% of Subtotal)	3.87	5.24	6.58	7.41	6.50	9.23	3.58	4.10	4.53	4.10
Control Surface Gaps	(0.36)	(0.487)	(0.612)	(0.689)	(0.604)	(0.858)	(0.333)	(0.381)	(0.426)	(0.381)
Nacelle Interference @ M ≤ 0.60	23.17	31.92	39.46	46.84	45.46	51.99	26.40	32.57	43.05	32.57
Contingency (5% of non N&P Items)	(2.154)	(2.967)	(3.569)	(4.354)	(4.226)	(4.833)	(2.454)	(3.027)	(4.072)	(3.027)
Total f/C _D = D/q ₀ S _w	1.65	2.26	2.30	3.32	3.23	3.69	1.87	2.31	3.06	2.31
Induced Drag Efficiency Factor	(0.153)	(0.210)	(0.260)	(0.309)	(0.300)	(0.343)	(0.174)	(0.215)	(0.284)	(0.215)
	0.16	0.22	0.28	0.33	0.32	0.36	0.18	0.23	0.30	0.23
	(0.015)	(0.020)	(0.026)	(0.030)	(0.030)	(0.033)	(0.017)	(0.021)	(0.028)	(0.021)
	0.31	0.42	0.44	0.48	0.57	0.59	0.40	0.36	0.38	0.36
	(0.029)	(0.039)	(0.040)	(0.045)	(0.052)	(0.055)	(0.037)	(0.036)	(0.054)	(0.036)
	0.76	1.30	1.67	-	-	2.28	-	1.60	1.26	1.60
	(0.071)	(0.121)	(0.155)	-	-	(0.212)	-	(0.149)	(0.118)	(0.149)
	1.08	1.48	1.82	2.18	2.15	2.37	1.26	1.57	2.12	1.57
	(0.100)	(0.138)	(0.169)	(0.202)	(0.200)	(0.220)	(0.117)	(0.146)	(0.197)	(0.146)
	27.13	37.60	46.47	53.15	51.73	61.28	30.11	38.67	50.38	38.67
	(2.522)	(3.495)	(4.319)	(4.940)	(4.808)	(5.696)	(2.799)	(3.594)	(4.683)	(3.594)
	0.02738	0.02573	0.02420	0.01898	0.01886	0.01808	0.02129	0.02264	0.01675	0.02264
	0.767	0.767	0.765	0.768	0.793	0.764	0.759	0.774	0.779	0.774

*Wing, vertical tail, and gear pod footprints removed from fuselage wetted area

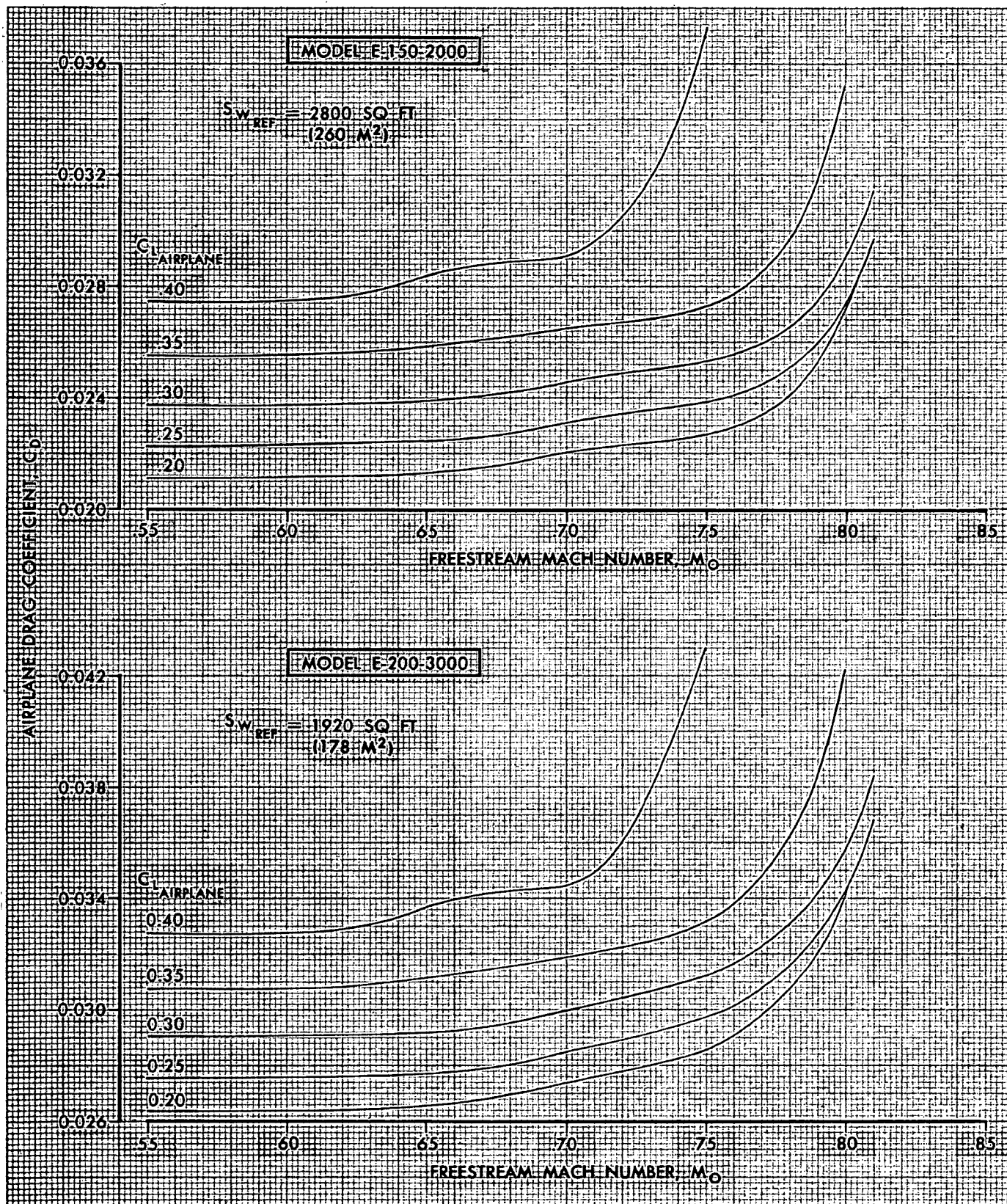


FIGURE B-26. ESTIMATED CRUISE-CONFIGURATION DRAG CHARACTERISTICS

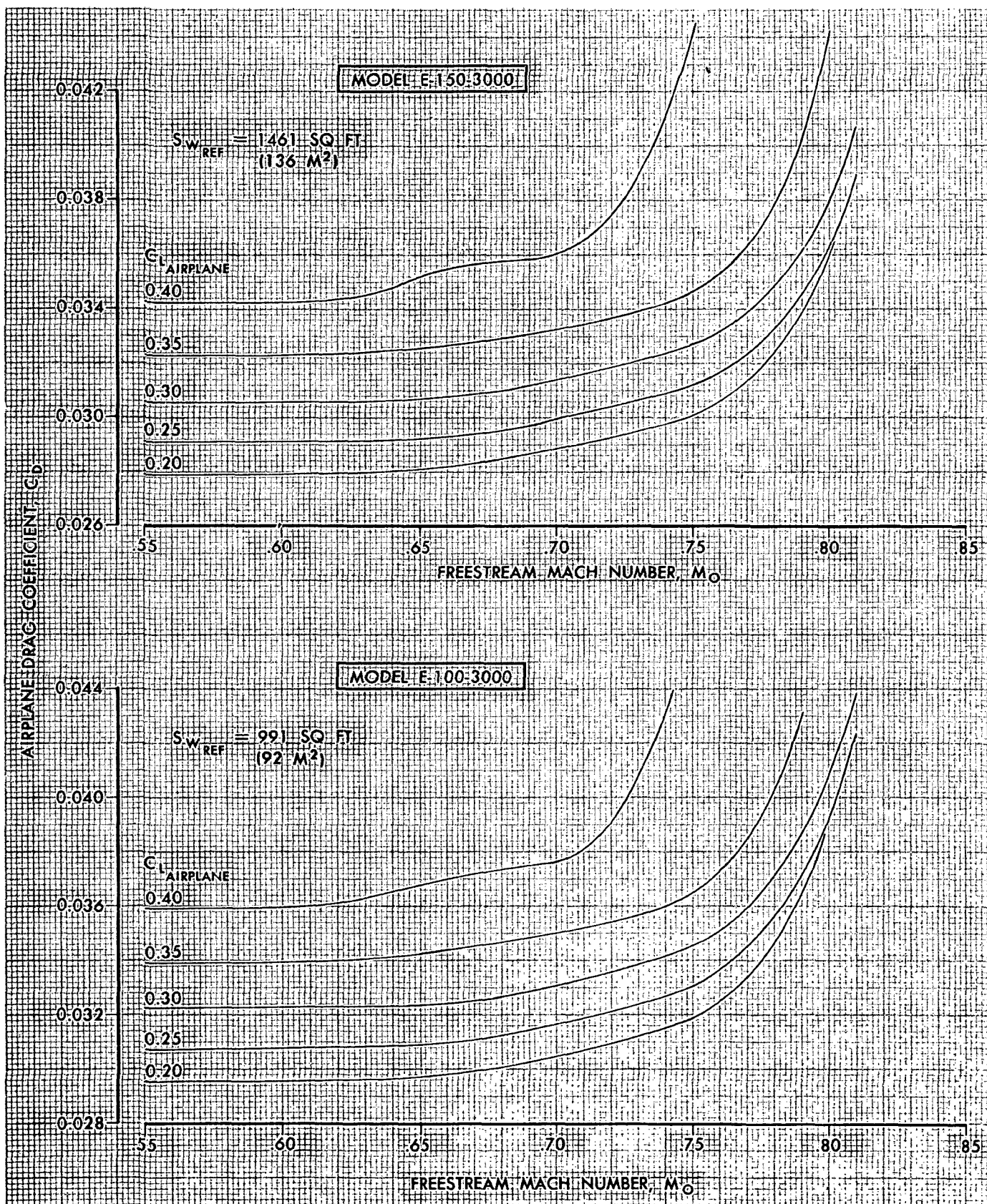


FIGURE B-27. ESTIMATED CRUISE-CONFIGURATION DRAG CHARACTERISTICS

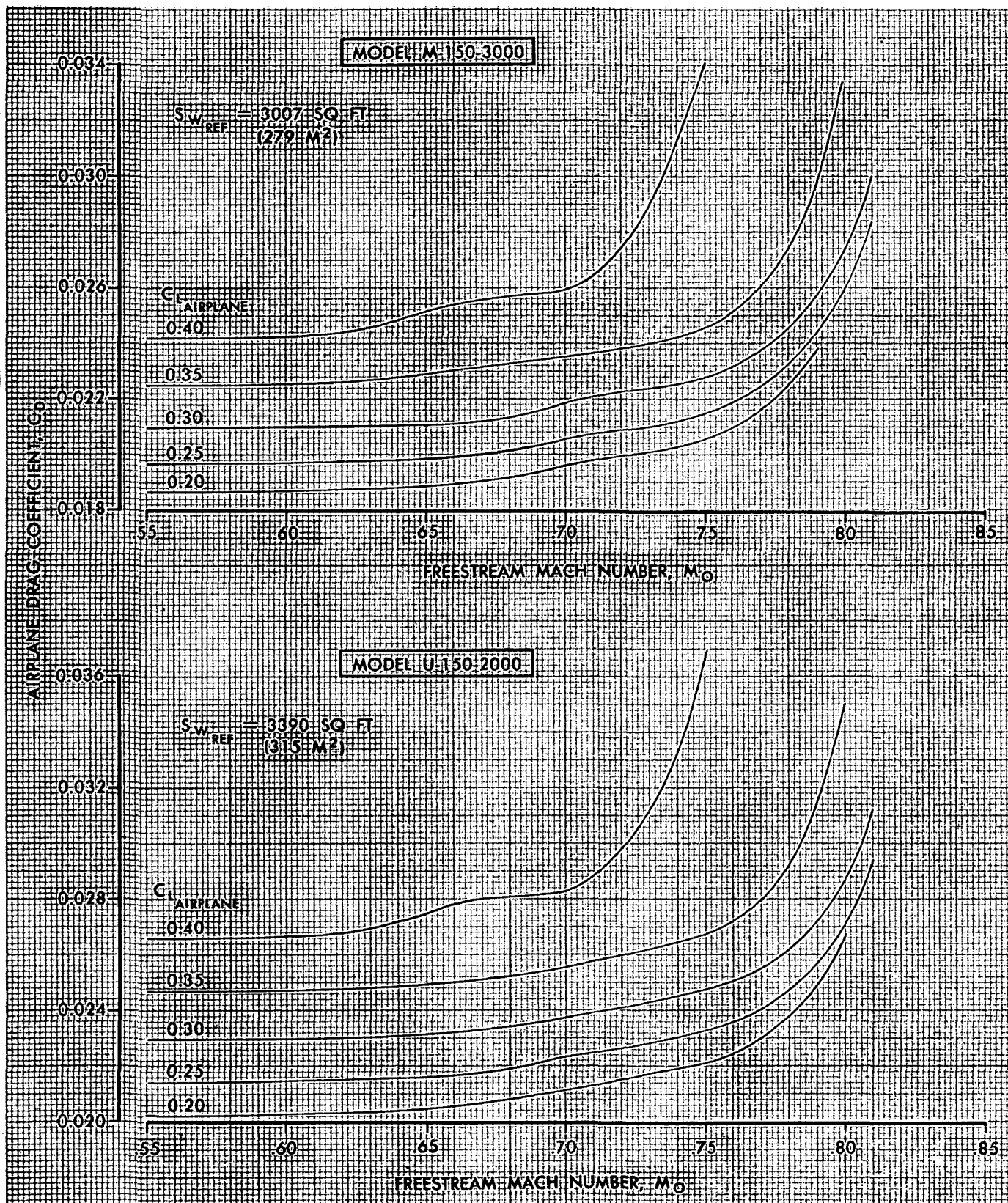


FIGURE B-28. ESTIMATED CRUISE-CONFIGURATION DRAG CHARACTERISTICS

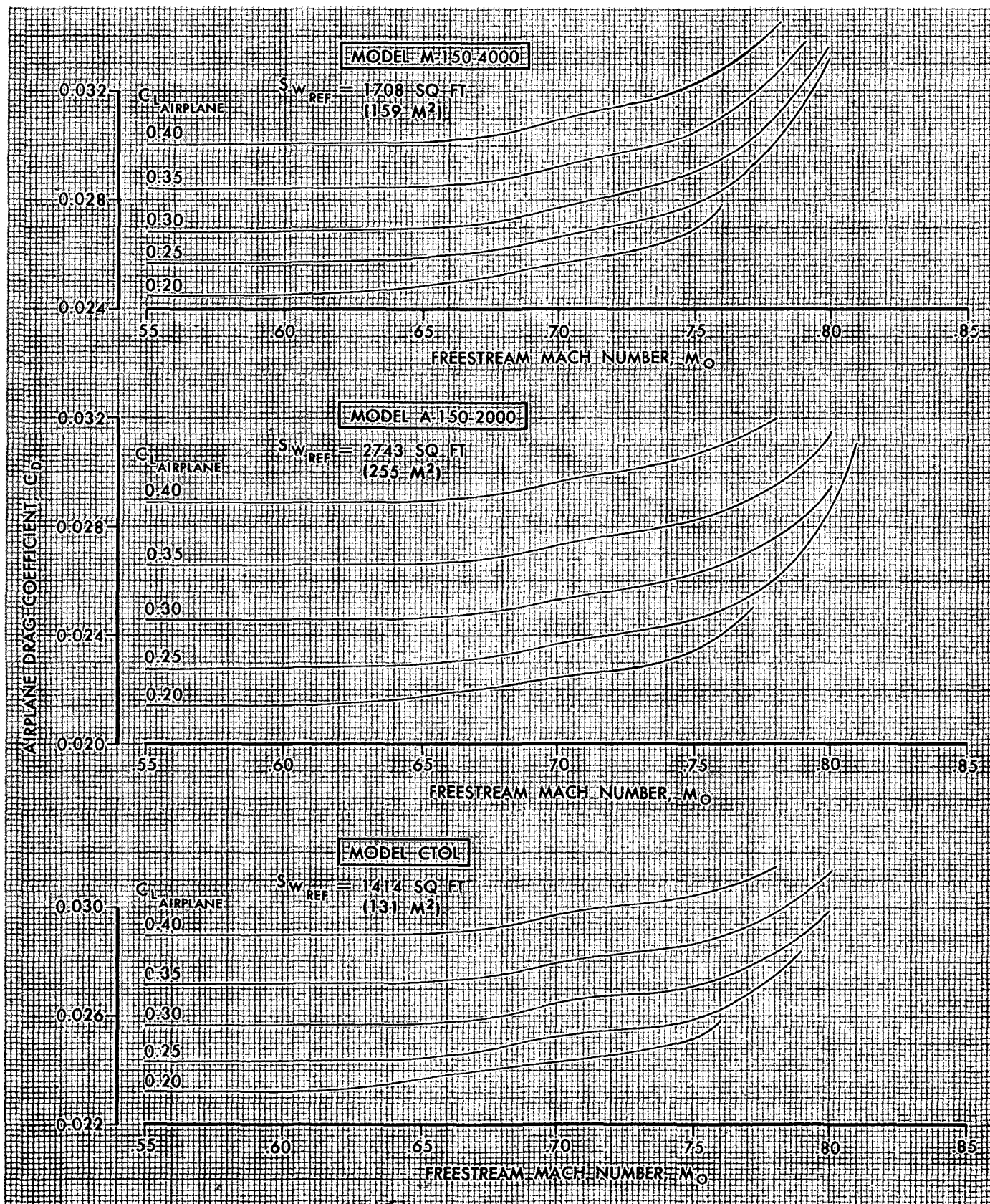


FIGURE B-29. ESTIMATED CRUISE-CONFIGURATION DRAG CHARACTERISTICS

APPENDIX C

ACOUSTIC ANALYSIS - FINAL DESIGN AIRCRAFT

C.1 Introduction

In order to develop acoustical treatment compatible with the noise goals of the program it was necessary to consider each of the propulsion system noise sources and the amount of suppression required for each. An airplane sideline noise goal of 95 EPNdB at 500 feet (152 m) at takeoff power was used for the final design aircraft. This goal was estimated to be a 2 PNdB relaxation of the goal of 95 PNdB used for the parametric aircraft because, at the relatively close 500 foot (152 m) sideline distance, the duration correction factor in the EPNL calculation reduces the maximum tone corrected perceived noise level by approximately 2 PNdB.

The following sections discuss the noise sources, duct lining treatment, 1980 technology factors and the propulsive lift flap interaction noise of each of the candidate STOL high lift concepts.

C.2 Acoustic Technology

C.2.1 Noise Sources. - Noise from turbofan engines consist of turbomachinery noise, combustion noise, and jet exhaust noise. Turbomachinery noise is produced by the fluctuating pressure fields on the various rotor and stator assemblies; it contains broadband and discrete frequency spectral components that are radiated from the inlet, fan discharge, and turbine discharge ducts.

Combustion noise consists of low-frequency broadband components radiated from the turbine discharge duct. Jet exhaust noise is generated outside the engine within the jet efflux and contains acoustical energy over a wide range of frequencies. Estimates of the maximum perceived noise levels for these sources were based on data supplied by the engine manufacturers, and supplemented by Douglas-developed techniques for predicting aircraft flyover noise levels.

Noise radiated from the inlet is a maximum in the forward quadrant and decreases rapidly in the aft quadrant after the airplane has passed the closest point of approach to the observer. The maximum values of the noise from the fan discharge, turbine discharge, and jet noise sources occur in the aft quadrant of acoustic angles between 100 degrees and 130 degrees from the inlet.

The maximum PNL produced by all the noise sources on the airplane was determined by combining, logarithmically, the contributions from all sources peaking in the aft quadrant. The contribution of inlet noise to the total aft-quadrant noise level was considered to be at least 9 PNdB less than the peak inlet noise level in the forward quadrant. The peak inlet noise was also considered to occur several seconds before the peak aft-quadrant noise.

C.2.2 Duct Linings. - An assessment of the acoustically absorptive duct linings and the number of splitters required in each engine installation was developed from various studies of duct linings for turbofan engines. The Douglas duct-lining design procedures are based on the results of laboratory impedance-tube and flow-resistance tests, duct-transmission-loss tests, static engine tests (JT3D, JT8D, JT9D, and CF6), and flyover-noise tests (DC-8, DC-9, and DC-10). Some of these test results are reported in References 13, 14, 15, and 16.

Analytical studies, References 17 and 18, are used, when feasible, to guide the selection of the acoustic design parameters.

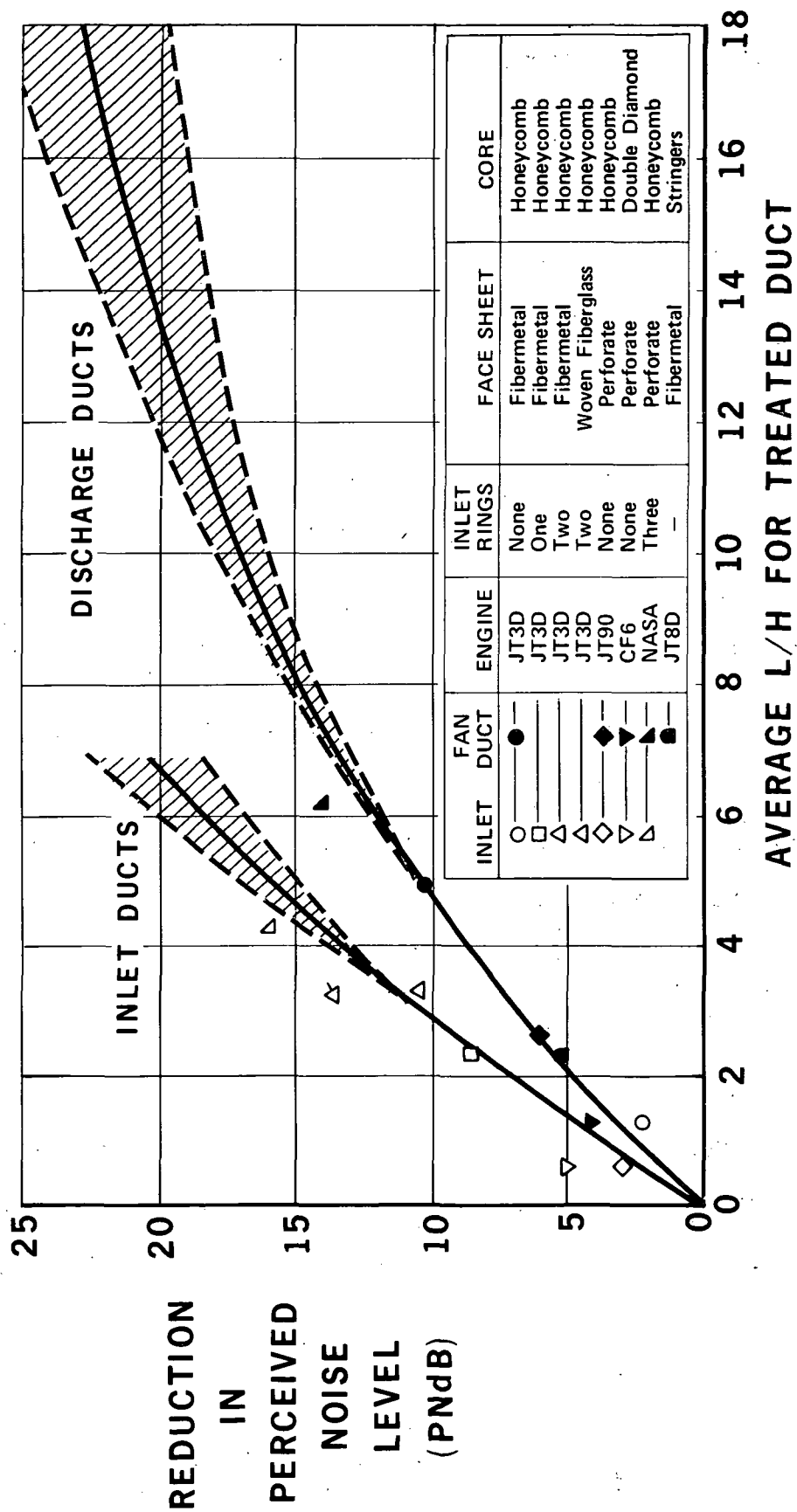
The various studies mentioned above concentrated on single-layer designs with only one porous face sheet and an impervious core. The variables that were studied included the acoustic impedance and the construction of the lining, the airflow over the surface of the lining, and the geometric arrangement of the treated surfaces within the duct. Tests were also conducted on multi-layer lining designs with impervious-core supports. The general result of these tests was the conclusion that somewhat larger attenuation bandwidths could be achieved with multi-layer designs.

A compilation of the test results for a variety of acoustically lined ducts is presented in Figure C-1. The JT3D results are from those reported in References 13 and 15. The NASA results are from those reported in References 19 and 20. The JT9D, CF6, and JT8D test results are unpublished.

Results are presented for engine operating conditions where the level of the blade-passage discrete-frequency fan noise was significantly above the level of the broadband fan noise at that frequency, that is, on the order of 20 to 25 dB. Results for a variety of duct-lining designs are included. The abscissa, in Figure C-1, is the average ratio, for a given treated duct, of the length of treatment (L) to the duct-passage height (H).

The PNL reductions are all relative to the noise radiated from a hard-walled reference inlet or fan-discharge duct. The inlet noise reduction for each configuration was taken at the corresponding angle of maximum PNL in the forward quadrant along a sideline; the reduction in fan discharge

PRELIMINARY DESIGN CHART FOR ACOUSTICALLY TREATED INLET AND DISCHARGE DUCTS



PR3-STOL-1558

FIGURE C-1

noise was taken in the aft quadrant. The dashed lines represent extrapolations beyond the measured data. The cross-hatching indicates the uncertainty in these extrapolations.

The data presented in Figure C-1 were used to evaluate the nacelle treatment designs that were developed in this study. The treated ducts that formed the basis for most of the test results had duct linings of the type known as single-degree-of-freedom (SDOF) linings with a single porous face sheet, an impervious supporting core, and an impervious backing sheet. Recent developments by Douglas and General Electric have shown that duct linings with porous cores can achieve greater attenuation bandwidths and greater PNL reductions than SDOF linings with the same average L/H ratios.

Depending on the details of the acoustical design, the new type of lining, sometimes termed multiple-degree-of-freedom (MDOF) lining, was considered to give one to three PNdB more noise reduction than equivalent SDOF duct linings at the same engine operating condition, the amount of increase depending on the L/H ratio of the duct in which it was installed. In evaluating the noise reduction of the duct lining, an additional credit was therefore allowed for the use of the MDOF type of lining.

The Douglas concept for a duct lining with the acoustical advantages of the MDOF approach is described as integrally-woven polyimide-impregnated fiberglass. The concept has evolved from a series of investigations conducted as part of a continuing Douglas program to develop improved acoustically absorptive duct linings. The new lining has an X-shaped porous core and is woven from fiberglass yarn on a loom that is capable of weaving in three mutually perpendicular planes. The loom simultaneously weaves the porous face

sheet, the porous X-core, and the impervious back sheet. The woven structure is then impregnated with a polyimide resin and cured in an oven. The porosity of the face sheet and core is determined by the diameter and twist of the yarn, the resin content, and the curing cycle. The result is a structure that is lightweight, strong, and durable. The woven fiberglass linings can be designed to be primary structural elements capable of carrying loads.

The lining designs envisioned for the treated ducts have the flexibility to permit the installation of linings with different acoustical resistances along the length of the lining. This technique of tailoring the acoustical impedance to match the varying characteristics of the acoustic and the aerodynamic fields has been successfully used to reduce JT3D fan noise, Reference 13, and the noise from the NASA Engine A, Reference 19.

An acoustic evaluation is presented in the following pages for each of the five STOL aircraft concepts with the engines selected for each. Estimates of the noise levels for the various sources in an unsuppressed airplane are shown, together with the levels for an airplane with noise-suppression treatment.

C.2.3 1980 Technology Factors. - Since the engine/airplane designs are to be consistent with the technology of the 1980 time period, estimates of improvements that could reasonably be expected to occur in noise-reduction technology were made. The noise-reduction goals are shown in Table C-1. Credit for appropriate noise reductions due to technology improvement was included in arriving at suppressed noise levels. The maximum credit shown in Table C-1 was not always used; instead, allowances were dependent on the amount of treatment involved.

TABLE C-1

NOISE REDUCTION IMPROVEMENTS FROM TECHNOLOGICAL ADVANCEMENTS

NOISE SOURCE	POSSIBLE TECHNOLOGICAL ADVANCEMENT	NOISE REDUCTION IMPROVEMENT GOAL
INLET	o FIXED GEOMETRY INLET WITH HIGH SUBSONIC VELOCITIES	7 PNdB for $M = 0.75$ 13 PNdB for $M = 0.9$
	o IMPROVED DUCT LINING	2 PNdB
FAN DISCHARGE AND TURBINE	o INTERNAL MIXING	3 PNdB
	o IMPROVED DUCT LINING	3 PNdB
JET	o MODIFY INITIAL MIXING ZONE	2-3 PNdB (for 1% reduction in F_g)
FLAP INTERACTION	o MODIFY WING AND FLAP	3 PNdB

It should be noted that the 1980 technology assumptions are highly important in achieving the STOL noise goals with reasonable levels of acoustic treatment. The technical risk associated with the technology factors and the lack of flight noise data for the study engines requires that a tolerance be placed on the absolute aircraft noise levels and that development be continued to realize these 1980 noise levels. The economic viability of the STOL concepts is highly dependent upon the stated noise goals and the 1980 technology assumptions because, at the high levels of treatment required, the additional noise reduction achieved by adding more and more treatment becomes less and less per unit of L/H ratio. A disproportionate amount of treatment would therefore be required to offset any increases in source noise.

C.3 Aircraft Noise Levels

C.3.1 EBF Concept. - Flap-interaction noise results from the impingement of the turbulent engine exhaust upon the wing and flap surfaces and from interaction with the leading and trailing edges of these structures in an externally blown flap configuration. NASA investigators, References 21-28 have conducted various model and full-scale tests of this phenomenon associated with EBF STOL airplanes and have estimated, for various flap deflections, the flyover noise levels that might be expected from engines with different exhaust velocities. The results of Douglas tests conducted under an in-house program have confirmed the general trends noted by the NASA investigators for engines with round exhaust nozzles.

PNL estimates for flap-interaction noise were based on the extrapolations given in References 21 and 24. The NASA data considered the

problems of extrapolating the sound-pressure levels measured around a model-scale test rig with unheated air to a flight condition for a full-scale EBF airplane. Use of the NASA extrapolations was considered reasonable for these study airplanes, because a flap located approximately four nozzle diameters downstream of the nozzle exit plane from an engine having a round exhaust nozzle would have a peak flap-impingement velocity approximately equal to the jet exit velocity.

The following equation for flap-interaction noise at takeoff power was developed from the relations given in the NASA data for estimating the maximum PNL on a 500-foot (152 m) sideline for the flap-interaction noise generated by a four-engine EBF airplane. The eighth power variation shown for the exhaust velocity term represents an average value for the data presented in Reference 19.

$$PNL_{T.O.} = 80 \log(V_E/500) + 10 \log(F_G/10,000) + \delta_F/10 + 86$$

where V_E is the exhaust velocity, in feet per second, at the nozzle exit calculated from the gross thrust and exhaust mass flow; F_G is the gross thrust per engine, in pounds, at the desired flight condition; and δ_F is the total flap deflection in degrees. This empirical relation was considered suitable for advanced design use until better information becomes available, and is applicable only to engines having round or annular exhaust nozzles.

The thrust term was included to scale the estimated PNL values to thrusts other than the 10,000 pounds (44,500 N) per engine value shown for all the NASA data. Gross thrust at the flight condition was chosen, rather than static gross thrust as in Reference 21, because inflight gross thrust (representing the momentum flux out of the nozzle measured relative to the wing) is a

measure of the force applied to the flaps and hence should be directly related to the level of flap-interaction noise.

Inclusion of the δ_F term permitted small adjustments to be made for takeoff and approach flap deflections different from those tested by the NASA.

The constant, of 86 PNdB, was obtained by fitting a mean straight line through the "flyover" data presented by NASA from measurements made at locations below the wing and subtracting a 2-PNdB factor to obtain equivalent "sideline" noise levels. The viewing angle expected for an externally blown flap STOL transport at the location of maximum PNL on the 500-foot (152 m) sideline during climbout made the 2-PNdB viewfactor more appropriate than the 5-PNdB viewfactor noted in Reference 21. The sideline data in Reference 19 were obtained with a viewing angle corresponding to that of an airplane on the ground at the time of the maximum PNL.

The viewfactor is highly important for determining whether the EBF can meet the sideline noise goal. The assumed viewfactor of 2 PNdB requires that the 3 PNdB 1980 technology assumption for flap interaction noise be used to meet either the parametric or final baseline noise goals. A more optimistic viewfactor would have meant that less acoustical treatment would have been required to reduce the turbomachinery noise so that the total aircraft noise would meet the noise goal. However, the noise beneath the aircraft and the length of a given noise contour around an airport during takeoff or approach would remain the same independent of the viewfactor. The flap noise levels for 1980 include a 1.0 PNdB reduction for a single slotted flap and a 1.5 PNdB reduction for forward velocity. These factors were estimated from model scale test data.

Table C-2 shows the hardwall component noise levels and the treatment required for 95 PNdB and 95 EPNdB 500 foot (152 m) sideline noise levels for an EBF aircraft. Estimates are also given for wall treatment only with 1980 technology. These estimates are valid for all of the EBF aircraft using the Allison PD287-3 engine. Different field lengths or passenger capacities would change the engine size from that shown. However, the effect of this change can be estimated by modifying each component noise level by $10 \log (F/F_{\text{ref}})$, where F_{ref} is 20,000 pounds (89,000 Newtons) rated takeoff thrust.

This correction would be a maximum of approximately 1 EPNdB for the airplanes considered in this study. Small changes to the treatment level (L/h) would be sufficient to adjust the noise level for small changes in thrust. Such accuracy would be misleading considering the 1980 technology factors, the lack of information on the effect of forward motion on flap-interaction noise, and the fact that the engines considered here have never been flown.

The calculations show that an external mixing nozzle was necessary to meet the goal of 95 PNdB at a 500 foot (152 m) sideline for the parametric aircraft. This nozzle would cause substantial penalties to be imposed on the aircraft. The external mixer was not included because the goal of 95 EPNdB for the final design aircraft made it unnecessary.

Possibilities of reducing the EBF flap interaction noise include lined ejector-shrouds around the nozzles, acoustical treatment of the flaps, recontouring of the flap and reduction of the number of separate flap segments. Table C-2 also shows the influence of the flap interaction noise "floor" on the effectiveness of acoustic treatment. As the flap noise floor

TABLE C-2

NOISE LEVELS OF EXTERNALLY BLOWN FLAP AIRPLANE
 4 Scaled PD287-3 Engines at 20,000 Lb (89,000 Newtons)/Engine Rated Thrust
 500 foot (152 m) Sideline, Flap Deflection = 20°

Noise Source	Maximum Perceived Noise Level, PNdB						
	Unsuppressed Noise Level	95 PNdB Goal L/h, Noise Level*	95 EPNdB Goal L/h, Noise Level*	Wall Treatment Only L/h, Noise Level*			
Inlet	100	1.5	92	1.5	92	.6	95
Fan Discharge	103	6.5	84	3.5	89	2.4	93
Turbine Discharge	98	4.5	84	2.6	88	2.6	88
Jet Exhaust	89	-	89	-	89	-	89
Flap Interaction	100	-	92***	-	94.5**	-	94.5**
All Sources	106		95		97		98
Effective Perceived Noise Level, EPNdB							
All Sources	104		93		95		96

*1980 Technology

**Round Tailpipe

***External Mixer Nozzle

is approached, additional treatment gives a very small reduction in overall noise. The economic penalties associated with acoustical treatment increase dramatically with small decreases in total aircraft noise as the noise floor is approached. For the reasons previously stated, this noise floor is somewhat uncertain so the treatment was reduced to investigate the effects of acoustical treatment on the airplane configuration. These noise levels are shown on the third column of Table C-2. Reducing the treatment in the fan discharge duct by an amount equivalent to 4 PNdB increases the total aircraft noise by one PNdB.

C.3.2 Upper Surface Blowing Concept. - The major acoustical feature of the upper surface blowing concept is the shielding of the aft generated turbomachinery noise. The existing model data, References 29, 30, and 31, is incomplete and assumptions had to be made concerning the amount of shielding. The data from References 29, 30, and 31 tends to show that the thrust deflector devices used to ensure attachment of the nozzle flow over the wing increase the noise level over the level of the jet alone. However, the wing gives some shielding of the high frequency jet noise. This phenomenon was approximated by assuming that the noise of the deflector device was equal to the lower surface blowing flap impingement noise. A noise reduction of 5 PNdB was then used to simulate the wing shielding. It was also assumed that the fan and turbine discharge noise would be reduced 5 PNdB by the wing shielding. 1980 technology factors were assumed for the turbomachinery noise and 5 PNdB was assumed as a technology improvement for wing-flap interaction. This flap noise level would be representative of an USB system without the noise of a separate flow attachment device.

Table C-3 shows the USB noise levels with an Allison PD287-22 engine. This engine cycle had higher tip speeds than the PD287-3 used for the EBF concept resulting in higher source noise. The wing shielding of the aft turbomachinery noise reduces the requirement for acoustic treatment for these sources. The USB concept, then, with the PD287-22 engine tends to be more inlet noise dominated. The configuration with wall treatment and 1980 technology assumptions is inlet noise dominated. Experience with the DC-9 and DC-10 aircraft (unpublished) has shown that the inlet noise is lower during flyover than during static operation. The inlet noise, however, is estimated from static test stand data. The noise levels in parentheses on the right hand column of Table C-3 exclude the inlet to show the contribution of the aft noise sources. The inlet noise for this case could be reduced by the addition of treated inlet rings.

The USB concept requires more large scale test data before the concept can be properly evaluated. One specific area of uncertainty is the magnitude of the turbomachinery noise shielding as a function of wing and nozzle dimensions and sideline versus overhead flight position. Another is the feasibility of attaching the flow of large diameter, low pressure ratio jets to the flap surface.

C.3.3 Mechanical Flap Concept. - The mechanical flap STOL concept is relatively straight forward from a noise assessment viewpoint because powered lift is not used. The PD287-23 engine chosen for the mechanical flap has a fairly high tip speed and therefore high turbomachinery noise. Extensive acoustic treatment is required to meet the noise goals. Table C-4 gives the noise level of the mechanical flap concept for several levels of treatment. The inlet noise is based on static test stand data. The high tip speed gives

TABLE C-3

NOISE LEVEL OF UPPER SURFACE BLOWING CONCEPT
4 PD287-22 Engines at 27,500 Lb (122,200 Newtons) Rated Thrust per Engine
500 foot (152 m) Sideline

Noise Source	Maximum Perceived Noise Level, PNdB			
	Unsuppressed Noise Level	Unsuppressed with Wing Shielding	Extensive Treatment L/h, Noise Level***	Wall Treatment L/h, Noise Level***
Inlet	108	108	2.5	.8
Fan Discharge	111	106	2.8	2.2
Turbine Discharge	101	96	2.1	2.1
Jet Exhaust	93			
Wing-Flap Interaction	103*	98**	93	93
All Sources	113	108	97	102 (100) ⁴
Effective Perceived Noise Level, EPNdB				
All Sources	111	106	95	100(98) ⁴

*25B noise assumption

**Assumed USB flap noise

***1980 Technology

4 Assume flight inlet noise reduces during flight

Table C-4

NOISE LEVEL OF MECHANICAL FLAP AIRPLANE
2 Scaled PD287-23 Engines at 35,000 Lb (155,700 Newtons)/Engine Rated Thrust
500 foot (152 m) Sideline

Noise Source	Maximum Perceived Noise Level, PNdB			
	Unsuppressed Noise Level	95 PNdB Goal L/h, Noise Level*	95 EPNdB Goal L/h, Noise Level*	Reduced Treatment L/h, Noise Level*
Inlet	117	4	4	4
Fan Discharge	115	13	10	9
Turbine Discharge	100	4	4	4
Jet Exhaust	95	-	-	-
All Sources	117	-	-	-
Effective Perceived Noise Level, EPNdB				
All Sources	115	93	95	97

*1980 Technology

**Estimate based on Static Data - Flight Inlet will Reduce Noise to About 95 PNdB.

a large multiple pure tone (MPT) component to the inlet noise. Past Douglas experience with static and flight noise data (unpublished) shows that the use of a flight inlet operated in the flight mode reduces these MPT noise sources. Therefore the "all source" noise on Table C-4 was estimated with the inlet contribution shown. A degree of risk, however, exists until an engine of this type is actually flown.

C.3.4 Augmentor Wing Concept. - Investigators at NASA and Boeing have conducted several tests to study noise characteristics of augmentor-wing ejector-flap systems. Noise from augmentor flaps is primarily generated during the turbulent mixing process that occurs between the jet sheet exhausting through the ejector flaps and the secondary or ambient flow.

Data presented in References 32-35 shows that noise from augmentor flaps is broadband in character and highly directional, with the peak noise radiated at an angle of about 45 degrees on both sides of the exhaust flow direction. Considering operational flap settings, aircraft angle of attack, and climb gradient, the peak noise is therefore directed nearly straight downward during takeoff.

Experimental results from References 32, 33 and 35 showed that the noise from slot nozzles used with augmentor flaps is proportional to the exit area of the nozzle and increases with increasing jet velocity. Above the critical nozzle pressure ratio, the sound contains discrete-frequency components related to turbulence in the exhaust flow interacting with the shock cells downstream of the nozzle. These components have a raucous sound characterized as screech.

Recently, extensive studies of the noise from augmentor flap systems have been reported in References 10, 36 and 27. In these reports, maximum PNL's on a 500-foot (152 m) sideline for a four-engine STOL airplane were derived from available model-scale test data scaled to represent the noise from an airplane with engines having a takeoff thrust rating of 20,000 pounds (89,000 Newtons) and a wing slot airflow of approximately 500 pounds per second (227 kg/sec) per semi-span. For a nozzle pressure ratio of 2.6, the 500 foot (152 m) sideline noise level was predicted to be 116 PNdB with a plain high-aspect-ratio slot nozzle at an airspeed of 100 knots (51.4 m/sec).

The noise suppression design recommended to suppress the jet noise from the augmentor flaps was developed from the results of the many tests described in References 10, 36, 37 and 38 and the results of previous Douglas tests on jet-noise suppressors and acoustically lined ducts.

Effective suppression of the noise from the augmentor flaps involves a combination of the proper choice of the geometry of the flaps and nozzles and the addition of acoustically absorptive treatment to the inner surfaces of the flap, shroud, and intake door. Addition of an acoustical shield below the nozzles is expected to produce at least some of the large noise reductions noted in Reference 35 that were associated with completely sealing off the lower flap. The principal features of the designs that were developed are discussed in Appendix D.

Data from References 10, 36, 37 and 38 showed that significant reductions in low-frequency noise can be achieved by replacing the long two-dimensional augmentor slot with a mixer nozzle consisting of a large number of nozzle elements. It has been shown that a lobed nozzle array achieved

greater noise reductions than a tubular nozzle array. A multi-element slot tends to shift the acoustical energy toward a frequency region where some of the energy can be absorbed by acoustically absorptive linings placed within the flaps. Therefore, although practical mixer nozzles tested to date have achieved only relatively small reductions in perceived noise level, when used in conjunction with absorptive treatment they have proven to be effective in achieving a substantial reduction in augmentor flap noise. In order to interrupt the acoustic feedback mechanism and suppress the screech sounds, screech shields consisting of rectangular plates extending downstream of the nozzle exit on one side of each nozzle were also included.

Acoustic design requirements for the suppression of augmentor flap noise were derived from the results presented in References 10 and 38. The values that were assumed for the various design parameters are given in Table C-5.

The absorptive linings on the flap surfaces require a wide absorption bandwidth to maximize the noise reduction. Within the constraint of the space available, a design was developed that uses a unique two-layer welded and bonded structure. Two-layer absorptive linings were also placed on the acoustic baffle door below the nozzle exits and ahead of the flap leading edge, the thickness of the lining constituting the total thickness of the door, except for the leading and the trailing edges.

C.3.5 Internally Blown Jet Flap Concept. - The internally blown jet flap is similar to the augmentor wing except the upper shroud is removed from the augmentor flap. References 23 and 19 were used to evaluate the jet flap. The internally blown flap noise levels are shown on Table C-6.

Table C-5

NOISE LEVEL OF AUGMENTOR WING AIRPLANE
4 Scaled PD287-43 Engines at 20,000 Lb (89,000 Newtons) Thrust Each
500 foot (152 m) Sideline Measuring Point

Noise Source	Maximum Perceived Noise Level - PNdB	
	Unsuppressed Noise Level	Suppressed with 1980 Technology
Inlet	119	Choked
Turbine Discharge	101	88
Primary Jet	90	90
Augmentor Flap	116	95
All Sources	119	97
All Sources	Effective Perceived Noise Level, EPNdB	
	117	95

Notes: Turbine L/h = 4.5
 Fan Duct requires treated L/h of 12 in augmentor ducting
 Augmentor flaps include multi-element nozzles, screech shields, lower baffles and
 MDOF acoustical treatment

Table C-6

NOISE LEVELS OF INTERNALLY BLOWN JET FLAP
4 Scaled PD287-43 Engines at 20,000 Lb (89,000 Newtons) Thrust Per Engine
500 Foot (152 m) Sideline Measuring Point

Noise Source	Maximum Perceived Noise Level - PNdB	
	Unsuppressed Noise Level	Suppressed Noise Level 1980 Technology
Inlet	119	Choked
Turbine Discharge	101	88
Primary Jet	90	90
Jet Flap	116	97
All Sources	119	98
All Sources	Effective Perceived Noise Level, EPNdB	
	117	96

Notes: Turbine L/h = 4.5
Fan Duct requires treated L/h - 12 in internal jet flap ducting
Jet Flap and wing nozzles include multi-element nozzles and screech shields

C.3.6 Conventional Takeoff and Landing Aircraft (CTOL). - A conventional aircraft for the 1980 time period was developed to use as a comparison to the STOL concepts. This aircraft has very extensive acoustical treatment compared to current aircraft. The noise sources were treated to exceed present FAR Part 36 noise levels. The treated noise level is about 98 EPNdB on a 500 foot (152 m) sideline measuring point. The noise levels at the FAA measuring points are summarized on Table C-7 for the hardwall and treated configurations. The EPNL values reflect CTOL airspeeds and measuring distances.

Table C-7

NOISE LEVEL OF CONVENTIONAL TAKEOFF AND LANDING AIRPLANE
2 Scaled GE13/F6A1 Engines Rated at 27,000 Lb (120,000 Newtons) Thrust Per Engine
FAR 36 Noise Measuring Locations, No Cutback

Noise Source	Maximum Perceived Noise Level, PNdB			
	1500 Ft Sideline Bare	Treated*	Takeoff, Alt - 2400', Bare	Treated* Approach, Alt = 370', Bare
Inlet	101	87	98	108
Fan Discharge	99	82	96	106
Turbine Discharge	84	81	81	100
Jet (Mixed) **	74	74	71	88
All Sources	100	86	97	108
Effective Perceived Noise Level, EPNdB				
All Sources	100	86	97	103

Treatment Level:

Source L/h
Inlet 4.0
Fan Discharge 7.0
Turbine Discharge 1.6

Current FAA Noise Levels

T.O. 98.5 EPNdB
App. 104 EPNdB
SL 104 EPNdB

*1980 Technology

**Jet Noise Assumes Mixing
of Primary & Fan Streams

APPENDIX D

PROPULSION INSTALLATION SUBSTANTIATION - FINAL DESIGN AIRCRAFT

This appendix contains the results of propulsion installation studies conducted on the engines selected for the final design aircraft. A summary of the propulsion installation losses pertinent to the calculation of aircraft performance is also given.

Thrust levels shown in the installation drawings were selected prior to final aircraft sizing and do not necessarily match the final engine thrust size.

D.1 Propulsion Installation

D.1.1 Externally Blown Flap. - The final design externally blown flap engine installation is shown in Figure D-1. The drawing is made for a 20,000 pound (88,964 N) S.L.S. thrust variable-pitch fan engine with a fan pressure ratio of 1.25.

Engine/Airframe Interrelation - The final design engine installation is shown matched to a wing cross section corresponding to the 50 percent semi-span cut of an 1800 square foot (167 m^2) wing with 7.0 aspect ratio, 0.3 taper ratio and 25 degrees of sweep at the quarter chord. These values were derived from previous studies and test experience as being typical for meeting externally blown flap wing requirements for high lift with minimum weight.

The nacelle is positioned relative to the wing by horizontally locating the fan exhaust plane forward of the wing L.E. by an amount equal to 10 percent of the wing chord at the inboard nacelle station; the vertical position is fixed by locating the top of the fan exhaust in the same horizontal plane as the lowest extremity of the drooped wing leading edge section.

EXTERNALLY BLOWN FLAP FINAL DESIGN ENGINE INSTALLATION

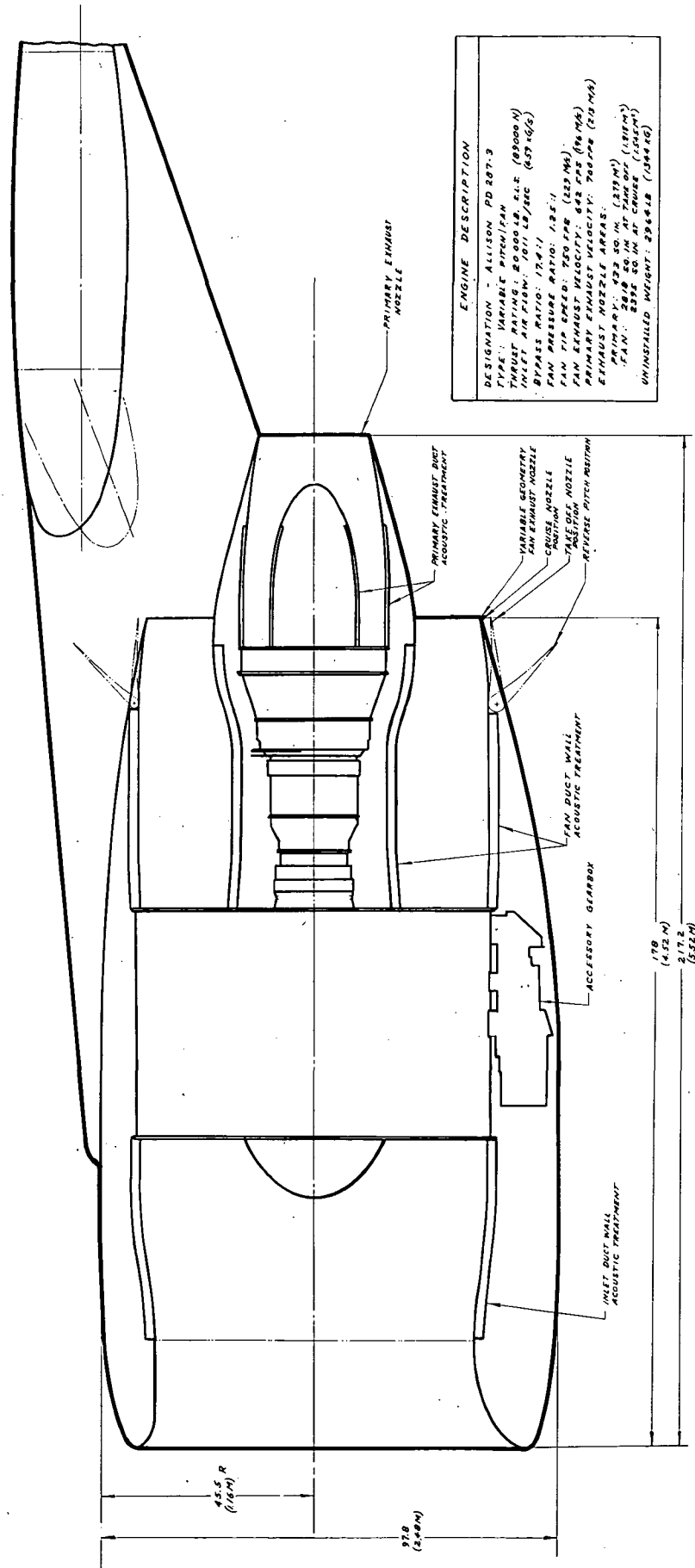


FIGURE D-1

PR3-STOL-I641A

Engine Inlet Geometry - The engine inlet throat area is sized to give an average throat Mach number no greater than 0.6 at takeoff power at sea level static conditions. The inlet is configured with a leading edge lip thickness that varies from 11 percent at the top to a maximum of 20 percent at the bottom. This lip design is consistent with maintaining acceptable inlet distortion levels at high angles of attack. The inlet length is dictated by the L/H ratio required to attain the desired level of acoustic attenuation as listed in Appendix C.

Nacelle External Shape - The maximum nacelle radii are sized primarily with regard to engine fan case clearance and with the accommodation of a fan exhaust duct which has been designed to the prescribed acoustic wall treatment L/H ratio. The nacelle/fan case clearance includes a volume allocation for the engine accessories and engine-mounted airframe system components such as C.S.D./generators, hydraulic pumps and pneumatic system controls and ducting. Size estimates of these components were based upon past experience with airplane requirements on the DC-8, DC-9 and DC-10 production programs. The diameter of the fan cowl trailing edge is dictated by boat-tail angle considerations. This diameter, in conjunction with the fan nozzle area requirements of the engine, sizes the core cowl maximum diameter.

The core cowl afterbody length is held to a minimum consistent with keeping the boat tail angle at a value that results in low aerodynamic drag.

Exhaust Duct Geometry - The fan duct flow area is sized to maintain duct Mach number below 0.45 through the acoustically lined duct between the engine fan case and the leading edge of the variable area exhaust nozzle vanes. At this point a reduction in duct area is initiated which continues to the

fan exhaust nozzle plane. A variable area is required at the fan nozzle in order to attain the proper match between takeoff and cruise performance. This is accomplished by having the last 19 inches (.483m) of the fan cowl broken up into finger-like vanes which can be actuated radially to demarcate varying nozzle diameters.

The primary exhaust duct has been kept to the minimum length consistent with meeting the nozzle area requirement and core cowl boat-tail angle drag considerations. An acoustically treated center plug is shown which is shaped to minimize flow losses as well as provide good acoustic L/H characteristics.

Accessibility - Access to the engine accessory section, located around the periphery of the engine fan case, is provided by fan cowl doors which are hinged at the top from the pylon structure. The accessory gear box is shown located on the bottom of the engine fan case since comparative experience of commercial airlines between this location and one on the engine core case demonstrates the superiority of the fan case location with respect to both accessibility and accessory service life due to the cooler environment.

Engine core case access is provided by splitting the fan duct vertically into half sections which are hinged from the pylon structure. This concept is basically the same as that which has been demonstrated in the DC-10 program.

Thrust Reversing - Reversed thrust is obtained by rotating the fan blades into reverse pitch. The effect of this feature upon the overall engine installation is the need for variable geometry in the nozzle to allow it to function as an inlet in the reverse mode. This requires an increase in area variation beyond that required between the takeoff and cruise values.

D.1.2 Upper Surface Blowing. - An upper-surface blowing lift concept engine installation using a 1.30 fan pressure ratio, fixed-pitch turbofan engine with a common-flow exhaust system is shown in Figure D-2. This installation matches a 27,500 pound (122,000 N) thrust engine to a wing cross-section corresponding to the 35 percent semi-span chord of a 3390 square foot (315 m²) wing with an 8.0 aspect ratio, 0.3 taper ratio and 25 degrees of sweep at the quarter chord.

Engine Airframe Interrelation - The positioning of the engine with respect to the wing was fixed with the following considerations:

- o The engine should be kept as far aft as possible to minimize installation weight, but should not be so far aft as to prohibit engine removal in a vertical plane forward of the primary wing structure.
- o The vertical positioning of the engine should be low enough to permit the nacelle dorsal line to conform to optimum boat-tail angle criterion (15 degrees maximum) while still permitting an acceptable fan duct flow transition from the underside of the gas generator to the upper surface of the wing.

**RATED THRUST = 27,500 LB SLS
(122,000 N)**

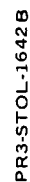


FIGURE D-2

- o The plane of the aft turbine should be forward of the wing spars and fuel tanks to comply with Federal Airworthiness Regulations requiring consideration in the design for rotor failures.

Engine Inlet Geometry and Nacelle External Lines - The engine inlet for the upper surface blowing engine installation follows identical guidelines listed for the externally blown flap installation. Similarly the external lines of the nacelle forward section are sized by the clearance requirements around the engine fan case and the fan exhaust duct for the accommodation of engine accessories, thrust reverser actuators and associated plumbing. Size estimates for these components were based on previous experience with the DC-8, DC-9 and DC-10 engine/airframe integration. The aft nacelle section external shape is primarily influenced by the requirement to spread out and attach the exhaust flow to the upper surface of the wing during hi-lift mode operations. This is accomplished by fairing the aft end of the nacelle to a D-shaped exhaust nozzle as shown in Figure D-2.

Exhaust Duct Geometry - To minimize duct pressure losses, the fan duct adjacent to the engine core is sized for 0.45 Mach number flow. This portion of the duct is lined with acoustic treatment as dictated by the L/H ratio required for the desired acoustic attenuation listed in Appendix C. As the junction of the fan duct with the primary duct is approached, the area of the fan duct is tailored to adjust the flow velocity to accomplish a match in static pressures of the fan and primary exhaust flows. The common flow exhaust duct is designed to accommodate the thrust reverser and variable geometry exhaust provisions with a flow area that minimizes duct pressure loss.

Thrust Reverser/Variable Geometry Nozzle - Thrust reversing is accomplished by diverting the combined fan exhaust and primary exhaust flow through a stationary cascade which is wrapped around the top half of the nacelle. The forward thrust flow path is blocked off by means of finger-like vanes, which in the retracted position form the cruise nozzle. These vanes in a partially extended position act to deflect and spread out the flow against the top wing surface during high lift mode operations

Engine Support Structural Arrangement - The location of the engine support structure relative to the engine has a very strong impact on engine maintainability. Commercial airlines have expressed a strong preference for keeping the engine removal/installation path completely vertical. In addition, direct access to the borescope ports located on the engine casing without removal of any nacelle components is required. Compliance with the first constraint virtually precludes the use of the most direct structural load path from the wing to the engine, (i.e., a structural beam cantilevered straight forward from the front spar to support the engine from its underside) and forces the use of side supports, top support, or a combination of both. A comparison of the advantages and disadvantages of the various engine support schemes is shown in Table D-1. The combined top and side support approach was selected for the baseline installation since it has the most favorable combination of low weight and ease of maintenance with the greatest overall torsional rigidity. The top support pylon structure attaches to wing primary structure commencing at the wing front spar and extending back along the upper wing skin approximately half way to the rear spar. An internal wing rib is required to carry the cantilevered load couple back to the rear spar of the wing. A fixed external fairing is required aft of the engine

Table D-1

ENGINE SUPPORT STRUCTURE SCHEMES FOR U.S.B. LIFT CONCEPT

ENGINE SUPPORT STRUCTURE LOCATION (RELATIVE TO ENGINE)	ADVANTAGE	DISADVANTAGE
Bottom	<ul style="list-style-type: none"> o Provides most direct load path from engine to wing structure. o Has least impact on fan exhaust ducting. 	<ul style="list-style-type: none"> o Cannot remove engine without horizontal translation. o Access for inspection and maintenance difficult. Will require additional support structure to support hinged fan duct sections.
Bottom with Support Structure Detachable from Wing	<ul style="list-style-type: none"> o Allows engine removal in vertical plane. 	<ul style="list-style-type: none"> o Requires support structure to be removed with engine (introduces extra interface for engine removal).
Single Side (either side of engine)	<ul style="list-style-type: none"> o Allows engine removal in vertical plane. 	<ul style="list-style-type: none"> o Since support beam acts as a torque tube, deflections will tend to be highest with this scheme, especially with regard to wing twisting. Torsional deflections cause problems that include large weight penalty solutions. o Commonality between starboard and port demountable assemblies is difficult to obtain without weight penalties.

Table D-1 (Continued)

ENGINE SUPPORT STRUCTURE LOCATION (RELATIVE TO ENGINE)	ADVANTAGE	DISADVANTAGE
Single Side (on Inboard Side of Engine)	<ul style="list-style-type: none"> o Keeps support structure cantilevered span to a minimum. 	<ul style="list-style-type: none"> o Support structure must be bent in plan view to stay within nacelle envelope. This accentuates the combined torsion/bending load already imposed on support.
Single Side (on Outboard Side of Engine)	<ul style="list-style-type: none"> o Permits DC-10 type fan duct hinged sections for engine access and removal (hinge line must be rotated 90° from vertical to outboard side) 	<ul style="list-style-type: none"> o Increases cantilevered span of support beam by approx. 36" (.914 m) relative to inboard side support on swept wing.
Both Sides	<ul style="list-style-type: none"> o Allows engine removal in vertical plane. o Permits DC-10 type fan duct hinged sections for engine access and removal (hinge line rotated 90° from vertical to outboard side) o Reduces deflections over single side mount by balancing torque loads. Tends to keep deflections along engine ϕ in phase with wing deflections. 	<ul style="list-style-type: none"> o Requires more structure and additional weight than with single side support.
Top	<ul style="list-style-type: none"> o Allows adaptation of DC-10 type nacelle with respect to hinging access doors and fan duct sections. o Allows engine removal in vertical plane. 	<ul style="list-style-type: none"> o Requires either bifurcating primary and fan ducts around thick, torque resistant structural support from wing to beam along top of nacelle, or bifurcating structure around fan/primary exhaust ducts with a banjo type structural shape.

Table D-1 (Concluded)

ENGINE SUPPORT STRUCTURE LOCATION (RELATIVE TO ENGINE)	ADVANTAGE	DISADVANTAGE
Combination of Top and One Side	<ul style="list-style-type: none"> o Allows engine removal in vertical plane. o Allows use of thin support beams (i.e., thin exhaust duct bifurcations). Since each pylon can be kept co-planar with engine c.g. and at a 90° plane angle to each other, large torque load pylon design requirements can be eliminated with the consequence that each pylon can be satisfactorily designed within a 6 inch (.152 m) width. o Overall nacelle design is lighter than pure top or side mount arrangements. 	<ul style="list-style-type: none"> o Requires bifurcation in primary and fan duct for structural support from wing to beam along top of nacelle. o Requires fan duct to be split into three hinged sections to provide engine access for maintenance and removal.

exhaust nozzle plane to house the upper engine support pylon where it attaches to the wing.

Accessibility - Access to the engine accessory section, located around the periphery of the engine fan case is provided by fan cowl doors which are hinged from structure projecting forward from the engine support pylon buried within the top of the nacelle. The accessory gearbox is located on the bottom of the engine fan case since comparative experience of commercial airlines between this location and a core case mounting demonstrates the superiority of the fan case with respect to both accessibility and accessory service life due to the cooler environment. Engine core case access is provided by splitting the fan duct into three sections arranged as follows: A duct section on the outboard side of each nacelle enclosing one half the total fan flow area is hinged from the top pylon and latches to an adjacent duct section along the bottom center line of the nacelle (similar to the DC-10 arrangement). On the inboard-upper quadrant of the nacelle, a fan duct section enclosing twenty five percent of the total fan flow area is hinged from the top pylon and latches to the side pylon structure. The remaining twenty five percent of the flow area is enclosed in a duct section in the lower inboard nacelle quadrant, which is hinged from the side engine support pylon, and which latches to the bottom of the fan outboard duct section. Engine removal is accomplished by opening the previously mentioned doors and fan duct sections together with an additional nacelle door, located beneath the primary exhaust duct. The remainder of the nacelle including the thrust reverser cascade (exclusive of the translating variable geometry exhaust nozzle assembly) is fixed cowl structure attached to the wing.

D.1.3 Augmentor Wing. - The final design augmentor wing lift concept engine installation using a 3.0 fan pressure ratio, two-flow turbofan engine is shown in Figure D-3 at a rated thrust of 13,000 pounds (57,800N). This installation shows the nacelle matched to a wing cross-section corresponding to the 45 percent semi-span (outboard engine location) of a 1,444 square foot (134 square meter) wing with a 6.5 aspect ratio, 0.3 taper ratio and 25 degrees of sweep at the quarter chord.

Engine Airframe Interrelation - The criteria for positioning the engine relative to the wing are:

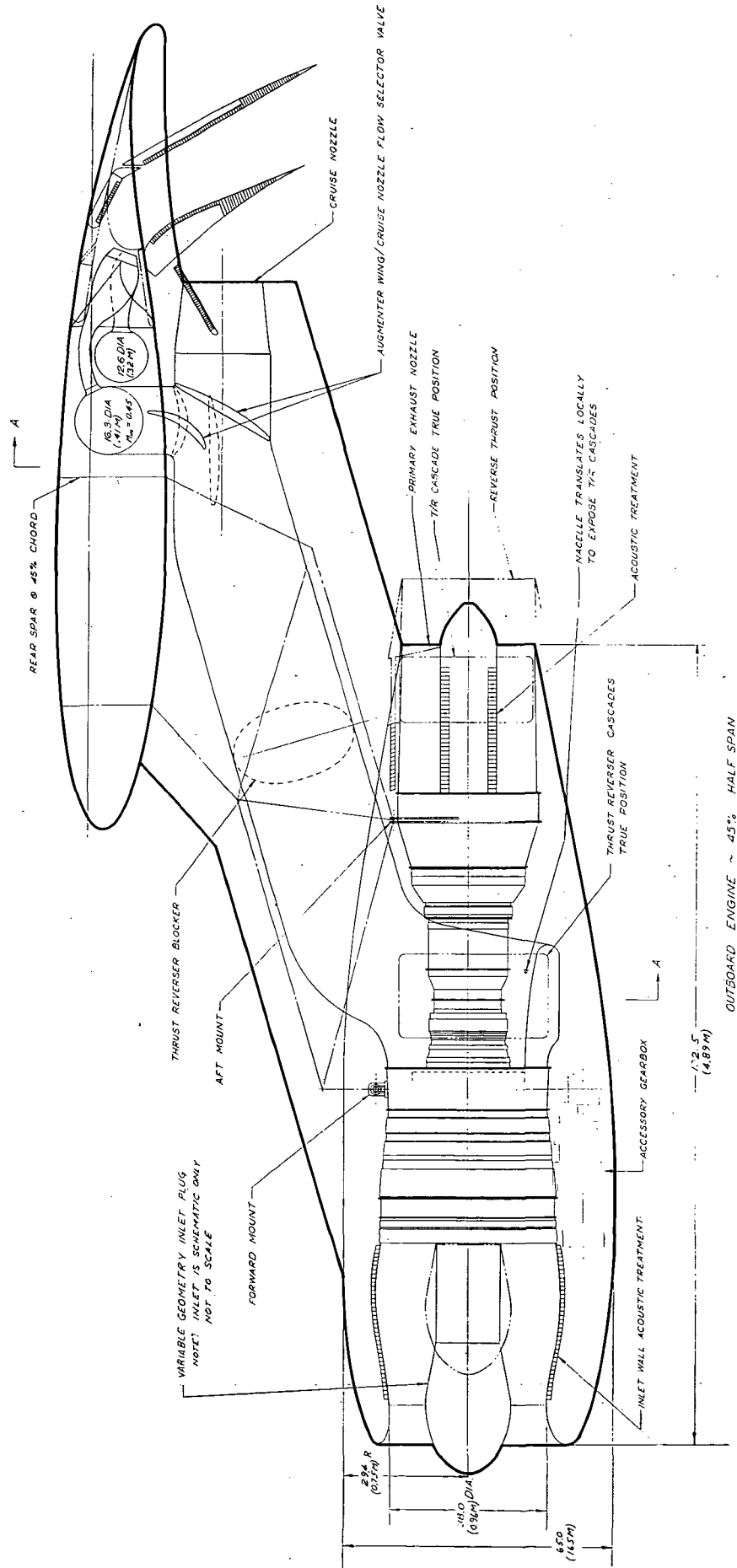
- (1) The primary exhaust plane is located no further aft than 25 percent of the wing chord to minimize nacelle/wing interference drag effects.
- (2) Vertical separation of the nacelle from the wing is kept to the minimum amount that permits the augmentor wing duct, sized for a cross-sectional area consistent with 0.45 Mach number flow, to fit between forward and aft pylon spars.

The leading edge of the pylon is shown cut back to permit installation of a continuous wing leading edge slat.

Engine Inlet Geometry - The engine inlet design is primarily driven by the noise attenuation needs which are satisfied by use of a variable geometry sonic inlet with a translating center bullet. The bullet is positioned in a forward position for takeoff, in which mode, the throat area is sized to produce near sonic velocity. In the cruise mode the bullet translates aft resulting in a larger throat area, lower air flow velocities and consequent lower pressure losses.

AUGMENTOR WING FINAL DESIGN ENGINE INSTALLATION

RATED THRUST = 13,000 LB SLS (57,800 N)



PR3-STOL-1643A

FIGURE D-3

Nacelle/Pylon External Shape - The external dimensions of the nacelle and pylon are primarily influenced by the unique requirement that all fan flow be diverted into the wing and discharged through nozzles to energize an ejector wing flap system. When the flaps are retracted, flow to these nozzles is blocked off by means of a diverter valve which directs the fan stream through a nozzle adjacent to the lower surface of the wing in the aft end of the pylon. The pylon thickness is dictated by the fan air duct dimensions which are sized for a duct flow Mach number of 0.45 in an effort to hold the duct pressure losses to practical values. Nacelle contours are set to accommodate the fan ducting and clearances around the engine accessory/gearbox located on the bottom of the engine fan case. Access to the engine accessory section for maintenance and inspection is provided by large nacelle access doors hinged from the pylon structure.

Thrust Reversers - Thrust reversing is accomplished with the use of a cascade type fan exhaust reverser and a cascade type primary exhaust spoiler. The fan exhaust reverser cascades are mounted on the sides of the engine nacelle alongside the engine high pressure compressor section. Upward reversed flow directivity (to minimize reinjection and reverse flow ground impingement) is accomplished by keeping the cascades within the top 210° portion of the nacelle perimeter and by tailoring the cascade vanes. The forward thrust fan flow stream is shut off by means of a blocker valve located in the fan duct through the pylon.

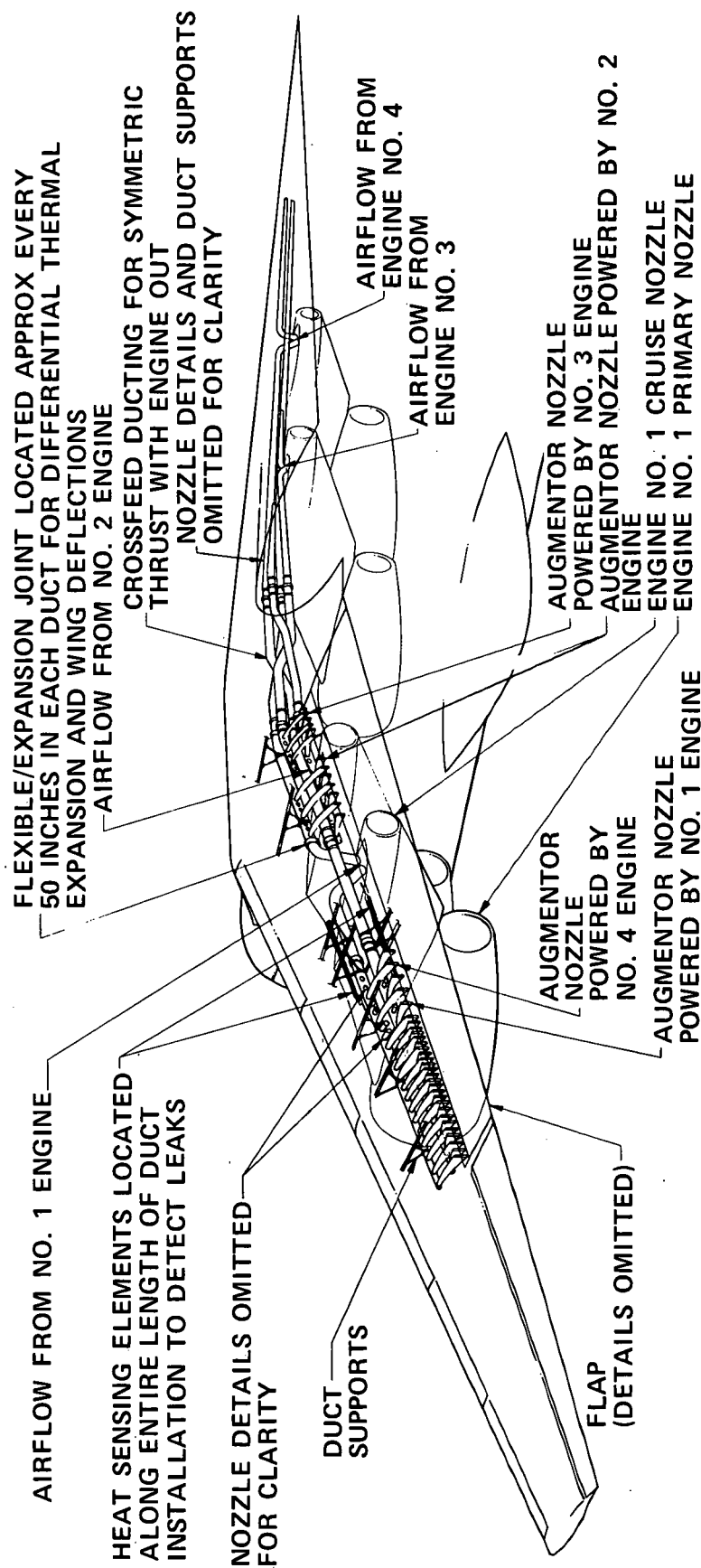
The primary spoiler is shown with an aft cowl section which translates aft to unport cascade vanes to the exhaust stream. Blocker doors hinge inward against a center bullet to close off the forward thrust flow path.

A considerable study effort was made to locate the fan reverser on the pylon where, it would seem, ideal reverse flow directivity could be attained (upward and forward), but without success. Locating the thrust reverser on the sides of the pylon would not only result in additional pylon width, but would preclude the use of the pylon walls as shear members and result in sizable structural weight penalties. Locating the thrust reverser in the pylon leading edge would be unacceptable since this would block the only available path through the pylon for engine/airframe sub-system ties (i.e., fuel, bleed air, hydraulics, electrical, controls and instrumentation).

Augmentor Wing Ducting - Although the design of augmentor wing flap system components was not within the scope of the study, certain conceptual design features of such a system had to be identified in order to make airplane weight and performance estimates. These features were derived from study experience gained in the NASA QUESTOL design studies and from the Boeing studies under NASA Contract (Reference 1). The resulting duct system arrangement is shown in Figure D-4 and features:

- o a four-engine independent-duct system which cross-flows 27 percent of the fan exhaust from each engine to the opposite side of the airplane to maintain reasonable roll moments during an engine-out condition.
- o a fan exhaust nozzle arrangement in which the nozzles from each engine pair (outboard pair, inboard pair) are interwoven along the augmentor flap entrance as recommended in the Boeing/NASA study (Reference 1).

AUGMENTOR WING WING DUCTING INSTALLATION



NOTES:

DUCT TEMP - 350°F MAX
DUCT PRESS 50 PSIG MAX

PR3-STOL-1608 A

FIGURE D-4

- o the wing ducting system broken into 50-inch segments joined by flexible couplings to allow for thermal expansion and wing bending deflections. Each duct section would be independently anchored to the wing structure with respect to airplane inertia loads, duct thrust, and axial and torsional loads resulting from duct pressurization.
- o ducts and nozzles to be fabricated from 2219-181 aluminum alloy, heat treated after welding.

An alternate to the independent-duct arrangement is the common-duct scheme in which the fan flow of all four engines is manifolded together. Despite its advantages with respect to wing ducting volume limitations, this arrangement was not selected because a satisfactory solution for maintaining the proper back pressure with an engine out has not been found. With a common duct, the augmentor discharge area would have to be reduced during an engine out condition and backflow into the failed engine prevented. Knowledge of which engine had failed and controls for the appropriate corrective action are also required. A common-duct system is undesirable also because of possible serious consequences of a single duct rupture, causing possible loss of more than one engine. Present commercial practice is to have independent operation of each engine so that failure of one will not result in loss of another. This is accomplished by complete system separation which starts at the fuel tank and is carried into separate nacelles and exhausts.

D.1.4 Mechanical Flap. - A mechanical flap lift concept engine installation using a 36,700 pound (163,000 N) thrust 1.50 fan pressure ratio, turbofan engine is shown in Figure D-5. The nacelle is shown matched to a wing cross-section corresponding to the 26 percent semi-span cut of a 2950 square foot (274 m²) wing with a 9.0 aspect ratio, 0.3 taper ratio, and 25 degrees of quarter chord sweep.

The mechanical flap engine installation follows identical guidelines to those described for the externally blown flap installation except that:

- o The nacelle is not close coupled to the wing lower surface as in the externally blown flap concept but rather, is located relative to the wing in accordance with attaining the best nacelle/wing drag characteristics for the individual airplane design.
- o Although there is no flap interaction noise on the mechanical flap, a higher noise level is inherently associated with the selected engine cycle which requires the use of acoustic rings in the inlet and fan exhaust duct.
- o Since a fixed pitch fan is used (as opposed to the variable pitch fan for the externally blown flap) the fan duct must be designed to accommodate a thrust reverser.

MECHANICAL FLAP FINAL DESIGN ENGINE INSTALLATION

**RATED THRUST = 36,700 LB SLS
(163,000 N)**

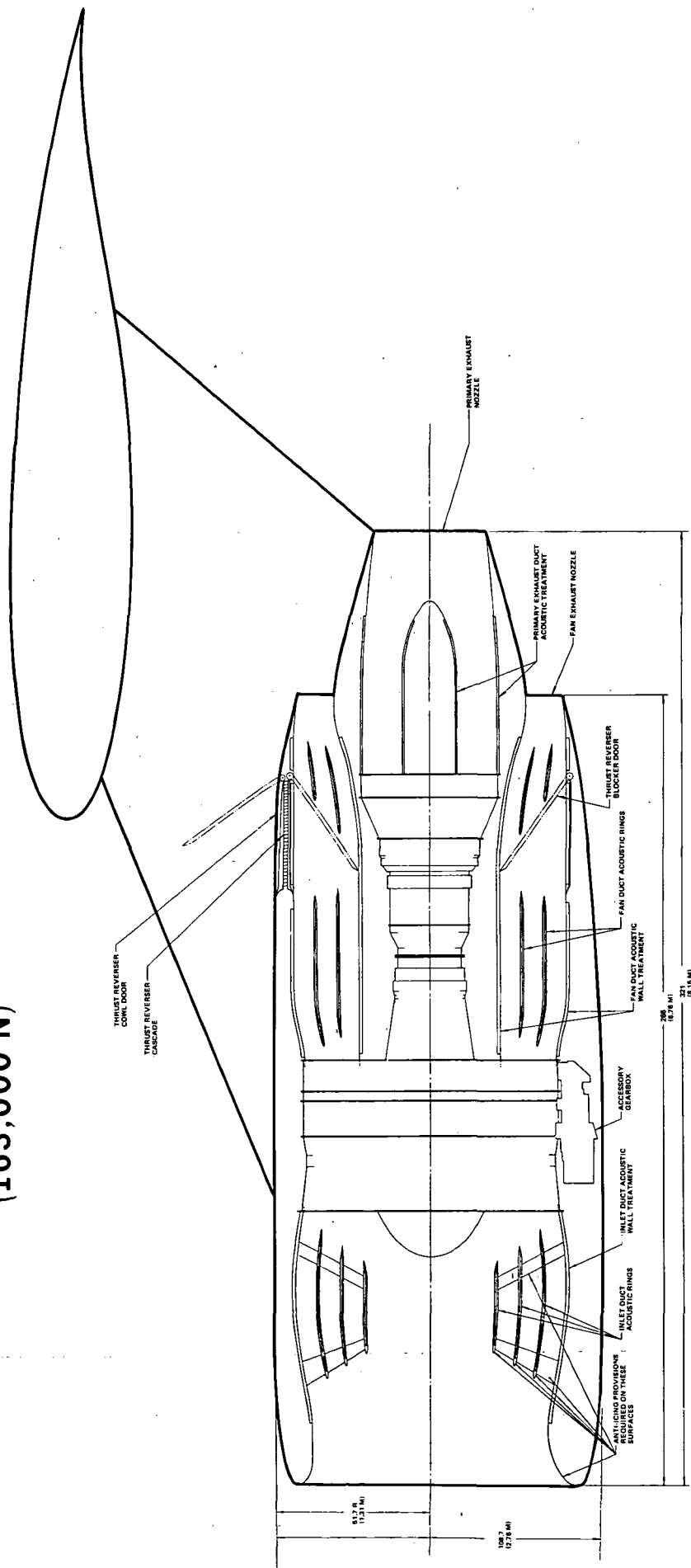


FIGURE D-5

The fan duct thrust reverser shown on Figure D-5 is a fixed cascade type with external cowl doors that are hinged at the aft end and which can thus be used to assist the cascade vanes in imparting a forward directivity to the fan exhaust flow. In response to the requirement for improved low speed capability of minimum re-ingestion and reverser flow ground impingement, upward directivity is imparted to the reversed thrust fan exhaust stream by limiting the cascades and external cowl doors to only the top 200 degree portion of the nacelle circumference. Blocker doors which hinge inward from the outer wall of the fan duct at the cascade trailing edge station are used to close off the forward thrust flow path during reverse thrust.

D.2 Installed Engine Performance (General)

Installed engine performance data were generated by correcting the engine manufacturer's reference engine performance values for the effects of installing the engine on the airplane.

To accomplish this, an existing general thermodynamic cycle matching computer program (SMOTE) was adjusted to match the cycle of each engine considered in the study. The quoted reference performance of each engine was successfully duplicated after a series of iterative adjustments to SMOTE. The installation effects, described below, were then mathematically described and combined with SMOTE to calculate installed propulsion system performance. This program was derived from Reference 40.

The installation effects are:

- o Inlet and exhaust system total pressure loss, including the applicable losses due to acoustic treatment.
- o Exhaust system nozzle performance differences relative to that included in the reference performance.
- o Scrubbing drag on those external surfaces that are washed by the engine exhaust flow.
- o Engine compressor airbleed and mechanical power extraction to supply the airplane accessory system requirements.
- o Fan airbleed to cool the compressor airbleed to acceptable values.
- o Those particular to a specific propulsive lift system.

D.2.1 Inlet Pressure Loss. - The inlet total pressure loss, shown in Table D-2, is calculated as flat-plate skin-friction loss on all surfaces, plus the form drag for the acoustic rings and supporting struts. A friction coefficient, 40 percent higher than that for smooth surfaces, was assumed for all acoustically treated surfaces. The increase in loss at low reciprocal mass flow ratio (takeoff condition) is due to high local velocities near the inlet leading edge at static conditions and low forward speeds. Also shown in the table is the effect of altitude on the inlet pressure loss. The skin friction coefficient increases with increasing altitude (decreasing Reynolds number). The method used to estimate the inlet pressure loss has been correlated with test data obtained from wind tunnel and full-scale boundary layer surveys on the inlets of DC-8, DC-9 and DC-10 aircraft.

D.2.2 Fan Duct and Nozzle Losses. - The exhaust system losses were evaluated using skin friction and form drag calculations for acoustically treated walls, rings and supporting struts in the same manner as for the inlet.

D.2.3 External Aerodynamic Losses. - The drag of the isolated nacelle at the typical cruise condition is included in the installed engine performance. The skin friction coefficient used to calculate drag is a function of the local Reynolds number. Local Reynolds number is calculated for both the freestream cruise condition and the fully expanded exhaust flows for both fan and primary exit conditions. Drag coefficients, D/q , are then calculated for the nacelle and pylon in the three flow regimes; free stream, fan nozzle discharge, and primary nozzle discharge. Depending on the nacelle configuration, the fan cowl and part of the pylon are exposed to free stream flow, while parts of the pylon and engine core cowl are exposed to fan nozzle discharge. Also, parts of the pylon may be exposed to primary nozzle discharge flow.

TABLE D-2 INSTALLATION LOSSES

Config- uration	Engine	Rating	Inlet Loss	Fan Duct	Primary Duct	Nozzle Velocity Coefficient		Drags		
			$\frac{\Delta P_T}{P_T}$	$\frac{\Delta P_T}{P_T}$	$\frac{\Delta P_T}{P_T}$	$C_{V_{Duct}}$	$C_{V_{PRI}}$	$\frac{D}{q_0}$	$\frac{D}{q_{Fan}}$	$\frac{D}{q_{PRI}}$
EBF	PD287-3	Takeoff	.031	.0073	.0072	.978	.977	1.310	.213	.043
		Cruise	.0185	.0084	0.0084	.978	.978	1.310	.213	.043
USB	PD287-22	Takeoff	.029	.0151	.0093	.975	.975	2.309	0.0	.072
		Cruise	.016	.0157	.012	.975	.975	2.309	0.0	.072
M.F.	PD287-23	Takeoff	.072	.03	.006	.978	.977	2.363	.369	.076
		Cruise	.065	.031	.007	.978	.977	2.363	.369	.076
AW	PD287-43	Takeoff	.042	.135	.005	None	.985	3.435	0.0	.0086
		Cruise	.026	.055	.006	.975	.985	1.800	.0343	.0086

Drag coefficients for these three flow regimes are shown in Table D-2.

D.2.4 Airbleed and Mechanical Power Extraction. - Engine compressor air-bleed is used for air conditioning and pressurizing the flight deck and crew compartment. Precoolers located in the pylons use fan bleed to cool the compressor airbleed. Figure D-6 shows the fan bleed requirement. Airbleed requirements are based on 14 CFM ($.0066 \text{ m}^3/\text{s}$) per passenger, where flow density is calculated using the DC-10 maximum cabin pressure schedule and a temperature of 70°F (21°C).

Mechanical power extraction is based on a statistical study of system requirements in several modes of flight. For all configurations, 150 HP (112 kW) per airplane was used for takeoff conditions, while 110 HP (82 kW) per airplane was used for cruise conditions.

D.3 Installed Engine Performance Particular to the Augmentor Wing

The performance of the augmentor ejector flap is based on the results of work accomplished by the Boeing Company under contract to NASA, with adjustments to these results to account for differences between the Boeing and Douglas configurations.

D.3.1 High Lift Configuration. - During high lift operation, gross thrust is calculated at the exit of the wing augmentor ejector flap, at the exit of the aileron blowing nozzles, and at the engine primary nozzle exit. The ram drag of the ejector flap secondary airflow is included in the installed engine performance.

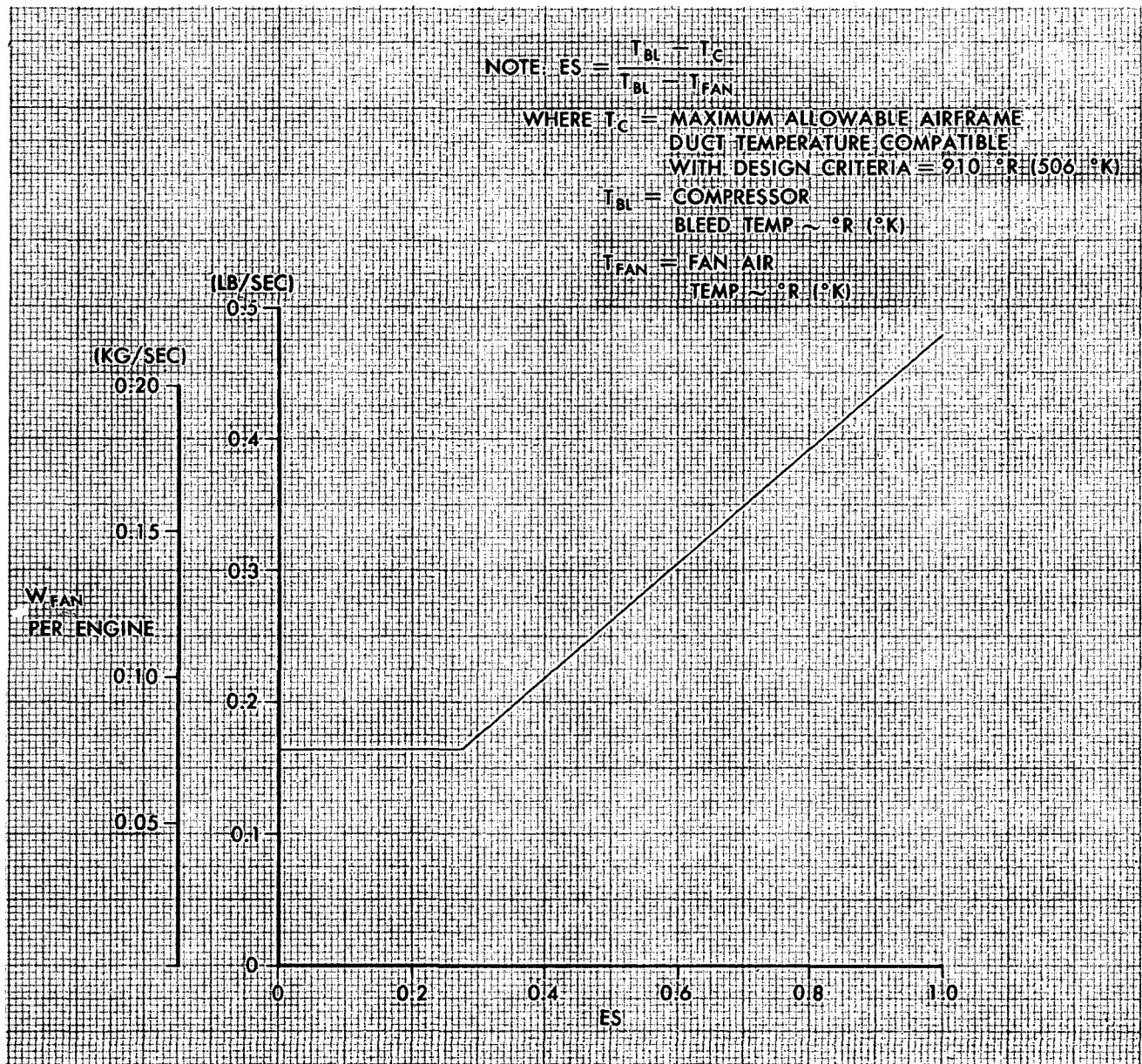


FIGURE D-6. FAN BLEED-HEAT EXCHANGER EFFECTIVITY

The augmentor wing ducting system is designed so that approximately 95 percent of the fan flow is supplied to the augmentor ejector flap primary nozzles. The remaining 5 percent is used for aileron blowing.

The gross thrust generated by the fan air exhausted through the aileron blowing nozzles is included in the thrust performance of the augmentor wing. A momentum recovery coefficient of 0.86 was used for the aileron blowing nozzle. The procedure for calculating the augmentor flap performance is illustrated in Appendix B. Appendix B also presents the ejector flap gross thrust augmentation and flow entrainment ratios for flap angles that are representative of takeoff and approach conditions.

D.3.2 Cruise Configuration. - During cruise operation installed net thrust is defined in the conventional manner by subtracting the ram drag of the engine inlet air flow from the gross thrust of the fan and primary exhaust streams.

D.3.3 Fan Exhaust Losses. - Performance losses due to the fan exhaust system are divided between those losses in the fan duct, from the fan exit to the flow diverter valves, and losses in the fan exhaust nozzle. The total pressure loss in the fan duct to the diverter valve was estimated to be 5.5 percent. Fan nozzle performance is based on a nozzle velocity coefficient of 0.975.

During high lift operation, an additional pressure drop of 9.9 percent was estimated from downstream of the flow diverter valve to the plenum just upstream of the ejector nozzle.

D.3.4 Primary Exhaust System Losses. - The primary exhaust system is a conventional acoustically treated tailpipe and convergent nozzle, except that

the tailpipe has an 18-degree bend so that the nozzle flow will not impinge on the flap during high lift operation.

D.4 Installation Loss Analyses

Tables D-3 and D-4 are summaries of the installation effects on engine performance at takeoff and cruise conditions for the baseline nacelle configurations considered in the study. The losses in each case are referenced to the required uninstalled thrust, F_{n_0} . The uninstalled sea level static takeoff thrust value for the selected engine size is denoted by $F_{n_{REF}}$.

D.5 Installed Propulsion System Performance Data

Installed propulsion system performance data for all significant aircraft operating conditions is shown in Figures D-7 through D-14. Performance for takeoff (maximum power) is presented in terms of gross thrust and ram drag in Figures D-7 through D-10. Installed fuel flow for any condition can be obtained from Figures D-11 through D-14 which show the generalized fuel flow parameter as a function of net thrust and Mach number.

**TABLE D-3
INSTALLATION LOSSES**

Configuration & Engine	Flight Condition	Alt	M ₀	T ₀	F _{N0}	W _{f0}	Loss Summary	Inlet Recovery $\frac{P_{T2}}{P_{T0}}$	Air Conditioning Bleed	Power Extraction	$\frac{\Delta P_{T,DUCT}}{P_T}$	$\frac{\Delta P_{T,PRI}}{P_T}$	C _{V,DUCT}	C _{V,PRI}	Drags				F _{NC} $\frac{\Delta F_N}{F_N}$	W _{fC} $\frac{\Delta W_f}{W_f}$
															D ₀	D _{FAN}	D _{PRI}			
E.B.F. PD287-3 F _{N,REF} = 18,260 lb (81.224 kN)	T.O.	0	.117	95°F (35°C)	14,749 lb (65.606 kN)	4,284 lb/hr (.5398 kg/s)	Amount	.9947	.62 lb/sec (.281 kg/sec)	37.5 HP (28. kW)	.0073	.0072	.978	.977	26 lb (118 N)	99 lb (443 N)	8 lb (36 N)	13,581 lb (60.411 kN)	4,212 lb/hr (.5307 kg/s)	
							$\Delta F_N/F_N$.023	.019	.001	.016	.003	.008	±0.0	.002	.007	0.0	.079	-	
							$\Delta W_f/W_f$.005	.012	±0.0	0.0	0.0	0.0	0.0	0.0	0.0	0.0	-	0.17	
	Cruise	20,000 Ft (6096 m)	.7	STD	4,210 lb (18.727 kN)	2,413 lb/hr (.304 kg/s)	Amount	.996	.62 lb/sec (.281 kg/sec)	27.5 HP (20.5 kW)	.0064	.008	.978	.977	436 lb (1939 N)	120 lb (534 N)	6 lb (27 N)	3,168 lb (14.09 kN)	2,359 lb/hr (.297 kg/s)	
							$\Delta F_N/F_N$.022	.040	-.003	.022	.005	.029	±0.0	.104	.028	.001	.248	-	
							$\Delta W_f/W_f$.004	.016	.002	0.0	0.0	0.0	0.0	0.0	0.0	0.0	-	.022	
U.S.B. PD287-22 F _{N,REF} = 29,490 lb (131.18 kN)	T.O.	0	.117	95°F (35°C)	24,095 lb (107.18 kN)	7,484 lb/hr (.943 kg/s)	Amount	.9974	.62 lb/sec (.413 kg/sec)	37.5 HP (28. kW)	.0151	.0093	.975	.975	47 lb (209 N)	38 lb (169 N)	0.0	22,167 lb (98.60 kN)	7,372 lb/hr (.929 kg/s)	
							$\Delta F_N/F_N$.009	.022	±0.0	.030	.003	.012	.001	.002	.001	0.0	.080	-	
							$\Delta W_f/W_f$.003	.012	±0.0	0.0	0.0	0.0	0.0	0.0	0.0	0.0	-	.015	
	Cruise	20,000 Ft (6096 m)	.7	STD	7,041 lb (31.32 kN)	4,199 lb/hr (.529 kg/s)	Amount	.998	.62 lb/sec (.413 kg/sec)	27.5 HP (20.5 kW)	.0157	.012	.975	.975	770 lb (3425 N)	42 lb (187 N)	0.0	5,295 lb (23.55 kN)	4,094 lb/hr (.516 kg/s)	
							$\Delta F_N/F_N$.011	.048	-.002	.034	.004	.039	.002	.106	.006	0.0	.248	-	
							$\Delta W_f/W_f$.002	.023	±0.0	0.0	0.0	0.0	0.0	0.0	0.0	0.0	-	.025	
M.F. PD287-23 F _{N,REF} = 37,000 lb (164.58 kN)	T.O.	0	.117	95°F (35°C)	31,474 lb (140.0 kN)	11,944 lb/hr (1.505 kg/s)	Amount	.9867	1.24 lb/sec (.562 kg/sec)	37.5 HP (28. kW)	.030	.006	.978	.977	48 lb (213 N)	294 lb (1308 N)	8 lb (35 N)	27,939 lb (124.28 kN)	11,661 lb/hr (1.469 kg/s)	
							$\Delta F_N/F_N$.036	.019	±0.0	.036	.003	.007	.001	.001	.009	0.0	.112	-	
							$\Delta W_f/W_f$.015	.008	±0.0	0.0	0.0	0.0	0.0	0.0	0.0	0.0	-	.024	
	Cruise	20,000 Ft (6096 m)	.7	STD	10,718 lb (47.673 kN)	6,706 lb/hr (.845 kg/s)	Amount	.9853	1.24 lb/sec (.562 kg/sec)	27.5 HP (20.5 kW)	.031	.007	.978	.977	788 lb (3505 N)	266 lb (1183 N)	11 lb (49 N)	7,971 lb (35.46 kN)	6,498 lb/hr (.819 kg/s)	
							$\Delta F_N/F_N$.045	.032	-.001	.055	.005	.019	.002	.073	.025	.001	.256	-	
							$\Delta W_f/W_f$.017	.014	±0.0	0.0	0.0	0.0	0.0	0.0	0.0	0.0	-	.031	

NOTE: 1) Not shown is the effect of pre-cooling fan bleed which is negligible.
2) The uninstalled value for C_{V DUCT} and C_{V PRI} is .985

TABLE D-4
SUMMARY OF ENGINE LOSSES FOR PROPULSIVE
LIFT CONFIGURATIONS

Configuration and Engine	Flight Condition	Alt	M ₀	T ₀	F ₀	W ₀	Loss Summary	Inlet $\frac{\Delta P}{P_0}$ $\frac{q_1}{P_0}$	Bleed A/C	Power Extraction	Fan Duct $\frac{\Delta P}{P_0}$ $\frac{T_1}{T_0}$	Core $\frac{\Delta P}{P_0}$ $\frac{T_1}{T_0}$	C _v Alleron	C _v Fan Duct	C _v Ejector Primary Nozzle	Drags			F ₀ $\frac{\Delta F}{F_0}$ $\frac{F_n}{F_0}$	W _c $\frac{\Delta W}{W_0}$ $\frac{W_f}{W_0}$	Ejector Thrust Augmentation	Ejector Ram Drag	F _{Aug} $\frac{\Delta F}{F_0}$ $\frac{F_n}{F_0}$
																D ₀	D _{fan}	D _{pri}					
F2027-J3 F _{0ref} = 19200 lb (85,406 kN)	Takeoff	0	0.117	95°F (35°C)	17,306 lb (78,591 kN)	10997 lb/hr (1,135 kg/s)	Amount $\frac{\Delta F}{F_0}$ $\frac{\Delta W}{W_0}$	0.042 0.036 0.022	0.62 lb/s (.114 kg/s) 0.010	37.5 HP (28.0 kW) 0.001	0.155 0.020 0.0	0.01 0.004 0.0	0.87 0.006 0.0	None	0.92	68 lb (302 N) 0.004 0.0	0.0 0.0 0.0	21 lb (93 N) 0.001 0.0	14,450 lb (64,277 kN) 0.165	10,250 lb/hr (1,291 kg/s) 0.033	5,515 lb (24,532 kN) -0.3187	3,833 lb (17,050 kN) .2214	15,858 lb (70,540 kN) 0.084
	Cruise	20,000 Ft (6096 m)	0.7	STD	7444 lb (31,778 kN)	6006 lb/hr (1,793 kg/s)	Amount $\frac{\Delta F}{F_0}$ $\frac{\Delta W}{W_0}$	0.026 0.011 0.006	0.62 lb/s (.114 kg/s) 0.011	27.5 HP (20.5 kW) 0.0	0.095 0.025 0.0	0.01 0.005 0.0	None	.975	None	601 lb (2,669 N) 0.004 0.0	6 lb 15 lb (27 N) (67 N) 0.003 0.002 0.0	5,982 lb (26,342 kN) 0.17	5,982 lb/hr (1,746 kg/s) 0.017	0.0 (0.0) 0.0	0.0 (0.0) 0.0	None (0.0) 0.0	

Note:

- 1) Not shown is the effect of precooler fan bleed which is negligible
- 2) The uninstalled value for C_v and C_{v,core} is .985
- 3) There is no installation effect for core engine C_v

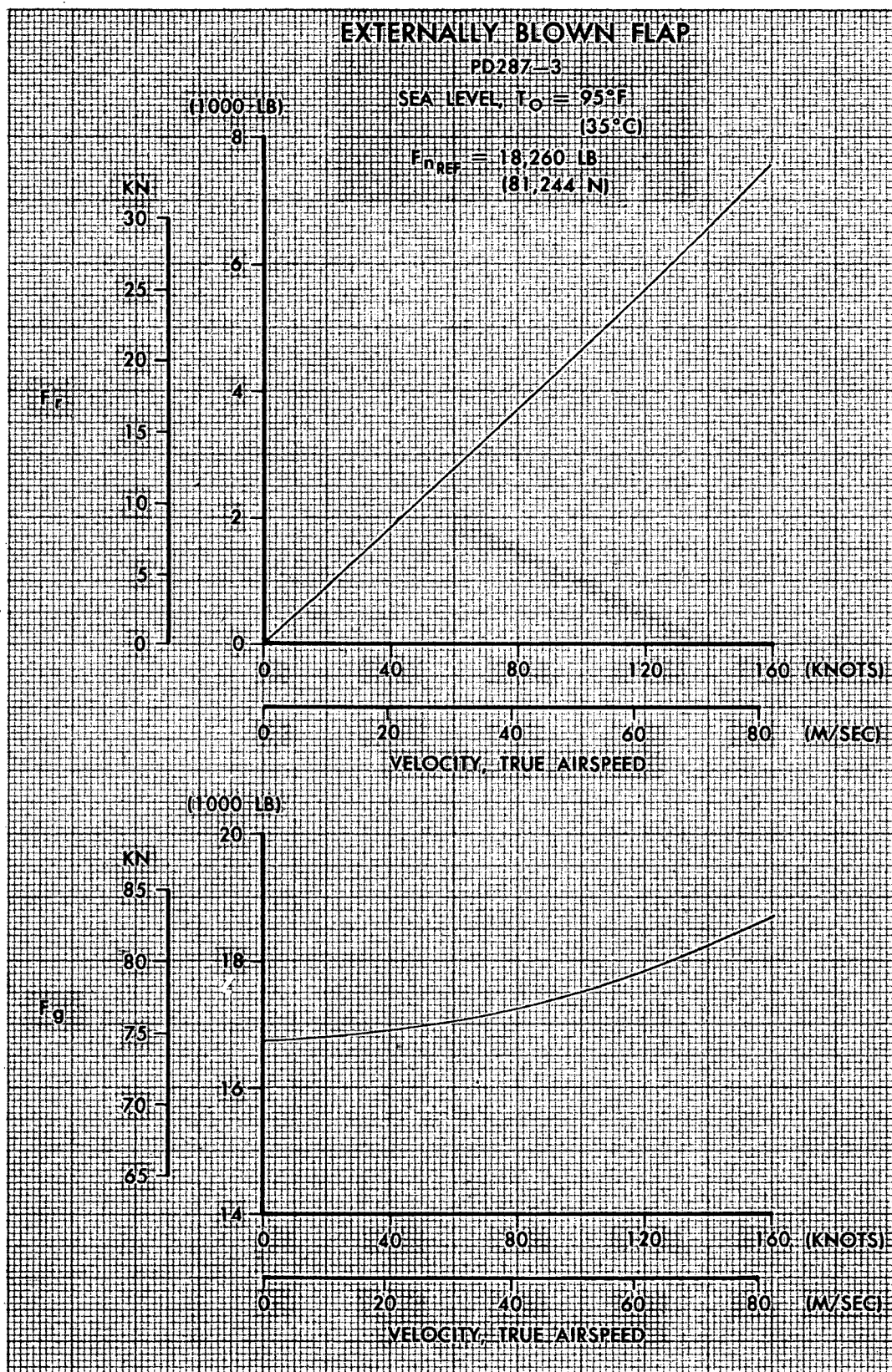


FIGURE D-7. GROSS THRUST AND RAM DRAG AT TAKEOFF POWER

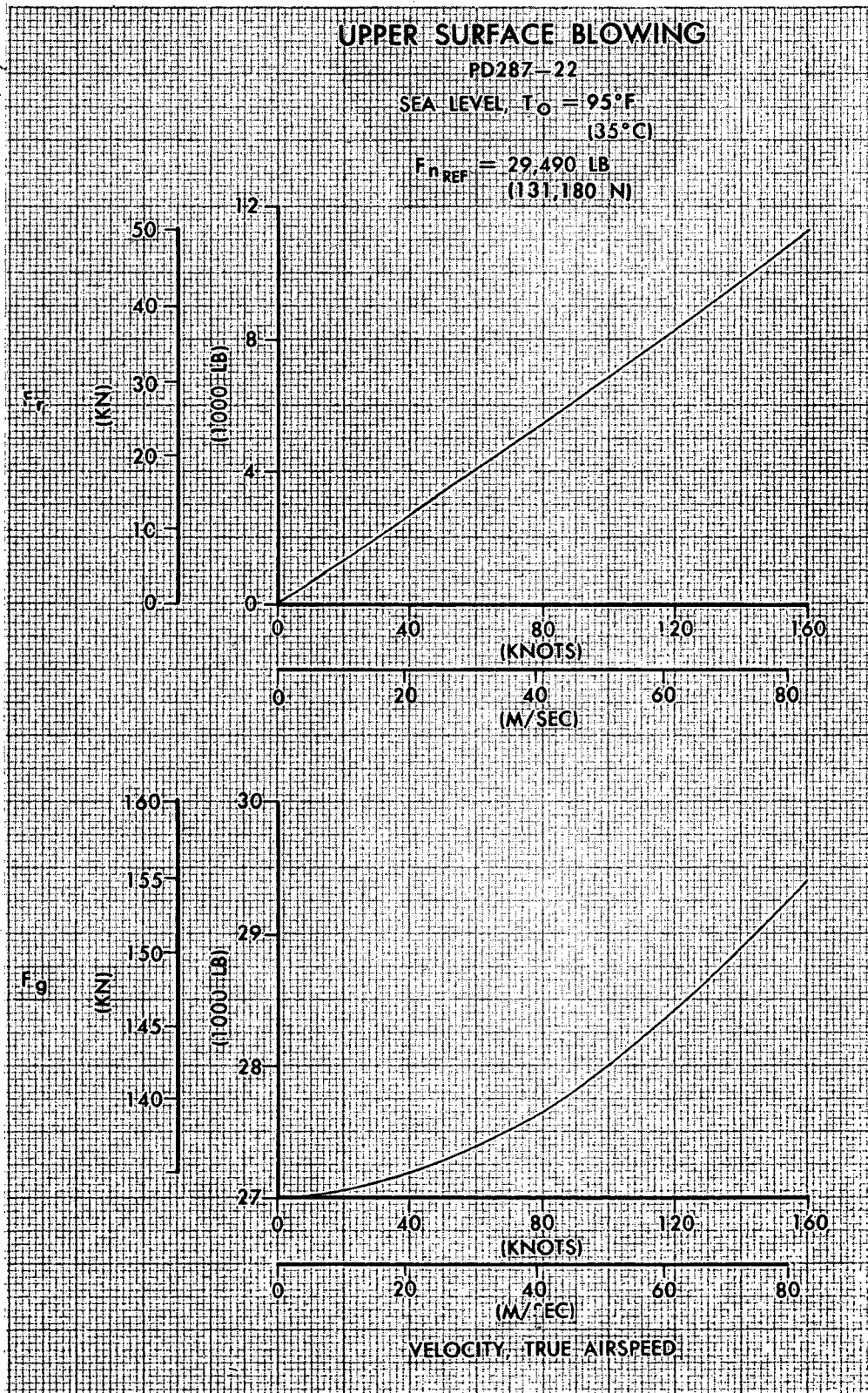


FIGURE D-8. GROSS THRUST AND RAM DRAG AT TAKEOFF POWER

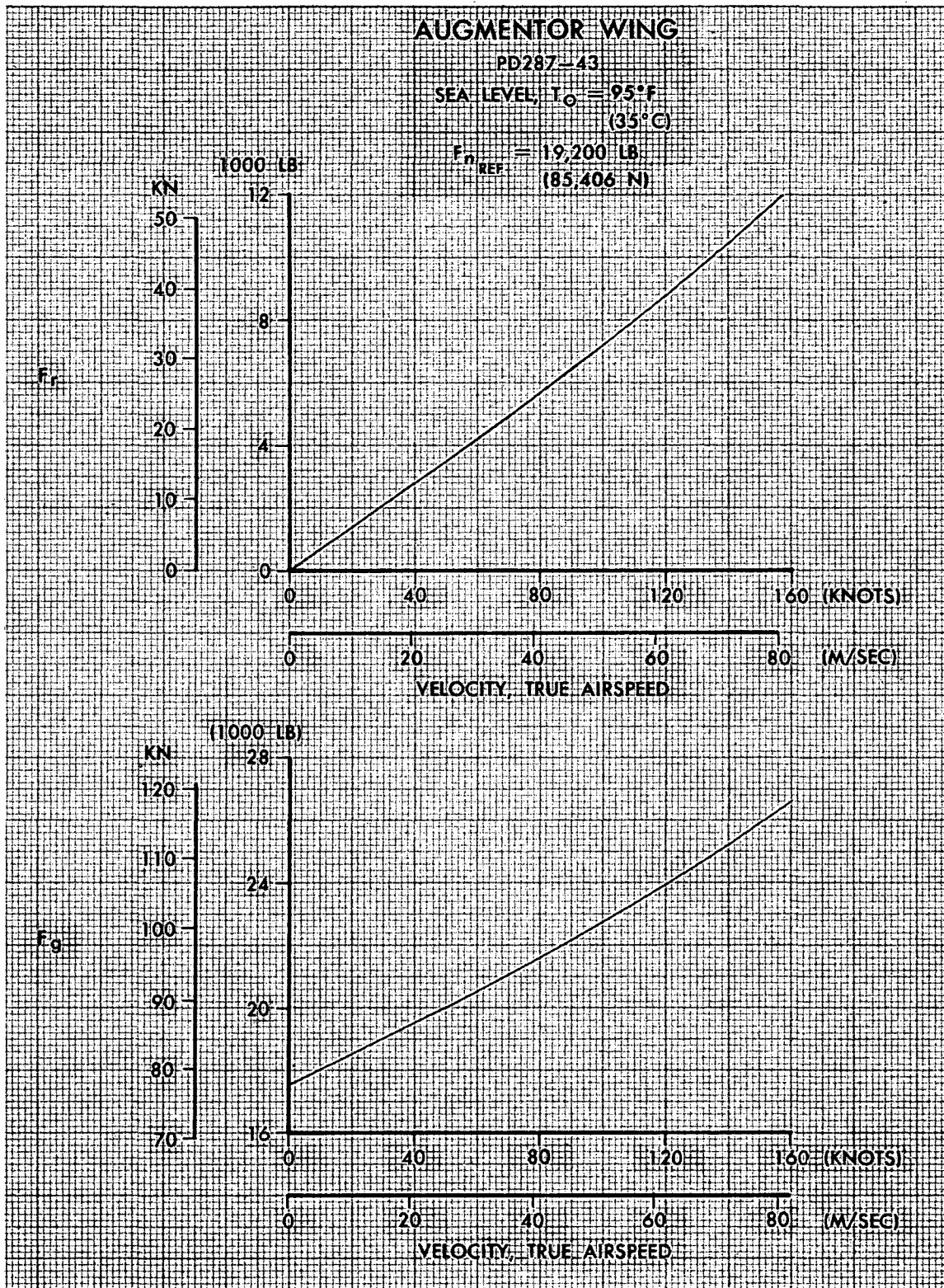


FIGURE D-9. GROSS THRUST AND RAM DRAG AT TAKEOFF POWER

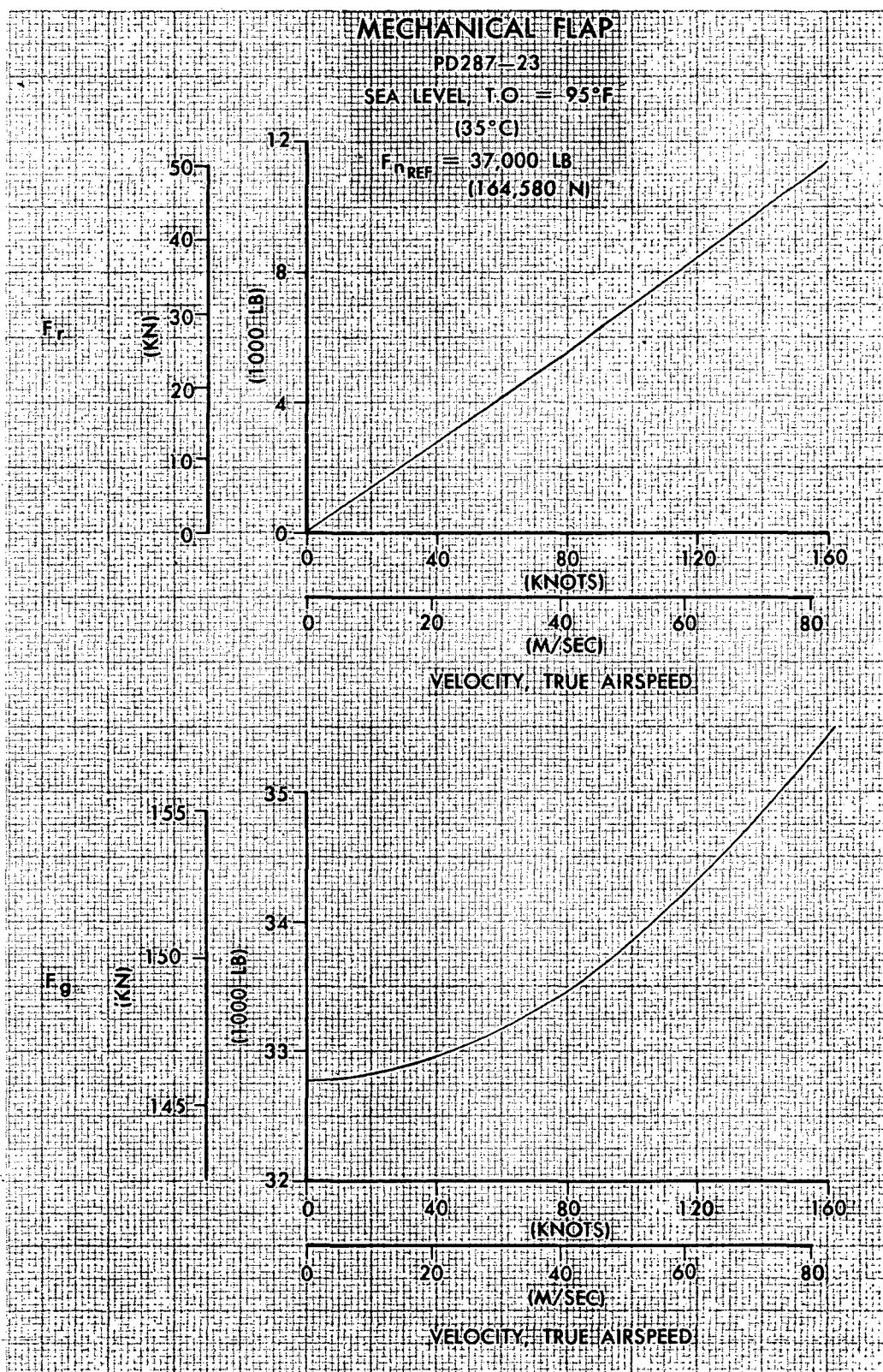


FIGURE D-10. GROSS THRUST AND RAM DRAG AT TAKEOFF POWER.

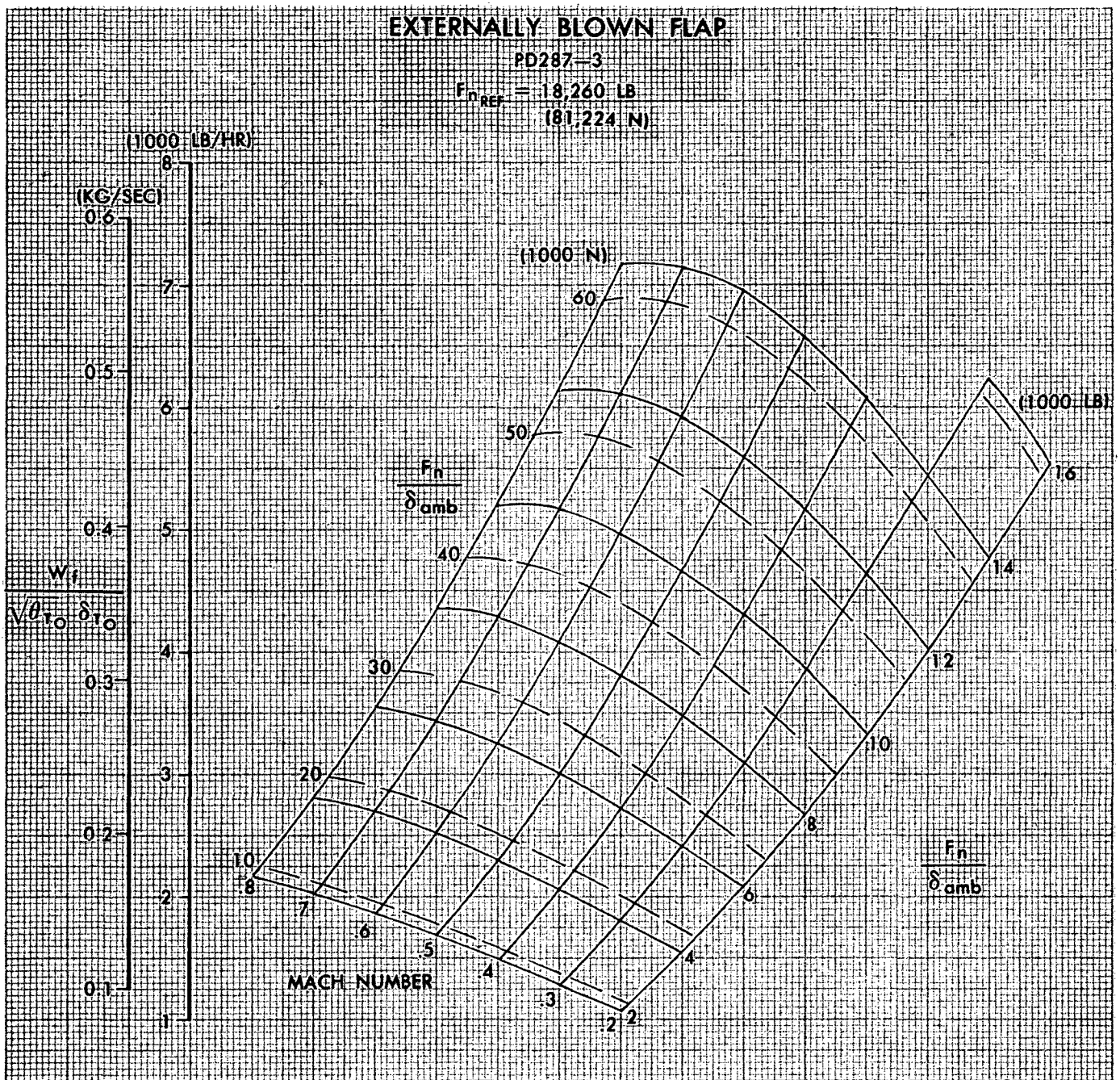


FIGURE D-11. GENERALIZED NET THRUST AND FUEL FLOW

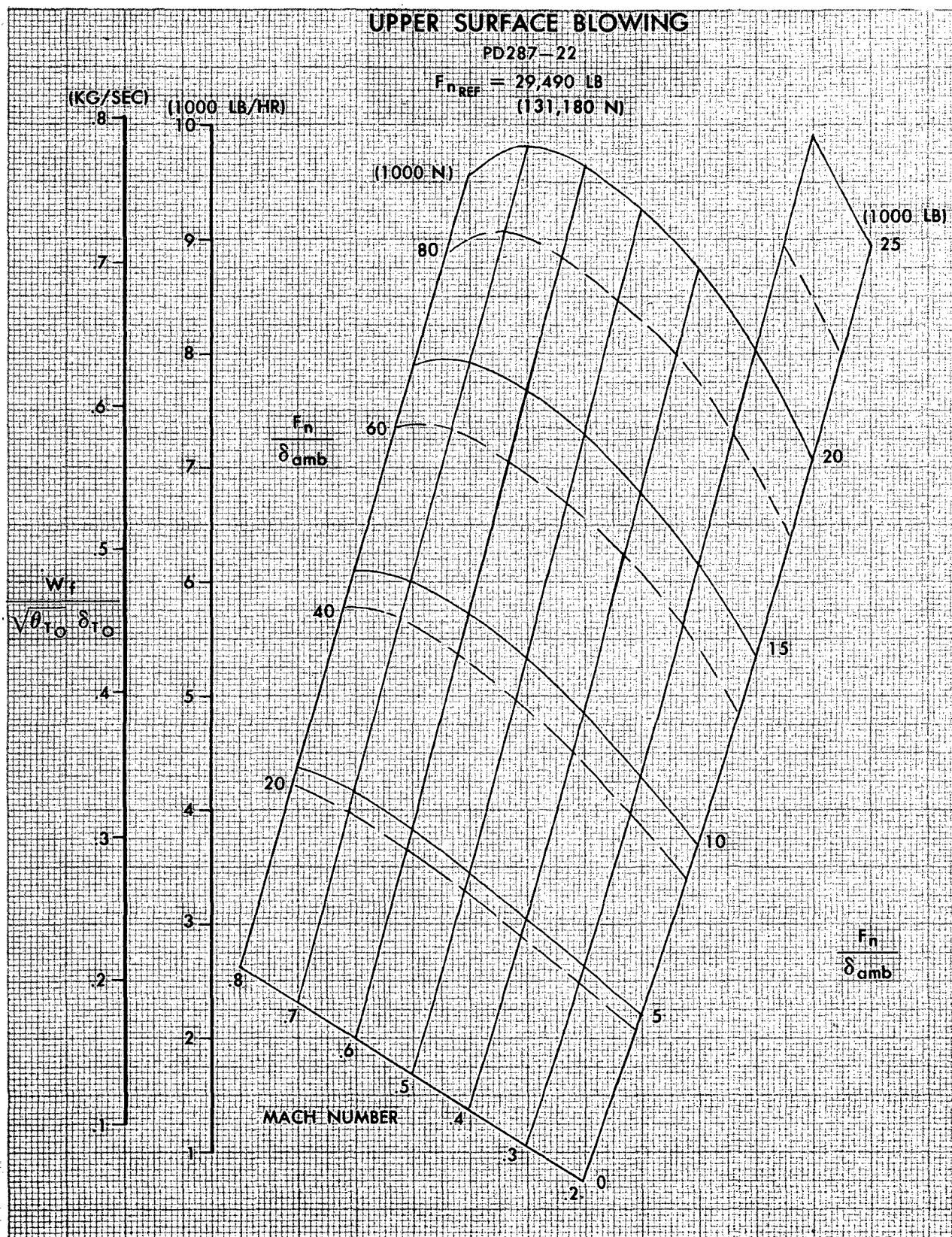


FIGURE D-12. GENERALIZED NET THRUST AND FUEL FLOW

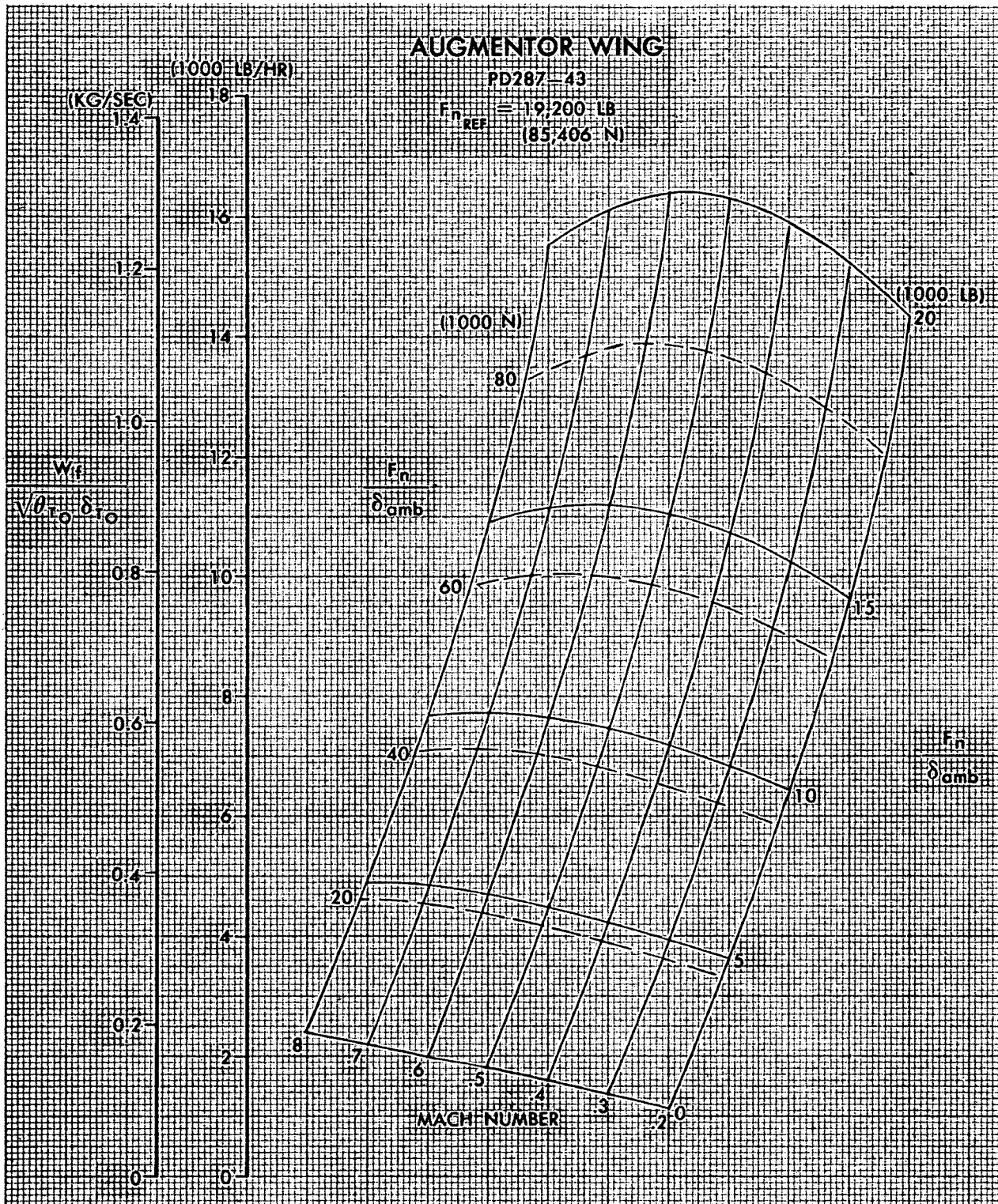


FIGURE D-13. GENERALIZED NET THRUST AND FUEL FLOW

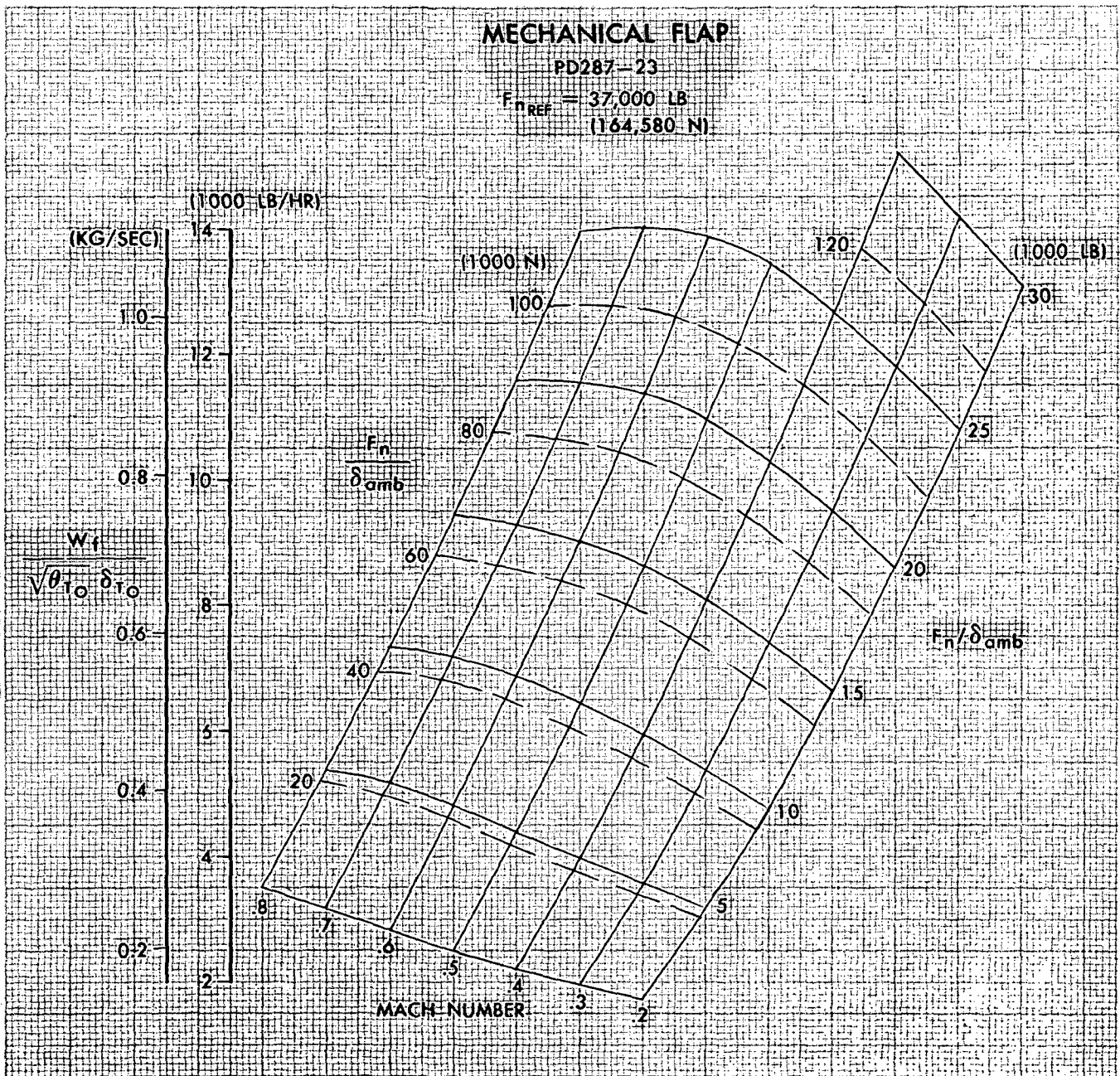


FIGURE D-14. GENERALIZED NET THRUST AND FUEL FLOW

APPENDIX E

MASS PROPERTIES DATA

This appendix presents the results of the detailed mass properties analyses of the eight final design aircraft. These data evolve through a multi-step process described as follows:

1. An initial aircraft functional weight breakdown is derived based on a three-view and preliminary design inputs for each point design. These preliminary design inputs have been developed during the parametric and systems analysis aircraft sizing studies. A preliminary balance check is also made.
2. Factors are derived from these first cycle weights for input into the parametric weight sensitivity program. The resulting matrix of weight values is integrated with the aerodynamic performance sizing program, and aircraft design weights are generated based on mission objectives.
3. The detail weights developed from step 2 are examined based on the degree of deviation from those of step 1. These refined functional group weights represent the final design aircraft.
4. Functional weights are distributed into five major sections (wing, fuselage, H-tail, V-tail, and power plant). This information is used to calculate final balance and moment of inertia values.

The data presented herein represent the final cycle 3 and 4 values and are divided into three sections. Section E.1 consists of the weight,

dimensional and structural data compatible with AN-9103 format. A brief weight substantiation of the final design aircraft, based on trend and comparative data, is given in Section E.2. The balance and moment of inertia data presented in Section E.3 include charts and nomographs to provide mass properties information for any combination of payload and fuel.

E.1 Weights, Dimensional and Structural Data

Table E-1 presents the summary weights for the eight final design aircraft, and Table E-2 contains the corresponding dimensional and structural data. Engine weights are based on those provided by the engine companies. The remaining weights are based on methodology developed from various commercial and military STOL programs (References 41 through 45) and from existing in-house efforts committed to the advancement of transport aircraft weight estimation techniques. Aircraft detail weights are calculated for over 400 components based on 300 inputs consisting of criteria, loads, geometry, and system descriptions. The weight equations utilize parametric relationships isolated during post design analysis of production transport aircraft. The weights for major structural components are derived by multi-station analysis techniques. The resulting accuracy analysis for predicting operational empty weight reflects a 0.8 percent deviation of the mean with a standard deviation of 1.8 percent.

E.2 Weight Substantiation

A brief substantiation example based on first level comparative weight trend curves is presented in this section. Deviations of the STOL vehicle component weights which are considered beyond normal tolerance, are

TABLE E-1
GROUP WEIGHT SUMMARY

HIGH LIFT CONCEPT NUMBER OF PASSENGERS FIELD LENGTH - FT (M) UNITS	EXTERNALLY BLOWN FLAP												AUGMENTOR WING				UPPER SURFACE BLN				MECHANICAL FLAP			
	100				150				200				150				150				150			
	3000	914.4	2000	609.6	914.4	3000	914.4	1500	609.6	914.4	3000	914.4	2000	609.6	914.4	3000	914.4	2000	609.6	914.4	3000	914.4	2000	609.6
	lb	kg	lb	kg	lb	kg	lb	kg	lb	kg	lb	kg	lb	kg	lb	kg	lb	kg	lb	kg	lb	kg	lb	kg
EMPTY WEIGHT SUMMARY:																								
WING GROUP	(12,180)	(5,525)	(33,445)	(15,170)	(18,070)	(8,196)	(11,199)	(24,690)	(11,199)	(33,200)	(15,059)	(41,470)	(18,811)	(37,520)	(17,019)	(22,210)	(10,074)							
BOX STRUCTURE	6,417	2,911	17,242	7,821	9,866	4,475	6,392	14,092	6,392	15,054	6,828	21,568	9,783	19,684	8,929	13,056	5,922							
SECONDARY STRUCTURE	1,393	632	3,310	1,501	1,916	869	1,082	2,386	1,082	5,700	2,585	4,065	1,844	4,017	1,822	2,533	1,149							
AILERONS	235	107	675	306	362	164	173	668	303	668	303	829	376	758	344	416	189							
FLAPS - TRAILING EDGE	2,966	1,345	8,812	3,997	4,266	1,935	2,572	5,670	2,572	8,226	3,731	10,824	4,910	8,746	3,967	3,933	1,784							
- LEADING EDGE	310	141	908	412	450	204	267	588	267	0	0	1,116	506	0	0	0	0							
SLATS	492	223	1,406	638	681	309	394	870	394	2,861	1,298	1,727	784	3,005	1,363	1,649	748							
SPOILERS	367	166	1,092	495	529	240	319	703	319	691	314	1,341	608	1,310	594	623	282							
TAIL GROUP	(2,970)	(1,347)	(11,995)	(5,441)	(4,625)	(2,098)	(6,155)	(2,792)	(12,390)	(5,620)	(14,070)	(6,382)	(8,335)	(3,781)	(3,380)	(1,533)								
STABILIZER - BASIC STRUCTURE	737	334	2,349	1,065	1,247	566	720	2,382	1,081	2,382	1,081	3,006	1,363	3,209	1,456	1,118	507							
FINS - BASIC STRUCTURE	950	431	4,784	2,170	1,415	642	912	2,010	912	5,016	2,275	5,410	2,454	3,209	1,456	1,118	507							
SECONDARY STRUCTURE (STAB. AND FINS)	200	91	637	289	298	135	379	172	647	293	718	326	490	222	217	98	186							
ELEVATORS	442	200	1,386	629	655	297	828	375	1,403	636	1,563	709	931	422	411	186	206							
RUDDER	386	175	2,025	919	628	285	394	869	394	2,116	960	2,455	1,114	1,276	579	453	206							
SLATS - STABILIZER	255	116	814	369	382	173	482	219	826	375	918	416	626	284	277	126								
BODY GROUP	(15,410)	(6,990)	(28,000)	(12,701)	(23,405)	(10,616)	(13,521)	(26,745)	(12,135)	(26,745)	(14,551)	(32,080)	(14,551)	(25,770)	(11,689)	(23,455)	(10,639)							
FUSELAGE - BASIC STRUCTURE	11,279	5,116	21,603	9,799	17,060	7,738	22,405	10,163	20,405	9,255	24,549	11,135	19,360	8,782	17,085	7,749								
SECONDARY STRUCTURE	560	254	519	236	519	236	618	280	519	235	1,356	615	525	238	520	236								
MAIN LANDING GEAR PODS	945	429	1,378	625	1,330	603	1,560	707	1,320	599	1,425	646	1,385	628	1,360	617								
ALSTAIRS	2,626	1,191	4,500	2,041	4,496	2,039	5,227	2,371	4,511	2,046	4,750	2,155	4,500	2,041	4,490	2,037								
DOORS, PANELS & MISC																								
ALIGNING GEAR GROUP	(4,370)	(1,982)	(8,230)	(3,733)	(6,260)	(2,839)	(3,658)	(8,930)	(4,051)	(9,540)	(4,327)	(8,020)	(3,638)	(6,545)	(2,969)									
MAIN GEAR																								
ROLLING ASSEMBLY	997	452	1,873	849	1,425	646	1,835	832	2,030	921	2,170	984	1,825	828	1,490	676								
GEAR STRUCTURE	2,165	982	4,075	1,848	3,102	1,407	3,993	1,811	4,424	2,007	4,722	2,142	3,971	1,801	3,242	1,471								
CONTROLS	313	142	592	269	453	205	582	264	646	293	688	312	579	263	473	214								
TOTAL MAIN GEAR	3,475	1,576	6,540	2,966	4,980	2,258	6,410	2,907	7,100	3,221	7,580	3,438	6,375	2,892	5,205	2,361								
NOSE GEAR																								
ROLLING ASSEMBLY	163	74	327	139	235	107	300	136	330	150	355	161	300	136	245	111								
GEAR STRUCTURE	553	251	1,046	475	789	358	1,023	464	1,134	514	1,212	550	1,017	461	828	376								
CONTROLS	179	81	337	153	256	116	332	151	366	166	393	178	328	149	267	121								
TOTAL NOSE GEAR	895	406	1,690	767	1,280	581	1,655	751	1,830	889	1,960	889	1,645	746	1,340	608								
SURFACE CONTROLS GROUP	(2,735)	(1,240)	(6,590)	(2,989)	(3,500)	(1,588)	(4,460)	(2,023)	(9,025)	(4,094)	(7,695)	(3,490)	(6,875)	(3,118)	(3,670)	(1,665)								
COCKPIT CONTROLS	85	39	85	39	85	39	85	39	85	39	85	39	85	39	85	39								
AUTOMATIC PILOT	230	104	240	109	240	109	250	113	240	109	240	109	240	109	240	109								
SYSTEM CONTROLS	2,420	1,097	6,265	2,841	3,175	1,440	4,125	1,871	8,700*	3,946*	7,370*	3,342	6,550	2,970	3,345	1,517								

*Includes 3,180 lb (1,442 kg) of augmentor ducting located in the wing.

TABLE E-1 (CONT)
GROUP WEIGHT SUMMARY

HIGH LIFT CONCEPT NUMBER OF PASSENGERS FIELD LENGTH - FT (M) UNITS	EXTERNALLY BLOWN FLAP										AUGMENTOR WING					UPPER SURFACE BLN					MECHANICAL FLAP															
	100					150					200					150					150															
	3000	914.4	lb	kg	lb	3000	914.4	lb	kg	lb	3000	914.4	lb	kg	lb	3000	914.4	lb	kg	lb	3000	914.4	lb	kg	lb	3000	914.4	lb	kg	lb	3000	914.4	lb	kg	lb	
ENGINE SECTION OR NACELLE GROUP	(5,000)	(2,268)			(10,020)	(4,545)	(7,090)	(3,216)			(8,900)	(4,037)	(7,690)	(3,488)							(14,390)	(6,527)	(8,400)	(3,810)	(7,370)	(3,343)										
INBOARD	2,500	1,134			5,010	2,272	3,545	1,608			4,450	2,018	3,845	1,744							7,195	3,263	6,590	2,989	5,782	2,623										
OUTBOARD	2,500	1,134			5,010	2,273	3,545	1,608			4,450	2,019	3,845	1,744							7,195	3,264	6,590	2,989	5,782	2,623										
SOUND SUPPRESSION RINGS	0	0			0	0	0	0			0	0	0	0							0	0	1,810	821	1,588	720										
PROPULSION GROUP	(9,170)	(4,159)			(17,505)	(7,940)	(12,380)	(5,616)			(15,480)	(7,022)	(23,040)	(10,451)							(23,730)	(10,764)	(15,780)	(7,157)	(13,390)	(6,074)										
ENGINE INSTALLATION	7,960	3,611			15,280	6,931	10,795	4,897			13,580	6,160	13,920	6,314							16,720	7,584	12,100	5,488	10,300	4,672										
EXHAUST SYSTEM	255	116			515	233	360	163			454	206	4,550*	2,064*							618	280	440	200	385	175										
COOLING SYSTEM	64	29			129	58	91	41			114	52	112	51							124	56	84	38	73	33										
FUEL SYSTEM	640	290			1,080	490	779	353			892	404	1,075	487							1,190	540	1,120	508	845	383										
ENGINE CONTROLS	60	27			65	30	65	30			70	32	65	30							65	30	50	23	50	23										
STARTING SYSTEM	191	86			436	198	290	132			370	168	378	171							421	191	271	123	237	108										
THRUST REVERSER	0	0			0	0	0	0			0	0	2,940	4,592							(950)	(431)	(950)	(431)	(950)	(431)										
AUXILIARY POWER PLANT GROUP	(775)	(352)			(950)	(431)	(950)	(431)			(1,120)	(508)	(950)	(431)							(950)	(431)	(950)	(431)	(950)	(431)										
INSTRUMENTS & NAVIGATIONAL EQUIP GROUP	(1,170)	(531)			(1,175)	(533)	(1,175)	(533)			(1,180)	(535)	(1,175)	(533)							(1,175)	(533)	(1,175)	(533)	(1,175)	(533)										
HYDRAULIC & PNEUMATIC GROUP	(1,775)	(805)			(3,565)	(1,617)	(2,285)	(1,036)			(2,870)	(1,302)	(3,130)	(1,420)							(4,010)	(1,819)	(3,250)	(1,474)	(2,090)	(948)										
HYDRAULIC SYSTEM	1,010	458			2,440	1,107	1,278	580			1,620	735	2,040	925							2,853	1,294	2,475	1,123	1,340	608										
PNEUMATIC SYSTEM	765	347			1,125	510	1,007	456			1,250	567	1,090	495							1,157	525	775	351	750	340										
ELECTRICAL GROUP	(2,230)	(1,012)			(2,590)	(1,175)	(2,590)	(1,175)			(3,150)	(1,425)	(2,590)	(1,175)							(2,590)	(1,175)	(2,540)	(1,152)	(2,540)	(1,152)										
ELECTRONICS GROUP	(1,690)	(767)			(1,760)	(798)	(1,760)	(798)			(1,910)	(866)	(1,760)	(798)							(1,760)	(798)	(1,760)	(798)	(1,760)	(798)										
EQUIPMENT	1,074	487			1,074	487	1,074	487			1,074	487	1,074	487							1,074	487	1,074	487	1,074	487										
INSTALLATION	616	280			686	311	686	311			836	379	686	311							686	311	686	311	686	311										
FURNISHINGS GROUP	(9,205)	(4,175)			(13,690)	(6,210)	(13,690)	(6,210)			(17,740)	(8,047)	(13,690)	(6,210)							(13,690)	(6,210)	(13,690)	(6,210)	(13,690)	(6,210)										
ACRCONDITIONING & ANTI-ICING EQUIP GRP	(1,460)	(662)			(2,165)	(982)	(1,960)	(889)			(2,310)	(1,048)	(2,160)	(980)							(2,240)	(1,016)	(2,195)	(996)	(2,005)	(909)										
ACRCONDITIONING	1,020	463			1,430	649	1,430	649			1,700	771	1,430	649							1,430	649	1,430	649	1,430	648										
ANTI-ICING	440	199			735	333	530	240			610	277	730	331							810	367	765	347	575	261										
AUXILIARY GEAR GROUP	(30)	(14)			(35)	(16)	(30)	(14)			(40)	(18)	(45)	(20)							(40)	(18)	(30)	(14)	(30)	(14)										
MANUFACTURER'S EMPTY WEIGHT	70,170	31,829			141,715	64,281	99,770	45,255			127,880	58,005	146,530	66,465							169,430	76,852	136,290	61,820	104,260	47,292										
OPERATIONAL ITEMS	(1,990)	(902)			(2,975)	(1,349)	(2,840)	(1,288)			(3,470)	(1,574)	(2,970)	(1,347)							(3,020)	(1,370)	(2,990)	(1,356)	(2,870)	(1,301)										
PILOT & CO PILOT @ 170# ea (77.1 kg ea)	340	154			340	154	340	154			340	154	340	154							340	154	340	154	340	154										
CABIN ATTENDANTS @ 130# ea (59.0 kg ea)	260	118			520	236	520	236			520	236	520	236							520	236	520	236	520	236										
CREW LUGGAGE & BRIEFCASES	130	59			170	77	170	77			170	77	170	77							170	77	170	77	170	77										
PASSENGER SERVICE ITEMS																																				
FOOD, BEVERAGE, & GALLEY EQUIPMENT	154	70			231	105	231	105			231	105	231	105							231	105	231	105	231	105										
CABIN SUPPLIES & LAVATORY SUPPLIES	301	136			439	199	439	199			588	267	439	199							439	199	439	199	439	199										
POTABLE WATER	250	113			375	170	375	170			500	227	375	170							375	170	375	170	375	170										
ENGINE OIL	145	66			235	106	195	89			245	111	205	93							255	116	195	89	175	79										
EVACUATION SLIDES	125	57			225	102	225	102			330	150	225	102							225	102	225	102	225	102										
UNUSABLE FUEL	285	129			440	200	345	156			400	181	465	211							465	211	495	224	395	179										

*Includes 4,170 lb (1,892 kg) of augmentor ducting and valves located in the engine pylon.

*Includes 4,170 lb (1,892 kg) of augmentor ducting and valves located in the engine pylon.

TABLE E-1 (CONT)

*Payload @ 200 lb/pax (90.7 kg/pax)
 **JP-4 @ 6.7 lb/gal (802.9 kg/m³)

TABLE E-2

HIGH LIFT CONCEPT	EXTERNALLY BLOWN FLAP										AUGMENTOR WING				UPPER SURFACE BLN				MECHANICAL FLAP												
											200				150				150												
											914.4				609.6				609.6												
											3000				2000				2000												
NUMBER OF PASSENGERS	.69	926	575	926	575	926	575	926	575	926	.69	926	575	926	575	926	.78	575	926	575	926	.76	575	926	575	926	.70	575	926	575	926
FIELD LENGTH - FT (m)	575	926	575	926	575	926	575	926	575	926	575	926	575	926	575	926	575	926	575	926	575	926	575	926	575	926	575	926	575	926	
DESIGN CRUISE MACH NO.																															
MISSION RANGE - S-MILES (km)																															
CONFIGURATION DATA																															
WING LOADING - LBS/FT ² (kg/m ²)	105	513	70.0	342	102	498	100	488	388	77.5	327	63.5	310	91	445																
ENGINE DESIGNATION	PD287-3	PD287-3	PD287-3	PD287-3	PD287-3	PD287-3	PD287-3	PD287-3	PD287-3	PD287-3	PD287-3	PD287-3	PD287-3	PD287-3	PD287-3																
SLS THRUST (UNINST)/TOGM	-508	-508	.527	.527	.490	.490	.478	.478	.361	.361	.519	.387	.387	.417	.417																
SLS THRUST (UNINST)/ENG - LB (N)	13,200	59,716	25,830	114,898	18,250	81,180	22,925	101,975	19,200	85,406	29,490	36,198	164,540	32,450	144,345																
NO. OF ACOUSTIC RINGS (INLET/EXH)	0	0	0	0	0	0	0	0	0	0	0	0	0	0	0																
NO. OF WING MID ENG/AIRPL	4	4	4	4	4	4	4	4	4	4	4	4	4	4	4																
MISSION FUEL WEIGHT/TOTGM	.1147	.1147	.1087	.1087	.1100	.1100	.1076	.1076	.1557	.1557	.1085	.1137	.1137	.1198	.1198																
DIMENSIONAL DATA																															
WING:																															
AREA - FT ² (m ²)	391	92.11	2,800	260.1	1,461	135.7	1,920	178.4	2,743	254.8	3,390	314.9	3,007	279.4	1,708																
MAC LENGTH - IN (cm)	146.5	372.1	246.2	625.3	177.8	451.6	203.7	517.4	268.8	682.8	270.9	688.1	240.6	611.1	181.3																
SPAN LENGTH - FT (m)	89.0	27.1	149.7	45.63	108.1	32.94	124.0	37.80	133.8	40.78	164.7	50.20	164.5	50.14	124.0																
ASPECT RATIO	8.0	8.0	8.0	8.0	8.0	8.0	8.0	8.0	6.5	6.5	8.0	8.0	9.0	9.0	9.0																
TAPER RATIO	.3	.3	.3	.3	.3	.3	.3	.3	.3	.3	.3	.3	.3	.3	.3																
SWEEP BACK AT 25% CHORD - DEGREE	25.0	25.0	25.0	25.0	25.0	25.0	25.0	25.0	25.0	25.0	25.0	25.0	25.0	25.0	25.0																
THEO ROOT CHORD LENGTH - IN (cm)	205.5	522.0	345.4	877.3	249.5	633.7	285.6	725.4	378.5	961.4	380.0	965.2	337.5	857.3	254.3																
THEO ROOT CHORD MAX t - IN (cm)	34.2	86.9	57.5	146	41.5	105	47.6	121	63.0	160	63.3	161	60.0	152	44.0																
THICKNESS BREAK CHORD LENGTH - IN (cm)	155.2	394.2	260.8	662.4	188.4	478.5	215.6	547.6	285.8	725.9	286.9	728.7	251	638	191.5																
THICKNESS BREAK CHORD MAX t - IN (cm)	21.5	54.6	36.1	91.7	26.1	66.3	29.9	75.9	39.6	101	39.7	101	34.8	88.4	26.5																
THEO TIP CHORD LENGTH - IN (cm)	61.6	157	103.6	263.1	74.8	190	85.7	218	113.5	288.3	114.0	289.6	101.2	257.0	76.3																
THEO TIP CHORD MAX t - IN (cm)	7.4	19	12.4	31.5	9.0	23	10.3	26.2	13.6	34.5	13.7	34.8	12.1	30.7	9.2																
LOC OF T/C BREAK - FRACTION OF b/2	.35	.35	.35	.35	.35	.35	.35	.35	.35	.35	.35	.35	.35	.35	.35																
AREAS: FT ² (m ²)																															
AILERONS (AFT OF HINGE LINE)	42	3.9	120	11.1	65	6.0	68	6.3	119	11.1	148	13.8	135	12.5	74																
LEADING EDGE FLAP	56	5.2	164	15.2	81	7.5	106	9.9	0	0	201	18.7	0	0	0																
TRAILING EDGE FLAP	232	21.6	688	63.9	333	30.9	443	41.2	505	46.9	846	78.6	875	81.3	393																
SLAT	62	5.8	178	16.5	86	8.0	110	10.2	362	33.6	219	20.3	380	35.3	209																
SPOILER	99	9.2	295	27.4	143	13.3	190	17.7	187	17.4	362	33.6	354	32.9	168																
HORIZONTAL TAIL																															
AREA - FT ² (m ²)	280	26.0	893	82.9	419	38.9	532	49.4	907	84.3	1,007	93.55	687	63.8	302																
MAC - LENGTH - IN (cm)	94.1	239	168.1	427.0	115.1	292.4	129.7	329.4	169.4	430.3	178.5	453.4	147.4	374.4	97.7																
SPAN - LENGTH - FT (m)	37.4	11.4	66.8	20.4	45.8	13.9	51.6	15.7	67.3	20.5	71.0	21.6	58.6	17.9	38.9																
ASPECT RATIO	5.0	5.0	5.0	5.0	5.0	5.0	5.0	5.0	5.0	5.0	5.0	5.0	5.0	5.0	5.0																
TAPER RATIO	.45	.45	.45	.45	.45	.45	.45	.45	.45	.45	.45	.45	.45	.45	.45																
SWEEP BACK AT 25% CHORD - DEGREE	25.0	25.0	25.0	25.0	25.0	25.0	25.0	25.0	25.0	25.0	25.0	25.0	25.0	25.0	25.0																
THEO ROOT CHORD LENGTH - IN (cm)	123.9	314.7	221.2	561.8	151.5	384.8	171	433.6	222.9	566.2	234.9	596.6	194.0	492.8	128.6																
THEO ROOT CHORD MAX t - IN (cm)	12.4	31.5	22.1	56.1	15.2	38.6	17.1	43.4	22.2	56.4	23.5	59.7	19.4	49.3	12.9																
THEO TIP CHORD LENGTH - IN (cm)	55.7	141	99.5	253	68.2	173	76.8	195	100.3	254.8	105.7	268.5	87.3	222	57.9																
THEO TIP CHORD MAX t - IN (cm)	5.6	14	10.0	25.4	6.8	17	7.7	20	10.0	25.4	10.6	26.9	8.7	22	5.8																
HORIZ TAIL ARM - IN (cm)	740	1,880	920	2,337	885	2,248	977	2,482	905	2,299	958	2,433	830	2,108	875																
HORIZ TAIL VOLUME	1,427	1,427	1,192	1,192	1,426	1,426	1,329	1,329	1,113	1,113	1,050	1,050	788	860	860																

TABLE E-2 (CONT)

[illegible]

*To Theoretical Loft Lines - No Cutouts, No Pods

further evaluated by considering second level parameter effects. The aircraft used in this example is the 150 passenger, 3000 foot (914 m) field length externally blown flap final design aircraft (Table E-1, Column 5). The statistical relationships given by these first level trend curves were not used to derive the final design weights but are presented only to show the STOL mass values relative to current production transports. If these first level trend curves were used to derive the weight, an 8.4 percent reduction in M.E.W. would result. A further M.E.W. reduction of 5.2 percent would result if the vehicle was resized based on constant mission performance.

E.2.1 Wing Structure. - Figure E-1 presents a correlation of wing box structure weight with a primary bending material index. The structural box includes all primary load carrying structure and associated splices, fasteners, bulkheads, and fuselage attach. The correlation of total STOL wing weight, Figure E-2, reflects the greater control surface (aileron, flap, leading edge flap, leading edge slat, and spoiler) requirements for this type of aircraft. These surfaces are 50 percent of the STOL wing area compared to only 36 percent of the DC-10 or DC-9 wing areas. The weight of the STOL control surfaces and secondary structure, 8,204 pounds (3,721 kg), is 5.6 pounds per square foot (27 kg/m^2) of wing area. This compares to only 4.4 pounds per square foot (22 kg/m^2) for the DC-10.

E.2.2 Tail Structure. - Figure E-3 presents a correlation of tail structure weight versus tail area. The unit weights for T-tail configurations are higher than for those with fuselage mounted horizontal surfaces, but usually T-tail arrangements require less total tail area. Note that the STOL tail weight includes 382 pounds (173 kg) for the addition of leading edge slats

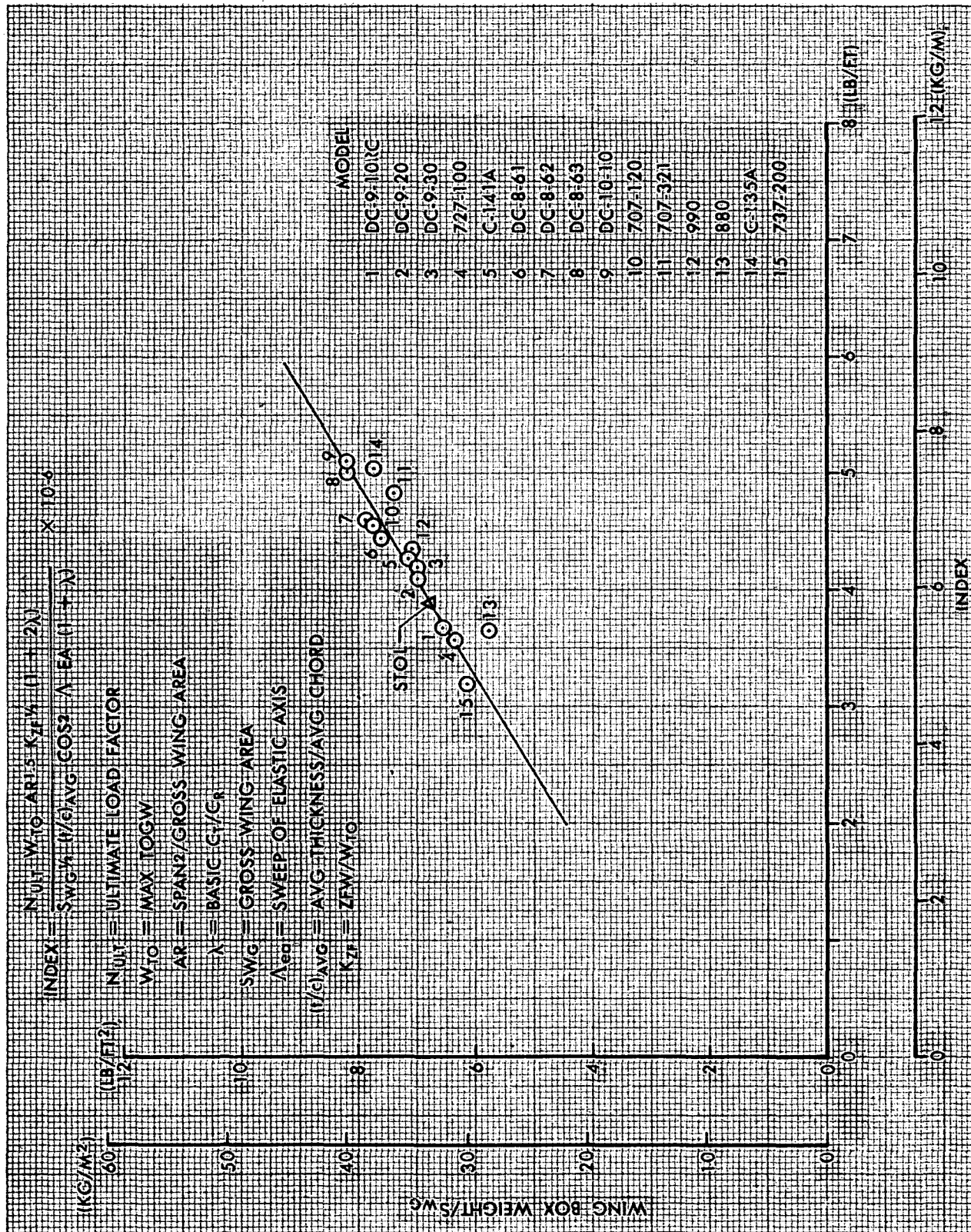


FIGURE E-1. WEIGHT TREND—WING BOX

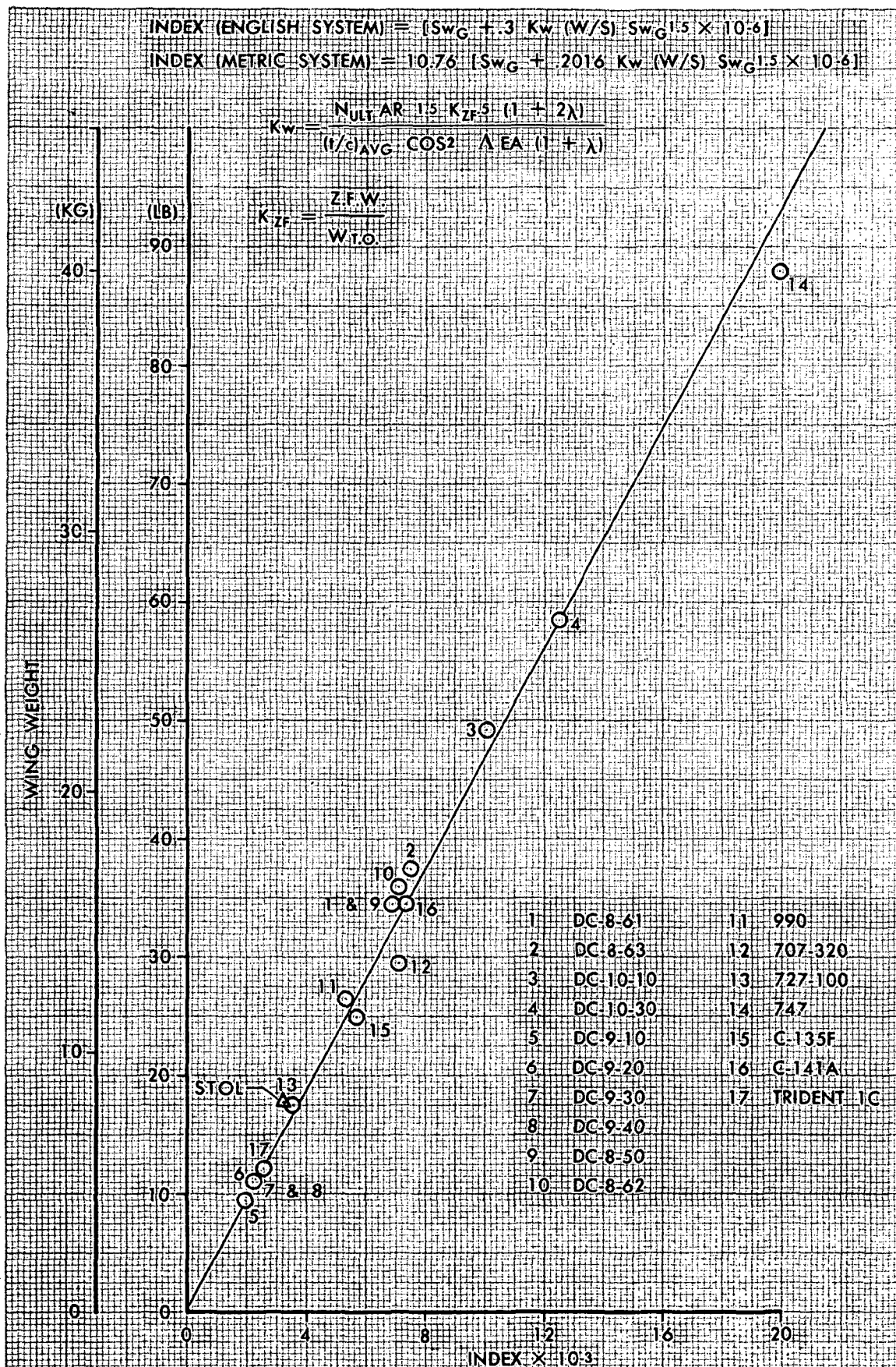


FIGURE E-2. WEIGHT TREND—WING GROUP

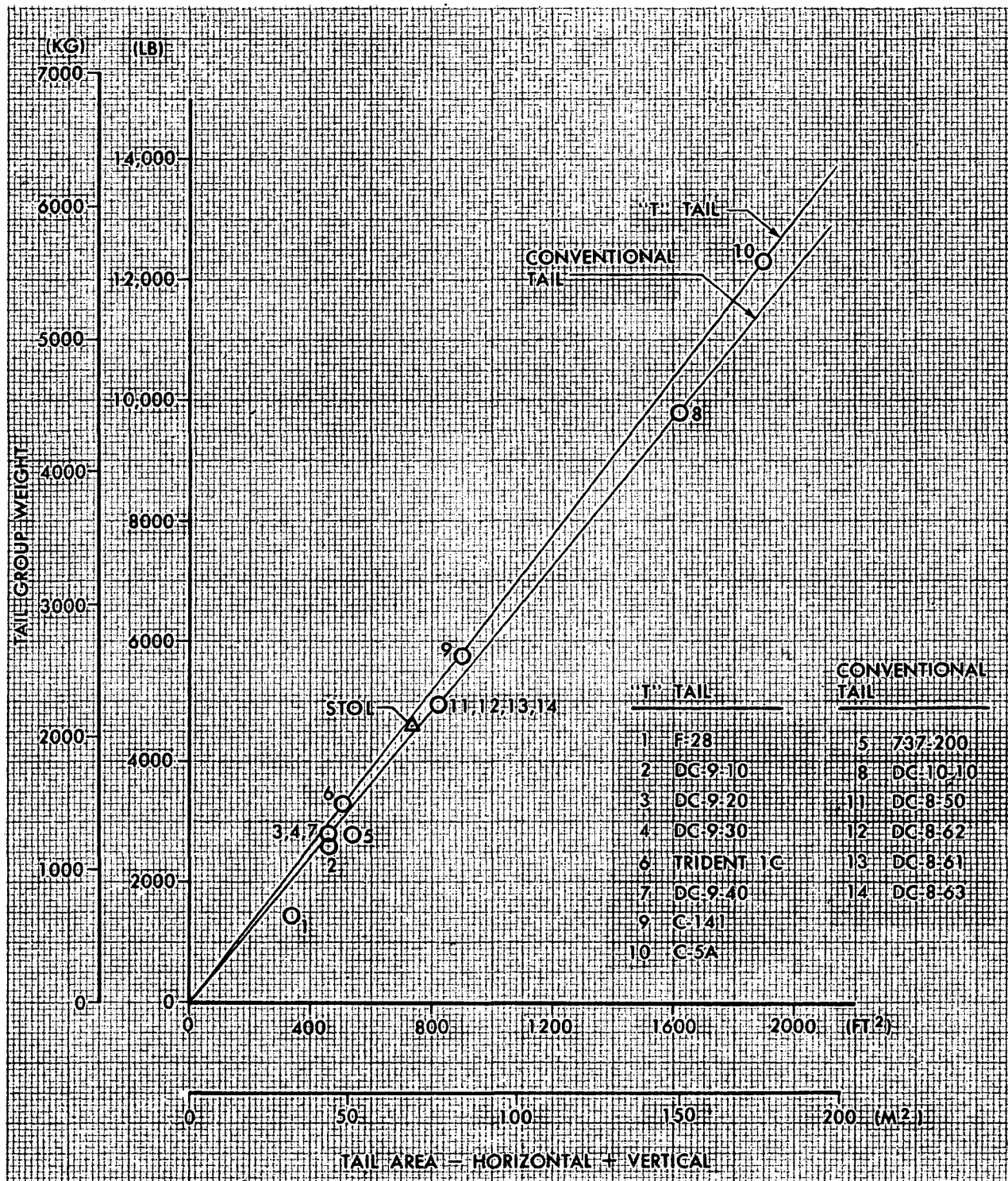


FIGURE E-3. WEIGHT TREND—TAIL GROUP

to the horizontal tail, but this increment is offset by a reduction in the required horizontal tail area.

E.2.3 Fuselage Structure. - Figure E-4 presents a correlation of fuselage structure weight with number of passengers. Passenger count is based on an all-coach configuration with a seat pitch of 34 inches (86 cm). The STOL point falls above the line reflecting a weight penalty for features unique to STOL. This penalty is explained in Table E-3 and includes the effect of a higher STOL wetted area per passenger due to the double aisle seating arrangement. Penalties in the wing, main landing gear and tail attach due to the high wing, fuselage mounted gear and large T-tail are also given. Weight penalties given as a function of wing and tail areas are based on detail calculations involving many parameters.

E.2.4 Landing Gear. - Figure E-5 presents the correlation of landing gear weight with takeoff gross weight. The STOL point falls above the normal trend curve due to the higher design sink speed of 15 fps (4.6 m/s) for STOL operations. The production transports shown on the correlation curve have design sink speeds of 10 fps (3.0 m/s) at landing gross weight and 6 fps (1.8 m/s) at takeoff gross weight.

E.2.5 Flight Control and Hydraulics. - Figure E-6 shows the weight trend of the flight control and hydraulic systems as a function of total control surface area. These are combined due to the inter-relationship between the systems and the differences in weight allocation among airframe companies. The systems are some of the hardest to correlate due to the number of surfaces, relative sizes among the surfaces, types of actuation; (i.e., screwjack, hydraulic cylinder, manual), and safety or redundancy requirements. The STOL

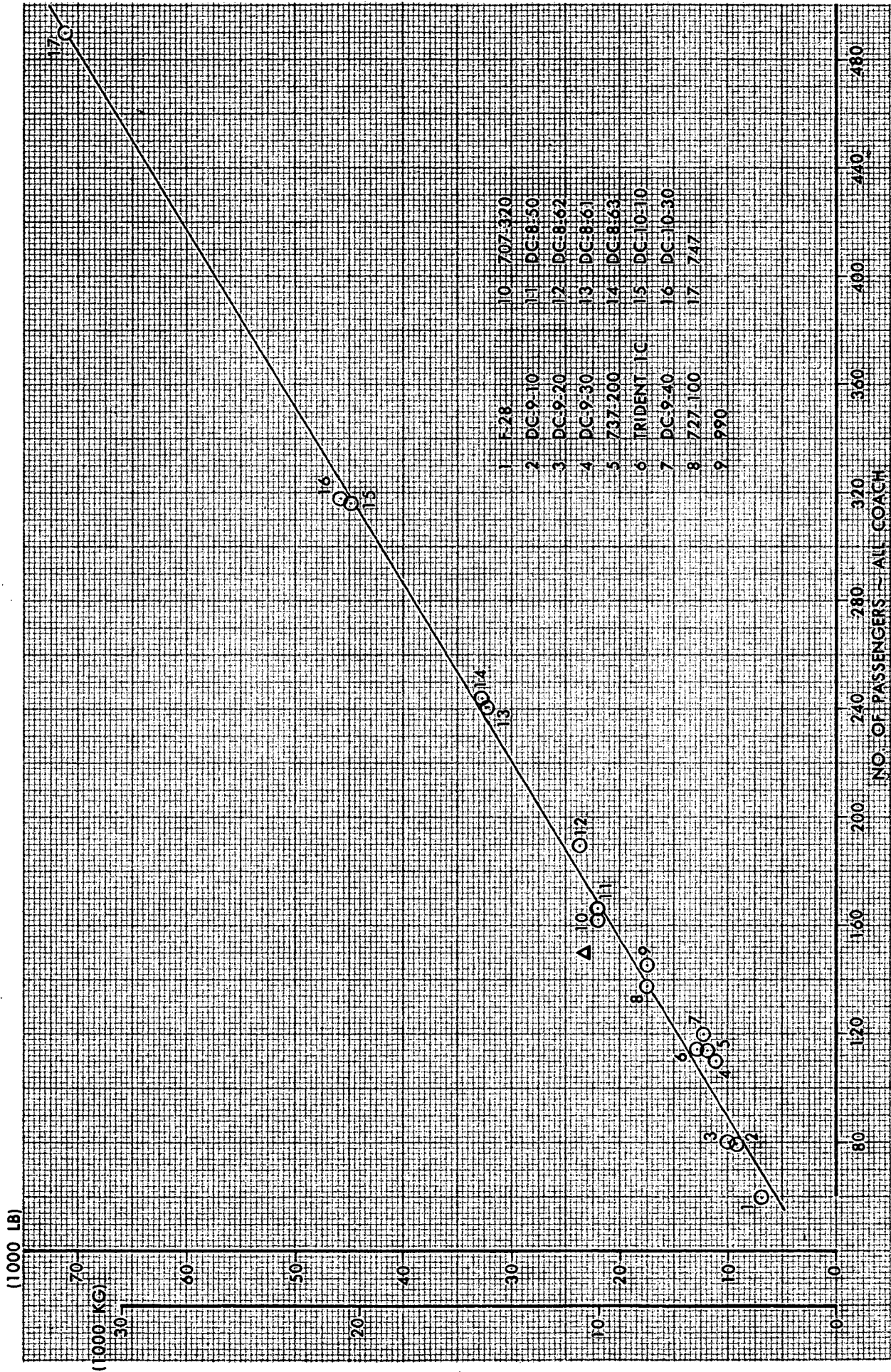


FIGURE E-4. WEIGHT TREND—FUSELAGE STRUCTURE

Table E-3

STOL FUSELAGE WEIGHT PENALTIES AND UNIT RATIOS

<u>Weight Penalties</u>	lb/airplane	kg/airplane
Fuselage Wetted Area Parameters		
$(34.9 \text{ ft}^2/\text{pass} - 30.6 \text{ ft}^2/\text{pass}) \times (2.4 \text{ lb/ft}^2)(150 \text{ pass})$	= +1,548	
$(3.24 \text{ m}^2/\text{pass} - 2.84 \text{ m}^2/\text{pass}) \times (11.7 \text{ kg/m}^2)(150 \text{ pass})$	=	+ 702
Wing & Gear Support		
$[(9.7 \text{ ft}^2/\text{pass})(1.89 \text{ lb/ft}^2) - (12.5 \text{ ft}^2/\text{pass})(.58 \text{ lb/ft}^2)](150 \text{ pass})$	= +1,664	
$[(.90 \text{ m}^2/\text{pass})(9.23 \text{ kg/m}^2) - (1.15 \text{ m}^2/\text{pass})(2.83 \text{ kg/m}^2)](150 \text{ pass})$	=	+ 755
Main Gear Pods and Doors		
$[(9.7 \text{ ft}^2/\text{pass})(.85 \text{ lb/ft}^2) - (12.5 \text{ ft}^2/\text{pass})(.23 \text{ lb/ft}^2)](150 \text{ pass})$	= + 806	
$[(.90 \text{ m}^2/\text{pass})(4.15 \text{ kg/m}^2) - (1.15 \text{ m}^2/\text{pass})(1.12 \text{ kg/m}^2)](150 \text{ pass})$	=	+ 366
Tail Support		
$[(2.1 \text{ ft}^2/\text{pass})(2.66 \text{ lb/ft}^2) - (1.8 \text{ ft}^2/\text{pass})(2.10 \text{ lb/ft}^2)](150 \text{ pass})$	= + 270	
$[(.20 \text{ m}^2/\text{pass})(12.99 \text{ kg/m}^2) - (.17 \text{ m}^2/\text{pass})(10.25 \text{ kg/m}^2)](150 \text{ pass})$	=	+ 122
TOTAL WEIGHT	+4,288	+ 1,945
<u>Unit Ratios</u>		
Fuselage Wetted Area Parameters		
STOL Wetted Area per Passenger	34.9 ft ² /pass	(3.24 m ² /pass)
Statistical Wetted Area per Passenger	30.6 ft ² /pass	(2.84 m ² /pass)
Average Fuselage Unit Weight*	2.4 lb/ft ²	(11.7 kg/m ²)
Wing Area (Trapezoidal) per Passenger		
STOL	9.7 ft ² /pass	(.90 m ² /pass)
Statistical	12.5 ft ² /pass	(1.15 m ² /pass)
V-Tail Area (exposed) per Passenger		
STOL	2.1 ft ² /pass	(.20 m ² /pass)
Statistical	1.8 ft ² /pass	(.17 m ² /pass)
Wing & Main Gear Support Weight/Wing Area		
High Wing (STOL)	1.89 lb/ft ²	(9.23 kg/m ²)
Low Wing	.58 lb/ft ²	(2.83 kg/m ²)
Main Gear Pod and Door Weight/Wing Area		
High Wing (STOL)	.85 lb/ft ²	(4.15 kg/m ²)
Low Wing	.23 lb/ft ²	(1.12 kg/m ²)
Tail Attach Weight/Tail Area		
STOL	2.66 lb/ft ²	(12.99 kg/m ²)
Statistical	2.10 lb/ft ²	(10.25 kg/m ²)
*Fuselage shell plus floors.		

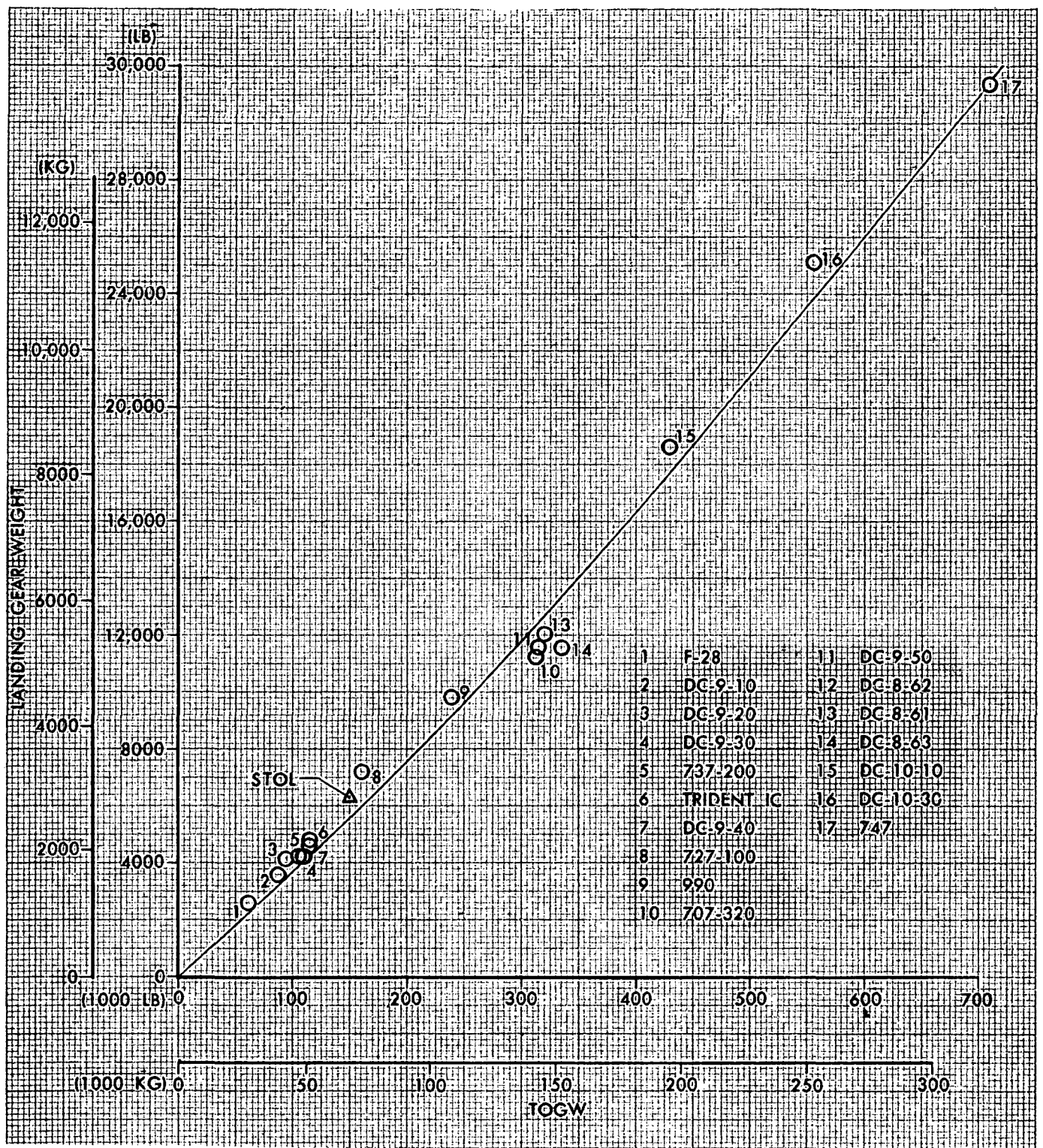


FIGURE E-5. WEIGHT TREND—LANDING GEAR

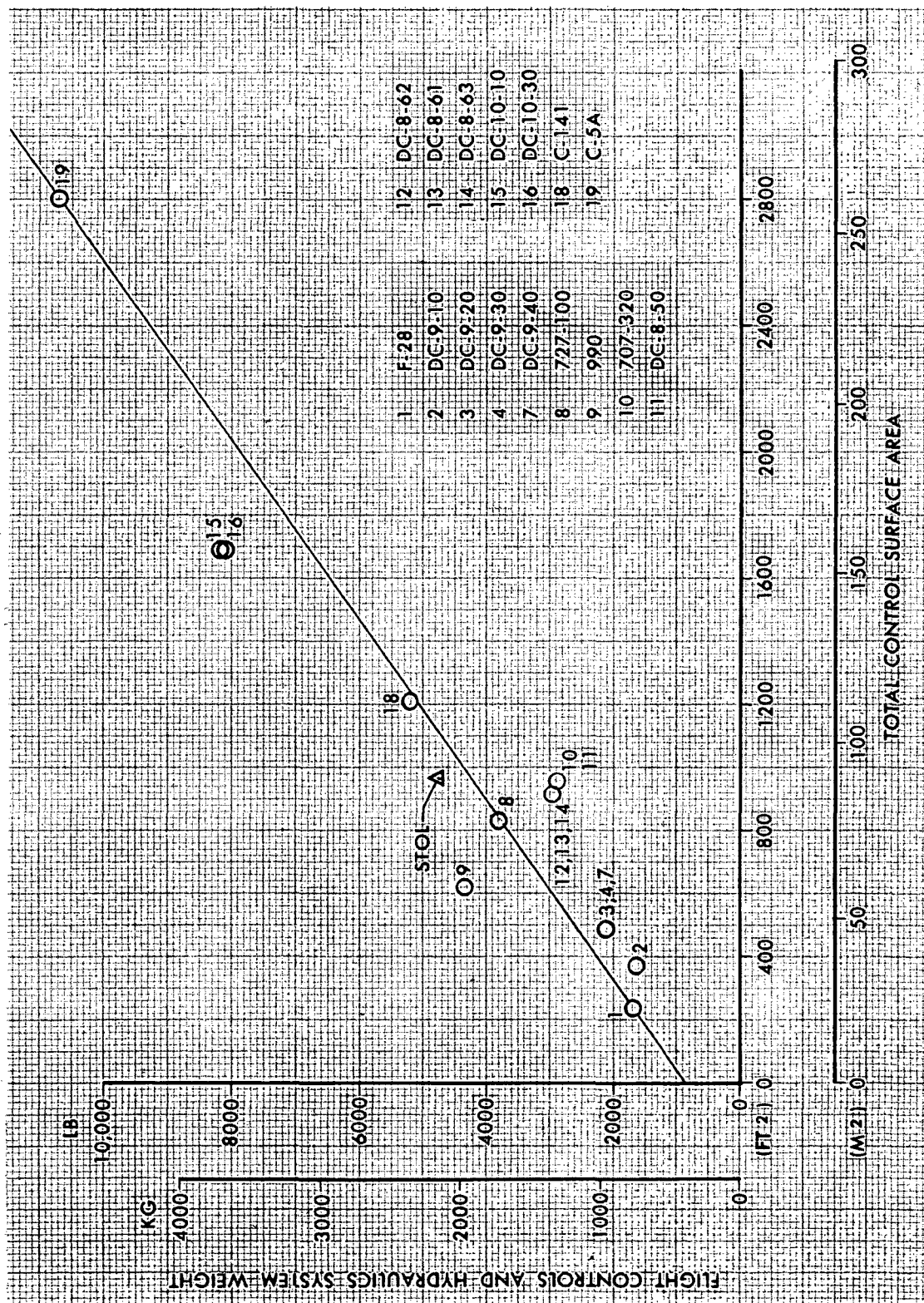


FIGURE E-6. WEIGHT TREND—FLIGHT CONTROLS AND HYDRAULIC SYSTEM

systems are not quite as heavy per unit area as the DC-10 systems.

E.2.6 Nacelle, Pylon, and Propulsion. - The engine weights are based on values supplied by General Electric and Allison. Figure E-7 shows the relationship of pylon unit weight to the size of the pylon and to the weight of the demountable power plant and its location relative to the wing. Note that the STOL values are higher than the average due to the unique positioning of the engine relative to the wing plus higher load factors, additive vectorally in three directions, during the STOL landing condition.

The nacelle weights are based on detailed component estimates which include the nose cowl lip, inner and outer inlet barrels, inner and outer fan cowlings, and core cowls. A few representative nacelle unit weights are shown in Table E-4 for comparison with the final design aircraft values. Unit values include the exhaust section weights and are based on a wetted area derived from the maximum nacelle diameter and the length from the nose cowl lip to the end of the tailpipe. Note that the thrust reversers are not required for the example aircraft because reverse thrust is accomplished by a change in fan pitch. This feature requires a variable-area nozzle.

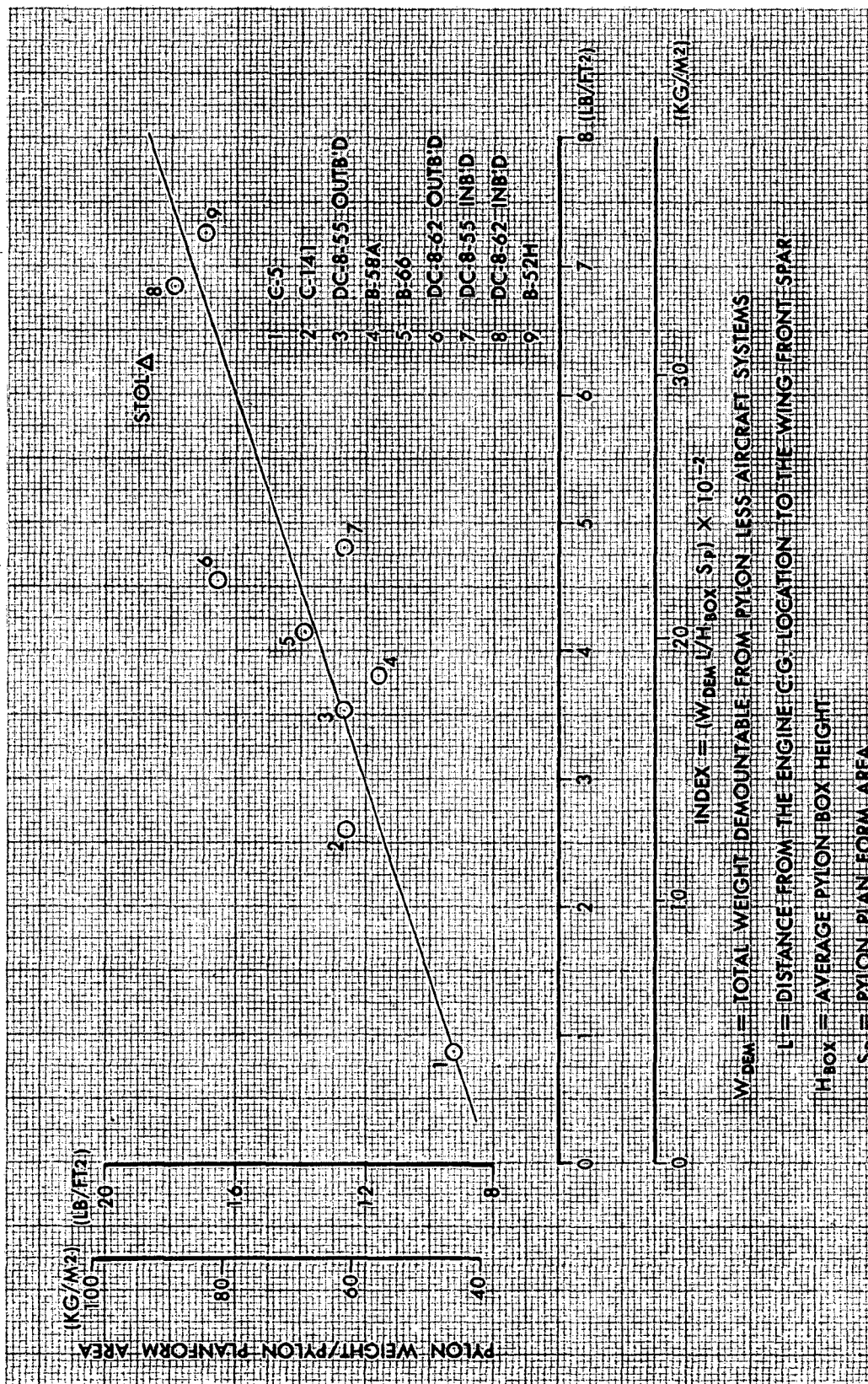


FIGURE E-7. PYLON UNIT WEIGHT COMPARISON

TABLE E-4. STOL NACELLE WEIGHT CORRELATION

Model	Unit Weight (Nacelle Plus Exhaust Section Minus Pylon)	
	lb/ft ² of nacelle wetted area	kg/m ² of nacelle wetted area
DC-8 Series 55 (JT3D-38)	1.9	9.3
DC-10 Series 10 (CF6-6D)	1.8	8.8
DC-10 Series 40 (JT9D-20)	2.2	10.7
C-5A (TF39)	1.5	7.3
STOL Final Design Aircraft	3.2	15.6
Less penalty for Sound Treatment	- .2	- 1.0
Less variable-area Nozzle Installation	- .4	- 1.9
Less portions of the Cowling normally replaced by Thrust Reversers	- .7	- 3.4
STOL ADJUSTED TO COMPARABLE CONFIGURATION	1.9	9.3

E.2.7 Instruments. - The STOL instrument weights are based on detail design requirements for instruments and warning systems monitoring flight, cabin, engine, and fuel activity. Since the weight of the instrument group is a function of many parameters, the trend curves shown in Figure E-8 indicate considerable scatter. Note that the curve titled "Flight, Navigational and Miscellaneous Instruments Weight" includes all instrument and warning subsystems other than the fuel and engine subsystems which are shown separately. The STOL flight/navigational instruments weight is higher than the average due primarily to the heads-up display system (HUD) and the requirement for the horizontal tail slat position indicating system.

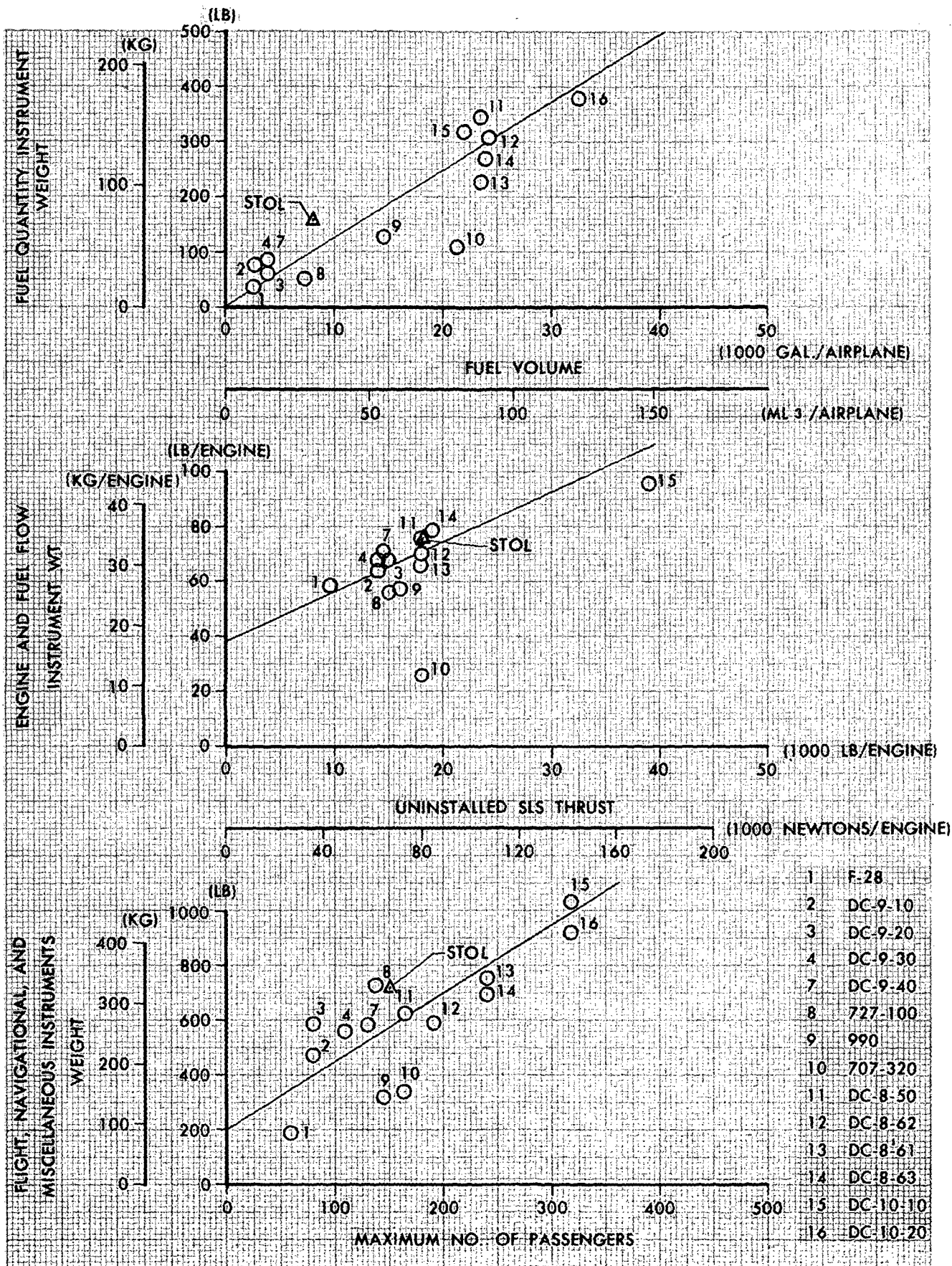


FIGURE E-8. WEIGHT TREND—INSTRUMENTS

E.2.8 APU, Pneumatics, and Air Conditioning. - Figure E-9 represents a weight trend of pneumatic related systems which are combined for the same reasons as given for the flight controls and hydraulics. All the aircraft shown in Figure E-9 have an APU; however, all of these aircraft have less than four engines. Therefore, a STOL weight exceeding the norm is attributed to the longer pneumatic duct runs between the four wing-mounted engines, the APU in the aft fuselage and the air conditioning units in the forward fuselage. Note that the fuselage pneumatic ducting also serves the STOL ice protection system.

E.2.9 Electrical System. - Figure E-10 shows the correlation of electrical system weights with maximum passenger load. The weights include AC and DC power supply and distribution systems and exterior/interior lighting systems.

E.2.10 Avionics. - Avionics weights are largely dependent on design definition and customer requirements. Table E-5 presents a tabulation of the DC-9, DC-10 and STOL avionics systems and their weights. STOL avionics requirements are discussed in Section 3.5

E.2.11 Furnishings. - The furnishings weight breakdown for the 6-abreast passenger seating configuration of the example aircraft is tabulated in Table E-6. The STOL furnishings weight is in close agreement with the statistical trend as shown in Figure E-11.

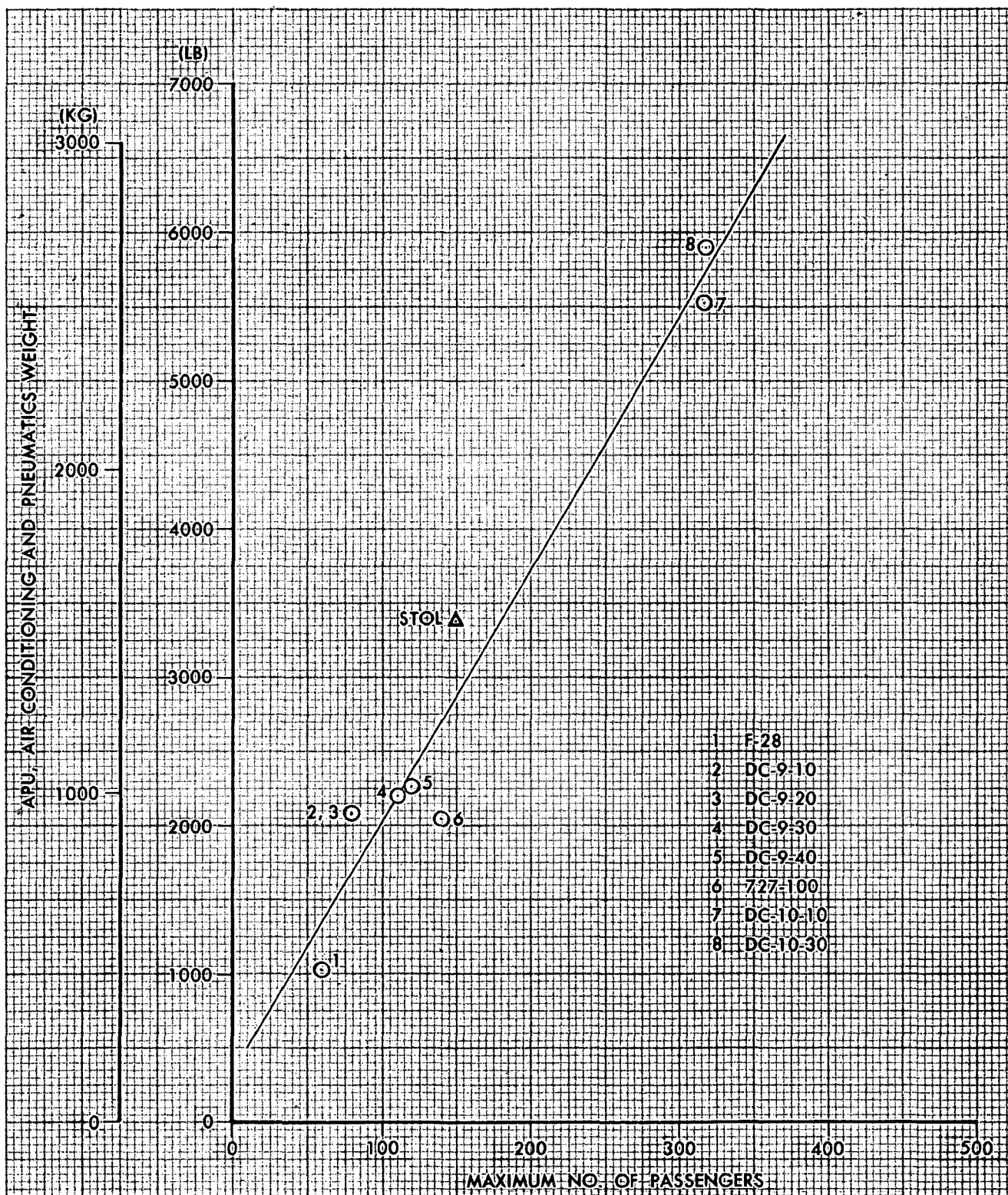


FIGURE E-9. WEIGHT TREND—APU, AIR CONDITIONING, PNEUMATICS

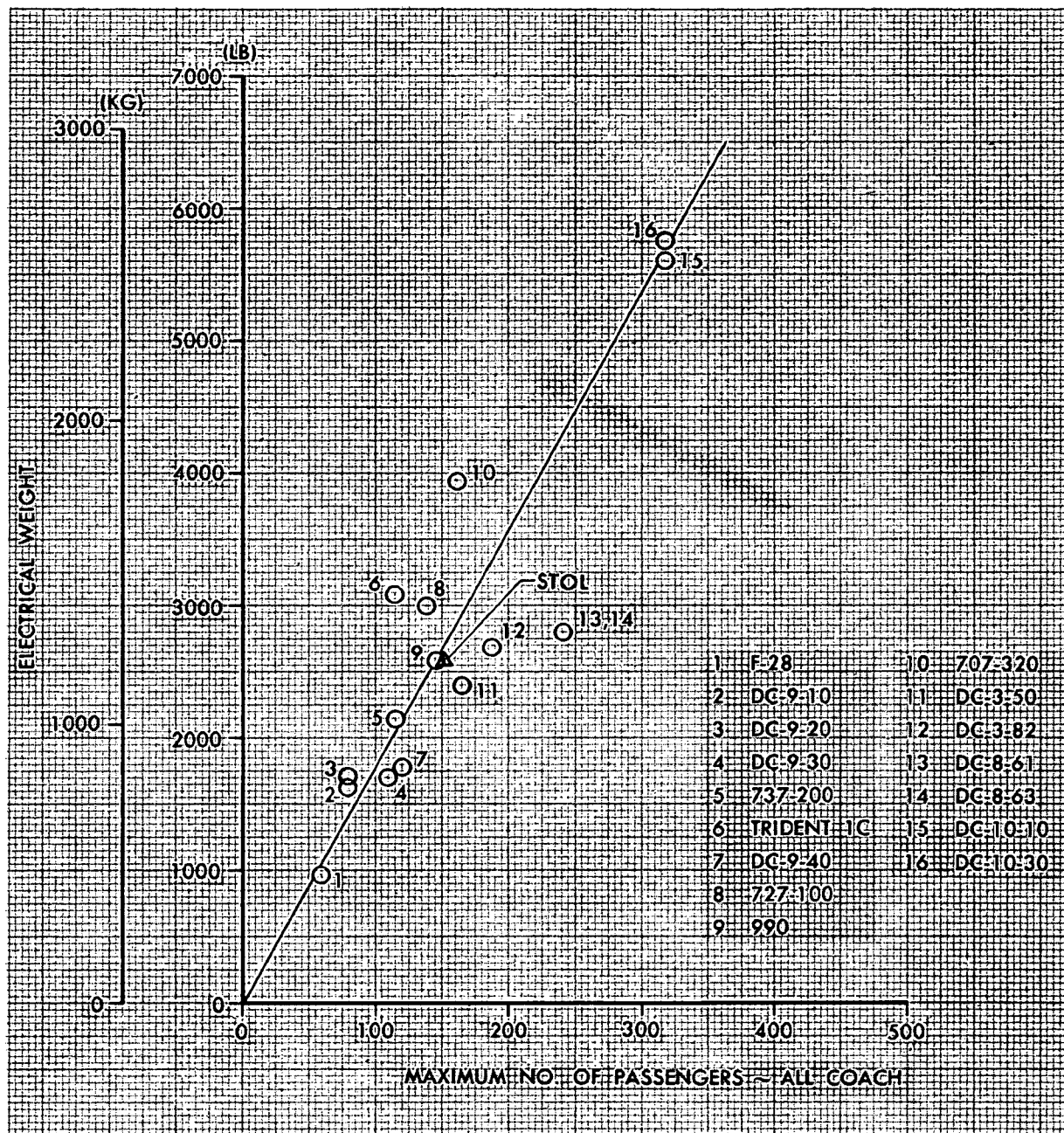


FIGURE E-10. WEIGHT TREND—ELECTRICAL GROUP

Table E-5

AVIONICS SYSTEM WEIGHT COMPARISON

	DC-9-30 ACA			DC-10-10 UAL			150 Pass EBF STOL		
	Req.	1b	kg	Req.	1b	kg	Req.	1b	kg
	(363)	(165)		(1112)	(504)		(670)	(304)	
o IFGCS (incl SCAS, autopilot, flight director, auto throttle, thrust management, area nav. and flight guidance displays.)									
SCAS									
Autopilot/flt director	--	--	--	--	--	--	} 370	}	168
Autothrottle/thrust management	229	104	104	638	289	289			
Area nav.	--	--	--	40	18	18			
Wire & instl	--	--	--	--	--	--	300		136
	134	61	61	434	197	197			
o ATTITUDE & HEADING SYSTEM									
Units	(1)	(56)	(25)	(2)	(76)	(34)	(2)	(116)	(53)
Wire & misc	33	15	15	52	23	23		92	42
	23	10	10	24	11	11		24	11
o AIR DATA SYSTEM									
Units	(1)	(104)	(47)	(2)	(103)	(47)	(2)	(182)	(83)
Wire & misc.	31	14	14	52	24	24		140	64
	73	33	33	51	23	23		42	19
o HEADS-UP DISPLAY SYSTEM									
Units	(0)	(0)	(0)	(0)	(0)	(0)	(1)	(58)	(26)
Wire & Misc.								24	11
								34	15
o INTERPHONE/INTERPHONE/PUBLIC ADDRESS SYSTEM									
Units	(1)	(99)	(45)	(1)	(348)	(158)	(1)	(216)	(98)
Speakers	11	5	5	95	43	43		59	27
Wire & misc	6	3	3	95	43	43		42	19
	82	37	37	158	72	72		115	52
o MARKER BEACON SYSTEM									
Units	(1)	(9)	(4)	(1)	(7)	(3)	(1)	(6)	(3)
Antenna	3	1	1	4	2	2		4	2
Wire & misc	1	1	1	1	--	--		1	--
	5	2	2	2	1	1		1	1

Table E-5

AVIONICS SYSTEM WEIGHT COMPARISON (Continued)

	DC-9-30 ACA			DC-10-10 UAL			150 Pass EBF STOL		
	Req.	lb	kg	Req.	lb	kg	Req.	lb	kg
o VOR/ILS SYSTEM Units Antenna Wire & misc.	(2)	(89) 39 1 49	(40) 18 -- 22	(2)	(147) 67 54 26	(67) 30 25 12	(2)	(136) 66 50 20	(62) 30 23 9
o ADF SYSTEM Units Antenna Wire & Misc.	(1)	(142) 19 82 41	(64) 9 37 18	(1)	(169) 11 133 25	(76) 5 60 11	(1)	(134) 11 105 18	(61) 5 48 8
o VHF COMM. SYSTEM Units Antenna Wire & misc.	(2)	(82) 43 30 9	(37) 20 13 4	(2)	(85) 34 36 15	(38) 15 16 7	(2)	(82) 41 30 11	(37) 18 14 5
o WEATHER RADAR SYSTEM Unit Antenna Indicator Wire & misc.	(1)	(124) 48 36 15 25	(56) 22 16 7 11	(2)	(275) 159 65 29 22	(125) 72 30 13 10	(1)	(125) 53 38 14 20	(57) 24 17 7 9
o AIDS		(0)	(0)		(46)	(21)		(0)	(0)
o COLLISION AVOIDANCE SYSTEM Units Antenna Wire & Misc.		(0) -- -- --	(0) -- -- --	Prov	(11) -- 7 4	(5) -- 3 2	(1)	(75) 64 7 4	(34) 29 3 2
o VOICE RECORDER SYSTEM Units Wire & misc.		(0) -- --	(0) -- --	(1)	(41) 22 19	(19) 10 9	(1)	(38) 22 16	(17) 10 7

Table E-5

AVIONICS SYSTEM WEIGHT COMPARISON (Continued)

	DC-9-30 ACA			DC-10-10- UAL			150 Pass EBF STOL		
	Req.	lb	kg	Req.	lb	kg	Req.	lb	kg
o MICROWAVE LANDING GUIDANCE SYSTEM		(0)	(0)		(0)	(0)	(2)	(100)	(45)
o MULTIPLEX SYSTEM		(0)	(0)		(240)	(109)		(140)	(63)
o ATC TRANSPONDER SYSTEM	(1)	(41)	(19)	(2)	(38)	(17)	(2)	(35)	(16)
Units	25	11	14	31	14	14		30	14
Antenna	1	1	2	4	2	1		2	1
Wire & misc.	15	7	3	3	1	1		3	1
o RADIO ALTIMETER SYSTEM	Prov	(37)	(17)	(2)	(96)	(44)	(2)	(62)	(28)
Units	--	--	--		51	23		34	15
Antenna	6	3	7		15	7		6	3
Wire & Misc.	31	14	14		30	14		22	10
o FLIGHT RECORDER SYSTEM	Prov	(5)	(2)	(1)	(72)	(33)	(1)	(61)	(28)
Units	--	--	--		51	23		54	25
Wire & misc.	5	2	10		21	10		7	3
o DME SYSTEM	Prov	(22)	(10)	(2)	(62)	(28)	(2)	(63)	(29)
Units	--	--	--		38	17		40	18
Antenna	2	1	4		9	4		9	4
Wire & misc.	20	9	7		15	7		14	7
o SELCAL SYSTEM	Prov	(2)	(1)	(1)	(12)	(5)	(1)	(12)	(5)
Units	--	--	--		9	4		9	4
Wire & misc.	2	1	1		3	1		3	1
o RADIO RACK STRUCTURE		(100)	(46)		(200)	(91)		(180)	(81)
SUB TOTAL WEIGHT		1275	578		3140	1424		2491	1130

AVIONICS SYSTEM WEIGHT COMPARISON (Continued)

Autopilot System	(Ref. Flight Control System)
Flight Director System	(Ref. Instrument System)
Autothrottle System	(Ref. Propulsion System)
Air Data System	(Ref. Instrument System)
Attitude & Heading System	(Ref. Instrument System)
Heads-Up Display System	(Ref. Instruments System)

TABLE E-6. STOL FURNISHINGS WEIGHT

	lb	kg
Cockpit and cabin seats and tracks	5,152	2,337
Lavatories (3) and water systems	861	391
Coffee bars (2)	540	245
Crew and passenger oxygen systems	304	138
Floor covering	530	240
Insulation above and below floor	1,224	555
Cabin window equipment	223	101
Cabin ceiling	785	356
Lining - above floor	716	325
Lining - below floor (cargo area)	919	417
Stowage and coatrooms	1,104	501
Partitions and doors	280	127
Instrument panels and consoles	104	47
Firex system	305	139
Emergency equipment	22	10
Cargo loading system	400	181
Miscellaneous furnishings	<u>221</u>	<u>100</u>
STOL FURNISHINGS WEIGHT	13,690	6,210

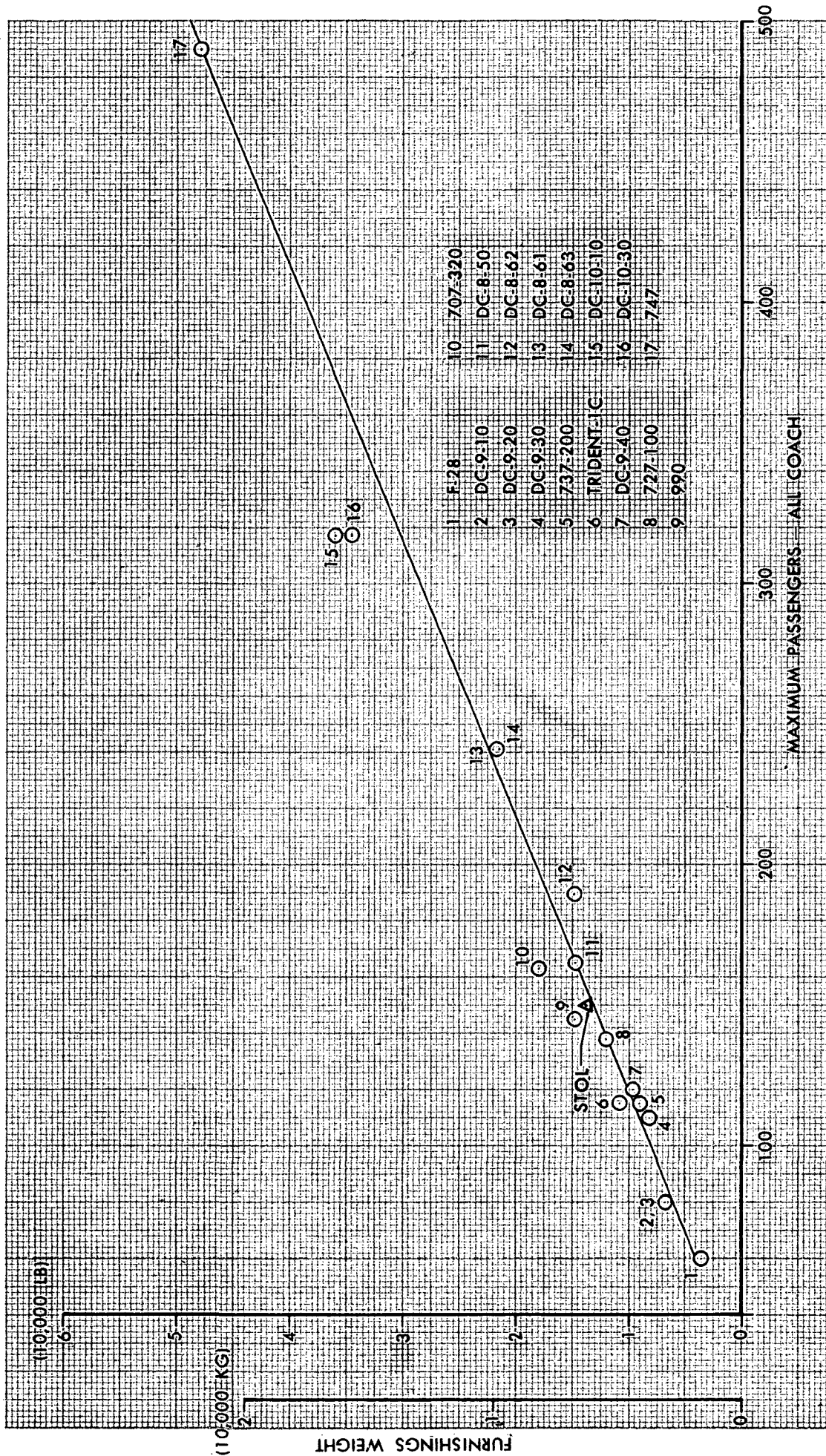


FIGURE E-11. WEIGHT TREND—FURNISHINGS

E.2.12 Ice Protection. - Ice protection is provided for the wing and horizontal tail leading edges, nacelle inlet lip, and windshield. Engine hot bleed air is used to deice the wing and stabilizer leading edges and to anti-ice the nacelles. The wing leading edge is protected outboard of the outer pylons only. The anti-icing system in the cockpit consists of electrically heated windows, electrically operated windshield wipers, and a rain repellent system. De-icing of the pitot tubes is also accomplished electrically. Table E-7 compares the STOL ice protection system weights with those for the similar DC-9 system. Differences between the systems are noted on the weight breakdown.

E.2.13 Operational Items. - Table E-8 presents the weight breakdown of the operational items for the example aircraft. Provisions are made for coffee service, plus normal passenger supplies such as newspapers and magazines. The weight allowances are based on DC-9 commuter experience.

Table E-7

WEIGHT SUMMARY - ICE PROTECTION SYSTEM

	DC-9-30		STOL	
	lb	kg	lb	kg
Ducts & Valves in Wing ^(a)	122	55	105	48
Ducts & Valves on Tail ^(b)	75	34	100	45
Ducts & Valves in Eng. Nacelle	70	32	186	84
Ducts & Valves in Fuselage ^(c)	80	36	Part of Pneu System	
Controls	20	9	25	11
Cockpit Window Anti-Ice ^(d)	27	12	46	21
Windshield-Wiper System ^(d)	15	7	48	22
Windshield - Rain Repellent ^(d)	12	6	11	5
Pitot De-Ice	<u>9</u>	<u>4</u>	<u>9</u>	<u>4</u>
TOTAL WEIGHT	430	195	530	240

Notes:

- (a) Wing: The STOL slat leading edge is de-iced outboard of the outboard engine pylon. The DC-9 entire slat leading edge is de-iced. The STOL aircraft uses titanium ducting versus steel on the DC-9.
- (b) Tail: Although the STOL aircraft uses titanium ducting to de-ice the horizontal tail slat, the weight is heavier than the steel ducting on the DC-9 due to the larger horizontal tail.
- (c) The STOL pneumatic system ducting runs from the wing engines to the APU in the aft fuselage and to the air conditioning units in the forward fuselage. This ducting also serves the wing ice protection system. On the DC-9, the engines, APU, and air conditioning units are located in the aft fuselage. Therefore, ducting is required from the engines to the wing ice protection system.
- (d) Cockpit window anti-ice, wiper system, and rain repellent system: The STOL windshields are the same size and design as those on the DC-10 and are therefore larger than on the DC-9. DC-10 weights are used for the STOL aircraft.

Table E-8

OPERATIONAL ITEMS WEIGHT SUMMARY
(150 Passenger Aircraft)

OPERATIONAL ITEMS	WEIGHT	
	lbs	kg
Pilots (2 @ 170 lbs each) (77.1 kg each)	340	154
Observer	0	0
Cabin Attendants (4 @ 130 lbs each)(59.0 kg each)	520	236
Crew Luggage	120	54
Briefcases	50	23
Galley Service Equipment & Beverage*	231	105
Cabin Supplies**	258	117
Lavatory Supplies	30	14
Oil (CSD, engine & APU)	195	89
Potable Water	375	170
Toilet Chemicals	126	57
Evacuation Slides	225	102
First Aid Equipment	25	11
Unusable Fuel	<u>345</u>	<u>156</u>
TOTAL OPERATIONAL ITEMS WEIGHT	2,840	1,288

*Galley Service Equipment & Beverage

Galley service equipment (cups, silverware, paperware)	=	.5 lb/pax (.2 kg/pax)
Refreshment meal (cookies, dry stores & liquids)	=	.5 lb/pax (.2 kg/pax)
Coffee Makers (3)	=	81 lb/airplane (37 kg/airplane)

**Cabin Supplies (Newspapers, magazines, coat hangers, headrest covers, sickness bags, kleenex and toilet tissue, towels and miscellaneous lavatory items.) = 1.72 lb/pax (.8 kg/pax)

E.3 Balance and Moments of Inertia

This section presents the balance and moments of inertia data for the eight final design aircraft. Table E-9 gives the weights and center of gravity (cg) locations for the major O.E.W. components. The aircraft balance location and the inclination of the principal axis for the O.E.W., Zero Fuel Weight and Takeoff Gross Weight are also included. For aircraft balance considerations, the payload is assumed to be loaded along the resultant of the passenger and belly cargo cg vectors (see Figure E-12).

An almost infinite number of aircraft balance and inertia conditions can be defined for each vehicle depending upon the payload and fuel loading desired. Therefore a series of charts and nomographs are presented to give the user the capability of investigating various payload, fuel, and gross weight combinations. These charts, Figures E-12(a) through (h), give the loading diagrams for a variety of weight conditions for each of the vehicles. In these figures moment is plotted against weight, and thus the loading vectors may be transferred to any part of the diagram so that the horizontal cg position for any combination of passengers, cargo and fuel can be easily determined. Forward and aft cg limits are shown on each figure.

Vertical cg positions are presented in Figure E-13. This nomograph is representative of all eight final design aircraft and provides the means for determining the delta vertical cg from the O.E.W. values shown in Table E-9. A sample calculation is given below.

Nomographs for determining aircraft pitching and rolling moments of inertia for the eight final aircraft are given in Figures E-14 and E-15.

TABLE E-9

WEIGHT, CENTER OF GRAVITY, AND PRINCIPAL AXIS SUMMARY

ITEM	WEIGHT		CENTER OF GRAVITY				PRINCIPAL AXIS (DEGREES)		
			PERCENT M.A.C.	HORIZONTAL (1)		VERTICAL (2)			
				IN	cm	IN		cm	
EBF-100 PAX-3000* FL (914.4 m)	LB	kg							
	WING	15,645	7,096		581.7	1478	150.0	381	
	H-TAIL	2,257	1,024		1309.6	3326	270.0	686	
	V-TAIL	1,588	720		1206.1	3064	177.0	450	
	FUSELAGE (INCL. LDG. GEAR)								
	POWER PLANT	37,361	16,947		521.5	1325	14.0	36	
		15,309	6,944		446.0	1133	39.0	99	
O.E.W.	72,160	32,731	27.3	558.3	1418	60.4	153	5.90	
Z.F.W. (P.L.=20,000LB, 9072 kg)	92,160	41,803	28.1	559.6	1421	53.4	136	4.92	
T.O.G.W.	104,100	47,219	28.3	559.9	1422	57.4	146	4.88	
EBF-150 PAX-2000* FL (609.6 m)	LB	kg							
	WING	40,472	18,358		789.8	2006	80.0	203	
	H-TAIL	6,612	2,999		1690.2	4293	380.0	965	
	V-TAIL	7,291	3,307		1481.6	3763	296.0	752	
	FUSELAGE (INCL. LDG. GEAR)								
	POWER PLANT	61,389	27,845		652.7	1658	14.0	36	
		28,926	13,121		577.0	1466	24.0	61	
O.E.W.	144,690	65,630	33.1	765.1	1943	65.5	166	11.45	
Z.F.W. (PL=30,000LB, 13,608 kg)	174,690	79,238	25.2	745.6	1894	60.3	153	10.21	
T.O.G.W.	196,000	88,904	25.5	746.3	1896	64.0	163	10.21	
EBF-150 PAX-3000* FL (914.4 m)	LB	kg							
	WING	22,450	10,183		703.0	1786	90.0	229	
	H-TAIL	3,371	1,529		1572.0	3993	330.0	838	
	V-TAIL	2,346	1,064		1449.0	3680	200.0	508	
	FUSELAGE (INCL. LDG. GEAR)								
	POWER PLANT	53,864	24,433		625.9	1590	14.0	36	
		20,579	9,334		544.0	1382	34.0	86	
O.E.W.	102,610	46,543	28.5	676.2	1718	49.4	125	6.07	
Z.F.W. (PL=30,000LB, 13,608 kg)	132,610	60,151	25.8	671.5	1706	42.2	107	5.05	
T.O.G.W.	149,000	67,585	26.6	672.9	1709	46.2	117	5.11	
(1) DISTANCE FROM FUSELAGE NOSE - GEAR UP									
(2) DISTANCE ABOVE FUSELAGE REFERENCE PLANE - GEAR UP									

TABLE E-9

WEIGHT, CENTER OF GRAVITY, AND PRINCIPAL AXIS SUMMARY (Continued)

ITEM	WEIGHT		PERCENT M.A.C.	CENTER OF GRAVITY		PRINCIPAL AXIS (DEGREES)
	LB	kg		HORIZONTAL IN	VERTICAL IN	
EBF-200 PAX-3000' FL (914.4 m)	30,120	13,662		783.1	100.0	
H-TAIL	4,079	1,850		1742.2	385.0	
V-TAIL	3,431	1,556		1599.2	247.0	
FUSELAGE (INCL. LDG. GEAR)	67,792	30,750		688.2	14.0	
POWER PLANT	25,928	11,761		606.0	26.0	
O.E.W.	131,350	59,579	27.1	750.3	53.7	6.78
Z.F.W. (P.L.=40,000 LB, 18,144kg)	171,350	77,723	23.5	742.9	46.2	5.61
T.O.G.W.	192,000	87,090	24.5	745.0	49.7	5.68
AW-150 PAX-2000' FL (609.6 m)	41,928	19,018		813.9	90.0	
H-TAIL	7,152	3,244		1694.8	504.0	
V-TAIL	7,752	3,516		1483.9	300.0	
FUSELAGE (INCL. LDG. GEAR)	60,838	27,596		652.6	14.0	
POWER PLANT	31,830	14,438		640.0	- 13.0	
O.E.W.	149,500	67,812	33.6	788.1	67.8	14.08
Z.F.W. (PL=30,000 LB, 13,608kg)	179,500	81,420	24.8	764.6	62.8	12.61
T.O.G.W.	212,600	96,434	24.9	764.8	68.3	12.69
USB-150 PAX-2000' FL (609.6 m)	49,766	22,573		809.3	110.0	
H-TAIL	7,502	3,403		1745.0	545.0	
V-TAIL	8,771	3,978		1511.8	320.0	
FUSELAGE (INCL. LDG. GEAR)	67,219	30,491		668.9	14.0	
POWER PLANT	39,192	17,777		568.0	121.0	
O.E.W.	172,450	78,222	31.0	776.2	104.7	12.45
Z.F.W. (PL=30,000 LB, 13,608 kg)	202,450	91,830	22.7	753.8	100.3	11.31
T.O.G.W.	227,100	103,011	23.2	755.1	103.7	11.33

TABLE E-9

[illegible]

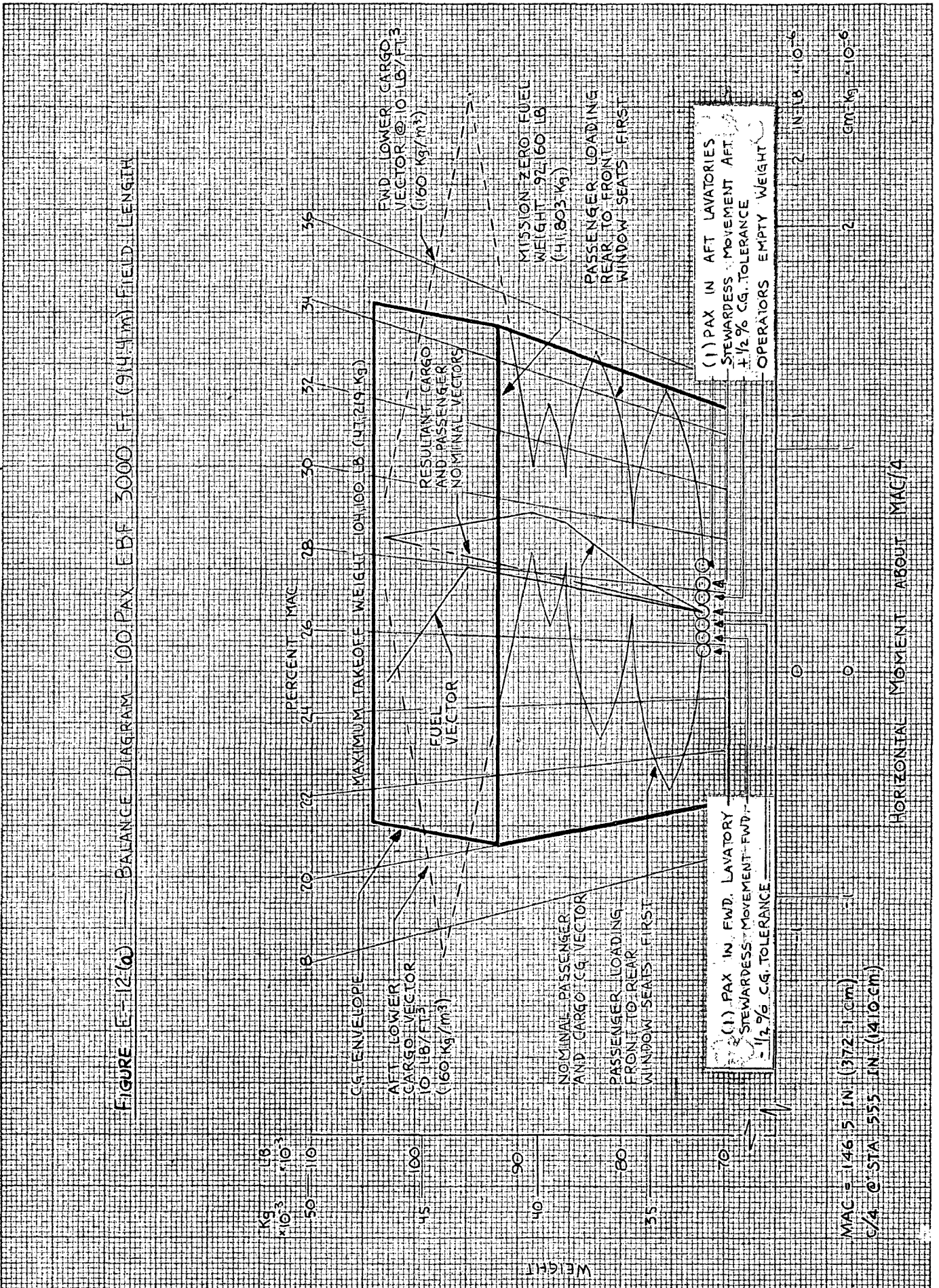


FIGURE E-12(b) --- BALANCE DIAGRAM 150 PAX EBF 2000 FT (609.6 m) FIELD LENGTH

PERCENT MAC
24 26 28 30 32 34 36

$kg \times 10^3$

200

190

180

170

160

150

140

130

120

110

100

90

80

70

60

50

40

30

20

10

0

-10

-20

-30

-40

-50

-60

-70

-80

-90

-100

CG ENVELOPE

AFT LOWER CARGO VECTOR @ 10 LB/FT³ (160 kg/m³)

FUEL VECTOR (TOGW LIMITED)

FWD LOWER CARGO VECTOR @ 10 LB/FT³ (160 kg/m³)

MISSION ZERO FUEL WEIGHT 174 690 LB (79 238 kg)

RESULTANT PASSENGER AND CARGO NOMINAL VECTORS

NOMINAL PASSENGER AND CARGO C.G. VECTOR

PASSENGER LOADING FRONT TO REAR WINDOW SEATS FIRST

PASSENGER LOADING REAR TO FRONT WINDOW SEATS FIRST

(1) PAX IN FWD LAVATORY STEWARDESS MOVEMENT FWD, -1/2 % C.G. TOLERANCE

(2) PAX IN AFT LAVATORIES STEWARDESS MOVEMENT AFT +1/2 % C.G. TOLERANCE OPERATORS EMPTY WEIGHT

MAC = 246.2 IN. (625.3 cm)
C/A C STA 745 IN. (1892 cm)

$in \times 10^{-6}$
 $cm \times 10^{-6}$

HORIZONTAL MOMENT ABOUT MAC/4

FIGURE 12(c) — BALANCE DIAGRAM — 150 PAX, EBF 3000 FT (914.4 m) FIELD LENGTH

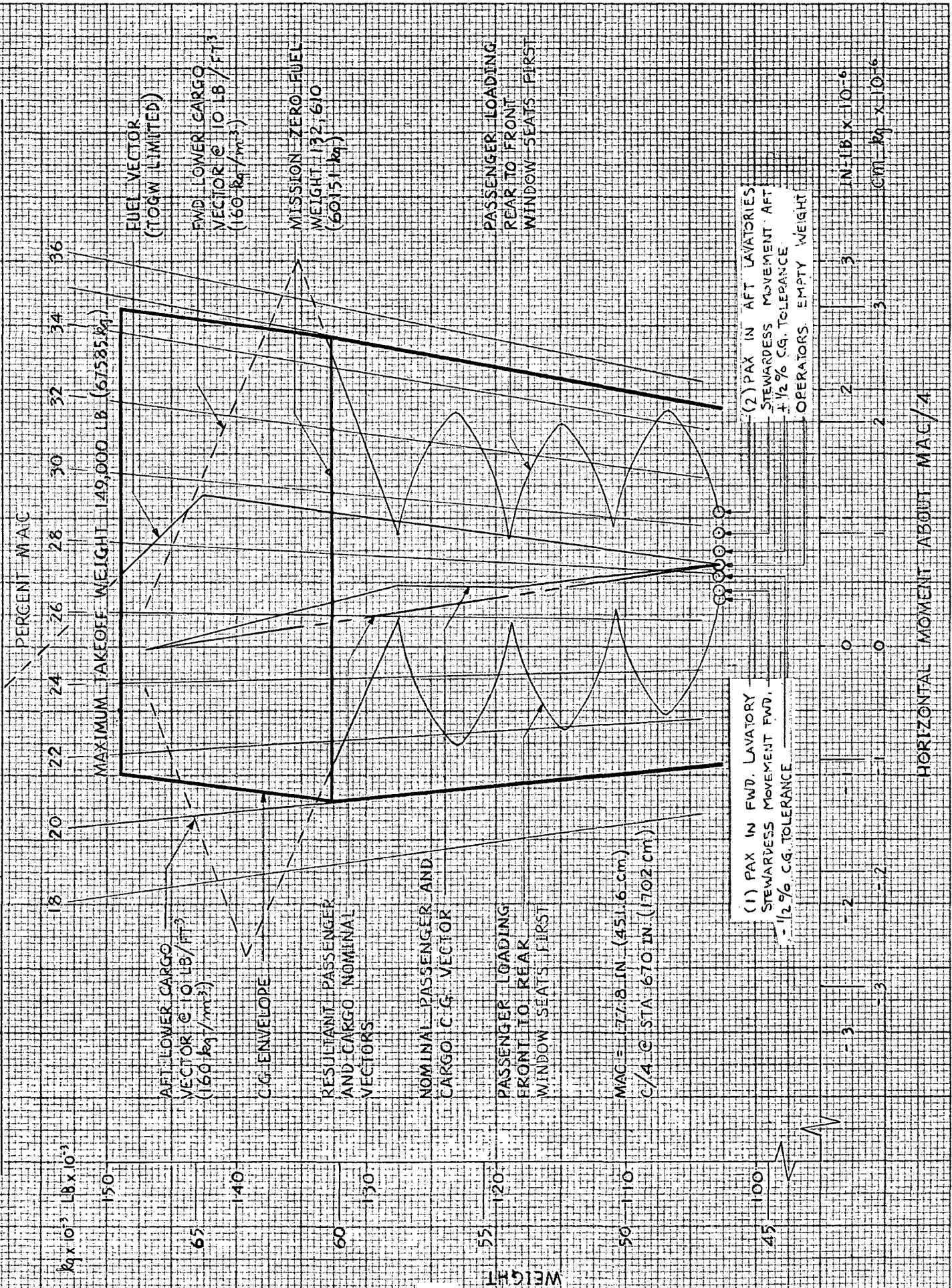
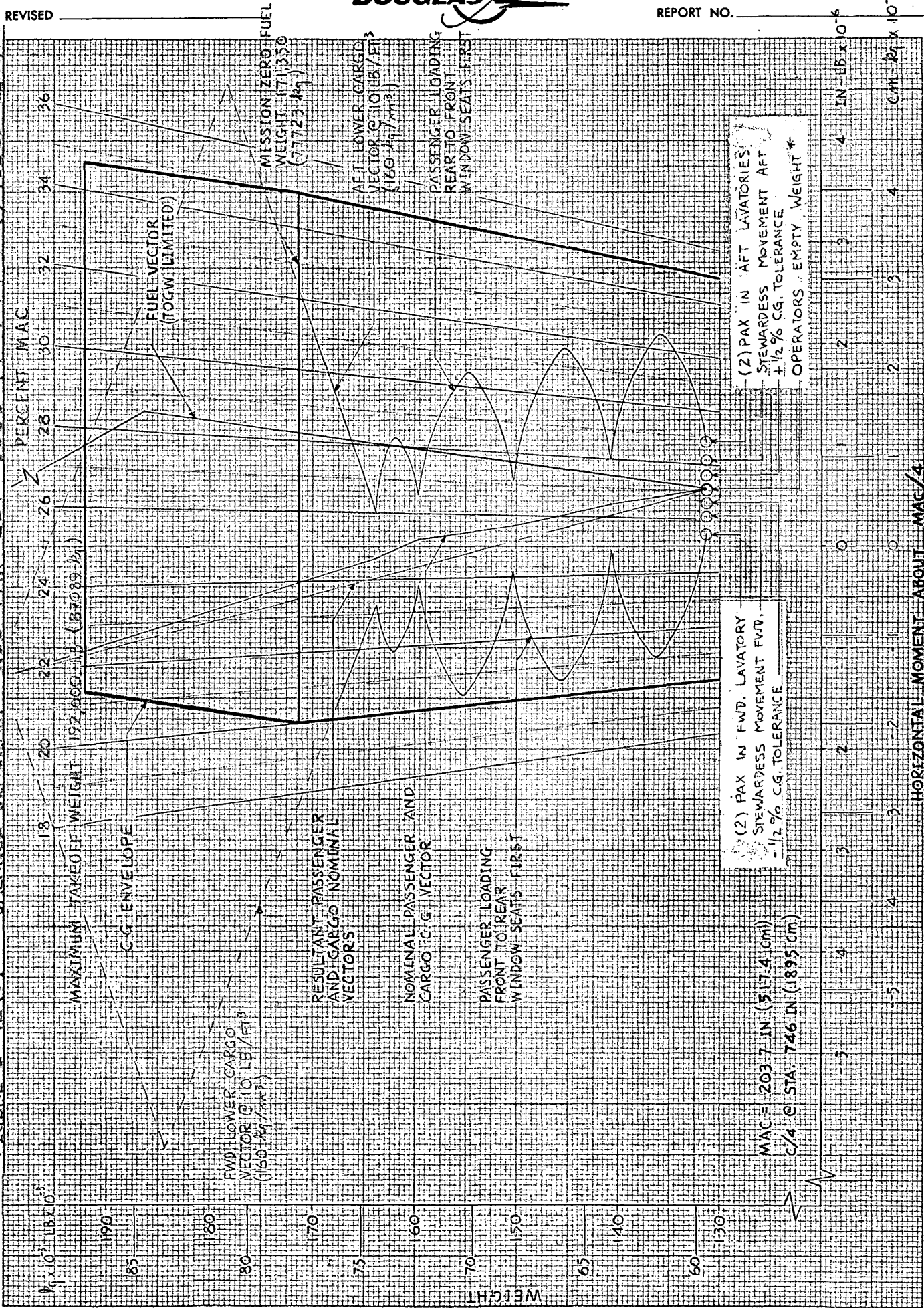
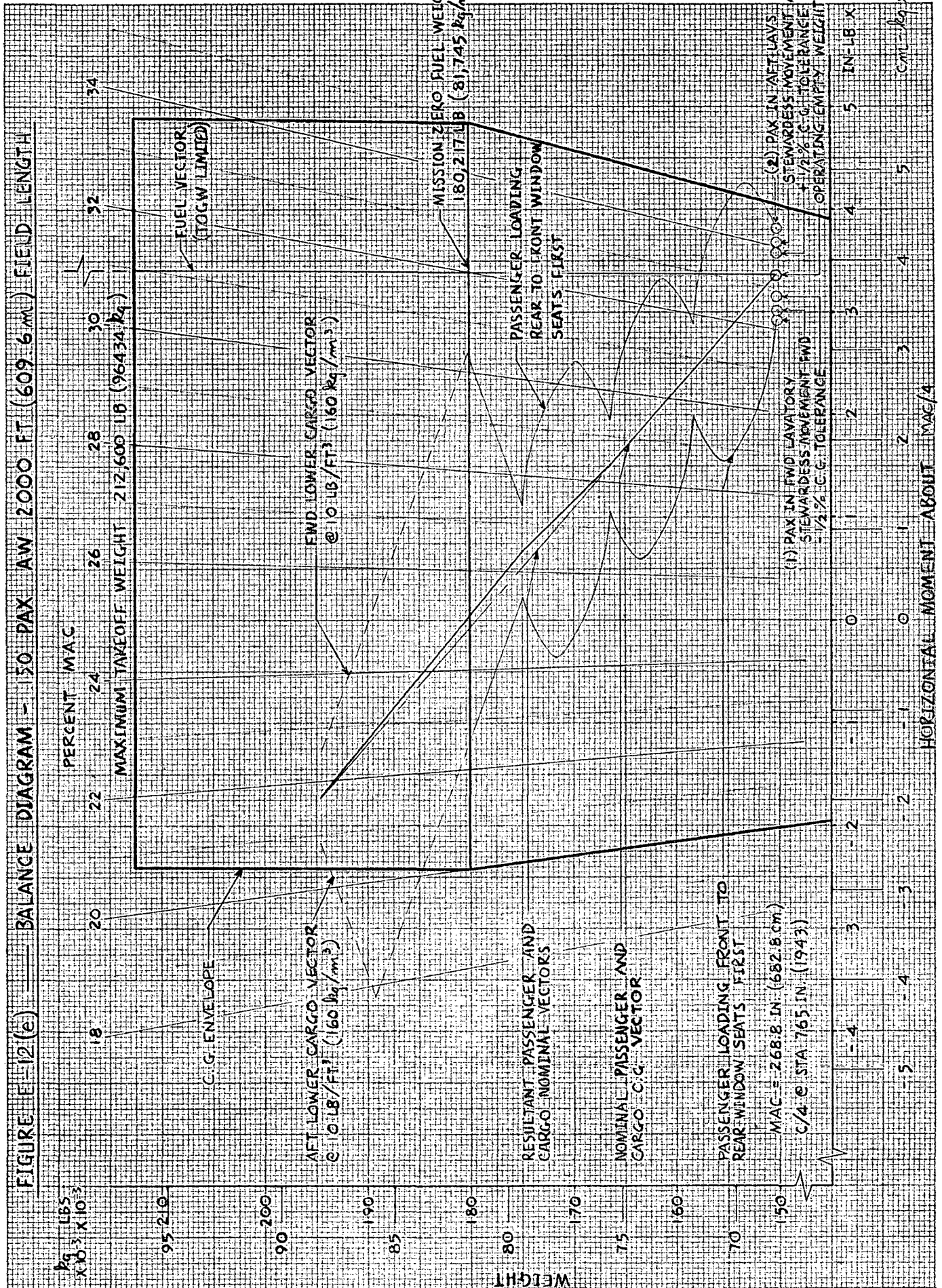
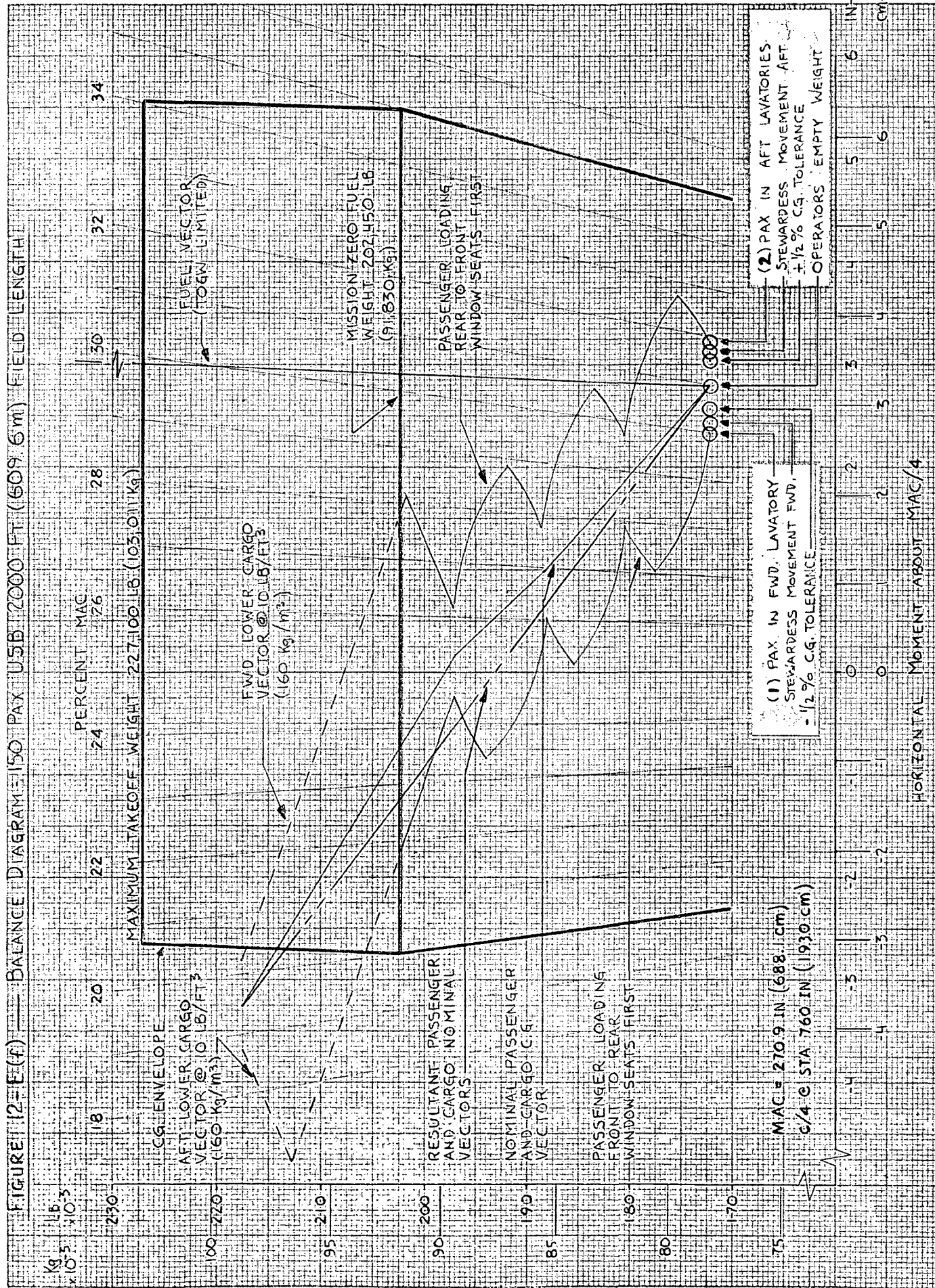


FIGURE E-12(d) — BALANCE DIAGRAM — 200 PAX EBF 3000 FT (914.4 m) FIELD LENGTH







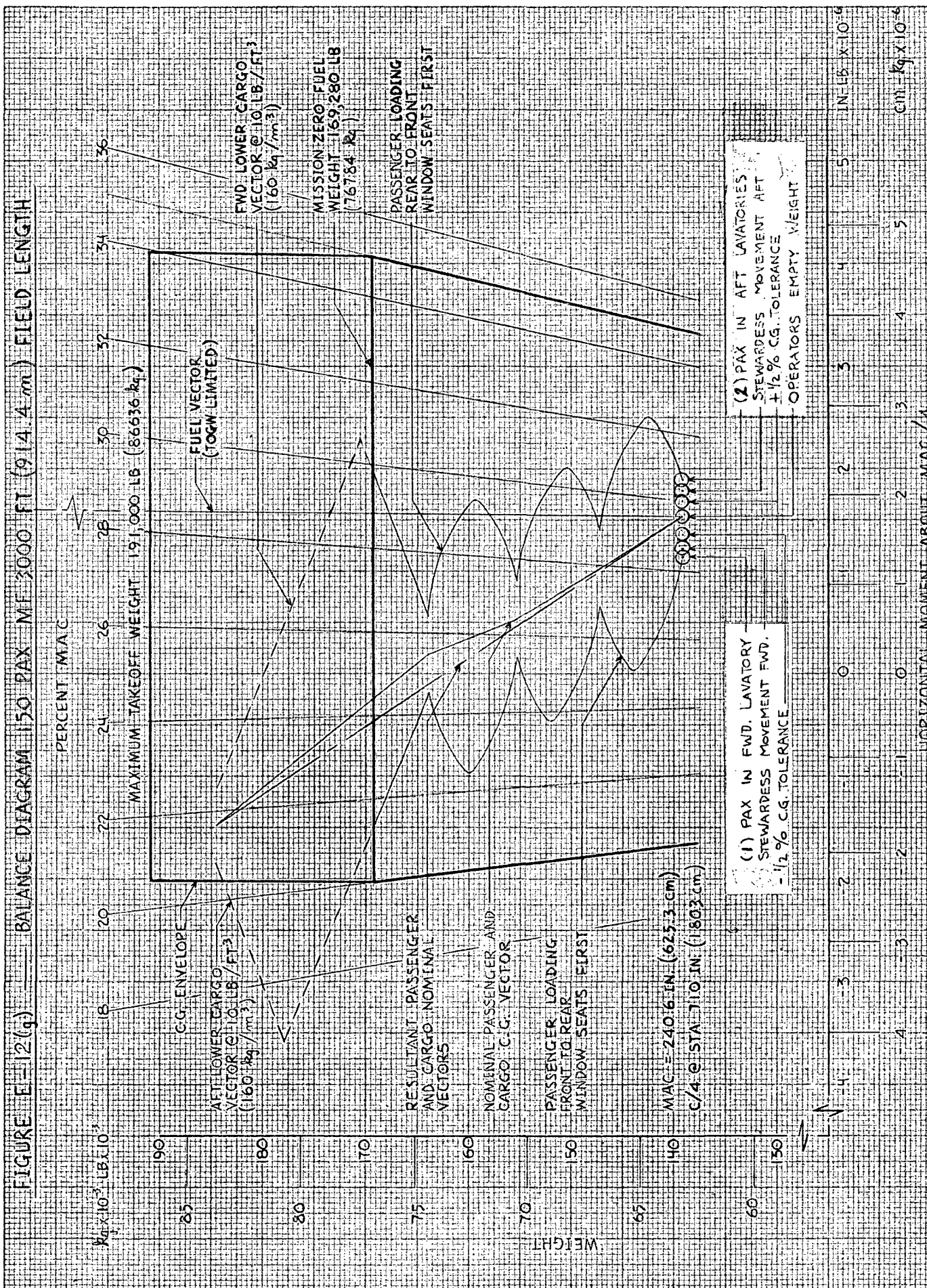




FIGURE E-12(h) BALANCE DIAGRAM 150 PAX ME 4000 FT (1219 m) FIELD LENGTH

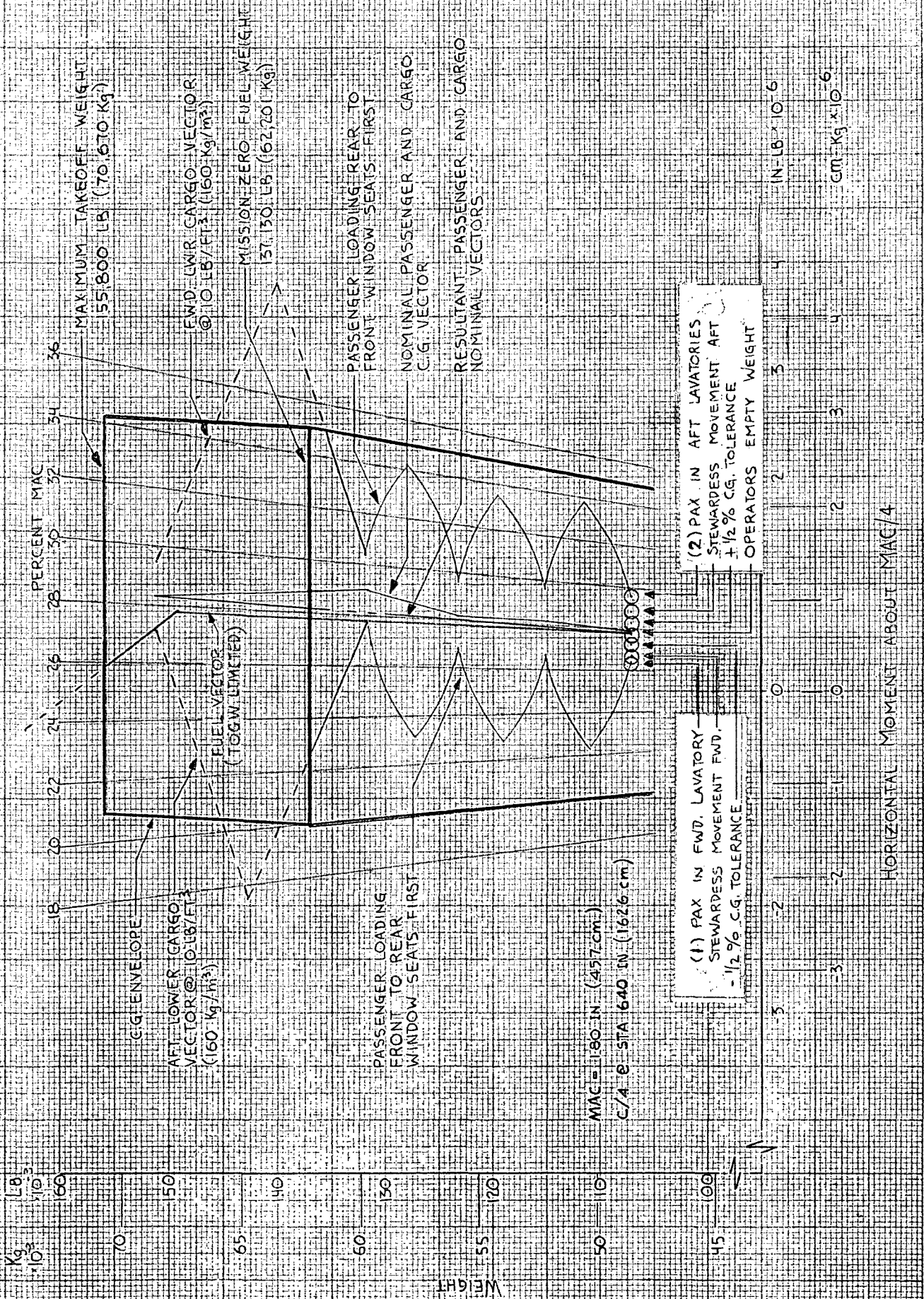


FIGURE E-13

VERTICAL CENTER OF GRAVITY

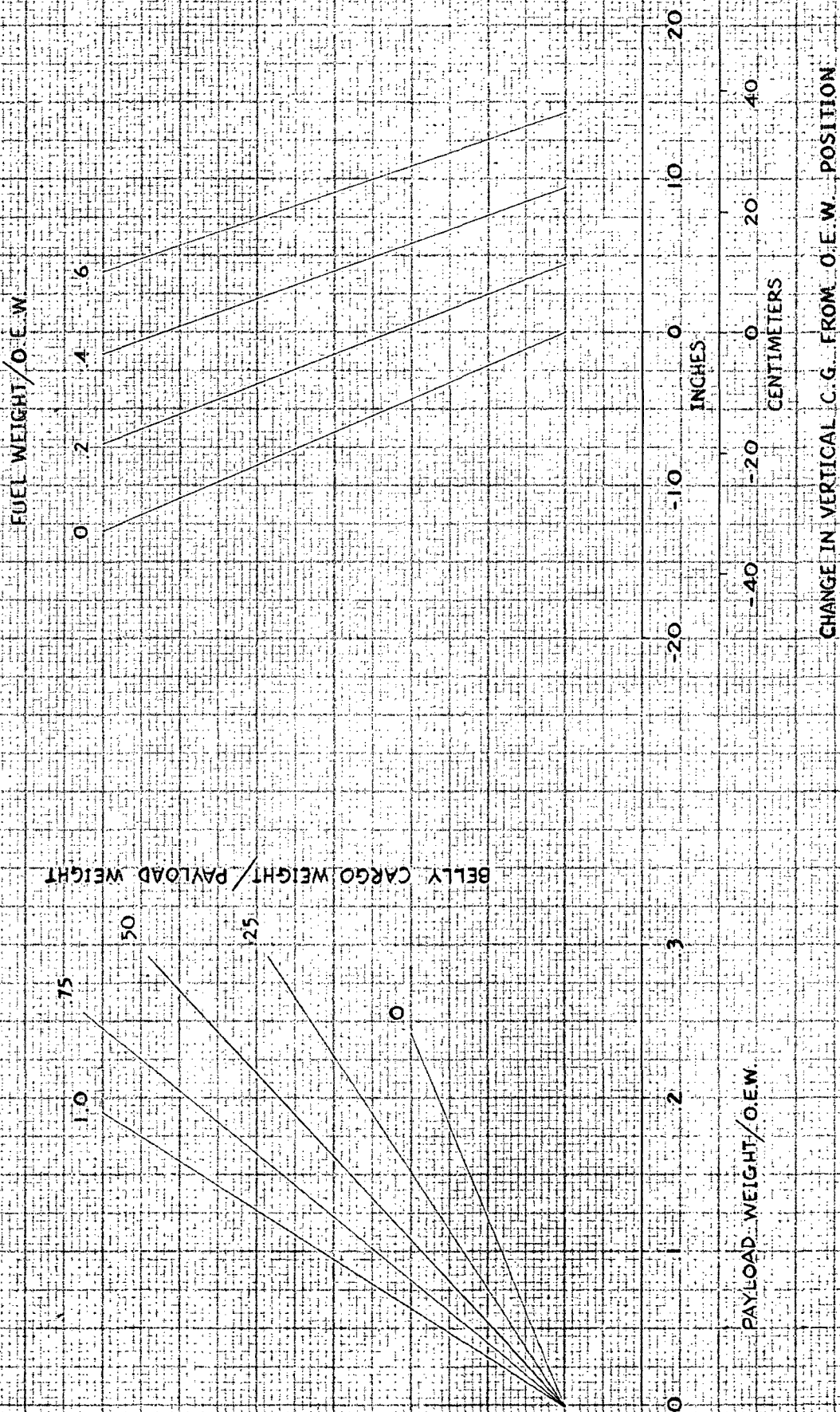
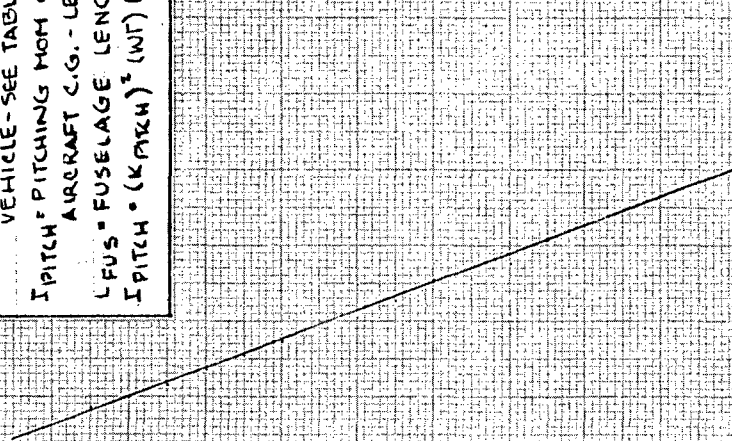




FIGURE E-14
 AIRPLANE PITCHING MOMENT OF INERTIA

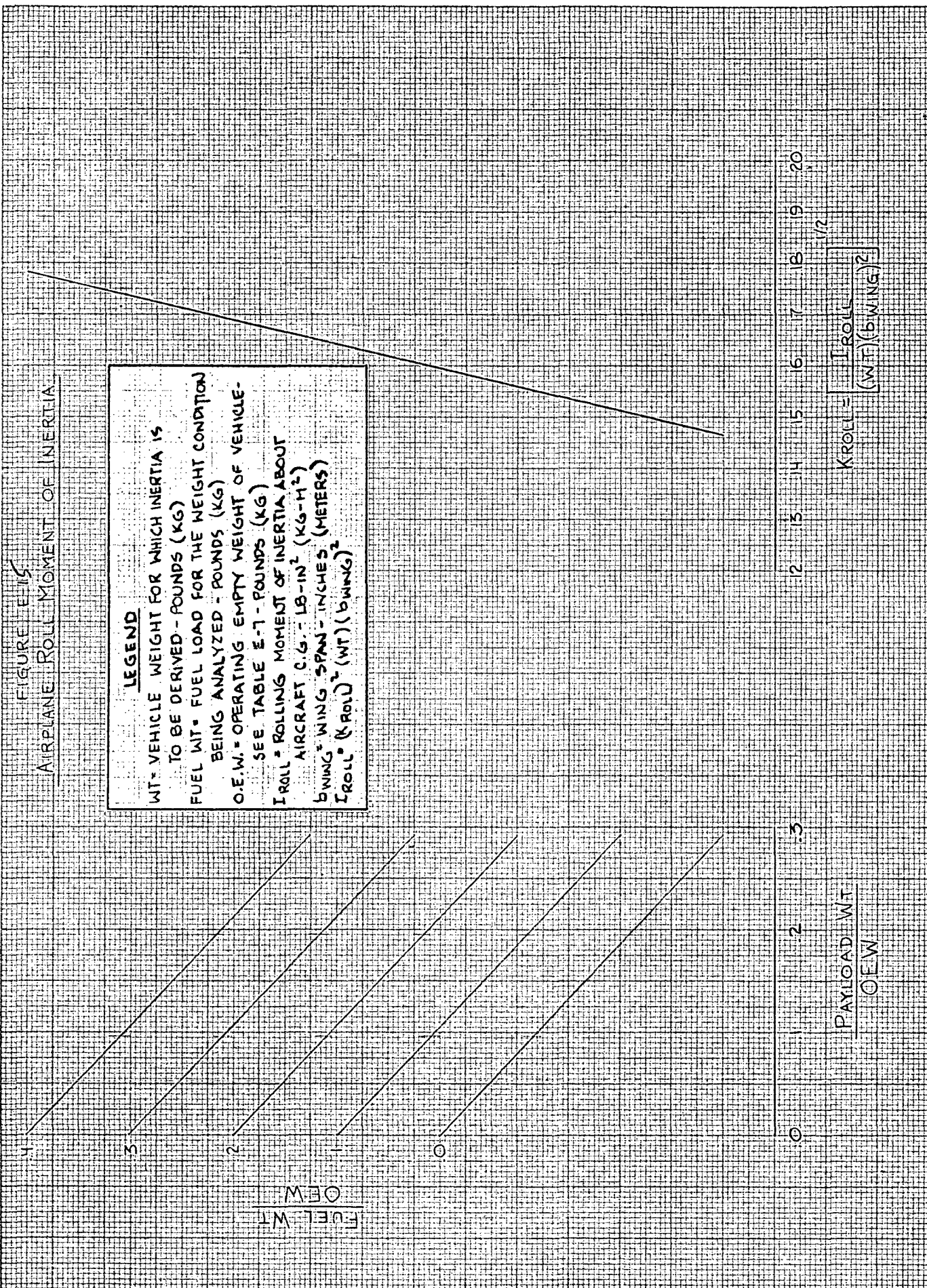
LEGEND

WT = VEHICLE WEIGHT FOR WHICH INERTIA IS TO BE DERIVED - POUNDS (KG)
 FUEL WT = FUEL LOAD FOR THE WEIGHT CONDITION BEING ANALYZED - LB (KG)
 O.E.W. = OPERATING EMPTY WEIGHT OF VEHICLE - SEE TABLE E-7 - LB (KG)
 I_{PITCH} = PITCHING MOM OF INERTIA ABOUT AIRCRAFT C.G. - LB-IN² (KG-M²)
 LFUS = FUSELAGE LENGTH - INCHES (METERS)
 I_{PITCH} = (K_{PITCH})² (WT) (LFUS)³

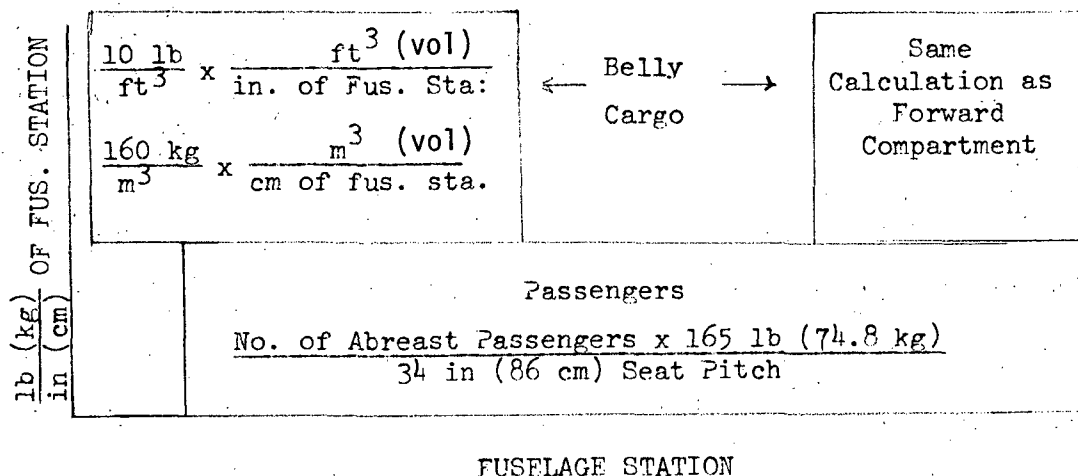


PAYLOAD WT
 OEW

FUEL WT
 OEW



Principal axis values are not given since variations over those shown in Table E-9 have been found to be negligible. Full payload is distributed throughout the cargo compartment in accordance with the following unit loading chart:



The moment of inertia nomographs assume the payload is homogeneously distributed throughout the cargo compartments.

In order to illustrate the use of the preceding charts and nomographs, a sample problem is given as follows: Balance and moment of inertia values are desired for the 150 passenger, 3000 foot (914 m) field length, final design EBF aircraft, for 50 percent load factor and baggage at 35 pounds (16 kg) per passenger at the maximum takeoff gross weight. The weight breakdown is as follows:

<u>Weight</u>	<u>lb</u>	<u>kg</u>
O.E.W. (Table E-7)	102,610	46,543
Passengers 75 x 165 lb ea. (74.8 kg ea)	12,375	5,613
Baggage 75 x 35 lb (16 kg)	2,625	1,191
Fuel	<u>31,390</u>	<u>14,238</u>
Takeoff Gross Weight	149,000	67,585

The pertinent tables and charts required for the example are reproduced in Figure E-16. From the loading diagram (E-16(b)), the TOGW horizontal cg is 27.9 percent MAC using nominal cg vectors. From the weight and balance summary (E-16(a)), the OEW vertical cg location is 49.4 inches (125 cm) above the fuselage reference plane. In the nomograph (E-16(c)), the approach line shows the delta cg value for payload/OEW (15,000/102,610) and fuel weight/OEW (31,390/102,610) is shown to be 4.0 inches (10 cm). The TOGW vertical cg for this condition is therefore 49.4 + 4.0 or 53.4 inches (136 cm).

Moment of inertia K factors for pitch and roll can be found in a similar manner by following the example arrows shown on the inertia nomograph (E-16(d) & (e)). Pitch, roll, and yaw values can therefore be determined as follows:

Figure E-16(a) - WEIGHT, CENTER OF GRAVITY, AND PRINCIPAL AXIS SUMMARY

ITEM	WEIGHT		CENTER OF GRAVITY		PERCENT M.A.C.	PRINCIPAL AXES (DEGREES)	
	LB	KG	HORIZONTAL (1) IN	VERTICAL (2) IN		(1)	(2)
EBF-150 PAX-3000* PL (914.4 m)							
WING	22,450	10,183	703.0	1786			
H-TAIL	3,371	1,529	1572.0	3993			
FUSELAGE (INCL. LOG. GEAR)	2,346	1,064	1449.0	3680			
POWER PLANT	20,579	9,334	625.9	1590			
O.E.W.	102,610	46,543	544.0	1382			
Z.E.W. (PL-3,000 LB. 608 kg)	132,610	60,151	676.2	1718	28.5		
T.O.G.W.	149,000	67,585	671.5	1706	25.8		
			672.9	1709	26.6		
(1) DISTANCE FROM FUSELAGE NOSE - GEAR UP							
(2) DISTANCE ABOVE FUSELAGE REFERENCE PLANE - GEAR UP							

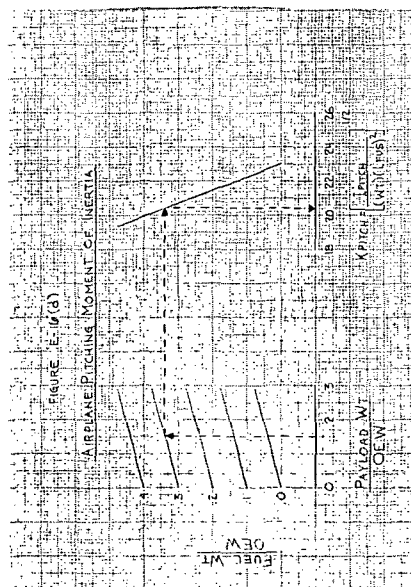
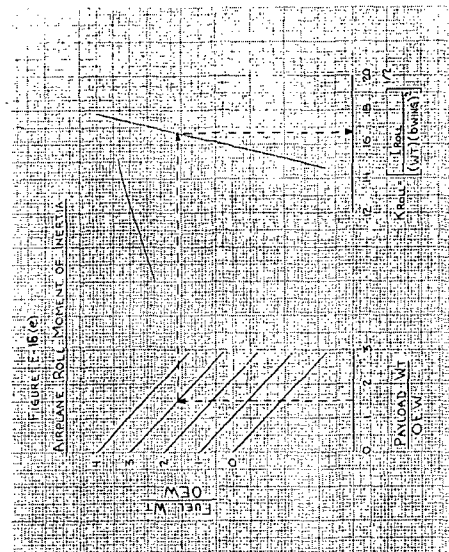
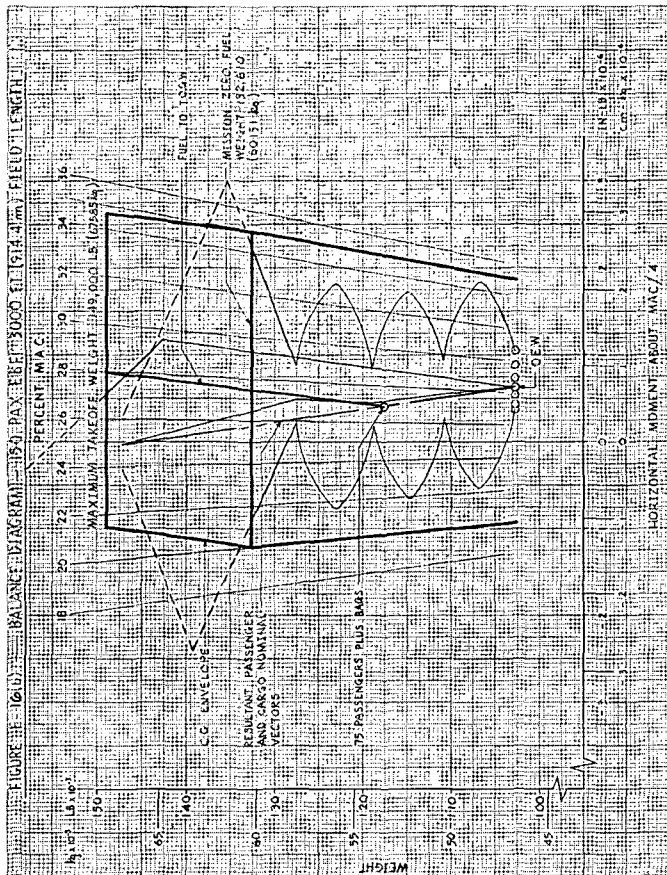


Figure E-16 SAMPLE PROBLEM CHARTS AND NOMOGRAPHS

Pitch (K = .204)

$$\begin{aligned}\text{English: } I_{\text{PITCH}} &= (.204)^2 (149,000 \text{ lb}) (1500 \text{ in})^2 \left(\frac{1 \text{ ft}^2}{4632 \text{ in}^2 - \text{ft/sec}^2} \right) \\ &= 3.01 \times 10^6 \text{ slug} - \text{ft}^2\end{aligned}$$

$$\text{Metric: } I_{\text{PITCH}} = (.204)^2 (67,585 \text{ kg}) (38.1 \text{ m})^2 = 4.08 \times 10^6 \text{ kg-m}^2$$

Roll (K = .167)

$$\begin{aligned}\text{English: } I_{\text{ROLL}} &= (.167)^2 (149,000 \text{ lb}) (1297 \text{ in})^2 \left(\frac{1 \text{ ft}^2}{4632 \text{ in}^2 - \text{ft/sec}^2} \right) \\ &= 1.51 \times 10^6 \text{ slug} - \text{ft}^2\end{aligned}$$

$$\text{Metric: } I_{\text{ROLL}} = (.167)^2 (67,585 \text{ kg}) (32.9 \text{ m})^2 = 2.04 \times 10^6 \text{ kg-m}^2$$

Yaw

$$\text{English: } I_{\text{YAW}} = (.94) (3.01 + 1.51) = 4.25 \times 10^6 \text{ slug-ft}^2$$

$$\text{Metric: } I_{\text{YAW}} = (.94) (4.08 + 2.04) = 5.75 \times 10^6 \text{ kg-m}^2$$

Page Intentionally Left Blank

APPENDIX F

FINAL DESIGN AIRCRAFT CONTROL SYSTEM, HANDLING QUALITIES, AND FLIGHT ENVELOPE

The discussions which follow describe in general terms the control systems, handling qualities and flight envelopes to which the final design aircraft have been designed. These descriptions are based upon the extensive research that the McDonnell Douglas Corporation has accomplished on STOL aircraft during the past five years. This experience is represented and integrated into the final designs.

F.1 Control System

The flight control systems consist of the mechanical flight control, trim, and fuel systems and a stability and control augmentation system. All control surfaces are operated by irreversible hydraulic actuators.

Longitudinal control is derived through a trailing-edge elevator. Longitudinal trim is achieved through adjustable stabilizer incidence, and control feel is supplied by an elevator load feel system in which force gradients are provided as functions of airspeed and stabilizer incidence.

Lateral control is derived through ailerons and spoilers. There are three spoiler segments on each wing panel. All three spoilers on both wing panels are used for direct lift control, landing spoilers, and speed brakes, but only the outboard two spoilers are used for lateral control. Lateral control forces are provided by a simple bungee system. There is a lateral control dead band equivalent to ± 5 percent of the total lateral control over which the spoilers do not operate. Most lateral trim requirements are thus accomplished by aileron deflection alone through the lateral

feel system.

Directional control is derived through a double-hinged rudder. Rudder pedal forces are supplied by a simple bungee system, and trim is accomplished through the feel system.

Direct lift control (DLC) is achieved through the symmetrical actuation of the spoilers which are located immediately forward of the wing flaps. When the wing flaps are lowered to the landing approach setting, the spoilers are raised to approximately 45 degrees TEU to provide a lift decrement of 0.15g at approach speeds. During the landing approach, the positioning of the spoiler can be varied to provide glide path control. The spoiler is lowered to its original position to provide a lift increment of 0.15g during the flare maneuver. DLC spoiler deflections are commanded by thumb switch on the throttle lever or a thumb switch on the control wheel/stick. DLC is primarily used for precise flight path control during the final part of landing approaches and is the primary landing flare control.

The Stability and Control Augmentation System (SCAS) consists of pitch and roll attitude stabilization with pitch and roll rate command proportional to control force and turn coordination and Dutch roll damping augmentation in the yaw channel. Although primarily designed for STOL mode operation the SCAS is operable throughout the flight envelope with appropriate gain changes with airspeed.

F.2 Flying Qualities

F.2.1 Longitudinal. -

Longitudinal Control Effectiveness

The critical longitudinal control effectiveness considerations in the STOL mode are takeoff rotation and landing flare. The 35-percent chord single-slotted elevator is designed to provide takeoff rotation capability at 90 percent of the desired rotation speed with the center of gravity at the forward permissible limit, 20 percent MAC.

The pitching acceleration capability in the STOL mode is 0.40 rad/sec². This is somewhat below that specified in MIL-F-83300, AGARD 408A, and TN D-5594 (References 46 through 48) but is considered to be adequate. Sufficient control is available to rotate the airplane as required to achieve desired short takeoff performance. The critical landing control requirement is satisfied by direct lift control.

In regard to the landing flare, aerodynamic ground effects in the form of reduced lift curve slope, reduced maximum lift, and nose down pitching moment change due to reduced downwash make the landing flare particularly difficult. The results of flight tests sponsored by NASA, flight simulator studies conducted by the contractor, and open-loop dynamic analyses indicate the landing flare is an open-loop process and that aircraft rotation alone does not provide sufficient lift to accomplish the flare. The results of contractor studies also indicate that flare control through thrust is not sufficiently precise with readily achievable thrust responses characteristics but that relatively precise flare control can be achieved through DLC with a 0.15g authority if consistent flare initiation heights between 30 and 40 feet (9.1 and 12.2 m) can be achieved.

A calculated time history of a typical DLC flare is shown in Figure F-1. The aircraft is rotated to a 10-degree nose-up attitude by longitudinal control application when the flare is initiated.

Static and Maneuvering Stability

The aircraft is stable with respect to angle of attack to angles well beyond the conceived operating envelope with the center of gravity at the aft permissible limit, 35 percent of MAC.

The longitudinal control feel system is designed such that control deflection force gradient are a function of airspeed and stabilizer incidence (thus center-of-gravity position) to provide relatively constant maneuvering force gradients with minimal effects of center-of-gravity location.

Dynamic Longitudinal Stability

The dynamic longitudinal stability of the unaugmented aircraft in the STOL mode is characterized by a relatively sluggish well-damped short period mode, a relatively high-frequency lightly-damped phugoid mode, and relatively strong coupling between the longitudinal modes. The frequency and damping of the two longitudinal modes are summarized as follows:

STOL MODE DYNAMIC LONGITUDINAL STABILITY SCAS OFF				
	Frequency rad/sec	Period sec	Damping Ratio	
Short Period	0.281	22.3	0.917	$T_{1/10} = 3.9 \text{ sec}$
Phugoid	0.288	21.8	0.047	$T_{1/2} = 50.9 \text{ sec}$

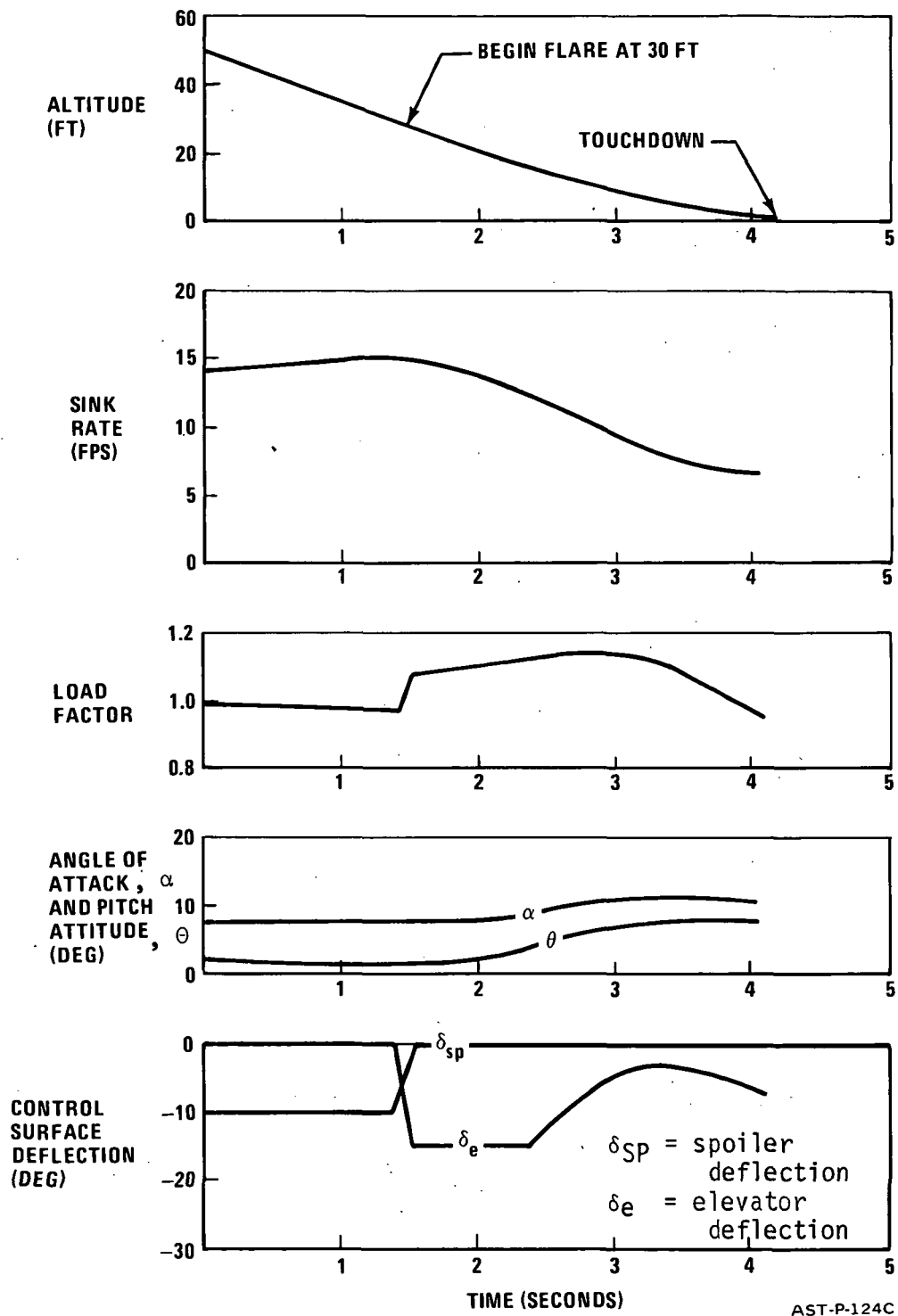


Figure F-1. Landing Flare Time History

In addition to the relatively sluggish short-period mode and the associated sluggish response to pitch commands, the aircraft has a low effective lift curve slope in the STOL mode. As a consequence of these low lift curve slopes and the strength of the coupling between the short-period and phugoid modes, longitudinal control of flight path is particularly poor. The strength of short-period and phugoid mode coupling can also be characterized by the vertical speed stability or slope of the flight path angle - speed curve ($d\gamma/dV$). The aircraft is well on the backside of the speed-drag or thrust required curve. As might be expected, it is necessary to control flight path angle and altitude through thrust and speed through longitudinal control under such conditions.

The longitudinal SCAS is designed to hold pitch attitude and provides pitch rate control proportional to longitudinal control force. As a consequence of the attitude-hold function, the SCAS effectively decouples the short-period and phugoid modes and provides excellent static stability. The effect of SCAS on the dynamic longitudinal stability is illustrated in the following tabular summary of the frequency and damping of the short-period and phugoid modes with SCAS on.

STOL MODE DYNAMIC LONGITUDINAL STABILITY
SCAS ON

	Frequency rad/sec	Period sec	Damping Ratio	
Short Period	3.96	1.59	0.35	$T_{1/10} = 3.88 \text{ sec}$
Phugoid	0.33	19.0	0.91	$T_{1/2} = 0.5 \text{ sec}$

It should be noted that flight path and altitude are still controlled by thrust, and speed is still controlled by longitudinal control with the SCAS on. Where as thrust is the primary altitude and flight path control, it is a relatively sluggish and gross control. Precise altitude control during the final approach is achieved through DLC.

F.2.2 Lateral-Directional. -

Control Effectiveness

Lateral control effectiveness in the STOL mode can be characterized in terms of rolling acceleration capability, one-second bank-angle change capability, or time required to accomplish a specific bank angle change (30 degrees, for example). These characteristics are summarized as follows for nominal STOL approach conditions:

Rolling Acceleration (Rad/sec²): $\ddot{\phi} = 0.54$

One Second Bank Angle Change (Deg): $\Delta\phi_{1 \text{ sec}} = 8.4$

Time to Bank 30 Degrees (Sec): $t_{30} = 1.8$

Directional control effectiveness can be characterized by the yawing acceleration capability; the steady-sideslip capability, and the asymmetric thrust control capability. Yawing acceleration capability in the STOL mode is primarily an indication of the ability to decrab during cross-wing landing flares; however, STOL cross wind landing approaches preferably would be made without rapid decrabbing prior to touchdown. A gradual transition from a crabbed approach to a steady sideslipping approach should be accomplished at an altitude of 100-150 feet, well before flare initiation. Steady sideslip capability is thus a much more meaningful directional control consideration.

The yawing-acceleration and steady-sideslip capabilities in the STOL mode are summarized as follows:

Yawing Acceleration (Rad/sec²): $\ddot{\psi} = 0.15$

Steady Sideslip Angle (Deg): $\beta_{\max} = 20$

Engine out, asymmetric thrust control in the STOL mode is of particular concern with externally-blown flap (EBF) STOL transport configurations and can be illustrated by the minimum speed at which maximum thrust asymmetries can be controlled and by the dynamics of the aircraft following an abrupt engine failure with the pilot attempting to maintain control. The minimum control speed in the takeoff and landing waveoff configurations is approximately 65 knots (33 m/sec). This speed is the minimum at which there is sufficient lateral and directional control to balance the maximum thrust asymmetry associated with one engine inoperative. Lateral control is a major consideration and the conventional 5-degree bank angle limitation is generally not critical. The minimum control speed quoted above provides a speed margin of 15 to 20 knots (7.7 to 10.3 m/sec) from anticipated STOL operating speeds.

A net rolling acceleration capability of 0.20 rad/sec² exists at anticipated STOL operating speeds after balancing the lateral asymmetry.

Contractor experience indicates a minimum rolling acceleration capability of at least 0.15 rad/sec² should exist under these conditions.

Time histories of the aircraft response to abrupt asymmetric engine failures obtained from fixed base flight simulator studies are shown in Figures F-2, F-3, F-4 and F-5 in takeoff and waveoff configurations with and without SCAS operation. The "SCAS-off" data show adequate control of the thrust asymmetry although the Dutch roll damping is particularly poor. The

Figure F-2.

RH OUTBOARD ENGINE CUT TIME HISTORY DURING TAKEOFF

$W/S = 80 \text{ LB/FT}^2$

$S_{f \text{ TOT}} = 23^\circ$

OB ENGINE @ 50% $b_{W/E}$

$T/W = .615$

$V_{e=0} = 100 \text{ KT}$

YAW DAMPER, TURN
COORDINATOR AND
SCAS OPERATIVE

4 ENGINE $C_{\mu} = 1.89$

3 ENGINE $C_{\mu} = 1.12$

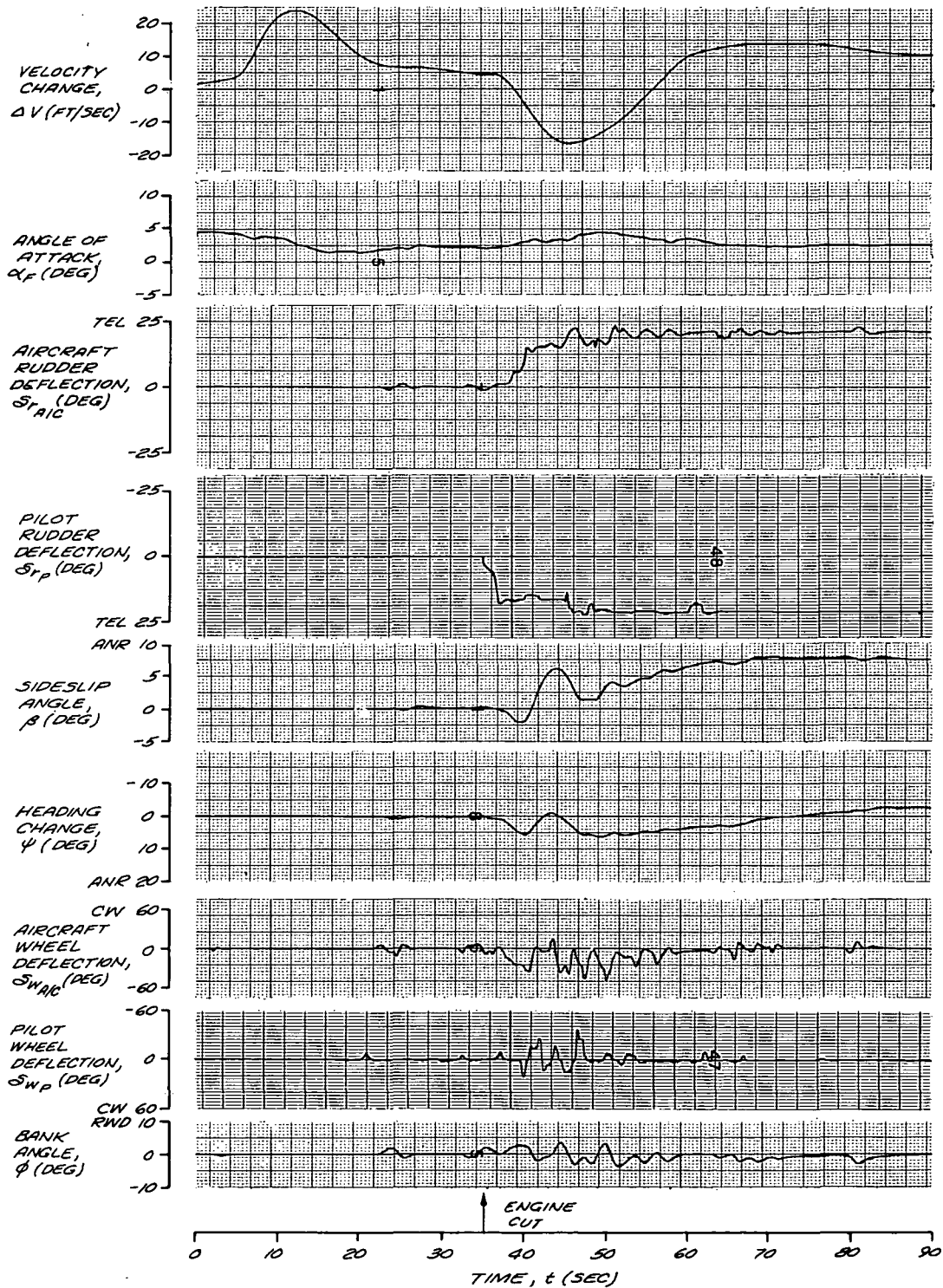


Figure F-3.

RH OUTBOARD ENGINE CUT TIME HISTORY DURING TAKEOFF

$W/S = 80 \text{ LB/FT}^2$

$S_{F \text{ TOT}} = 23^\circ$

OB ENGINE @ 50% $b_{W/2}$

$T/W = .615$

UNAugMENTED
AIRCRAFT

4 ENGINE $C_{\mu} = 1.49$

$V_{ct=0} = 100 \text{ KT}$

3 ENGINE $C_{\mu} = 1.12$

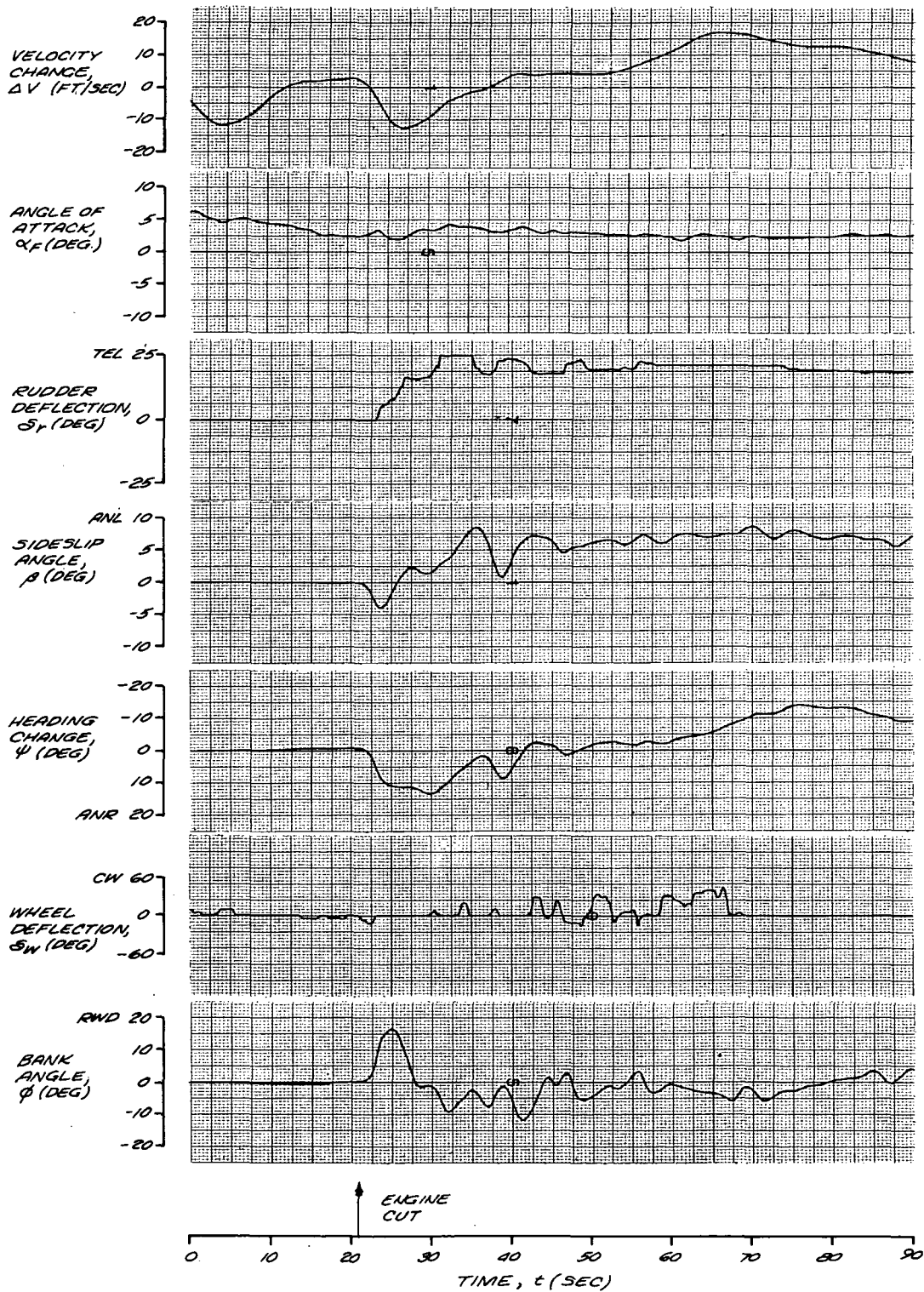


Figure F-4.

RH OUTBOARD ENGINE CUT TIME HISTORY DURING WAVEOFF

$W/S = 80 \text{ LB/FT}^2$

$S_{f \text{ TOT}} = 46^\circ$

OB ENGINE @ 50% b_{WIZ}

$T/W = 0.615$

YAW DAMPER, TURN
COORDINATOR AND
SCAS OPERATIVE

4 ENGINE $C_{\mu} = 2.31$

3 ENGINE $C_{\mu} = 1.73$

$V_{c, t=0} = 80 \text{ KT}$

NOTE: SIMULATION INCLUDED
MODERATE TURBULENCE

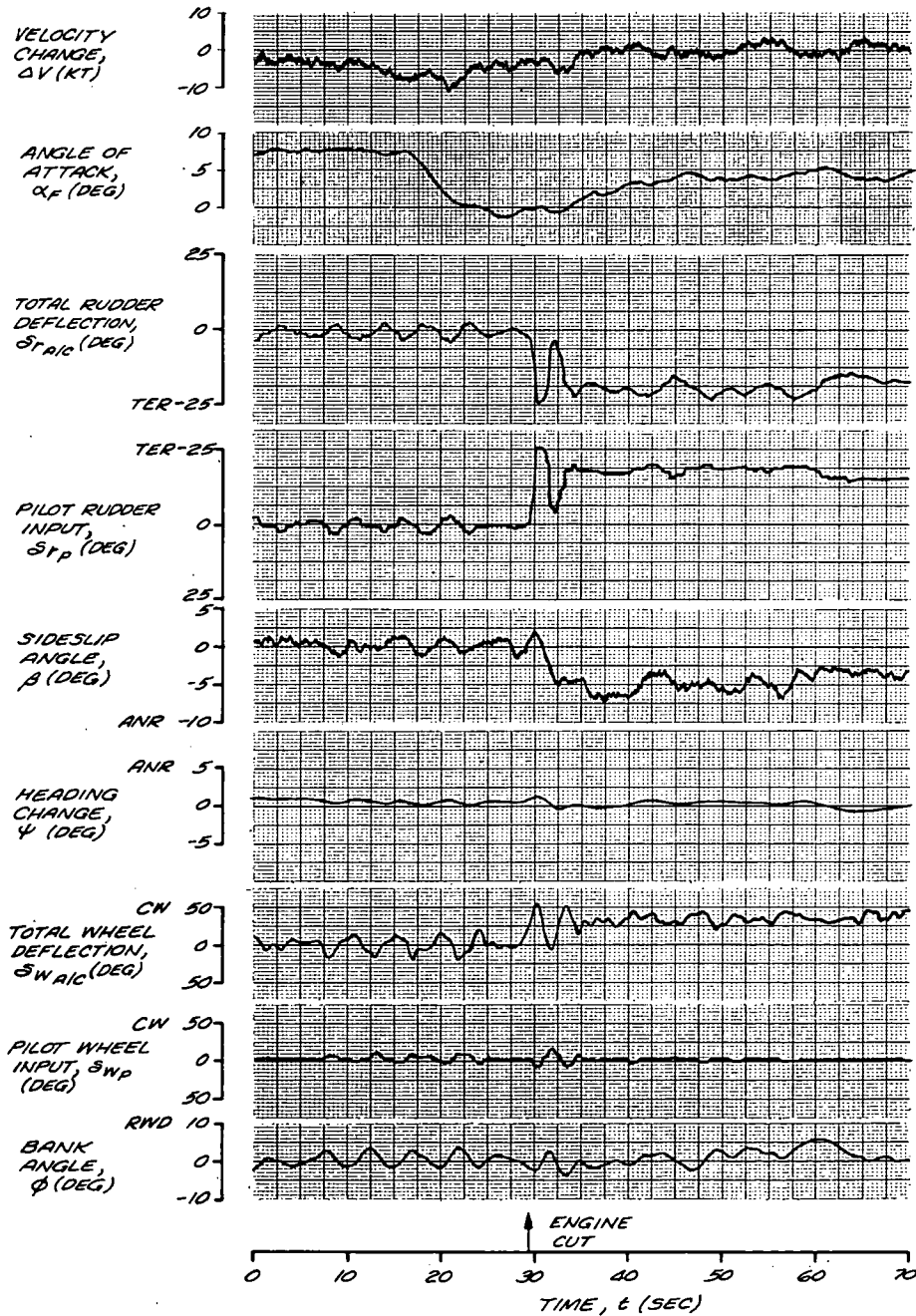


Figure F-5.

RH OUTBOARD ENGINE CUT TIME HISTORY DURING WAVEOFF

$W/S = 80 \text{ LB/FT}^2$

$S_F \text{ TOT} = 46^\circ$

OB ENGINE @ 50% $b_{W/E}$

$T/W = 0.615$

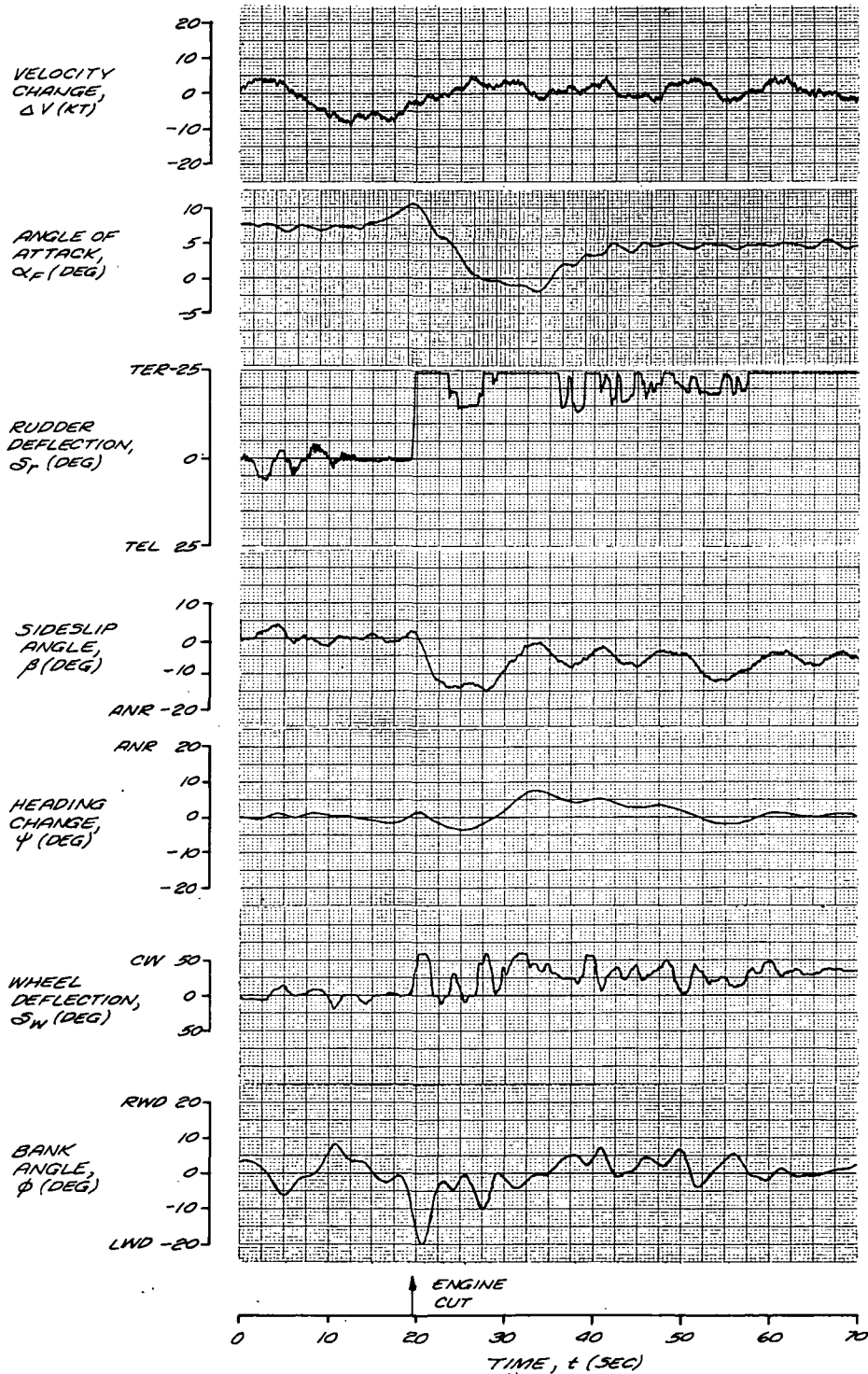
UNAUGMENTED
AIRCRAFT

4 ENGINE $C_\mu = 2.31$

$V_{c t=0} = 80 \text{ KT}$

3 ENGINE $C_\mu = 1.73$

NOTE: SIMULATION INCLUDED
MODERATE TURBULENCE



"SCAS-on" data show very little disturbance and relatively little pilot control activity as a result of the engine failure. Both the steady state and dynamic engine failure control characteristics appear to be satisfactory. In light of the tendency of the SCAS to mask an asymmetric thrust failure, auditory warning of the failure may be necessary.

The static lateral-directional stability characteristics as indicated by the lateral and directional control deflections and bank angle per unit sideslip angle in steady sideslips in the STOL mode are summarized as follows:

$$\text{Directional Stability: } \frac{d\delta_r}{d\beta} = 1.01$$

$$\text{Lateral Stability: } \frac{d\delta_a}{d\beta} = 0.22$$

$$\text{Side force curve slope: } \frac{d\phi}{d\beta} = 0.30$$

These data show that the airplane possesses positive controls fixed static directional stability and dihedral effect and has negative side force curve slope. For example, increasing left rudder, right aileron, and right bank angle are required for increasing right steady sideslips.

The maximum attainable steady sideslip angle is 20 degrees. This permits steady sideslipping approaches in 90 degree cross winds in excess of 25 knots (12.9 m/sec) at normal STOL approach speeds of 85 knots (43.7 m/sec). A bank angle of 6.5 degrees is required in this situation. Crabbed cross-wind landing approaches require excessive directional control power to decrab the airplane rapidly prior to touchdown unless cross wind landing gear are used. In view of the improved visibility and control precision associated with sideslipping approaches, transition to sideslipping approaches is

accomplished on final approach at an altitude of 100 to 150 feet.

Dynamic Lateral-Directional Stability

The dynamic lateral-directional stability characteristics in the STOL mode at normal STOL operational speeds without SCAS are summarized as follows:

1. The Dutch roll mode has a period of 7.9 seconds and damps to half amplitude in 5.5 seconds.
2. The spiral mode is unstable and doubles amplitude in 8 seconds.
3. The roll mode time constant is 1.2 seconds.

These characteristics are not sufficiently good to be considered satisfactory but are considered acceptable for emergency operation.

The result of fixed base flight simulator tests conducted by the contractor confirms this conclusion.

SCAS operation improves these characteristics appreciably:

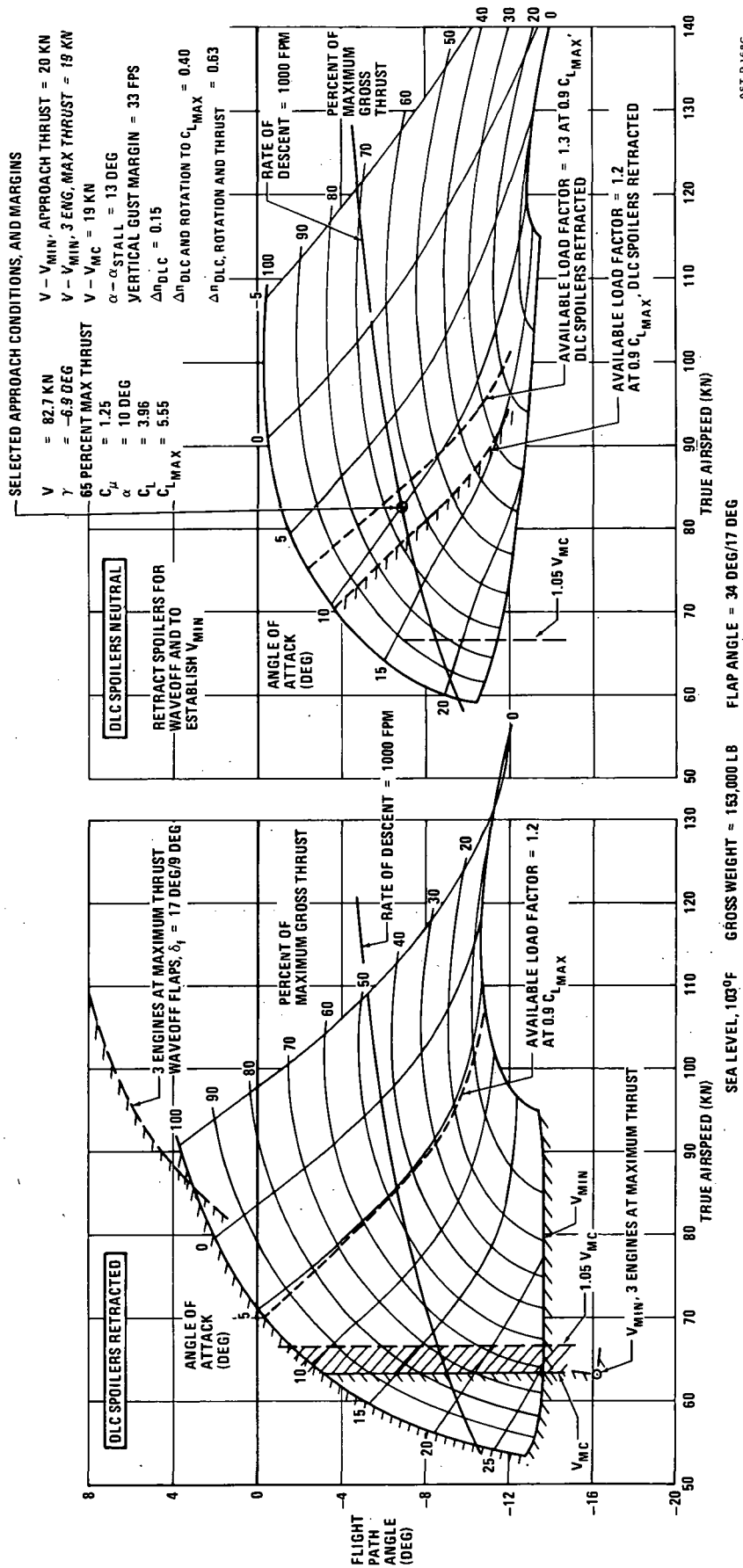
1. Dutch roll damping with SCAS on is increased to the point that the time to damp to half amplitude is reduced to 0.78 seconds. The period is reduced to 2.95 seconds.
2. The spiral mode is stabilized by SCAS operation to give a 2.7 second time to damp to half amplitude. This represents a major flying quality improvement.
3. The roll mode time constant is reduced from 1.2 to 0.8 seconds.

F.3 STOL Flight Envelope

Typical STOL mode operating conditions are illustrated in the speed-flight-path-angle (V - γ) envelope of Figure F-6 in which constant angle of attack and thrust lines are presented. The desire to continue an approach after an engine failure makes it necessary to limit thrust level in the approach to a maximum of 65 percent. Pilot perception of altitude and sink rate requires limitation of the approach sink rate to a maximum of 1000 feet per minute (5.1 m/sec). Maneuverability considerations require some maneuvering margin from the stall. Although there is little flight experience upon which to base such criteria, the contractor feels the available maneuvering load factor should be at least 1.2 and has thus established a requirement for 1.2g at 0.9 $C_{L_{max}}$. Inasmuch as DLC is the primary maneuvering device, the maneuvering margin is established with the DLC spoilers closed. An angle-of-attack margin from the stall of at least 10 degrees is also considered to be desirable. This corresponds to a 25-foot-per-second (7.6 m/sec) vertical gust at a nominal approach speed of 85 knots (43.7 m/sec).

It is essential that anticipated operating speeds be well above minimum control speeds with maximum thrust asymmetries associated with an engine failure. However there are no established criteria regarding how large the speed margin should be. It is suggested that minimum operating speeds be at least 5 percent or 5 knots (2.6 m/sec) above the minimum asymmetric thrust control speed. Inasmuch as the minimum control speed is 64 knots (33 m/sec) this criterion does not appear to be critical. It is also recommended that a net lateral control power of at least 0.15 radians per second squared exist with an engine out at minimum operating speeds. A net rolling acceleration capability

Figure F-6
TYPICAL STOL MODE OPERATING CONDITIONS



AST-P-168C

of 0.20 radians per second squared exists with an engine inoperative at recommended minimum STOL operating speeds.

As indicated in Figure F-6, one-g stall speed (V_{MIN}) is greatly affected by thrust. In this case the recommended minimum STOL landing approach speed, 82.7 knots (42.5 m/sec), is 12.5 knots (6.4 m/sec) above the approach power stall speed. Maintenance of adequate maneuver and stall angle margins appears to provide adequate stall speed margins.

F.4 Conclusions

The flying qualities of unaugmented propulsive lift STOL transport aircraft are not satisfactory for operational use. A fairly sophisticated stability and control augmentation system is therefore required to improve the basic handling qualities to the currently acceptable standards. The summary presented in this appendix is characteristic of all propulsive lift systems. The mechanical flap type of aircraft will exhibit much of the handling quality characteristics of conventional aircraft with the exception of degradations which occur as a result of lower flying speeds. Difficulty in achieving satisfactory handling qualities increases as the field length or operating speeds are decreased. Existing state-of-the-art concepts, however, are available and adequate to provide excellent handling qualities for all aircraft of this study.

APPENDIX G

RIDE QUALITIES

G.1 Introduction Ride Qualities

Aircraft with relatively low wing loadings are more responsive to turbulence upsets than high wing loading aircraft at comparable airspeeds.

The primary objective of this study was to investigate the ride quality characteristics of a typical low wing loading propulsive lift (EBF used as typical) aircraft and to explore the effects of various stability and control augmentation concepts on aircraft response to turbulence. A complete design study of the ride qualities of all the final design aircraft is beyond the scope of this study. Rather the work reported in this section is intended to identify some of the potential problems which must be addressed to provide satisfactory ride qualities for low wing loading STOL aircraft.

The aircraft chosen for the study had a wing loading of 65 psf (317 kg/m^2). This is close to the value of 70 psf (342 kg/m^2) for the EBF 2000 foot (610 m) 150 passenger final design aircraft (Section 2.3). This initial study concentrated on aircraft dynamic behavior in the approach mode and used the Dryden turbulence model from the flying qualities specification MIL-F-8785B (Reference 2) to provide external disturbances. A basic RMS value of 10 ft/sec (3.04 m/sec) was chosen for the turbulence model as representing a realistic level of gust activity for the approach mode. Ride qualities characteristics were evaluated on the basis of normal acceleration activity for the longitudinal axis and lateral acceleration excursions for the lateral/directional axes.

The systems discussed in this report apply specifically to the approach mode. Cruise and transition flight regimes may require different system configurations due to restrictions on the types of control surfaces available and the change in aircraft dynamic characteristics.

G.2 Longitudinal Axis

Longitudinal transfer functions for augmented and unaugmented aircraft are shown in Table G-1. Figure G-1 shows an example block diagram of the type of augmentation system studied. This particular configuration utilizes pitch rate feedback to spoiler surfaces. The turbulence model is shown as providing vertical gust disturbance inputs to the closed loop system (W_G).

The basic unaugmented aircraft frequency response characteristic for normal acceleration due to vertical gust is shown on Figure G-2. A peak in the acceleration response occurs at a frequency of 0.3 rad/sec due to the lightly damped phugoid mode of the basic aircraft. This characteristic shows the magnitude of the aircraft normal acceleration for sinusoidal vertical gusts applied at each frequency value. The gust model then applies the appropriate frequencies pertinent to atmosphere turbulence in the vertical plane and an estimate of aircraft normal acceleration excursions can be made from the power spectral density characteristic as discussed below. Figure G-3 shows a power spectral density plot of normal acceleration activity for the basic aircraft. The corresponding standard deviation or RMS normal acceleration value (calculated from the area under the power spectral density curve) is approximately 4.2 ft/sec² (1.3 m/sec²) or 0.13g for this case. The effect of pitch rate and normal acceleration feedback on aircraft response to a vertical gust is shown in Figure G-4. Curve A shows the effect of pitch rate and normal acceleration

Table G-1

LONGITUDINAL TRANSFER FUNCTIONS

APPROACH CONDITION

$$Wt = 121,875 \text{ lbs (55,281 kg), Wing loading} = 65 \text{ lbs/ft}^2 \text{ (317 kg/m}^2\text{)}$$

$$V_{EAS} = 73 \text{ kts (37.5 m/sec), C.G.} = 25\%$$

$$\alpha = 6.7^\circ, \quad \gamma = -6.7^\circ$$

$$\text{VERTICAL GUST MODEL } H_W(S) = \frac{10.0 (S + 0.144)}{(S + 0.25)^2}$$

$$\frac{A_Z}{W_{GUST}} \text{ (Basic Aircraft)}$$

$$= \frac{0.65 (S^2 + 0.034S + 0.123)(S + 1.2)S}{(S^2 + 1.87S + 1.16)(S^2 + 0.027S + .08)}$$

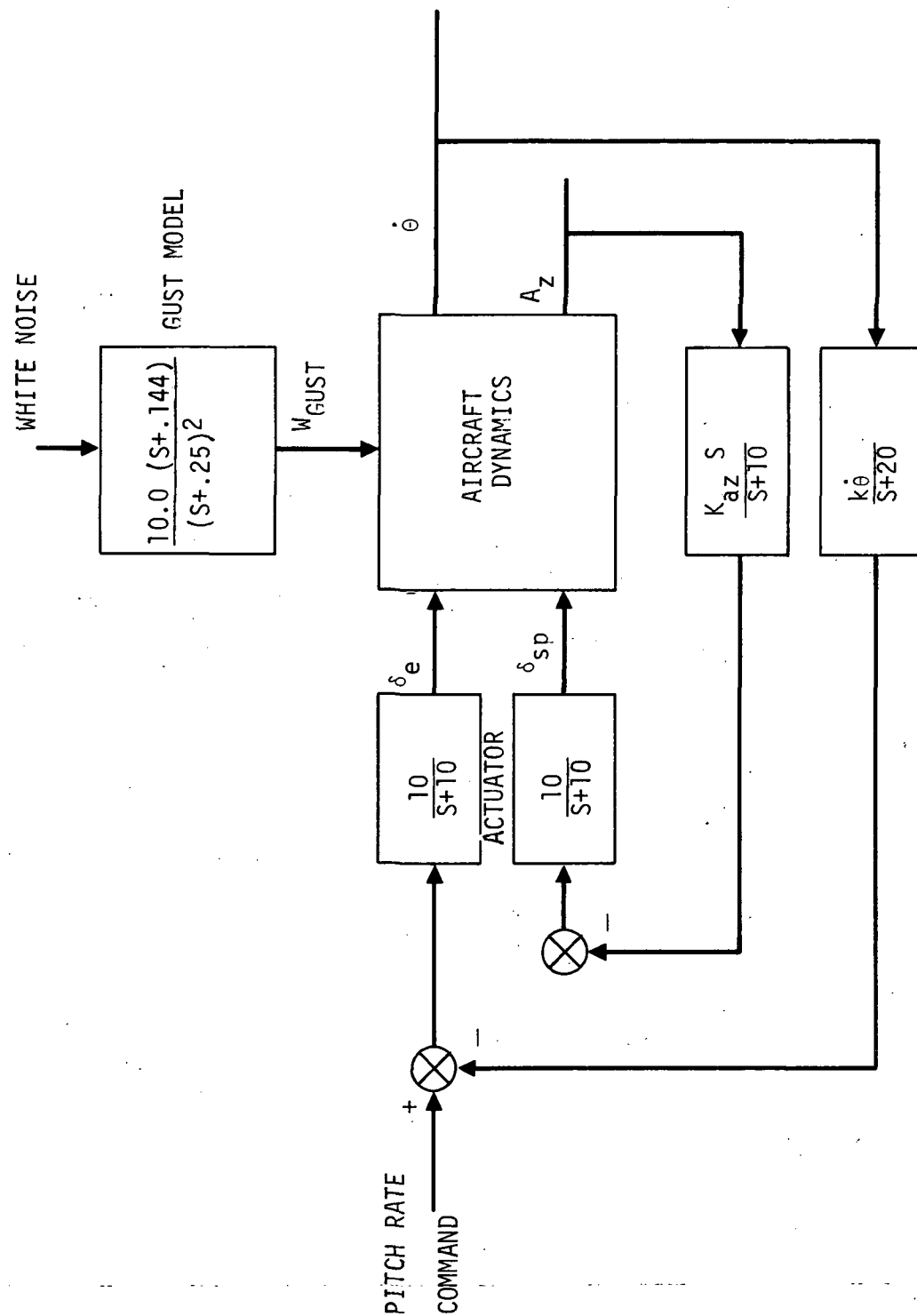
$$\frac{A_Z}{W_{GUST}} \text{ (Basic Aircraft + } \dot{\theta}/\delta_e + A_Z/\delta_e \text{ loops closed)}$$

$$= \frac{0.65 (S^2 + 0.12S + 0.02)(S^2 + 7.4S + 57.6)(S + 23.7)(S + 10.0)S}{(S^2 + 0.098S + 0.02)(S^2 + 7.08S + 89.4)(S + 22.7)(S + 7.4)(S + .6)}$$

$$\frac{A_Z}{W_{GUST}} \text{ (Basic Aircraft + } \dot{\theta}/\delta_e + A_Z/\delta_{sp} \text{ loops closed)}$$

$$= \frac{0.65 (S^2 + 20.S + 100.)(S + 10.)(S + 10)(S - 4.)(S + 0.16)(S - .12)S}{(S^2 + 9.8S + 107.)(S^2 + 18.0 + 89.5)(S + 20.)(S + .56)(S + .09)(S + .03)}$$

(Normal Acceleration Measured at C.G.)



LONGITUDINAL RIDE CONTROL SYSTEM (APPROACH)

Figure 6-1

BASIC AIRCRAFT NORMAL ACCELERATION/VERTICAL GUST

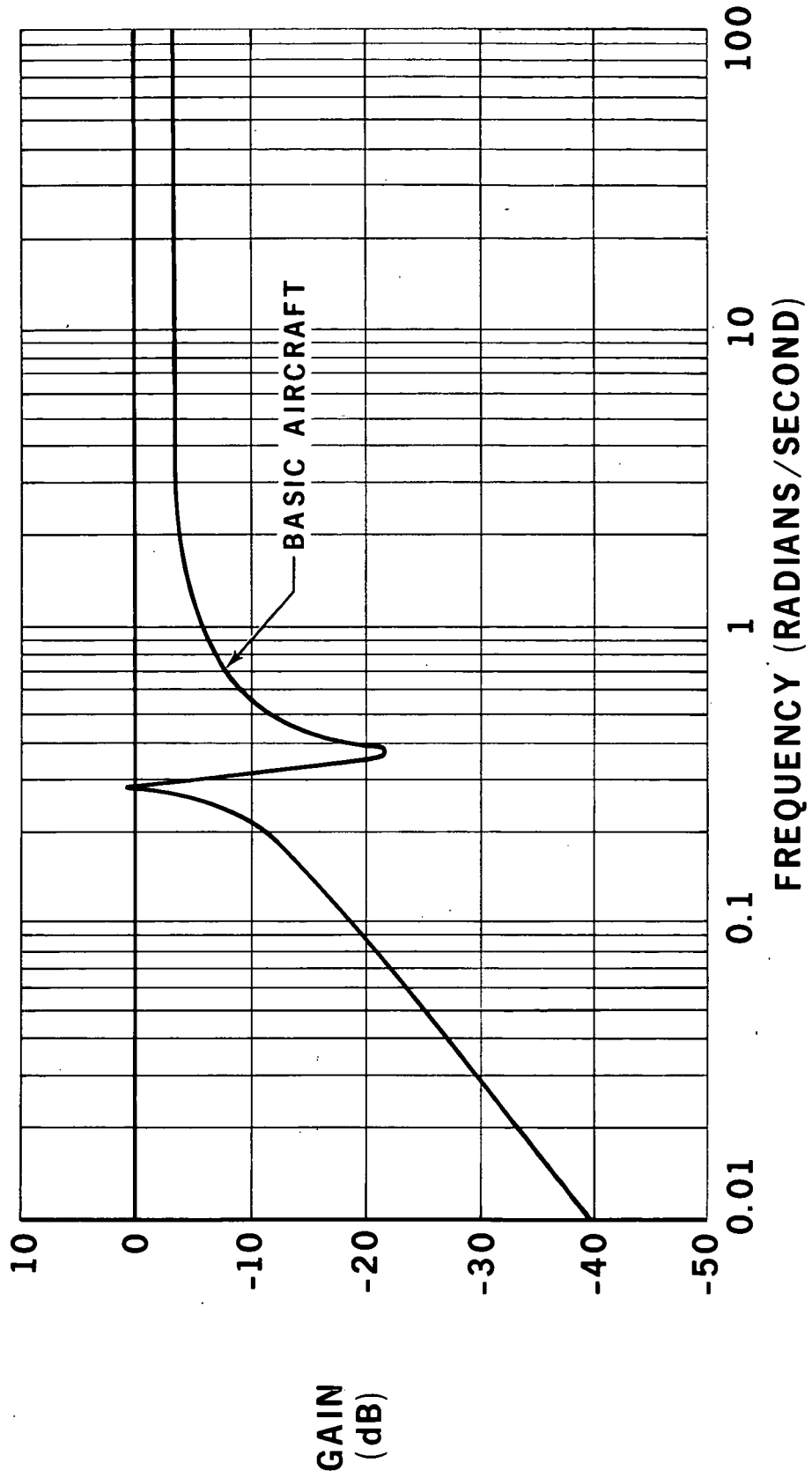


FIGURE G-2

PR3-STOL-1540

POWER SPECTRUM OF NORMAL ACCELERATION

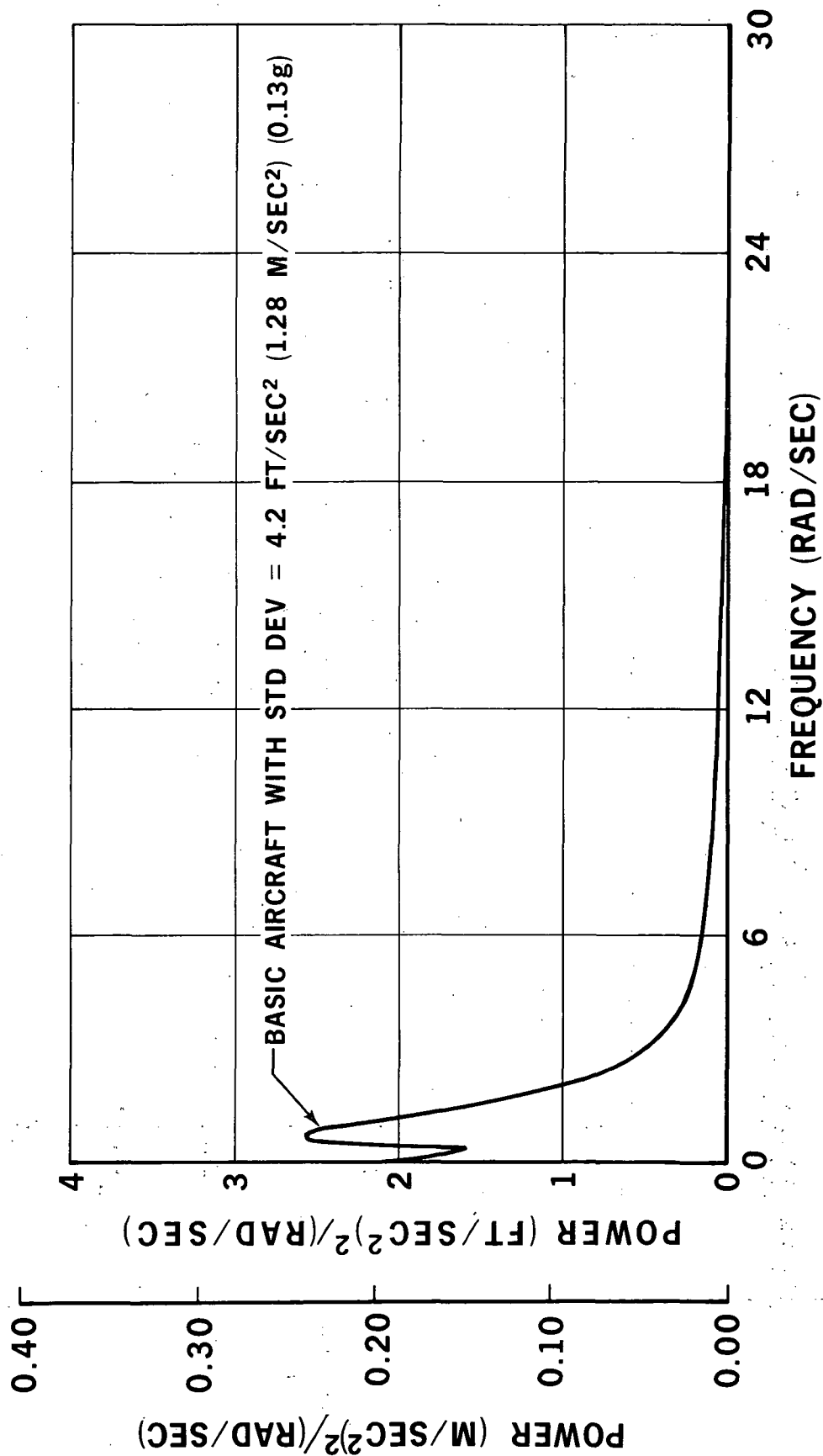
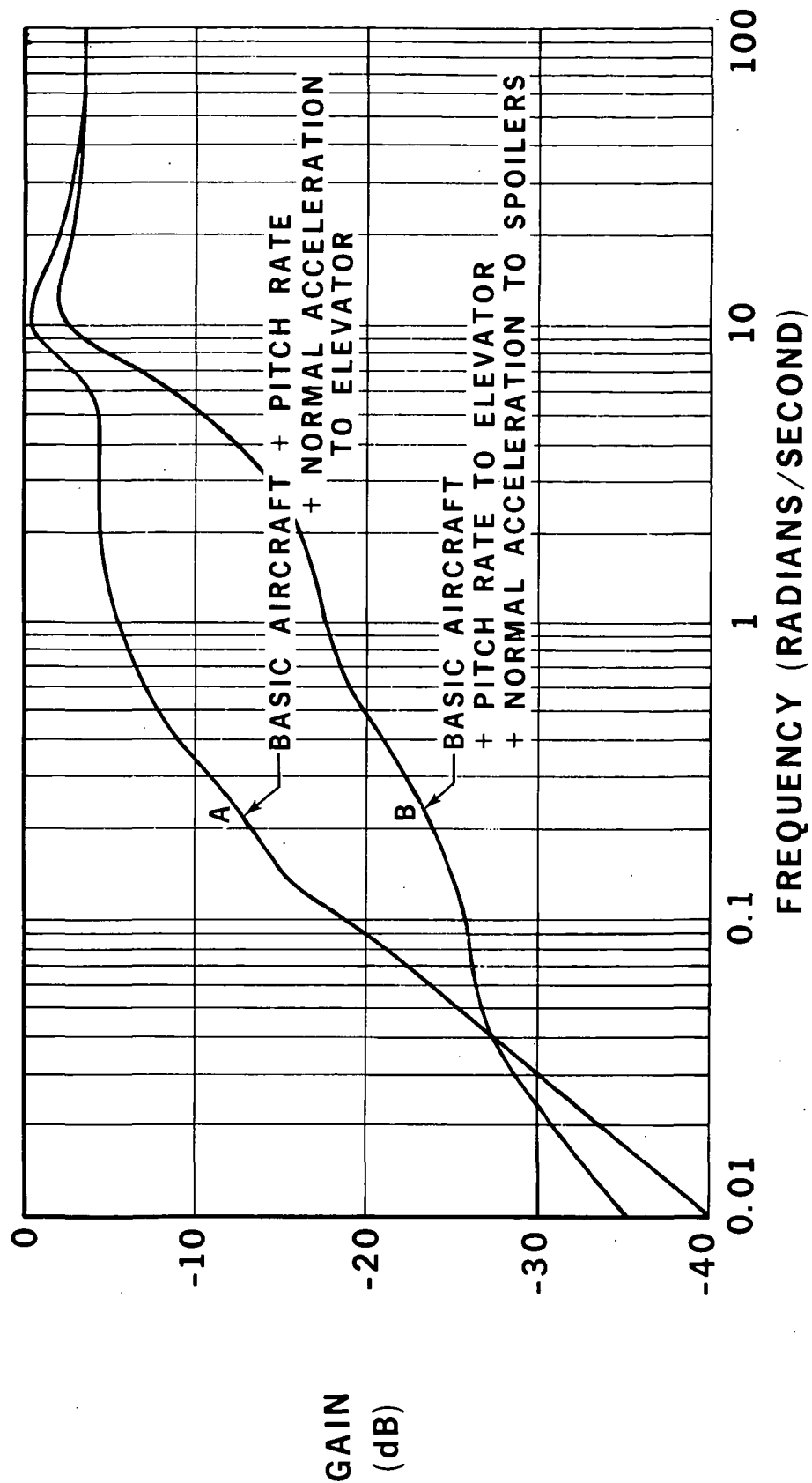


FIGURE G-3

PR3-STOL-1538

NORMAL ACCELERATION/VERTICAL GUST



PR3-STOL-1541

FIGURE G-4

feedback to the elevator. Curve B illustrates the effect of pitch rate feedback to the elevator and normal acceleration feedback to spoiler surfaces. It is evident that although the basic aircraft dynamic modes are fairly well damped in either case, feedback of normal acceleration to spoilers produces lower levels of aircraft acceleration in the critical frequency range 0.1 to 10.0 rads/sec.

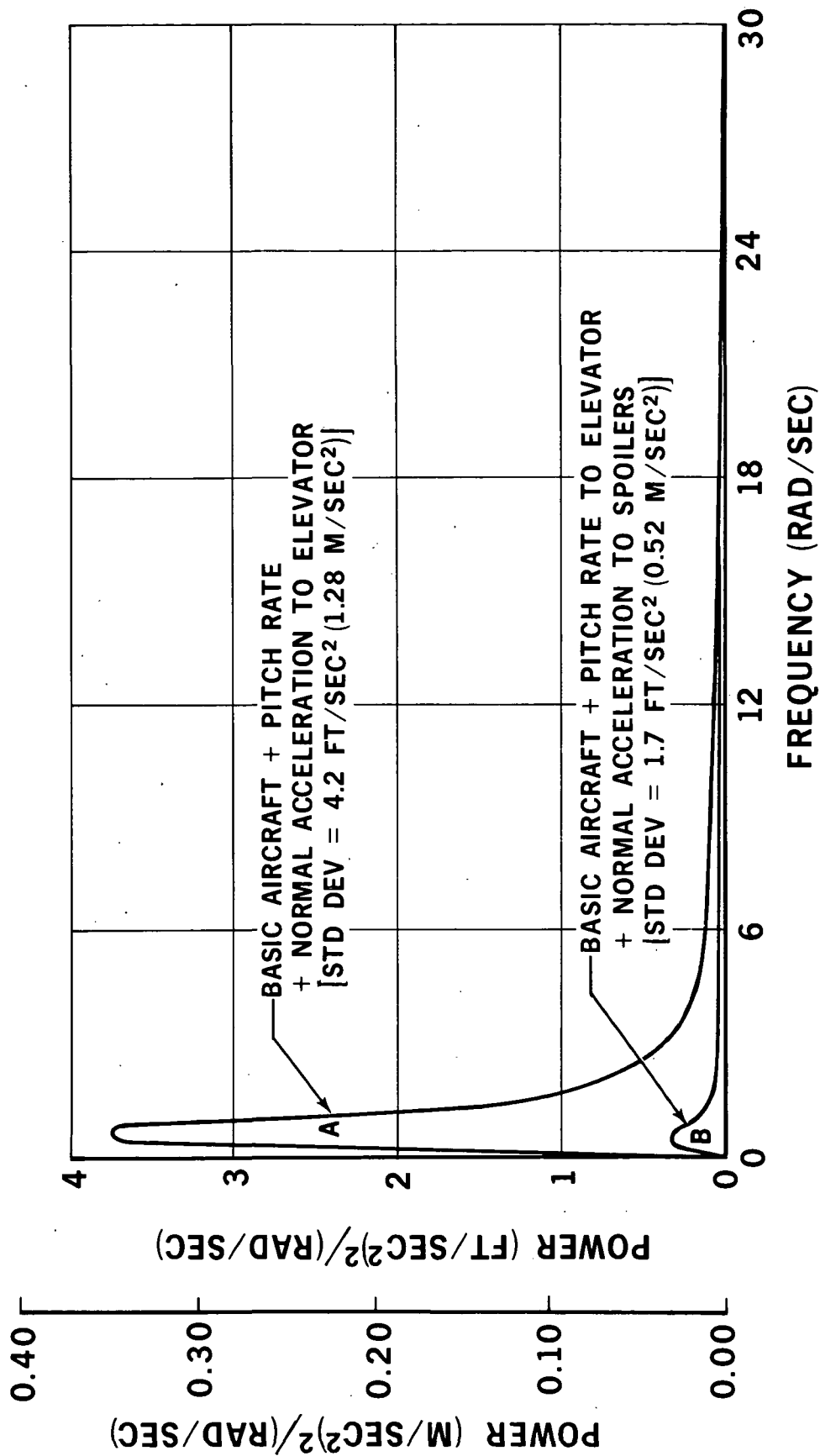
Power spectral density plots for the above two cases as shown in Figure G-5 also indicate much less activity with acceleration feedback to spoilers, the standard deviation for Case A (acceleration feedback to elevator) being approximately 0.13g and for Case B (acceleration feedback to spoilers) being in the region of 0.05g.

Acceleration activity was computed for forward, mid and aft aircraft locations and the results are summarized in Figure G-6. For the purposes of comparison a basic acceptance criterion for normal acceleration activity was extracted from Reference 1. This criterion states that acceptable levels of normal acceleration should be less than 0.1g and the boundary is indicated in Figure G-6. It will be observed that both the basic aircraft and the augmentation system utilizing pitch rate and normal acceleration to the elevator have acceleration levels higher than 0.1g. Feedback of normal acceleration to spoiler surfaces, however, provides sufficient gust suppression to lower RMS acceleration values to less than 0.1g for the three aircraft locations studied.

G.3 Lateral/Directional Axes

Lateral/directional transfer functions for unaugmented aircraft are shown in Table G-2. It will be observed that the basic aircraft has a lightly

POWER SPECTRUM OF NORMAL ACCELERATION

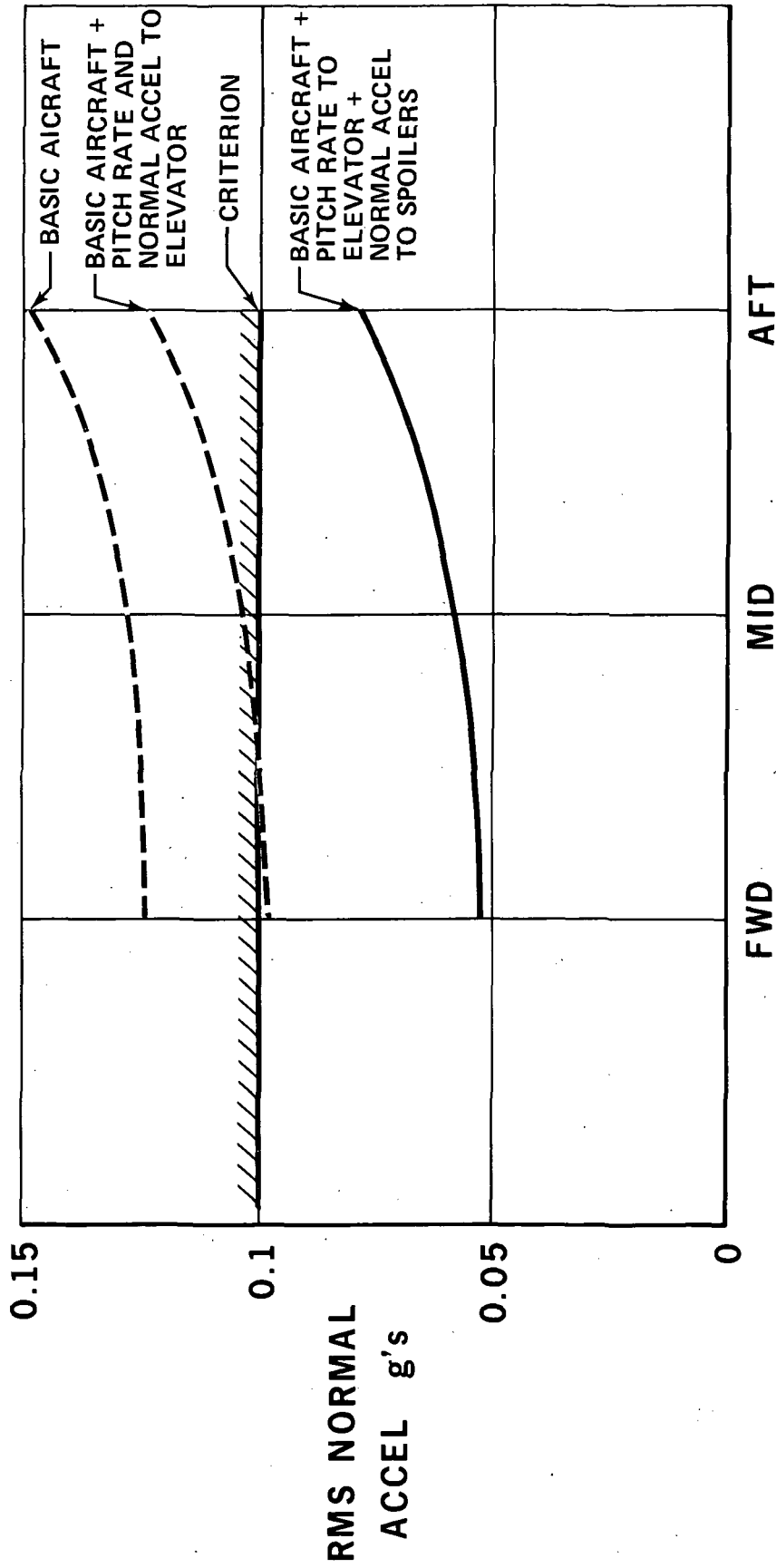


PR3-STOL-1539

FIGURE G-5

AIRCRAFT NORMAL ACCELERATION

ACTIVITY IN TURBULENCE



C.G. POSITION

FIGURE G-6

Table G-2

LATERAL TRANSFER FUNCTIONS

$$\text{LATERAL GUST MODEL } H_{\beta}(s) = \frac{3.0 (s+0.12)}{(s+0.21)^2}$$

$$\frac{A_y}{\beta_{\text{GUST}}} \text{ (Basic Aircraft)}$$

$$= \frac{0.41 (s^2 - 0.36s + 0.167)(s - 0.03)s}{0.99(s^2 + 0.095s + 0.63)(s + 0.98)(s - 0.035)}$$

DUTCH ROLL MODE ($\zeta_0 = 0.06$)	ROLL MODE CONSTANT	UNSTABLE SPIRAL MODE
--	--------------------------	----------------------------

$$\frac{A_y}{\beta_{\text{GUST}}} \text{ (Basic Aircraft + Yaw Damper + } A_y/\delta_r \text{ loops closed)}$$

$$= \frac{0.41(s^2 - 0.075s + 0.003)(s + 0.65)(s - 0.42)s}{0.99(s^2 + 0.3s + 0.45)(s + 0.94)(s + 0.5)(s - 0.016)}$$

$$\frac{A_y}{\beta_{\text{GUST}}} \text{ (Basic Aircraft + Yaw Damper + } \dot{\phi}/\delta_A + \phi/\delta_A \text{ loops closed)}$$

$$= \frac{0.41 (s^2 + 0.1s + 0.18)(s + 6.0)(s + 1.2)(s + 0.065)s}{0.98(s^2 + 7.4s + 16.7)(s^2 + 0.38s + 0.4)(s + 0.47)(s + 0.057)}$$

(Normal Acceleration Measured at C.G.)

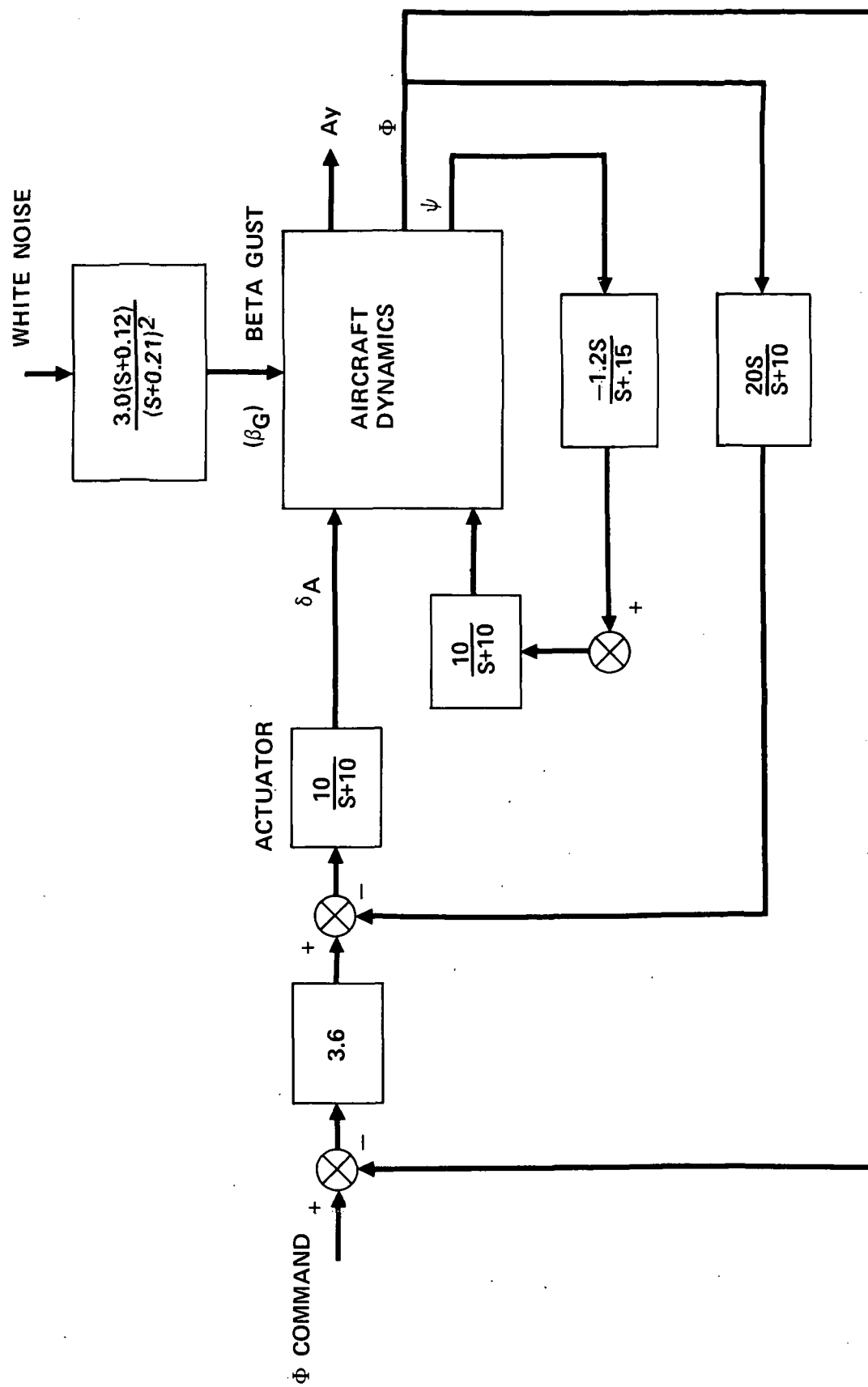
damped dutch roll mode ($\zeta = 0.06$) and an unstable spiral mode which doubles amplitude in 20 seconds.

An example of the type of augmentation system studied for the lateral/directional axes is shown in block diagram form in Figure G-7. Washed out yaw rate feedback to rudder is used to provide damping of the dutch roll mode. The basic aircraft unstable spiral mode is stabilized by means of a combination of roll rate and roll attitude feedback to ailerons. The turbulence model is shown as providing external sideslip type disturbance inputs to the aircraft (β_G).

The basic aircraft lateral acceleration response characteristics to side gust is shown in Figure G-8. Peak response activity occurs at the frequency of the lightly damped dutch roll mode ($\omega_d = 0.8$ rad/sec).

Figure G-9 shows a power spectral density plot for basic aircraft lateral acceleration activity. The standard deviation is approximately 1.6 ft/sec² (0.49 m/sec²) or 0.05g.

The effect of utilizing yaw rate and lateral acceleration feedback to rudder is shown in Figure G-10. The dutch roll mode is now fairly well damped although lateral acceleration gains are still relatively large in the frequency range of 0.1 to 1.0 rad/sec. If a desired level of dutch roll damping is maintained using yaw rate feedback to rudder and the basic aircraft spiral mode is stabilized with a combination of roll rate and roll attitude feedback to rudder, then the results are as shown in Figure G-11. Lateral acceleration response for this case is less than for the previous case with lateral acceleration feedback to rudder (critical frequency range of 0.1 to 10.0 rad/sec).

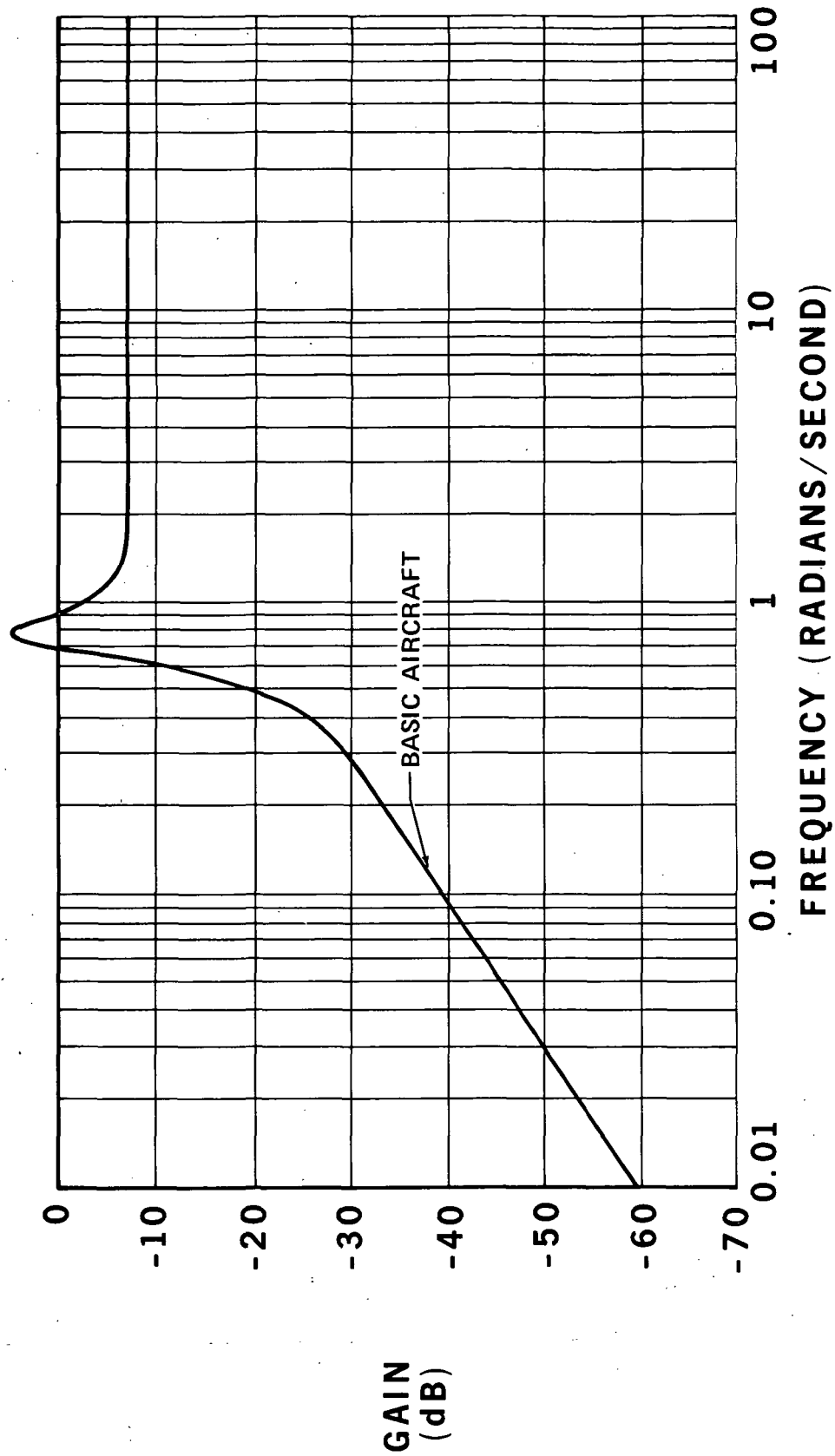


LATERAL CONTROL SYSTEM

FIGURE G-7

BASIC AIRCRAFT LATERAL ACCELERATION ACTIVITY

LATERAL ACCELERATION/BETA GUST



PR3-STOL-1552

FIGURE G-8

BASIC AIRCRAFT LATERAL ACCERATION ACTIVITY

POWER SPECTRUM OF LATERAL ACCELERATION

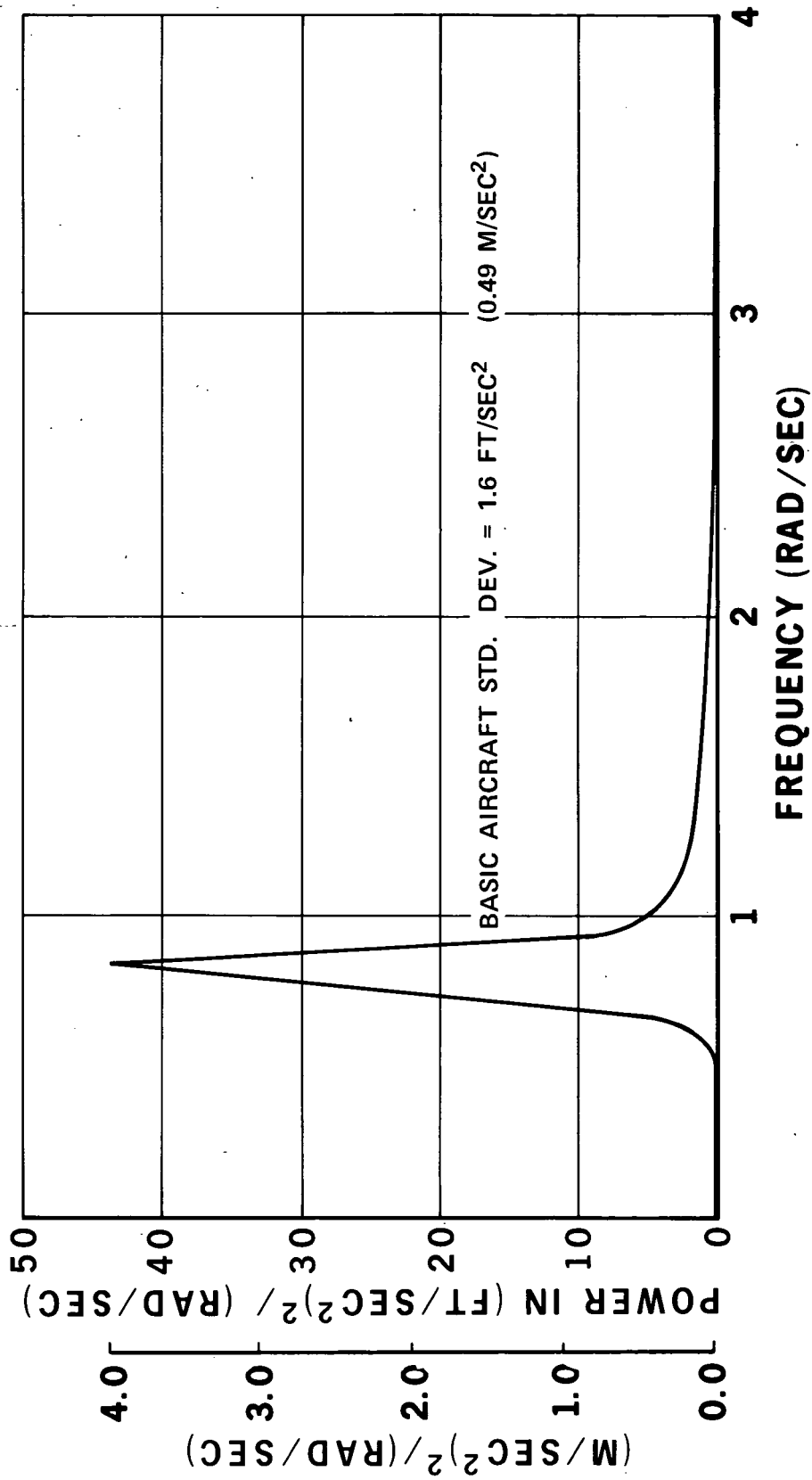
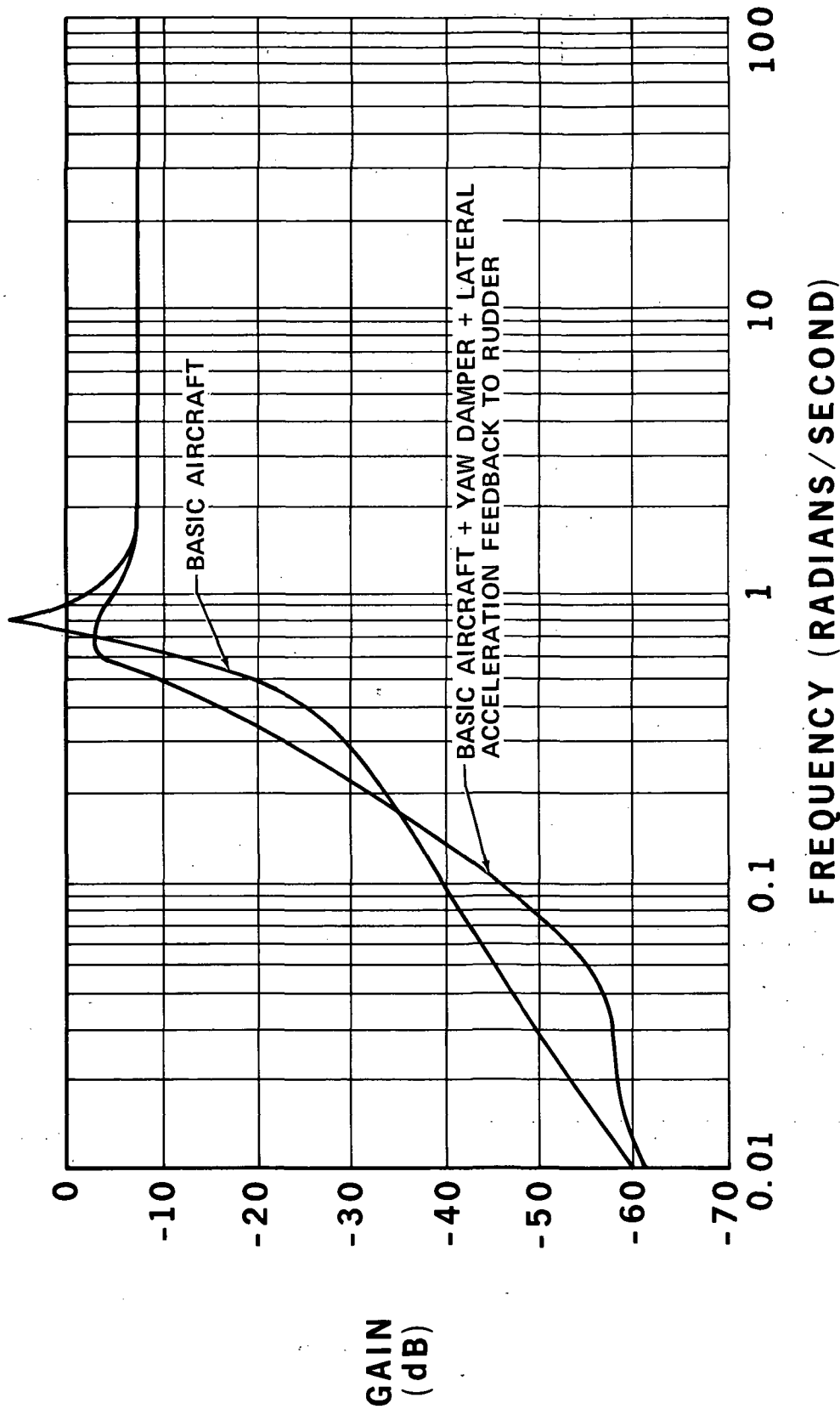


FIGURE G-9

PR3-STOL-1546

EFFECT OF YAW RATE + LATERAL ACCELERATION FEEDBACK TO RUDDER

LATERAL ACCELERATION/BETA GUST (B_G)



PR3-STOL-1553

FIGURE G-10

EFFECT OF ROLL RATE AND ROLL ATTITUDE FEEDBACK TO AILERONS

LATERAL ACCELERATION/BETA GUST

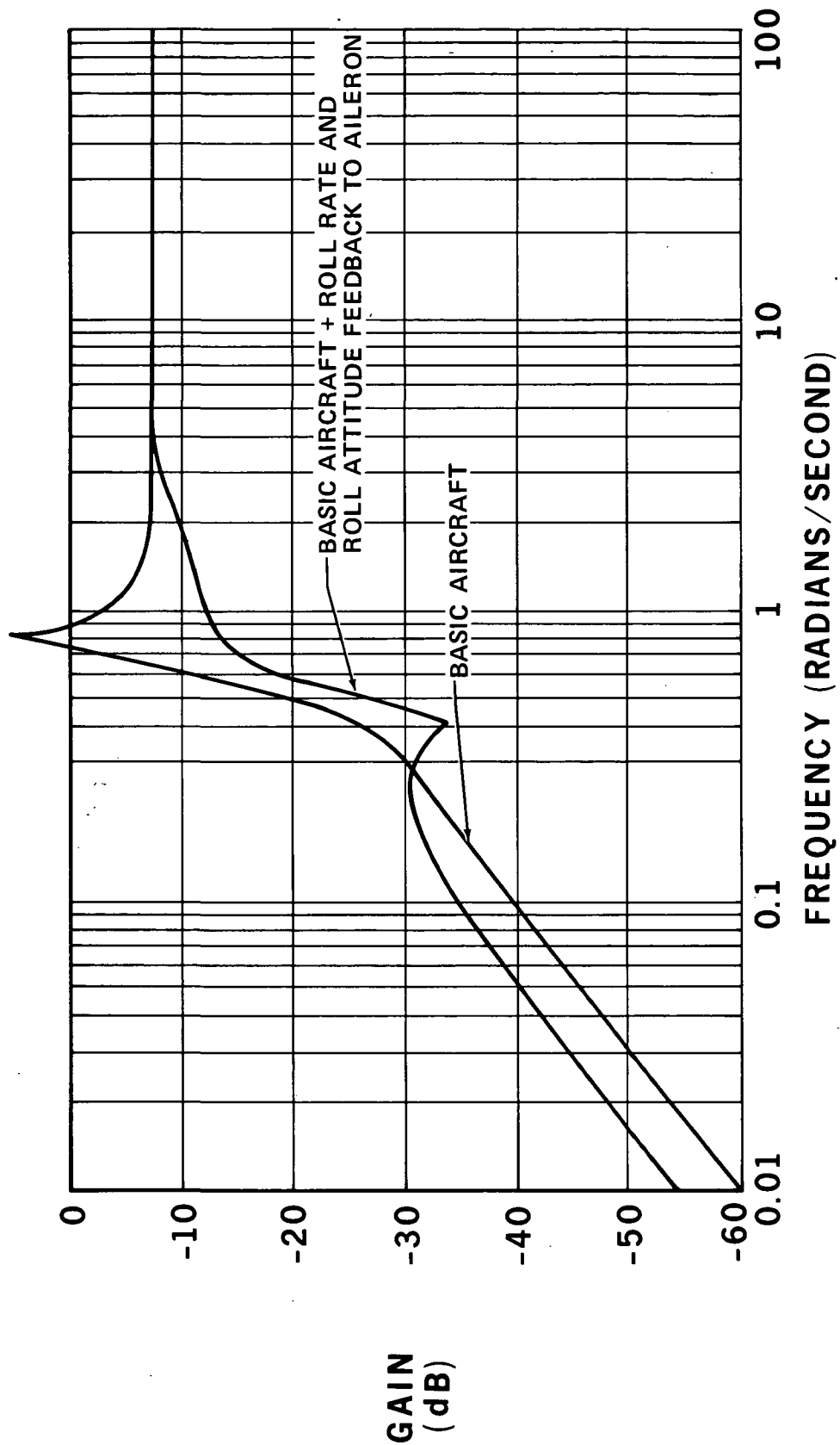


FIGURE G-11

PR3-STOL-1551

The corresponding power spectral density plots are shown in Figure G-12. The standard deviation values for roll rate and attitude feedback to rudder (0.6 ft/sec^2 (0.18 m/sec^2) versus 1.22 ft/sec^2 ($.37 \text{ m/sec}^2$)). Results are summarized on Figure G-13 for RMS lateral acceleration values measured at three aircraft locations.

It will be observed that the aft CG location produces the largest values of RMS lateral acceleration. Basic aircraft activity is in the region of $0.18g$ at the aft location. A basic acceptance criterion of $0.06g$ was extracted from Reference 49 and is shown on Figure G-13 for purposes of comparison. The augmentation system with roll rate and roll attitude feedback to aileron represents the only case where lateral acceleration activity is less than $0.06g$ at the aft location.

G.4 Conclusions - Ride Qualities

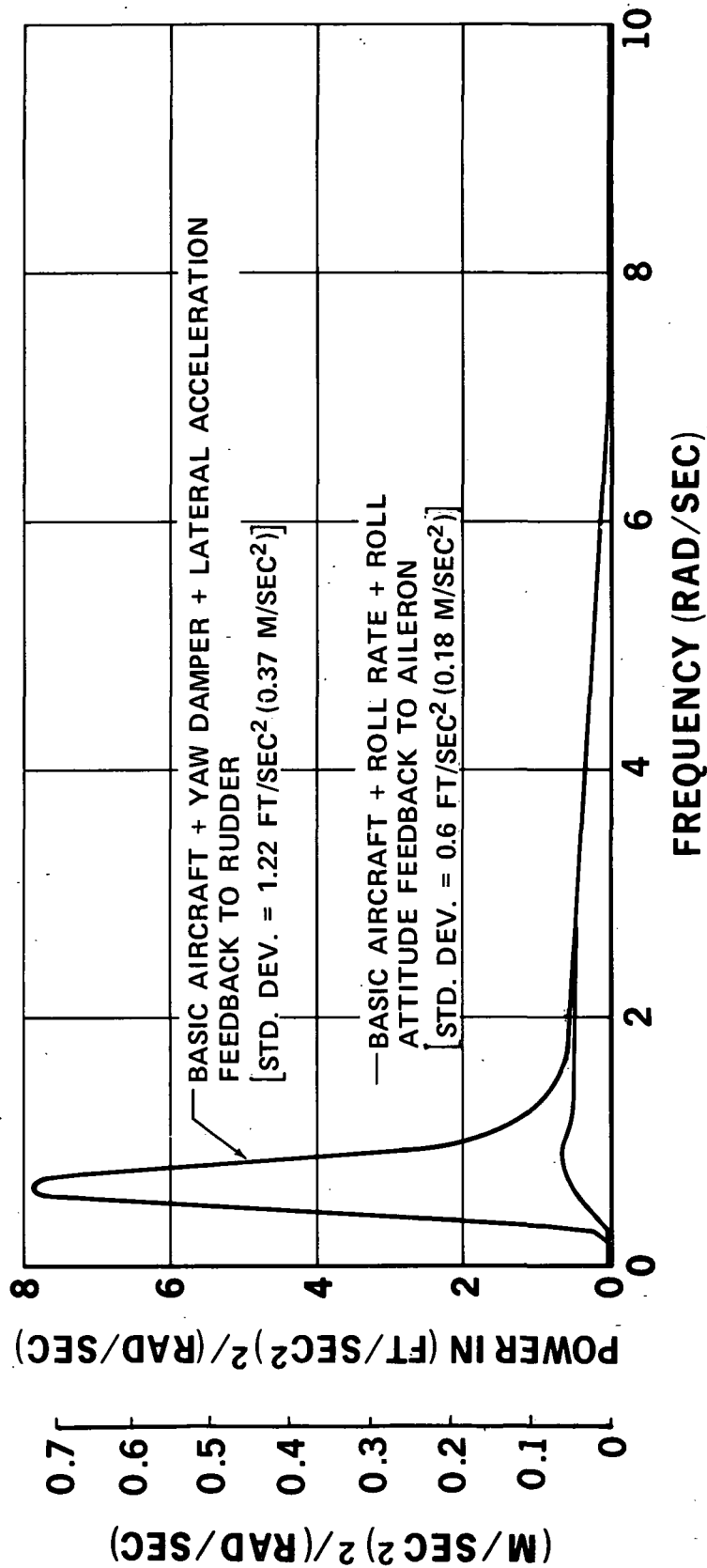
Use of elevator surfaces for improvement in longitudinal ride qualities for the STOL approach mode does not appear to be very effective.

This study has indicated that an effective method of reducing normal acceleration activity in turbulence is to utilize normal acceleration feedback to spoiler surfaces and to use pitch rate feedback to elevator as a means of providing the necessary damping signals. Since the use of spoiler surfaces in cruise or transition flight regimes is not feasible, it will be necessary to explore alternate solutions for those conditions.

In the lateral/directional axes lateral acceleration feedback to rudder appears to be undesirable for the following reasons.

BASIC AIRCRAFT LATERAL ACCELERATION ACTIVITY

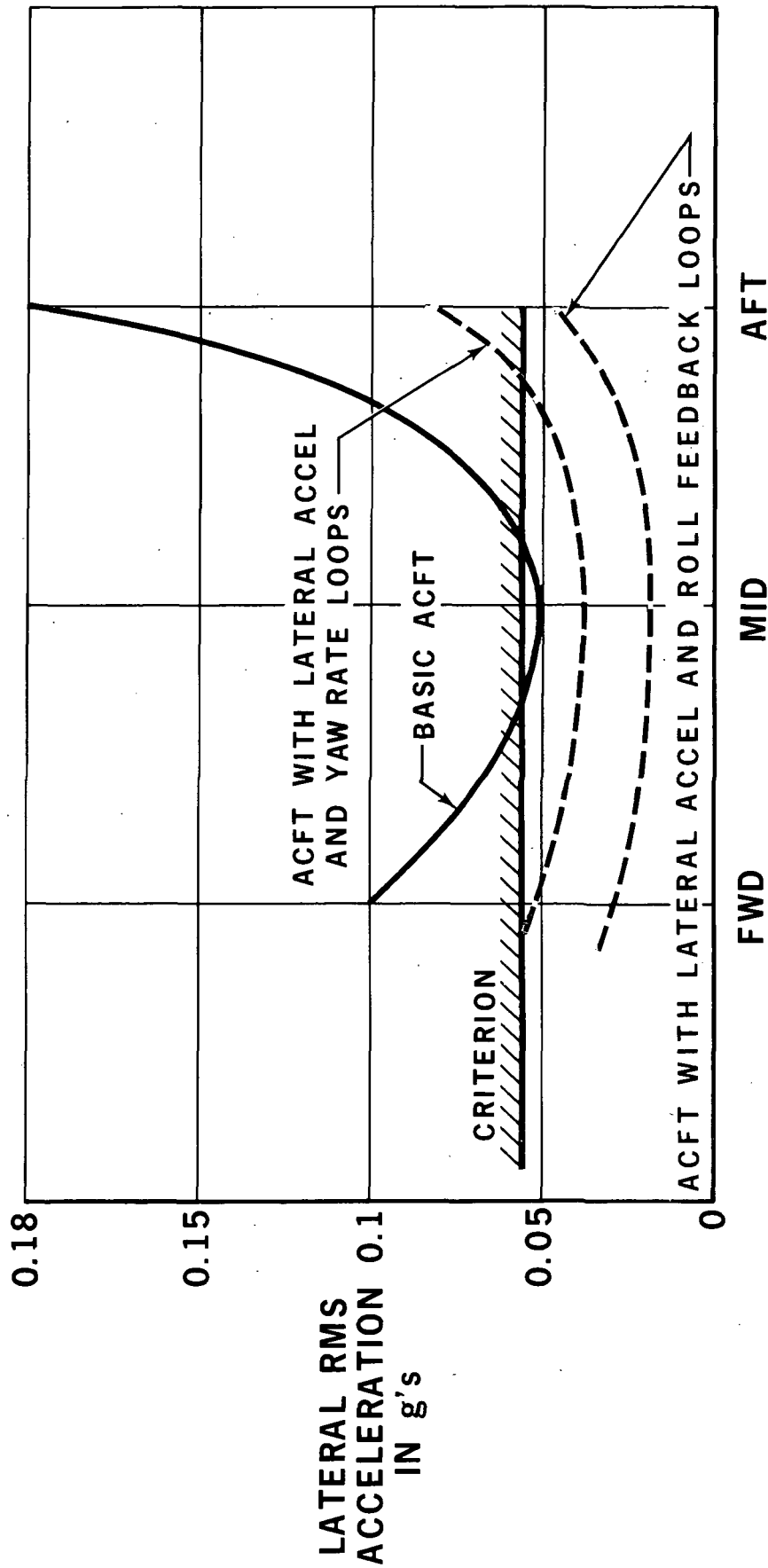
POWER SPECTRUM OF LATERAL ACCELERATION



PR3-STOL-1550

FIGURE G-12

AIRCRAFT LATERAL ACCELERATION ACTIVITY IN TURBULENCE



C.G. POSITION

FIGURE G-13

PR3-STOL-1542

- o The spiral mode is destabilized.
- o The basic damping of the dutch roll mode is reduced.
- o This type of feedback is not sufficiently effective to reduce lateral accelerations at the aft position to an acceptable level.

The use of roll rate and roll attitude feedback to the ailerons in conjunction with a conventional yaw damper does reduce lateral acceleration levels to an acceptable level and also provides adequate stability for the basic aircraft spiral mode. Since the basic spiral mode is normally stable in the cruise flight regime it is possible that lateral acceleration feedback to rudder would be sufficiently effective to provide satisfactory ride qualities in this condition.